

**Specifics of Forced-Convection Heat Transfer in a Vertical 7-Element
Bundle Cooled with Upward Flow of Supercritical Water**

by

Scott E. Clark

A thesis submitted to the
School of Graduate and Postdoctoral Studies in partial
fulfilment of the requirements for the degree of

Master of Applied Science in Nuclear Engineering

Faculty of Energy Systems and Nuclear Science (FESNS)
University of Ontario Institute of Technology (Ontario Tech University)

Oshawa, Ontario Canada

August 17, 2020

© Scott E. Clark, P. Eng.

THESIS EXAMINATION INFORMATION

Submitted by: Scott E. Clark

Master of Applied Science in Nuclear Engineering

Thesis title:

Specifics of Forced-Convection Heat Transfer in a Vertical 7-Element Bundle Cooled with Upward Flow of Supercritical Water

An oral defense of this thesis took place on July 29th, 2020 in front of the following examining committee:

Examining Committee:

Chair of Examining Committee	Dr. Hossam Gaber, FESNS, UOIT
Research Supervisor	Dr. Igor Pioro, FESNS, UOIT
Examining Committee Member	Dr. Jennifer McKellar, FESNS, UOIT
Examining Committee Member	Dr. Rachid Machrafi, FESNS, UOIT
Thesis Examiner	Dr. Fedor Naumkin, Faculty of Science, UOIT

The above committee determined that the thesis is acceptable in form and content and that a satisfactory knowledge of the field covered by the thesis was demonstrated by the candidate during an oral examination. A signed copy of the Certificate of Approval is available from the School of Graduate and Postdoctoral Studies.

ABSTRACT

Current Generation II/III/III+ Nuclear Power Plants (NPPs) are no longer economically competitive partially due to low thermal efficiencies.

Six Generation IV NPP concepts were proposed having increased thermal efficiency, with Canada investigating the SuperCritical Water Reactor (SCWR) concept. However, determining Heat Transfer specifics for SuperCritical Water in bundle configurations is required.

Many empirical Nusselt number (**Nu**) correlations derived from bare tubes are available, with only one derived from a bundle. No assessments of **Nu** correlations are available for 7-rod bundle datasets, representing the centre of 37-element bundles currently used in Canadian NPPs.

A **Nu** correlation derived from a 7-rod bundle dataset is proposed, and assessed against 35 common **Nu** correlations, using Root Mean Square error and graphical investigation. The assessment indicates the proposed **Nu** correlation is the most suitable for 7-rod bundles and bare tubes.

One typical Canadian SCWR design is confirmed based on maximum fuel centreline and sheath temperatures.

Keywords: Heat Transfer Nusselt number Correlation; SuperCritical Water Reactor (SCWR); Nuclear Engineering; Fuel Bundle; Small Modular Reactor (SMR);

AUTHORS DECLARATION

I hereby declare that this thesis consists of original work of which I have authored. This is a true copy of the thesis, including any required final revisions, as accepted by my examiners.

I authorize the University of Ontario Institute of Technology (Ontario Tech University) to lend this thesis to other institutions or individuals for the purpose of scholarly research. I further authorize University of Ontario Institute of Technology (Ontario Tech University) to reproduce this thesis by photocopying or by other means, in total or in part, at the request of other institutions or individuals for the purpose of scholarly research. I understand that my thesis will be made electronically available to the public.



Scott Clark

STATEMENT OF CONTRIBUTIONS

I hereby certify that I am the sole author of this thesis and that no part of this thesis has been published or submitted for publication. I have used standard referencing practices to acknowledge ideas, research techniques, or other materials that belong to others. Furthermore, I hereby certify that I am the sole source of the creative works and/or inventive knowledge described in this thesis.

ACKNOWLEDGEMENTS

I would like to thank my supervisor, Dr. Igor Pioro, for his support throughout my entire graduate degree. The completion of this thesis project would not be possible without his encouragement and direction.

I would also like to give thanks to my amazing parents, Barb & Barry Smith, and Les Clark and Pat McKee, who have given me unconditional support and guidance through all of my endeavors, and continue to inspire me to be the best I can be on a daily basis.

Also, I would not be here without the unwavering support of my fiancée Justian Shouldice. Without you I would not be completing a Master's degree. I thank you from the bottom of my heart for all the sacrifices made, and promise to spend the rest of my life making up for it.

Additionally, I would like to thank my predecessors whom I have never had the privilege of meeting: Sarah Mokry, Sahil Gupta, and Khalil Sidawi. Without your contributions to this field my work would not have been possible.

Finally, I would like to thank and acknowledge the University of Ontario Institute of Technology (UOIT/Ontario Tech University), and specifically the entire Faculty of Energy Systems and Nuclear Science (FESNS), from professors to the administration, for providing a wonderful experience for me - from research and teaching to navigating the logistics of this degree and financial aid - you have all provided me with a truly enriching period in my life.

NOMENCLATURE

Symbol	Description	Unit	Formula
A	Area	m^2	
C_p	Specific Heat Capacity	$J/kg \cdot K$	
$\overline{C_p}$	Average Specific Heat Capacity	$J/kg \cdot K$	$\overline{C_p} = \frac{H_w - H_b}{T_w - T_b}$
D	Diameter	m	
D_{hy}	Hydraulic-Equivalent Diameter	m	$D_{hy} = \frac{4 \cdot A_{fl}}{p_{wet}}$
Err	Error	$\%$	
f_f	Friction Factor	-	
G	Mass Flux	$kg/m^2 \cdot s$	
\dot{g}	Energy Generation Density	W/m^3	
g	Gravity (9.81)	m/s^2	
H	Specific Enthalpy	J/kg	
h	Heat Transfer Coefficient (HTC)	$W/m^2 \cdot K$	
k	Thermal Conductivity	$W/m \cdot K$	
L	Length	m	
\dot{m}	Mass Flowrate	kg/s	
P	Pressure	Pa	
p	Perimeter	m	
q	Heat Flux	W/m^2	
\dot{Q}	Heat Flow	J/s	
q^+	Non-Dimensional Heat Flux	-	$q^+ = \frac{q \cdot \beta_b}{G \cdot \overline{C_p}}$
S	Specific Entropy	$J/kg \cdot K$	
T	Temperature	$^{\circ}C$	
V	Velocity	m/s	
x	Distance along heated length	m	

Greek Letters

Symbol	Description	Unit	Formula
α	Thermal Diffusivity	m ² /s	$\alpha = \frac{k}{\rho \cdot c_p}$
β	Volumetric Expansivity	1/K	
μ	Dynamic Viscosity	Pa·s	
ν	Kinematic Viscosity	m ² /s	
π_A	Acceleration Coefficient	-	$\pi_{A,b} = \frac{q \cdot \beta_b}{G \cdot c_{p,b}}$
ρ	Density	kg/m ³	
$\bar{\rho}$	Average Density	kg/m ³	$\bar{\rho} = \frac{\int_{T_b}^{T_w} \rho(T) \cdot dT}{T_w - T_b} \approx \frac{\rho_b + \rho_w}{2}$

Non-Dimensional Numbers

Symbol	Description	Formula
Bo ⁺	Modified Bond Number	$\mathbf{Bo}^+ = \frac{\mathbf{Gr}_b}{\mathbf{Re}_b^{3.5} \cdot \mathbf{Pr}_b^{0.8}}$
Gr	Grashof Number	$\mathbf{Gr}_b = \frac{(\rho_b - \rho_w) \cdot g \cdot D^3}{\rho_b \cdot \nu_b^2}$
$\overline{\mathbf{Gr}}$	Average Grashof Number	$\overline{\mathbf{Gr}}_b = \frac{(\rho_b - \bar{\rho}) \cdot g \cdot D_{hy}^3}{\rho_b \cdot \nu_b^2}$
Gr [*]	Modified Grashof Number	$\mathbf{Gr}^* = \frac{g \cdot \beta_b \cdot D^4 \cdot q}{k_b \cdot \nu_b^2}$
Nu	Nusselt Number	$\mathbf{Nu} = \frac{h \cdot D}{k}$
Pr	Prandtl Number	$\mathbf{Pr}_b = \frac{c_{p,b} \cdot \mu_b}{k_b}$
$\overline{\mathbf{Pr}}$	Average Prandtl Number	$\overline{\mathbf{Pr}}_b = \frac{\bar{c}_p \cdot \mu_b}{k_b} = \frac{\nu}{\alpha}$
Re	Reynolds Number	$\mathbf{Re} = \frac{G \cdot D_{hy}}{\mu}$

Subscripts and Superscripts

Symbol	Description
A625	Alloy 625
avg	Average
b	Bulk
c	characteristic (length)
cr	Critical
D	Diameter
DB	Dittus-Boelter, (1930)
dht	Deteriorated Heat Transfer
ext	External
f	Film
fl	Flow
h	Heated
ID	Internal Diameter
in	Inlet
int	Internal
MEA	Mokry, Et Al. (2011)
out	Outlet
pc	Pseudo-Critical
UO2	Uranium Dioxide
vl	Volumetric
w	Wall
wet	Wetted
Z4	Zircaloy-4

Abbreviations

Symbol	Description
AC	Alternating Current
AECL	Atomic Energy of Canada Ltd.
ARIS	Advanced Reactors Information System
BOC	Beginning Of Cycle
BWR	Boiling Water Reactor
CANDU	CANada Deuterium Uranium reactor
CF	Capacity Factor
CHF	Critical Heat Flux
CNNC	China National Nuclear Corporation
CNSC	Canadian Nuclear Safety Commission
CO ₂	Carbon Dioxide
CRL	Chalk River Laboratories
CT	Calandria Tube
D ₂ O	Heavy Water
DAE	Department of Atomic Energy (India)
DC	Direct Current
DHT	Deteriorated Heat Transfer
DOE	Department Of Energy
EGP	Power Heterogeneous Loop Reactor (in Russian abbreviations) (Russia)
EOC	End Of Cycle
EQ	Equation
FNR	Fast Neutron Reactor
GCR	Gas Cooled Reactor
GE	General Electric
GFP	Global First Power
GFR	Gas-cooled Fast Reactor
GIF	Generation IV International Forum
GWe	Giga-Watt electrical
H ₂ O	Water
HDI	Human Development Index

HT	Heat Transfer
HTC	Heat Transfer Coefficient
IAEA	International Atomic Energy Agency
ID	Internal Diameter
IEA	International Energy Agency
IHT	Improved/enhanced Heat Transfer
LFR	Lead-cooled Fast Reactor
LWGR	Light Water Graphite-moderated Reactor
LWR	Light Water cooled Reactor
MAE	Mean Average Error
ME	Mean Error
MHI	Mitsubishi Heavy Industries
MMR	Micro Modular Reactor
MPa	Mega Pascal
MS	MicroSoft
MSR	Molten Salt Reactor
MtCO ₂	Mega tonnes of CO ₂ emissions from energy sources
MTM	Ministry of Heavy Machine Building (in Russian abbreviations) (Russia)
MW _{el}	Mega-Watt Electrical
MW _{th}	Mega-Watt Thermal
NHT	Normal Heat Transfer
NIST	National Institute of Standards and Technology
NPP	Nuclear Power Plant
NRC	Nuclear Regulatory Commission
OD	Outer Diameter
OPG	Ontario Power Generation
P-T	Pressure-Temperature
PHWR	Pressurized Heavy Water Reactor
PT	Pressure Tube
PV	Pressure Vessel
PWR	Pressurized Water Reactor

RBMK	Reactor of Large Capacity Channel Type (in Russian abbreviations) (Russia)
REFPROP	REFerence PROPerties
RMS	Root Mean Square
SC	SuperCritical
SCF	SuperCritical Fluid
sCO ₂	supercritical CO ₂
SCW	SuperCritical Water
SCWR	SuperCritical Water-cooled Reactor
SD	Standard Deviation
SFR	Sodium-cooled Fast Reactor
SMR	Small Modular Reactor
SS	Stainless Steel
SSR	SuperSafe© Reactor
TWh	Tera-Watt hours
US	United States
USNC	Ultra Safe Nuclear Corporation
USSR	Union of Soviet Socialist Republics
VB	Visual Basic
VHTR	Very High Temperature Reactor
WNA	World Nuclear Association

TABLE OF CONTENTS

THESIS EXAMINATION INFORMATION	ii
ABSTRACT.....	iii
AUTHORS DECLARATION.....	iv
STATEMENT OF CONTRIBUTIONS.....	v
ACKNOWLEDGEMENTS	vi
NOMENCLATURE.....	vii
TABLE OF CONTENTS	xiii
LIST OF FIGURES.....	xix
LIST OF TABLES	xxvii
1 INTRODUCTION	1
1.1 THESIS OVERVIEW	1
1.2 ELECTRICITY, GLOBAL WARMING, AND NPPs	3
1.3 POWER GENERATION BASICS AND IMPORTANT FACTORS	7
1.3.1 ADDITIONAL IMPORTANT FACTORS	12
1.4 DISADVANTAGES OF NPPs.....	13
1.5 ADVANTAGES OF NPPs	14
1.6 INTRODUCTION SUMMARY	15
2 LITERATURE REVIEW	16
2.1 CATEGORIES OF NPP.....	16
2.1.1 SMR (<300 MW _{el}).....	16
2.1.2 Larger Reactors (>700 MW _{el}).....	17
2.2 CANADIAN SCWR DESIGNS	22
2.2.1 Reactor Designs	23

2.2.2	Fuel Channel Design.....	24
2.2.3	Fuel Element Design.....	26
2.2.4	Fuel Design	28
2.2.5	Issues Facing SCWR.....	30
2.3	GENERAL TERMS.....	31
2.4	SPECIFICS OF SCW THERMOPHYSICAL PROPERTIES.....	33
2.5	SPECIFICS OF SCW HEAT TRANSFER.....	35
2.5.1	Heat Transfer Regimes	35
2.5.2	DHT Predictions	37
2.5.3	Long bare tubes Cooled with SCW	38
2.5.4	Short bare tubes Cooled with SCW	39
2.5.5	1-rod (Annular) Bundle Cooled with SCW	40
2.5.6	3-rod Bundle Cooled with SCW	41
2.5.7	7-rod Bundle Cooled with SC R-12.....	42
2.5.8	7-rod Bundle Cooled with SCW	43
2.6	PREVIOUS Nu CORRELATIONS SUMMARY.....	45
2.7	PREVIOUS ASSESSMENT STUDIES	59
2.8	LITERATURE REVIEW SUMMARY	64
2.8.1	Conclusions.....	64
2.8.2	Objectives of Research	66
3	METHODOLOGY	67
3.1	EXPERIMENTAL SETUP	67
3.1.1	BARE TUBE	68
3.1.2	7-ROD BUNDLE.....	72
3.2	DESCRIPTION.....	78

3.3	CALCULATIONS	80
3.3.1	HT Characteristics	80
3.3.2	Assessment.....	80
3.3.3	New Nu Correlation.....	83
3.3.4	Sheath Temperature	89
3.3.5	Fuel Centreline Temperature	89
4	RESULTS	93
4.1	SPECIFICS OF THERMOPHYSICAL PROPERTIES OF SCW COMPARED TO SUBCRITICAL WATER	93
4.2	NUMERICAL ANALYSIS AND COMPARISONS	98
4.2.1	7-ROD BUNDLE.....	98
4.2.2	BARE TUBE	114
4.2.3	COMBINED RESULTS	119
4.3	DEVELOPMENT OF NEW Nu CORRELATION.....	121
4.3.1	PHASE 1	124
4.3.2	PHASE 2	125
4.3.3	PHASE 3	126
4.3.4	NEW Nu CORRELATION COMPARISONS.....	129
4.4	GRAPHICAL ANALYSIS AND COMPARISONS	132
4.4.1	7-ROD BUNDLE DATA	133
4.4.2	BARE TUBE DATA	166
4.4.3	GRAPHICAL RESULTS SUMMARY	170
4.5	SIMULATED T_{Sheath} AND $T_{\text{Fuel CL}}$	171
4.5.1	SIMULATED 7-ROD BUNDLES	172
4.5.2	SIMULATED PROPOSED SCW DESIGNS	179

4.5.3	SIMULATIONS SUMMARY	181
5	DISCUSSION.....	183
5.1	NPP & SCWR	183
5.2	LITERATURE REVIEW	183
5.3	EXPERIMENTAL RESULTS	184
5.3.1	DHT Regime	184
5.3.2	IHT Regime	185
5.3.3	Central & Peripheral Rods	185
5.4	NEW Nu CORRELATION	185
5.5	Nu CORRELATION ASSESSMENTS	186
5.6	GRAPHICAL RESULTS	186
5.7	SHEATH AND FUEL CENTRELINE TEMPERATURES	187
6	CONCLUSIONS.....	188
7	FUTURE WORK.....	190
	REFERENCES.....	191
	APPENDIX A: CODE USED.....	210
A.1	Code Parameters	212
A.1.1	Fluid Options	212
A.1.2	Additional Formulas	212
A.1.3	Error Range	212
A.1.4	Non-Convergences.....	212
A.2	Modules	213
A.3	Code Body	213
A.3.1	ThesisMainCode Module.....	213
A.3.2	SupportCode Module	219

A.3.3	RefPropCode Module	228
A.3.4	PrintCode Module	231
A.3.5	Misc.....	239
A.3.6	HeadersCode Module.....	243
A.3.7	GetPropertiesCode Module.....	256
A.3.8	CalculateCorrelations Module	259
A.3.9	Fluid_Select Form.....	278
A.3.10	Parameter_Data Form	279
A.3.11	Parameters_Check Form	281
A.3.12	Prop_Order Form	283
A.3.13	Raw_Or_Parameter Form	284
APPENDIX B: VERIFICATION OF CODE FUNCTION.....		286
B.1	Test 27_22	286
B.2	Test 27_53	287
B.3	Test 27_86	288
B.4	Test 27_88	289
B.5	Test 49_8	290
B.6	Test 51_9	291
APPENDIX C: SUPPLEMENTARY DATA.....		292
C.1	T_{pc} AND C_p – PRESSURE LOOKUP TABLE.....	292
C.2	ERROR TABLES FOR ALL Nu CORRELATIONS	294
C.2.1	7-rod Data Sorted by HTC RMS	294
C.2.2	7-rod Data Sorted by T_w RMS	295
C.2.3	bare tube Data Sorted by HTC RMS	296
C.2.4	bare tube Data Sorted by T_w RMS	297

C.3	CALCULATIONS	298
C.3.1	Sample Calculation for Nu Correlations.....	298
C.3.2	Hydraulic Diameter Calculations.....	307
C.3.3	Sheath and Fuel Centreline Temperature Calculations.....	312
APPENDIX D: PERMISSIONS OBTAINED		315
D.1	WNA PERMISSION FOR USE OF CONTENT	315
D.2	THOMAS PANEBIANCO PERMISSION FOR HDI WORLDMAP	316
APPENDIX E: AUTHORS WORKS		317
E.1	PUBLICATIONS	317
E.2	CONFERENCES ATTENDED	317

LIST OF FIGURES

FIGURE 1-1: IMPACT OF ELECTRICAL-ENERGY CONSUMPTION ON HDI.....	3
FIGURE 1-2: HDI GLOBAL VALUES (2018).....	4
FIGURE 1-3: GLOBAL CO ₂ EMISSIONS FROM FUEL COMBUSTION (2017).....	4
FIGURE 1-4: ELECTRICITY GENERATION MIX, 2018	5
FIGURE 1-5: ONTARIO (2014/15).....	6
FIGURE 1-6: BRUCE NPP (CAPACITY 6384 MW _{EL}).....	6
FIGURE 1-7: DIRECT THERMAL CYCLE (SINGLE LOOP, RANKINE CYCLE)	7
FIGURE 1-8: INDIRECT POWER CYCLE (DOUBLE LOOP, RANKINE CYCLE)	8
FIGURE 1-9: CAPACITY FACTOR OF VARIOUS ENERGY SOURCES IN ONTARIO FOR SELECTED WORKING DAYS IN (A) WINTER, (B) SUMMER.....	10
FIGURE 1-10: CARBON FOOTPRINT FROM VARIOUS POWER PLANTS.....	12
FIGURE 1-11: DEATHS PER TWH BY ENERGY GENERATION SOURCE	13
FIGURE 2-1: SMR CATEGORIES	16
FIGURE 2-2: GLOBAL # OF NPP BY TYPE, AND # OF FORTHCOMING UNITS (2020).....	17
FIGURE 2-3: CANDU FUEL-CHANNEL DESIGN	19
FIGURE 2-4: PHOTOS OF FUEL BUNDLES: (A) 37-ELEMENT CANDU STYLE, (B) 43-ELEMENT CANFLEX STYLE.....	19
FIGURE 2-5: GIF COUNTRIES AND GEN IV CONCEPTS	20
FIGURE 2-6: PRESSURE-TEMPERATURE DIAGRAM OF WATER WITH TYPICAL OPERATING CONDITIONS	22
FIGURE 2-7: PRELIMINARY CONCEPT OF THE PT TYPE SCWR	23
FIGURE 2-8: RECENT CONCEPT OF THE PT TYPE SCWR.....	24
FIGURE 2-9: CANADIAN SCWR FUEL-CHANNEL CONCEPT	25
FIGURE 2-10: FUEL CHANNEL BOTTOM SHOWING VARIOUS COMPONENTS AND FLOW DIRECTION	25
FIGURE 2-11: 37-ELEMENT BUNDLE DIMENSIONS.....	26
FIGURE 2-12: CONCEPTUAL 64-ELEMENT FUEL BUNDLE AND CHANNEL DESIGN.....	27
FIGURE 2-13: THERMAL CONDUCTIVITIES OF ALLOY 625 AND UO ₂	28

FIGURE 2-14: HEAT GENERATION IN A TYPICAL FUEL ELEMENT.....	29
FIGURE 2-15: PRESSURE-TEMPERATURE DIAGRAM FOR WATER	32
FIGURE 2-16: TEMPERATURE-ENTROPY DIAGRAM FOR WATER.....	32
FIGURE 2-17: THERMOPHYSICAL PROPERTIES OF WATER 25 MPA.....	34
FIGURE 2-18: DHT REGIMES IN BARE TUBES	36
FIGURE 2-19: SCW LONG BARE TUBE EXPERIMENTAL RESULTS (D=10 MM)38	
FIGURE 2-20: SCW SHORT BARE TUBE EXPERIMENTAL RESULTS (D=6.28 MM)	39
FIGURE 2-21: SCW 1-ROD EXPERIMENTAL RESULTS ($D_{HY} = 2.67$ MM)	40
FIGURE 2-22: SCW 3-ROD EXPERIMENTAL RESULTS ($D_{HY} = 2.40$ MM)	41
FIGURE 2-23: SC F-R12 7-ROD EXPERIMENTAL RESULTS ($D_{HY} =$ NOT LISTED)	42
FIGURE 2-24: SCW 7-ROD EXPERIMENTAL RESULTS ($D_{HY} = 2.38/2.76$ MM)	44
FIGURE 2-25: EFFECT OF AVERAGE SPECIFIC HEAT CAPACITY AND PRANDTL NUMBER	45
FIGURE 3-1: SKD-1 LOOP SCHEMATIC.....	69
FIGURE 3-2: 3-D IMAGE OF 7-ROD BUNDLE	72
FIGURE 3-3: RADIAL CROSS SECTION OF 7-ROD BUNDLE.....	73
FIGURE 3-4: SCW LOOP SCHEMATIC	74
FIGURE 3-5: COPPER PLUG COATED WITH SILICONE RESIN.....	75
FIGURE 3-6: PHASE 1 OF NU CORRELATION DEVELOPMENT, MANUALLY CALCULATE EXPONENTS	85
FIGURE 3-7: PHASE 2 OF NU CORRELATION DEVELOPMENT, ITERATE TO FINALIZE EXPONENTS	85
FIGURE 3-8: PHASE 3 OF NU CORRELATION DEVELOPMENT, CALCULATE CONSTANT	86
FIGURE 3-9: FUEL ROD CENTRELINE TEMPERATURE	91
FIGURE 4-1: DENSITY OF WATER, SUB-CRITICAL TO SC PRESSURES	93
FIGURE 4-2: THERMAL CONDUCTIVITY OF WATER, SUB-CRITICAL TO SC PRESSURES.....	94

FIGURE 4-3: SPECIFIC HEAT CAPACITY OF WATER, SUB-CRITICAL TO SC PRESSURES.....	94
FIGURE 4-4: SPECIFIC ENTHALPY OF WATER, SUB-CRITICAL TO SC PRESSURES.....	95
FIGURE 4-5: DYNAMIC VISCOSITY OF WATER, SUB-CRITICAL TO SC PRESSURES.....	95
FIGURE 4-6: KINEMATIC VISCOSITY OF WATER, SUB-CRITICAL TO SC PRESSURES.....	96
FIGURE 4-7: PRANDTL NUMBER OF WATER, SUB-CRITICAL TO SC PRESSURES	96
FIGURE 4-8: VOLUMETRIC EXPANSIVITY OF WATER, SUB-CRITICAL TO SC PRESSURES.....	97
FIGURE 4-9: THERMAL DIFFUSIVITY OF WATER, SUB-CRITICAL TO SC PRESSURES.....	97
FIGURE 4-10: TRIAL #1 – HT PROFILE AND THERMOPHYSICAL PROPERTIES, 7-ROD	99
FIGURE 4-11: TRIAL #2 – HT PROFILE AND THERMOPHYSICAL PROPERTIES, 7-ROD	100
FIGURE 4-12: TRIAL #3 – HT PROFILE AND THERMOPHYSICAL PROPERTIES, 7-ROD	101
FIGURE 4-13: TRIAL #4 – HT PROFILE AND THERMOPHYSICAL PROPERTIES, 7-ROD	102
FIGURE 4-14: TRIAL #5 – HT PROFILE AND THERMOPHYSICAL PROPERTIES, 7-ROD	103
FIGURE 4-15: TRIAL #6 – HT PROFILE AND THERMOPHYSICAL PROPERTIES, 7-ROD	104
FIGURE 4-16: TRIAL #7 – HT PROFILE AND THERMOPHYSICAL PROPERTIES, 7-ROD	105
FIGURE 4-17: TRIAL #8 – HT PROFILE AND THERMOPHYSICAL PROPERTIES, 7-ROD	106

FIGURE 4-18: PROFILES OF SCW BULK-FLUID, WALL TEMPERATURES, AND HTC ACROSS THE HEATED LENGTH OF THE CENTRAL ROD VARYING HEAT FLUX (ADJUSTED AXIS').....	107
FIGURE 4-19: PROFILES OF SCW BULK-FLUID, WALL TEMPERATURES, AND HTC ACROSS THE HEATED LENGTH OF THE CENTRAL AND PERIPHERAL ROD (ADJUSTED AXIS').....	108
FIGURE 4-20: PROFILES OF SCW BULK-FLUID AND WALL TEMPERATURES, AND HTC ACROSS THE HEATED LENGTH OF THE CENTRAL ROD VARYING PRESSURE (ADJUSTED AXIS').....	109
FIGURE 4-21: CORRELATION PREDICTIONS FOR HTC, 7-ROD DATASET.....	110
FIGURE 4-22: TOP NU CORRELATION PREDICTIONS FOR HTC, 7-ROD DATASET	111
FIGURE 4-23: NU CORRELATION PREDICTIONS FOR T_w , 7-ROD DATASET.	111
FIGURE 4-24: TOP NU CORRELATION PREDICTIONS FOR T_w , 7-ROD DATASET	112
FIGURE 4-25: TEST 70_07	114
FIGURE 4-26: TEST 15_14	115
FIGURE 4-27: TEST 49_13	115
FIGURE 4-28: NU CORRELATION PREDICTIONS FOR HTC, BARE TUBE DATASET	116
FIGURE 4-29: TOP NU CORRELATION PREDICTIONS FOR HTC, BARE TUBE DATASET	117
FIGURE 4-30: NU CORRELATION PREDICTIONS FOR T_w , BARE TUBE DATASET	117
FIGURE 4-31: TOP NU CORRELATION PREDICTIONS FOR T_w , BARE TUBE DATASET	118
FIGURE 4-32: COMPARISON OF Q_{AVG}/Q_{DHT} AND HTC_{AVG} IN 7-ROD BUNDLES AND BARE TUBES.....	119
FIGURE 4-33: PHASE 1 - STEP 1	124
FIGURE 4-34: PHASE 1 - STEP 2	124
FIGURE 4-35: PHASE 1 - STEP 3	124

FIGURE 4-36: PHASE 1 - STEP 4	124
FIGURE 4-37: PHASE 2 - STEP 1	125
FIGURE 4-38: PHASE 2 - STEP 2	125
FIGURE 4-39: PHASE 2 - STEP 3	125
FIGURE 4-40: PHASE 2 - STEP 4	125
FIGURE 4-41: PHASE 3 – CONSTANT CALCULATION (FIRST ITERATION)	126
FIGURE 4-42: HTC COMPARISON BETWEEN EXPERIMENTAL AND CALCULATED BY CLARK VALUES FOR 7-ROD BUNDLE	128
FIGURE 4-43: T_w COMPARISON BETWEEN EXPERIMENTAL AND CALCULATED BY CLARK VALUES FOR 7-ROD BUNDLE	128
FIGURE 4-44: HTC COMPARISON BETWEEN EXPERIMENTAL AND CALCULATED BY CLARK VALUES FOR BARE TUBE	128
FIGURE 4-45: T_w COMPARISON BETWEEN EXPERIMENTAL AND CALCULATED BY CLARK VALUES FOR BARE TUBE	128
FIGURE 4-46: TOP HTC NU CORRELATIONS, 7-ROD BUNDLE	129
FIGURE 4-47: TOP T_w NU CORRELATIONS, 7-ROD BUNDLE DATASET	129
FIGURE 4-48: TOP HTC NU CORRELATIONS, BARE TUBE DATASET	130
FIGURE 4-49: TOP T_w NU CORRELATIONS, BARE TUBE DATASET	130
FIGURE 4-50: T_w AND HTC VARIATIONS ALONG 0.485M 7-ROD BUNDLE TRIAL #1-1	135
FIGURE 4-51: T_w AND HTC VARIATIONS ALONG 0.485M 7-ROD BUNDLE TRIAL #2-1	136
FIGURE 4-52: T_w AND HTC VARIATIONS ALONG 0.485M 7-ROD BUNDLE TRIAL #3-1	137
FIGURE 4-53: T_w AND HTC VARIATIONS ALONG 0.485M 7-ROD BUNDLE TRIAL #4-1	138
FIGURE 4-54: T_w AND HTC VARIATIONS ALONG 0.485M 7-ROD BUNDLE TRIAL #5/#6-1	139
FIGURE 4-55: T_w AND HTC VARIATIONS ALONG 0.485M 7-ROD BUNDLE TRIAL #7-1	140

FIGURE 4-56: T_w AND HTC VARIATIONS ALONG 0.485M 7-ROD BUNDLE TRIAL	
#8-1	141
FIGURE 4-57: T_w AND HTC VARIATIONS ALONG 0.485M 7-ROD BUNDLE TRIAL	
#1-2	143
FIGURE 4-58: T_w AND HTC VARIATIONS ALONG 0.485M 7-ROD BUNDLE TRIAL	
#2-2	144
FIGURE 4-59: T_w AND HTC VARIATIONS ALONG 0.485M 7-ROD BUNDLE TRIAL	
#3-2	145
FIGURE 4-60: T_w AND HTC VARIATIONS ALONG 0.485M 7-ROD BUNDLE TRIAL	
#4-2	146
FIGURE 4-61: T_w AND HTC VARIATIONS ALONG 0.485M 7-ROD BUNDLE TRIAL	
#5/#6-2	147
FIGURE 4-62: T_w AND HTC VARIATIONS ALONG 0.485M 7-ROD BUNDLE TRIAL	
#7-2	148
FIGURE 4-63: T_w AND HTC VARIATIONS ALONG 0.485M 7-ROD BUNDLE TRIAL	
#8-2	149
FIGURE 4-64: T_w AND HTC VARIATIONS ALONG 0.485M 7-ROD BUNDLE TRIAL	
#1-3	151
FIGURE 4-65: T_w AND HTC VARIATIONS ALONG 0.485M 7-ROD BUNDLE TRIAL	
#2-3	152
FIGURE 4-66: T_w AND HTC VARIATIONS ALONG 0.485M 7-ROD BUNDLE TRIAL	
#3-3	153
FIGURE 4-67: T_w AND HTC VARIATIONS ALONG 0.485M 7-ROD BUNDLE TRIAL	
#4-3	154
FIGURE 4-68: T_w AND HTC VARIATIONS ALONG 0.485M 7-ROD BUNDLE TRIAL	
#5/#6-3	155
FIGURE 4-69: T_w AND HTC VARIATIONS ALONG 0.485M 7-ROD BUNDLE TRIAL	
#7-3	156
FIGURE 4-70: T_w AND HTC VARIATIONS ALONG 0.485M 7-ROD BUNDLE TRIAL	
#8-3	157

FIGURE 4-71: T_w AND HTC VARIATIONS ALONG 0.485M 7-ROD BUNDLE TRIAL #1-4	159
FIGURE 4-72: T_w AND HTC VARIATIONS ALONG 0.485M 7-ROD BUNDLE TRIAL #2-4	160
FIGURE 4-73: T_w AND HTC VARIATIONS ALONG 0.485M 7-ROD BUNDLE TRIAL #3-4	161
FIGURE 4-74: T_w AND HTC VARIATIONS ALONG 0.485M 7-ROD BUNDLE TRIAL #4-4	162
FIGURE 4-75: T_w AND HTC VARIATIONS ALONG 0.485M 7-ROD BUNDLE TRIAL #5/#6-4	163
FIGURE 4-76: T_w AND HTC VARIATIONS ALONG 0.485M 7-ROD BUNDLE TRIAL #7-4	164
FIGURE 4-77: T_w AND HTC VARIATIONS ALONG 0.485M 7-ROD BUNDLE TRIAL #8-4	165
FIGURE 4-78: T_w AND HTC VARIATIONS ALONG 4 M BARE TUBE TEST 70_07	167
FIGURE 4-79: T_w AND HTC VARIATIONS ALONG 4 M BARE TUBE TEST 15_14	168
FIGURE 4-80: T_w AND HTC VARIATIONS ALONG 4 M BARE TUBE TEST 49_13	169
FIGURE 4-81: SHEATH & FUEL ROD TEMPERATURE ALONG 8 BUNDLES - TRIAL #1	172
FIGURE 4-82: SHEATH & FUEL ROD TEMPERATURE ALONG 5 BUNDLES - TRIAL #2	173
FIGURE 4-83: SHEATH & FUEL ROD TEMPERATURE ALONG 5 BUNDLES - TRIAL #3	174
FIGURE 4-84: SHEATH & FUEL ROD TEMPERATURE ALONG 5 BUNDLES - TRIAL #4	175
FIGURE 4-85: SHEATH & FUEL ROD TEMPERATURE ALONG 5 BUNDLES - TRIAL #5 & #6	176

FIGURE 4-86: SHEATH & FUEL ROD TEMPERATURE ALONG 4 BUNDLES - TRIAL #7	177
FIGURE 4-87: SHEATH & FUEL ROD TEMPERATURE ALONG 4 BUNDLES - TRIAL #8	178
FIGURE 4-88: SHEATH & FUEL ROD TEMPERATURE WITH 37-ELEMENT BUNDLES	179
FIGURE 4-89: SHEATH & FUEL ROD TEMPERATURE WITH 64-ELEMENT BUNDLE	180
FIGURE A-1: BASIC ALGORITHM FOR PROGRAM	211
FIGURE A-2: VBA MACRO MODULES	213
FIGURE B-1: T_w AND HTC VARIATIONS ALONG 1 M BARE TUBE, TEST 27_22	286
FIGURE B-2: T_w AND HTC VARIATIONS ALONG 1 M BARE TUBE, TEST 27_53	287
FIGURE B-3: T_w AND HTC VARIATIONS ALONG 1 M BARE TUBE, TEST 27_86	288
FIGURE B-4: T_w AND HTC VARIATIONS ALONG 1 M BARE TUBE, TEST 27_88	289
FIGURE B-5: T_w AND HTC VARIATIONS ALONG 1 M BARE TUBE, TEST 49_8	290
FIGURE B-6: T_w AND HTC VARIATIONS ALONG 1 M BARE TUBE, TEST 51_9	291
FIGURE C-1: EXAMPLE OF NON-CONVERGENCE	306
FIGURE C-2: TOTAL FLOW AREA OF 7-ROD FUEL BUNDLE.....	308

LIST OF TABLES

TABLE 1-1: MAXIMUM GROSS THERMAL EFFICIENCIES OF TYPICAL NPPS AND THERMAL POWER PLANTS	11
TABLE 2-1: GENERAL CHARACTERISTICS OF NPPS	18
TABLE 2-2: NPPS OPERATIONAL IN CANADA AS OF MAY 2020.....	18
TABLE 2-3: GEN IV NPP REACTOR STYLES	21
TABLE 2-4: DHT PREDICTIONS	37
TABLE 2-5: DYADYAKIN AND POPOV 7-ROD BUNDLE CONFIGURATIONS ...	43
TABLE 2-6: DYADYAKIN AND POPOV 7-ROD SCW PARAMETERS	43
TABLE 2-7: HEAT TRANSFER NU CORRELATIONS	46
TABLE 3-1: UNCERTAINTY OF PRIMARY PARAMETERS FOR SKD-1 LOOP ...	69
TABLE 3-2: TEST MATRIX FOR SKD-1 LOOP	70
TABLE 3-3: DATA REDUCTION PARAMETERS FOR SKD-1 LOOP (KIRILLOV ET AL., 2005)	71
TABLE 3-4: UNCERTAINTY OF PRIMARY PARAMETERS FOR SCW LOOP	76
TABLE 3-5: TEST MATRIX FOR SCW LOOP	76
TABLE 3-6: DATA REDUCTION PARAMETERS FOR SCW LOOP.....	77
TABLE 3-7: DIMENSIONS OF ESSENTIAL THERMOPHYSICAL PROPERTIES ..	83
TABLE 3-8: Π -TERMS (MOKRY ET AL., 2009)	84
TABLE 3-9: LAYER SIZES FOR $T_{\text{FUEL CL}}$ (7-ROD PARAMETERS EXAMPLE).....	92
TABLE 4-1: TOP NU CORRELATIONS FOR BOTH HTC AND T_w , 7-ROD DATA	113
TABLE 4-2: TOP NU CORRELATIONS FOR BOTH HTC AND T_w , RAZUMOVSKIY DATA	118
TABLE 4-3: RMS COMPARISON FOR TOP NU CORRELATIONS FOR BOTH RAZUMOVSKIY AND KIRILLOV DATASETS	120
TABLE 4-4: ASSESSMENT OF NEW NU CORRELATION BASED ON 7-ROD BUNDLE DATASET	122
TABLE 4-5: ASSESSMENT OF NEW NU CORRELATION BASED ON BARE TUBE DATASET	122

TABLE 4-6: HEAT FLUX AND MASS FLUX PARAMETERS IN 7-ROD DATA SET	123
TABLE 4-7: ASSESSMENT OF NEW NU CORRELATION BASED ON 7-ROD AND BARE TUBE DATASETS	126
TABLE 4-8: ASSESSMENT OF FINAL NU CORRELATION BASED ON 7-ROD AND BARE TUBE DATASETS	127
TABLE 4-9: TEST MATRIX FOR NEW NU CORRELATION	127
TABLE 4-10: RMS COMPARISON FOR CLARK AND TOP NU CORRELATIONS FOR BOTH RAZUMOVSKIY AND KIRILLOV DATASETS	131
TABLE C-1: T_{PC} AND C_P VALUES UP TO $P = 40$ MPA.....	292
TABLE C-2: INPUT PARAMETERS FOR SAMPLE CALCULATION	299
TABLE C-3: INITIAL BULK FLUID THERMOPHYSICAL PROPERTIES	299
TABLE C-4: 1 ST ITERATION PROPERTIES.....	300
TABLE C-5: 2 ND ITERATION PROPERTIES	301
TABLE C-6: 3 RD ITERATION PROPERTIES	302
TABLE C-7: 4 TH ITERATION PROPERTIES	303
TABLE C-8: TEMPERATURE AT H_{l+1}	304
TABLE C-9: FUEL CENTRELINE LAYER TEMPERATURES	313

1 INTRODUCTION

1.1 THESIS OVERVIEW

Nuclear Power Plants (NPPs) are an excellent source of low-carbon power generation, and provide extremely reliable power to electrical grids. However, new construction of NPPs face challenges due to economic competition and public perception of safety performance.

Low-cost fossil fuel thermal power plants have achieved significant cost reductions through increased gross thermal efficiency. This has given fossil fuel thermal power plants a competitive advantage in open power markets, rendering NPPs non-competitive (Duffey & Pioro, 2019). Also, well known NPP disasters at Three Mile Island in 1979, Chernobyl in 1986, and Fukushima Daiichi in 2011, have further put NPPs at a competitive disadvantage due to public hysteria over radiation.

To overcome these challenges a new generation of NPPs must be developed with better gross thermal efficiency and safety features than the current Gen II/III/III+ NPPs.

The Generation IV International Forum (GIF) began in January of 2000 when the U.S. Department of Energy (US DOE), Office of Nuclear Energy, Science and Technology invited representatives from nine (9) countries to collaborate on the development of Gen IV NPPs. (GIF, 2019). Over the past decade working with GIF, more than 100 experts have evaluated over 130 different reactor concepts and selected six (6) reactor concepts to pursue for further research and development (GIF, Generation IV Systems, 2019):

- | | |
|-----------------------------------|--|
| 1) Gas-cooled Fast Reactor (GFR) | 4) Sodium-cooled Fast Reactor (SFR) |
| 2) Lead-cooled Fast Reactor (LFR) | 5) Very High Temperature Reactor (VHTR) |
| 3) Molten Salt Reactor (MSR) | 6) SuperCritical Water-cooled Reactor (SCWR) |

Canada initially focused on the VHTR and SCWR, then in 2012 moved forward with only developing the SCWR NPP concept due to previous CANDU experience, existing infrastructure, 60+ years of nuclear R&D experience with water based NPPs, and the ability to combine SCW fossil fuel plant and boiling water reactor technologies (Pynn et al., 2016).

SCWRs offers higher thermal efficiency (~45-50%) compared to current NPPs (~30-35%), and lower capital costs per kWh of electricity, including the possibility a passive safety system when using a Pressure Tube (PT) reactor design (Peiman et al., 2012).

While the majority of existing NPPs worldwide are classified as 'large' NPP ($> 700 \text{ MW}_{\text{el}}$), the focus for future installations has shifted towards Small Modular Reactors (SMRs) ($\leq 300 \text{ MW}_{\text{el}}$). SMRs have the projected benefits of modularity and mass manufacturing. With modularity, SMRs can be paired together to increase the desired output, allowing operators to more closely follow the fluctuating power demands over time on a year-to-year basis. SMRs can also be installed in existing installations where old reactors are taken offline, and can make use of existing balance of plant facilities (turbine, generator, etc). Mass manufacturing of SMRs in a centralized large-scale facility, instead of the current practice of on-site construction, will provide a reduction in cost as parts can be standardized and ordered in larger quantities (Pioro, 2016).

One major challenge facing the design of Supercritical Water (SCW) NPPs (Large or Small) is accurately calculating the heat removal rate with the SCW coolant from the reactor core. This is vital to design engineers as it allows for the determination of the maximum expected sheath and fuel centreline temperatures.

While the vast majority of Heat Transfer (HT) occurs within the Normal HT (NHT) regime, SCW exhibits two additional regimes that result in unpredictable temperature swings – Deteriorated HT (DHT), where the HT is lower than expected; and Improved HT (IHT), where the HT is higher than expected.

Bundle geometries impede coolant flow that distorts the flow patterns and alters the HT characteristics, which is expected to result in differences when compared to bare tubes. Previously, Dyadyakin and Popov (1977) performed experiments with SCW in a 7-rod bundle and developed the only Nusselt number (**Nu**) correlation for bundle configurations currently available in literature. However, their experimental data was proprietary. More recently, Razumovskiy, et al. (2008) & (2015) performed experiments with SCW in 7-rod & 1-rod/3-rod bundle configurations, and produced data available to the author.

1.2 ELECTRICITY, GLOBAL WARMING, AND NPPs

Electricity is vital to the world today, with a higher level of electrical consumption per capita generally associated with higher standards of living, and greater technological developments across areas such as industry, agriculture, and health care. The Human Development Index (HDI) measures factors such as life expectancy, education, and economic prosperity of citizens living in a country. Figure 1-1 below shows the relationship between HDI and electrical consumption per capita, with low-income countries consuming less electricity, and high-income countries consuming more electricity.

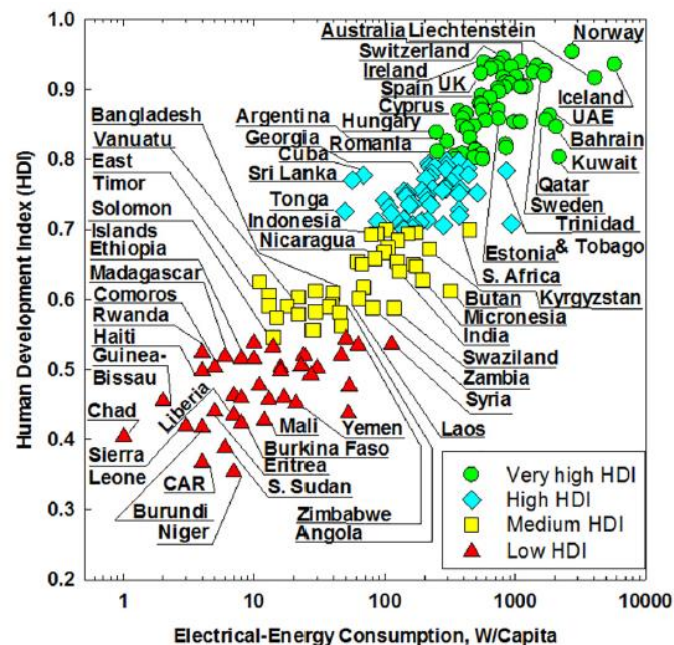


Figure 1-1: Impact of Electrical-Energy consumption on HDI
(courtesy of I.L. Pioro (Pioro et al., 2019)) (Copyright of ASME)

Figure 1-2 shows the global distribution of HDI, with African countries ranking amongst the lowest, and North America, Europe, and parts of South East Asia ranking highest.

Figure 1-3 shows the global CO₂ emissions by country. Countries that have higher HDI produce more electricity, and on average, contribute more to global CO₂ emissions. The Centre for Climate and Energy Solutions (2017) estimated 72% of global greenhouse gas emissions came from the energy sector in 2017. The top 10 contributors to global CO₂ emissions according to the IEA (2017) in 2017 were (in order); China, USA, India, Russia, Japan, Germany, South Korea, Iran, Canada, and Saudi Arabia.

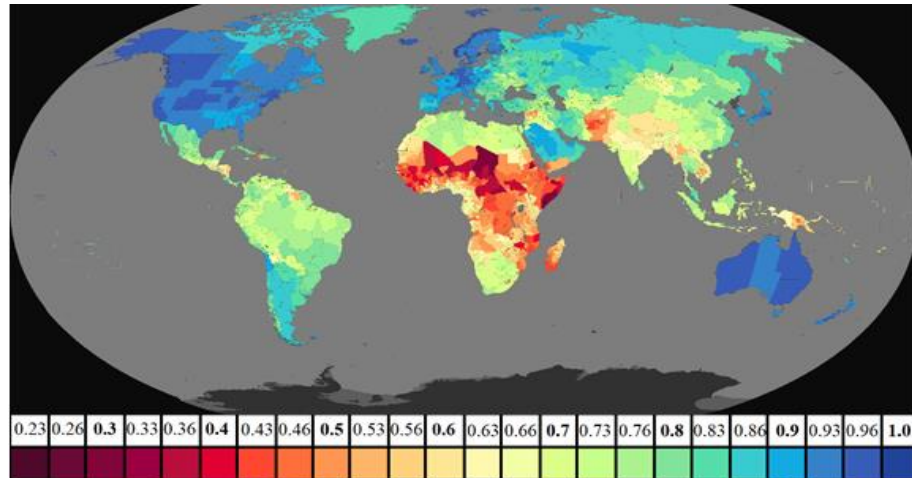


Figure 1-2: HDI Global Values (2018)
 (courtesy of Thomas Panebianco, 2020)
 (Created using data from UNDP (2018), and Global Data Lab (2020))

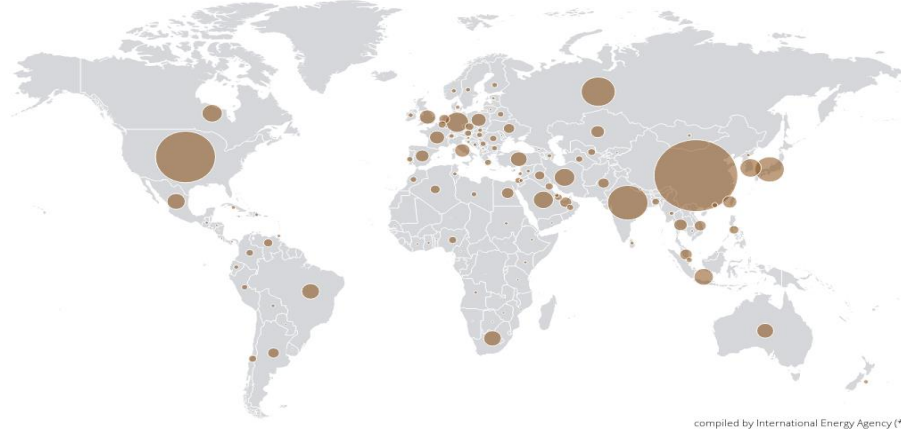


Figure 1-3: Global CO₂ Emissions from Fuel Combustion (2017)
 (compiled by the IEA (2017)) (Copyright of IEA)

Different methods of power generation produce varying levels of CO₂ emissions. These methods fall into two categories; 1) **Renewables**; hydro (through dams), solar, wind, geothermal, tidal, and biomass, and 2) **Non-Renewables**; coal, natural gas, oil, and nuclear. Nuclear is unique among the non-renewables with significantly lower CO₂ emissions (Figure 1-10).

Electrical grids require base load sources that provide reliable power, and peak load sources to handle the spikes in demand. This mix of power generation sources greatly effects CO₂ emissions.

In 2018, nuclear power accounted for approximately 10% of the electricity generated globally. Figure 1-4 shows the breakdown of generation methods for selected countries.

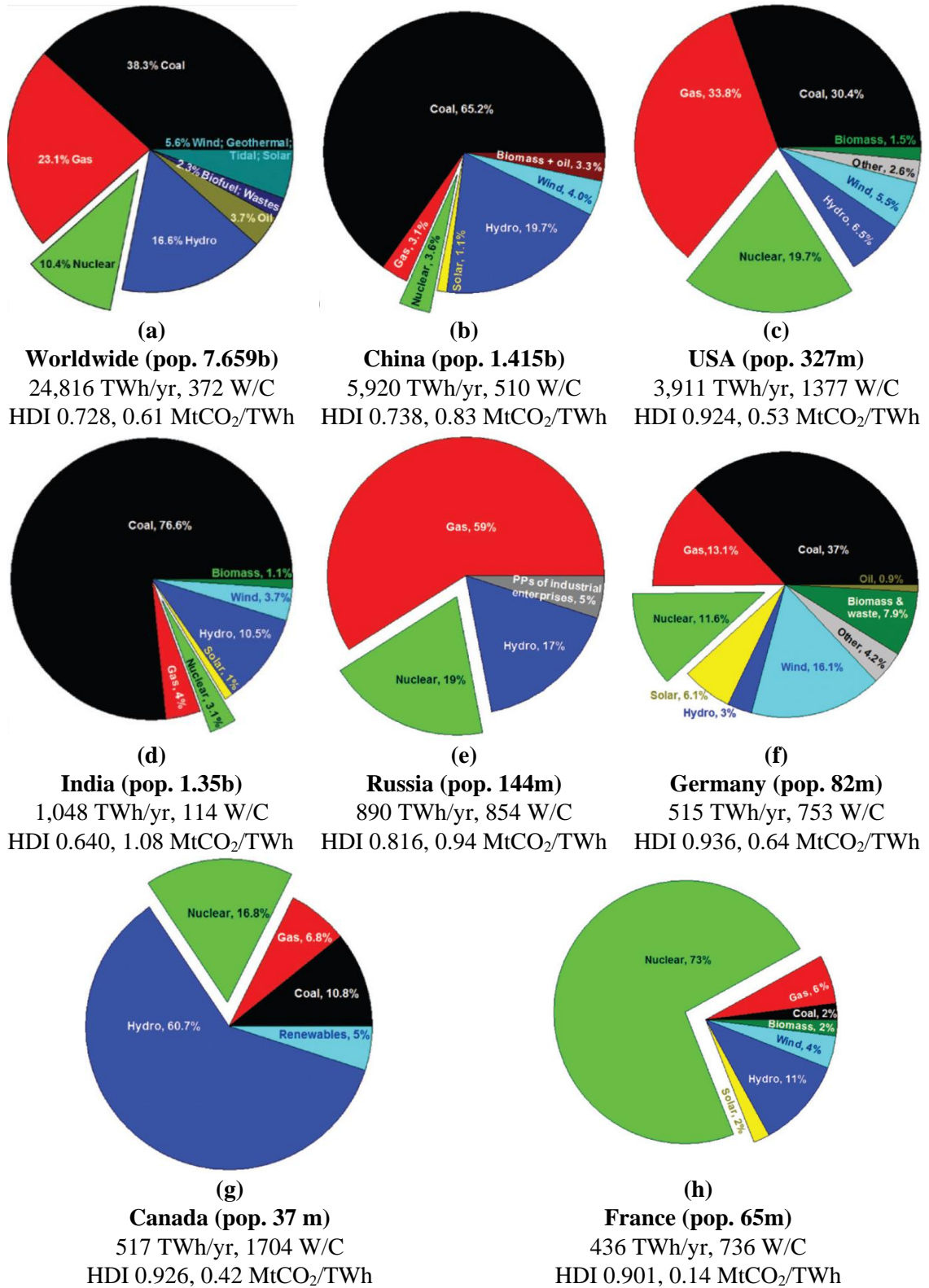


Figure 1-4: Electricity Generation Mix, 2018

(courtesy of I.L. Pioro, adapted from (Pioro et al. 2019)) (Copyright of ASME)
(MtCO₂ 2017 data, Electricity/Heat Producers, IEA (2020)) (W/C=W per Capita)

As shown in Figure 1-4, higher energy production by coal and gas leads to higher CO₂ emissions. While Germany has the highest mix of renewable energy (not including hydro), due to their reliance on non-renewables (coal and gas) their CO₂ emissions generated per TWh are high. This was not always the case, as Germany operated many nuclear power plants prior to 2011. After the NPP disaster at Fukushima Daiichi in 2011, public antinuclear sentiments were high and thousands of protesters took to the streets, leading the German government to legislate the closure of the NPPs in Germany. As renewables are not as reliable as nuclear power, coal and gas plants were built to provide the base-load. This resulted in higher CO₂ emissions as a result of the closure of the NPPs (Oberhaus, 2020).

The electrical-energy generation profile in the province of Ontario is similar to France, with the main source being nuclear power, followed by hydro-electric, natural gas, and then wind. The largest NPP in the world is located in Ontario, named the Bruce NPP, with two separate plants each housing 4 CANDU style reactors, Bruce A and Bruce B. The breakdown of electrical-energy generation in Ontario is shown in Figure 1-5, while a photo of the Bruce NPP is shown in Figure 1-6.

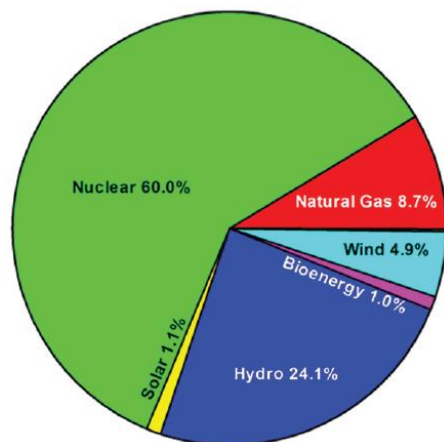


Figure 1-5: Ontario (2014/15)
(courtesy of I.L. Pioro (Pioro et al., 2019)) (Copyright of ASME)



Figure 1-6: Bruce NPP (Capacity 6384 MW_{el})
(courtesy I.L. Pioro (Pioro et al., 2019))
(Copyright of ASME)

1.3 POWER GENERATION BASICS AND IMPORTANT FACTORS

All forms of electrical-energy, other than solar, generate electricity by turning a turbine that turns a generator, creating electricity. With wind, tidal, and hydro-electric, the turbine is turned directly due to the flowing forces of nature (wind, tides, water falling).

For fossil fuel based power plants, fuel is converted to heat through a chemical reaction (burning) used to boil water, converting water to pressurized steam, which is then directed through the turbine. NPPs operate by using nuclear sources as fuel, such as UO₂ pellets. This fuel undergoes carefully controlled nuclear reactions that produce heat emission. This heat is transferred to the primary water coolant, which is either converted to steam (direct thermal cycle - Figure 1-7), or is used to convert secondary water to steam (indirect thermal cycle - Figure 1-8), that drives the turbine.

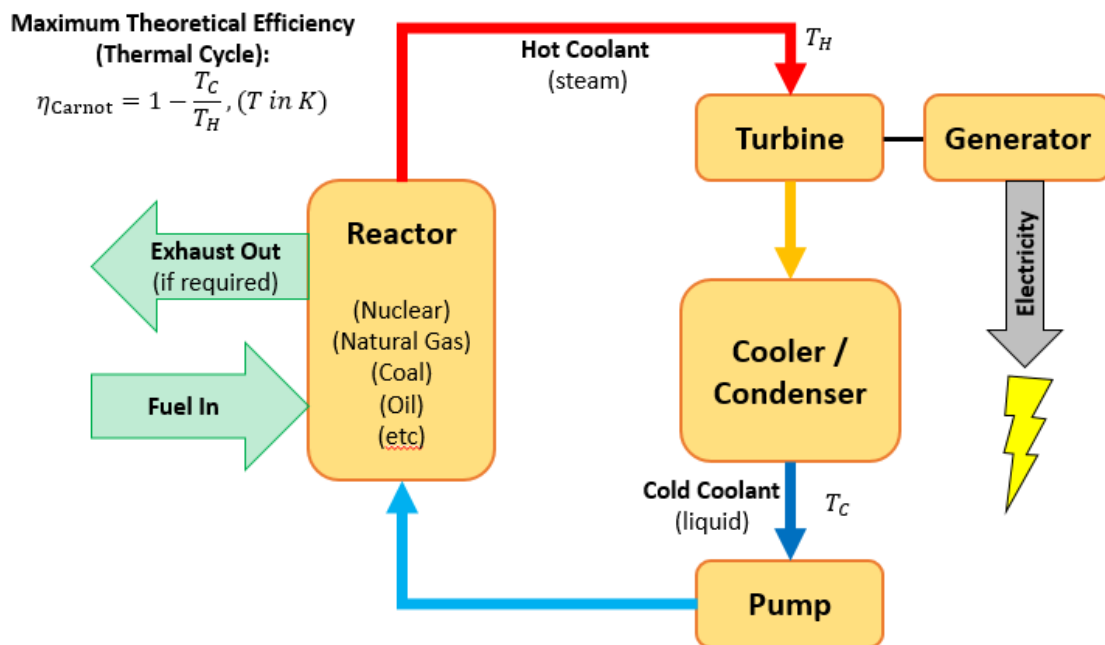


Figure 1-7: Direct Thermal Cycle (Single Loop, Rankine Cycle)

The direct thermal cycle shown typically uses water as the coolant. When using a gas coolant that does not condense, the pump is a compressor, making it a direct Brayton cycle. The maximum theoretical thermal efficiency is determined by the Carnot equation (shown in Figure 1-7), while the actual efficiency is less due to system losses. When it is desirable to keep the coolant separate from the turbine, as is the case with most NPPs due to radioactivity concerns, a second loop is enacted, heated by the first loop Figure 1-8.

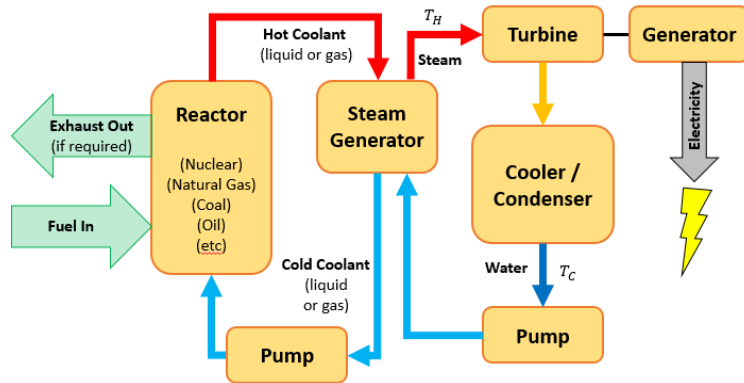


Figure 1-8: Indirect Power Cycle (Double Loop, Rankine Cycle)

According to Pioro et al. (2019), there are two important factors for power plant consideration:

1) Gross Efficiency

- A measure of the total energy output of a process against the total energy input.

The gross efficiency does not account for the energy consumed by the NPP to continue the process, referred to as the net efficiency.

- Table 1-1 demonstrates that the current fleet of NPPs are significantly lower in thermal efficiency when compared with combined cycle gas and supercritical coal-fired power plants.
 - This has placed an economic strain on the NPP industry, and partially explains the lack of new NPP construction.
 - The maximum operating temperature of the coolant must be below the boiling temperature to prevent burnout, that can lead to unpredictably high temperatures potentially causing the sheath to rupture and/or the fuel to melt, resulting in a release of radiation. As a result, the temperatures at the inlet of the turbine are lower, resulting in lower maximum gross thermal efficiency (demonstrated by the Carnot equation in Figure 1-7).

2) Capacity Factor (CF)

- A measure of the actual energy generated over a period of time against the installed capacity over the same period of time.
- For various methods of power generation, the CF varies significantly (ie. If the sun is not shining, solar power cannot be used). Examples can be seen in Figure 1-9.
 - Note, gas/biofuel is used for peak power demand in Ontario, not base load demand, leading to artificially lower CF shown in Figure 2-9
- NPPs have the highest capacity factor of all power plant types, with a theoretical CF of 100%. However, due to planned outages and aging plants requiring more maintenance, the average CF is roughly 90%. Combined cycle, coal and hydroelectric are ~50%, while wind and solar are ~40% and 30%, respectively.

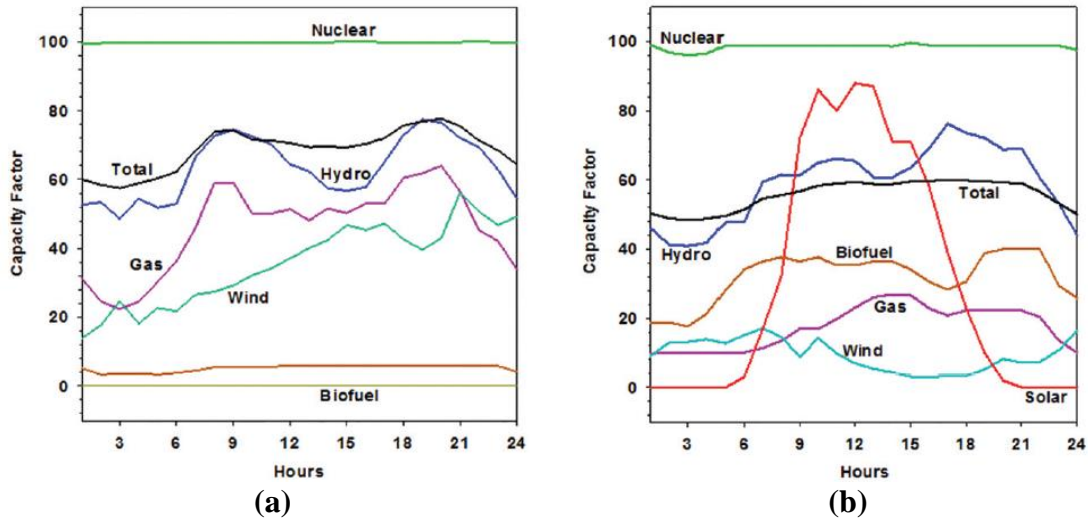


Figure 1-9: Capacity Factor of Various Energy Sources in Ontario for selected working days in (a) Winter, (b) Summer

(courtesy of I.L. Pioro (Pioro et al., 2019)) (Copyright of ASME)

Table 1-1: Maximum Gross Thermal Efficiencies of Typical NPPs and Thermal Power Plants

(adapted from Pioro et al. (2019))

Thermal Power Plant Type (Fuel Type) Cycle, conditions at turbine inlet, and/or at the coolant exiting the reactor)	Maximum Gross Thermal Efficiency
Combined-cycle power plant (Natural Gas/Liquefied Natural Gas) Brayton, $P_{in}=2.5$ MPa, $T_{in}=1650^{\circ}\text{C}$ (Exhaust Gasses) Steam Rankine Cycle, $P_{in}=12.5$ MPa, $T_{in}=620^{\circ}\text{C}$	Up to 62%
Supercritical-pressure coal-fired power plant (Coal) Steam Rankine Cycle, $P_{in}=23.5\text{-}38$ MPa, $T_{in}=540\text{-}625^{\circ}\text{C}$	Up to 55%
Internal combustion engine generators (Natural Gas) Diesel and Otto cycle with natural gas fuel	Up to 50%
Subcritical-pressure coal-fired plant (Coal) Steam Rankine Cycle, $P_{in}=17$ MPa, $T_{in}=540^{\circ}\text{C}$	Up to 43%
Advanced Gas-cooled Reactor (AGR) (Nuclear) Coolant – CO_2 , $P=4$ MPa, $T_{out}=290\text{-}650^{\circ}\text{C}$ Secondary Loop – Steam Rankine Cycle, $P_{in}=17$ MPa, $T_{in}=560^{\circ}\text{C}$	Up to 42%
Sodium Fast Reactor (SFR) Coolant – Liquid Sodium Steam Rankine Cycle, $P_{in}=14.2$ MPa, $T_{in}=505^{\circ}\text{C}$	Up to 40%
Pressurized Water Reactor (PWR) (Gen III+) Coolant – Water, $P=15.5$ MPa, $T_{out}=327^{\circ}\text{C}$ Steam Rankine Cycle, $P_{in}=7.8$ MPa, $T_{in}=293^{\circ}\text{C}$	Up to 36-38%
PWR (Gen III) Coolant – Water, $P=15.5$ MPa, $T_{out}=292\text{-}329^{\circ}\text{C}$ Steam Rankine Cycle, $P_{in}=6.9$ MPa, $T_{in}=285^{\circ}\text{C}$	Up to 34-36%
Boiling Water Reactor (BWR) Rankine Cycle, $P_{in}=7.2$ MPa, $T_{in}=288^{\circ}\text{C}$	Up to 34%
Pressurized Heavy Water Reactor (PHWR) Coolant – Heavy Water, $P=11$ MPa, $T_{out}=260\text{-}310^{\circ}\text{C}$ Steam Rankine Cycle, $P_{in}=4.7$ MPa, $T_{in}=260^{\circ}\text{C}$	Up to 32%
PWR SMR NPP (RITM-200M, Russia – not yet in operation) Coolant – Water, $P=15.7$ MPa, $T_{out}=277\text{-}313^{\circ}\text{C}$ Steam Rankine Cycle, $P_{in}=3.82$ MPa, $T_{in}=295^{\circ}\text{C}$	Up to 31%
PWR SMR NPP (KLT-40S, Russia) Coolant – Water, $P=12.7$ MPa, $T_{out}=280\text{-}316^{\circ}\text{C}$ Steam Rankine Cycle, $P_{in}=3.72$ MPa, $T_{in}=290^{\circ}\text{C}$	Up to 26%

1.3.1 ADDITIONAL IMPORTANT FACTORS

Additional important factors facing power generating plants are the contribution to global warming, and overall safety. According to the Centre for Climate and Energy Solutions (2017), 72% of global greenhouse gas emissions come from the energy sector.

Many studies have been published on the life-cycle assessments of various power generating plants and their associated CO₂ emissions. The vast majority of available studies produce similar trends shown in Figure 1-10, showing NPPs have a very low carbon footprint compared to fossil fuel power plants, and are similar to hydro and wind.

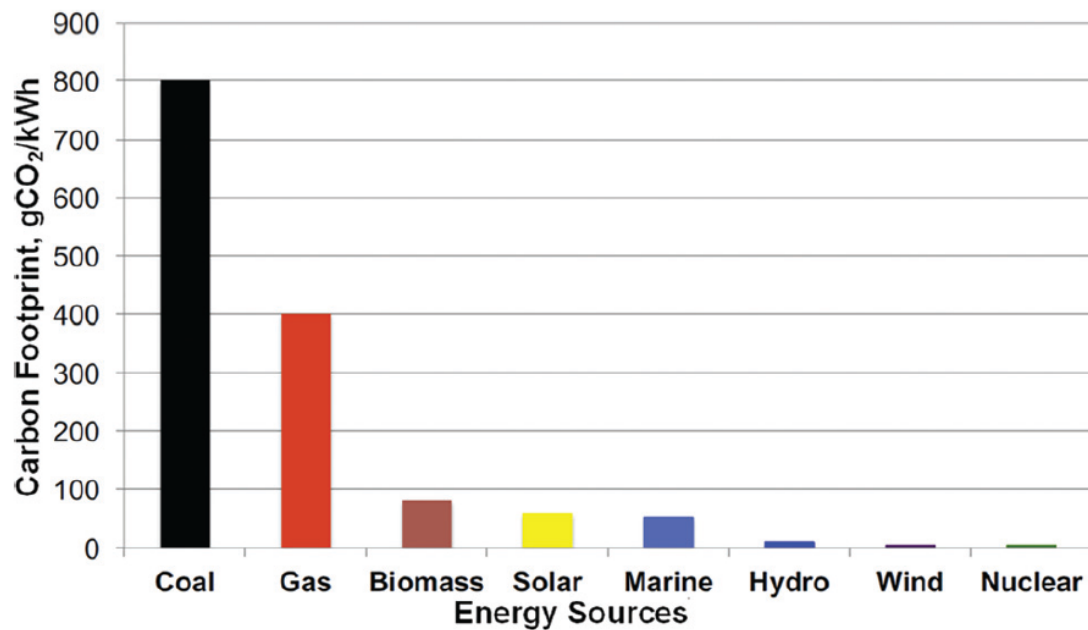


Figure 1-10: Carbon Footprint from Various Power Plants
(courtesy of I.L. Pioro (Pioro et al., 2019)) (Copyright of ASME)

Figure 1-11 shows the deaths associated with each power generation type on a per TWh basis. Due to the extreme precautions taken in the nuclear industry, very little worker and/or public deaths come as a result of NPP operation worldwide.

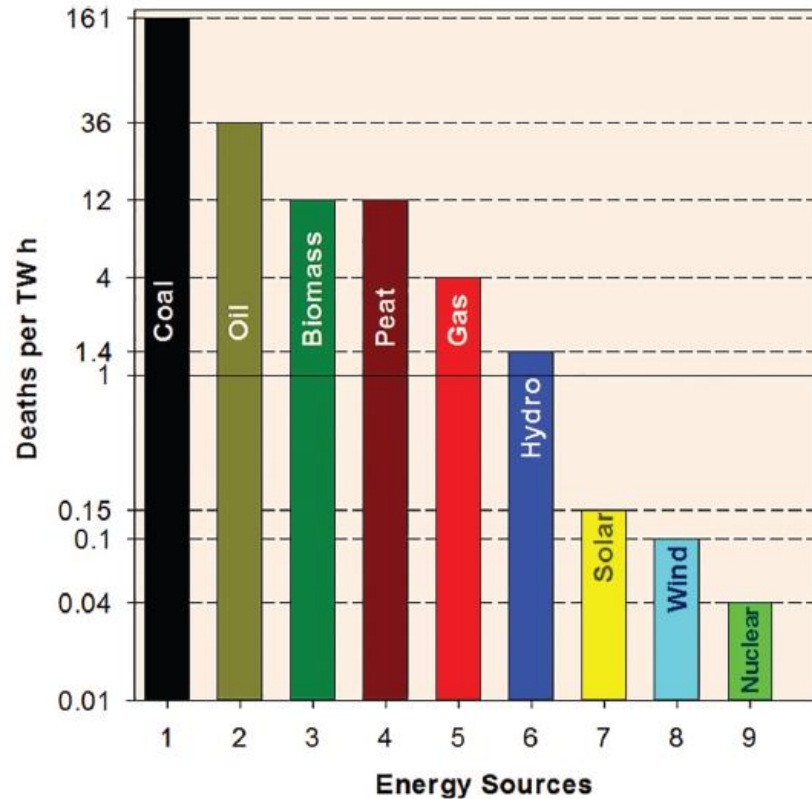


Figure 1-11: Deaths per TWh by energy generation source
(courtesy of I.L. Pioro (Pioro et al., 2019)) (Copyright of ASME)

1.4 DISADVANTAGES OF NPPs

Today, the public perception of nuclear power is largely negative in the West due to concerns over nuclear proliferation and nuclear waste concerns, in addition to fear of a nuclear meltdown as experienced in the three large scale NPP disasters at Three Mile Island in 1979, Chernobyl in 1986, and recently Fukushima Daiichi in 2011 (Office of Nuclear Energy, 2020).

In addition to the lower gross thermal efficiencies of NPPs, other economic factors such as the lack of a mature supply chain, changing regulations, subsidies provided for renewable technologies distorting the power markets, and lower natural gas prices all contribute to disadvantages of NPPs.

The negative public perception of NPPs, low thermal efficiency and economic factors have all combined to create an unfavorable situation for building new NPPs (Lesser, 2019).

1.5 ADVANTAGES OF NPPs

However, according to Pioro et al. (2019) the advantages of NPPs are considerable:

- 1) Nuclear material is a concentrated and reliable source of nearly limitless energy, that can run at high capacity factors not reliant upon weather conditions;
 - With global warming increasing, some NPPs in Europe that use water for cooling the condenser/coolers from the ocean, seas, and/or rivers had to shut down due to low water levels or high water temperatures.
- 2) Due to the high capacity factors and long operating cycles (NPPs can run without shutting down for upwards of 18 months to 2 years), NPPs are well suited for continuous base-load operations;
- 3) As shown in Figure 1-10, there are negligible emissions of CO₂ and relatively small amounts of waste generated when compared with fossil-fuel thermal power plants;
- 4) Relatively small amount of fuel is required to supply electricity due to the concentrated fuel
 - Energy Generation values (MJ/kg) that are 3 to 4 orders of magnitude larger than fossil- or bio-fuels according to the World Nuclear Association (2018)
- 5) With the advent of electric vehicles, NPPs are well suited to provide the base-load for overnight re-charging.

Due to the advantages of NPPs, they should be considered as the best method for power generation within the next several decades.

However, in order to compete in the challenging energy market today, NPPs must become more economically advantageous than the current fleet offers through increasing the gross thermal efficiency.

1.6 INTRODUCTION SUMMARY

Electrical-power generation is the key factor for increasing the HDI of a region.

Major sources for electrical-energy in the world today are thermal power plants, fueled by coal, natural gas, hydro-electric (dams), and nuclear, while a minor sources include oil and renewables in selected countries.

Renewables are attractive in some locations, where government incentives offer competitive advantages. However, renewables have significantly lower capacity factors and are unreliable as base-load sources of power, ensuring that electrical grids must have larger grid systems to overcome these intermittent renewable sources, often including coal and gas power plants.

At present, nuclear power is considered one of the most abundant fuel sources for base-load electrical generation for the foreseeable future. Advances in fuel recycling, utilizing alternative fuels such as thorium, and building fast-neutron-spectrum reactors will combine to decrease the radioactive waste generated by NPPs, leading nuclear fuel to become a more sustainable source of power.

Despite the high capacity factors, low carbon emissions, and relatively safe operation of NPPs, the existing fleet (Gen II/III/III+) is no longer economically competitive with the high efficiency natural gas combined cycle and coal-fired plants. While partially due to low gas and coal prices, this is also due to higher levels of regulation imposed upon the nuclear industry due to previous NPP disasters, resulting in higher capital costs for NPPs.

Therefore, enhancements to thermal efficiency (reaching at least $> 40\%$) are needed in Gen IV reactors to compete in world markets (without government subsidies if possible), in addition to improvements in safety and design.

2 LITERATURE REVIEW

2.1 CATEGORIES OF NPP

There are a wide variety of NPP's in operation today, utilizing different configurations, coolants, moderators, and many other parameters. However, when referring to NPP's today, two main categories are typically discussed:

- 1) Small Modular Reactors (SMR) <300 MW_{el}
- 2) Large Reactors >700 MW_{el}
 - a. Generation II/III/III+
 - b. Generation IV

2.1.1 SMR (<300 MW_{el})

SMRs are a 'hot topic' in the industry at present time. According to the World Nuclear Association (WNA) (2020), the interest in SMRs is driven by a desire to reduce the impact of capital costs, and to provide power away from large grid systems. The classification of SMR used to refer to 'Small and Medium Reactors', which are reactors less than 300 & 700 MW_{el}. In this thesis, the SMR abbreviation will only refer to Small Modular Reactors.

As reported by Pioro et al. (2019) , there are 55 SMR concepts, separated into 6 categories (Figure 2-1) designed to be modular, pre-built in a factory to reduce capital costs, and have simplified designs.

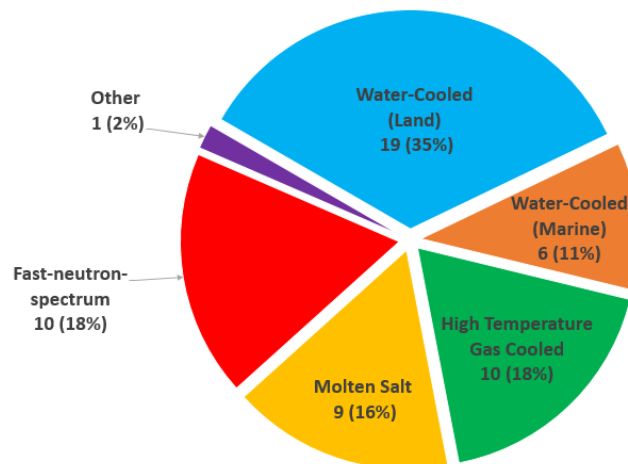


Figure 2-1: SMR Categories
(adapted from Pioro et al (2019).)

Currently 26 Small and Medium Reactors are in operation around the world (Pioro et al., 2019). However, none of these fall into the 55 concepts as they are neither modular, pre-built, or have simplified designs. Of these 55 SMR concepts, only two have been constructed thus far (KLT-40S) and installed on a barge, destined for a northern city in Russia. In addition, one SMR is being constructed in Argentina, and one SMR is reaching the experimental phase in Japan (Pioro et al., 2019). In Canada, the Canadian Nuclear Safety Commission (CNSC) has entered into pre-licensing design reviews with 9 SMR vendors, with various types of SMRs proposed.

2.1.2 Larger Reactors (>700 MW_{el})

2.1.2.1 Gen II/III/III+

There are six main categories of larger NPPs operating throughout the world today (Figure 2-2), with a total of 440 NPPs worldwide.

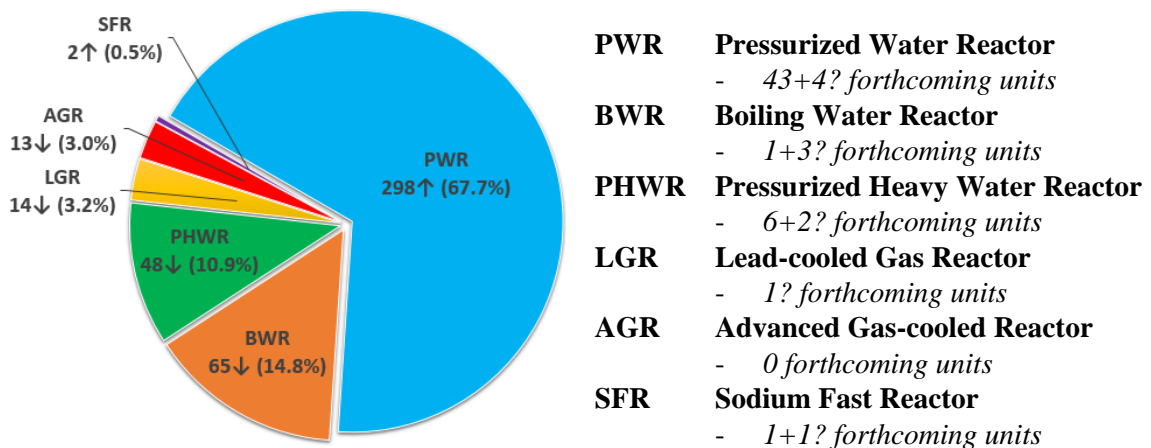


Figure 2-2: Global # of NPP by Type, and # of Forthcoming Units (2020)

(adapted from Pioro et al. (2019))

(arrows indicate change in fleet since 2011, prior to Fukushima Daiichi disaster)

Examining the forthcoming units in Figure 2-2, the only type of NPPs planned to be built on a larger scale in the near future is the PWR type. Unless additional NPPs are built, the total amount remaining in service over the next 10 – 15 years will decrease. Additionally, it appears that the LGR, AGR, and BWR NPP technologies are becoming obsolete as very few are planned to be built.

The general characteristics of the existing Gen II/III/III+ NPPs are shown in Table 2-1. Combined, approximately 96% of all reactors worldwide use water as a coolant (water cooled), leading to a large amount of experience with water cooled reactors.

Table 2-1: General Characteristics of NPPs
(courtesy of I.L. Pioro)

NPP Type	Thermal Cycle	Coolant (outlet conditions)			Moderator
		Fluid	Pressure (MPa)	Temp. (°C)	
PWR	Indirect	Water	15	~329	Water
BWR	Direct	Water	7	~288	Water
PHWR	Indirect	Heavy Water	11	~310	Heavy Water
LGR	Indirect	Water	7	~284	Graphite
AGR	Indirect	CO ₂	4	~650	Graphite
SFR	Indirect ×2	Sodium (liquid)	0.1	~550	None

The PHWR type is exclusively used in Canada with the style of reactor being the CANada Deuterium Uranium (CANDU) reactor. The following NPPs remain operational today:

Table 2-2: NPPs Operational in Canada as of May 2020
(WNA, 2020)

NPP Name	Model of Units	Number of Units	Installed Capacity	Grid Connection
Operator: Bruce Power, Ontario				
- Bruce A	CANDU 791 (×2)/750A (×2)	4 units	2964 MW _{el}	1977 - 1979
- Bruce B	CANDU 750B (×4)	4 units	3261 MW _{el}	1984 - 1988
Operator: Ontario Power Generation (OPG), Ontario				
- Darlington	CANDU 850 (×4)	4 units	3524 MW _{el}	1990 - 1993
- Pickering	CANDU 500A (×2)/500B(×4)	6 units	3080 MW _{el}	1971 – 1974 1982 - 1986
NB Power, New Brunswick				
- Point Lepreau	CANDU 6	1 unit	660 MW _{el}	1982

PHWRs utilize fuel channels with a pressure tube design in an indirect thermal cycle (Figure 2-3). UO_2 fuel pellets are loaded into fuel pins, made of zircaloy-4 sheaths (cladding). The fuel pins together are known as the fuel bundle. Both the 37-element and the 43-element (CANFLEX) fuel bundle designs contain a centre rod and inner ring arrangement similar to the 7-rod design, which will be tested in this thesis (Figure 2-4).

The heavy water coolant flows inside of the pressure tube, removing heat from the fuel bundles, produced by the UO_2 fuel. This heat is transferred to the secondary water, creating steam, that is directed to the turbine to generate electricity.

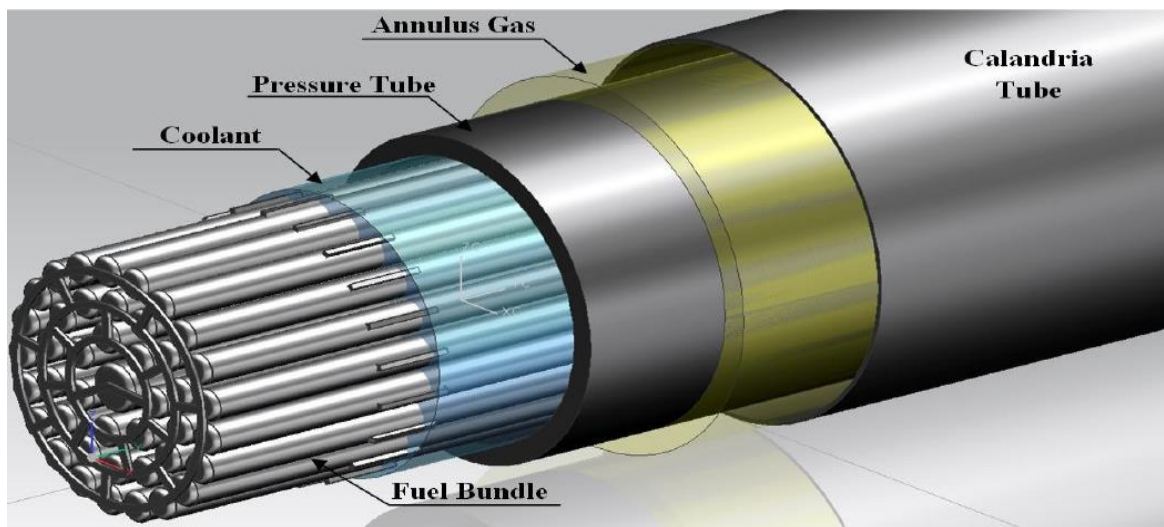
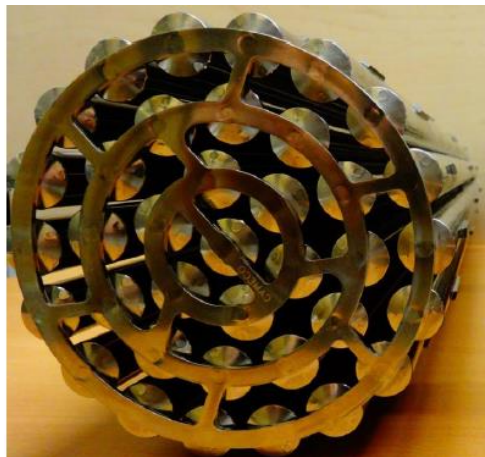
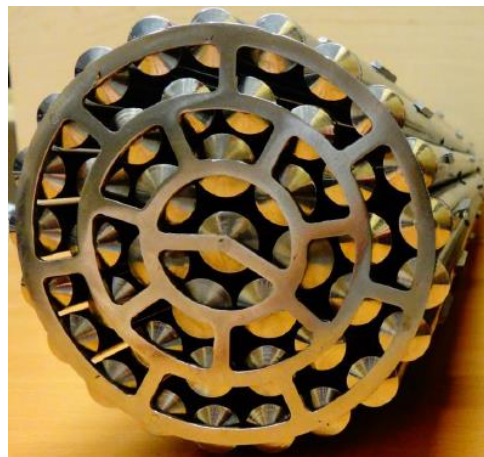


Figure 2-3: CANDU fuel-channel design
(courtesy of W. Peiman (Pioro & Duffey, 2007)) (Copyright of ASME)



(a)



(b)

Figure 2-4: Photos of fuel bundles: (a) 37-element CANDU style, (b) 43-element CANFLEX style
(courtesy of I.L. Pioro)

2.1.2.2 Gen IV

In January of 2000, the US DOE Office of Nuclear Energy, Science and Technology invited a group of senior governmental representatives from nine countries to collaborate on the development of Generation IV concepts. This group became known as the Generation IV International Forum (GIF) Policy Group, who then formed a subsequent group consisting of Senior Technical Experts, that first met in April of 2000. As of July, 2011, there are 13 members of the GIF who agreed to an extension of the GIF Charter to continue development of the Gen IV concepts (Pioro, 2016). 11 of these members can be seen below in Figure 2-5.












System	AU	CA	CN	EU	FR	JP	KR	RU	CH	GB	US
											
GFR				✓	✓	✓					
SCWR		✓	✓	✓		✓		✓			
SFR			✓	✓	✓	✓	✓	✓		✓	✓
VHTR	✓		✓	✓	✓	✓	✓		✓	✓	✓
LFR				P		P	P	P			P
MSR	P			P	P			P	P		P
✓ Signatory to the System Arrangement P Signatory to the Memorandum of Understanding Argentina, Brazil, and South Africa are inactive											

Figure 2-5: GIF Countries and Gen IV Concepts
(adapted from GIF (Grosch, 2019))

One of the goals of the Gen IV reactors is to increase the gross thermal efficiencies. As shown in Figure 1-7, increasing the inlet temperature to the turbine will raise the theoretical gross thermal efficiency. The expected efficiencies of the Gen IV designs being researched are listed in Table 2-3.

Canada's sole focus for Gen IV larger reactors is the SCWR concept, accompanied by four other members: China, Europe, Japan, and Russia.

Table 2-3: Gen IV NPP Reactor Styles
(Pioro, 2016)

NPP Power Plant Type Cycle, conditions at turbine inlet, and/or at the coolant exiting the reactor)	Maximum Gross Thermal Efficiency
Very High Temperature Reactor (VHTR) (Direct) Brayton Cycle, Coolant – He, $P=7$ MPa, $T_{in}/T_{out}=640/1000^{\circ}\text{C}$ Steam Rankine Cycle (possible indirect backup)	$\geq 55\%$
Gas Fast Reactor (GFR) (Direct) Brayton Cycle, Coolant – He, $P=9$ MPa, $T_{in}/T_{out}=490/850^{\circ}\text{C}$ Steam Rankine Cycle (possible indirect backup)	$\geq 50\%$
SuperCritical Water Reactor (SCWR) <u>Canadian Concept:</u> (Direct) Coolant – H_2O , $P=25$ MPa, $T_{in}/T_{out}=350/625^{\circ}\text{C}$ Steam Rankine Cycle (possible indirect backup with reheat) High Temperature Steam Superheat	45-50%
Molten Salt Reactor (MSR) (Indirect) Coolant – Na-F salt with dissolved uranium fuel, $T_{out}=700\text{-}800^{\circ}\text{C}$ Brayton cycle, CO_2 (Steam Rankine Cycle as possible backup)	$\sim 50\%$
Lead-cooled Fast Reactor (LFR) <u>Russian design BREST-OD-300*:</u> (Indirect) Coolant – liquid Pb, $P=0.1$ MPa, $T_{in}/T_{out}=420/540^{\circ}\text{C}$ Steam Rankine Cycle, $P_{in}=17$ MPa, $T_{in}=505^{\circ}\text{C}$ High Temperature Steam Superheat (design in other countries based on sCO_2 Brayton indirect cycle)	$\sim 41\text{-}43\%$
Sodium Fast Reactor (SFR) <u>Russian design BN-600:</u> (Indirect) 1 st Cycle Coolant – liquid Na, $P=0.1$ MPa, $T_{in}/T_{out}=380/550^{\circ}\text{C}$ 2 nd Cycle – liquid Na, $T_{in}/T_{out}=320/520^{\circ}\text{C}$ Steam Rankine Cycle, $P_{in}=14.2$ MPa, $T_{in}=505^{\circ}\text{C}$ Steam Superheat, $P_{in}=2.45$ MPa, $T_{in}=505^{\circ}\text{C}$	$\sim 40\%$

2.2 CANADIAN SCWR DESIGNS

Gen II/III/III+ water cooled NPPs operate with subcritical pressures (BWR, CANDU, PWR shown in Figure 2-6), therefore the maximum temperature of the coolant is limited by the boiling temperature (saturation line in Pressure-Temperature (P-T) diagram - Figure 2-6). This limit avoids boiling that leads to burnout – a condition characterized by steam acting as an insulative barrier to heat transfer, producing unpredictably high temperatures that can lead to sheath failure or fuel meltdown, resulting in the possible release of radiation to the public.

SCWRs are designed to operate with coolant water above the critical point (373.95°C / 22.064 MPa – shown in Figure 2-6). As SCW has no distinct gas or liquid phase, no boiling occurs in SCWRs, avoiding the burnout regime. This allows SCWRs to achieve coolant temperatures at the turbine inlet above 373.95°C , leading to greater gross thermal efficiencies. In addition, as the temperature crosses the pseudo-critical (pc) point, unique properties of SCW are exploited to further increase the thermal efficiency.

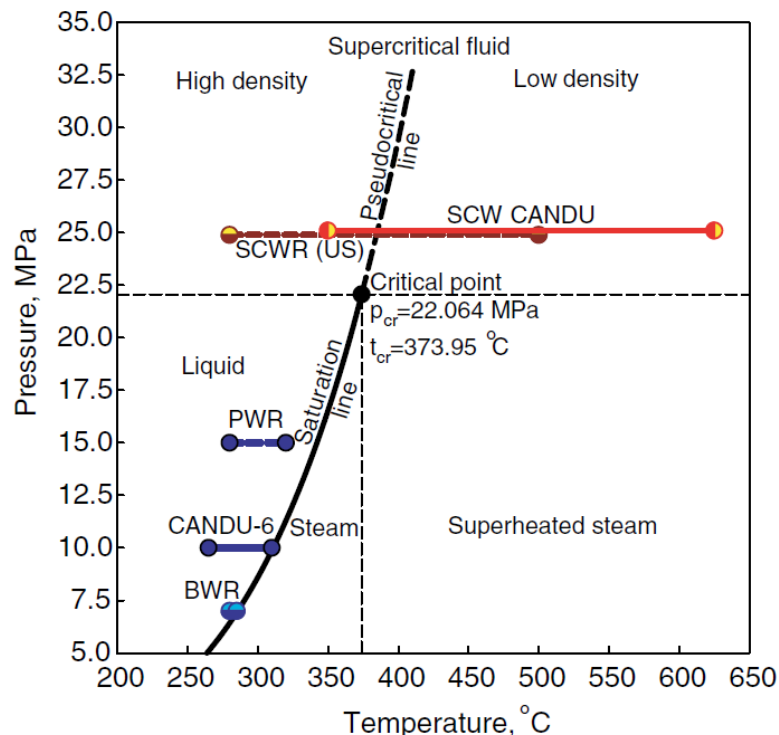


Figure 2-6: Pressure-Temperature diagram of water with typical operating conditions

(courtesy of I. L. Pioro (Pioro & Duffey, 2007)) (Copyright of ASME)

2.2.1 *Reactor Designs*

The Canadian SCW concept uses the Pressure-Tube (PT) design in a direct power cycle (Figure 1-7) configuration, while other SCW designs make use of a Pressure Vessel (PV).

Yetisir et al. (2011) from AECL proposed a SCWR design based upon CANDU experience. This is a direct-cycle concept, drawing on the BWR and CANDU reactors. The expected thermal efficiency is 50%. The coolant is light water, while the moderator surrounding the fuel channels inside the Calandria vessel is heavy water.

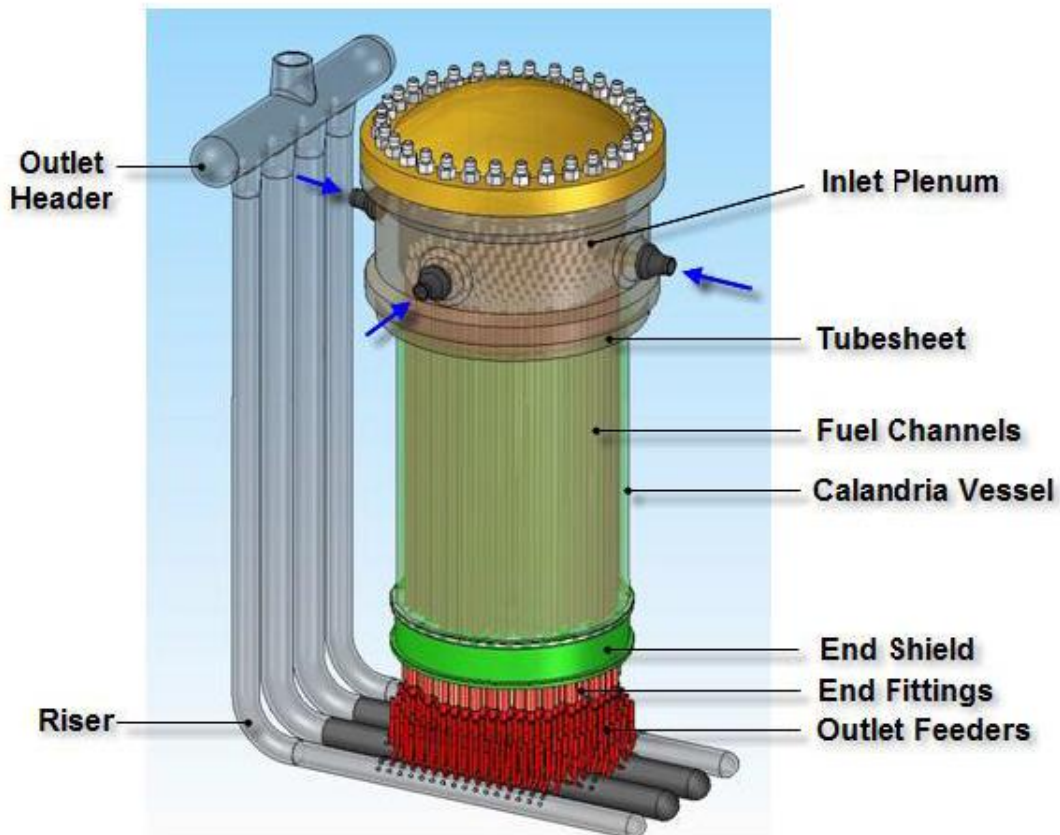


Figure 2-7: Preliminary Concept of the PT type SCWR
(Yetisir et al., 2011) (Copyright of CNL)

This SCWR design is anticipated to generate 2540 MW_{th} (1200 MW_{el}), with 336 fuel channels. The channels are designed for a coolant with an inlet temperature of 350°C and an outlet temperature of 625°C, at a pressure of 25 MPa (Yetisir et al., 2011).

This concept utilizes a vertical fuel channel, with off-power refueling, eliminating on-line fueling by using enriched recycled fuels. Figure 2-7 shows the conceptual design of the SCWR with major design components.

In addition, Duffey, et al. (2011) and Yetisir et al. (2012) published the concept of the SCWR SMR referred to as the SuperSafe© Reactor (SSR), having similar features to the SCWR concept in Figure 2-7. This conceptual design was projected to produce 670 MW_{th} (300 MW_{el}) using 108 fuel channels with SCW coolant at the turbine inlet (25 MPa, 625°C), and high efficiencies (up to 50%).

More recently, Yetisir et al. (2016) have proposed a similar version of the SCWR (Figure 2-8), with the same design parameters ($T_{in/out}=350/625^{\circ}\text{C}$, $P=25\text{MPa}$) utilizing a fuel channel with a central flow tube, allowing water to flow downwards to the bottom of the channel, before being forced upwards through the fuel bundles. This design feature allows for the inlet and outlet flow features to be located at the top of the reactor. This current design utilizes 336 channels, a per channel power of 9.97 MW (heated length of 5 m) and a mass flowrate of 5.13 kg/s, at the beginning of cycle (Domínguez et al., 2016)

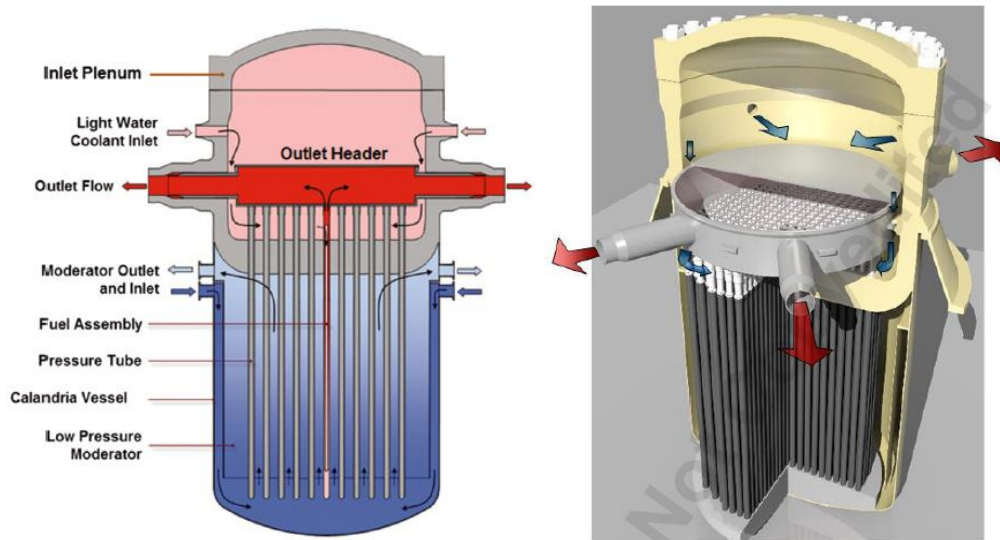


Figure 2-8: Recent Concept of the PT type SCWR
(Yetisir,et al. (2016) & (2018)) (Copyright of CNL)

2.2.2 *Fuel Channel Design*

The design initially proposed by Yetisir et al. (2011) (Figure 2-9) considered a 37-element fuel bundle, 12 in a fuel channel), with the centre rod and inner ring composing of a 7-rod configuration, currently used in CANDU operations. The 43-Element CANFLEX® bundles were also considered in the safety analysis (IAEA, 2014). Coolant flows around the Fuel bundle inside of a pressure tube.

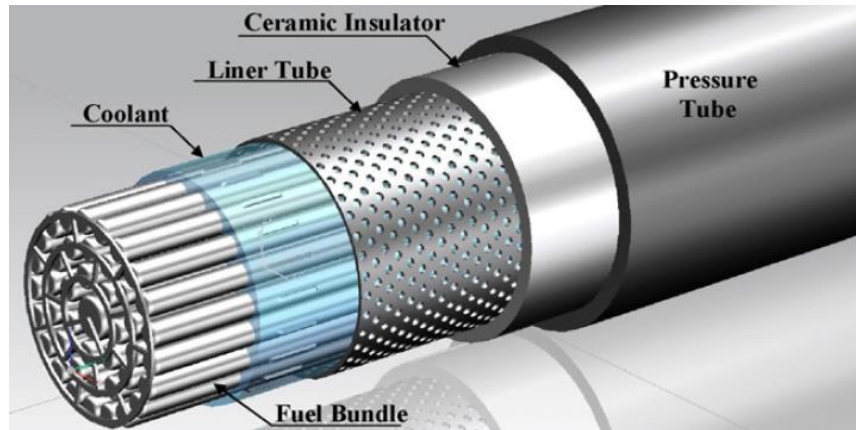


Figure 2-9: Canadian SCWR fuel-channel concept
(courtesy of W. Peiman (Peiman et al., 2012)) (Copyright of IntechOpen)

This design, similar to the design of a CANDU fuel channel shown in Figure 2-3, allows the PT to be protected by the ceramic insulator and be in direct contact with the moderator, avoiding the high temperatures expected by the SCW coolant.. The liner tube would protect the ceramic insulator from damage due to changing the fuel bundle during refueling (Yetisir et al., 2011).

Yetisir et al. (2018) also proposed a completely new fuel channel design where water flows vertically down the fuel channel through a central flow tube that is separated from the fuel bundles, and then rises vertically, being forced through the fuel bundles that are arranged radially around the centre as shown in Figure 2-10.

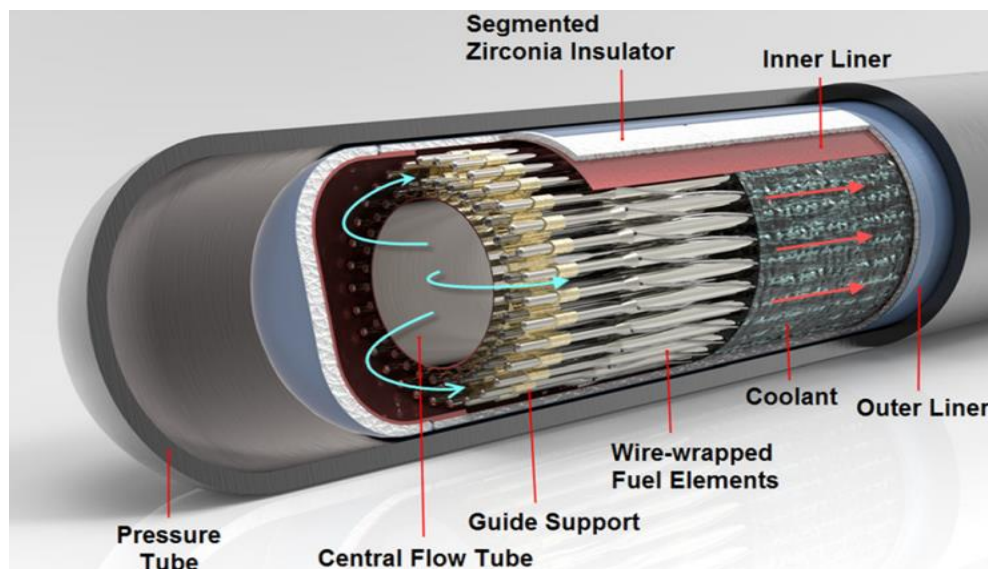


Figure 2-10: Fuel channel bottom showing various components and flow direction
(Yetisir et al., 2018) (Copyright of ASME)

This newly proposed fuel bundle design is a 64-element, double ring configuration (32 elements in each ring), with the central flow tube design aspect (Figure 2-12). This design aspect helps to meet the “No-core-melt” safety goal of the Canadian SCWR, as in a LOCA event, the central flow tube can have flashed steam interrupting its natural flow circulation.

Despite this flow interruption, the created void in the central flow tube leads to a negative coefficient of void reactivity due to the neutron moderation activity of the water in the central flow tube. This safety consideration requires future work, though initial analysis suggests that in a total station blackout condition the fuel element maximum temperature is not exceeded (Yetisir et al., 2018).

While this 64-element bundle does not have the same 7-rod bundle interior as the 37-element bundle, it is still a bundle geometry, and must be considered in any future research.

2.2.3 *Fuel Element Design*

The sheath cladding of the 37-element bundle for the CANDU PHWR fuel bundles is made of Zircaloy-4, with a minimum wall thickness of 0.38 mm, and outside diameter of 13.08 mm (Page, 1976). Figure 2-11 shows the relevant dimensions of the 37-element bundle (Colton et al., 2017) (Page, 1976), including the PT (not included is the length of each bundle, 495.3 mm in length, fuel length of 485 mm). Page (1976) reported the nominal channel power of 12 MW, and a total of 12 bundles per channel.

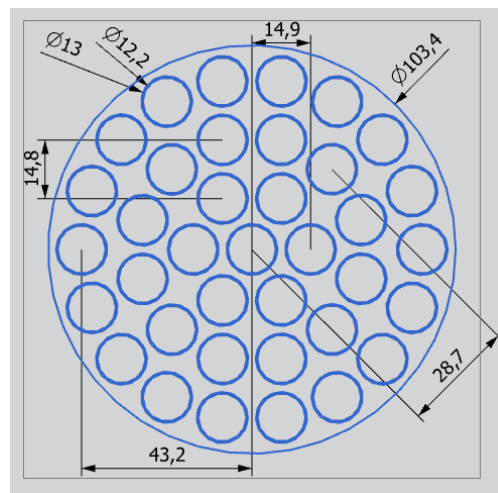


Figure 2-11: 37-Element Bundle Dimensions
(created from dimensions listed by Colton, et al. (2017))

This 37-element bundle contains three main types of pitch arrangements; triangular, square, and a 7-rod bundle (1 inner rod surrounded by 6 rods). The inner rod of the 7-rod bundle is anticipated to experience the highest surface temperature due to the geometry.

The CANFLEX® 43-element bundles are similar to the 37-element bundles, with three rings of fuel elements circling a centre fuel rod. However, the CANFLEX® central ring has 7 fuel rods compared to 6 in the 37-element bundle (8-rod bundle central pitch arrangement). The centre fuel rod and the fuel rods of the central ring of the CANFLEX® are all 13.42 mm in diameter with a wall temperature of 0.36 mm, while the outer ring fuel rods are all 11.36 mm in diameter with a wall thickness of 0.33 mm (Kim et al., 2011).

The maximum surface temperature of the sheath for the 37-element and CANFLEX® bundles is 850°C and 804°C, respectively (Yetisir et al., 2011).

The 64-element double ring features fuel rods 9.5, 10 mm in diameter (inner and outer ring, respectively), with a liner tube inner diameter of 144 mm, the centre flow outer diameter of 94 mm, and hydraulic diameter of 6.74 mm. Each rod is a total of 5 metres in heated length (Domínguez et al., 2016).

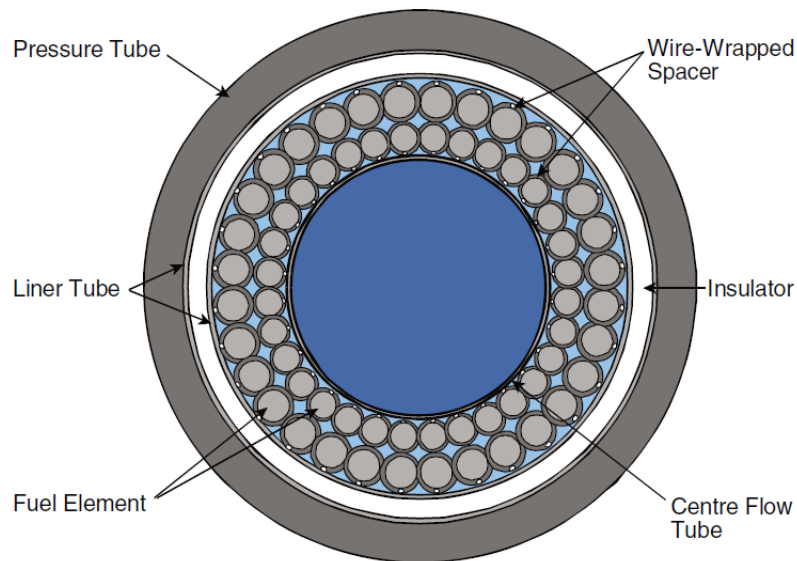


Figure 2-12: Conceptual 64-Element Fuel Bundle and Channel design
(Domínguez et al., 2016) (Copyright of CNL)

The cladding for the newly proposed fuel bundle design by Yetisir et al. (2018) is still undecided. Zircaloy-4 experiences severe oxidation after a few hundred hours of operation

(IRSN, 2015), in addition to low strength at the elevated temperatures (Chow & Khartabil, 2007), and should not be considered as a cladding material.

The suggested cladding material is a Nickel based material such as Alloy 625 or 800H, with a thickness of 0.4 mm (Yetisir et al., 2018). Alloy 625 has a lower thermal conductivity than 800H. According to Kaschnitz et al. (2019), the thermal conductivity of Alloy 625 can be described as:

$$k_{A625} \left(\frac{W}{m \cdot K} \right) = 9.7116 + 0.0176 \cdot T, \quad T \text{ in } ^\circ C \quad (2.1)$$

For the SMR SSR, Yetisir et al. (2012) proposed a similar 78-element SCWR fuel assembly, with 3 rings of fuel elements surrounding a centre flow tube.

2.2.4 Fuel Design

Uranium Dioxide (UO₂) has been used in the fuel of CANDU operations for some time, in addition to all LWR in the US (Phillipot et al., 2011). It is a ceramic and has low thermal conductivity relative to metal fuels. At temperatures of 800 to 1400°C it becomes plastic, and above these temperatures grain growth occurs leading to cracking (Page, 1976). The industrial accepted maximum limit for UO₂ fuel pellets is 1850°C (Peiman et al., 2012). Fink (2000) reported the thermal conductivity as relationship as:

$$k_{UO_2} \left(\frac{W}{m \cdot K} \right) = \left[\frac{100}{6.548 + 23.533 \cdot \frac{T}{1000}} \right] + \left[\frac{6400}{\left(\frac{T}{1000} \right)^{2.5}} \right] \cdot e^{\left(-\frac{16350}{T} \right)}, T \text{ in } K \quad (2.2)$$

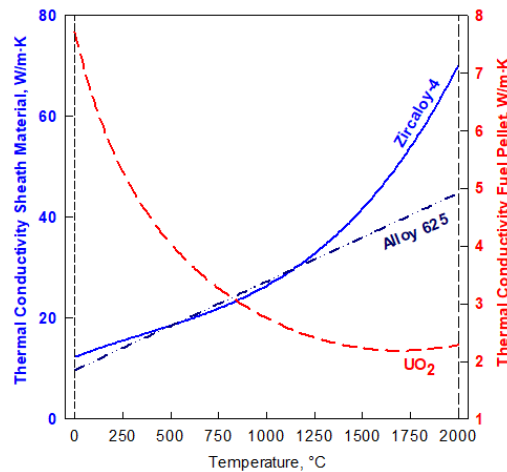


Figure 2-13: Thermal Conductivities of Alloy 625 and UO₂

Figure 2-13 was created to show the thermal conductivity of sheath materials Zircaloy-4 and Alloy 625, in addition to the fuel pellet UO_2 .

Recently, thorium based fuels has re-emerged as an attractive fuel source for the following three reasons; 1) scarce supply of nuclear fuel, 2) disposal of nuclear waste, 3) nuclear proliferation. Thorium offers an attractive option to resolve all three of these issues. It is estimated that the thorium reserves are three times more abundant in nature when compared to natural uranium reserves (Liu & Cai, 2014). In addition, the thermal conductivity of thorium dioxide is higher than uranium dioxide (IAEA, 2005).

Fuel is what provides the energy for heating up the coolant. In a typical nuclear reactor, the heat generation rate (\dot{q}) typically follows a cosine shape across the heated length due to the geometry of the reactor (Figure 2-14). The change of this heat generation rate will lead to a variable heat flux (q) across the heated length.

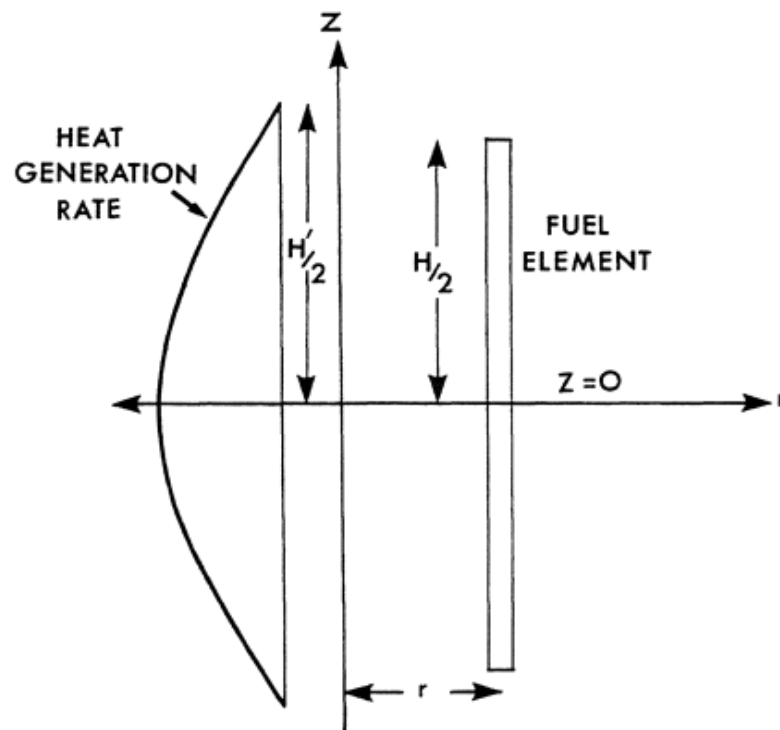


Figure 2-14: Heat Generation in a Typical Fuel Element
(Cameron, 1982) (Copyright of Plenum Press)

In this thesis only a constant heat flux will be examined as this will be a part of future work to perform simulations to determine accurate cosine shapes.

2.2.5 *Issues Facing SCWR*

In order to progress the SCWR concept, several challenges must be addressed (Pioro, 2016):

- 1) Prediction of HT in SCW needs to be validated with bundle experiments.
 - Domínguez et al. (2016) predicted the HT using a CFD based approach, and a HT approach based on four **Nu** correlations for bare tubes: Dittus-Boelter (1930), Bishop et al. (1964), Jackson (2002), and Mokry et al. (2009)
 - Both approaches showed acceptable temperatures for sheath (cladding)
 - No **Nu** correlation based on bundle geometries was utilized
 - No Fuel Centreline temperatures were reported
- 2) Alloys to handle the design peak cladding conditions (850°C / 25 MPa) need to be identified.
 - Alloy 625 is suggested (Yetisir et al., 2018)
- 3) Peak coolant conditions that lead to stress corrosion cracking need to be identified.
- 4) Water chemistry issues such as predicting and controlling water radiolysis and corrosion product transport require reconciliation.

The starting point for determining the suitable **Nu** correlations required for the SCWR in the bundle geometries outlined, is to examine those available based on bare tubes and other geometries.

In depth studies are made by Dr. Pioro and Dr. Duffey (Pioro & Duffey, 2007) for **Nu** correlations available in open literature.

2.3 GENERAL TERMS

SCW is looked upon favorably for its ability to store tremendous energy due to the thermophysical properties changing near the critical/pc point, in particular the specific heat capacity (Figure 2-17). To understand these properties, general terms must be understood.

Some terms as defined by Pioro and Duffey (2007) are listed below:

Compressed fluid is a fluid at a pressure above the critical pressure but at a temperature below the critical temperature.

Critical point (also called a *critical state*) is the point where the distinction between the liquid and gas (or vapor) phases disappears, i.e., both phases have the same temperature, pressure and volume. The *critical point* is characterized by the phase state parameters T_{cr} , P_{cr} , and ρ_{cr} which have unique values for each pure substance.

Pseudocritical point (characterized with P_{pc} and T_{pc}) is a point at a pressure above the critical pressure and at a temperature ($T_{pc} > T_{cr}$) corresponding to the maximum value of the specific heat capacity for this particular pressure.

- A look up table specifying pc points for pressures increasing by 0.1 MPa was compiled and listed in Appendix C.1.

Supercritical fluid is a fluid at pressures and temperatures that are higher than the critical pressure and critical temperature. However, in the present monograph, the term *supercritical fluid* includes both terms—a *supercritical fluid* and *compressed fluid*.

Supercritical steam is actually supercritical water because at supercritical pressures there is no difference between phases. However, this term is widely (and incorrectly) used in the literature in relation to supercritical steam generators and turbines.

Superheated steam is a steam at pressures below the critical pressure but at temperatures above the critical temperature.

A P-T phase diagram for Water illustrates the general terms (Figure 2-15), and is useful for determining the phase at any given pressure and temperature combination.

Above the critical point, no distinct liquid or gaseous states exist, only liquid-like and gas-like regions. The transition between these regions occurs as the fluid crosses the pc point, shown in Figure 2-15 and Figure 2-16.

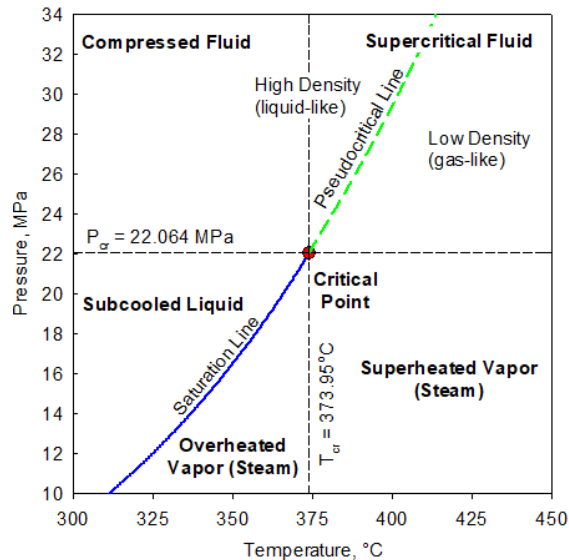


Figure 2-15: Pressure-Temperature Diagram for Water
(created by data from NIST REFPROP 10.0)

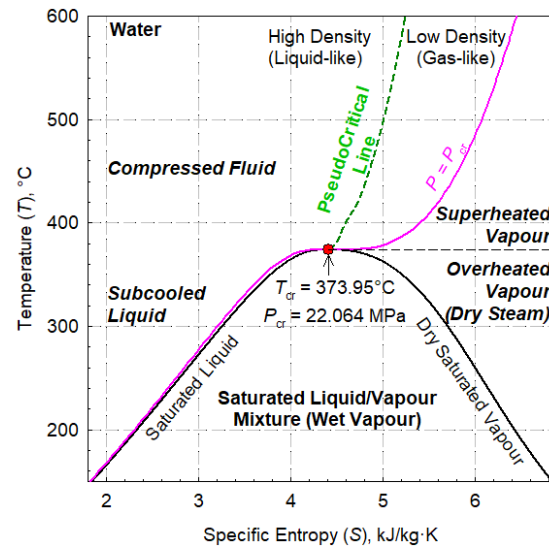


Figure 2-16: Temperature-Entropy Diagram for Water
(created by data from NIST REFPROP 10.0)

For thermodynamic calculations, it is convenient to observe the Temperature-Specific Entropy (T-S) diagram (Figure 2-16). The area under the T-S curve for a process equates to the heat transferred to or from a system.

Between the Saturated Liquid and the Dry Saturated Vapour curves of the T-S diagram, is the region where boiling occurs. As the critical point is the peak of this curve, any temperature higher will not experience boiling, and thus avoid any burnout regimes.

2.4 SPECIFICS OF SCW THERMOPHYSICAL PROPERTIES

All thermophysical properties experience a gradual change with increasing temperature.

However, in a range about the pc point there are sharp fluctuations in properties. Figure 2-17 shows the property changes for SCW at 25 MPa, the proposed pressure for the Canadian SCWR concept. These properties are described below:

The density (ρ) decreases with increasing temperature, showing a sharp decrease about the pc point, while decreasing gradually outside of the pc range.

The thermal conductivity (k) decreases with increasing temperature until it reaches an absolute minimum. There are two phases of decrease, one in the liquid-like region that is gradual, and one in the gas-like region immediately after crossing the pc point that is sudden. After reaching a minimum at $\sim 520^\circ\text{C}$, the thermal conductivity starts to increase slowly.

The specific heat capacity (C_p) experiences a sharp peak at 384.89°C at the pc point. The temperature corresponding to this peak is what defines the pc point for the given pressure of SCW at 25 MPa. A table listing temperatures corresponding to the peak C_p values for pressures from the critical pressure up to 40 MPa, intervals of 0.1 MPa, was compiled and listed in Appendix C.1

The bulk-fluid enthalpy (H) experiences a sharp increase at the pc point, with gradual increases outside of the pc point.

The dynamic viscosity (μ), similar to the density, experiences a sharp decrease about the pc point, while decreasing gradually outside of the pc point.

The Prandtl number (**Pr**), is defined by C_p , μ , and k . As μ and k experience similar trends, and due to the magnitude of the sharp increase of C_p , the Prandtl number experiences similar characteristics to the C_p . The Prandtl number experiences a sharp peak at the pc point, and gradually decreases as the temperature moves away from the pc point.

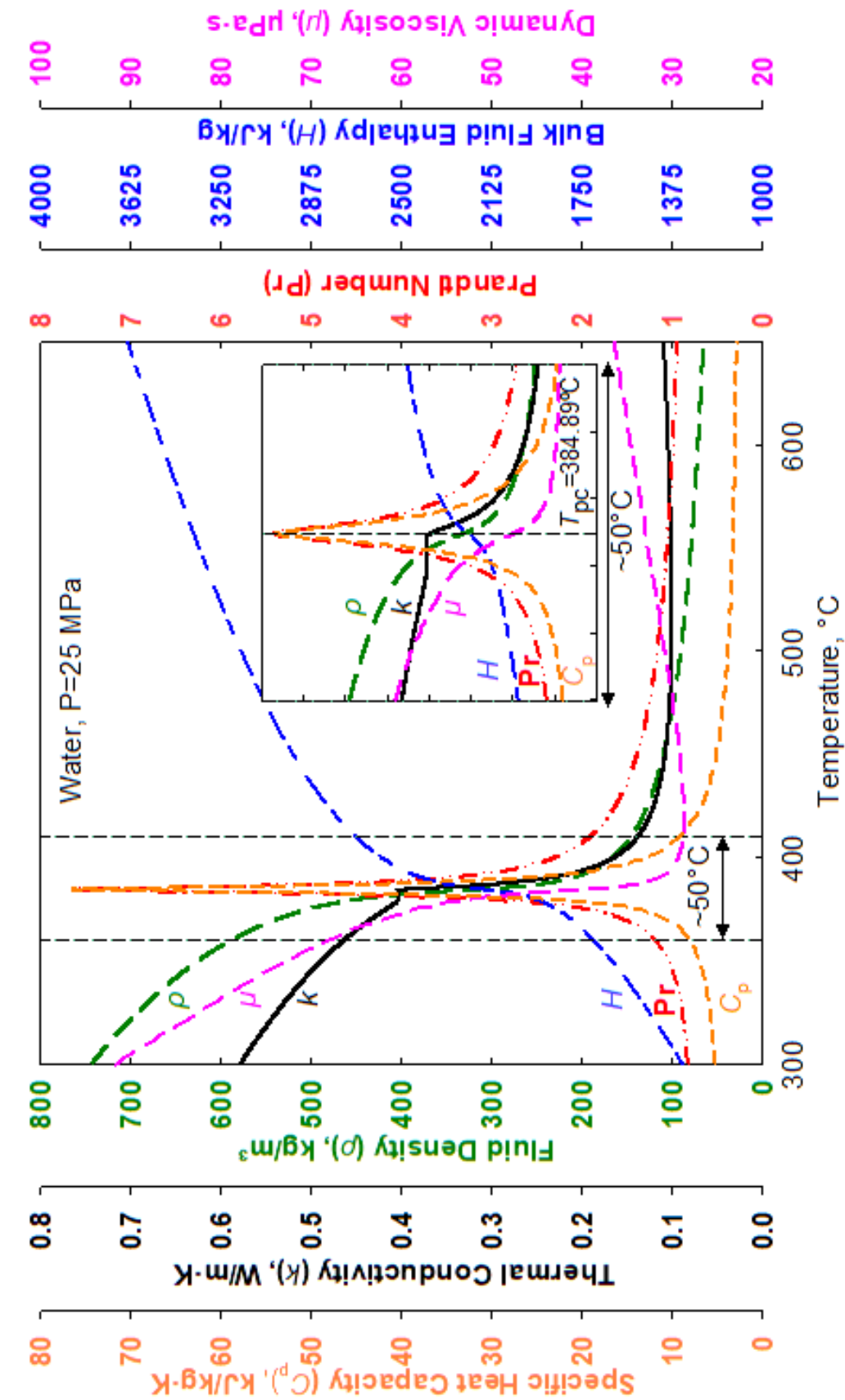


Figure 2-17: Thermophysical Properties of Water 25 MPa
(created with NIST REFPROP 10.0)

2.5 SPECIFICS OF SCW HEAT TRANSFER

2.5.1 *Heat Transfer Regimes*

Some general terms relating to the HT regimes are described by Pioro and Duffey (2007):

Deteriorated heat transfer (DHT) is characterized with lower values of the wall heat transfer coefficient compared to those at the normal heat transfer; and hence has higher values of wall temperature within some part of a test section or within the entire test section.

Improved heat transfer (IHT) is characterized with higher values of the wall heat transfer coefficient compared to those at the normal heat transfer; and hence lower values of wall temperature within some part of a test section or within the entire test section. In our opinion, the improved heat-transfer regime or mode includes peaks or “humps” in the heat transfer coefficient near the critical or pseudocritical regions.

Normal heat transfer (NHT) can be characterized in general with wall heat transfer coefficients similar to those of subcritical convective heat transfer far from the critical or pseudocritical regions, when are calculated according to the conventional single-phase Dittus-Boelter type **Nu** correlations.

Pseudo-boiling is a physical phenomenon similar to subcritical pressure nucleate boiling, which may appear at supercritical pressures. Due to heating of the supercritical fluid with a bulk-fluid temperature below the pseudocritical temperature (high-density fluid, i.e., “liquid”), some layers near a heating surface may attain temperatures above the pseudocritical temperature (low-density fluid, i.e., “gas”). This low-density “gas” leaves the heating surface in the form of variable density (bubble) volumes. During the pseudo-boiling, the wall heat transfer coefficient usually increases (improved heat-transfer regime).

Pseudo-film boiling is a physical phenomenon similar to subcritical pressure film boiling, which may appear at supercritical pressures. At pseudo-film boiling, a low-density fluid (a fluid at temperatures above the pseudocritical temperature, i.e., “gas”) prevents a high-density fluid (a fluid at temperatures below the pseudocritical temperature, i.e., “liquid”) from contacting (“rewetting”) a heated surface. Pseudo-film boiling leads to the deteriorated heat transfer regime.

The three HT regimes as described by Pioro and Duffey (2007) (NHT / IHT / DHT) are illustrated in Figure 2-18:

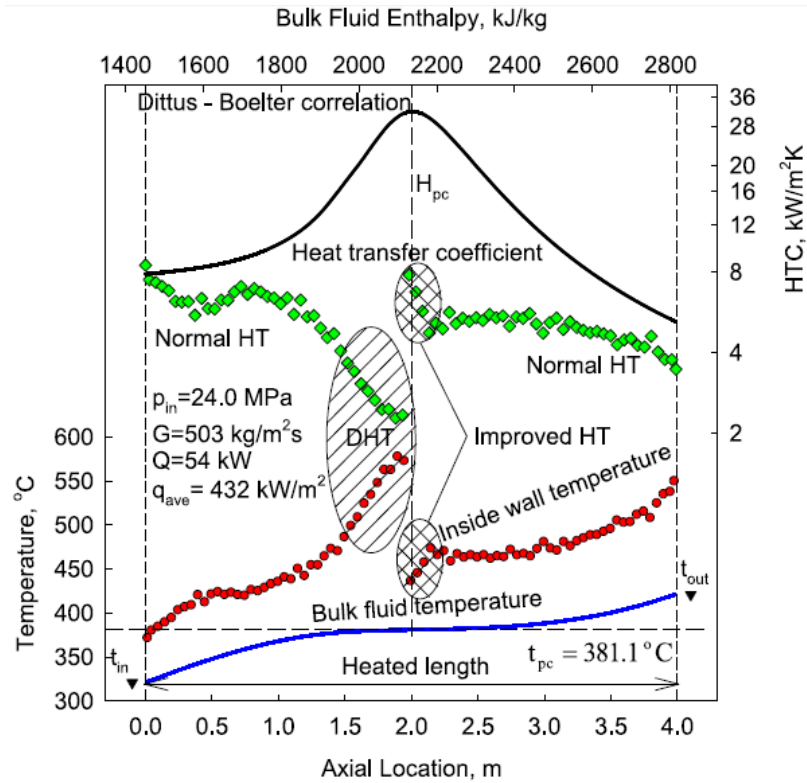


Figure 2-18: DHT Regimes in bare tubes
(courtesy of I.L. Pioro (Pioro, 2019)) (Copyright of ASME)

As described by Pioro and Duffey (2007), Figure 2-18 demonstrates the NHT regime for the first 1.5 m of the trial.

Next, pseudo-film boiling occurs as the bulk-fluid temperature crosses the pc point between 1.5 to 2.0 m, leading to a DHT regime resulting in a reduced HTC and an increase in wall temperature (T_w).

After the DHT regime ends, pseudo-boiling occurs, resulting in a brief IHT regime (2.0 to ~2.25 m).

The NHT regime resumes for the remainder of the trial (~2.25 to 4 m).

2.5.2 DHT Predictions

Various authors have proposed prediction methods for whether DHT will appear based on the initial parameters, however none can predict the moment of DHT occurring along the heated length. Table 2-4 lists common DHT appearance predictions, where q_{dht} represents the minimum heat flux where DHT is predicted to occur.

Table 2-4: DHT Predictions

AUTHOR	DHT PREDICTION
Styrikovich, et al. (1967)	$q_{dht} = 580 \cdot G$ (2.3)
Kondrat'ev (1971)	$q_{dht} = 5.815 \times 10^{-17} \cdot \text{Re}_b^{1.7} \cdot \left(\frac{P \text{ (MPa)}}{0.101325} \right)^{4.5}$ (2.4)
Yamagata, et al. (1972)	$\frac{q}{G^{1.2}} < 0.2$ (2.5)
Jackson & Hall (1979)	$\frac{\overline{\text{Gr}}_b}{\text{Re}^{2.7}} < 10^{-5}$ for vertical tubes $\frac{\overline{\text{Gr}}_b}{\text{Re}^{2.7}} < 10^{-3}$ for horizontal tubes (2.6)
Jackson, et al. (1989)	$\text{Bo}^+ = \frac{\text{Gr}_b}{\text{Re}_b^{3.5} \text{Pr}_b^{0.8}} < 5.6 \times 10^{-7}$ (2.7)
Kirillov, et al. (1990)	$\left(1 - \frac{\rho_w}{\rho_b} \right) \cdot \frac{\text{Gr}}{\text{Re}^2} < 0.4$ OR $\frac{\text{Gr}}{\text{Re}^2} < 0.6$ (2.8)
Kitoh, et al. (2001)	$q_{dht} = 200 \cdot G^{1.2}$ (2.9)
Gabaraev, et al. (2003)	$q_{dht} = 7.9 \times 10^{-4} \cdot G \cdot \left(\frac{P}{P_{cr}} \right)^{1.5}$ (2.10)
Mokry, et al. (2011)	$q_{dht} = -58.97 + 0.745 \cdot G$ (2.11)
Jackson (2013)	$\frac{\overline{\text{Gr}}_b}{\text{Re}_b^{2.7} \text{Pr}_b^{0.5}} < 10^{-5}$ (2.12)
Kong, et al. (2019)	$q_{dht} = 0.457 \cdot G \left(1 - 0.035 \left(\frac{D_{ID}}{20} \right)^{1.96} \cdot \left(\frac{P \text{ (MPa)}}{22.1} \right)^{7.16} \right)$ (2.13)

2.5.3 Long bare tubes Cooled with SCW

Mokry et al. (2009) and (2011), analyzed long bare tubes cooled with SCW experimental data from the Institute for Physics and Power Engineering (IPPE) supercritical-test facility in Russia. IHT/NHT/DHT regimes were observed, with DHT occurring in trials when the average heat flux (q_{avg}) was larger than the q_{dht} predicted by (2.11), and as the T_b approached and crossed the T_{pc} . Increasing the ratio of $q_{avg}/q_{dht} \geq 1.07$ (ratio of heat flux to mass flux function- q_{dht}) prolonged the DHT effect, while lower q_{avg}/q_{dht} and higher G led to higher HTC values. At high G and low q_{avg}/q_{dht} , HTC values were unstable.

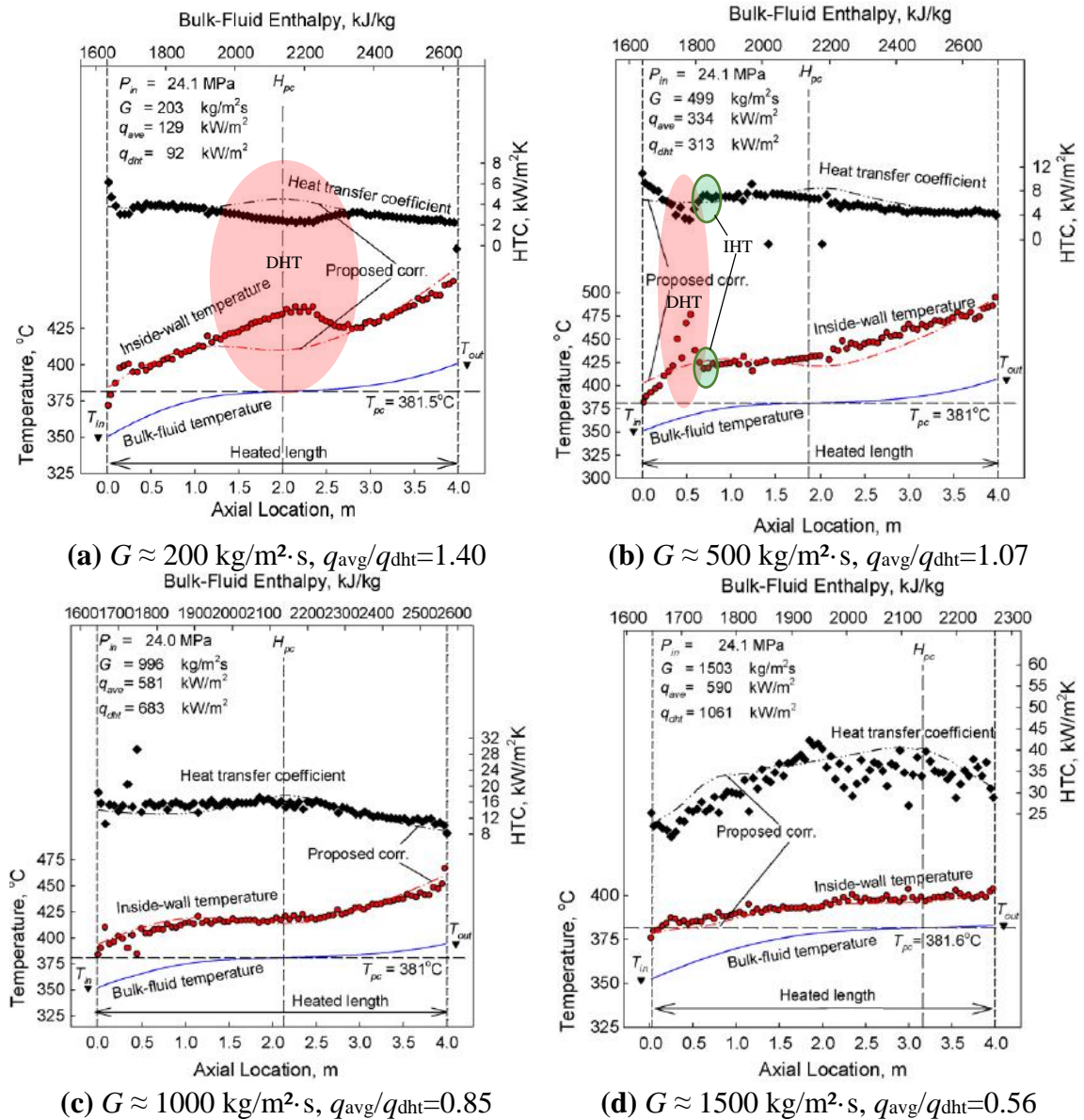


Figure 2-19: SCW Long bare tube Experimental Results (D=10 mm)
 (courtesy of I.L. Pioro (Mokry et al., 2011)) (Copyright of Elsevier)

2.5.4 Short bare tubes Cooled with SCW

Zvorykin et al. (2018) analyzed short bare tube cooled with SCW experimental data from the National Technical University of Ukraine supercritical-test facility. In short bare tubes, only two regimes of HT were observed (NHT/DHT) due to the short length of the heated section (0.6 m). DHT occurred in trials when $q_{\text{avg}}/q_{\text{dht}} \geq 1.15$, with the effect of DHT becoming more severe as $q_{\text{avg}}/q_{\text{dht}}$ grew larger. The mass flux remains constant through the trials, with only slight HTC decreases observed with increasing ratios of $q_{\text{avg}}/q_{\text{dht}}$, suggesting the mass flux has a greater effect on HTC compared to the ratio of $q_{\text{avg}}/q_{\text{dht}}$.

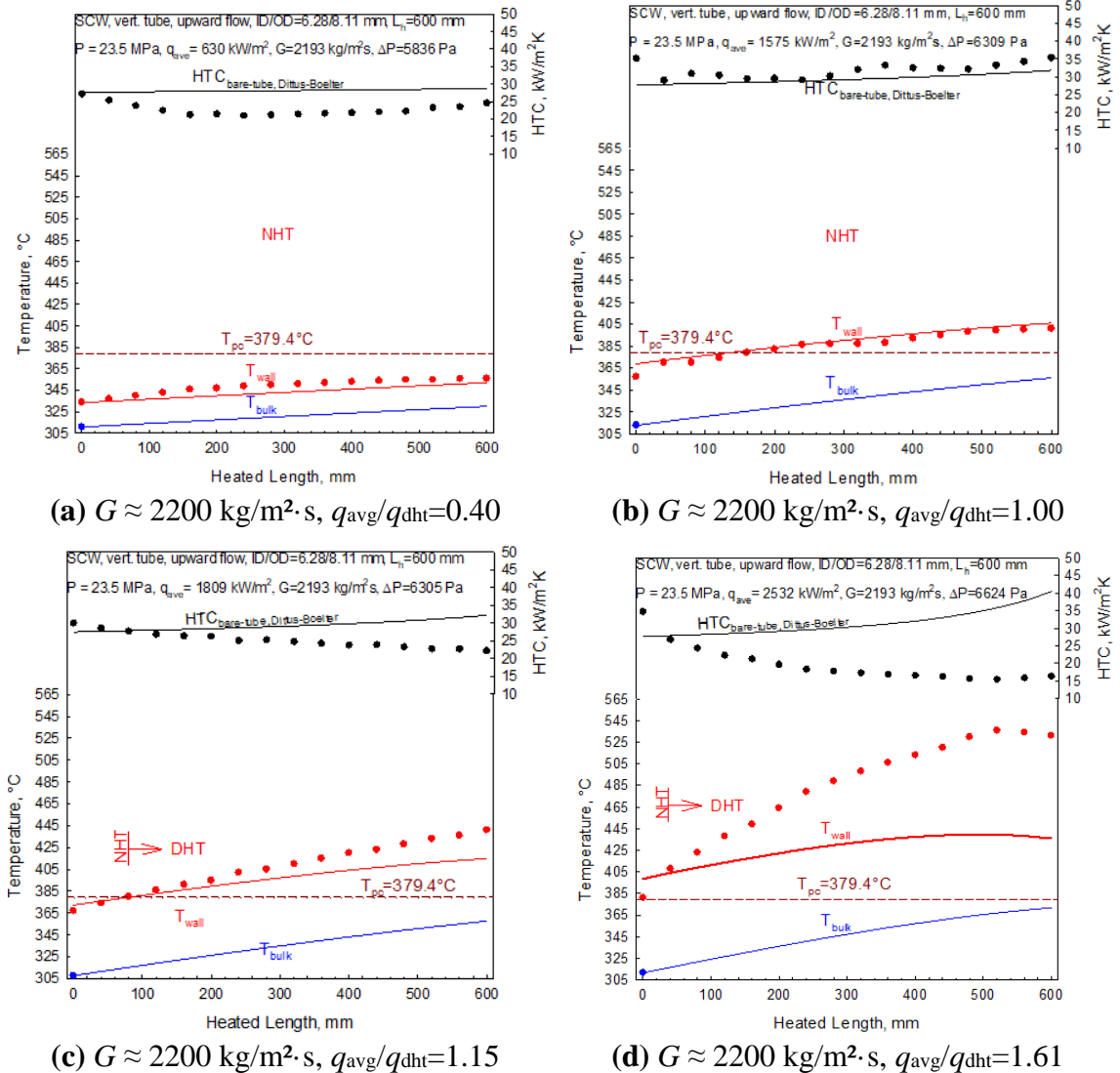


Figure 2-20: SCW Short bare tube Experimental Results (D=6.28 mm)
(courtesy of I.L. Pioro (Zvorykin et al., 2018)) (Copyright of ASME)

2.5.5 1-rod (Annular) Bundle Cooled with SCW

Razumovskiy et al. (2015) analyzed a 1-rod (annular) bundle (Figure 2-21 (d)) cooled with SCW experimental data from the National Technical University of Ukraine supercritical-test facility. In the 1-rod experiments, only two regimes of HT were observed (NHT/DHT) due to the short length of the heated section (0.485 m). DHT occurred when $q_{avg}/q_{dht} \geq 1.78$. The mass flux and average HTC values in these trials were similar to the short bare tube results shown in section 2.5.4.

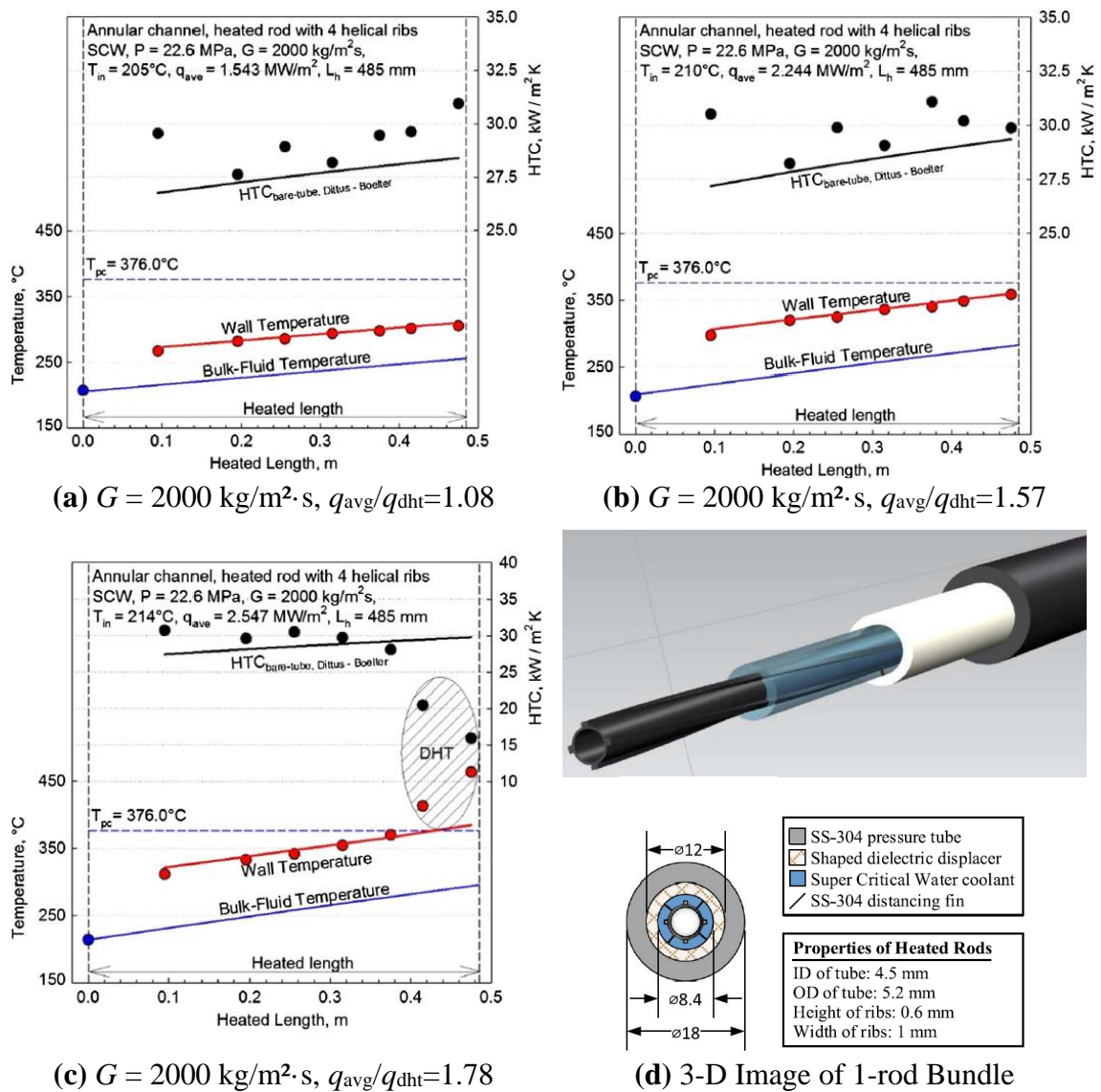


Figure 2-21: SCW 1-rod Experimental Results ($D_{hy} = 2.67 \text{ mm}$)
(courtesy of I.L. Pioro (Razumovskiy et al., 2015)) (Copyright of ASME)

2.5.6 3-rod Bundle Cooled with SCW

Razumovskiy et al. (2015) also analyzed a 3-rod bundle cooled with SCW experimental data from the National Technical University of Ukraine supercritical-test facility. This 3-rod is representative of a triangular pitch seen in the 37-element bundle.

In the 3-rod experiments, all three regimes of HT were observed (NHT/DHT/IHT). DHT was observed when $q_{avg}/q_{dht} \geq 1.64$. The mass flux and average HTC values in these trials were similar to the short bare tube results shown in section 2.5.4.

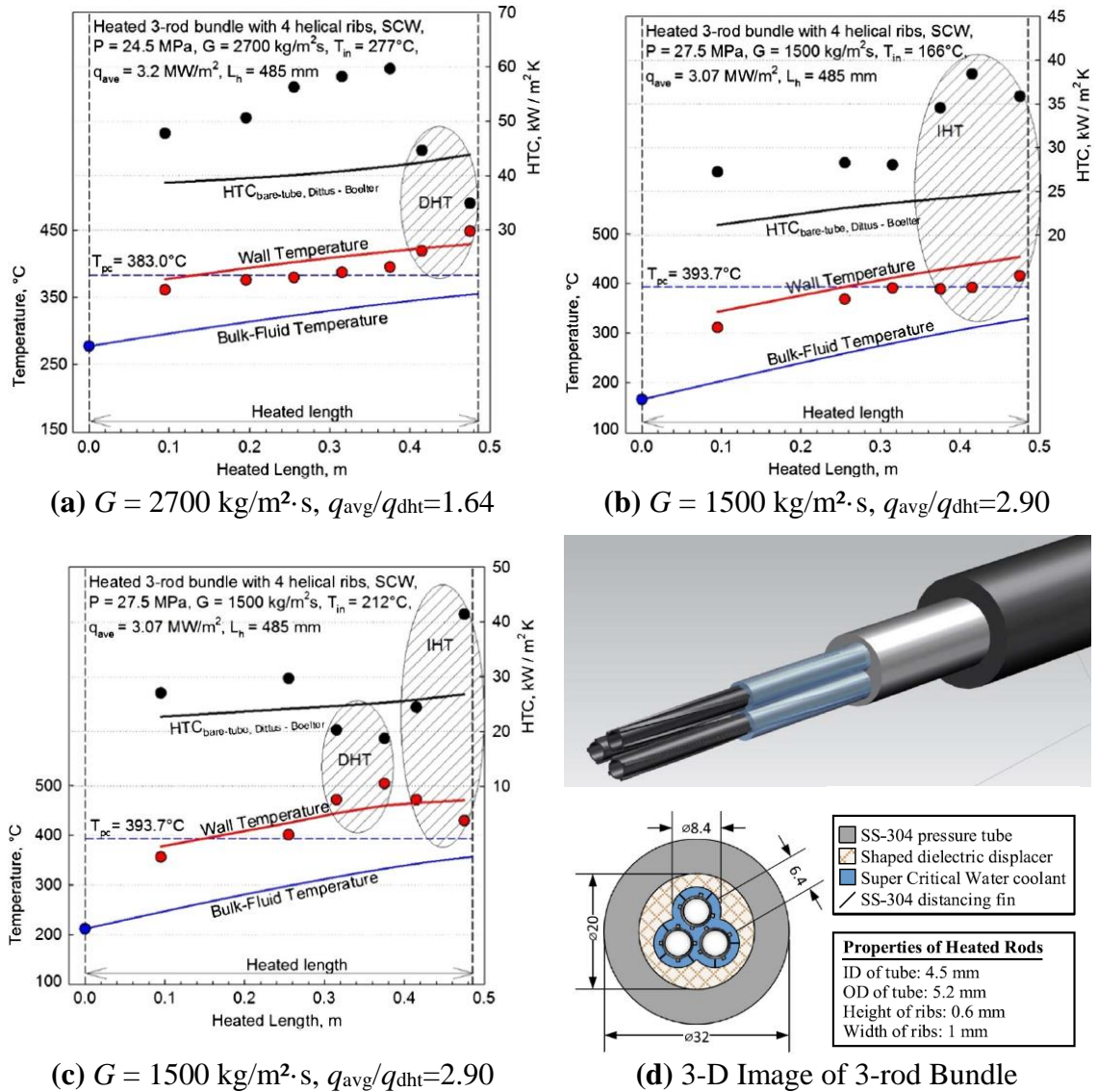


Figure 2-22: SCW 3-rod Experimental Results ($D_{hy} = 2.40 \text{ mm}$)
 (courtesy of I.L. Pioro (Razumovskiy et al., 2015)) (Copyright of ASME)

2.5.7 7-rod Bundle Cooled with SC R-12

Richards et al. (2013) analyzed experimental data for a 7-rod bundle cooled with SuperCritical (SC) Freon R-12 (F-R12) from the Institute for Physics and Power Engineering (IPPE) supercritical-test facility in Russia. This 7-rod is representative of the 7-rod internal pitch seen in the 37-element bundle.

In the 7-rod experiments, all three regimes of HT were observed (NHT/DHT/IHT). DHT was observed when $q_{avg}/q_{dht} \geq 0.008$. Thus, in a 7-rod bundle cooled with SC F-R12, all three regimes can occur.

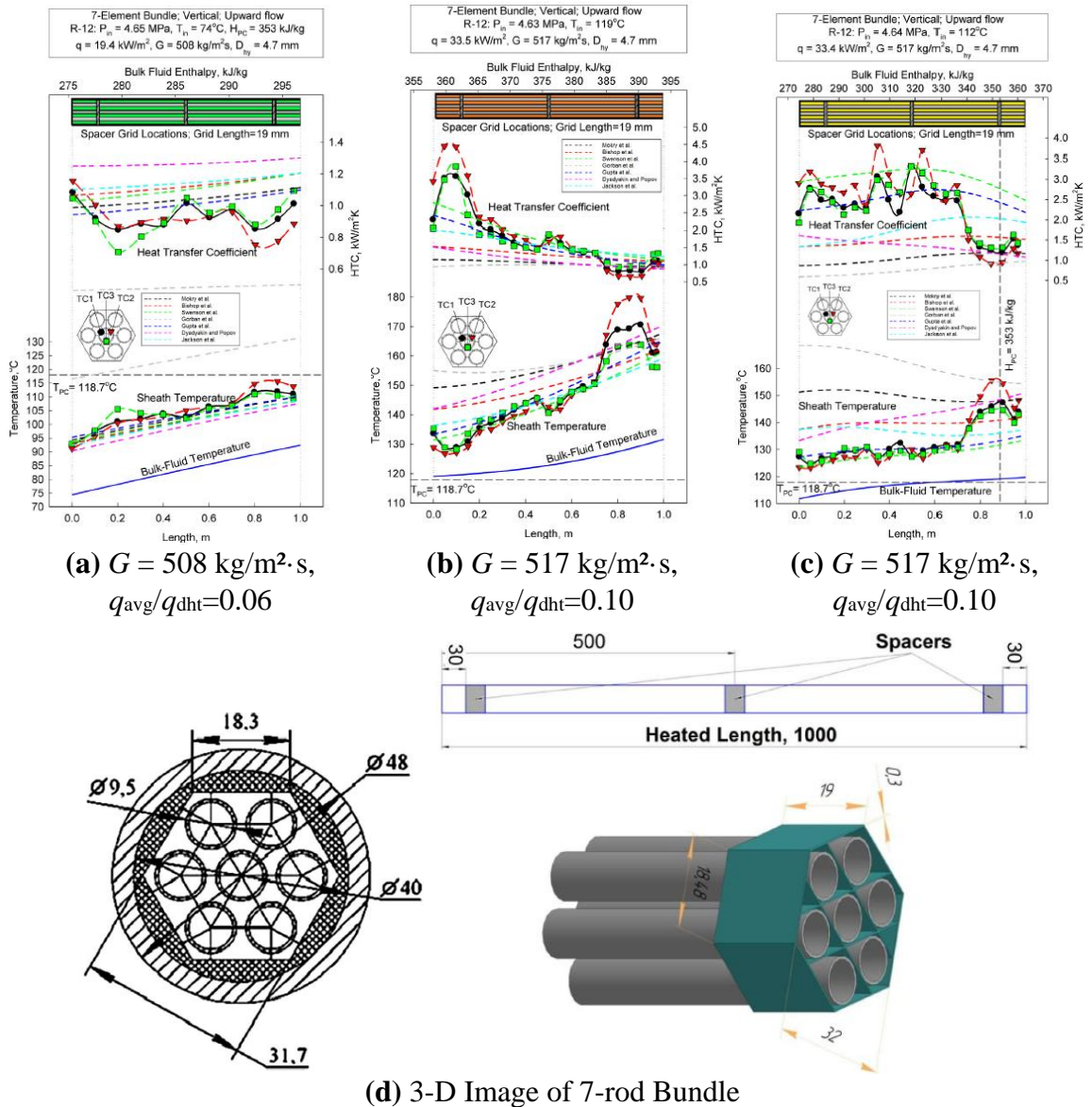


Figure 2-23: SC F-R12 7-rod Experimental Results (D_{hy} = not listed)
(courtesy of I.L. Pioro (Richards et al., 2013)) (Copyright of Elsevier)

2.5.8 7-rod Bundle Cooled with SCW

2.5.8.1 Dyadyakin and Popov (1977)

Dyadyakin and Popov (1977) conducted experiments for a 7-rod bundle, cooled with SCW. There were five bundle configurations tested (Table 2-5), for the parameters listed in Table 2-6. The rods were each 5.2 mm in diameter, with a total length of 0.5 m. Each rod had four helical fins of 0.6 mm in height and thickness of 1 mm. These helical fins were wrapped in a helical pitch (400 mm) around the rods. The PT was hexagonal in cross section. These 7-rod bundles are representative of the 7-rod internal pitch of the 37-element bundle.

Table 2-5: Dyadyakin and Popov 7-rod Bundle Configurations
(Dyadyakin & Popov, 1977)

Test Section #:	1	2	3	4	5
A_f (mm ²)	112	134	113	121	102
D_{hy} (mm)	2.35	2.77	2.38	2.53	2.15

Table 2-6: Dyadyakin and Popov 7-rod SCW Parameters
(Dyadyakin & Popov, 1977)

P MPa	T_b °C	H_b kJ/kg	q MW/m ²	G kg/m ² ·s
24.5	90–570	400–3400	<4.7	500–4000

Dyadyakin and Popov (1977) used their data to create the only **Nu** correlation for HTC based upon SCW in a bundle geometry configuration.

The results of their trials were not published in open literature, however Razumovskiy et al. (2008) reported that the Dyadyakin and Popov (1977) experiments did not experience any DHT regimes in their trials.

2.5.8.2 Razumovskiy et al. (2008)

Razumovskiy et al. (2008) also analyzed a 7-rod bundle cooled with SCW experimental data from the National Technical University of Ukraine supercritical-test facility. This 7-rod is representative of a centre rod and inner ring pitch seen in the 37-element bundle. This is the dataset that will become the focus of this assessment in later chapters.

In the 7-rod experiments, Razumovskiy et al. (2008) reported that two regimes were encountered (NHT/DHT) and the Dyadyakin and Popov (1977) Nu correlation fit the data the best. However, no evidence was provided or information listed, other than the wall temperature, T_w (exterior sheath temperature), plotted against the heated length.

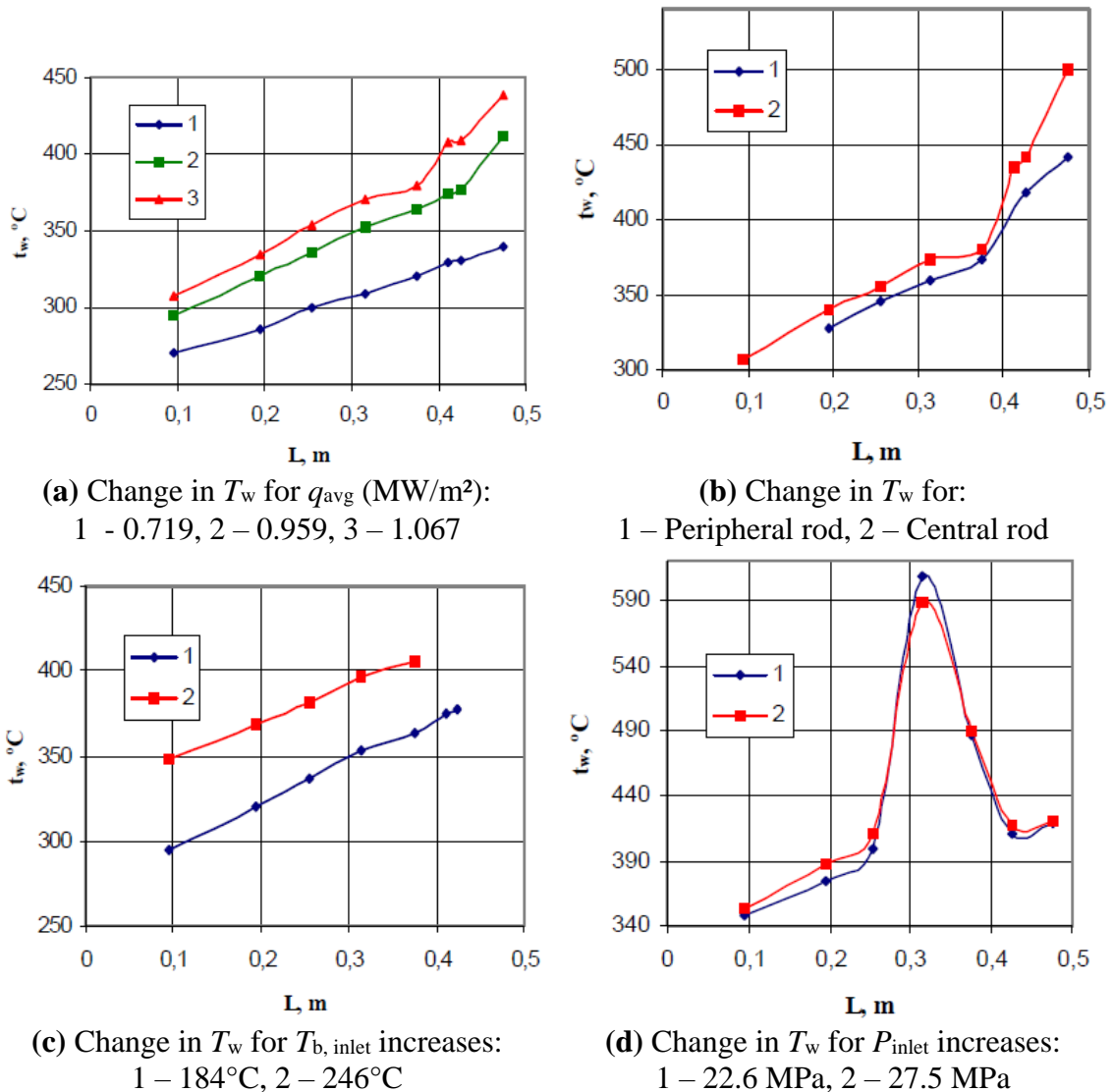


Figure 2-24: SCW 7-rod Experimental Results ($D_{hy} = 2.38/2.76$ mm)
(courtesy of I.L. Pioro (Razumovskiy et al., 2008)) (Copyright of ASME)

2.6 PREVIOUS Nu CORRELATIONS SUMMARY

Listed in Table 2-7 is a summary of common Heat Transfer Nu Correlations for determining turbulent flow inside tubes found in literature.

One important Nu correlation is that of Petukhov et al. (1961) Nu correlation Eq. (5), due to the introduction of the average specific heat, and average Prandtl number. As these parameters are used in the Nu correlations shown in this section to predict HTC and T_w , large spikes in values lead to erroneous predictions. By averaging out the specific heat and Prandtl number, these large peaks do not occur, as shown in Figure 2-25.

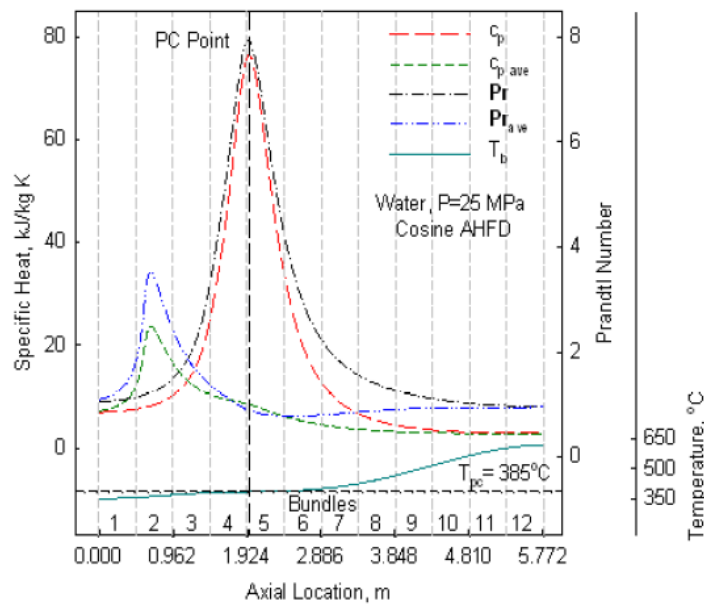


Figure 2-25: Effect of Average Specific Heat Capacity and Prandtl Number
(courtesy of I.L. Pioro (Mokry et al., 2009)) (Copyright of ASME)

Another important Nu correlation is that of Dyadyakin & Popov (1977) correlation Eq. (16). This is the only Nu correlation currently in literature that has been specifically developed for a bundle geometry test data (7-rod) cooled with SCW.

In addition, each Nu correlation is classified into three categories:

- 1) **Dittus-Boelter type**
 - Reynolds and Prandtl numbers only
- 2) **Dittus-Boelter type with modifier(s)**
 - Reynolds and Prandtl numbers, and non-dimensional modifiers
- 3) **Dittus-Boelter type with modifier(s) and buoyancy effects**
 - Reynolds, Prandtl, and Grashof numbers, and non-dimensional modifiers

Table 2-7: Heat Transfer Nu Correlations

	<p>Eq. (1)</p> <p>Nu_b = $0.023 \cdot \text{Re}_b^{0.8} \cdot \text{Pr}_b^n$ <i>where;</i> $n = 0.3$ for cooling, 0.4 for heating;</p> <p>Nu_b = Nusselt Number $= \frac{h \cdot L_C}{k_b}$ <i>h</i> = Heat Transfer Coefficient (HTC) $\left(\frac{\text{W}}{\text{m}^2 \cdot \text{K}}\right)$ <i>k</i> = Thermal Conductivity $\left(\frac{\text{W}}{\text{m} \cdot \text{K}}\right)$</p> <p>Re_b = Reynolds Number $= \frac{\rho_b \cdot V \cdot L_C}{\mu_b} = \frac{G \cdot D_{hy}}{\mu_b}$ <i>ρ</i> = Density (kg/m³) <i>V</i> = Velocity (m/s) <i>μ</i> = Dynamic Viscosity (Pa · s) <i>L_C</i> = Characteristic Length (m) <i>G</i> = Mass Flux $\left(\frac{\text{kg}}{\text{m}^2}\right)$</p> <p>Pr_b = Prandtl Number $= \frac{C_{p_b} \cdot \mu_b}{k_b}$ <i>D_{hy}</i> = Hydraulic Diameter (m) <i>C_p</i> = Specific Heat Capacity $\left(\frac{\text{J}}{\text{kg} \cdot \text{K}}\right)$</p>	<p>Eq. (2)</p> <p>Nu_D = $0.027 \cdot \text{Re}_b^{0.8} \cdot \text{Pr}_b^{1/3} \cdot \left(\frac{\mu_b}{\mu_w}\right)^{0.14}$</p>
<p>Dittus & Boelter (1930)</p> <p>Water, Oils, gases bare tubes Type 1</p>	<p>$0.6 \leq \text{Pr}_b \leq 160$ $10,000 \leq \text{Re}_b \leq 120,000$ $10 \leq \frac{L}{D}$</p>	<p>$0.7 \leq \text{Pr}_b \leq 16,700$ $10,000 \leq \text{Re}_b$ $D_{hy} = 19 \text{ mm}$ $10 \leq L/D$</p>
<p>Sieder & Tate (1936)</p> <p>Oils bare tube Type 2</p>		

Table 2-7: Heat Transfer Nu Correlations, continued

<p>Bringer & Smith (1957)</p> <p>Water, CO₂ bare tube Type 1</p>	<p>Eq. (3)</p> $\text{Nu}_z = C \cdot \text{Re}_z^{0.77} \cdot \text{Pr}_w^{0.55}$ <p>where; $C = 0.0266$ for water, 0.0375 for CO₂</p> $z = \begin{cases} T_b & E < 0 \\ T_{pc} & 0 \leq E \leq 1 \\ T_w & E > 1 \end{cases} \quad E = (T_{pc} - T_b)/(T_w - T_b)$	<p>CO₂</p> <p>$30,000 \leq \text{Re}_b \leq 300,000$ $P \text{ (MPa)} \approx 8.3$ $21 \leq T_b \text{ (}^\circ\text{C)} \leq 49$ $D_{hy} = 4.5 \text{ mm}$</p> <p>Water</p> <p>$P \text{ (MPa)} \approx 34.5$ $T_b \text{ (}^\circ\text{C)} \approx 482$ (within $\pm 15\%$)</p>
<p>Miropol'skiy & Shitsman (1957)</p> <p>Water bare tubes Type 1</p>	<p>Eq. (4)</p> $\text{Nu}_b = 0.023 \cdot \text{Re}_b^{0.8} \cdot \text{Pr}_{\min}^{0.8}$ <p>where; Pr_{\min} = the minimum of Pr_b and Pr_w</p>	<p>$0.4 \leq P \text{ (MPa)} \leq 27.4$ $T_b \text{ (}^\circ\text{C)} \leq 420$ $420 \leq q \text{ (kW/m}^2\text{)} \leq 8,400$ $170 \leq G \text{ (kg/m}^2 \cdot \text{s)} \leq 3,000$ $D_{hy} = 7.8, 8.2 \text{ mm}$ (within $\pm 15\%$)</p>
<p>Petukhov et al. (1961)</p> <p>Water & CO₂ bare tubes Type 2</p>	<p>Eq. (5)</p> $\text{Nu}_b = \text{Nu}_0 \cdot \left(\frac{\mu_b}{\mu_w}\right)^{0.11} \cdot \left(\frac{k_b}{k_w}\right)^{-0.33} \cdot \left(\frac{\bar{C}_p}{C_{pb}}\right)^{0.35}$ <p>where; $\text{Nu}_0 = \frac{(f_f/8) \cdot \text{Re}_b \cdot \bar{\text{Pr}}_b}{12.7 \sqrt{f_f/8} \cdot (\bar{\text{Pr}}_b^{2/3} - 1) + 1.07}$</p> <p>$f_f = (1.82 \cdot \log_{10} \text{Re}_b - 1.64)^{-2}$, $\bar{\text{Pr}}_b = \bar{C}_p \cdot \frac{\mu_b}{k_b}$, $\bar{C}_p = \frac{H_w - H_b}{T_w - T_b}$</p>	<p>$0.85 \leq \text{Pr}_b \leq 65$ $20,000 \leq \text{Re}_b \leq 860,000$ $22.3 \leq P \text{ (MPa)} \leq 32.0$ $0.9 \leq \mu_w/\mu_b \leq 3.6$ $1.0 \leq k_w/k_b \leq 6.0$ $0.07 \leq \bar{C}_p/C_{pb} \leq 4.5$ (within $\pm 15\%$)</p>

Table 2-7: Heat Transfer Nu Correlations, continued

<p>Domin (1963)</p> <p>Water bare tube Type 1 & 2</p>	$\text{Nu}_b = \begin{cases} 0.1 \cdot \text{Re}_b^{0.66} \cdot \overline{\text{Pr}}_b^{-1.2} & \text{Case 1} \\ 0.036 \cdot \text{Re}_b^{0.8} \cdot \overline{\text{Pr}}_b^{-0.4} \cdot \left(\frac{\mu_w}{\mu_b}\right) & \text{Case 2} \end{cases}$ <p>where; Case 1 = $T_w \geq 350^\circ\text{C}$ Case 2 = $250 < T_w < 350^\circ\text{C}$</p>	<p>Eq. (6)</p>	$22 \leq P \text{ (MPa)} \leq 26$ $600 \leq G \text{ (kg/m}^2 \cdot \text{s)} \leq 5,100$ $580 \leq q \text{ (kW/m}^2\text{)} \leq 4,500$ $D_{\text{hy}} = 2.0, 4.0 \text{ mm}$ <p>(within $\pm 20\%$)</p>
<p>Bishop et al. (1964)</p> <p>Water bare tube, Whistled Circular Tubes, Annular Channels Type 2</p>	$\text{Nu}_b = 0.0069 \cdot \text{Re}_b^{0.9} \cdot \overline{\text{Pr}}_b^{0.66} \cdot \left(\frac{\rho_w}{\rho_b}\right)^{0.43} \cdot \left(1 + 2.4 \frac{D}{x}\right)$	<p>Eq. (7)</p>	$22.8 \leq P \text{ (MPa)} \leq 27.6$ $651 \leq G \text{ (kg/m}^2 \cdot \text{s)} \leq 3,662$ $310 \leq q \text{ (kW/m}^2\text{)} \leq 3,460$ $282 \leq T_b \text{ (}^\circ\text{C)} \leq 527$ $2.5 \leq D_{\text{hy}} \text{ (mm)} \leq 5.1$ $30 \leq L/D \leq 565$ <p>(within $\pm 15\%$)</p>
<p>Swenson et al. (1965)</p> <p>Water bare tubes Type 2</p>	$\text{Nu}_w = 0.0459 \cdot \text{Re}_w^{0.923} \cdot \overline{\text{Pr}}_w^{0.613} \cdot \left(\frac{\rho_w}{\rho_b}\right)^{0.231}$ <p>where; $\overline{\text{Pr}}_w = \overline{C}_p \cdot \frac{\mu_w}{k_w}$</p>	<p>Eq. (8)</p>	$75,000 \leq \text{Re}_b \leq 3,160,000$ $22.8 \leq P \text{ (MPa)} \leq 41.4$ $542 \leq G \text{ (kg/m}^2 \cdot \text{s)} \leq 2,150$ $200 \leq q \text{ (kW/m}^2\text{)} \leq 1,800$ $75 \leq T_b \text{ (}^\circ\text{C)} \leq 576$ $93 \leq T_w \text{ (}^\circ\text{C)} \leq 649$ $D_{\text{hy}} \text{ (mm)} = 9.4$ <p>(within $\pm 15\%$)</p>

Table 2-7: Heat Transfer Nu Correlations, continued

<p>Krasnoshchekov et al. (1967)</p> <p>Water & CO₂ bare tubes Type 2</p>	$\mathbf{Nu}_b = \mathbf{Nu}_0 \cdot \left(\frac{\rho_w}{\rho_b} \right)^{0.3} \cdot \left(\frac{C_p}{C_{pb}} \right)^n$ <p>where;</p> $n = \begin{cases} 0.4 & \frac{T_w}{T_{pc}} \leq 1 \text{ OR } \frac{T_b}{T_{pc}} \geq 1.2 \\ x = 0.22 + 0.18 \cdot \frac{T_w}{T_{pc}} & 1 \leq \frac{T_w}{T_{pc}} \leq 2.5 \\ x + (5 \cdot x - 2) \left(1 - \frac{T_b}{T_{pc}} \right) & 1 \leq \frac{T_b}{T_{pc}} \leq 1.2 \end{cases}, T \text{ in K}$	<p>Eq. (9)</p>	<p>$0.85 \leq \mathbf{Pr}_{avg} \leq 65$ $80,000 \leq \mathbf{Re}_b \leq 500,000$ $22.5 \leq P \text{ (MPa)} \leq 26.5$ $460 \leq q \text{ (kW/m}^2\text{)} \leq 2,600$ $1.6 \leq D_{hy} \text{ (mm)} \leq 20$ $0.09 \leq \rho_w/\rho_b \leq 65$ $0.9 \leq T_w/T_{pc} \leq 2.5$ $0.02 \leq Cp_{avg}/Cp_b \leq 4.0$ (within $\pm 20\%$)</p>
<p>Ornatsky et al. (1970)</p> <p>Water bare tubes Type 2</p>	$\mathbf{Nu}_b = 0.023 \cdot \mathbf{Re}_b^{0.8} \cdot \mathbf{Pr}_{min}^{0.8} \cdot \left(\frac{\rho_w}{\rho_b} \right)^{0.3}$	<p>Eq. (10)</p>	<p>$22.6 \leq P \text{ (MPa)} \leq 29.7$ $450 \leq G \text{ (kg/m}^2 \cdot \text{s)} \leq 3,000$ $400 \leq q \text{ (kW/m}^2\text{)} \leq 1,810$ $3 = D_{hy} \text{ (mm)}$ (within $\pm 15\%$)</p>
<p>Giarratano et al. (1971)</p> <p>Helium bare tube Type 2</p>	$\mathbf{Nu}_b = 0.0259 \cdot \mathbf{Re}_b^{0.8} \cdot \mathbf{Pr}_b^{0.4} \cdot \left(\frac{T_w}{T_b} \right)^{-0.716}, \quad T \text{ in K}$	<p>Eq. (11)</p>	<p>Developed for Helium</p>

Table 2-7: Heat Transfer Nu Correlations, continued

<p>Yamagata et al. (1972)</p> <p>Water bare tubes Type 2</p>	$\mathbf{Nu}_b = 0.0135 \cdot \mathbf{Re}_b^{0.85} \cdot \mathbf{Pr}_b^{0.8} \cdot F_c$ <p>where;</p> $F_c = \begin{cases} 1.0 & E > 1 \\ 0.67 \cdot \mathbf{Pr}_{pc}^{-0.05} \cdot \left(\frac{\bar{C}_p}{\bar{C}_{pb}}\right)^{n_1} & 0 \leq E \leq 1 \\ \left(\frac{\bar{C}_p}{\bar{C}_{pb}}\right)^{n_2} & E < 0 \end{cases}$ $n_1 = 1.49 - 0.77 \cdot (1 + 1/\mathbf{Pr}_{pc}); \quad n_2 = 1.44 \cdot (1 + 1/\mathbf{Pr}_{pc}) - 0.53$	<p>Eq. (12)</p> <p>22.6 ≤ P (MPa) ≤ 29.4 310 ≤ G (kg/m² · s) ≤ 1,830 116 ≤ q (kW/m²) ≤ 930 230 ≤ T_b (°C) ≤ 540 7.5, 10 = D_{hy} (mm) (within ± 20%)</p>
<p>Zukauskas (1972)</p> <p>Various fluids bare tubes Type 2</p>	$\mathbf{Nu}_b = C \cdot \mathbf{Re}_b^m \cdot \mathbf{Pr}_b^n \cdot \left(\frac{\mathbf{Pr}_b}{\mathbf{Pr}_w}\right)^{0.25}$ <p>where;</p> <p>if $\mathbf{Pr}_b \lesssim 10$, $n = 0.37$ if $\mathbf{Pr}_b > 10$, $n = 0.36$ $1 \leq \mathbf{Re}_b \leq 40$, $C = 0.75$, $m = 0.4$ $40 \leq \mathbf{Re}_b \leq 1000$, $C = 0.51$, $m = 0.5$ $1000 \leq \mathbf{Re}_b \leq 2 \times 10^5$, $C = 0.26$, $m = 0.6$ $2 \times 10^5 \leq \mathbf{Re}_b \leq 10^6$, $C = 0.076$, $m = 0.7$</p>	<p>0.71 ≤ Pr_b ≤ 112 10,000 ≤ Re_b ≤ 1,000,000</p>
<p>Jackson & Fewster (1975)</p> <p>Water bare tube Type 2</p>	$\mathbf{Nu}_b = 0.0183 \cdot \mathbf{Re}_b^{0.82} \cdot \mathbf{Pr}_b^{-0.5} \cdot \left(\frac{\rho_w}{\rho_b}\right)^{0.3}$	<p>Eq. (14)</p> <p>113,000 = Re_b 6.5 ≤ P (MPa) ≤ 7.58 0 ≤ q (kW/m²) ≤ 56.9 19 = D_{hy} (mm) (within ± 15%)</p>

Table 2-7: Heat Transfer Nu Correlations, continued

<p>Gnielinski (1976)</p> <p>Various Fluids bare tubes Type 2</p>	$\text{Nu}_b = \frac{(f_p/8) \cdot (\text{Re}_b - 1000) \cdot \text{Pr}_b}{1 + 12.7 \sqrt{f_p/8} \cdot (\text{Pr}_b^{2/3} - 1)}$ <p>where; $f_p = (0.790 \cdot \ln \text{Re}_b - 1.64)^{-2}$</p>	<p>Eq. (15)</p>	$0.5 \leq \text{Pr}_b \leq 2000$ $3,000 \leq \text{Re}_b \leq 5,000,000$
<p>Dyadyakin & Popov (1977)</p> <p>Water 7-rod Bundle Type 2</p>	$\text{Nu}_b = 0.021 \cdot \text{Re}_b^{0.8} \cdot \overline{\text{Pr}_b}^{-0.7} \cdot F \cdot \left(1 + 2.5 \cdot \frac{D_{\text{hy}}}{x}\right)$ <p>where; $F = \left(\frac{\rho_w}{\rho_b}\right)^{0.45} \cdot \left(\frac{\mu_b}{\mu_{\text{in}}}\right)^{0.2} \cdot \left(\frac{\rho_b}{\rho_{\text{in}}}\right)^{0.1}$</p> <p style="text-align: center;">$x = \text{distance along heated length (m)}$</p>	<p>Eq. (16)</p>	$24.5 = P \text{ (MPa)}$ $500 \leq G \text{ (kg/m}^2 \cdot \text{s)} \leq 4,000$ $q \text{ (kW/m}^2) \leq 4700$ $90 \leq T_b \text{ (}^\circ\text{C)} \leq 570$ $5.2 = D_{\text{hy}} \text{ (mm)}$ $(\text{within } \pm 20\%)$
<p>Watts & Chou (1982)</p> <p>Water bare tubes Type 3</p>	$\text{Nu}_b = \begin{cases} \text{Nu}_1 \cdot [1 - 3000 \cdot \gamma]^{0.295} & \gamma < 10^{-4} \\ \text{Nu}_1 \cdot [7000 \cdot \gamma]^{0.295} & \gamma > 10^{-4} \end{cases}$ <p>where; $\text{Nu}_1 = 0.021 \cdot \text{Re}_b^{0.8} \cdot \overline{\text{Pr}_b}^{-0.55} \cdot \left(\frac{\rho_w}{\rho_b}\right)^{0.35}$, $\gamma = \frac{\overline{\text{Gr}_b}}{\text{Re}_b^{2.7} \cdot \text{Pr}_b^{-0.5}}$</p> $\overline{\text{Gr}_b} = \frac{(\rho_b - \bar{\rho}) \cdot g \cdot D^3}{\rho_b \cdot \nu_b^2}, \quad \bar{\rho} = \frac{1}{T_w - T_b} \cdot \int_{T_b}^{T_w} \rho(T) \cdot dT$	<p>Eq. (17)</p>	$0.85 \leq \text{Pr}_b \leq 2.30$ $6,500 \leq \text{Re}_b \leq 300,000$ $25.0 = P \text{ (MPa)}$ $130 \leq G \text{ (kg/m}^2 \cdot \text{s)} \leq 1,000$ $170 \leq q \text{ (kW/m}^2) \leq 450$ $150 \leq T_b \text{ (}^\circ\text{C)} \leq 350$ $(\text{within } \pm 20\%)$

Table 2-7: Heat Transfer Nu Correlations, continued

<p>Petukhov, et al. (1983)</p> <p>Water, CO₂, He bare tubes Type 2</p>	$\text{Nu}_b = \frac{(\xi/8)}{12.7\sqrt{\xi/8} \cdot (\text{Pr}_b^{2/3} - 1) + 1 + \text{Re}_b} \cdot \text{Re}_b \cdot \text{Pr}_b$ <p>Eq. (18)</p> <p>where;</p> $\xi = \frac{1}{(1.82 \cdot \log \text{Re}_b - 1.64)^2} \cdot \left(\frac{\rho_w}{\rho_b}\right)^{0.4} \cdot \left(\frac{\mu_w}{\mu_b}\right)^{0.2}$	<p>7.7 ≤ P (MPa) ≤ 8.9 1,000 ≤ G (kg/m² · s) ≤ 4,100 384 ≤ q (kW/m²) ≤ 1,053 (within ± 15%)</p>
<p>Gorban et al. (1990)</p> <p>Freon-12 bare tubes Type 1</p>	$\text{Nu}_b = 0.0059 \cdot \text{Re}_b^{0.9} \cdot \text{Pr}_b^{-0.12}$ <p>Eq. (19)</p>	<p>Developed for Freon-12</p>

Table 2-7: Heat Transfer Nu Correlations, continued

<p>Griem (1996)</p> <p>Water bare tube Type 1</p>	<p>Nu_G = 0.0169 · Re_b^{0.8356} · Pr_{b,G}^{0.432} · φ Eq. (20)</p> <p>where;</p> $\mathbf{Pr}_{b,G} = \frac{C_{p,G} \cdot \mu_b}{k_G}, \quad k_G = \frac{k_b + k_w}{2}, \quad C_{p_G} = \frac{C_{p_{Max,1}} + C_{p_{Max,2}} + C_{p_{AVG}}}{3}$ <p>$C_{p_{Max,1}}$ = greatest value of $C_{p_b}, C_{p_{bf}}, C_{p_f}, C_{p_{fw}}, C_{p_w}$</p> <p>$C_{p_{Max,2}}$ = second greatest value of $C_{p_b}, C_{p_{bf}}, C_{p_f}, C_{p_{fw}}, C_{p_w}$</p> <p>$C_{p_{avg}}$ = average of remaining three values of $C_{p_b}, C_{p_{bf}}, C_{p_f}, C_{p_{fw}}, C_{p_w}$</p> <p>$C_{p_{bf}}$ = value of C_p at T_{bf}, $T_{bf} = \frac{T_b + T_f}{2}$</p> <p>$C_{p_{fw}}$ = value of C_p at T_{fw}, $T_{fw} = \frac{T_f + T_w}{2}$</p> <p>if $H_b > 1740 \frac{kJ}{kg}$, $\phi = 1$, if $H_b < 1540 \frac{kJ}{kg}$, $\phi = 0.82$</p> <p>if $1540 < H_b < 1740 \frac{kJ}{kg}$, $\phi = 0.0009 \cdot H_b - 0.566$</p> $HTC = \frac{Nu_G \cdot k_G}{D}$	<p>22.0 ≤ P (MPa) ≤ 27.0</p> <p>300 ≤ G (kg/m² · s) ≤ 2,500</p> <p>200 ≤ q (kW/m²) ≤ 700</p> <p>D_{hy} = 10, 14, 20 mm</p> <p>(within ± 20%)</p>
---	--	--

Table 2-7: Heat Transfer Nu Correlations, continued

<p>Hu (2001)</p> <p>Water bare tubes Type 2</p>	$\mathbf{Nu_b} = 0.0068 \cdot \mathbf{Re_b^{0.9}} \cdot \mathbf{Pr_b^{-0.63}} \cdot \left(\frac{\rho_w}{\rho_b}\right)^{0.17} \cdot \left(\frac{k_w}{k_b}\right)^{0.29}$ <p>Eq. (21)</p>	$23.0 \leq P \text{ (MPa)} \leq 30.0$ $300 \leq G \text{ (kg/m}^2 \cdot \text{s)} \leq 900$ $100 \leq q \text{ (kW/m}^2\text{)} \leq 400$ <p>(within $\pm 20\%$)</p>
<p>Kitoh et al. (2001)</p> <p>Water Numerical Simulation in bare tubes Type 1</p>	$\mathbf{Nu_b} = 0.15 \cdot \mathbf{Re_b^{0.85}} \cdot \mathbf{Pr_b^n}$ <p>where; $n = 0.69 - 81000/q_{\text{det}} + F_c \cdot q$</p> $F_c = \begin{cases} 2.9 \times 10^{-8} + 0.11/q_{\text{det}} & 0 \leq H_b < 1.5 \text{ MJ/kg} \\ -8.7 \times 10^{-8} - 0.65/q_{\text{det}} & 1.5 \leq H_b < 3.3 \text{ MJ/kg} \\ -9.7 \times 10^{-7} + 1.30/q_{\text{det}} & 3.3 \leq H_b < 4 \text{ MJ/kg} \end{cases}$ <p>$q_{\text{det}} = 200 \cdot G^{1.2} = \text{deteriorated heat flux (W/m}^2\text{)}$ $G = \text{mass flux (kg/m}^2 \cdot \text{s)}, \quad q = \text{heat flux (W/m}^2\text{)}$</p> <p>Eq. (22)</p>	$100 \leq G \text{ (kg/m}^2 \cdot \text{s)} \leq 1,750$ $0 \leq q \text{ (kW/m}^2\text{)} \leq 1,800$ $20 \leq T_b \text{ (}^\circ\text{C)} \leq 550$ <p>(within $\pm 15\%$)</p>

Table 2-7: Heat Transfer Nu Correlations, continued

<p>Jackson (2002)</p> <p>Water and CO₂ bare tubes Type 2</p>	<p>Eq. (23)</p> $\text{Nu}_b = 0.0183 \cdot \text{Re}_b^{0.82} \cdot \text{Pr}_b^{0.5} \cdot \left(\frac{\rho_w}{\rho_b}\right)^{0.3} \cdot \left(\frac{\bar{C}_p}{C_{pb}}\right)^n$ <p>where;</p> $n = \begin{cases} 0.4 & T_b < T_w < T_{pc} \text{ or } 1.2T_{pc} \leq T_b < T_w \\ 0.4 + 0.2 \left(\frac{T_w}{T_{pc}} - 1\right) & T_b < T_{pc} \leq T_w \\ 0.4 + 0.2 \left(\frac{T_w}{T_{pc}} - 1\right) \left[1 - 5 \left(\frac{T_w}{T_{pc}} - 1\right)\right] & T_{pc} < T_b \leq 1.2T_{pc} \text{ and } T_b < T_w \end{cases}, T \text{ in K}$	<p>80,000 ≤ Re_b ≤ 500,000 23.4 ≤ P (MPa) ≤ 29.3 700 ≤ G (kg/m² · s) ≤ 3,600 46 ≤ q (kW/m²) ≤ 2,600 1.6 ≤ D_{hy} (mm) ≤ 20 (within ± 20%)</p>
<p>Xu & Guo (2005)</p> <p>Water bare tubes Type 2</p>	<p>Eq. (24)</p> $\text{Nu}_b = 0.02269 \cdot \text{Re}_b^{0.8079} \cdot \overline{\text{Pr}}_b^{-0.9213} \cdot F$ <p>where;</p> $F = \left(\frac{\mu_w}{\mu_b}\right)^{0.8687} \cdot \left(\frac{\rho_w}{\rho_b}\right)^{0.6638}$	<p>23.0 ≤ P (MPa) ≤ 30.0 600 ≤ G (kg/m² · s) ≤ 1,200 100 ≤ q (kW/m²) ≤ 600 12.0 = D_{hy} (mm) (within ± 20%)</p>
<p>Kuang et al. (2008)</p> <p>Water bare tubes (ducts) Type 3</p>	<p>Eq. (25)</p> $\text{Nu}_b = 0.0239 \cdot \text{Re}_b^{0.759} \cdot \overline{\text{Pr}}_b^{0.833} \cdot F \cdot (\text{Gr}^*)^{0.014} (q^+)^{-0.021}$ <p>where;</p> $F = \left(\frac{\rho_w}{\rho_b}\right)^{0.31} \left(\frac{k_w}{k_b}\right)^{0.0863} \left(\frac{\mu_w}{\mu_b}\right)^{0.832}$ $\text{Gr}^* = \frac{g\beta D^4 q}{k\nu^2} \quad g = \text{gravity (m/s}^2\text{)}$ $q^+ = \frac{q\beta}{GC_p} \quad \beta = \text{Thermal Expansivity (1/K)}$ <p>Gr = Grashof number q^+ = non – dimensional heat flux</p>	<p>22.8 ≤ P (MPa) ≤ 31.0 380 ≤ G (kg/m² · s) ≤ 3,600 233 ≤ q $\left(\frac{kW}{m^2}\right)$ ≤ 3,474 (within ± 30%)</p>

Table 2-7: Heat Transfer Nu Correlations, continued

Yu et al. (2009) Water bare tubes Type 3	$\mathbf{Nu}_b = 0.01378 \mathbf{Re}_b^{0.9078} \overline{\mathbf{Pr}}_b^{-0.6171} F(\mathbf{Gr}^*)^{-0.012} (q^+)^{-0.0605}$ <p>where; $F = \left(\frac{\rho_w}{\rho_b} \right)^{0.4356}$</p>	Eq. (26)	$22.6 \leq P \text{ (MPa)} \leq 41.0$ $90 \leq G \text{ (kg/m}^2 \cdot \text{s)} \leq 2,441$ $90 \leq q \text{ (kW/m}^2\text{)} \leq 1,800$ $1.5 \leq D_{hy} \text{ (mm)} \leq 38.1$ <p>(within $\pm 30\%$)</p>
Cheng et al. (2009) Water bare tubes Type 2	$\mathbf{Nu}_b = 0.023 \cdot \mathbf{Re}_b^{0.8} \cdot \overline{\mathbf{Pr}}_b^{-1/3} \cdot F$ <p>where; $F = \min(F_1, F_2)$,</p> $F_1 = 0.85 + 0.776 \cdot (\pi_A \cdot 10^3)^{2.4}, \quad \pi_A = \frac{\beta_b}{C_{Pb}} \cdot \frac{q}{G},$ $F_2 = \frac{0.48}{(\pi_{A,PC} \cdot 10^3)^{1.55}} + 1.21 \cdot \left(1 - \frac{\pi_A}{\pi_{A,PC}} \right), \quad \pi_{A,PC} = \frac{\beta_{pc}}{C_{Ppc}} \cdot \frac{q}{G}$	Eq. (27)	$22.5 \leq P \text{ (MPa)} \leq 25$ $700 \leq G \text{ (kg/m}^2 \cdot \text{s)} \leq 3500$ $300 \leq q \text{ (kW/m}^2\text{)} \leq 2000$ $300 \leq T_b \text{ (}^\circ\text{C)} \leq 450$ $D_{hy} \text{ (mm)} = 10, 20$ <p>(within $\pm 30\%$)</p>
Mokry et al. (2009) Water bare tubes Type 2	$\mathbf{Nu}_b = 0.0061 \cdot \mathbf{Re}_b^{0.904} \cdot \overline{\mathbf{Pr}}_b^{-0.684} \cdot \left(\frac{\rho_w}{\rho_b} \right)^{0.564}$	Eq. (28)	$24.0 \approx P \text{ (MPa)}$ $200 \leq G \text{ (kg/m}^2 \cdot \text{s)} \leq 1,500$ $0 \leq q \text{ (kW/m}^2\text{)} \leq 729$ <p>(within $\pm 15\%$)</p>
Gupta et al. (2011) Water bare tubes Type 2	$\mathbf{Nu}_w = 0.0033 \cdot \mathbf{Re}_w^{0.94} \cdot \overline{\mathbf{Pr}}_w^{-0.76} \cdot \left(\frac{\rho_w}{\rho_b} \right)^{0.16} \cdot \left(\frac{\mu_w}{\mu_b} \right)^{0.4}$	Eq. (29)	$24.0 \approx P \text{ (MPa)}$ $200 \leq G \text{ (kg/m}^2 \cdot \text{s)} \leq 1,500$ $70 \leq q \text{ (kW/m}^2\text{)} \leq 1,250$ $320 \leq T_b \text{ (}^\circ\text{C)} \leq 350$ $320 \leq T_w \text{ (}^\circ\text{C)} \leq 350$ <p>(within $\pm 15\%$)</p>

Table 2-7: Heat Transfer Nu Correlations, continued

<p>Gupta et al. (2013)</p> <p>CO₂ bare tubes Type 2</p>	$\text{Nu}_b = 0.01 \cdot \text{Re}_b^{0.89} \cdot \overline{\text{Pr}}_b^{-0.14} \cdot F$ <p>where; $F = \left(\frac{\rho_w}{\rho_b}\right)^{0.93} \cdot \left(\frac{k_w}{k_b}\right)^{0.22} \cdot \left(\frac{\mu_w}{\mu_b}\right)^{-1.13}$</p> $\text{Nu}_w = 0.0038 \cdot \text{Re}_w^{0.96} \cdot \overline{\text{Pr}}_w^{-0.14} \cdot F$ <p>where; $F = \left(\frac{\rho_w}{\rho_b}\right)^{0.84} \cdot \left(\frac{k_w}{k_b}\right)^{-0.75} \cdot \left(\frac{\mu_w}{\mu_b}\right)^{-0.22}$</p> $\text{Nu}_f = 0.0043 \cdot \text{Re}_f^{0.94} \cdot \left(\frac{\rho_w}{\rho_b}\right)^{0.57} \cdot \left(\frac{k_w}{k_b}\right)^{-0.52}$ <p>Eq. (30)</p> <p>Eq. (31)</p> <p>Eq. (32)</p>	<p>Developed for sCO₂</p>
<p>Chen & Fang (2014)</p> <p>Water bare tubes Type 3</p>	$\text{Nu}_b = 0.46 \cdot \text{Re}_b^{0.16} \cdot F \cdot \left(\frac{\overline{C}_p}{C_{p,b}}\right)^{0.88} \cdot \left(\frac{\text{Gr}_b^*}{\text{Gr}_b}\right)^{0.81}$ <p>where;</p> $F = \left(\frac{\text{Pr}_w}{\text{Pr}_b}\right)^{0.1} \cdot \left(\frac{\nu_w}{\nu_b}\right)^{-0.55}, \quad \text{Gr}_b = \frac{(\rho_b - \rho_w) \cdot g \cdot D^3}{\rho_b \cdot \nu_b^2}$ <p>Eq. (33)</p>	<p>22.0 ≤ P (MPa) ≤ 34.3 100 ≤ G (kg/m² · s) ≤ 3600 129 ≤ q $\left(\frac{\text{kW}}{\text{m}^2}\right)$ ≤ 1,735 7.5 ≤ D_{hy} (mm) ≤ 26.0 (within ± 30%)</p>
<p>Wang & Li (2014)</p> <p>Water bare tubes Type 2</p>	$\text{Nu}_b = 0.00684 \cdot \text{Re}_b^{0.89765} \cdot \overline{\text{Pr}}_b^{0.68625} \cdot F$ <p>where; $F = \left(\frac{\rho_w}{\rho_b}\right)^{0.31142} \cdot \left(\frac{k_w}{k_b}\right)^{0.26185}$</p> <p>Eq. (34)</p>	<p>0.4 ≤ P (MPa) ≤ 41.3 201 ≤ G (kg/m² · s) ≤ 2,500 q $\left(\frac{\text{kW}}{\text{m}^2}\right)$ ≤ 8400 2.5 ≤ D_{hy} (mm) ≤ 26.0 (within ± 20%)</p>

Table 2-7: Heat Transfer Nu Correlations, continued

Lei et al. (2019) Water bare tubes Type 2	$\mathbf{Nu_b} = 0.00728 \cdot \mathbf{Re_b^{0.891}} \cdot \mathbf{Pr_b^{0.6}} \cdot \left(\frac{\rho_w}{\rho_b} \right)^{0.49}$ Eq. (35)	$0.57 \leq \mathbf{Pr_b} \leq 8.5$ $4,270 \leq \mathbf{Re_b} \leq 7,400,000$ $0.09 \leq \rho_w / \rho_b \leq 0.93$
---	--	--

2.7 PREVIOUS ASSESSMENT STUDIES

Previously several authors have analyzed various **Nu** correlations with a wide range of conclusions:

Zahlan et al. (2011), compiled an exhaustive water dataset from over 40 authors consisting of over 36,000 data points, and reduced to just over 24,000 after removing unreliable data and outliers ($P = 22.3$ to 34.5 MPa, $G = 90$ to 5000 kg/m²·s, $q_{avg} = 72$ to 5457 kW/m², $T_b = 17$ to 564°C , I.D. = 2 to 38 mm, bare tubes and other geometries).

Zahlan et al. (2011) compared 16 different **Nu** correlations, 14 of which are considered in this thesis:

Eq. (1)	Dittus-Boelter (1930)	Eq. (17)	Watts and Chou (1982)
Eq. (2)	Sieder and Tate (1936)	Eq. (20)	Griem (1996)
Eq. (7)	Bishop et al. (1964)	Eq. (22)	Kitoh et al. (2001)
Eq. (8)	Swenson et al. (1965)	Eq. (23)	Jackson (2002)
Eq. (9)	Krasnoshchekov et al. (1967)	Eq. (25)	Kuang et al. (2008)
Eq. (12)	Yamagata et al. (1972)	Eq. (28)	Mokry et al. (2009)
Eq. (15)	Gnielinski (1976)	Eq. (29)	Gupta et al. (2011)

Zahlan et al. (2011) compared data in three regions, liquid-like, gas-like, and close to the critical or pc point. The conclusion was the Mokry et al. (2009) correlation Eq. (28) was the most accurate predictor of HTC by Root Mean Square (RMS) error method for all regions, while the Gupta et al. (2011) correlation Eq. (29), Bishop et al. (1964) correlation Eq. (7), Swenson et al. (1965) correlation Eq. (8), and the Watts and Chou (1982) correlation Eq. (17) were also accurate across the three phases. These findings were reported by the IAEA in 2014 as part of TECDOC-1746 (IAEA, 2014).

Jäger et al. (2011) used the datasets from six experiments with water to validate the newly inputted routines into the TRAC/RELAP Advanced Computational Engine (TRACE) computer simulation program. The TRACE program is the Nuclear Regulatory Commission (NRC) flagship thermal-hydraulics analysis tool. It was originally developed for LWR, but was recognized to have invalid parameters for the supercritical region. The

six experiments used for the datasets are for supercritical water ($P = 22.6$ to 31 MPa, $G = 500$ to 2150 kg/m²·s, $q_{avg} = 116$ to 1577 kW/m², I.D. = 7.5 to 26 mm, bare tubes, vertical upwards flow).

Jäger et al. (2011) compared 15 different **Nu** correlations, 12 of which are considered in this thesis:

Eq. (4)	Miropol'skiy and Shitsman (1957)	Eq. (12)	Yamagata et al. (1972)
Eq. (5)	Petukhov et al. (1961)	Eq. (17)	Watts and Chou (1982)
Eq. (6)	Domin (1963)	Eq. (20)	Griem (1996)
Eq. (7)	Bishop et al. (1964)	Eq. (22)	Kitoh et al. (2001)
Eq. (8)	Swenson et al. (1965)	Eq. (23)	Jackson (2002)
Eq. (9)	Krasnoshchekov et al. (1967)	Eq. (25)	Kuang et al. (2008)

Jäger, et al. (2011) concluded that the most suitable **Nu** correlation from those tested is the Bishop et al. (1964) correlation Eq. (7), though the metric was not defined.

Wang and Li (2014) compiled a dataset of just over 1900 data points for supercritical water flowing vertically upwards in a bare tube.

Wang and Li (2014) compared 16 different **Nu** correlations including one of their own, all of which are considered in this thesis:

Eq. (1)	Dittus-Boelter (1930)	Eq. (12)	Yamagata et al. (1972)
Eq. (3)	Bringer and Smith (1957)	Eq. (14)	Jackson and Fewster (1975)
Eq. (4)	Miropol'skiy and Shitsman (1957)	Eq. (19)	Gorban et al. (1990)
Eq. (5)	Petukhov et al. (1961)	Eq. (21)	Hu (2001)
Eq. (7)	Bishop et al. (1964)	Eq. (22)	Kitoh et al. (2001)
Eq. (8)	Swenson et al. (1965)	Eq. (23)	Jackson (2002)
Eq. (9)	Krasnoshchekov et al. (1967)	Eq. (25)	Kuang et al. (2008)
Eq. (10)	Ornatsky et al. (1970)	Eq. (34)	Wang and Li (2014)

Wang and Li (2014) concluded that the Swenson et al. (1965) correlation Eq. (8), and the Hu (2001) correlation Eq. (21) were the predictors of HTC based on Mean Average Error (MAE).

Chen et al. (2015) compiled experiments from nine different laboratories with 3220 data points for water ($P = 22$ to 41 MPa, $G = 200$ to 2500 kg/m²·s, $q_{avg} = 0$ to 1800 kW/m², $T_b = 50$ to 576°C , I.D. = 7.5 to 26 mm, bare tubes, vertical upwards flow).

Chen et al. (2015) compared 26 different **Nu** correlations, 20 of which are considered in this thesis;

Eq. (1)	Dittus-Boelter (1930)	Eq. (19)	Gorban et al. (1990)
Eq. (3)	Bringer and Smith (1957)	Eq. (20)	Griem (1996)
Eq. (4)	Miropol'skiy and Shitsman (1957)	Eq. (21)	Hu (2001)
Eq. (5)	Petukhov et al. (1961)	Eq. (22)	Kitoh et al. (2001)
Eq. (7)	Bishop et al. (1964)	Eq. (23)	Jackson (2002)
Eq. (8)	Swenson et al. (1965)	Eq. (24)	Xu and Guo (2005)
Eq. (9)	Krasnoshchekov et al. (1967)	Eq. (25)	Kuang et al. (2008)
Eq. (10)	Ornatsky et al. (1970)	Eq. (26)	Yu et al. (2009)
Eq. (12)	Yamagata et al. (1972)	Eq. (28)	Mokry et al. (2009)
Eq. (17)	Watts and Chou (1982)	Eq. (29)	Gupta et al. (2011)

Chen et al. (2015) concluded that for the entire database, the Mokry et al. (2009) correlation Eq. (28) was the most accurate predictor of HTC by RMS, while the Swenson et al. (1965) correlation Eq. (8), and the Gupta et al. (2011) correlation Eq. (29) were also in the top five by RMS.

Sidawi (2016) gathered data from Razumovskiy et al. (2015) for 1-rod and 3-rod bundles, using supercritical water flowing upwards in a vertical tube ($P = 22.6, 24.5, 27.5$ MPa, $G = 1500, 2000, 2700$ kg/m²·s, $q_{avg} = 1543$ to 3200 kW/m², $T_b = 166$ to 227°C). This dataset consisted of 35 points for 1-rod bundle (annular channel), and 25 points for the 3-rod bundle. Sidawi also obtained over 500 data points for a 2x2 square rod bundle with vertical upwards flow using supercritical water from the test facility SWAMUP at the Shanghai Jiao Tong University (2015) ($P = 23, 25, 26$ MPa, $G = 500$ to 1500 kg/m²·s, $q_{avg} = 400$ to 1500 kW/m², $T_b = 310$ to 390°C , $D_{hy} = 6.98$ mm).

Sidawi (2016) compared 7 **Nu** correlations, all of which are considered in this thesis:

Eq. (1)	Dittus-Boelter (1930)	Eq. (16)	Dyadyakin and Popov (1977)
Eq. (7)	Bishop et al. (1964)	Eq. (23)	Jackson (2002)
Eq. (8)	Swenson et al. (1965)	Eq. (28)	Mokry et al. (2009)
Eq. (9)	Krasnoshchekov et al. (1967)		

Sidawi (2016) concluded that the Dittus-Boelter (1930) correlation Eq. (1) and the Jackson (2002) correlation Eq. (23) showed the best agreement for predicting Wall Temperature

for 1-rod (annular), 3-rod, and 2x2 rod channels, while demonstrating that some **Nu** correlations do not converge to a single wall temperature.

Gschnaidtner et al. (2018) compiled a comprehensive dataset from 40 authors consisting of over 8500 points obtained through experiments with upward flow of supercritical water in vertical bare tubes. ($P = 22$ to 34.4 MPa, $G = 55$ to 3700 kg/m²·s, $q_{avg} = 37$ to 4522 kW/m², $T_b = 20$ to 554°C , I.D. = 1.57 to 38 mm, bare tubes, vertical upwards flow).

Gschnaidtner et al. (2018) compared 11 different **Nu** correlations, all of which are considered in this thesis:

Eq. (1)	Dittus-Boelter (1930)	Eq. (27)	Cheng et al. (2009)
Eq. (7)	Bishop et al. (1964)	Eq. (28)	Mokry et al. (2009)
Eq. (8)	Swenson et al. (1965)	Eq. (29)	Gupta et al. (2011)
Eq. (17)	Watts and Chou (1982)	Eq. (33)	Chen and Fang (2014)
Eq. (18)	Petukhov et al. (1983)	Eq. (34)	Wang and Li (2014)
Eq. (23)	Jackson (2002)		

Gschnaidtner et al. (2018) concluded that the Swenson et al. (1965) correlation Eq. (8) and the Gupta et al. (2011) correlation Eq. (29) gave the best results, followed by the Mokry et al. (2009) correlation Eq. (28) and the Wang and Li (2014) correlation Eq. (34). Gschnaidtner et al. (2018) also recommended that the trend of adding more complex **Nu** correlation modifier modifiers was not found to increase the prediction accuracy, and should be avoided for future **Nu** correlations.

Lei et al. (2019) gathered approximately 3000 data points on supercritical water from open literature for supercritical water and used this to compare **Nu** correlations, and also propose a new **Nu** correlation ($P = 22.5$ to 41 MPa, $G = 100$ to 2150 kg/m²·s, $q_{avg} = 100$ to 1800 kW/m², I.D. = 1.5 to 26 mm, bare tubes, vertical upwards flow).

Lei et al. (2019) compared 22 different **Nu** correlations, all of which are considered in this thesis:

Eq. (1)	Dittus-Boelter (1930)	Eq. (17)	Watts and Chou (1982)
Eq. (3)	Bringer and Smith (1957)	Eq. (19)	Gorban et al. (1990)

Eq. (4)	Miropol'skiy and Shitsman (1957)	Eq. (20)	Griem (1996)
Eq. (5)	Petukhov et al. (1961)	Eq. (21)	Hu (2001)
Eq. (6)	Domin (1963)	Eq. (22)	Kitoh et al. (2001)
Eq. (7)	Bishop et al. (1964)	Eq. (23)	Jackson (2002)
Eq. (8)	Swenson et al. (1965)	Eq. (24)	Xu and Guo (2005)
Eq. (9)	Krasnoshchekov et al. (1967)	Eq. (25)	Kuang et al. (2008)
Eq. (10)	Ornatsky et al. (1970)	Eq. (26)	Yu et al. (2009)
Eq. (12)	Yamagata et al. (1972)	Eq. (33)	Chen and Fang (2014)
Eq. (14)	Jackson and Fewster (1975)	Eq. (35)	Lei et al. (2019)

Lei et al. (2019) concluded that their newly proposed **Nu** correlation was the most accurate predictor of HTC by RMS.

Recently, [Debrah et al. \(2019\)](#) performed an assessment of heat transfer **Nu** correlations in a square rod geometry as is proposed in the European SCWR fuel bundle design. While this is one of the first studies on a bundle configuration since Dyadyakin and Popov (1977), it has no experimental basis. Instead the assessment was performed against the data collected through a simulation performed by Waata (2006) based on the simulation performed with the Monte-Carlo N-Particle code (MCNP) and the sub-channel code Sub-channel Thermal-hydraulics Analysis of a Fuel Assembly under Supercritical conditions (STAFAS).

Debrah et al. (2019) compared 13 different **Nu** correlations, 12 of which are considered in this thesis:

Eq. (1)	Dittus-Boelter (1930)	Eq. (18)	Petukhov et al. (1983)
Eq. (4)	Miropol'skiy and Shitsman (1957)	Eq. (20)	Griem (1996)
Eq. (7)	Bishop et al. (1964)	Eq. (27)	Cheng et al. (2009)
Eq. (9)	Krasnoshchekov et al. (1967)	Eq. (28)	Mokry et al. (2009)
Eq. (10)	Ornatsky et al. (1970)	Eq. (29)	Gupta et al. (2011)
Eq. (16)	Dyadyakin and Popov (1977)	Eq. (33)	Chen and Fang (2014)

Debrah et al. (2019) concluded that the Cheng et al. (2009) correlation Eq. (27) is best suited for predicting HTC in a bundle rod geometry.

2.8 LITERATURE REVIEW SUMMARY

2.8.1 *Conclusions*

As of March 2020, 440 larger NPPs (>700 MW_{el}) are in operation worldwide, in addition to 26 Small and Medium sized reactors (<300 MW_{el}). However, very few NPPs are planned to be built in the foreseeable future, aside from PWRs. Within the next 25 years, BWRs and PHWRs will decrease to negligible numbers, while in the next 15 years, all AGRs and LGRs will be shut down permanently.

Over 55 SMR concepts have been developed, and while many Small and Medium Reactors have been built over the 30 – 40 years, none fit the description of modular, simpler design, and factor built, and therefore no true SMRs have been built. Two SMRs, both the KLT-40S versions, are currently being built to be put onto a Russian ship to provide power in northern remote regions.

Two Canadian SCWR designs have been proposed, with a 37-element fuel bundle arrangement and a 64-element fuel bundle arrangement. Issues facing SCWR are related to verifying previous HT **Nu** correlations with bundle geometries. Specifically, for the 37-element bundle design, experiments with a 7-rod bundle must be used to assess the performance of common HT **Nu** correlations.

SCW thermophysical properties change rapidly and continuously, close to the pc point. In particular, the specific heat capacity experiences an extremely large peak that is used to determine the pc point.

Many authors have proposed prediction methods to determine if DHT will occur along a heated length. However, no current prediction method exists to determine exactly when DHT will occur along the heated length, how long it will last, or the severity.

The ratio of heat flux (q_{avg}) to predicted deteriorated heat flux in bare tubes (q_{dht}), as expressed in (2.11), is a useful tool to numerically assess whether DHT will occur, as heat flux and mass flux appear to be the major parameters affecting HT characteristics.

$$\frac{q_{avg}}{G} \rightarrow \frac{q_{avg}}{-58.87 + 0.745 \cdot G} = \frac{q_{avg}}{q_{dht}}$$

In bare tubes cooled with SCW, DHT is observed when the ratio of q_{avg}/q_{dht} is greater than 1. In bundle geometries, DHT occurs when the ratio of q_{avg}/q_{dht} is greater than 1.6 to 1.8. For any geometry, with higher mass flux comes higher HTC, and within the DHT regime the HTC can be reduced by as much as 50% in some cases. Within the IHT regime the HTC can be increased by as much as 30% in some cases.

As bundles introduce greater turbulence to a system, and bundle experiments did not experience DHT effects until much higher q_{avg}/q_{dht} ratios, it is concluded that additional turbulence results in DHT not occurring until the heat flux (q_{avg}) to mass flux function (q_{dht}) is much higher than in bare tubes.

In addition, bundles cooled with SC F-R12 experience a much lower HTC than bundles or bare tubes cooled with SCW. Bundles cooled with SC F-R12 also experience DHT at a ratio of $q_{avg}/q_{dht} > 0.008$, significantly lower than in bundles cooled with SCW. Therefore, SC F-R12 is much less effective as a coolant, and experiences DHT at much lower mass flux values when compared with bare tubes cooled with SCW.

Numerous assessments have been made in the past 10 years to study the applicability of **Nu** correlations to various data-sets, including bare tubes, 1-rod (annular), 3-rod, and 2x2 Rod channels.

The results have generally concluded that the Mokry, et al. (2009) correlation Eq. (28) and the Swenson et al. (1965) correlation Eq. (8) were the best for bare tubes, while there are limited and mixed results for bundle configurations. No **Nu** correlation exists that can predict accurately in the DHT range.

As of this writing, only one **Nu** correlation assessment has been performed on a 7-rod bundle cooled with SCW. It concluded that the Dyadyakin and Popov (1977) correlation Eq. (16) is the most suitable (Razumovskiy et al., 2008). However, it is unknown which **Nu** correlations were assessed, the method of assessment, or metrics examined.

It is important to properly assess a 7-rod bundle (6 + 1 configuration) cooled with SCW, as the central rod in the proposed fuel bundle configuration in Figure 2-9 is in a 7-rod bundle ring. 1-rod and 3-rod configurations may be useful for understanding sub-channels, however the central rod will experience the highest temperatures.

2.8.2 *Objectives of Research*

The objectives this thesis are as follows:

- 1) Analyze recent experimental data for a vertical 7-rod bundle with helical ribs cooled with upward flow of SCW, and understand the specifics of HT in bundle geometry.
- 2) Compare the 35 known **Nu** correlations using the 7-rod bundle data to determine the most suitable **Nu** correlation for predicting HTC and T_w in the 7-rod bundle.
 - Any correlation that is suitable in the 7-rod bundle must also predict acceptably in a bare tube to provide confidence that scaling up to any of the proposed SCWR designs will yield reliable results.
- 3) If no **Nu** correlations provide suitable performance in both a 7-rod bundle and a bare tube, propose a new **Nu** correlation based on the 7-rod bundle data.
- 4) Compare data in the DHT regime in a 7-rod bundle, using the q_{dht} expression for bare tubes.
- 5) Using the most suitable **Nu** correlation for the 7-rod bundle, determine if any of the 7-rod dataset parameters or the typical SCWR designs are suitable for use in future SCWR NPPs based on maximum sheath and fuel centreline temperatures (using assumed sheath materials, fuels, and parameters).

3 METHODOLOGY

3.1 EXPERIMENTAL SETUP

SCW experimental loops are extremely expensive to implement, requiring sophisticated equipment and measuring techniques. As a result, many of the studies performed are proprietary and are not published in open literature (Pioro & Duffey, 2007).

In this thesis, the datasets obtained to compare existing **Nu** correlations and testing of new **Nu** correlations were obtained from two sources:

- 1) SKD-1 Loop (Kirillov et al., 2005)
 - Institute of Physics and Power Engineering (IPPE, Obninsk, Russia)
 - 4 metre bare tube

- 2) SCW Loop (Razumovskiy et al., 2008)
 - National Technical University of Ukraine, Kiev Polytechnic Institute (Igor Sikorsky Kyiv Polytechnic Institute, Kyiv, Ukraine)
 - 0.485 metre bundles inside of tube (7-rod)

3.1.1 BARE TUBE

The following description is taken from Kirillov et al. (2005), and a simple schematic can be seen in Figure 3-1.

The SKD-1 Loop is a high temperature/pressure pumped vertically upwards flowing loop. The loop is able to handle pressures up to 28 MPa at the outlet, and fluid temperatures up to 500°C. Distilled and de-ionized water were used as the fluid in the SKD-1 loop.

From the pump, the fluid passes through a flowmeter, preheater, test section, mixer, main coolers, and back to the pump. Pressurization was achieved through high pressure nitrogen, and power was delivered via 600 kW (A/C) power supply.

The test section was a vertical stainless steel (similar to SS-304, 12Cr18Ni10Ti) circular tube, with 10 mm ID, 2 mm wall thickness, and an average surface roughness of 0.63 (0.8 μm). This corresponds to the equivalent D_{hy} of typical SCW reactor fuel bundles proposed.

Two lengths were used: 1 metre and 4 metre.

Water was heated via AC current passing through the tube wall from the inlet to the outlet power terminals via copper clamps. The test section was wrapped with thermal insulation to minimize heat loss.

The test section current and voltage were used to calculate the power, and the pressure was only measured at the inlet. Mass flowrate was calculated using measurements via the Differential Pressure cell that measured the pressure drop across a small orifice plate. Ambient temperature was also measured.

Temperature of the bulk fluid (T_b) at the inlet (T_{in}) and outlet (T_{out}) were measured using ungrounded sheathed thermocouples, installed just downstream of the mixing chambers. This was done to ensure a true T_b was measured, as opposed to single point temperature resulting from the cross-sectional temperature distribution. These thermocouples were calibrated *in situ*.

21 thermocouples for the one-metre tube, and 81 thermocouples for the four-metre tube, were contact welded to the outer walls of the tubes at intervals of 50 mm. These thermocouples were calibrated *in situ*, and provided the T_w measurements.

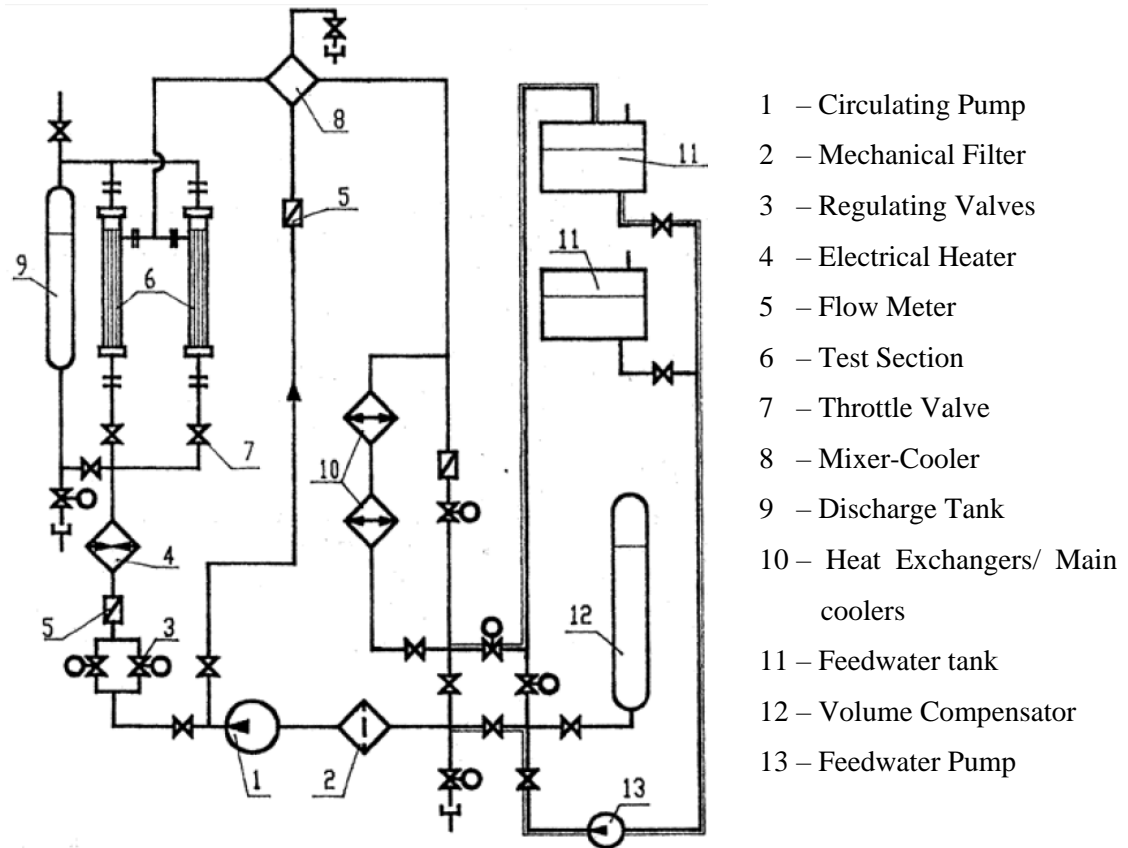


Figure 3-1: SKD-1 Loop Schematic
 (courtesy of I. L. Pioro (Kirillov et al., 2005))

Table 3-1 lists the uncertainty of the described primary parameters for the SKD-1 Loop, while Table 3-2 lists the Test Matrix for the SKD-1 Loop, indicating the parameters tested for the dataset provided.

Table 3-1: Uncertainty of Primary Parameters for SKD-1 Loop
 (Kirillov et al., 2005)

PARAMETER	MAXIMUM UNCERTAINTY
Test-section power	$\pm 1.0\%$
Inlet Pressure	$\pm 0.25\%$
Wall Temperatures	$\pm 3.0\text{ }^{\circ}\text{C}$
Mass-Flow Rate	$\pm 1.5\%$
Heat Loss	$\leq 3.0\%$

Table 3-2: Test Matrix for SKD-1 Loop
(Kirillov et al., 2005)

P MPa	T_{in} °C	T_{out} °C	T_w °C	q kW/m ²	G kg/m ² ·s
24.5-25	300-380	360-390	<700	90-1050	200, 500, 1000
24	320-350	380-406	<700	160-900	500, 1000, 1500

The heat flux for the loop is not constant, and changes with imperfections of the tube (thicker/thinner material, chemical composition, etc) leading to slightly more or less heat flux as a result of the electrical conductivity experienced. The q_{avg} used throughout this thesis is the average value of the heat flux, calculated at each thermocouple location as mentioned previously.

Custom software was utilized for the Data Acquisition System (DAS). This allowed the loop to gain stabilization of the primary parameters before moving forward to a new power level and/or new flow conditions. The primary parameters used by the SKD-1 test loop are listed in Table 3-2.

While the heat loss was tested and showed only minor losses, these were still used in the heat transfer calculations to adjust for the heat loss.

In order to calculate the exact parameters, the equations listed in Table 3-3 were used, while the bulk fluid temperature in the cross section was calculated using local pressure and local enthalpy where an external wall thermocouple was located.

Table 3-3: Data Reduction Parameters for SKD-1 Loop (Kirillov et al., 2005)

PARAMETER	SI UNIT	EQUATION	DESCRIPTION
External Wall Temperature	°C	$T_w^{\text{ext}} = T_w^{\text{int}} + \frac{q_{vl}}{4 \cdot k_{wl}} \left[\left(\frac{D_{\text{ext}}}{2} \right)^2 - \left(\frac{D}{2} \right)^2 \right] - \frac{q_{vl}}{2 \cdot k_{wl}} * \left(\frac{D_{\text{ext}}}{2} \right) \ln \left(\frac{D_{\text{ext}}}{D} \right)$ (3.1)	
Flow Area	m ²	$A_{\text{fl}} = \pi \cdot D^2 / 4$ (3.2)	D – Inner Diameter (m)
Mass Flux	kg/m ² · s	$G = \dot{m} / A_{\text{fl}}$ (3.3)	\dot{m} – mass flowrate (kg/s)
Total Heated Area	m ²	$A_{\text{h}} = \pi \cdot D \cdot L_{\text{h}}$ (3.4)	L_{h} – Tube Heated Length (m)
Local Heated Area	m ²	$A_{\text{hl}} = \pi \cdot D \cdot L_{\text{hl}}$ (3.5)	L_{hl} – Local heated Length (50 mm)
Power	W	$POW = V \cdot I$ (3.6)	V – test section voltage drop (Volts) I – Electrical Current (Amps – A)
Local Power	W	$POW_1 = I^2 \cdot R_1$ (3.7)	R_1 – Local Resistance (Ohms – Ω)
Average Heat Flux	W/m ²	$q = POW / A_{\text{h}}$ (3.8)	POW – Power (W)
Local Heat Flux	W/m ²	$q_1 = \frac{POW_1 - HL_1}{A_{\text{hl}}}$ (3.9)	HL_1 – Local Heat Loss based on external wall Temp measurements
Volumetric Heat Flux	W/m ²	$q_{vl} = POW_1 / \frac{\pi}{4} \cdot (D_{\text{ext}}^2 - D^2) \cdot L_{\text{hl}}$ (3.10)	D_{ext} – Exterior Diameter (m)
Outlet Pressure	Pa	$P_{\text{out}} = P_{\text{in}} - \Delta P_{\text{TS}}$ (3.11)	P_{in} – Pressure in (Pa) ΔP_{TS} – P Drop across test section (Pa)
Tube wall local Thermal Conductivity	W/m · K	$k_{wl} = f(T_w^{\text{avg}}, P_{\text{in}})$ (3.12)	$T_w^{\text{avg}} = (T_w^{\text{ext}} + T_w^{\text{int}}) / 2$ T_w^{ext} – External wall temp (°C) T_w^{int} – Internal wall temp (°C)

3.1.2 7-ROD BUNDLE

Razumovskiy produced two papers, one detailing the SCW loop for use with a 7-rod bundle (Razumovskiy et al., 2008), and a second detailing the SCW loop for use with a 1-rod and 3-rod bundle (Razumovskiy et al., 2015). The loop remained virtually unchanged between these two experiments, and with the exception of the power supply (DC for 7-rod, AC for 1- and 3-rod), only the bundles used differed.

The following description of the SCW loop is taken from both of these papers (Razumovskiy et al. (2008) and Razumovskiy et al (2015)), with a simple schematic of the SCW loop shown in Figure 3-4.

The SCW Loop is an “open” stainless-steel vertical upwards flowing loop. The operating range is up to 28 MPa, and water temperatures up to 700 °C. Chemically desalinated water (pH = 7.5, average hardness = 0.2 µg-equiv/kg) was used as the fluid in the SCW loop. Power was delivered via 90 kW power supply.

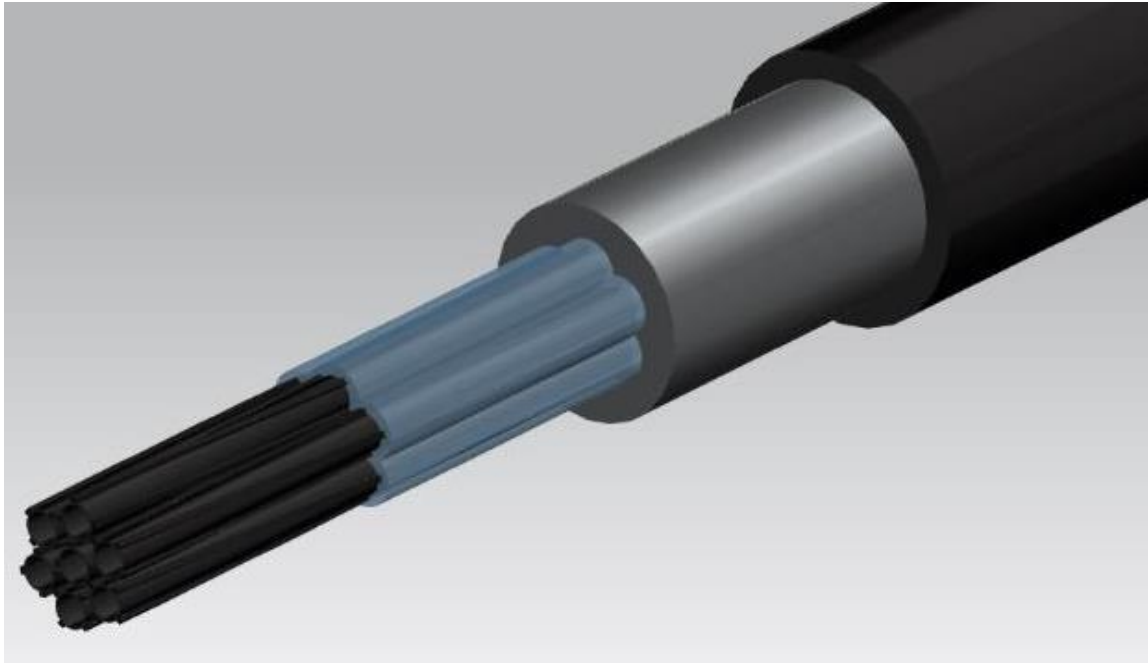


Figure 3-2: 3-D Image of 7-rod Bundle
(Clark et al., 2019)

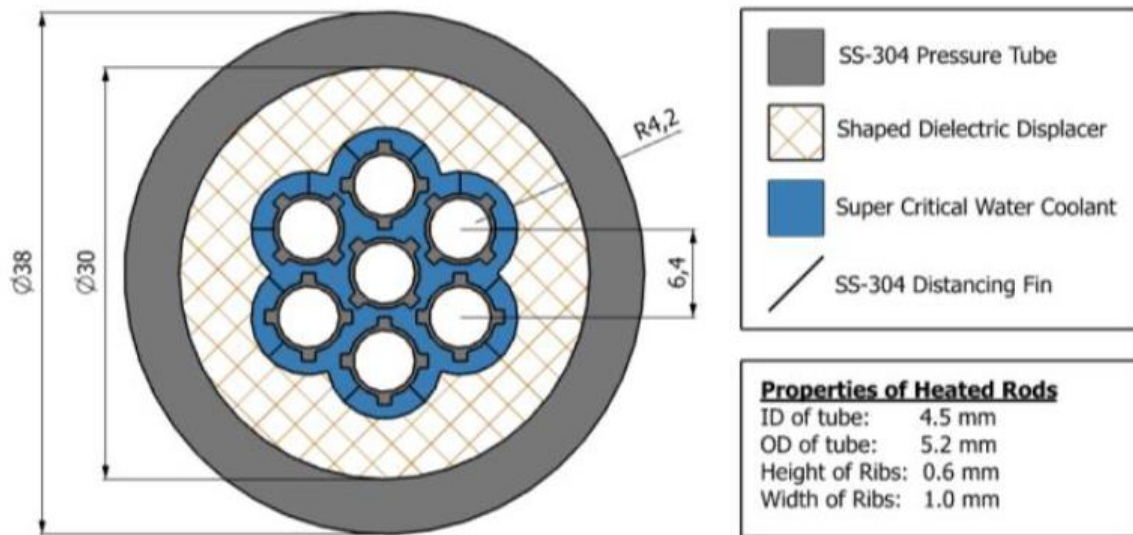
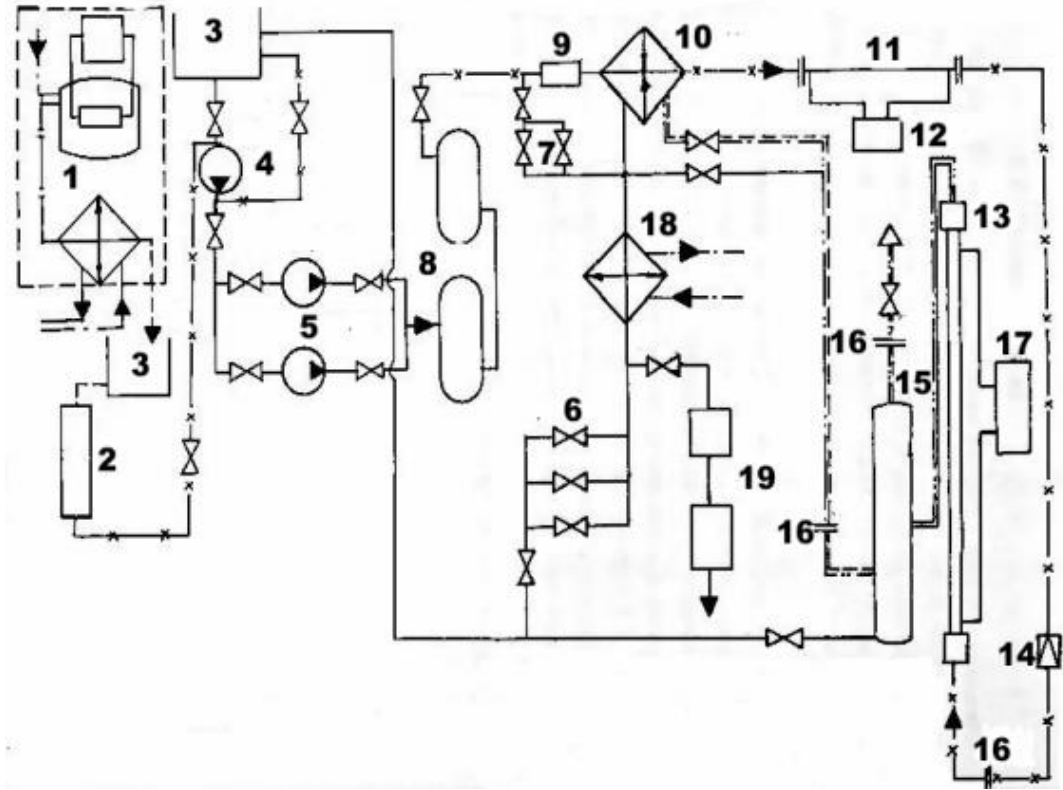


Figure 3-3: Radial Cross Section of 7-rod Bundle
(Clark et al., 2019)

Figure 3-2 and Figure 3-3 show the bundle geometry for the 7-rod bundle. SCW flows through the gap between the heated rods and the displacer. Rods were directly heated, with current passing through the wall of the rods.

The bundle elements were 485 mm heated length tubes (Ukrainian SS similar to SS-304) of 5.2 mm OD and 4.5 mm ID, with four helical ribs of 0.6 mm height and 1 mm width that were wound over the tubes with a 400 mm pitch. Calibrated SS fins of 0.1 mm thickness were welded to the rods to provide a 1 mm gap between the rod ribs and the displacer. The displacers were inserted into pressure tubes of 18/12-mm (1-rod), 32/20 mm (3-rod), and 38/30 mm (7-rod) OD/ID diameters.



- | | |
|----------------------------|--------------------------------|
| 1 – Electro-distillator | 11 – Electrical Preheater |
| 2 – Ion-exchange Filter | 12 – Dynamotor |
| 3 – Accumulator Reservoirs | 13 – Test Section |
| 4 – Boosting Pump | 14 – Throttling Valve |
| 5 – Plunger Pumps | 15 – Damping Reservoir |
| 6 – Regulating Valves | 16 – Electro-isolating Flanges |
| 7 – Regulating Valves | 17 – Main Power Supply |
| 8 – Damping Reservoir | 18 – Cooler |
| 9 – Turbine Flow Meter | 19 – Throttling Valves |
| 10 – Heat Exchanger | |

Figure 3-4: SCW Loop Schematic

(courtesy of I. L. Pioro (Razumovskiy et al., 2008)) (Copyright of ASME)

Hydraulic equivalent diameters (D_{hy}) were listed as 2.67 mm (1-rod), 2.40 mm (3-rod), and 2.38 mm for Central sub-channel and 2.76 mm for Peripheral sub-channels (7-rod), determined through the following equation:

$$D_{hy} = \frac{4 \cdot A_{fl}}{p_{wet}}, \quad \text{where } p_{wet} \text{ is the wetted perimeter} \quad (3.13)$$

Wall temperatures on the OD of the rods were calculated using ID temperature measurements with seven thermocouples installed along the heated length on the ID surface of a heated rod at 95, 195, 255, 315, 375, 415, 475 mm from the inlet of the heated section (the first thermocouple is past the entrance region, i.e. $L/D_{hy} > 25$). Each thermocouple was tightly engraved into a copper plug of a diameter equal to the inner diameter of the rod (Figure 3-5). These plugs were covered in a silicone resin that is heat-resistant to provide electrical insulation. Good contact and high thermal conductivity of the copper plugs allowed the measurement of an average temperature in each cross section with good response time. This was verified with isothermal tests.

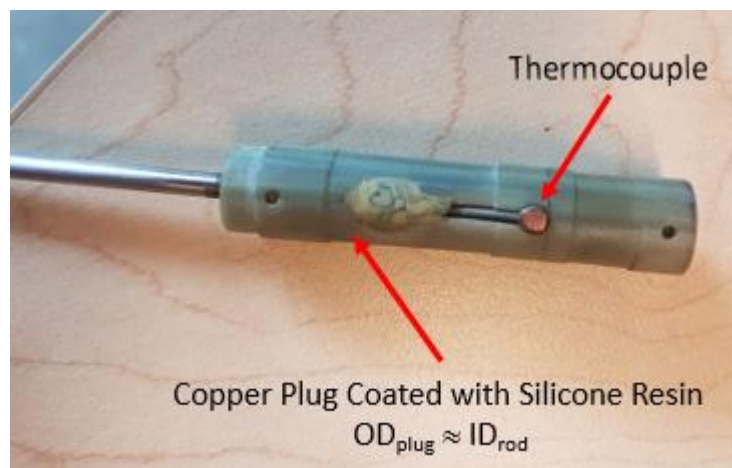


Figure 3-5: Copper Plug Coated with Silicone Resin

Bulk fluid temperatures were measured using chromel-alumel ungrounded sheathed thermocouples of 0.2 mm diameter wire inserted into the fluid flow inside the mixing chambers. Similar to the SKD-1 Loop, this was purposefully done to obtain a true bulk temperature.

Table 3-4 lists the uncertainty for the SCW loop, while Table 3-5 lists the test matrix.

Table 3-4: Uncertainty of Primary Parameters for SCW Loop
(Razumovskiy et al. (2008) and (2015))

PARAMETER	MAXIMUM UNCERTAINTY
MEASURED PARAMETERS	
Inlet Pressure	$\pm 0.2\%$
Bulk Fluid Temp	$\pm 3.4\%$
Wall Temp	$\pm 3.2\%$
MEASURED PARAMETERS	
Mass-Flow Rate	$\pm 2.3\%$
Heat Flux	$\pm 3.5\%$
HTC	$\pm 12.7\%$
Heat Loss	$\leq 3.4\%$

Table 3-5: Test Matrix for SCW Loop
(Razumovskiy et al. (2008) and (2015))

<i>TEST</i>	<i>P</i> MPa	<i>T_{in}</i> °C	<i>T_{out}</i> °C	<i>G</i> kg/m ² ·s	<i>q</i> MW/m ²	<i>q/G</i> kJ/kg
1-rod	22.6	166		1500	1.25	
	24.5	↓	-	↓	↓	-
3-rod	27.5	277		2700	3.2	
7-rod	22.6	125	290	700	0.50	<1.5
	24.5	↓	↓	↓	↓	
	27.5	325	379	1500	1.60	

Since the rods were electrically heated, the resistance of a rod is directly dependent on local wall temperatures along the heated length. This leads to the heat flux varying slightly along the heated length. It was found that for $q \leq 2.244$ MW/m² the HTC variations were less than 5%, however for $q = 2.547$ MW/m² it varied by 8.5%.

Similar to the SKD-1 Loop, data reduction was required to calculate the parameters for the SCW Loop (listed in Table 3-6). For parameters that require calculation, NIST REFPROP 10.0 software was used. In all test sections, pressure losses along the heated length were considered to be negligible.

Table 3-6: Data Reduction Parameters for SCW Loop
(Razumovskiy et al., 2008)

PARAMETER	SI UNIT	EQUATION	DESCRIPTION
External Wall Temperature	°C	$T_w^{\text{ext}} = T_w^{\text{int}} + \frac{q_{vl}}{4 \cdot k_{wl}} \left[\left(\frac{D_{\text{ext}}}{2} \right)^2 - \left(\frac{D}{2} \right)^2 \right] - \frac{q_{vl}}{2 \cdot k_{wl}} \cdot \left(\frac{D_{\text{ext}}}{2} \right)^2 \ln \left(\frac{D_{\text{ext}}}{D} \right) \quad (3.14)$	
Enthalpy	J/kg	$H_{b(i+1)} = H_{b(i)} + \frac{q_{(i)} \cdot dx \cdot p_h}{A_{fl} \cdot G} \quad (3.15)$	dx – distance along heated length (m)
Bulk Fluid Temperature	°C	$T_{b,calc} = f(P_{in}, H_{b(i)}) \quad (3.16)$	
Heat Transfer Coefficient (HTC)	W/m ² · K	$HTC_{(i)} = \frac{q_{(i)}}{T_{w,o} - T_{b,calc}} \quad (3.17)$	L_h – Tube Heated Length (m)

3.2 DESCRIPTION

Four separate methods will be utilized to meet the objectives of this research, based upon the two datasets shown in section 3.1. The 7-rod dataset is of particular interest as it represents the centre rod and the inner ring of the 37-element bundle. These four methods are described below:

1) EXPERIMENTAL RESULTS SHOWING HT CHARACTERISTICS

The 7-rod datasets and selected bare tube datasets will be plotted to determine the HT characteristics.

2) COMPARATIVE STUDY THROUGH ERROR ASSESSMENT

These datasets will be used to assess the performance of the previous **Nu** correlations identified in section 2.7. The assessment will be performed as follows:

1. Using the data from the 7-rod datasets and the bare tube datasets, the predictions for each previous **Nu** correlation will be calculated
2. The error for each previous **Nu** correlation predictions for HTC and T_w when compared with the experimental data will be calculated. The methods of computing error will be:
 - a. Standard Deviation (SD)
 - b. Mean (or average) Error (ME)
 - c. Mean Absolute Error (MAE)
 - d. Root Mean Square error (RMS)

These steps are not performed by hand. Instead, a program was built in MS Excel using VB macros linked to NIST REFPROP 10.0 to calculate thermophysical properties. The code for the program is listed in APPENDIX A:CODE USED.

3) **DEVELOPMENT OF NEW Nu CORRELATION**

The first step in creating a new Nu correlation to predict the HTC is to perform a dimensional analysis by the Buckingham Pi theorem. Once this is performed, the expression for HTC can be determined as a function of the identified HT parameters.

Based upon the assessment, terms from the most suitable previous Nu correlation will be selected.

With the terms known, the method as outlined by Mokry et al. (2011) is employed to determine the coefficients for the terms using the 7-rod datasets, and select bare tube datasets. The 7-rod datasets will have the DHT points removed for determining the Nu correlation. The bare tube datasets will not have the DHT points removed due to the difficulty in determining the clear DHT.

This is completed using computer code. This new Nu correlation is then assessed using the same error methods from the Assessment section.

4) **SIMULATED SHEATH AND FUEL CENTRELINE TEMPERATURES**

Once a new Nu correlation is determined, simulations are run to determine what the surface temperature of the sheath would be using the methods outlined in the Assessment section.

Using the surface temperature of the sheath, the inner sheath temperature will be determined. Once the inner surface temperature of the sheath (T_{sheath}) is determined, the fuel centreline ($T_{\text{fuel CL}}$) will be determined.

To determine the fuel centreline, the fuel will be subdivided into layers, 0.5 mm thick, and the inner temperature of these layers will be calculated. This will be repeated until the layer is less than 0.5 mm thick, after which, the layers will decrease in size by factors of 10 until a steady inner temperature is reached (ΔT between layers $< 0.1^\circ\text{C}$), indicating the true fuel centreline temperature (see Table 3-9 for example). Sample calculations can be found in section C.3.3.

The simulations will determine the maximum fuel bundle length using the parameters from the 7-rod bundle trials and the proposed SCWR designs, based on industry accepted maximum T_{sheath} and $T_{\text{fuel CL}}$.

3.3 CALCULATIONS

3.3.1 *HT Characteristics*

No calculations are required for the HT Characteristics

3.3.2 *Assessment*

3.3.2.1 **HTC and T_w Predictions**

The majority of **Nu** correlations shown in section 2.6 use a parameter that requires a known wall temperature. However, the T_w is not known at the beginning of the calculation, and therefore must first be guessed.

A good first approximation for T_w can be obtained through the Dittus-Boelter **Nu** correlation, as this uses bulk fluid temperature only.

An example using the Mokry et al. (2009) correlation Eq. (28) is shown below, with the first step being to obtain the HTC (h_{DB}) and T_w calculated by Dittus-Boelter ($T_{w,DB}$):

$$\mathbf{Re}_b = \frac{\rho_b V_b D_{hy}}{\mu_b} = \frac{\rho_b \left(\frac{\dot{V}}{A_{fl}} \right) D_{hy}}{\mu_b} = \frac{\rho_b \left(\frac{\dot{m}/\rho_b}{A_{fl}} \right) D_{hy}}{\mu_b} = \frac{G \cdot D_{hy}}{\mu_b} \quad (3.18)$$

$$\mathbf{Nu}_{DB} = 0.023 \cdot \mathbf{Re}_b^{0.8} \cdot \mathbf{Pr}_b^{0.4} \quad \text{Eq. (1)}$$

$$h_{DB} = \frac{\mathbf{Nu}_{DB} \cdot k_b}{D_{hy}} \quad (3.19)$$

$$T_{w,DB} = T_b + \frac{q_{avg}}{h_{DB}} \quad (3.20)$$

The next step is to use this $T_{w,DB}$ as an initial guess to determine the fluid properties at the T_w (using NIST REFPROP 10.0 for thermophysical properties):

Using these properties (@DB), the T_w can then be computed using the Mokry, et al. (2009) equation. This is an iterative process where the average properties must first be computed:

$$\overline{C_P} = \frac{H_{w@DB} - H_b}{T_{w@DB} - T_b} \quad (3.21)$$

$$\overline{\mathbf{Pr}}_b = \frac{\overline{C_P} \cdot \mu_b}{k_b} \quad (3.22)$$

$$\mathbf{Nu}_{MEA} = 0.0061 \cdot \mathbf{Re}_b^{0.904} \cdot \overline{\mathbf{Pr}}_b^{0.684} \cdot \left(\frac{\rho_{w@DB}}{\rho_b} \right)^{0.564} \quad (3.23)$$

$$h_{\text{MEA}} = \frac{\text{Nu}_{\text{MEA}} \cdot k_b}{D_{\text{hy}}} \quad (3.24)$$

$$T_{\text{w,MEA}} = T_b + \frac{q_{\text{avg}}}{h_{\text{MEA}}} \quad (3.25)$$

$$T_{\text{w},1-2} = |T_{\text{w,MEA}} - T_{\text{w,DB}}| \quad (3.26)$$

If this temperature difference is less than 0.1°C , then the prediction matches and the solution has converged. The temperature is chosen as the parameter to base the calculations on, as this allows designers to calculate the fuel centreline temperature and sheath temperature.

If the temperature difference is greater than 0.1°C , then the calculated wall temperature ($T_{\text{w,MEA}}$) is used as the temperature to determine the average properties. The wall temperature is again calculated, and then the temperature difference is examined again:

$$\overline{C}_P' = \frac{H_{\text{w@MEA}} - H_b}{T_{\text{w@MEA}} - T_b} \quad (3.27)$$

$$\overline{\text{Pr}}_b' = \frac{\overline{C}_P' \cdot \mu_b}{k_b} \quad (3.28)$$

$$\text{Nu}'_{\text{MEA}} = 0.0061 \cdot \text{Re}_b^{0.904} \cdot (\overline{\text{Pr}}_b')^{0.684} \cdot \left(\frac{\rho_{\text{w,MEA}}}{\rho_b} \right)^{0.564} \quad (3.29)$$

$$h'_{\text{MEA}} = \frac{\text{Nu}'_{\text{MEA}} \cdot k_b}{D_{\text{hy}}} \quad (3.30)$$

$$T'_{\text{w,MEA}} = T_b + \frac{q_{\text{avg}}}{h'_{\text{MEA}}} \quad (3.31)$$

$$T_{\text{w},1-2} = |T'_{\text{w,MEA}} - T_{\text{w,MEA}}| \quad (3.32)$$

This process is repeated until the temperature difference is less than 0.1°C , indicating a convergent solution. Non-convergent solutions are possible also (see section C.3.1.3). Non-convergences typically occur as the T_w prediction crosses the T_{pc} , indicating the presence of both gas-like and liquid-like density regions in this area of non-convergence. If the process repeats more than 60 times, the process is stopped to avoid an endless loop. In these cases, it is evidence of a non-convergent solution.

3.3.2.2 Error Calculations

Once the HTC values and T_w have been determined for each **Nu** correlation along the heated path, the error from the predicted values to the measured values is calculated.

Error is defined below, where x is any property that is being examined (ex. HTC or Wall Temperature).

$$Err_i = \left[\frac{x_{i,calculated}}{x_{i,measured}} - 1 \right]; \quad n = \text{number of data points} \quad (3.33)$$

- 1) Mean Error (ME)
(Wang & Li, 2014)

$$ME = \frac{\sum_{i=1}^n Err_i}{n} \quad (3.34)$$

- 2) Mean Average Error (MAE)
(Gupta et al., 2013)

$$MAE = \frac{\sum_{i=1}^n |Err_i|}{n} \quad (3.35)$$

- 3) Standard Deviation (SD)
(Wang & Li, 2014)

$$SD = \sqrt{\frac{\sum_{i=1}^n (Err_i - ME)^2}{n - 1}} \quad (3.36)$$

- 4) Root Mean Square error (RMS)
(Gupta et al., 2013)

$$RMS = \sqrt{\frac{\sum_{i=1}^n Err_i^2}{n}} \quad (3.37)$$

The ME provides a measure of the error of the **Nu** correlation predictions, where positive values mean the **Nu** correlation typically over predicts and negative values equate to an under prediction. However, as the ME does not take signs into account, large positive and large negative numbers can cancel themselves out, leading to low ME numbers and erroneous observations. While the ME is included in the error analysis for an overall measure of whether a correlation over or under predicts, it is not suitable for determining the best overall **Nu** correlation.

The MAE provides a suitable measure of the average error of the **Nu** correlation predictions as it converts all errors to a positive value. It cannot provide an overall measure of whether the prediction is over predicting or under predicting. However, the MAE averages out all errors, and therefore if there are many small errors and one large error, the average error may still be small. The MAE is used in the error analysis, however is not considered to be the most important error evaluation.

The SE provides a measure of the magnitude of the errors from the average. However, it is not suitable for determining the best **Nu** correlation as it uses the ME. If the ME is a large value, the SE is reduced, leading to erroneous results. While the SE is included in the error analysis for reference, it is not suitable for determining the best overall **Nu** correlation.

The RMS provides a measure of the magnitude of the errors, without influence of positive or negative errors. As RMS uses the squared value of errors, unlike MAE, when many small errors are paired with one large error, the RMS will be larger. It is desirable to use a **Nu** correlation that predicts close to the measured values without any large variations, therefore the RMS is the most suitable method to calculating error and will be used to determine the best overall **Nu** correlation.

3.3.3 New **Nu** Correlation

As HTC is not an independent variable, and is affected by a fluids flow characteristics and thermophysical properties, it is important to identify a set of variables that affect HTC, and their basic dimensions in order to calculate HTC:

- 1) Mass (M) 2) Length (L) 3) Temperature (K) 4) Time (T)

Note: The symbols used for the dimensions have overlap with other symbols used in this paper. Please be aware that these symbols apply only to the discussion of the dimensions in this section

Table 3-7 lists the essential thermophysical properties as identified by Piro and Duffey (2007), and their associated dimensions.

Table 3-7: Dimensions of Essential Thermophysical Properties

VARIABLE	DESCRIPTION	SI UNITS	DIMENSIONS
<i>HTC</i>	Heat Transfer Coefficient	W/m ² ·K	M·T ⁻³ ·K ⁻¹
<i>D</i>	ID of tube	m	L
<i>ρ_b</i>	Density of fluid at T _b	kg/m ³	M·L ⁻³
<i>ρ_w</i>	Density of fluid at T _w	kg/m ³	M·L ⁻³
<i>μ_b</i>	Dynamic Viscosity at T _b	Pa·s	M·L ⁻¹ ·T ⁻¹
<i>μ_w</i>	Dynamic Viscosity at T _w	Pa·s	M·L ⁻¹ ·T ⁻¹
<i>k_b</i>	Thermal Conductivity at T _b	W/m·K	M·L·T ⁻³ ·K ⁻¹
<i>k_w</i>	Thermal Conductivity at T _w	W/m·K	M·L·T ⁻³ ·K ⁻¹
<i>C_{p,b}</i>	Specific Heat Capacity T _b	J/kg·K	L ² ·T ⁻² ·K ⁻¹
<i>V</i>	Velocity of fluid	m/s	L·T ⁻¹

The Buckingham Π -theorem (Munson et al., 2012) can be used to determine a generalized correlation for HTC by performing a dimensional analysis of parameters.

$$h = f(D, \rho_b, \rho_w, \mu_b, \mu_w, k_b, k_w, C_{p,b}, V) \quad (3.38)$$

By considering the dimensions discussed, six unique dimensionless Π -terms were determined.

$$\Pi_1 = f(\Pi_2, \Pi_3, \Pi_4, \Pi_5, \Pi_6) \quad (3.39)$$

In general terms:

$$\mathbf{Nu}_b = C \times x_1^{n_1} \cdot x_2^{n_2} \cdot x_3^{n_3} \cdot x_4^{n_4} \dots x_{n-1}^{n_{n-1}} \cdot x_n^{n_n} \quad (3.40)$$

or as per Table 3-8:

$$Nu_b = C \times \mathbf{Re}_b^{n_1} \cdot \mathbf{Pr}_b^{n_2} \cdot \left(\frac{\rho_w}{\rho_b}\right)^{n_3} \cdot \left(\frac{\mu_w}{\mu_b}\right)^{n_4} \cdot \left(\frac{k_w}{k_b}\right)^{n_5} \quad (3.41)$$

Table 3-8: Π -terms (Mokry et al., 2009)

Π -TERMS	DIMENSIONLESS GROUP	NAME
Π_1	$\frac{h \cdot D}{k_b}$	Nusselt Number, Nu
Π_2	$\frac{\rho_b \cdot V \cdot D}{\mu_b}$	Reynolds Number, Re
Π_3	$\frac{C_{p,b} \cdot \mu_b}{k_b}$	Prandtl Number, Pr
Π_4	$\frac{\rho_w}{\rho_b}$	Density Ratio
Π_5	$\frac{\mu_w}{\mu_b}$	Dynamic Viscosity Ratio
Π_6	$\frac{k_w}{k_b}$	Thermal Conductivity Ratio

The methodology follows three main phases, as outlined by Mokry et al. (2009):

Phase 1 – Manually determine starting exponents (n) for each term (x).

Phase 2 – Iterate to determine exponents for each term

Phase 3 – Calculate the Constant

Based upon the dimensional analysis, and all previous **Nu** correlations, the first two terms are fixed ($x_1^{n_1} = \mathbf{Re}_b^{n_1}, x_2^{n_2} = \mathbf{Pr}_b^{n_2}$). However, future dimensional analysis may result in

additional terms. At this stage, the methodology will remain in general terms, and in later sections of this paper exact terms will be described. The flow charts below (Figure 3-6 to Figure 3-8) show an overview of the phases, and their relevant steps.

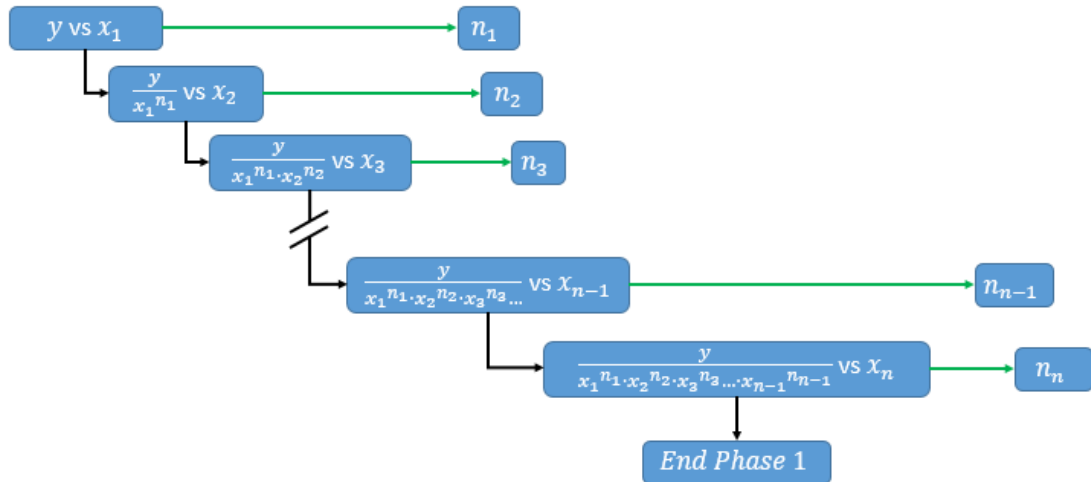


Figure 3-6: Phase 1 of Nu Correlation Development, Manually Calculate Exponents

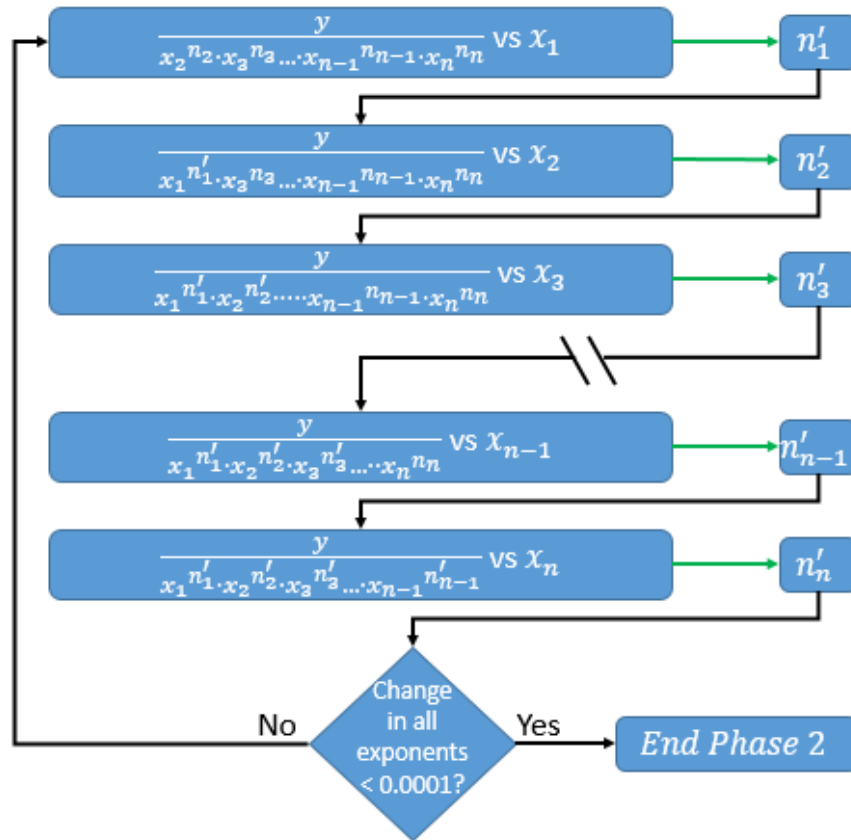


Figure 3-7: Phase 2 of Nu Correlation Development, Iterate to Finalize Exponents

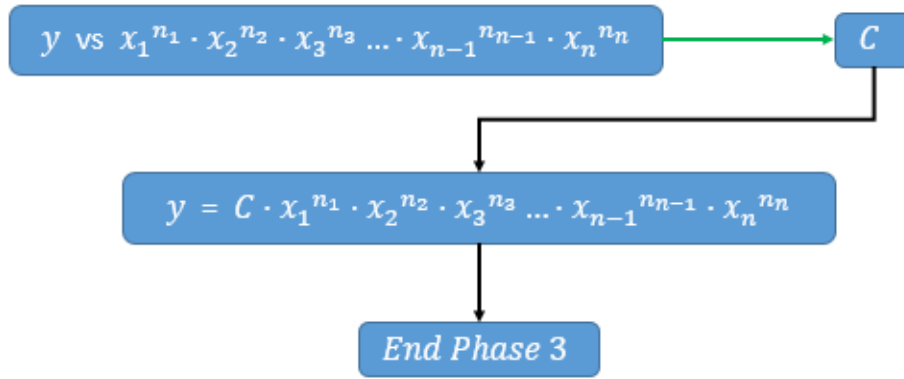


Figure 3-8: Phase 3 of Nu Correlation Development, Calculate Constant

3.3.3.1 Phase 1

The difference between Phase 1 and Phase 2 is that the exponents (n_i) all begin at 0, until they are tested.

3.3.3.1.1 Step 1

In this step, all exponents other than n_1 are set to 0 for (3.40):

In order to obtain the new value of n_1 , the following logarithmic relation is employed:

$$\text{Nu}_b = C \times x_1^{n_1} \cdot x_2^0 \cdot x_3^0 \cdot x_4^0 \dots x_{n-1}^0 \cdot x_n^0 \quad (3.42)$$

$$\begin{aligned} &\rightarrow \frac{\text{Nu}_b}{x_2^0 \cdot x_3^0 \cdot x_4^0 \dots x_{n-1}^0 \cdot x_n^0} = C \cdot x_1^{n_1} \\ &\rightarrow \log\left(\frac{\text{Nu}_b}{x_2^0 \cdot x_3^0 \cdot x_4^0 \dots x_{n-1}^0 \cdot x_n^0}\right) = \log(C) + \log(x_1^{n_1}) \\ &\rightarrow \log\left(\frac{\text{Nu}_b}{x_2^0 \cdot x_3^0 \cdot x_4^0 \dots x_{n-1}^0 \cdot x_n^0}\right) = \log(C) + n_1 \cdot \log(x_1) \\ &\rightarrow \log\left(\frac{\text{Nu}_b}{x_2^0 \cdot x_3^0 \cdot x_4^0 \dots x_{n-1}^0 \cdot x_n^0}\right) = n_1 \cdot \log(x_1) + \log(C) \end{aligned} \quad (3.43)$$

and is now of the form:

$$y = mx + b \quad (3.44)$$

To calculate m (n_1) and b (C) the following linear regression relationship as described by Brown (2000) is used:

$$m = \frac{n(\sum xy) - (\sum x)(\sum y)}{n(\sum(x^2)) - (\sum x)^2} \quad (3.45)$$

$$b = \frac{(\sum y)(\sum(x^2)) - (\sum x)(\sum xy)}{n(\sum(x^2)) - (\sum x)^2} \quad (3.46)$$

Each exponent can also be described by the R^2 parameter, a ‘goodness of fit’ parameter. Pearson’s expression can be used to determine the R^2 parameter using the formula as described by Chee (2015):

$$R^2 = \left[\frac{n(\sum xy) - (\sum x)(\sum y)}{\sqrt{[n(\sum x^2) - (\sum x)^2] \cdot [n(\sum y^2) - (\sum y)^2]}} \right]^2 \quad (3.47)$$

The larger the R^2 value, which ranges between -1 and 1, the better the fit of the data. A value of 0 means there is no correlation between the data, while -1 means a perfect negative correlation, and 1 meaning a perfect positive correlation.

A sample calculation can be found in section C.3.1.1.

3.3.3.1.2 Step 2 to n

With a value for n_1 determined, the next value to determine is n_2 , while all other values remain at 0.

By repeating the same process as in 3.3.3.1.1, the value of n_2 can be determined after setting it to an initial value of 1.

$$\frac{\mathbf{Nu}_b}{x_1^{n_1} \cdot x_3^0 \cdot x_4^0 \dots x_{n-1}^0 \cdot x_n^0} = C \cdot x_2^{n_2} \quad (3.48)$$

$$\begin{aligned} \rightarrow \log \left(\frac{\mathbf{Nu}_b}{x_1^{n_1} \cdot x_3^0 \cdot x_4^0 \dots x_{n-1}^0 \cdot x_n^0} \right) &= \log(C) + \log(x_2^{n_2}) \\ \rightarrow \log \frac{\mathbf{Nu}_b}{x_1^{n_1} \cdot x_3^0 \cdot x_4^0 \dots x_{n-1}^0 \cdot x_n^0} &= n_2 \cdot \log(x_2) + \log(C) \end{aligned} \quad (3.49)$$

As this is now in the same form as (3.44), equations (3.45) and (3.46) can be used to determine n_2 .

This process can be repeated until all exponential terms have been calculated.

$$\log \left(\frac{\mathbf{Nu}_b}{x_1^{n_1} \cdot x_2^{n_2} \cdot x_3^{n_3} \cdot x_4^{n_4} \dots x_{n-1}^{n_{n-1}}} \right) = n_n \cdot \log(x_n) + \log(C) \quad (3.50)$$

A sample calculation can be found in section C.3.1.2.

3.3.3.2 Phase 2

The second phase is identical to the first phase, with the major difference being that all exponents now have values, and are not set to 0 or 1. The cycle is described by the equations below:

$$\log \frac{\mathbf{Nu}_b}{x_2^{n_2} \cdot x_3^{n_3} \cdot x_4^{n_4} \dots x_{n-1}^{n_{n-1}} \cdot x_n^{n_n}} = n_1 \cdot \log(x_1) + \log(C) \quad (3.51)$$

$$\log \frac{\mathbf{Nu}_b}{x_1^{n_1} \cdot x_3^{n_3} \cdot x_4^{n_4} \dots x_{n-1}^{n_{n-1}} \cdot x_n^{n_n}} = n_2 \cdot \log(x_2) + \log(C) \quad (3.52)$$

$$\log \frac{\mathbf{Nu}_b}{x_1^{n_1} \cdot x_2^{n_2} \cdot x_3^{n_3} \cdot x_4^{n_4} \dots x_n^{n_n}} = n_{n-1} \cdot \log(x_{n-1}) + \log(C) \quad (3.53)$$

$$\log \frac{\mathbf{Nu}_b}{x_1^{n_1} \cdot x_2^{n_2} \cdot x_3^{n_3} \cdot x_4^{n_4} \dots x_{n-1}^{n_{n-1}}} = n_n \cdot \log(x_n) + \log(C) \quad (3.50)$$

Equations (3.51) to (3.53), and (3.50) are of the same type of (3.44), and therefore equations (3.45) and (3.46) can be used to determine each exponential term (from n_1 to n_n).

Phase 2 is an iterative process, repeating the cycle of equations (3.51) to (3.53), and (3.50). From one cycle to the next the exponential terms change as they converge to one unique value.

This cycle is repeated until all exponential values (from n_1 to n_n) converge to a unique solution (within ± 0.0001). Once this is accomplished, Phase 2 is complete.

3.3.3.3 Phase 3

Finally, the Constant for the entire equation can be calculated without the logarithmic function:

$$\mathbf{Nu}_b = C \cdot (x_1^{n_1} \cdot x_2^{n_2} \cdot x_3^{n_3} \cdot x_4^{n_4} \dots x_{n-1}^{n_{n-1}} \cdot x_n^{n_n}) \quad (3.40)$$

which is of the same type as (3.44), with $b = 0$, and therefore equations (3.45) and (3.46) can be used to calculate the constant (C).

3.3.4 Sheath Temperature

The surface temperature of the sheath exterior is determined by the wall temperature predictions as outlined in section 3.3.2.1. To calculate the temperature of the interior of the sheath, a simple relation can be determined from the thermal conductivity first principles formula (Bergman et al., 2017):

$$\begin{aligned}
 \dot{Q} &= -kA \frac{dT}{dx} & (3.54) \\
 \rightarrow \text{for a cylinder} \rightarrow \dot{Q} &= -kA \frac{dT}{dr} = -k(2\pi rL) \frac{dT}{dr} \\
 \rightarrow \int_{r_{int}}^{r_{ext}} \frac{\dot{Q}}{r} dr &= \int_{T_{int}}^{T_{ext}} -k_{A625}(2\pi L) dT \rightarrow \dot{Q} \int_{r_{int}}^{r_{ext}} \frac{1}{r} dr = -k_{A625}(2\pi L) \int_{T_{int}}^{T_{ext}} dT \\
 \rightarrow \dot{Q} [\ln r_{ext} - \ln r_{int}] &= -k_{A625}(2\pi L) [T_{ext} - T_{int}] \\
 \rightarrow \dot{Q} \cdot \ln \left(\frac{r_{ext}}{r_{int}} \right) &= k_{A625}(2\pi L) [T_{int} - T_{ext}] \\
 \rightarrow T_{int} = T_{ext} + \frac{\dot{Q}}{k_{A625}(2\pi L)} \cdot \ln \left(\frac{r_{ext}}{r_{int}} \right) &= T_{ext} + \frac{q \cdot 2\pi L r_{ext}}{k_{A625}(2\pi L)} \cdot \ln \left(\frac{r_{ext}}{r_{int}} \right) \\
 T_{int} = T_{ext} + \frac{q \cdot r_{ext}}{k_{A625}} \cdot \ln \left(\frac{r_{ext}}{r_{int}} \right) & \quad (3.55)
 \end{aligned}$$

From section 2.2.3 the thermal conductivity for Alloy 625 is described as:

$$k_{A625} \left(\frac{W}{m \cdot K} \right) = 9.7116 + 0.0176 \cdot T, \quad T \text{ in } ^\circ C \quad (2.1)$$

3.3.5 Fuel Centreline Temperature

To determine the fuel centreline temperature, the energy generation must be taken into account. From Bergman et al. (2017), the conservation of energy on a rate basis is expressed as:

$$Energy_{in} + Energy_{generated} - Energy_{out} = Energy_{stored} \quad (3.56)$$

Fourier's law is expressed as:

$$q_x = -k \frac{\partial T}{\partial x} \quad (3.57)$$

Combining (3.56) and (3.57), in steady state operations for cylindrical coordinates, is expressed as:

$$\frac{1}{r} \frac{\partial}{\partial r} \left(kr \frac{\partial T}{\partial r} \right) + \frac{1}{r^2} \frac{\partial}{\partial \phi} \left(k \frac{\partial T}{\partial \phi} \right) + \frac{\partial}{\partial z} \left(k \frac{\partial T}{\partial z} \right) + \dot{Q} = 0 \quad (3.58)$$

As the interest is in one dimension (the radial dimension), some terms can be cancelled:

$$\frac{1}{r} \frac{\partial}{\partial r} \left(kr \frac{\partial T}{\partial r} \right) + \dot{Q}(W) = 0 \quad (3.59)$$

With some rearranging and evaluating the first integral:

$$\partial T (k) = \partial r \left(-\dot{Q}r + \frac{C_1}{r} \right) \quad (3.60)$$

As Thermal conductivity is not constant, (3.60) and (2.2) are combined and expressed as below:

$$\int \left(\left[\frac{100}{6.548 + 23.533 \cdot \frac{T}{1000}} \right] + \left[\frac{6400}{\left(\frac{T}{1000} \right)^{2.5}} \right] \cdot e^{\left(-\frac{16350}{T} \right)} \right) dt = \int \left(-\dot{Q}r + \frac{C_1}{r} \right) dr \quad (3.61)$$

While the right side of this expression is can be readily solved, the left side is not.

To determine the fuel centreline temperature, an approximation to account for the variable Thermal Conductivity is made by dividing the fuel pellet into layers 0.5 mm in thickness, moving to thinner layers closer to the centreline. This allows the thermal conductivity to remain as a constant, while being recalculated for each layer.

Figure 3-9 illustrates the fuel rod design, with the sheath and attached ribs in steel, and layers of the fuel rod colored.

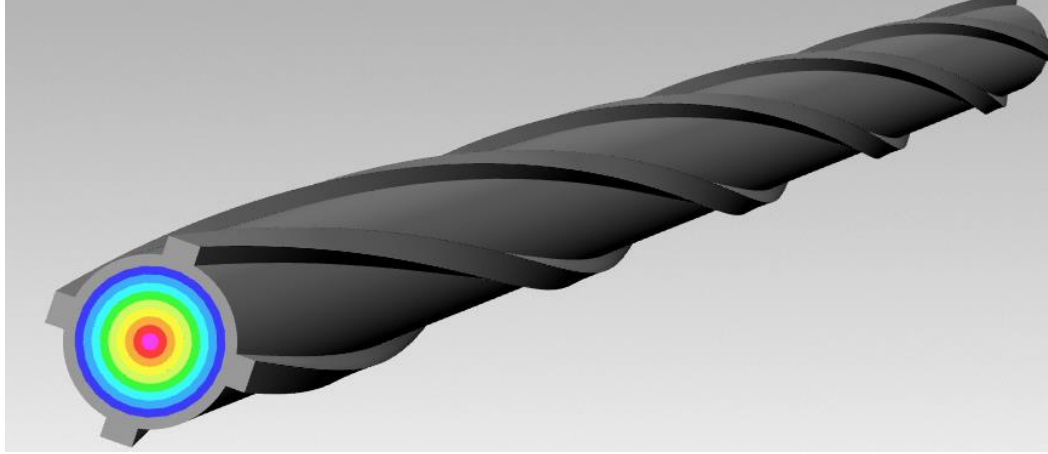


Figure 3-9: Fuel Rod Centreline Temperature

It is convenient to use the energy generation term to calculate the fuel rod centreline temperature. Under steady conditions, the rate of heat transfer from the system must equal to the rate of energy generation. As stated by Cengel and Ghajar (2015):

$$\dot{Q} = \dot{g}V \quad (3.62)$$

Therefore, from (3.57) for cylindrical coordinates by Cengel and Ghajar (2015):

$$-kA \frac{dT}{dr} = \dot{g}V \quad (3.63)$$

Treating thermal conductivity as constant for this process, and expanding terms:

$$\rightarrow -k(2\pi rL) \frac{dT}{dr} = \dot{g}(\pi r^2 L) \rightarrow dT = -\frac{\dot{g}}{2k} r dr \quad (3.64)$$

Integrating from an inner radius to an outer radius and evaluating:

$$\int_{T(r=0)}^{T(r=i)} dT = -\frac{\dot{g}}{2k} \int_{r_o}^{r_i} r dr \rightarrow T_i - T_o = -\frac{\dot{g}}{4k} (r_i^2 - r_o^2)$$

Rearranging, and a final expression is derived:

$$T_i = T_o + \frac{\dot{g}}{4k_{UO_2}} (r_o^2 - r_i^2) \quad (3.65)$$

Equation (3.65) can then be used to determine the temperature inside of the first layer.

Based on this T , a new Thermal Conductivity can be calculated with (2.2), and a new internal T can be calculated. This process is repeated until the T calculated remains stable and does not increase ($>0.1^{\circ}\text{C}$), which, is taken as the true fuel centreline T .

An example of the layering for the 7-rod fuel size (OD = 4.5 mm) is listed in Table 3-9.

Table 3-9: Layer Sizes for $T_{\text{fuel CL}}$ (7-rod Parameters example)

Layer	Layer Size OD (mm)	Layer Size ID (mm)		Layer	Layer Size OD (mm)	Layer Size ID (mm)
1	4.5	4.0		6	2.0	1.5
2	4.0	3.5		7	1.5	1.0
3	3.5	3.0		8	1.0	0.5
4	3.0	2.5		9	0.5	0.1
5	2.5	2.0		10	0.1	0.01

4 RESULTS

4.1 SPECIFICS OF THERMOPHYSICAL PROPERTIES OF SCW COMPARED TO SUBCRITICAL WATER

Figure 4-1 through Figure 4-9 show selected thermophysical properties for two categories of water; **(a)** Sub-critical water at the pressures listed in Table 2-1 for typical Gen II/III/III+ reactor pressures, and **(b)** critical and SC pressures used in the 7-rod dataset by Razumovskiy et al. (2008).

Of importance to SCWR designs is the continuous property changes, as opposed to the jump in properties when compared with sub-critical due to boiling. In addition, the peak experienced in specific heat capacity allows for SCWR to take advantage of the ability for SCW to store tremendous amounts of energy when close to the pc and critical point. While boiling is not an issue and C_p peaks while crossing the pc point, properties such as density, thermal conductivity, and dynamic viscosity all experience significant reductions that can lead to a DHT regime.

All properties shown in this section were obtained using NIST REFPROP 10.0 (Lemmon et al., 2018).

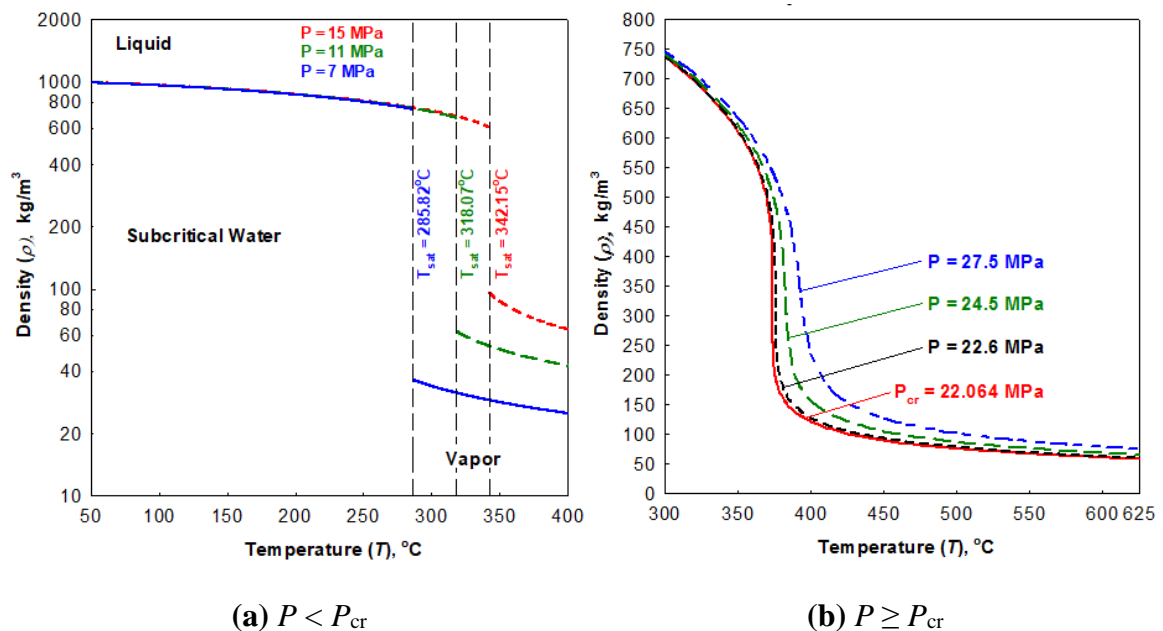


Figure 4-1: Density of Water, Sub-critical to SC Pressures

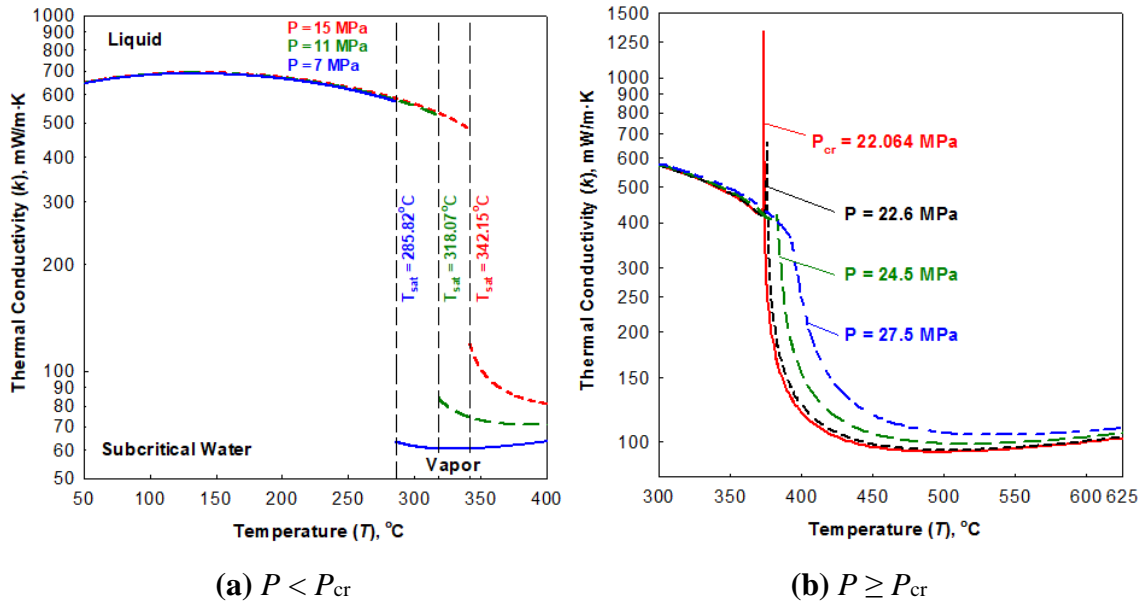


Figure 4-2: Thermal Conductivity of Water, Sub-critical to SC Pressures

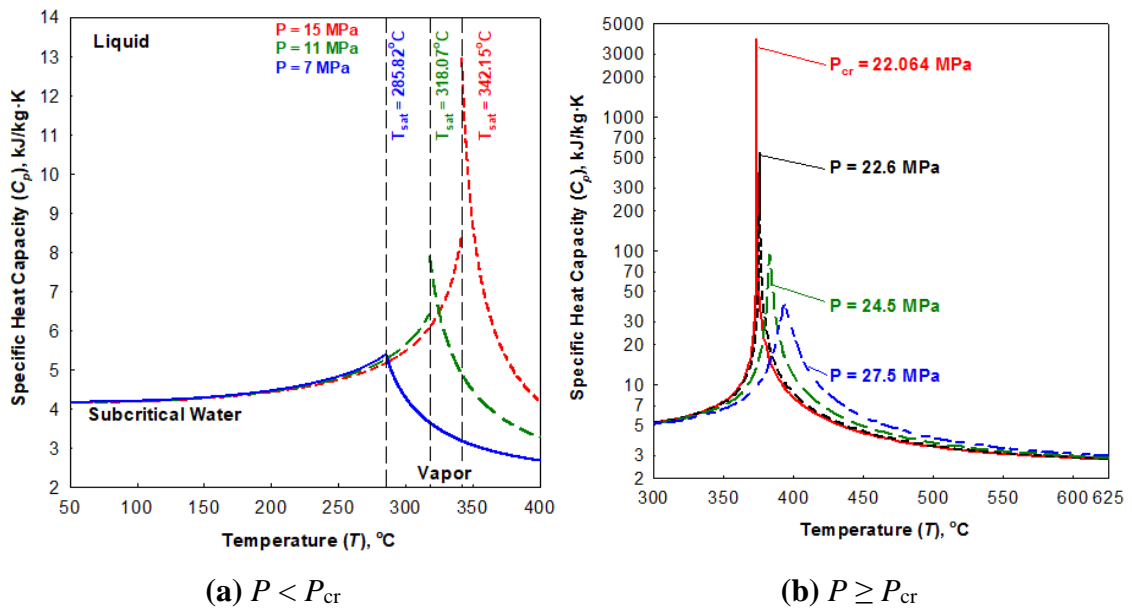


Figure 4-3: Specific Heat Capacity of Water, Sub-critical to SC Pressures

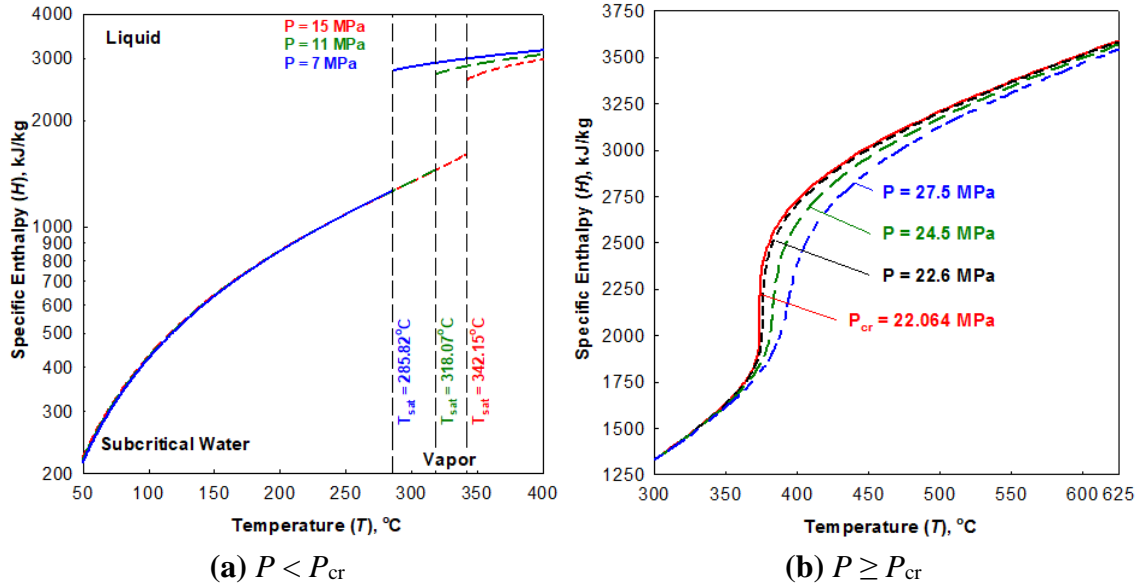


Figure 4-4: Specific Enthalpy of Water, Sub-critical to SC Pressures

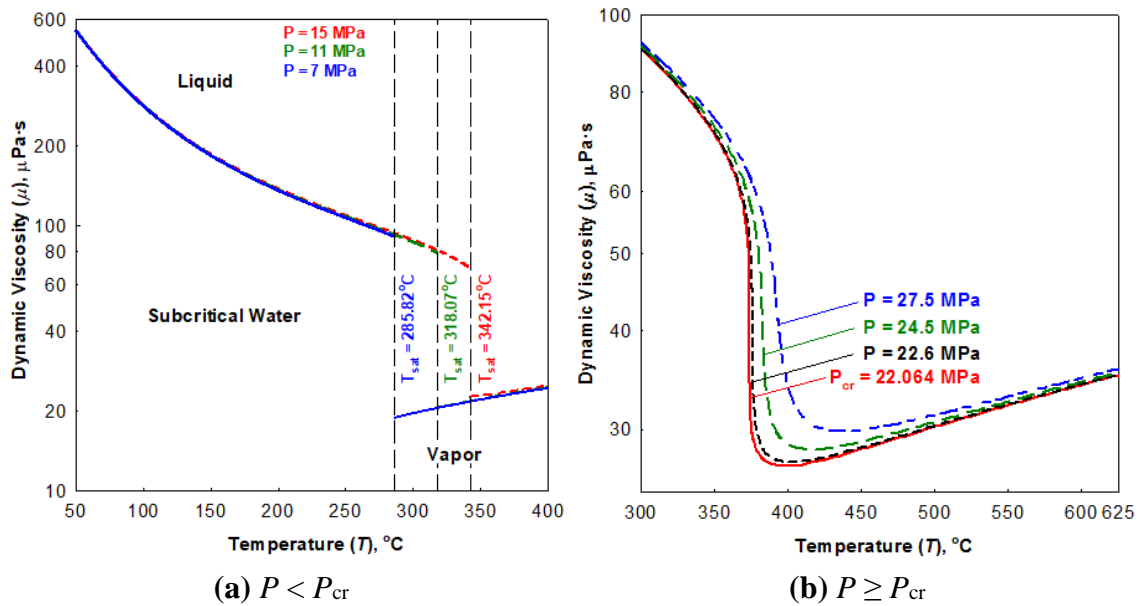


Figure 4-5: Dynamic Viscosity of Water, Sub-critical to SC Pressures

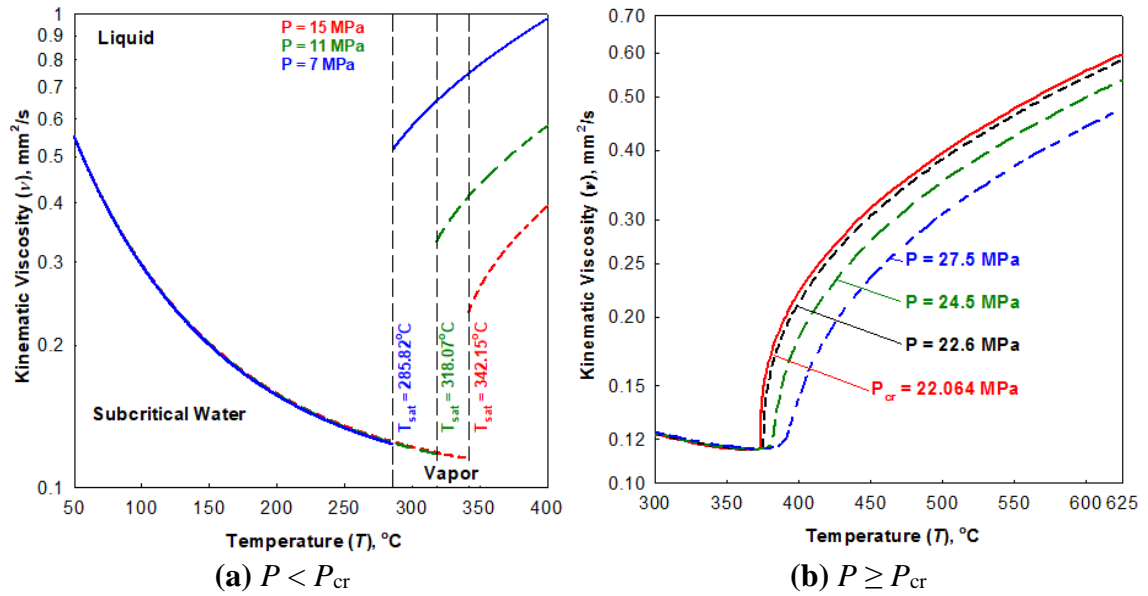


Figure 4-6: Kinematic Viscosity of Water, Sub-critical to SC Pressures

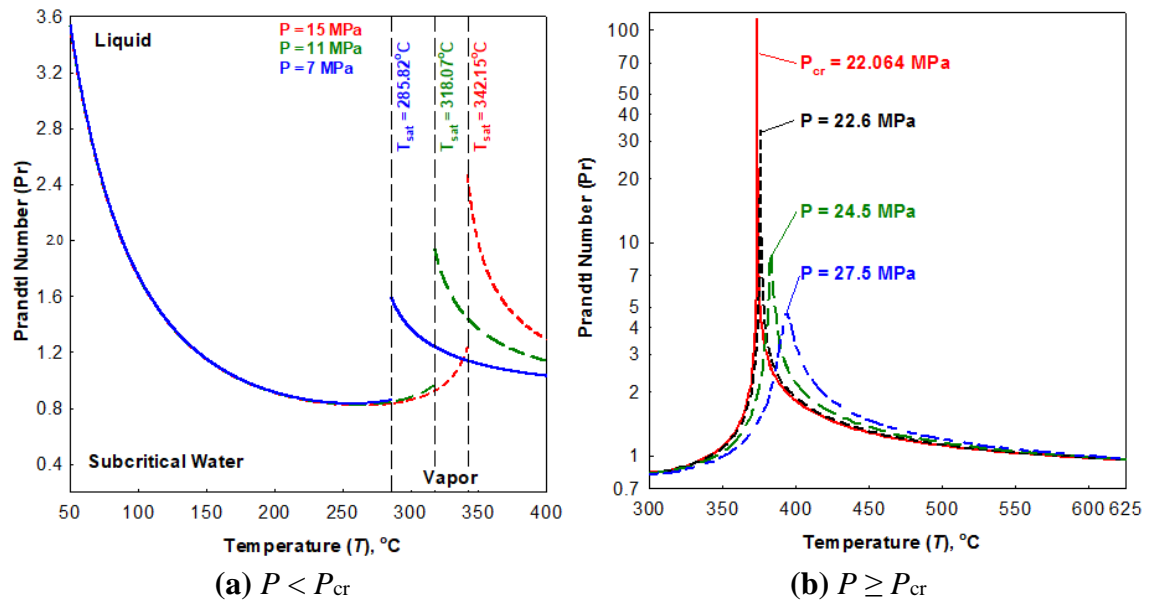


Figure 4-7: Prandtl Number of Water, Sub-critical to SC Pressures

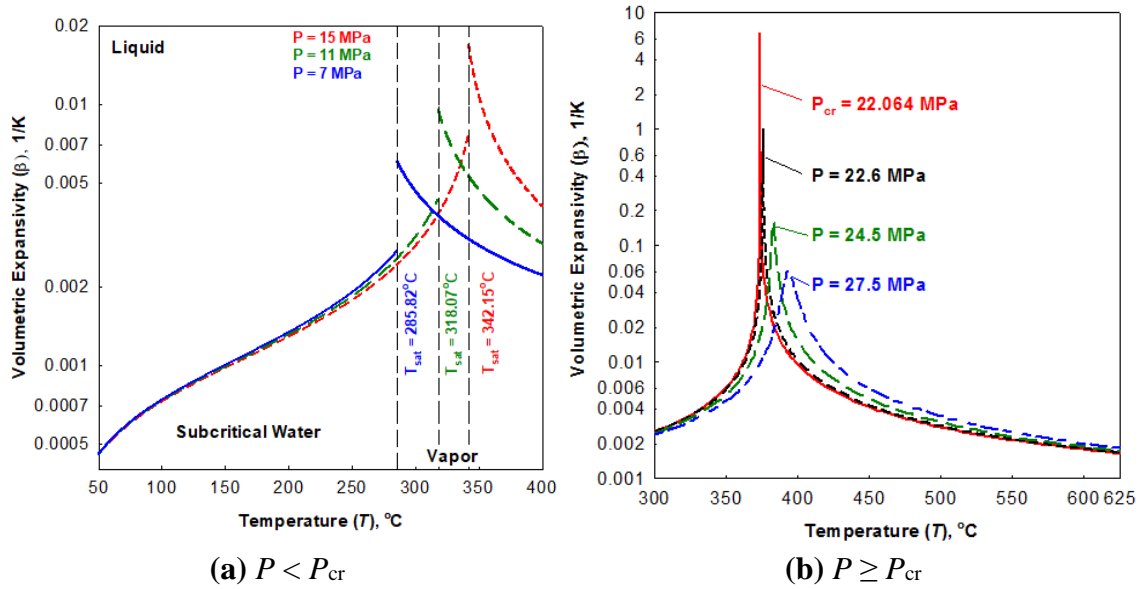


Figure 4-8: Volumetric Expansivity of Water, Sub-critical to SC Pressures

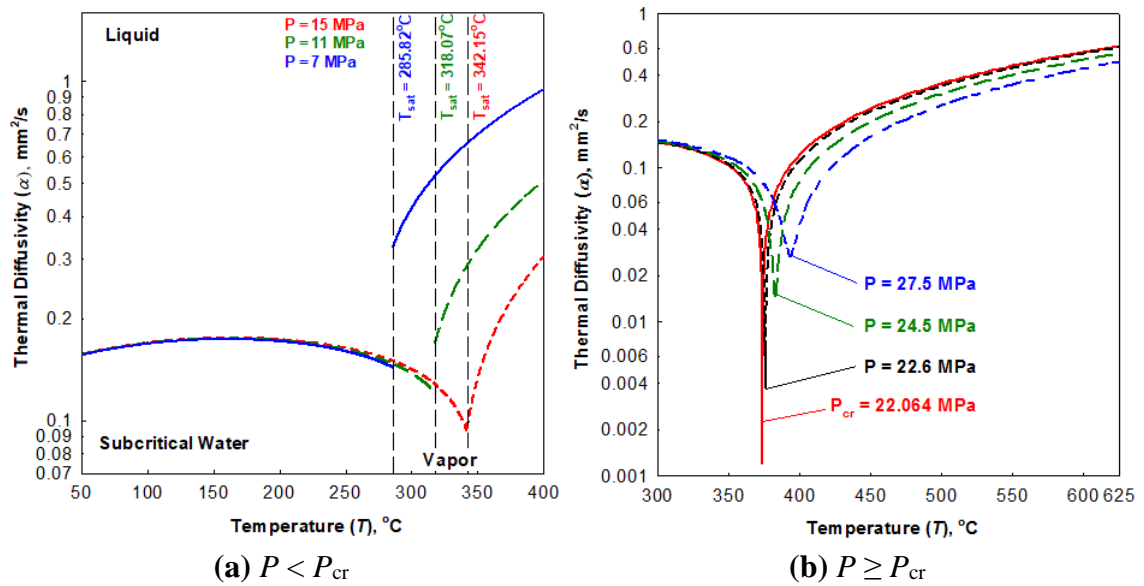


Figure 4-9: Thermal Diffusivity of Water, Sub-critical to SC Pressures

4.2 NUMERICAL ANALYSIS AND COMPARISONS

4.2.1 7-ROD BUNDLE

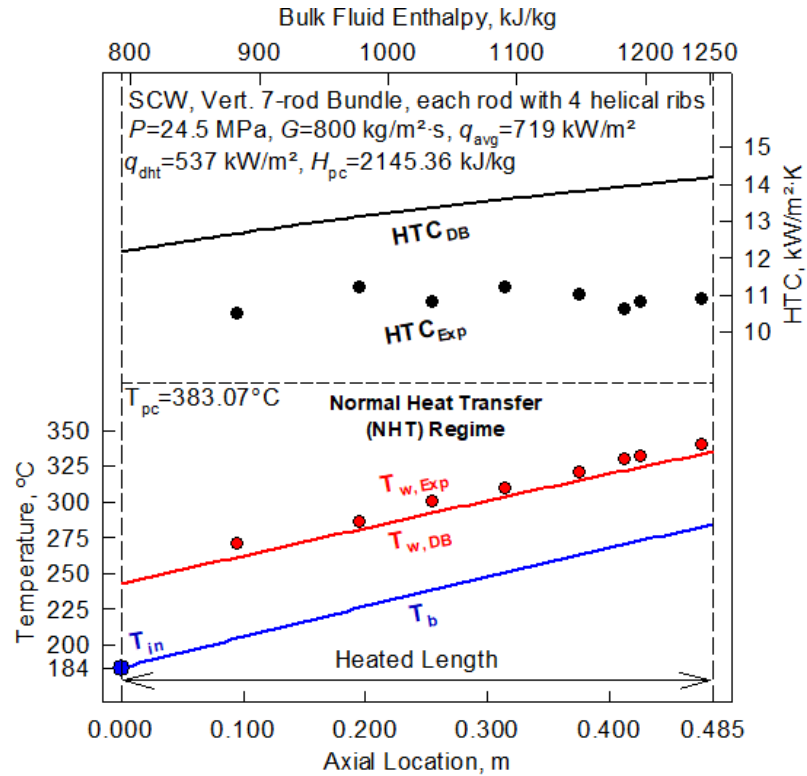
4.2.1.1 Results

The data obtained from Razumovskiy et al. (2008) consists of 60 data points from 8 tests, obtained with the test apparatus as described in section 3.1.1. Listed below in Figure 4-10 through Figure 4-17 are shown the eight tests (trials) for the 7-rod datasets. These figures were created to show the bulk fluid temperature calculated using the reduction parameters from Table 3-3 and Table 3-6, the outside-wall temperatures (T_w) are calculated from the inside wall temperatures obtained through thermocouples, the calculated HTC, and the Dittus-Boelter Eq. (1) predictions for both T_w and HTC, using properties calculated using NIST REFPROP 10.0 (Lemmon et al., 2018). Also listed is the q_{dht} as predicted by Mokry et al. from Table 2-4, as well as the pc temperatures (T_{pc}).

The basic thermophysical properties for SCW based on the bulk-fluid temperature (T_b) and the wall temperature (T_w) are also shown with each trial. These properties are shown across the heated length for each, and are calculated using NIST REFPROP 10.0 (Lemmon et al., 2018).

Each trial along with the associated thermophysical properties is shown. Then a comparison of these trials is shown with each trial having the same T and HTC axis to allow for direct comparisons of each graph.

Finally, some observed trends are listed are also listed in reference to the HTC, T_w , and T_b profiles, the trends of the ratio of q_{avg}/q_{dht} and this effect on the trials, and the effects of changing flowrate and pressure.



(a) HTC, T_w , and T_b profiles along heated length of central rod

$$P=24.5 \text{ MPa}, G=800 \text{ kg/m}^2\cdot\text{s}, q_{avg}/q_{dht} = 1.34$$

Symbols = Experimental Data; Curves = Calculated Values; (DB – Dittus-Boelter)

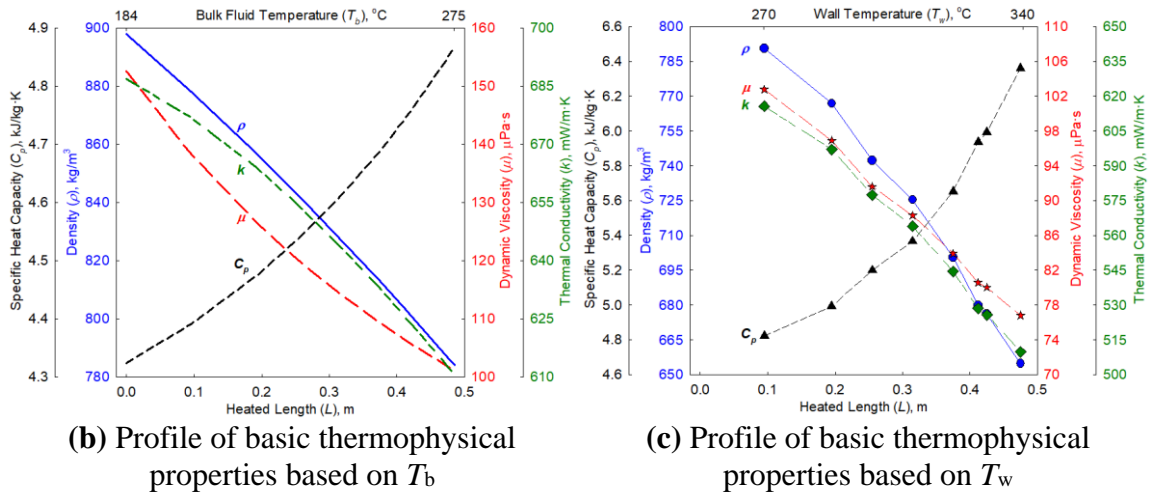
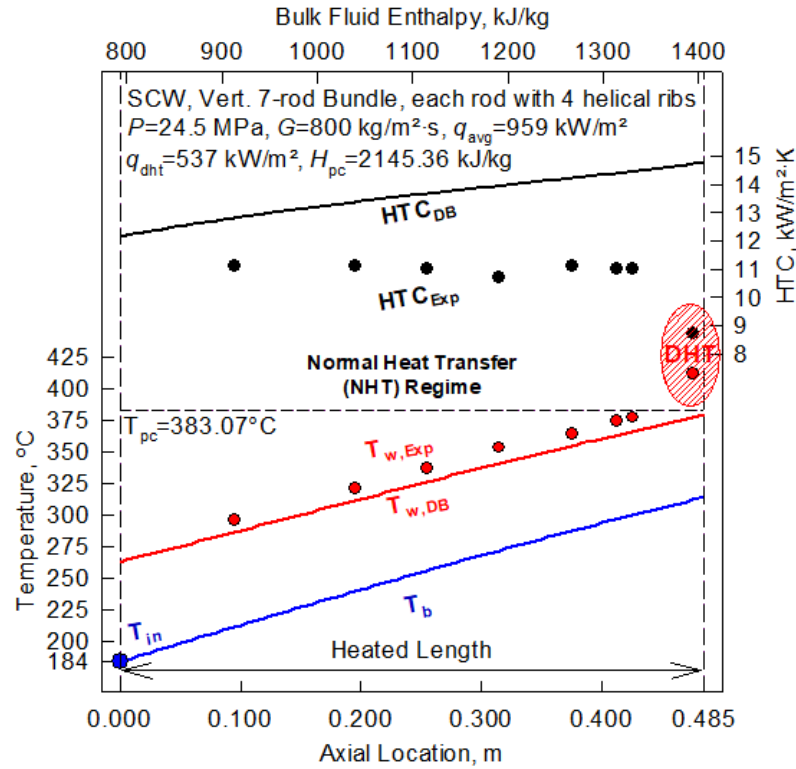


Figure 4-10: Trial #1 – HT Profile and Thermophysical Properties, 7-rod

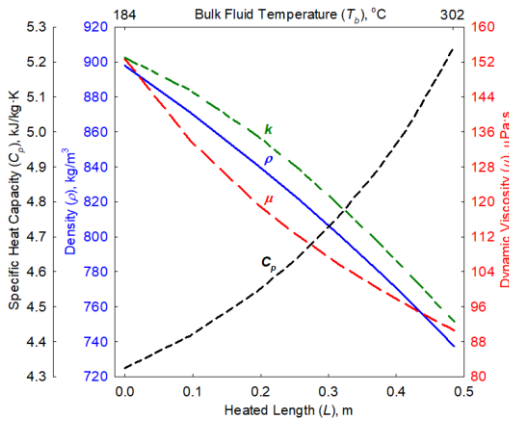
Trial #1 in Figure 4-10 (a) experienced only the NHT regime. The ratio of q_{avg}/q_{dht} is 1.34, and the temperature profile is stable. The inlet T_b is low relative to the T_{pc} , leading to the T_b and T_w being below the T_{pc} for the entire heated length.



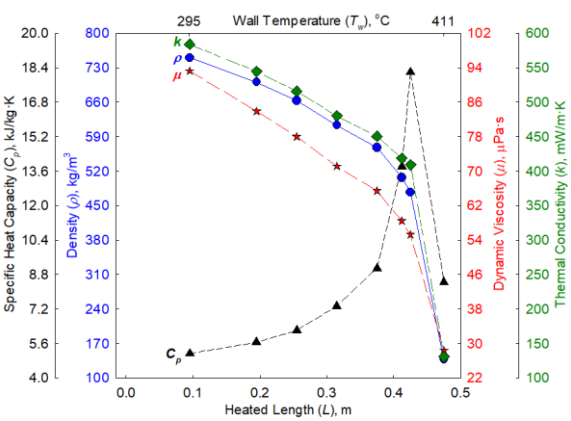
(a) HTC, T_w , and T_b profiles along heated length of central rod

$P=24.5$ MPa, $G=800$ kg/m²·s, $q_{avg}/q_{dht} = 1.79$

Symbols = Experimental Data; Curves = Calculated Values; (DB – Dittus-Boelter)



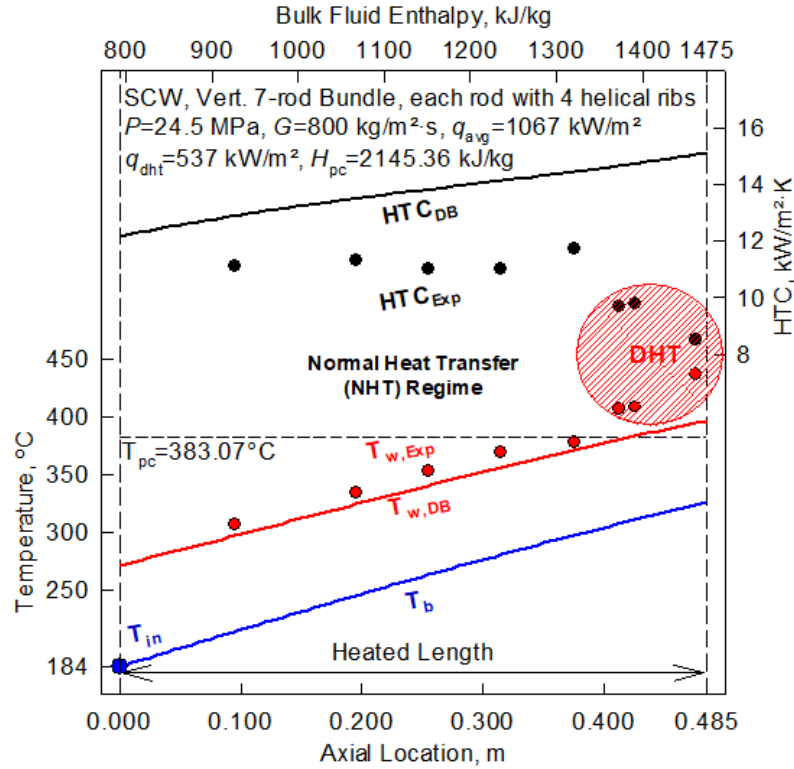
(b) Profile of basic thermophysical properties based on T_b



(c) Profile of basic thermophysical properties based on T_w

Figure 4-11: Trial #2 – HT Profile and Thermophysical Properties, 7-rod

Trial #2 in Figure 4-11 (a) experienced the DHT and NHT regimes. The ratio of q_{avg}/q_{dht} is 1.79. T_b remains below T_{pc} for the entire trial. However, with the higher q_{avg} , the T_w crosses the pc point at the end of the heated length, leading to a DHT regime as soon as the SCW enters the gas-like region based on T_w thermophysical properties.



(a) HTC, T_w , and T_b profiles along heated length of central rod

$$P=24.5 \text{ MPa}, G=800 \text{ kg/m}^2\cdot\text{s}, q_{avg}/q_{dht} = 1.99$$

Symbols = Experimental Data; Curves = Calculated Values; (DB – Dittus-Boelter)

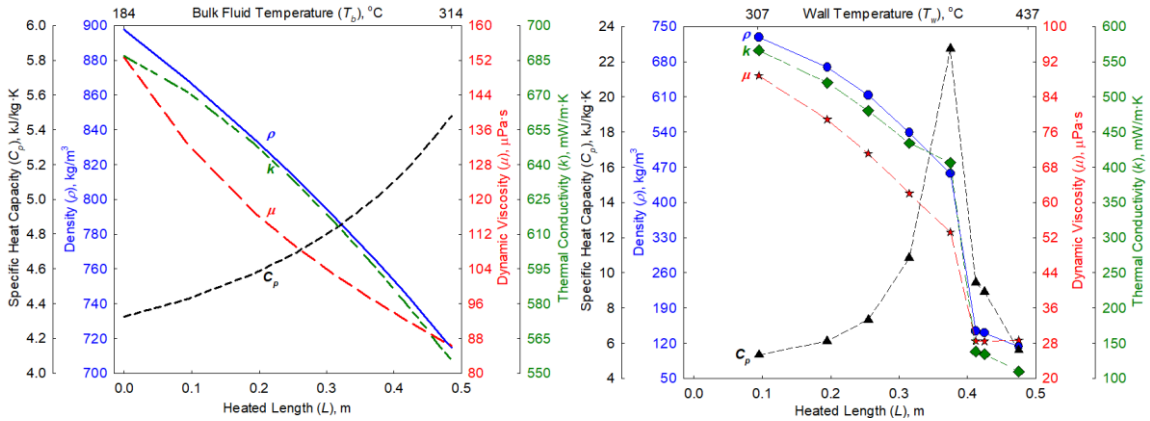
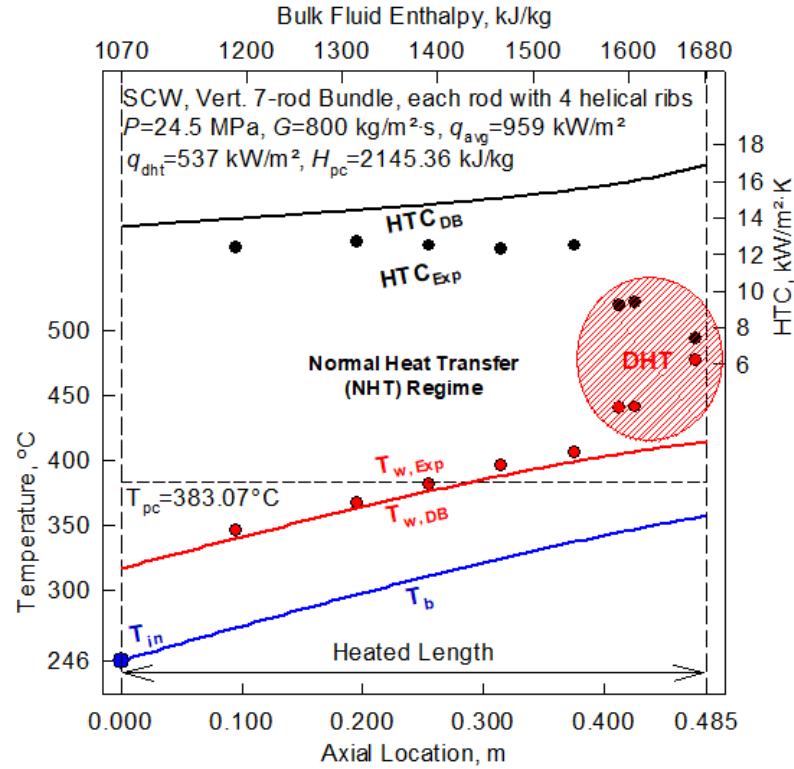


Figure 4-12: Trial #3 – HT Profile and Thermophysical Properties, 7-rod

Trial #3 in Figure 4-12 (a) experienced the DHT and NHT regimes. The ratio of q_{avg}/q_{dht} is 1.99. T_b remains below T_{pc} for the entire trial, while T_w crosses the pc point earlier, and with a longer DHT regime, than Trial #2. The DHT begins as soon as the SCW enters the gas-like region based on T_w thermophysical properties.



(a) HTC, T_w , and T_b profiles along heated length of central rod

$$P=24.5 \text{ MPa}, G=800 \text{ kg/m}^2\cdot\text{s}, q_{avg}/q_{dht} = 1.79$$

Symbols = Experimental Data; Curves = Calculated Values; (DB – Dittus-Boelter)

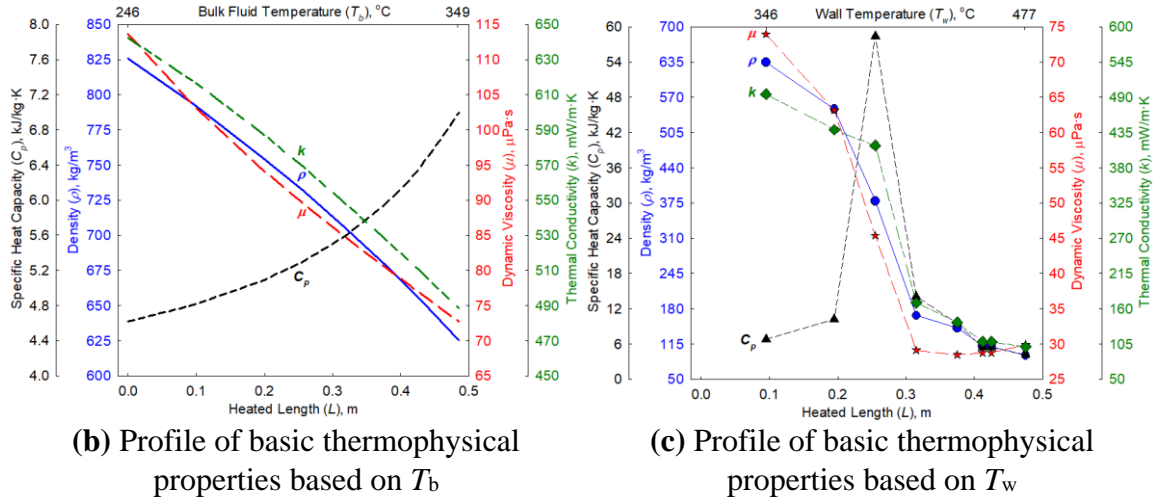
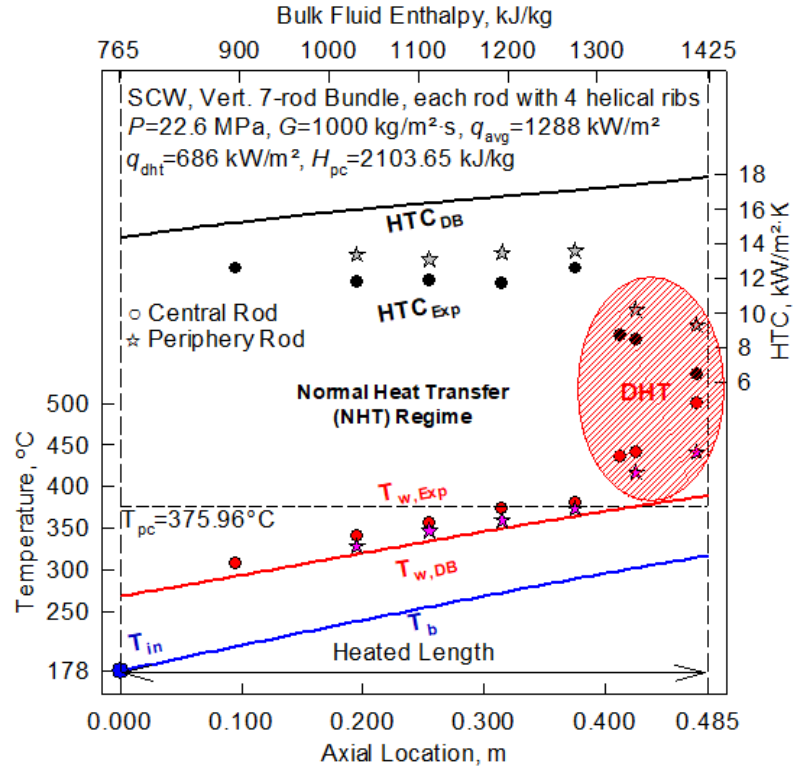


Figure 4-13: Trial #4 – HT Profile and Thermophysical Properties, 7-rod

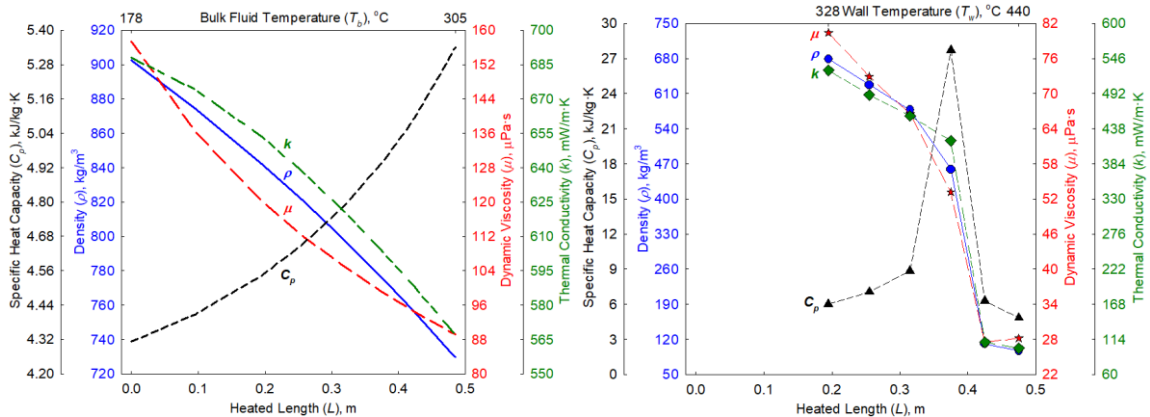
Trial #4 in Figure 4-13 experiences the DHT and NHT regimes, and only differs from Trial #2 with a higher inlet T_b (same G and ratio of q_{avg}/q_{dht}). T_b still remains below T_{pc} for the entire trial, while T_w crosses the pc point earlier, and with a longer DHT regime, than Trial #2. However, the DHT begins after the SCW has entered the gas-like region based on T_w thermophysical properties.



(a) HTC, T_w , and T_b profiles along heated length of periphery rod

$P=22.6$ MPa, $G=1000$ kg/m²·s, $q_{avg}/q_{dht} = 1.88$

Symbols = Experimental Data; Curves = Calculated Values; (DB – Dittus-Boelter)

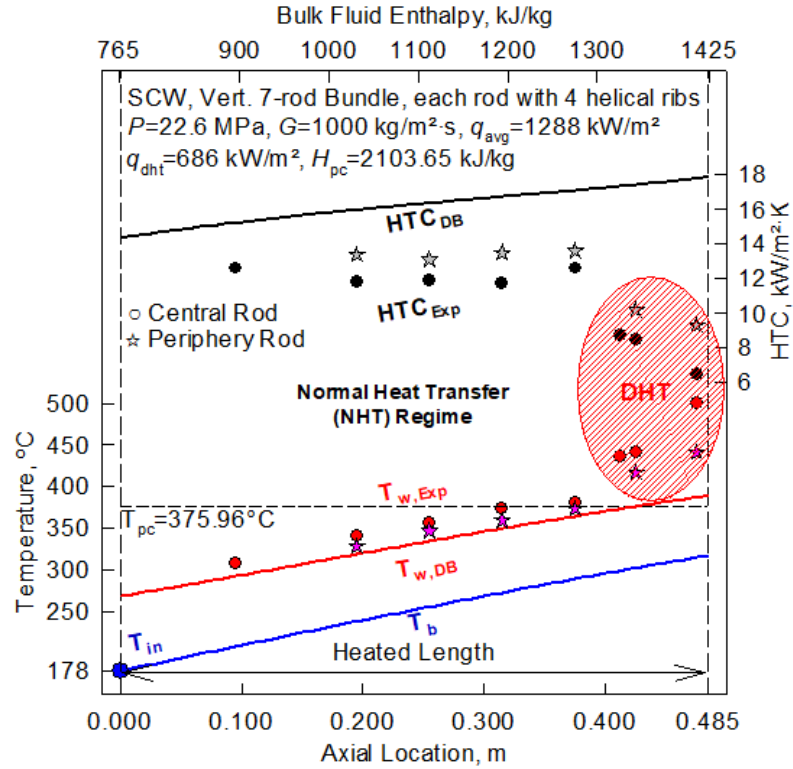


(b) Profile of basic thermophysical properties based on T_b

(c) Profile of basic thermophysical properties based on T_w

Figure 4-14: Trial #5 – HT Profile and Thermophysical Properties, 7-rod

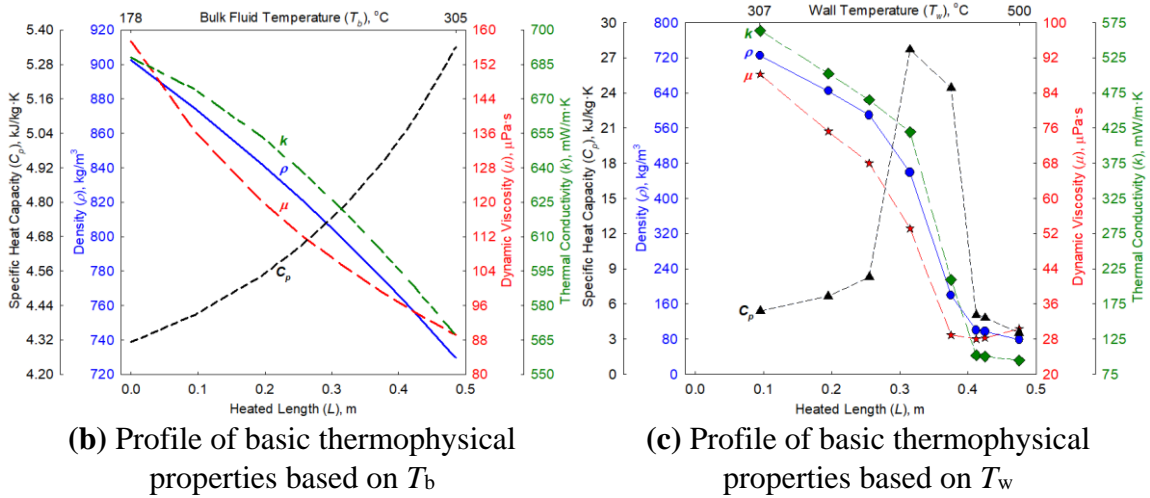
Trial #5 in Figure 4-14 (a) experienced the DHT and NHT regimes. The ratio of q_{avg}/q_{dht} is 1.88. T_b remains below T_{pc} for the entire trial, while T_w crosses the pc point near the end of the heated length. The DHT begins as soon as the SCW enters the gas-like region based on T_w thermophysical properties. Trial #5 (peripheral rods) had two less thermocouple location readings than Trial #6 (central rod).



(a) HTC, T_w , and T_b profiles along heated length of central rod

$$P=22.6 \text{ MPa}, G=1000 \text{ kg/m}^2 \cdot \text{s}, q_{\text{avg}}/q_{\text{dht}} = 1.88$$

Symbols = Experimental Data; Curves = Calculated Values; (DB – Dittus-Boelter)

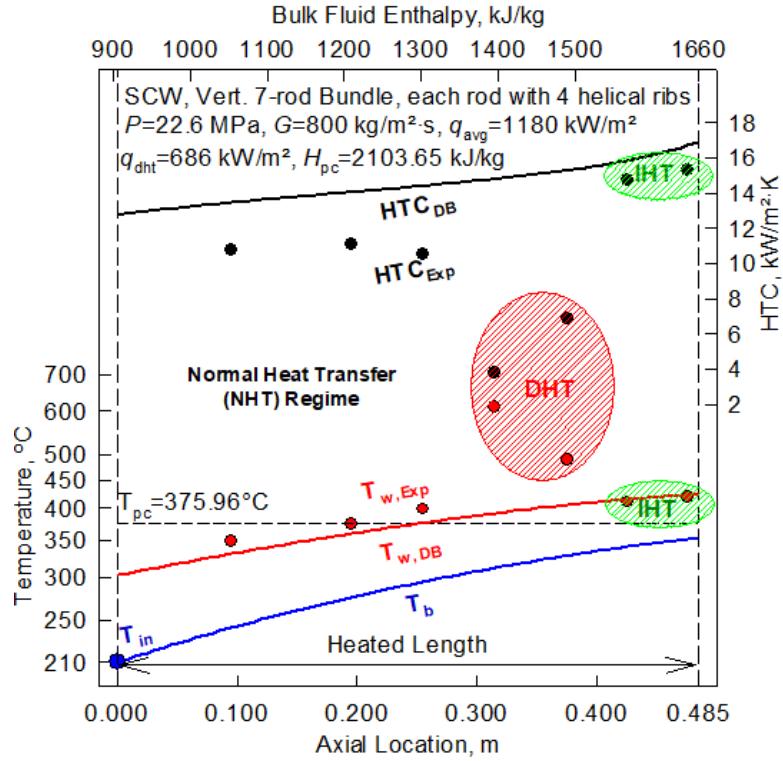


(b) Profile of basic thermophysical properties based on T_b

(c) Profile of basic thermophysical properties based on T_w

Figure 4-15: Trial #6 – HT Profile and Thermophysical Properties, 7-rod

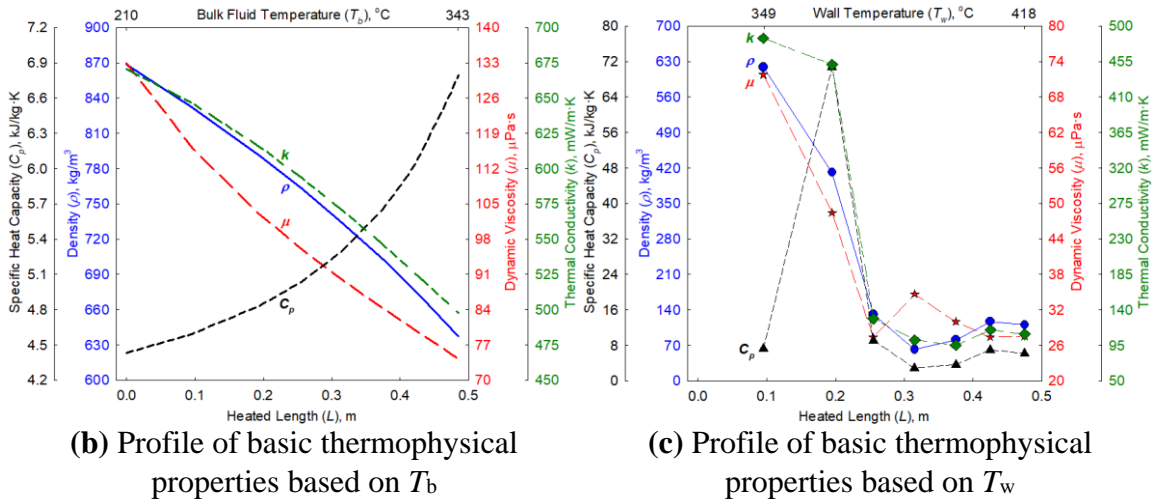
Trial #6 in Figure 4-15 (a) experienced the DHT and NHT regimes. The ratio of $q_{\text{avg}}/q_{\text{dht}}$ is 1.88. T_b remains below T_{pc} for the entire trial, while T_w crosses the pc point near the end of the heated length. The DHT begins just after the SCW enters the gas-like region, with the C_p beyond the peak, based on T_w thermophysical properties.



(a) HTC, T_w , and T_b profiles along heated length of central rod

$P=22.6$ MPa, $G=800$ kg/m²·s, $q_{avg}/q_{dht} = 2.20$

Symbols = Experimental Data; Curves = Calculated Values; (DB – Dittus-Boelter)

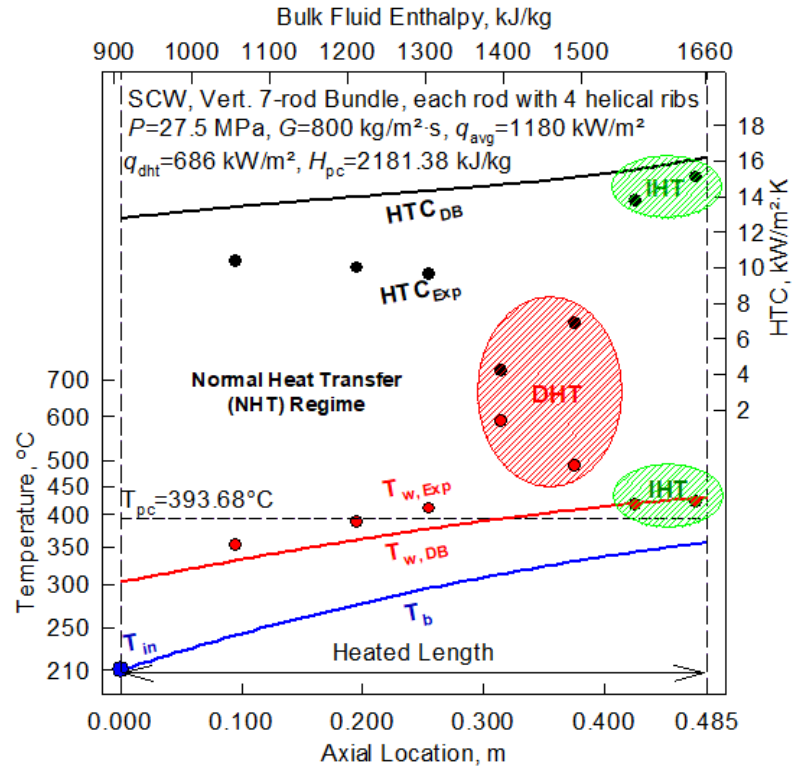


(b) Profile of basic thermophysical properties based on T_b

(c) Profile of basic thermophysical properties based on T_w

Figure 4-16: Trial #7 – HT Profile and Thermophysical Properties, 7-rod

Trial #7 in Figure 4-16 (a) experienced all 3 regimes (DHT/NHT/IHT). The ratio of q_{avg}/q_{dht} is 2.20. T_b remains below T_{pc} for the entire trial, while T_w crosses the pc point near the middle of the heated length. The DHT begins after the SCW enters the gas-like region, based on T_w thermophysical properties. The DHT regime results in a drop in HTC ($> 50\%$) and spike in T_w (+ ~200°C). An IHT regime follows with an increased HTC and lower T_w .



(a) HTC, T_w , and T_b profiles along heated length of central rod

$P=27.5$ MPa, $G=800$ kg/m²·s, $q_{avg}/q_{dht} = 2.20$

Symbols = Experimental Data; Curves = Calculated Values; (DB – Dittus-Boelter)

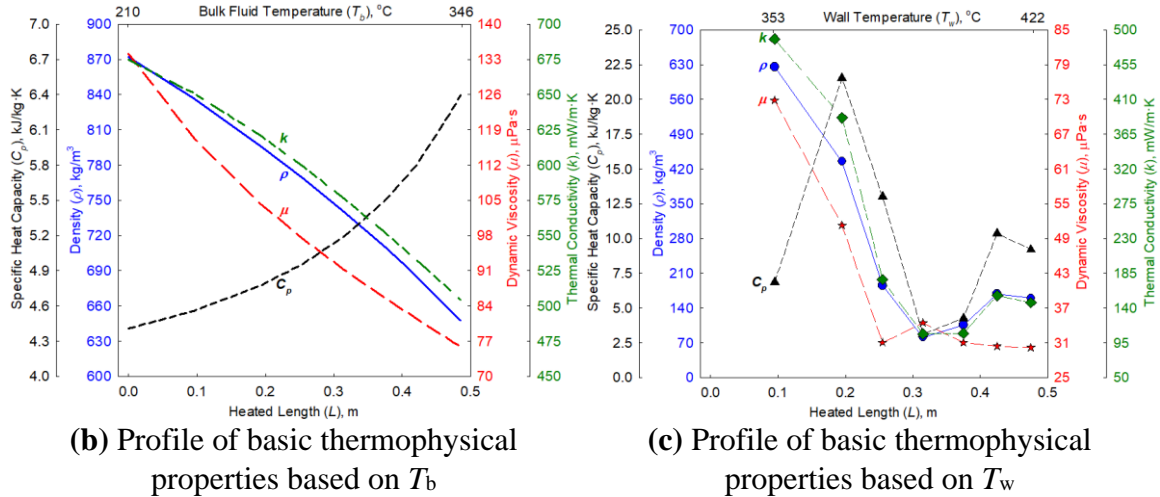


Figure 4-17: Trial #8 – HT Profile and Thermophysical Properties, 7-rod

Trial #8 in Figure 4-17 (a) experienced all 3 regimes (DHT/NHT/IHT). All Trial #8 parameters are identical to Trial #7, except P . The HT profile of Trial #8 is nearly identical to Trial #7, with the DHT occurring just past the middle of the heated length.

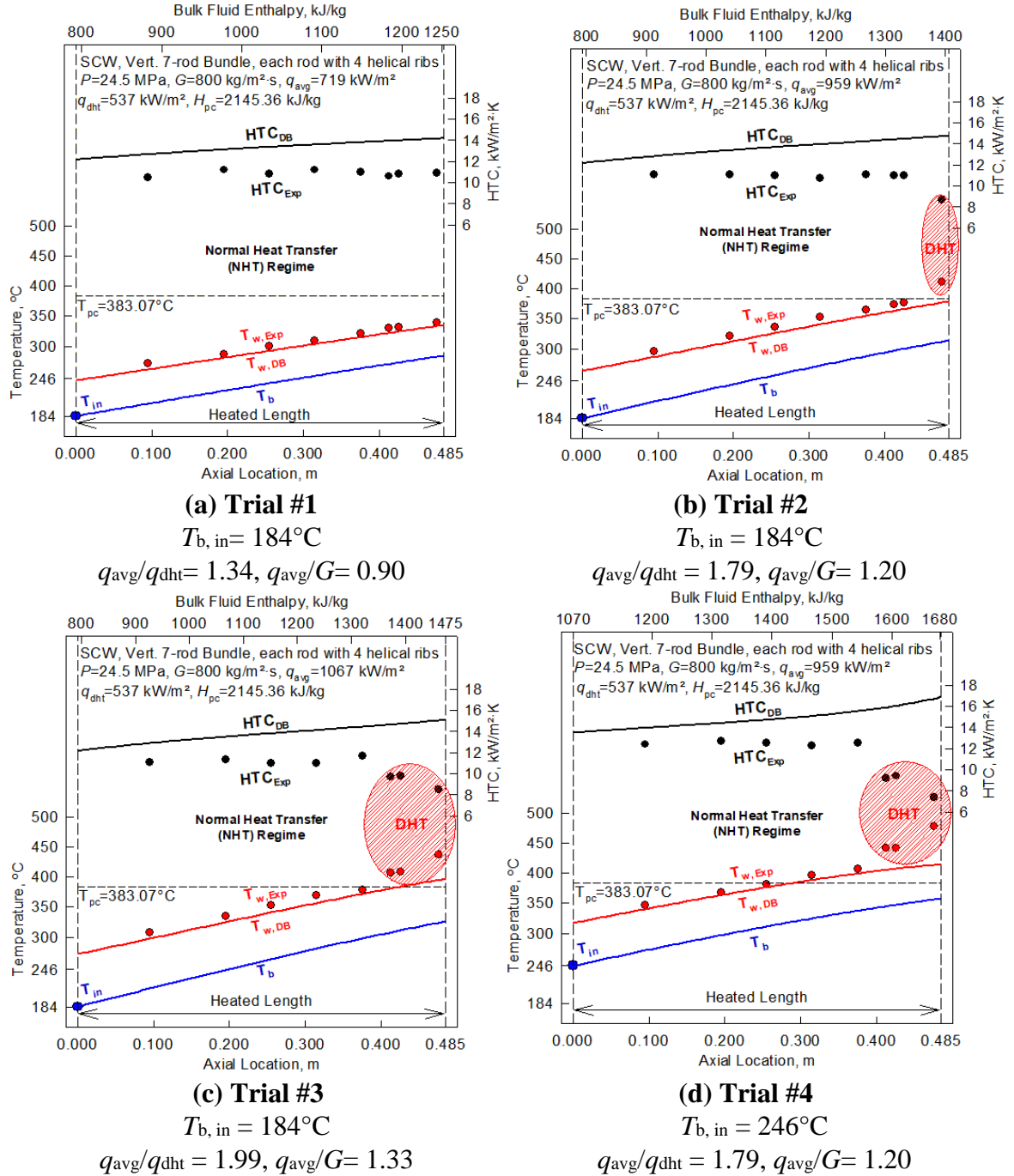


Figure 4-18: Profiles of SCW Bulk-Fluid, Wall Temperatures, and HTC across the Heated Length of the Central Rod varying Heat Flux (adjusted Axis')

The results from Trial #1 to #3 demonstrate that increasing the ratio of q_{avg}/q_{dht} increases the rate of ΔT over the heated length, leading to T_w crossing the pc point earlier in the trials.

The results from Trial #2 and #4 demonstrate that the DHT effect can be more severe with higher inlet T_b , despite having identical ratios of q_{avg}/q_{dht} .

Trial #3 and #4 demonstrate that the onset of DHT does not consistently occur once the measured wall temperatures cross the pc point (indicating that SCW near the wall has entered the gas-like region). This suggests additional factors (geometry, entrance effects, etc) play a role in the onset of DHT in addition to the thermophysical properties.

The results from Trial #1 to #4 demonstrate that increasing the q_{avg} has only a slight effect on the average HTC, while the onset of DHT has a dramatic effect on the HTC values ($HTC_{dht} \approx \frac{2}{3} HTC_{nht}$).

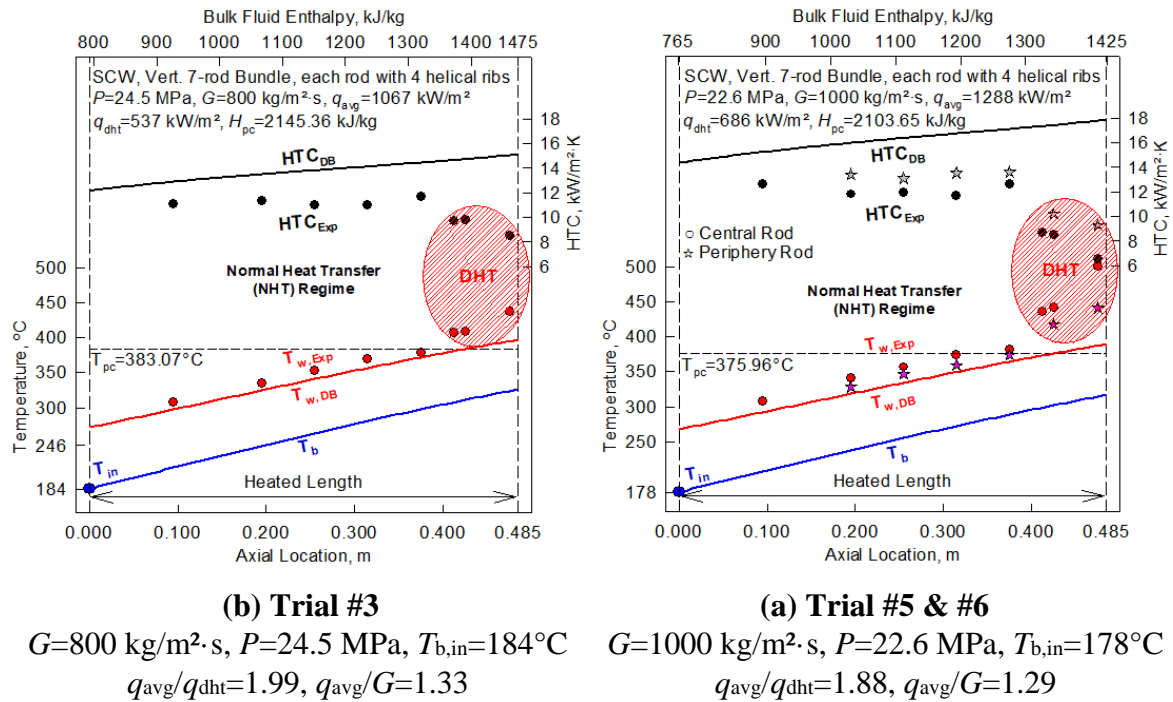


Figure 4-19: Profiles of SCW Bulk-Fluid, Wall Temperatures, and HTC across the Heated Length of the Central and Peripheral Rod (adjusted Axis')

Trial #5 and #6 demonstrate that the central rod in the 7-rod bundle experiences higher temperatures than the periphery rod, likely the result of the geometry.

Comparing Trial #5 and #6 to Trial #3, the HTC profiles are similar in shape despite different parameters (higher G in #5/#6, approximately same ratio of q_{avg}/q_{dht}). This suggests the HTC profiles in Trials #1 to #6 would follow a similar shape given a longer heated length, with the rate of ΔT over the heated length changing with varying parameters.

Additionally, when comparing Trial #5 and #6 to Trial #3, the effect of DHT is more severe for Trial #5 and #6. This suggests that DHT effects may be more severe at higher G .

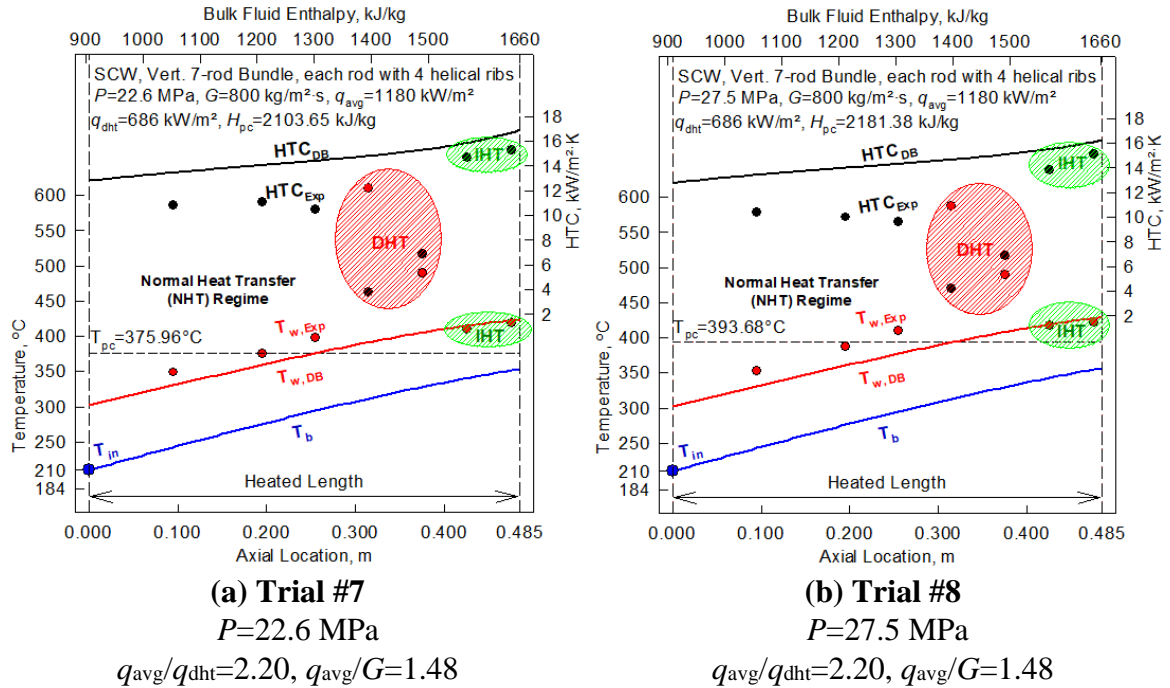


Figure 4-20: Profiles of SCW Bulk-Fluid and Wall Temperatures, and HTC across the Heated Length of the Central Rod varying Pressure (adjusted Axis')

Trial #7 and #8 demonstrate that changing pressure does not significantly alter the HTC and T_w profiles, and it does not lead to a more severe DHT effect.

However, the ratios of $q_{\text{avg}}/q_{\text{dht}}$ and q_{avg}/G is larger for these trials when compared to Trial #1 to #6, and a different temperature profile was encountered, with the IHT regime emerging after the DHT regime. This demonstrates that with the higher ratio of $q_{\text{avg}}/q_{\text{dht}}$ (and q_{avg}/G), the ΔT is greater, leading to the T_w crossing the pc point in the middle of the heated length. The DHT regime that occurs immediately after the T_w crosses the T_{pc} is more severe, leading to a greater decrease in HTC and a higher spike in T_w .

This suggests that with a longer heated length for Trials #1 to #6, the IHT regime may be encountered also.

For 7-rod bundles, the onset of DHT appears to be unpredictable, not depending upon thermophysical properties alone. In addition, the DHT effect appears to be more severe at higher ratios of $q_{\text{avg}}/q_{\text{dht}}$, and higher G . The IHT effect must be explored more thoroughly, though this is not anticipated to have negative consequences for designers.

4.2.1.2 Analysis

After performing all the calculations outlined in section 3.3.2 for each **Nu** correlation in the 7-rod bundles (Razumovskiy et al., 2008), the SD, ME, MAE, and RMS were computed for each **Nu** correlation for the entire dataset. The MAE and RMS for each **Nu** correlation for the HTC are shown below in Figure 4-21. See section C.2 for a table of values.

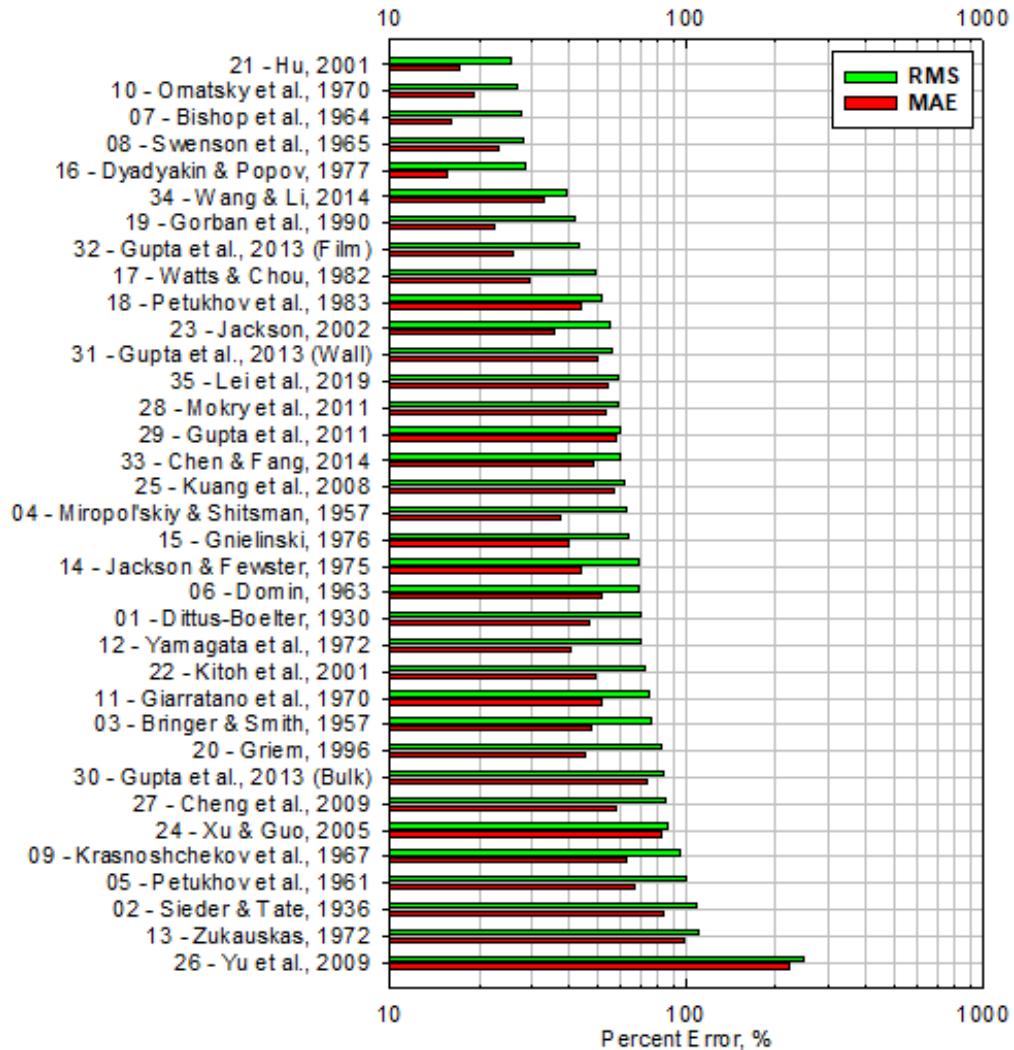


Figure 4-21: Correlation Predictions for HTC, 7-rod Dataset

Previous **Nu** correlations listed in section 2.6 are listed as accurate to within $\pm 30\%$. Expanding this, and looking closer at the **Nu** correlations with less than 40% RMS error (Figure 4-22), it is clear that the Hu (2001) correlation Eq. (21) has the lowest RMS, while the Dyadyakin and Popov (1977) correlation Eq. (16) has the lowest MAE.

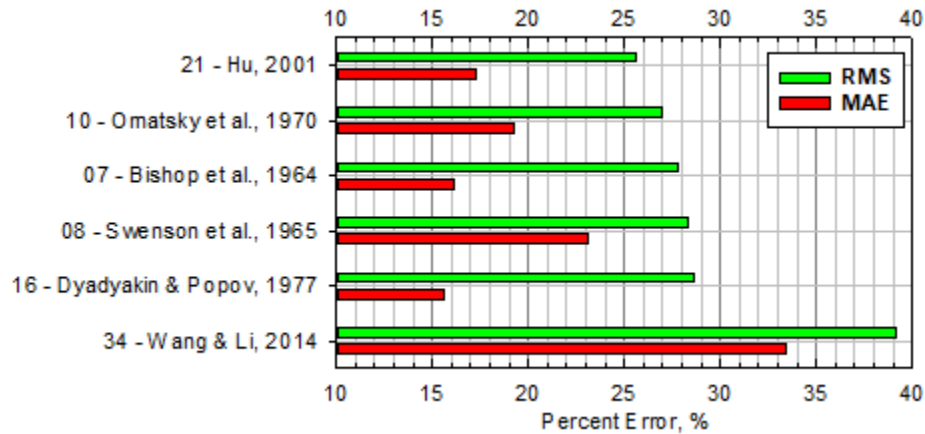


Figure 4-22: Top Nu Correlation Predictions for HTC, 7-rod Dataset

The MAE and the RMS are shown below in Figure 4-23. Unexpectedly, the **Nu** correlations with the closest T_w predictions for the same dataset are not the same **Nu** correlations as those with the closest HTC predictions.

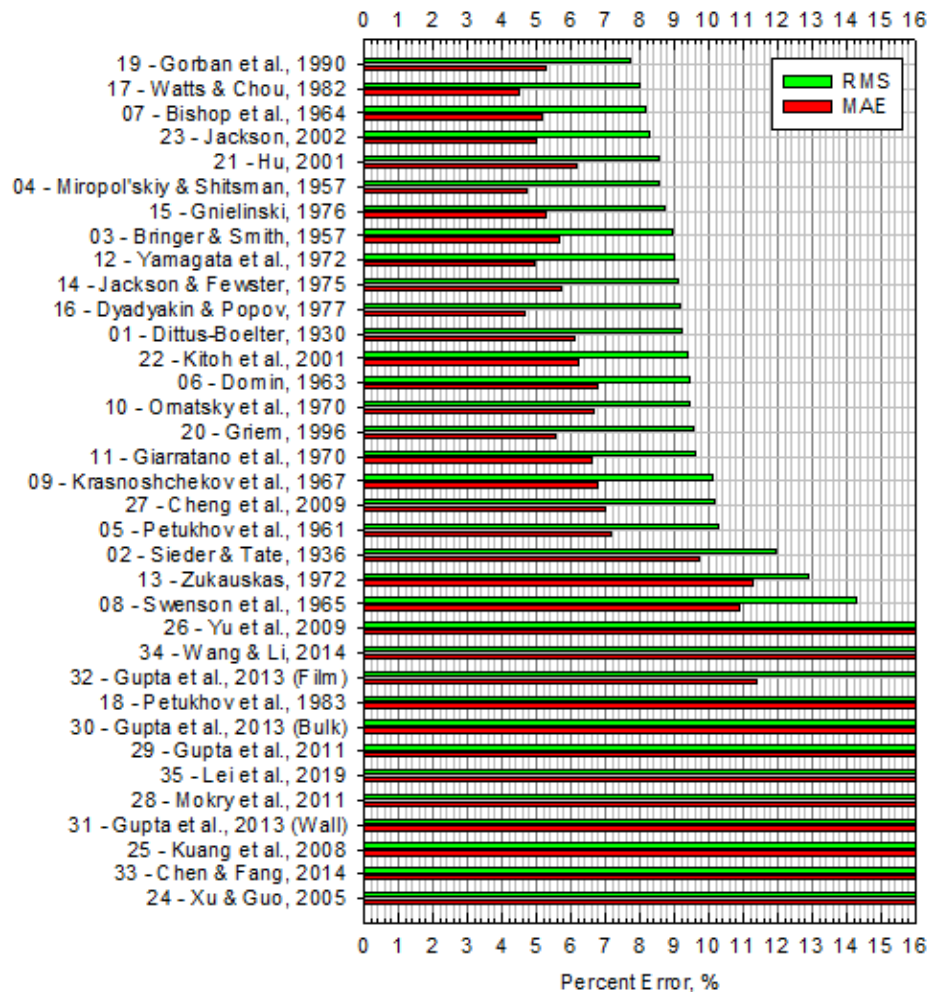


Figure 4-23: Nu Correlation Predictions for T_w , 7-rod Dataset

While predicting the HTC is of vital importance for designers, predicting T_w is also important to ensure that materials such as the sheath and fuel centreline, do not exceed maximum temperatures. While previous **Nu** correlations do not mention an accuracy, it is desired to only look at **Nu** correlations that produce low RMS error for T_w .

Looking closer at the **Nu** correlations with less than 10% RMS error for T_w , the Watts and Chou (1982) correlation Eq. (17) has the lowest MEA, while the Gorban, et al. (1990) correlation Eq. (19) has the lowest RMS.

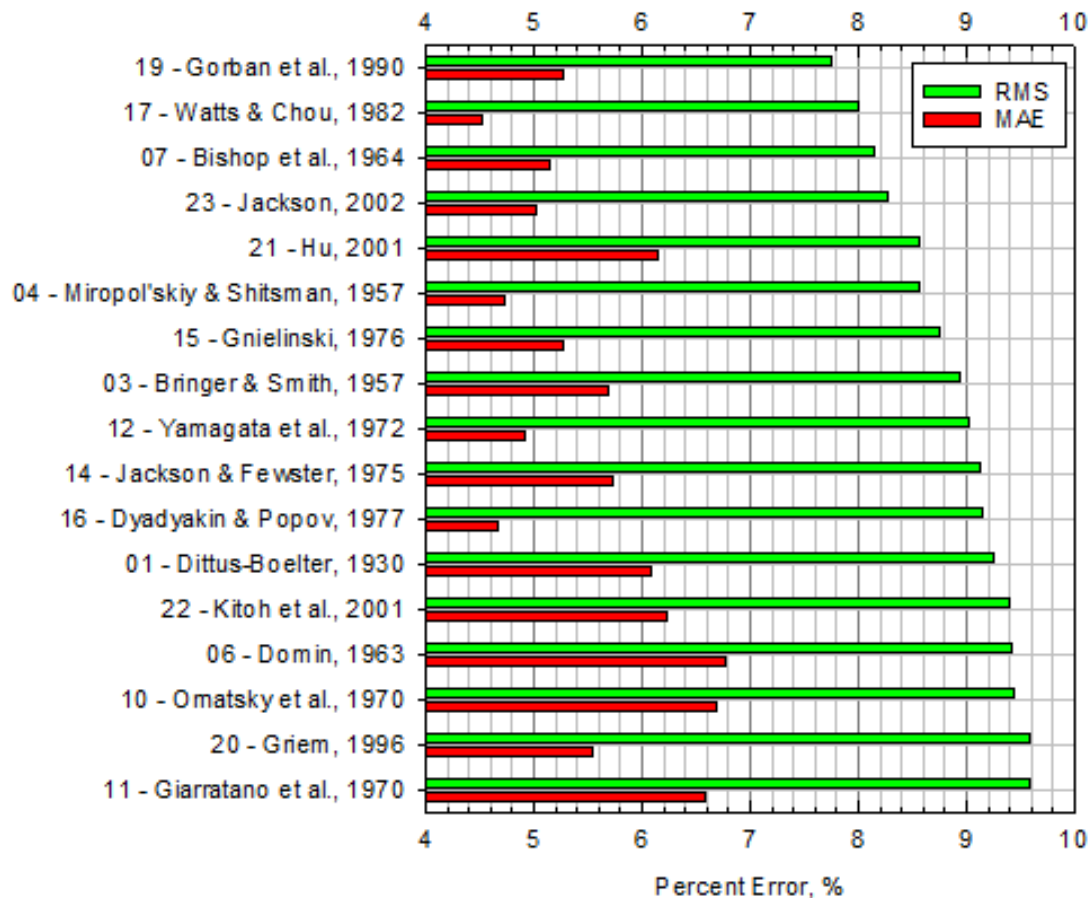


Figure 4-24: Top Nu Correlation Predictions for T_w , 7-rod Dataset

Looking at the combined results (HTC and T_w), there are only four **Nu** correlations with both a RMS of less than 40% for HTC and less than 10% for T_w , all listed in Table 4-1 below (Green for best among the four, Red for worst among the four).

Table 4-1: Top Nu Correlations for both HTC and T_w , 7-rod Data

Nu Correlations	HTC		T_w	
	<i>MEA</i>	<i>RMS</i>	<i>MEA</i>	<i>RMS</i>
Eq. (7): Bishop et al. (1964)	16.1%	27.8%	5.2%	8.2%
Eq. (21): Hu (2001)	17.2%	25.6%	6.2%	8.6%
Eq. (16): Dyadyakin & Popov (1977)	15.6%	28.6%	4.7%	9.1%
Eq. (10): Ornatsky et al. (1970)	19.2%	26.9%	6.7%	9.4%

Based on this data, all four **Nu** correlations are suitable for use in 7-rod bundles. It is recommended that the Hu (2001) correlation Eq. (21) is the best **Nu** correlation for the 7-rod bundle, while the Dyadyakin and Popov (1977) correlation Eq. (16) also deserves consideration for the low MEA error and similar RMS values for both HTC and T_w .

As the SCWR designs currently being examined include a 37-element bundle with a 7-rod bundle in the middle, and a 64-element bundle arranged in an annulus configuration, it is also important that these four **Nu** correlations are also able to predict in other datasets to provide confidence in their predictions for each of the SCWR designs being proposed.

By looking at the bare tube results, and comparing with the 7-rod bundle results, it will be determined if any **Nu** correlations are suitable for use to predict the SCWR sheath and fuel centreline temperatures.

4.2.2 BARE TUBE

4.2.2.1 Results

The data obtained from Kirillov et al. (2005) consists of 7074 data points from 88 tests, obtained with the test apparatus as described in section 3.1.1 using water. Below are three created graphs of the 88 tests, showing the bulk-fluid temperature calculated using the reduction parameters from section 3.1.1, the T_w calculated from the inner-wall temperature obtained through thermocouples, the calculated HTC, and the Dittus-Boelter Eq. (1) predictions for both T_w and HTC, with properties calculated from NIST REFPROP 10.0 (Lemmon et al., 2018). As Mokry et al. (2011) already examined this dataset, only a limited analysis will be presented.

Figure 4-25 shows the data gathered for a 4 metre length tube, with an average heat flux slightly above the deteriorated heat flux as predicted by Mokry et al. (2009), shown in Table 2-4. The bulk-fluid temperature crosses the pc point near the end of the tube.

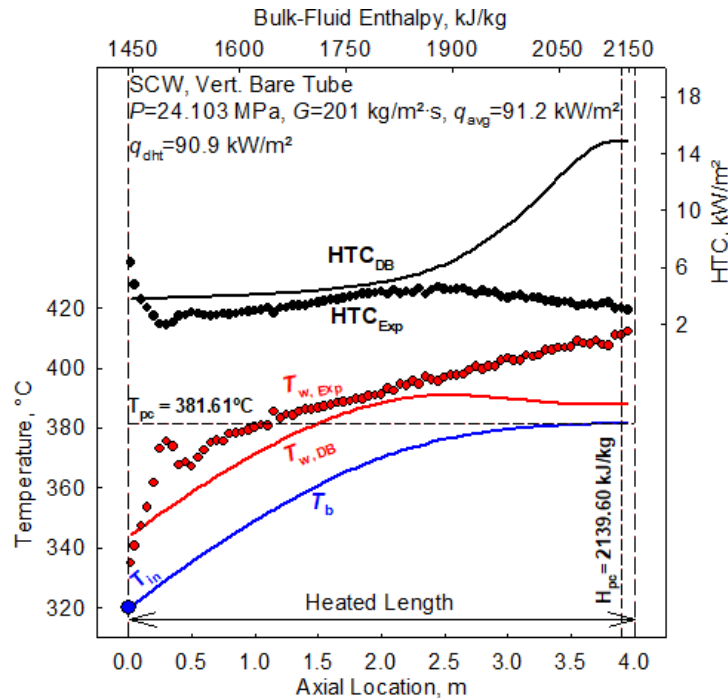


Figure 4-25: Test 70_07
Water, bare tube, ID = 10 mm

Figure 4-26 shows the data gathered for a 4 metre length tube, with an average heat flux well above the deteriorated heat flux as predicted by Mokry et al. (2009), shown in Table 2-4. The bulk-fluid temperature crosses the pc point in the middle of the tube.

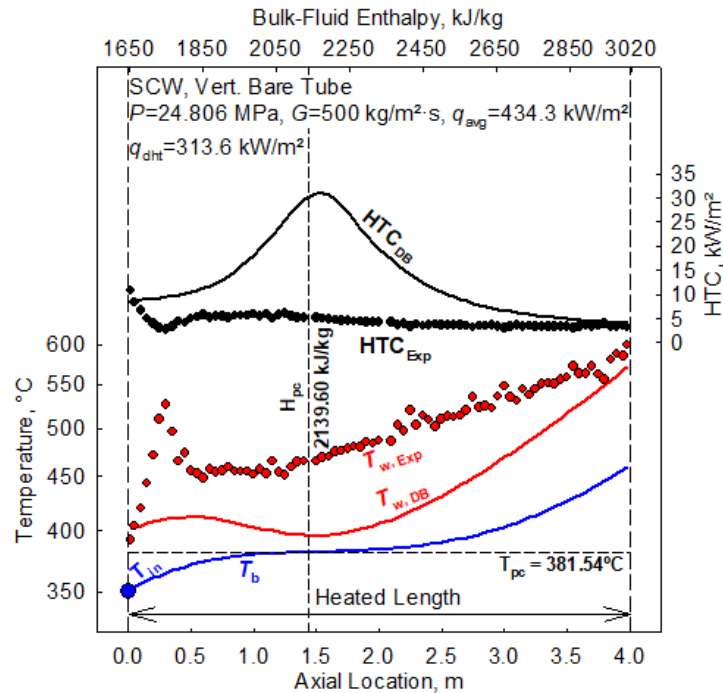


Figure 4-26: Test 15_14
Water, bare tube, ID = 10 mm

Figure 4-27 shows the data gathered for a 4 metre length tube, with an average heat flux well above the deteriorated heat flux as predicted by Mokry et al. (2009), shown in Table 2-4. The bulk-fluid temperature crosses the pc in the middle of the tube.

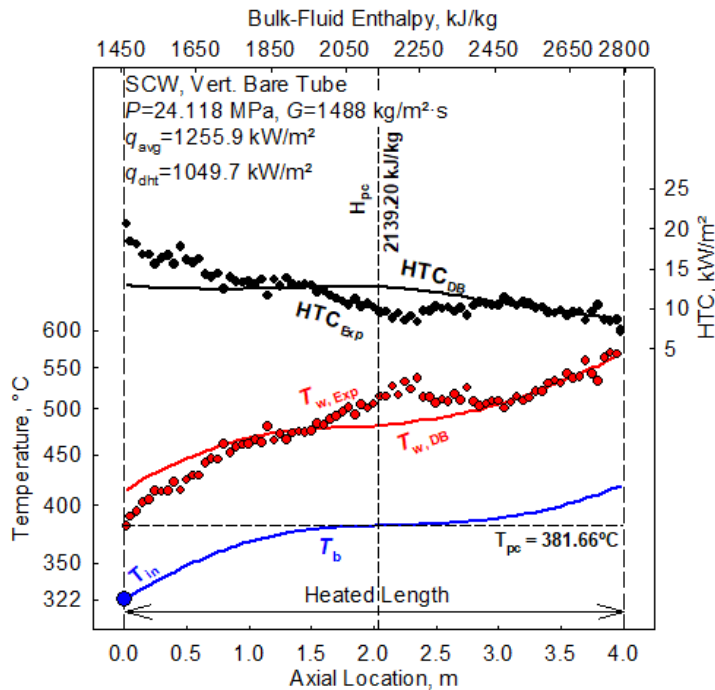


Figure 4-27: Test 49_13
Water, bare tube, ID = 10 mm

4.2.2.2 Analysis

After performing all the calculations for the bare tube dataset (Kirillov et al., 2005), the RMS and MEA for the HTC predictions are shown below in Figure 4-28. The top **Nu** correlations for the bare tube dataset are largely different from the 7-rod dataset. See section C.2 for a table of values.

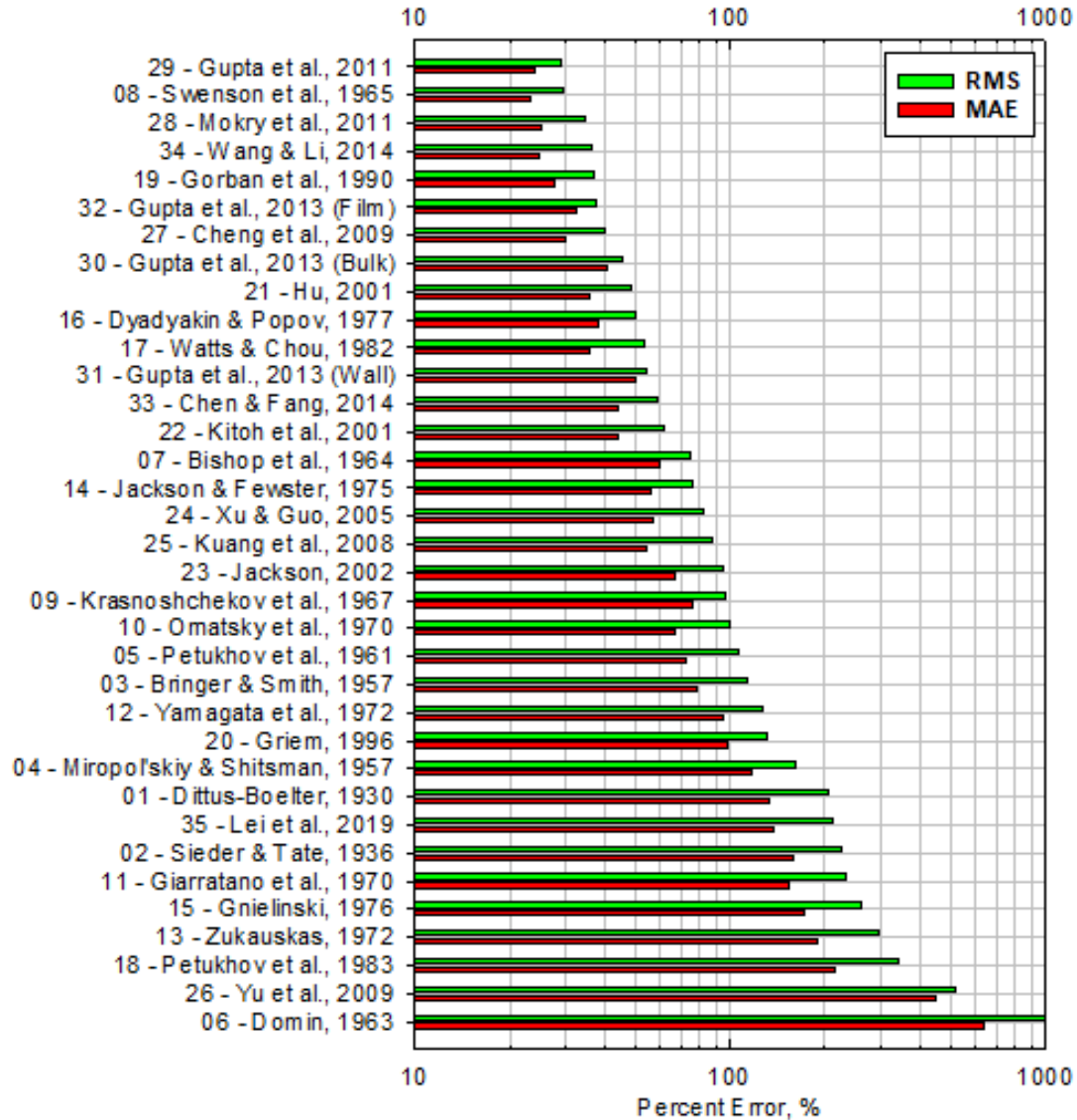


Figure 4-28: Nu Correlation Predictions for HTC, bare tube Dataset

Examining the top **Nu** correlations for the bare tube dataset, with an RMS below 40% (Figure 4-29), the Gupta, et al. (2011) correlation Eq. (29) has the lowest RMS, while the Swenson, et al. (1965) has the lowest MEA.

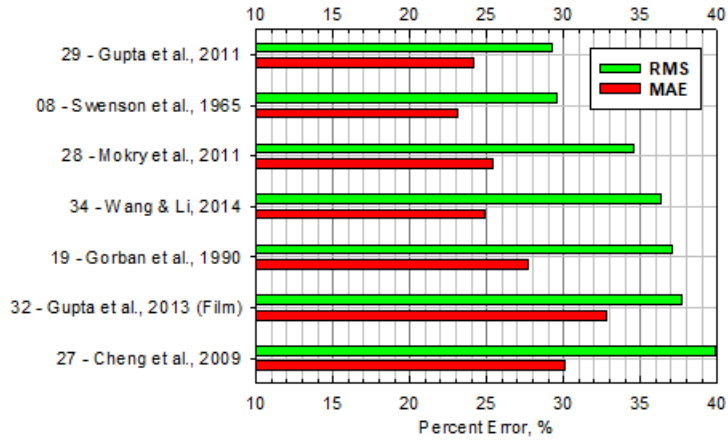


Figure 4-29: Top Nu Correlation Predictions for HTC, bare tube Dataset

In general, the T_w predictions are closer to the experimental values for bare tubes in comparison to the 7-rod data. Unlike the 7-rod dataset, the top HTC **Nu** correlations in the bare tube dataset are also amongst the top **Nu** correlations for T_w , as seen in Figure 4-30.

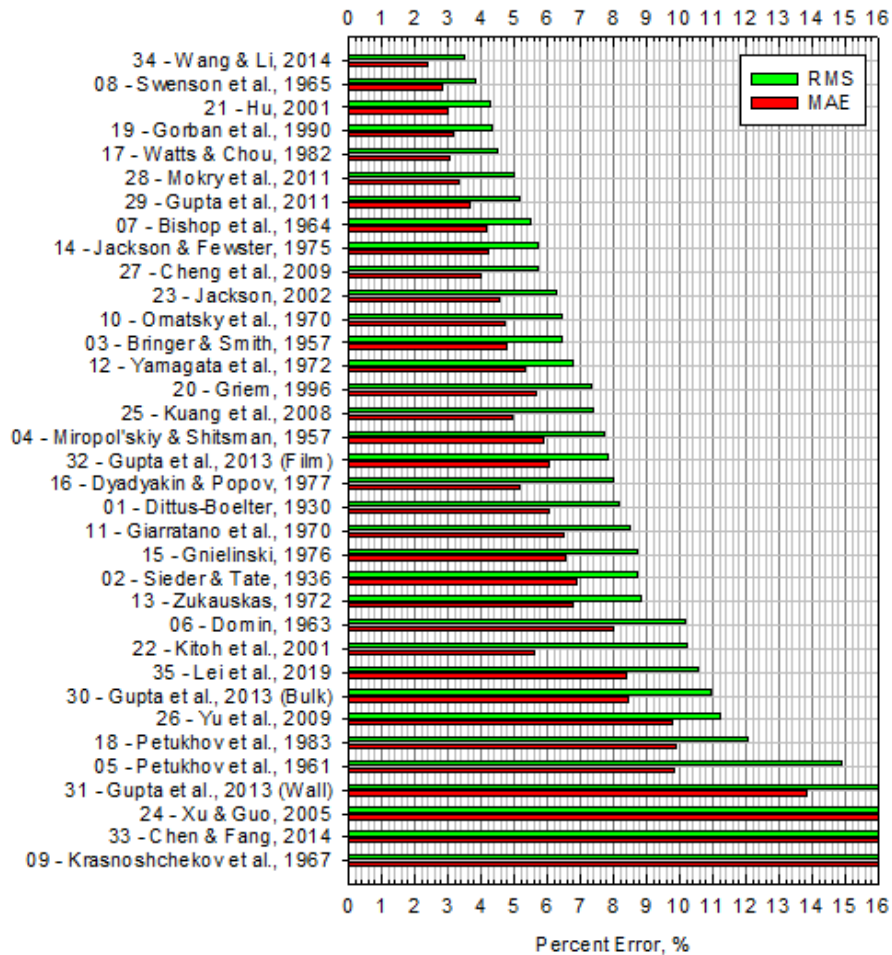


Figure 4-30: Nu Correlation Predictions for T_w , bare tube Dataset

Examining the top **Nu** correlations for T_w , with an RMS less than 10%, the Wang and Li (2014) correlation Eq. (34) is shown to be the best by both RMS and MEA standards.

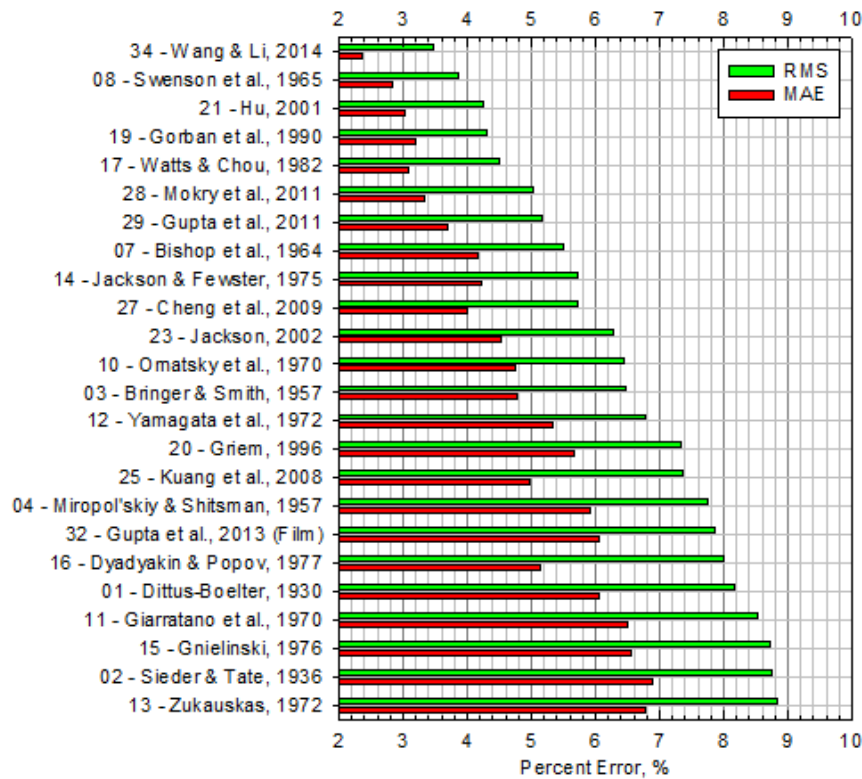


Figure 4-31: Top Nu Correlation Predictions for T_w , bare tube Dataset

There are 7 **Nu** correlations with an RMS below 40% for HTC, and an RMS below 10%, for T_w , all listed in Table 4-2 (Green for best in category, Red for worst in category).

Table 4-2: Top Nu Correlations for both HTC and T_w , Razumovskiy Data

Nu Correlations	HTC		T_w	
	MEA	RMS	MEA	RMS
Eq. (34): Wang and Li (2014)	24.9%	36.3%	2.4%	3.5%
Eq. (8): Swenson, et al. (1965)	23.1%	29.6%	2.8%	3.9%
Eq. (19): Gorbun, et al. (1990)	27.7%	37.0%	3.2%	4.3%
Eq. (28): Mokry, et al. (2009)	25.4%	34.6%	3.3%	5.0%
Eq. (29): Gupta, et al. (2011)	24.1%	29.3%	3.7%	5.2%
Eq. (27): Cheng, et al. (2009)	30.1%	39.9%	4.0%	5.7%
Eq. (32): Gupta, et al. (2013) Film	32.8%	37.7%	6.1%	7.9%

Based on this data, all 7 **Nu** correlations are suitable for use in bare tubes, with the Gupta et al. (2011) correlation Eq. (29) having the lowest HTC RMS error, and the Wang and Li (2014) correlation Eq. (34) having the lowest T_w RMS error.

4.2.3 COMBINED RESULTS

4.2.3.1 HTC Observations

The relationship of average HTC (HTC_{avg}) throughout a trial, and the ratio of q_{avg}/q_{dht} of the 7-rod bundles and the bare tubes (Figure 4-32) is a power function. The HTC_{avg} value is heavily influenced by both the mass flux (G) and the ratio of q_{avg}/q_{dht} in bare tubes.

For bare tubes, at low G levels, the HTC_{avg} values are low, while at high G levels the HTC_{avg} values are high. This is not confirmed in 7-rod bundles due to small sample size.

For bare tubes, at lower G 's the HTC_{avg} is not as sensitive to the ratio of q_{avg}/q_{dht} as at high G 's. However, the SD (error bars in Figure 4-32) is large at low (unstable HTC) and high (DHT influence) ratios of q_{avg}/q_{dht} , and is small close to a ratio of 1. For the 7-rod bundle, the ratio of q_{avg}/q_{dht} only slightly effects the HTC_{avg} , with large SD occurring at higher q_{avg}/q_{dht} ratios due to DHT influence.

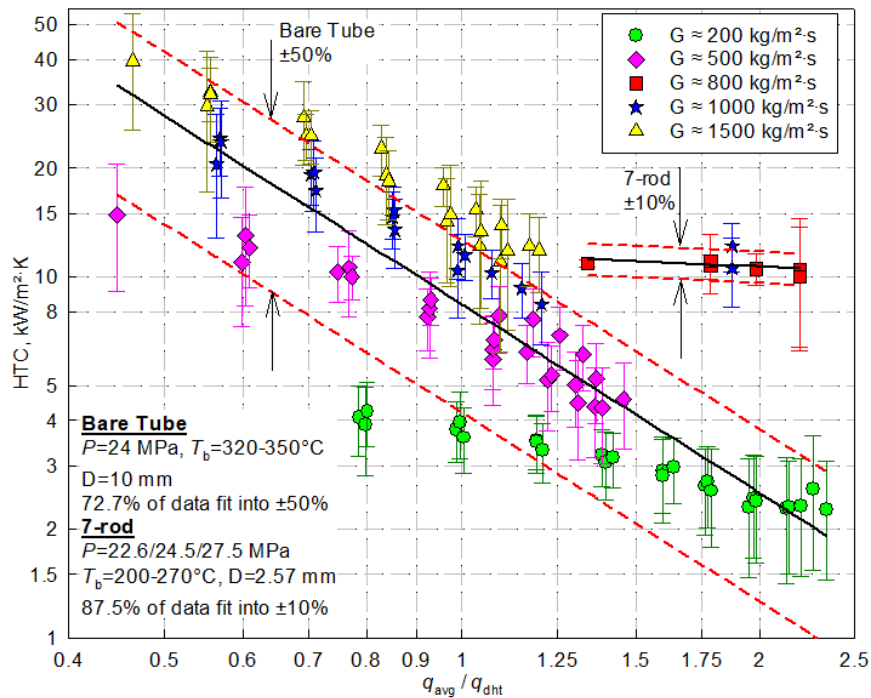


Figure 4-32: Comparison of q_{avg}/q_{dht} and HTC_{avg} in 7-rod Bundles and bare tubes

The HTC_{avg} in 7-rod bundles is more stable with increasing q_{avg} than in bare tubes. Also, the HTC_{avg} value is only slightly higher in 7-rod bundles than in bare tubes for similar G . This suggests that turbulence, introduced by the 7-rod bundle geometry with 4 helical ribs on each rod, only slightly increases the HTC_{avg} above that experienced in bare tubes.

4.2.3.2 Combined 7-rod and bare tube Analysis

When examining both sets of data (7-rod and bare tube), it becomes clear that no single **Nu** correlation is suitable for use across both geometries. As mentioned previously, to have high confidence while designing systems, choosing a **Nu** correlation to predict HTC and T_w in a 37-element, 64-element annulus bundle, or any another configuration, the **Nu** correlation chosen should be reliable with as many datasets as possible, in configurations. In this thesis, a 7-rod bundle dataset and a bare tube dataset were available and tested.

While the expanded RMS error of 40% for HTC was used as a cutoff to eliminate more erroneous **Nu** correlations, no single **Nu** correlation has an RMS error of less than 40% for HTC, and an RMS error of less than 10% for T_w , for both the 7-rod bundle datasets and the bare tube datasets.

Expanding further, 3 **Nu** correlations can be shown to have an RMS error of less than 50% for HTC and less than 15% for T_w for both 7-rod bundle and bare tube. These are listed below in Table 4-3.

Table 4-3: RMS Comparison for Top Nu Correlations for both Razumovskiy and Kirillov Datasets

Nu Correlations	HTC		T_w	
	7-rod	bare tube	7-rod	bare tube
Eq. (8): Swenson, et al. (1965)	28.3%	29.6%	14.3%	3.9%
Eq. (19): Gorman, et al. (1990)	42.2%	37.0%	7.8%	4.3%
Eq. (21): Hu (2001)	25.6%	48.5%	8.6%	4.3%

All three **Nu** correlations will also produce large errors for any given configuration, however the Hu (2001) correlation Eq. (21) and the Gorman et al. (1990) correlation Eq. (19) both provide low RMS error for T_w for both 7-rod bundle and bare tube datasets. As each provide large RMS error for HTC, neither **Nu** correlation provides a designer with confidence.

Therefore, a new **Nu** correlation will be determined to more accurately predict the HTC and T_w in both bare tubes and 7-rod bundle configurations.

4.3 DEVELOPMENT OF NEW **Nu** CORRELATION

From the analysis performed in section 4.2.3.2, three **Nu** correlations were examined as potential terms for developing the new **Nu** correlation:

- 1) Swenson et al. (1965) correlation Eq. (8) uses primarily wall temperature based properties, along with averaged properties, and produces high errors (RMS ~ 15%) when predicting wall temperature in the 7-rod bundle.
- 2) The Gorban et al. (1990) correlation Eq. (19) uses bulk fluid properties and has large RMS errors when predicting HTC for both 7-rod bundles and bare tubes.
- 3) The Hu (2001) correlation Eq. (21) uses primarily bulk-fluid properties, and averaged properties, and provides amongst the best predictions for 7-rod bundles (HTC & T_w). While the prediction of wall temperature for bare tubes is acceptable, the prediction of HTC has significant error (~50% RMS).

Due to the better performance in 7-rod bundles, and the property type (bulk-fluid and average), the Hu (2001) correlation Eq. (21) was selected as the basis for the new **Nu** correlation:

$$\mathbf{Nu}_b = C \cdot \mathbf{Re}_b^{n_1} \cdot \overline{\mathbf{Pr}}_b^{n_2} \cdot \left(\frac{\rho_w}{\rho_b}\right)^{n_3} \cdot \left(\frac{k_w}{k_b}\right)^{n_4} \quad (4.1)$$

As the **Nu** correlation was not developed by hand, but through the code as described in APPENDIX A:CODE USED, any parameters that had a very low correlation were not discarded automatically. The advantages of carrying these terms is as the **Nu** correlation undergoes several iterations, these terms with a low correlation initially (low R^2) ended up experiencing large increases in correlation.

Initially, a **Nu** correlation was created using the data from Razumovskiy, et al. (2008) 7-rod Bundle dataset, edited to remove the DHT regime zones shown in section 4.1.

After 380 iterations, a convergent **Nu** correlation was determined that was unsuitable for both the 7-rod data from Razumovskiy, et al. (2008) and for the 4 m bare tube data from Kirillov, et al. (2005) as shown in Table 4-4.

$$\mathbf{Nu}_b = 0.1099 \cdot \mathbf{Re}_b^{0.6389} \cdot \overline{\mathbf{Pr}}_b^{1.1323} \cdot \left(\frac{\rho_w}{\rho_b}\right)^{1.1080} \cdot \left(\frac{k_w}{k_b}\right)^{-0.5152} \quad (4.2)$$

Table 4-4: Assessment of New Nu Correlation based on 7-rod bundle Dataset

Nu Correlation	HTC RMS		T_w RMS	
	<i>7-rod</i>	<i>bare tube</i>	<i>7-rod</i>	<i>bare tube</i>
New Nu Correlation 7-rod data only	70.01%	266.48%	9.24%	218.50%

The second attempt at producing a **Nu** correlation came from using the Kirillov, et al. (2005) dataset, with no modification.

After 22 iterations, a convergent **Nu** correlation was determined. While this produced a **Nu** correlation that was suitable for the bare tube data from Kirillov, et al. (2005), it was not suitable for the 7-rod data from Razumovskiy, et al (2008), though had better performance than (4.2).

$$\mathbf{Nu}_b = 0.0060 \cdot \mathbf{Re}_b^{0.904} \cdot \overline{\mathbf{Pr}}_b^{0.6471} \cdot \left(\frac{\rho_w}{\rho_b}\right)^{0.4361} \cdot \left(\frac{k_w}{k_b}\right)^{0.1397} \quad (4.3)$$

Table 4-5: Assessment of New Nu Correlation based on bare tube Dataset

Correlation	HTC RMS		T_w RMS	
	<i>7-rod</i>	<i>bare tube</i>	<i>7-rod</i>	<i>bare tube</i>
New Nu Correlation bare tube data only	48.60%	31.04%	37.60%	4.34%

As described in section 4.2.3.2, at higher q_{avg}/q_{dht} ratios DHT occurs earlier in the heated length. In addition, in bundle geometries DHT is experienced as the T_w approaches the pc point, while in bare tubes DHT is experienced as the T_b approaches the pc point.

It was decided to combine the 7-rod dataset with the bare tube dataset in an effort to create a **Nu** correlation that could satisfy both requirements. To avoid dilution, only select bare tube datasets could be used, as each bare tube trial had 10x more data than the each 7-rod trial.

When examining the ratios of q_{avg}/q_{dht} and q_{avg}/G of the 7-rod data, seven of the eight trials available to the author from Razumovskiy, et al. (2008) had a q_{avg}/G ratio above 1, and all had q_{avg}/q_{dht} ratios higher than in the bare tube datasets, as can be seen below in Table 4-6.

Table 4-6: Heat Flux and Mass Flux Parameters in 7-rod Data Set

Trial	q_{avg} (kW/m ²)	G (kg/m ² ·s)	Ratio of q / G	q_{dht} (kW/m ²)	q_{avg}/q_{dht}
1	719	800	0.899	537	1.34
2	959	800	1.199	537	1.79
3	1067	800	1.334	537	1.99
4	959	800	1.199	537	1.79
5	1288	1000	1.288	686	1.88
6	1288	1000	1.288	686	1.88
7	1180	800	1.475	537	2.20
8	1180	800	1.475	537	2.20

Of the 88 trials from Kirillov, et al. (2005) datasets available to the author, the ratios of q_{avg}/G varied from 0.281 to 1.058. In order to develop a **Nu** correlation that would satisfy both the Razumovskiy et al. (2008) and Kirillov et al. (2005) datasets, three test datasets from the Kirillov, et al. (2005) experiments were added to the Razumovskiy, et al. (2008) datasets. To maximize the range of mass fluxes and ratio of q_{avg}/G , while not minimizing the effects of the 7-rod data, the following three tests were selected to be combined:

- 1) Test 70_07 – lowest ratio q_{avg}/G (0.45) of the low-mass fluxes (201 kg/m²·s) with $q_{avg}/q_{dht} > 1$.
- 2) Test 15_14 – highest ratio q_{avg}/G (0.87) and q_{avg}/q_{dht} of the mid-mass fluxes (500 kg/m²·s) without experiencing severe DHT regime.
- 3) Test 49_13 – highest ratio q_{avg}/G (0.84) of the high-mass fluxes (1488 kg/m²·s)

As the 7-rod dataset contained G in the range of 800 – 1100, the bare tube data with G in this range was not selected. A unique dataset of 284 points consisting of the 7-rod data and bare tube data was then used in the iteration steps below to develop the new **Nu** correlation.

4.3.1 PHASE 1

Figure 4-33 to Figure 4-36 shows each step of phase 1 for the development of the new **Nu** correlation. The generic term $a_i^{n_i}$ was used in place of the parameter labels in each of the proceeding graphs due to limitations in the software.

The dots represent data points, while the solid red line represents the mean of the sample. The dashed lines represent error bands about the mean of the sample.

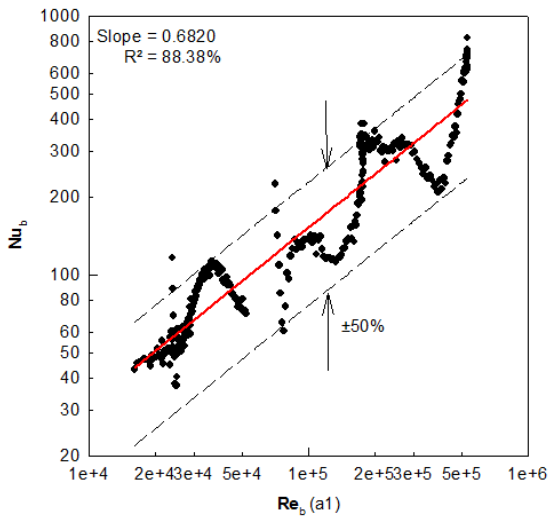


Figure 4-33: Phase 1 - Step 1

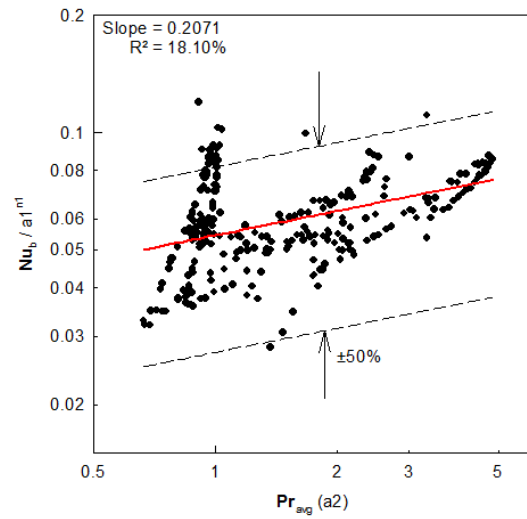


Figure 4-34: Phase 1 - Step 2

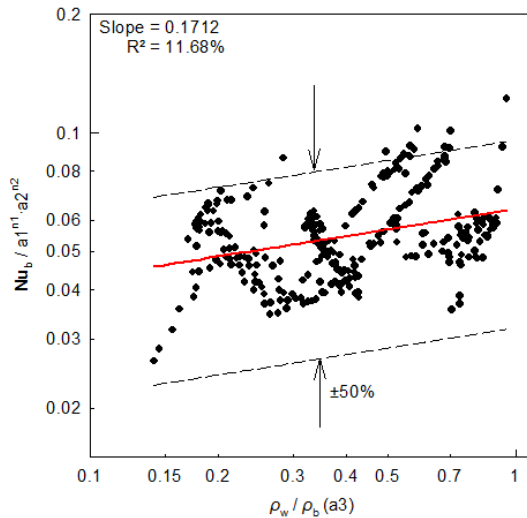


Figure 4-35: Phase 1 - Step 3

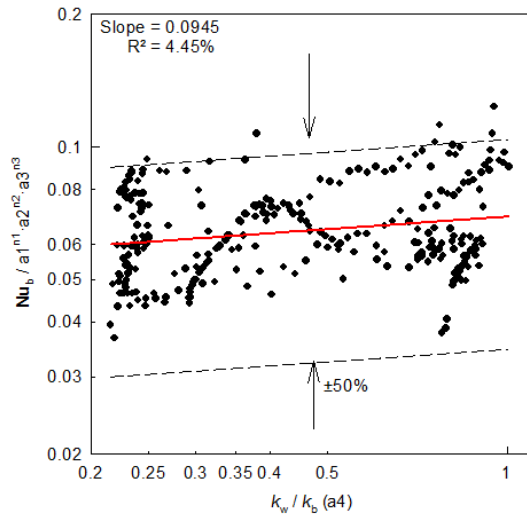


Figure 4-36: Phase 1 - Step 4

4.3.2 PHASE 2

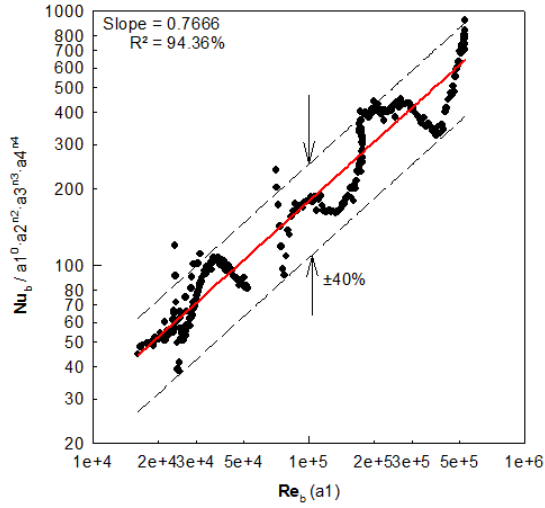


Figure 4-37: Phase 2 - Step 1

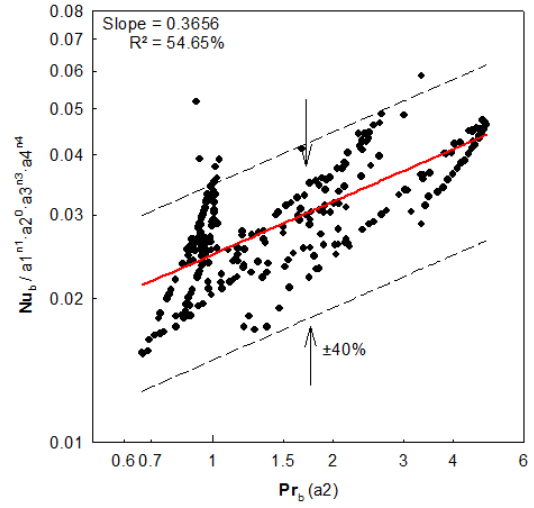


Figure 4-38: Phase 2 - Step 2

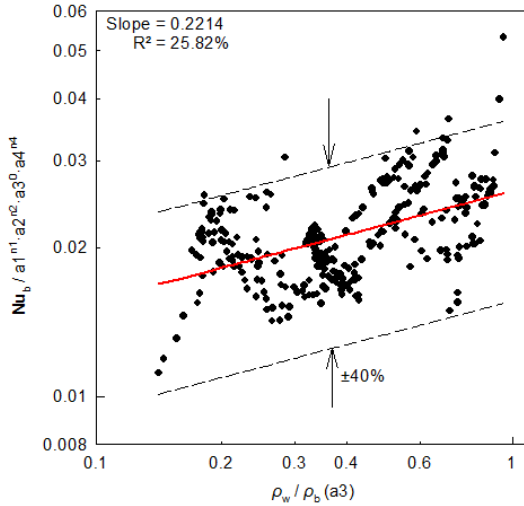


Figure 4-39: Phase 2 - Step 3

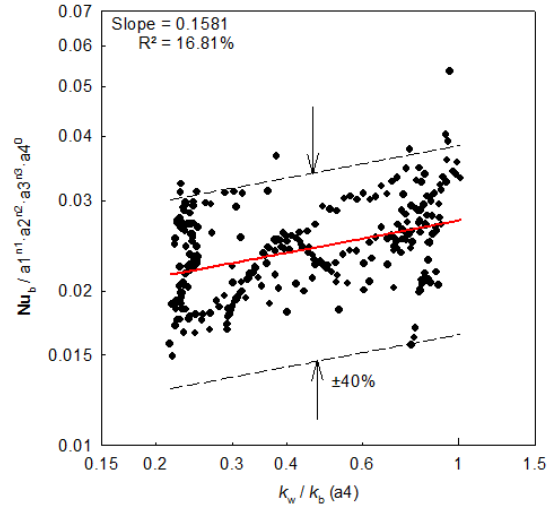


Figure 4-40: Phase 2 - Step 4

Figure 4-37 to show each step the first iteration for phase 2 of the development of the new **Nu** correlation.

4.3.3 PHASE 3

While the Constant is not required to be calculated until the end of Phase 2, the computer algorithm developed calculated it at the end of every iteration.

Figure 4-41 shows the Constant calculation for Phase 3 after the first iteration of Phase 2.

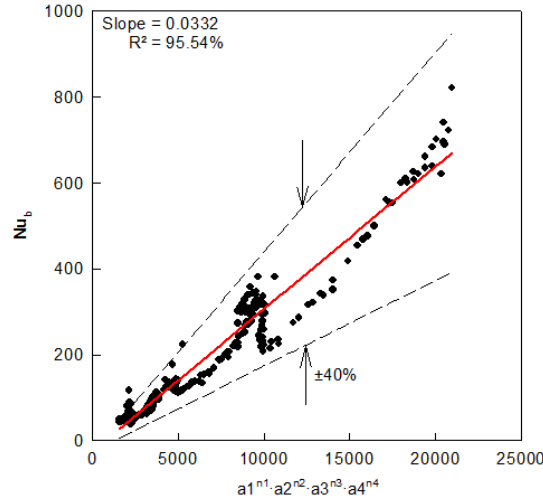


Figure 4-41: Phase 3 – Constant Calculation (first iteration)

4.3.3.1 Initial Nu Correlation

After the 63rd iteration, the values of all exponents converged to their unique values as described in section 3.3.3, the constant was calculated, and the **Nu** correlation values were obtained (4.4).

$$\mathbf{Nu}_b = 0.0126 \cdot \mathbf{Re}_b^{0.8367} \cdot \mathbf{Pr}_b^{0.4399} \cdot \left(\frac{\rho_w}{\rho_b}\right)^{-0.0707} \cdot \left(\frac{k_w}{k_b}\right)^{0.4874} \quad (4.4)$$

Table 4-7: Assessment of New Nu Correlation based on 7-rod and bare tube Datasets

Nu Correlation	HTC RMS		T_w RMS	
	7-rod	bare tube	7-rod	bare tube
Initial 7-rod and bare tube data combination	26.0%	27.0%	8.5%	3.5%

This **Nu** correlation provides excellent prediction for both the 7-rod bundle and bare tube datasets. However, the RMS error for T_w is higher than other **Nu** correlations. As T_w is used to determine the centreline temperature of fuel, of high importance for designing SCWR, it is desirable to reduce the RMS of T_w as much as possible.

4.3.3.2 Final Nu Correlation

After some trial and error approaches, the final **Nu** correlation to be proposed was obtained (named Clark, et al. 2020, Eq. (36)), with lower RMS for T_w and higher RMS for HTC:

$$\text{Nu}_b = 0.0129 \cdot \text{Re}_b^{0.841} \cdot \overline{\text{Pr}}_b^{0.5} \cdot \left(\frac{\rho_w}{\rho_b}\right)^{-0.07} \cdot \left(\frac{k_w}{k_b}\right)^{0.53} \quad \text{Eq. (36)}$$

Table 4-8: Assessment of Final Nu Correlation based on 7-rod and bare tube Datasets

Nu Correlation	HTC RMS		T_w RMS	
	7-rod	bare tube	7-rod	bare tube
Clark et al. (2020)	26.5%	29.0%	7.4%	3.3%

The test matrix for this new **Nu** correlation is listed in Table 4-9.

Table 4-9: Test Matrix for new Nu Correlation

Geometry	P MPa	$T_{b, \text{in}}$ °C	$T_{b, \text{out}}$ °C	T_w °C	q_{avg} kW/m ²	G kg/m ² ·s
7-rod	22.6, 24.5, 27.5	178 to 246	273 to 348	271 to 610	719 to 1288	800, 1000
bare tube	23.9 to 24.4	320 to 354	380 to 516	330 to 643	72 to 1308	201 to 1506

For the 7-rod bundle, the Clark et al. (2020) correlation Eq. (36) predicts the HTC values within $\pm 25\%$ for $q_{\text{avg}}/q_{\text{dht}}$ ratios of 1.0 to 2.0 (Figure 4-42). For ratios of $q_{\text{avg}}/q_{\text{dht}}$ between 2.0 and 2.5, there the HTC can be over-predicted by Eq. (36).

For the 7-rod bundle, the Clark et al. (2020) correlation Eq. (36) predicts the T_w values within $\pm 10\%$ for $q_{\text{avg}}/q_{\text{dht}}$ ratios of 1.0 to 2.0 (Figure 4-43). For ratios of $q_{\text{avg}}/q_{\text{dht}}$ between 2.0 and 2.5, the T_w can be under-predicted by Eq. (36) by as much as 150°C.

For the bare tubes, the Clark et al. (2020) correlation Eq. (36) predicts the HTC values within $\pm 35\%$ for q_{avg}/q_{dht} ratios of 0 to 2.5 (Figure 4-44). For ratios of q_{avg}/q_{dht} below 1.0, the HTC prediction is conservative by Eq. (36).

For bare tubes, the Clark et al. (2020) correlation Eq. (36) predicts the T_w values within $\pm 10\%$ for q_{avg}/q_{dht} ratios of 0.0 to 1.0, and 2.0 to 2.5 (Figure 4-45). For ratios of q_{avg}/q_{dht} between 1.0 and 2.0, the T_w can be under-predicted by Eq. (36) by as much as 150°C .

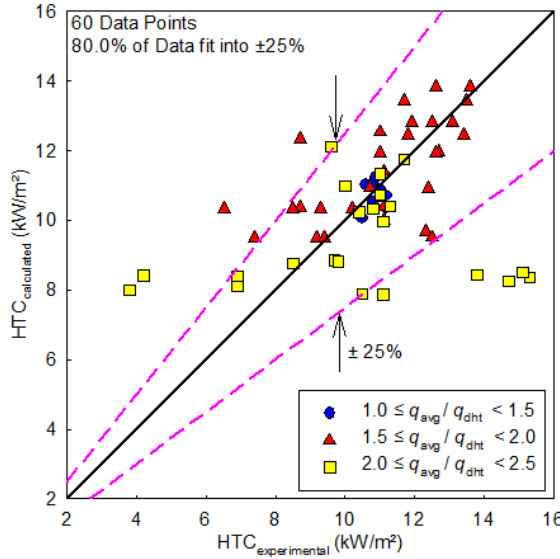


Figure 4-42: HTC Comparison between Experimental and Calculated by Clark values for 7-rod bundle

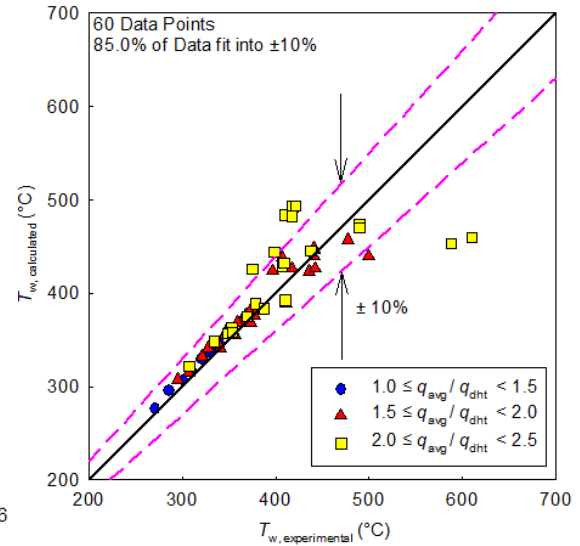


Figure 4-43: T_w Comparison between Experimental and Calculated by Clark values for 7-rod bundle

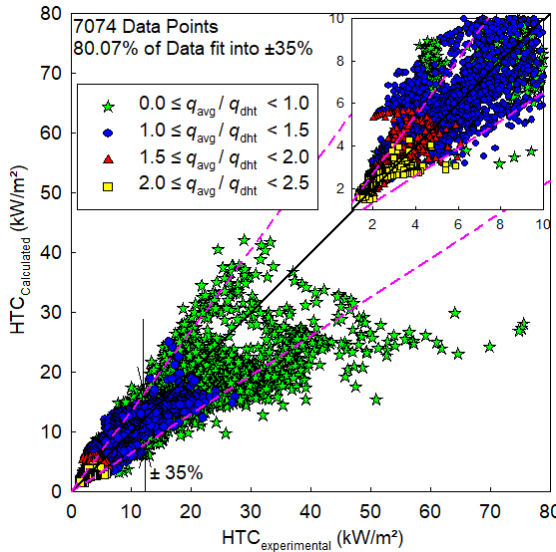


Figure 4-44: HTC Comparison between Experimental and Calculated by Clark values for bare tube

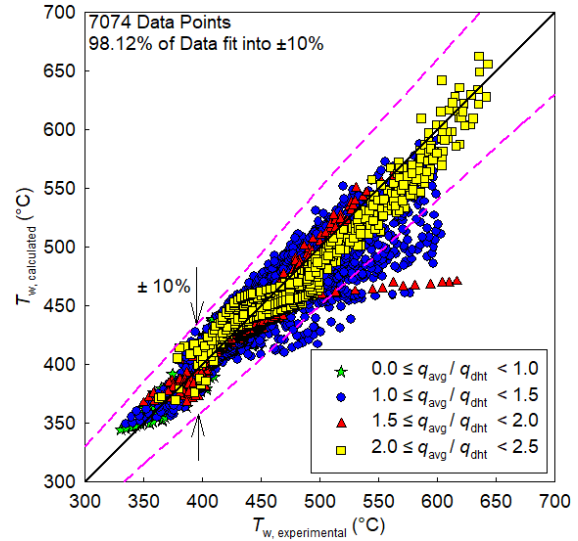


Figure 4-45: T_w Comparison between Experimental and Calculated by Clark values for bare tube

4.3.4 NEW NU CORRELATION COMPARISONS

Figure 4-46 for the 7-rod dataset shows that the Clark et al. (2020) correlation Eq. (36) provides the second best prediction of HTC by RMS next to Hu, while also providing the second best prediction of HTC by MAE next to Dyadyakin and Popov.

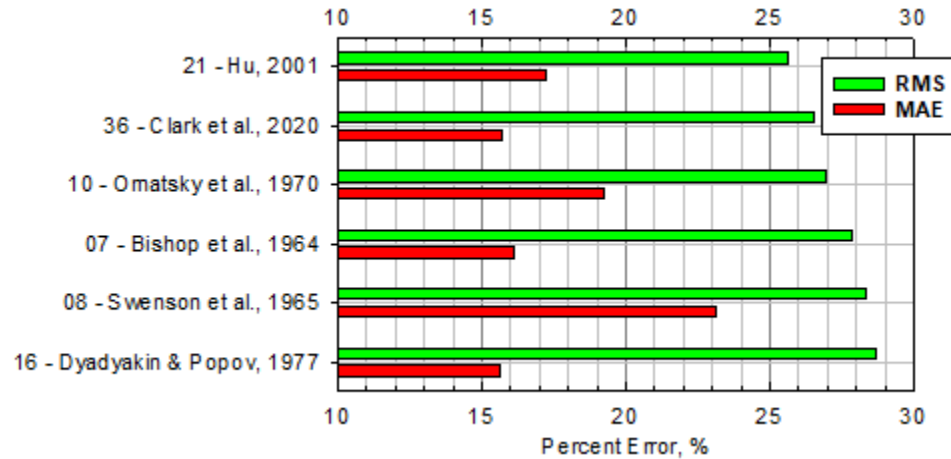


Figure 4-46: Top HTC Nu Correlations, 7-rod Bundle

Figure 4-47 for the 7-rod dataset shows that the Clark et al. (2020) correlation Eq. (36) provides the best predictor of T_w by RMS, while being amongst the top 5 predictors of T_w by MAE.

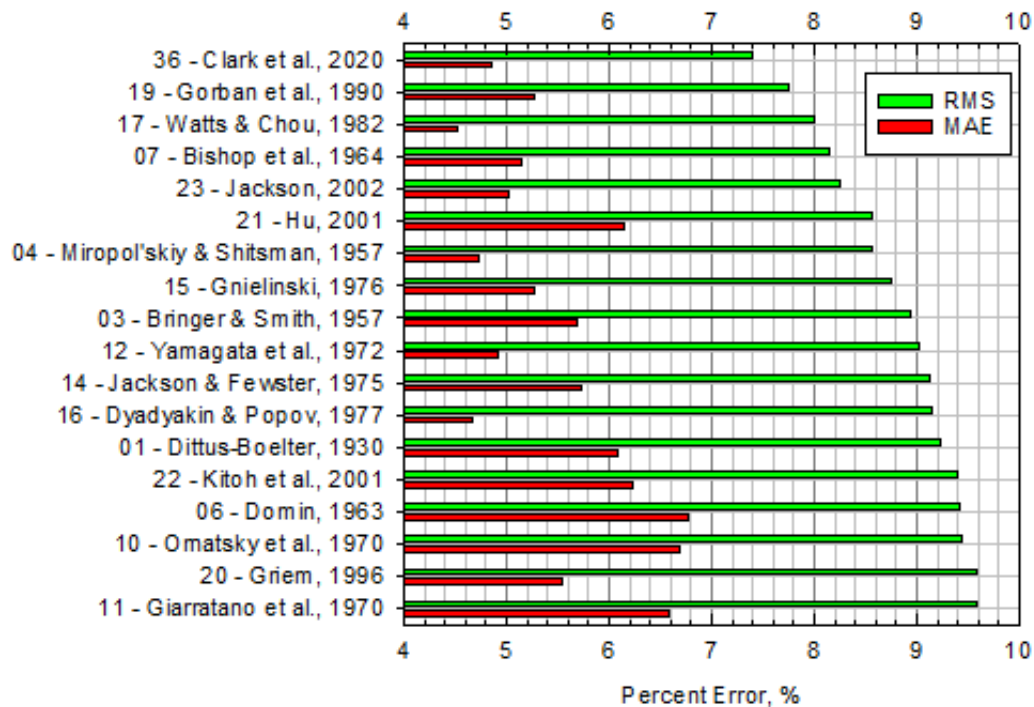


Figure 4-47: Top T_w Nu Correlations, 7-rod Bundle Dataset

Figure 4-48 for the bare tube dataset shows that the Clark et al. (2020) correlation Eq. (36) is the best predictor of HTC by both RMS and MAE methods.

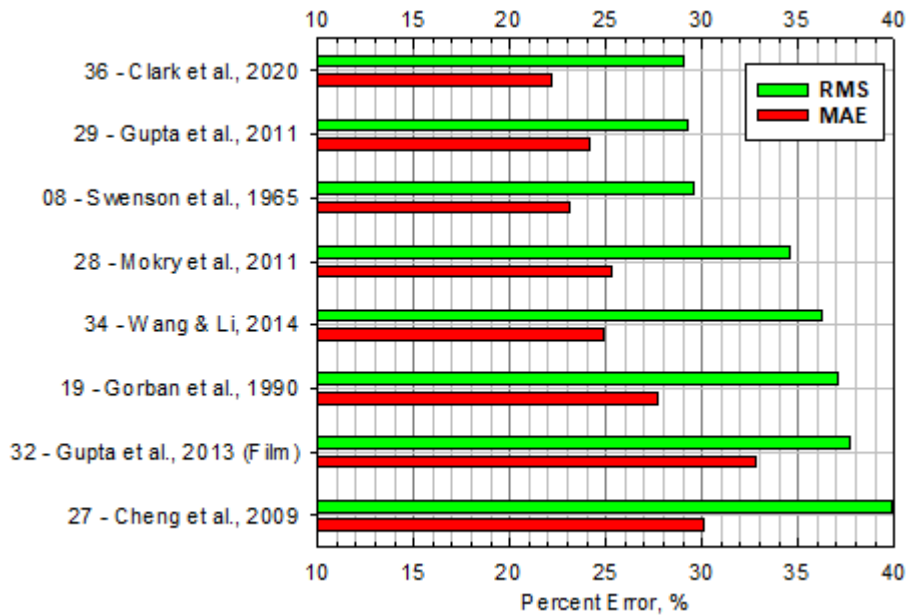


Figure 4-48: Top HTC Nu Correlations, bare tube Dataset

Figure 4-49 shows that the Clark et al. (2020) correlation Eq. (36) is the best predictor of T_w by RMS, and is the second best predictor of T_w by MEA, next to Wang and Li.

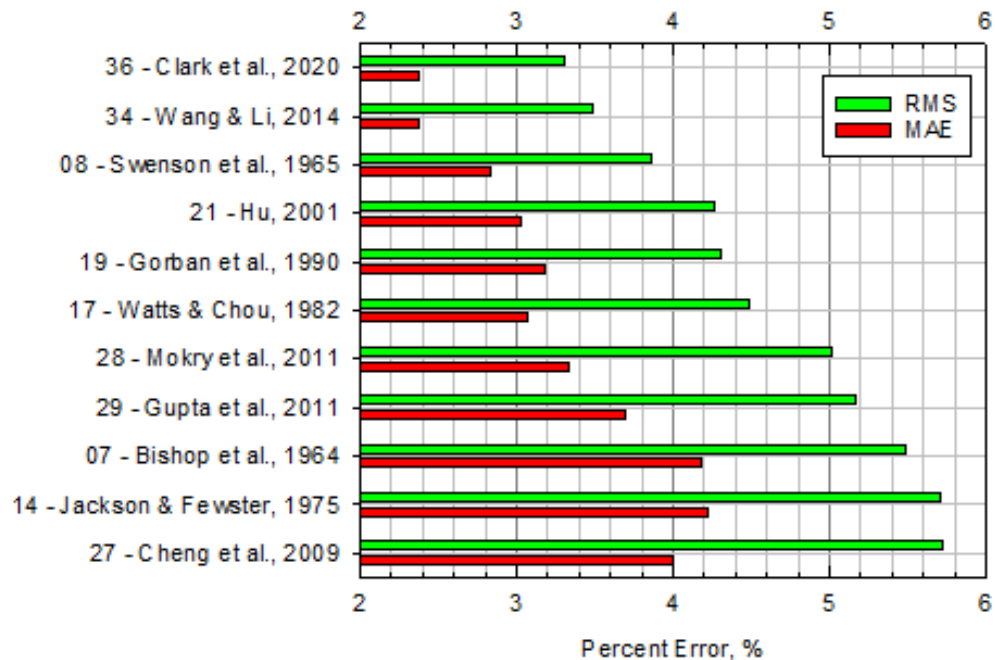


Figure 4-49: Top T_w Nu Correlations, bare tube Dataset

Re-examining the top **Nu** correlations from the Razumovskiy, et al. (2008) and Kirillov, et al. (2005) datasets, reveals that the Clark correlation Eq. (36) is the only **Nu** correlation that has an HTC RMS less than 30% and T_w RMS less than 10% for both datasets.

Table 4-10 shows the list of **Nu** correlations with an HTC prediction of less than 50% by RMS for 7-rod and bare tubes, and a T_w prediction less than 20% by RMS (Green for best in category, Red for worst in category).

Table 4-10: RMS Comparison for Clark and Top Nu Correlations for both Razumovskiy and Kirillov Datasets

Nu Correlations	HTC RMS		T_w RMS	
	<i>7-rod</i>	<i>bare tube</i>	<i>7-rod</i>	<i>bare tube</i>
Eq. (36): Clark, et al. (2020)	26.5%	29.0%	7.4%	3.3%
Eq. (8): Swenson, et al. (1965)	28.3%	29.6%	14.3%	3.9%
Eq. (21): Hu (2001)	25.6%	48.5%	8.6%	4.3%
Eq. (19): Gorban, et al. (1990)	42.2%	37.0%	7.8%	4.3%

4.4 GRAPHICAL ANALYSIS AND COMPARISONS

An important goal is to predict the T_w accurately at all regimes for SCW (NHT/DHT/IHT) in order to predict the fuel centreline temperature ($T_{\text{fuel CL}}$) and maximum sheath temperature (T_{sheath}). While the Clark, et al. (2020) correlation statistically outperforms other **Nu** correlations, it is desirable to visually see how various **Nu** correlations perform across the heated length, in addition to overall trends.

Four sets of graphs for the 7-rod bundle trials are listed below in section 4.4.1. One set of graphs (Set 4) for the three bare tube trials is also listed below in section 4.4.2. Each set of graphs contains the measured HTC and T_w , and the predictions of each by the Dittus-Boelter **Nu** correlation, in addition to four separate sets of **Nu** correlations:

SET 1

Mokry et al. (2011)	Eq. (28)
Dyadyakin & Popov (1977)	Eq. (16)
Lei et al. (2019)	Eq. (35)
Clark et al. (2020)	Eq. (36)

SET 2

Sieder & Tate (1936)	Eq. (2)
Gnielinski (1976)	Eq. (15)
Giarratano et al. (1970)	Eq. (11)
Zukauskas (1972)	Eq. (13)

SET 3

Gupta et al. (2011)	Eq. (29)
Gupta et al. Bulk (2013)	Eq. (30)
Gupta et al. Wall (2013)	Eq. (31)
Gupta et al. Film (2013)	Eq. (32)

SET 4

Swenson et al. (1965)	Eq. (8)
Gorban et al. (1990)	Eq. (18)
Hu (2001)	Eq. (21)
Clark et al. (2020)	Eq. (36)

Section 4.4.3 shows the predicted T_{sheath} and $T_{\text{fuel CL}}$ (assuming A625 sheath and UO₂ fuel with constant heat flux), using the Clark, et al. (2020) correlation Eq. (36) to predict T_w .

It was desirable to know how many 7-rod bundles could be used if an SCWR used 7-rod bundles with the stated parameters from each Trial. This process was then repeated for the 37- and 64-element bundles with the parameters listed in section 2.2.1 and 2.2.3.

All proceeding graphs will be displayed on a full page to enhance the clarity for the reader, with a brief introduction prior to each set, and a summary in section 4.4.3.

4.4.1 7-ROD BUNDLE DATA

4.4.1.1 Set 1

Set 1 consists of the Dittus-Boelter (1930) correlation Eq. (1), the Mokry et al. (2009) correlation Eq. (28), the Dyadyakin and Popov (1977) correlation Eq. (16), the Lei et al. (2019) correlation Eq. (35), and the Clark et al. (2020) correlation Eq. (36).

Figure 4-50 through Figure 4-56 show the experimentally determined values for HTC and T_w for Trials #1 through #8 (symbols), the calculated values for T_b based upon the experiments, and the values predicted by the **Nu** correlations in Set 1 (solid lines).

In Figure 4-50, the T_b and the predicted T_w for all **Nu** correlations in Set 1 remained below the T_{pc} (383.07°C) throughout Trial #1, and increased linearly. The average HTC values for all predicted values also increased linearly.

The Dyadyakin and Popov (1977) correlation Eq. (16) contains an entrance effect modifier:

$$\left(1 + 2.5 \cdot \frac{D_{hy}}{x}\right) \quad \text{from Eq. (16)}$$

As a result, the initial HTC prediction spikes due to the short axial length (x) in comparison with the D_{hy} . At an axial location of roughly 0.100 metres, the entrance effect modifier term approaches 1 and ceases to have an effect on the predictions.

The four **Nu** correlations in Set 1 provide conservative predictions of the measured HTC and T_w values throughout Trial #1, while the Dittus-Boelter (1930) correlation Eq. (1) over-predicts the HTC and under-predicts the T_w values throughout Trial #1.

Of the four **Nu** correlations in Set 1 for Trial #1, the Dyadyakin and Popov (1977) correlation Eq. (16) and the Clark et al. (2020) correlation Eq. (36) appear to follow the trends of the HTC and T_w the closest.

Figure 4-51 shows the predicted values for Set 1 for Trial #2. The T_b remains below the T_{pc} , while the T_w predictions for the four **Nu** correlations in Set 1 cross the T_{pc} at various stages throughout the trial.

The Lei et al. (2019) correlation Eq. (35) and the Mokry et al. (2009) correlation Eq. (28) both experience significant jumps in their predictions as they cross the T_{pc} . The Clark et al.

(2020) correlation Eq. (36) experiences a short period of non-convergence as the predictions cross the T_{pc} , where the HTC values are over-predicted (for more on non-convergences, see section A.1.4).

Both the Clark et al. correlation Eq. (36) and the Dyadyakin and Popov (1977) correlation Eq. (16) appear to follow the trends of the HTC and T_w the closest.

Figure 4-52 shows the predicted values for Set 1 for Trial #3. The T_b remains below the T_{pc} , while the T_w predictions for the four **Nu** correlations in Set 1 cross the T_{pc} at various stages throughout the trial.

Similar to Trial #2, as the predictions cross the T_{pc} , the Lei et al. (2019) correlation Eq. (35) and the Mokry et al. (2009) both experience significant jumps, and the Clark et al. (2020) correlation Eq. (36) experiences a short period of non-convergence.

Both the Clark et al. correlation Eq. (36) and the Dyadyakin and Popov (1977) correlation Eq. (16) appear to follow the trends of the HTC and T_w the closest.

Figure 4-53 & Figure 4-54 show the predicted values for Set 1 for Trial #4 and Trial #5/#6. The T_b remains below the T_{pc} , while the T_w predictions for the four **Nu** correlations in Set 1 cross the T_{pc} at various stages throughout the trial.

The same trends in Trial #2 & Trial #3 are observed in Trial #4 and Trial #5/#6, while the Clark et al. correlation Eq. (36) and the Dyadyakin and Popov (1977) correlation Eq. (16) appear to follow the trends of the HTC and T_w the closest.

Figure 4-55 and Figure 4-56 show the results of Trial #7 and #8, that follow the same trends observed in Trial #2 through #5/#6. In addition, the Dittus-Boelter (1930) correlation Eq. (1) predicts the IHT extremely well.

None of the **Nu** correlations predict the onset of the DHT regime, or the onset of the IHT regime. The Clark et al. correlation Eq. (36) and the Dyadyakin and Popov (1977) correlation Eq. (16) appear to follow the values of the HTC and T_w the closest, with the Clark et al. correlation Eq. (36) being closer the IHT values of the two.

4.4.1.1.1 Set 1 – Trial #1

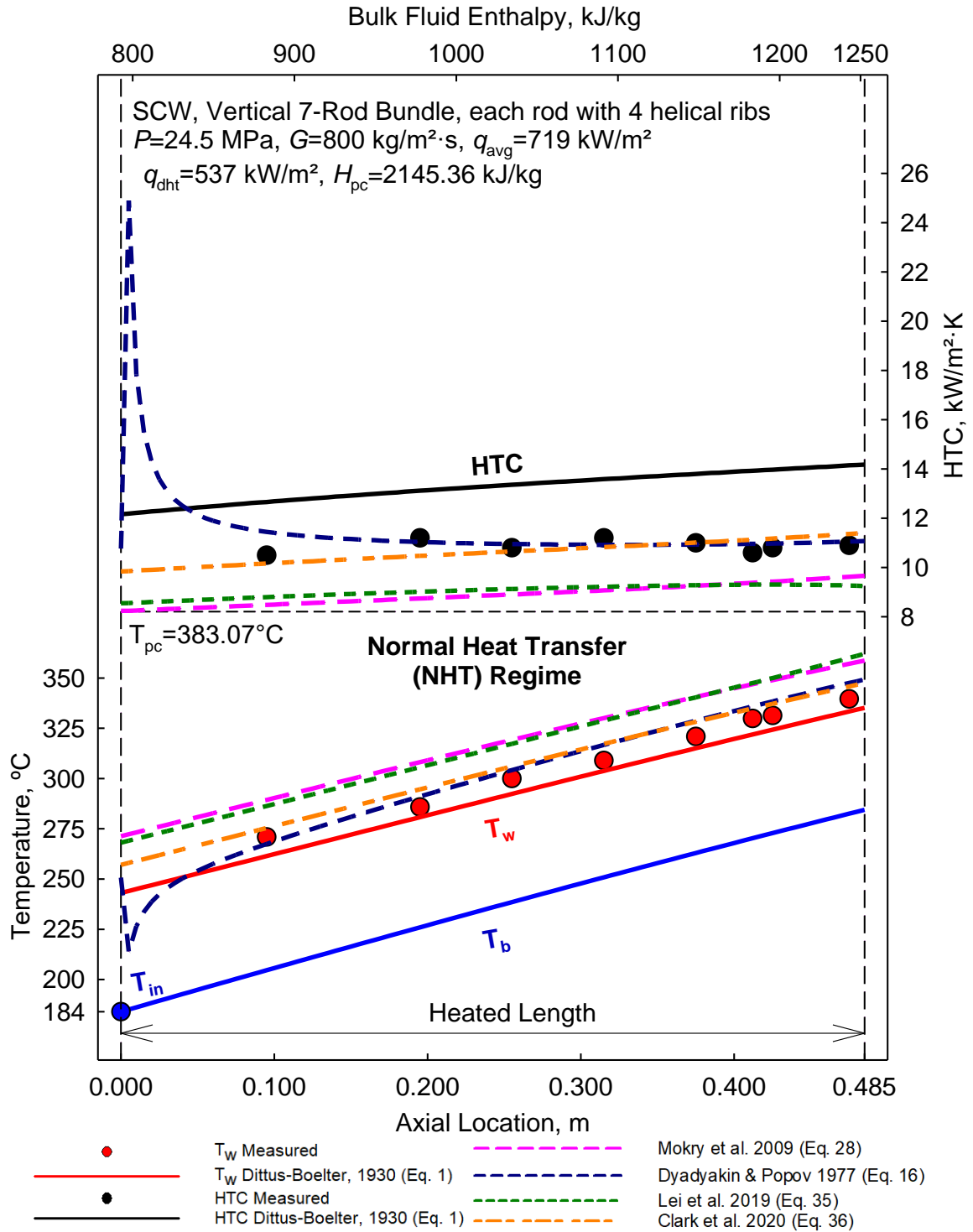


Figure 4-50: T_w and HTC Variations along 0.485m 7-rod Bundle Trial #1-1

$$q_{avg} / q_{dht} = 1.34, q_{avg} / G = 0.90, D_{hy} = 2.57 \text{ mm}$$

4.4.1.1.2 Set 1 – Trial #2

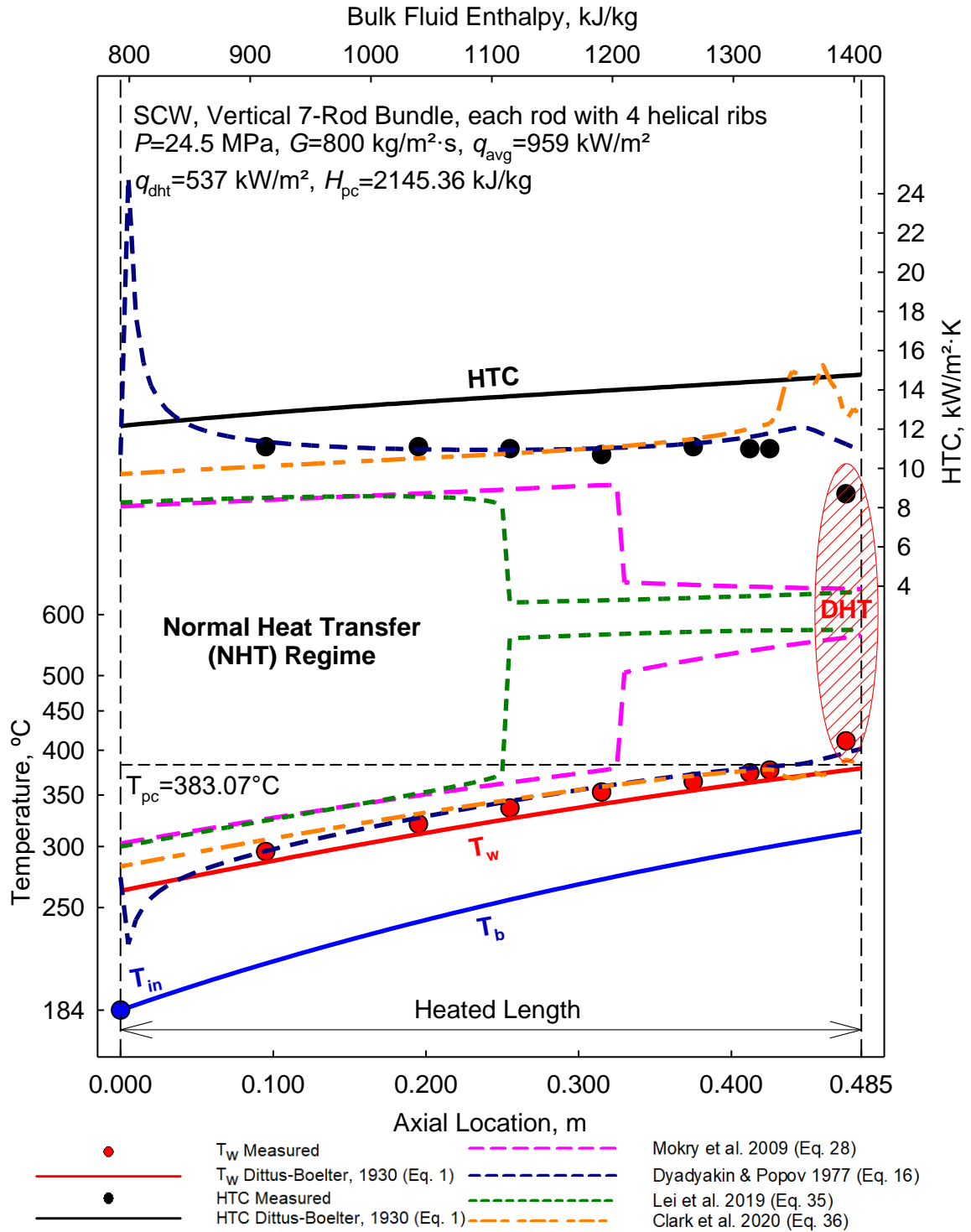


Figure 4-51: T_w and HTC Variations along 0.485m 7-rod Bundle Trial #2-1

$$q_{avg} / q_{dht} = 1.79, q_{avg} / G = 1.20, D_{hy} = 2.57 \text{ mm}$$

4.4.1.1.3 Set 1 – Trial #3

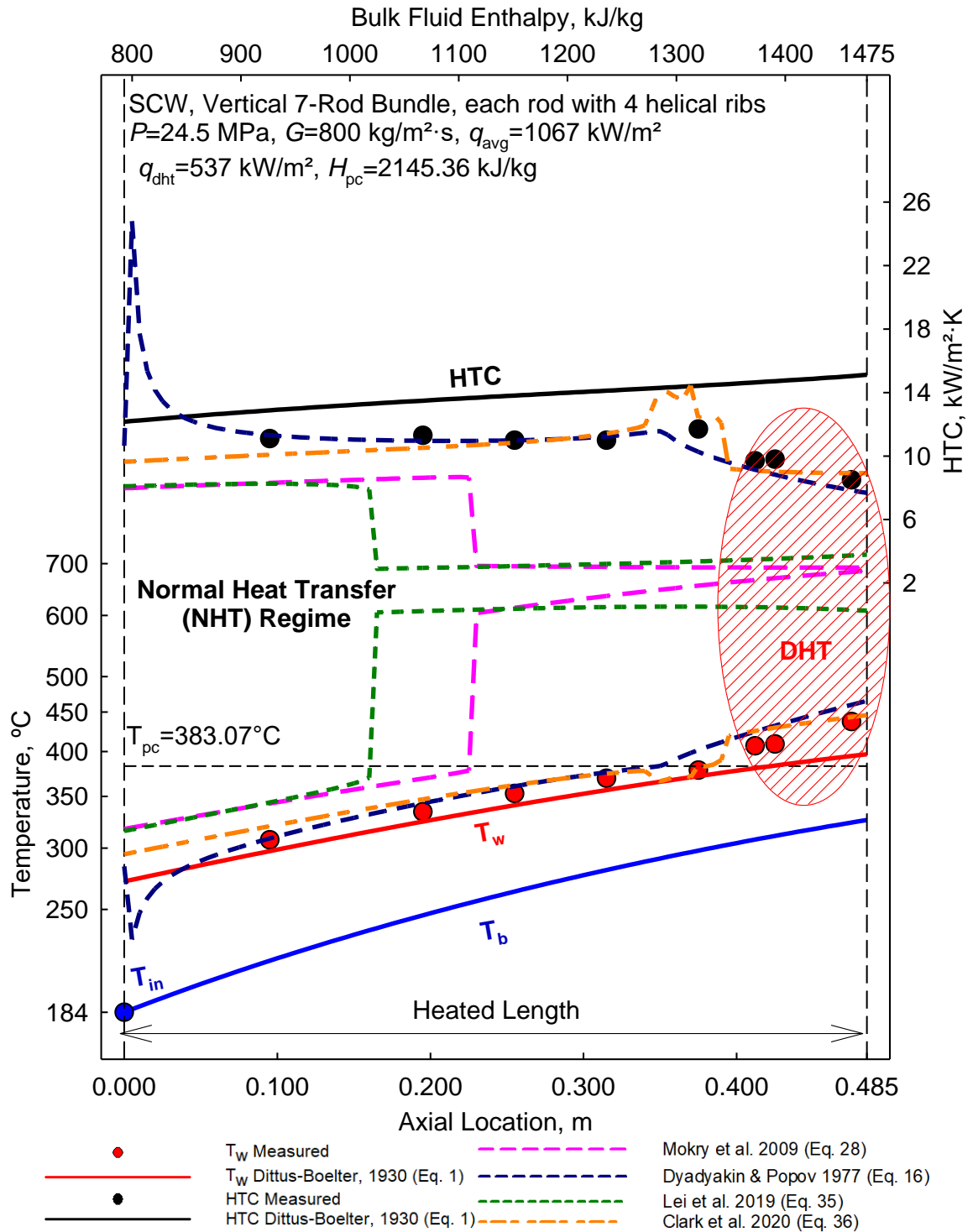


Figure 4-52: T_w and HTC Variations along 0.485m 7-rod Bundle Trial #3-1

$$q_{avg} / q_{dht} = 1.99, q_{avg} / G = 1.33, D_{hy} = 2.57 \text{ mm}$$

4.4.1.1.4 Set 1 – Trial #4

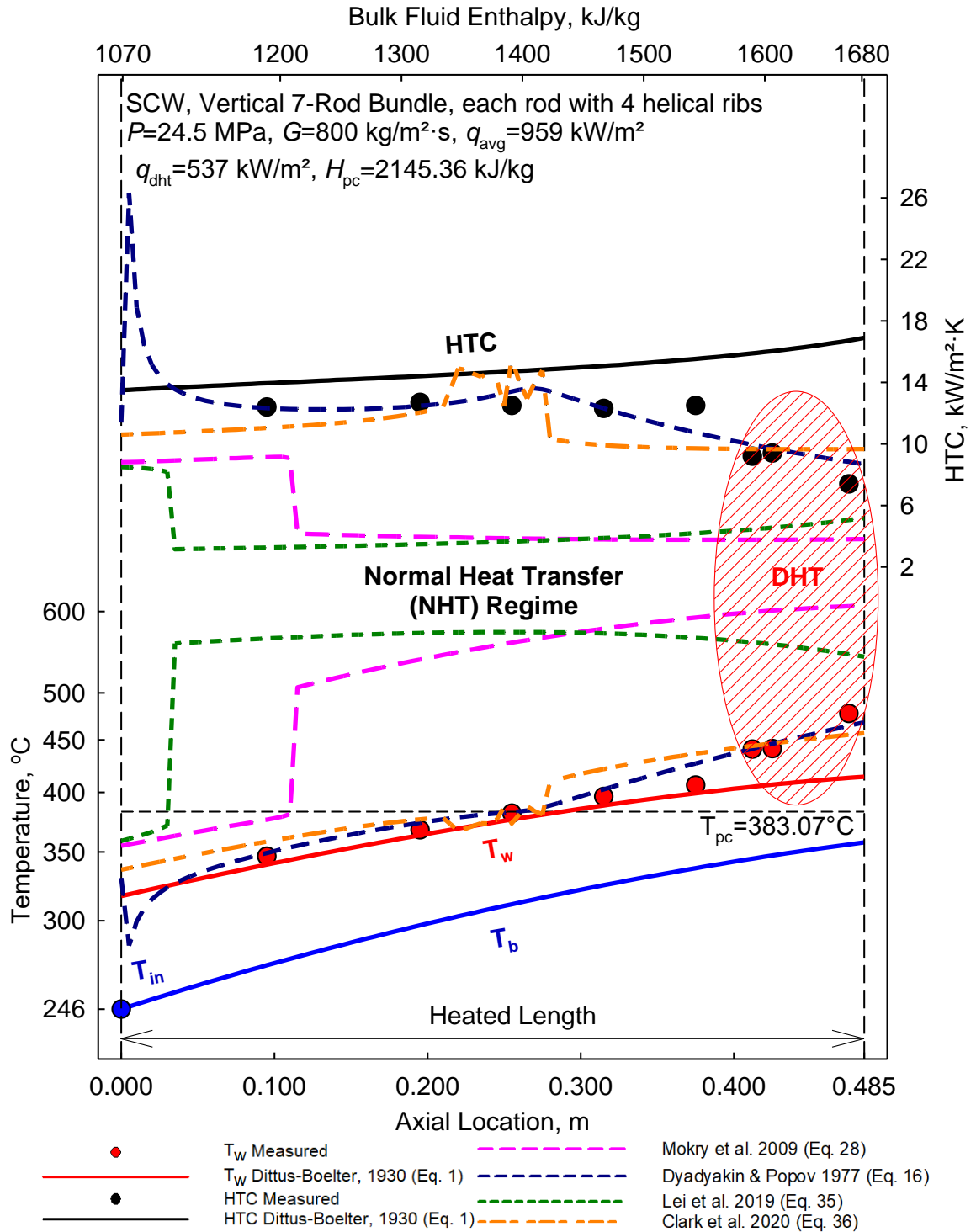


Figure 4-53: T_w and HTC Variations along 0.485m 7-rod Bundle Trial #4-1

$$q_{avg} / q_{dht} = 1.79, q_{avg} / G = 1.20, D_{hy} = 2.57 \text{ mm}$$

4.4.1.1.5 Set 1 – Trial #5/#6

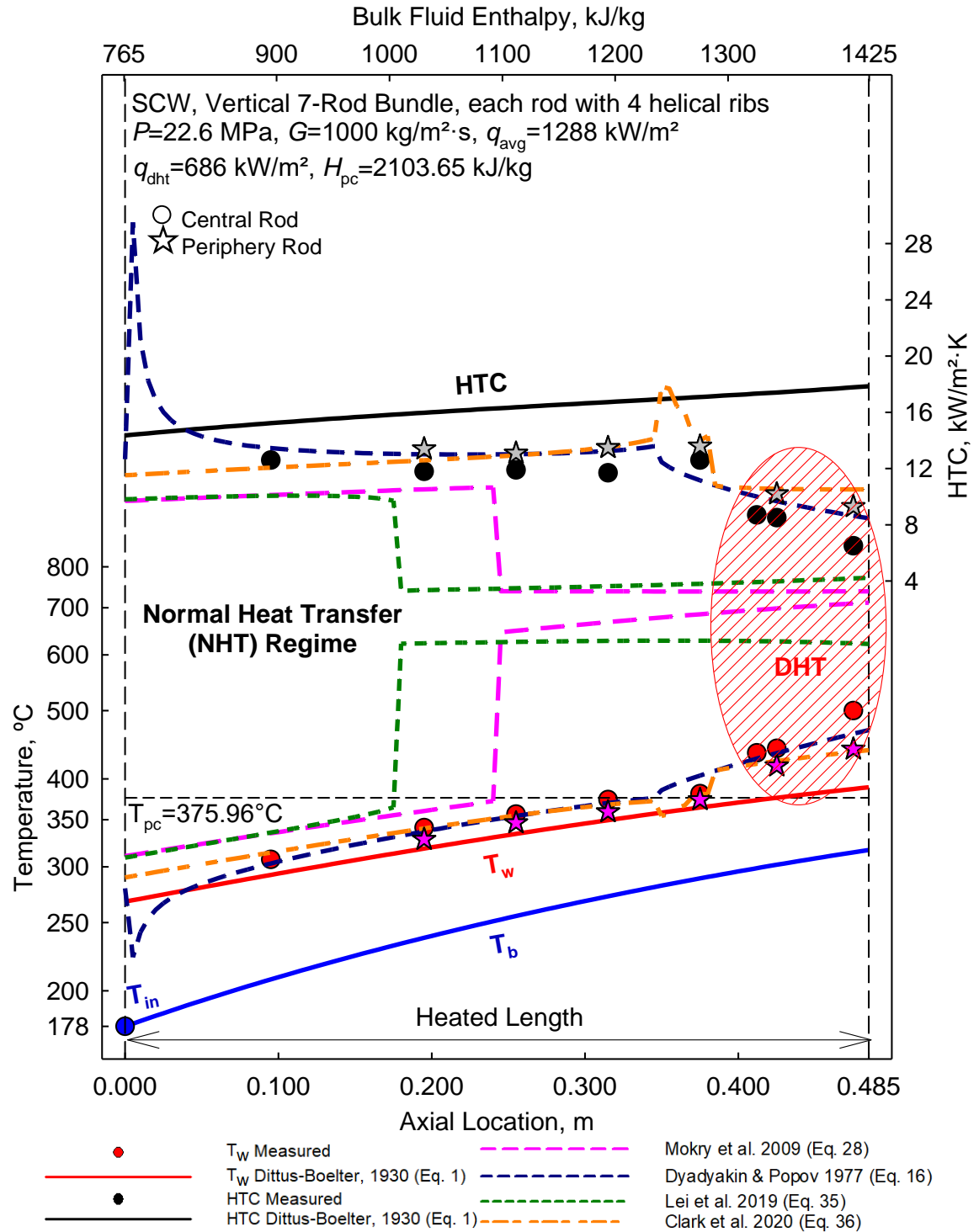


Figure 4-54: T_w and HTC Variations along 0.485m 7-rod Bundle Trial #5/#6-1

$$q_{avg} / q_{dht} = 1.88, q_{avg} / G = 1.29, D_{hy} = 2.57 \text{ mm}$$

4.4.1.1.6 Set 1 – Trial #7

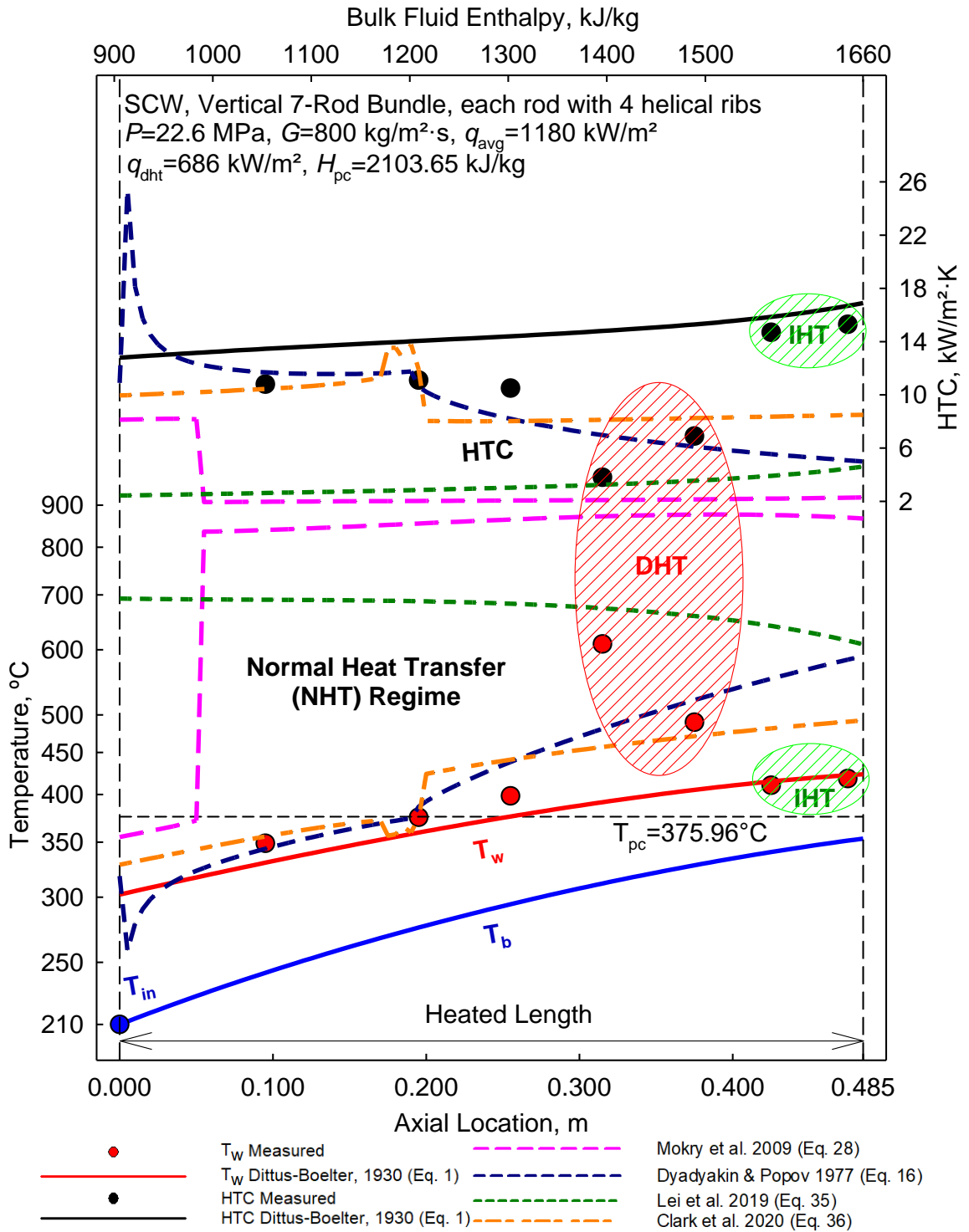


Figure 4-55: T_w and HTC Variations along 0.485m 7-rod Bundle Trial #7-1

$$q_{avg} / q_{dht} = 2.20, q_{avg} / G = 1.48, D_{hy} = 2.57 \text{ mm}$$

4.4.1.1.7 Set 1 – Trial #8

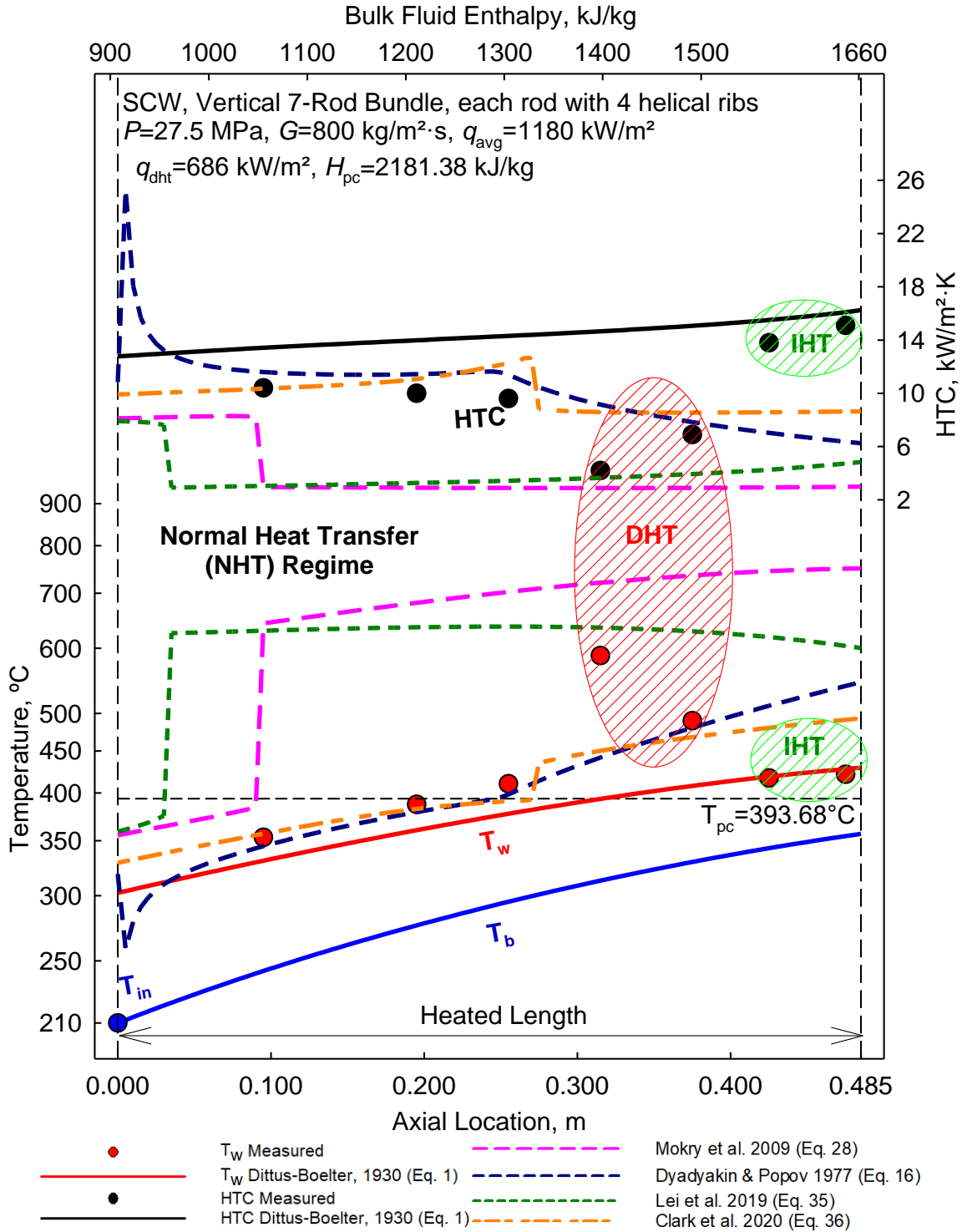


Figure 4-56: T_w and HTC Variations along 0.485m 7-rod Bundle Trial #8-1

$$q_{avg} / q_{dht} = 2.20, q_{avg} / G = 1.48, D_{hy} = 2.57 \text{ mm}$$

4.4.1.2 Set 2

Set 2 consists of the Dittus-Boelter (1930) correlation Eq. (1), the Sieder and Tate (1936) correlation Eq. (2), the Gnielinski (1976) correlation Eq. (15), the Giarratano et al. (1970) correlation Eq. (11), and the Zukauskas (1972) correlation Eq. (13).

Similar to Set 1 in section 4.4.1.1, Figure 4-57 through Figure 4-63 show the experimentally determined values for HTC and T_w for Trials #1 through #8 (symbols), the calculated values for T_b based upon the experiments, and the values predicted by the **Nu** correlations in Set 2 (solid lines).

While the T_b and the predicted T_w for all **Nu** correlations in Set 2 remained below the T_{pc} (383.07°C) throughout Trials #1 and #2, the predictions for T_w for all **Nu** correlations in Set 2 crossed the T_{pc} at various points throughout Trials #3 through #8.

The Gnielinski (1976) correlation Eq. (15) and the Giarratano et al. (1970) correlation Eq. (11) predictions are nearly identical to those of the Dittus-Boelter (1930) correlation Eq. (1) predictions for all trials.

The Sieder and Tate (1936) correlation Eq. (2) consistently over-predicts the HTC and under-predicts the T_w for all trials, while experiencing a small jump in predictions as the T_w prediction crosses the T_{pc} .

The Zukauskas (1972) correlation Eq. (13) also consistently over-predicts the HTC and under-predicts the T_w for all trials. However, as it crosses the T_{pc} point, there is a small band of non-convergence.

4.4.1.2.1 Set 2 – Trial #1

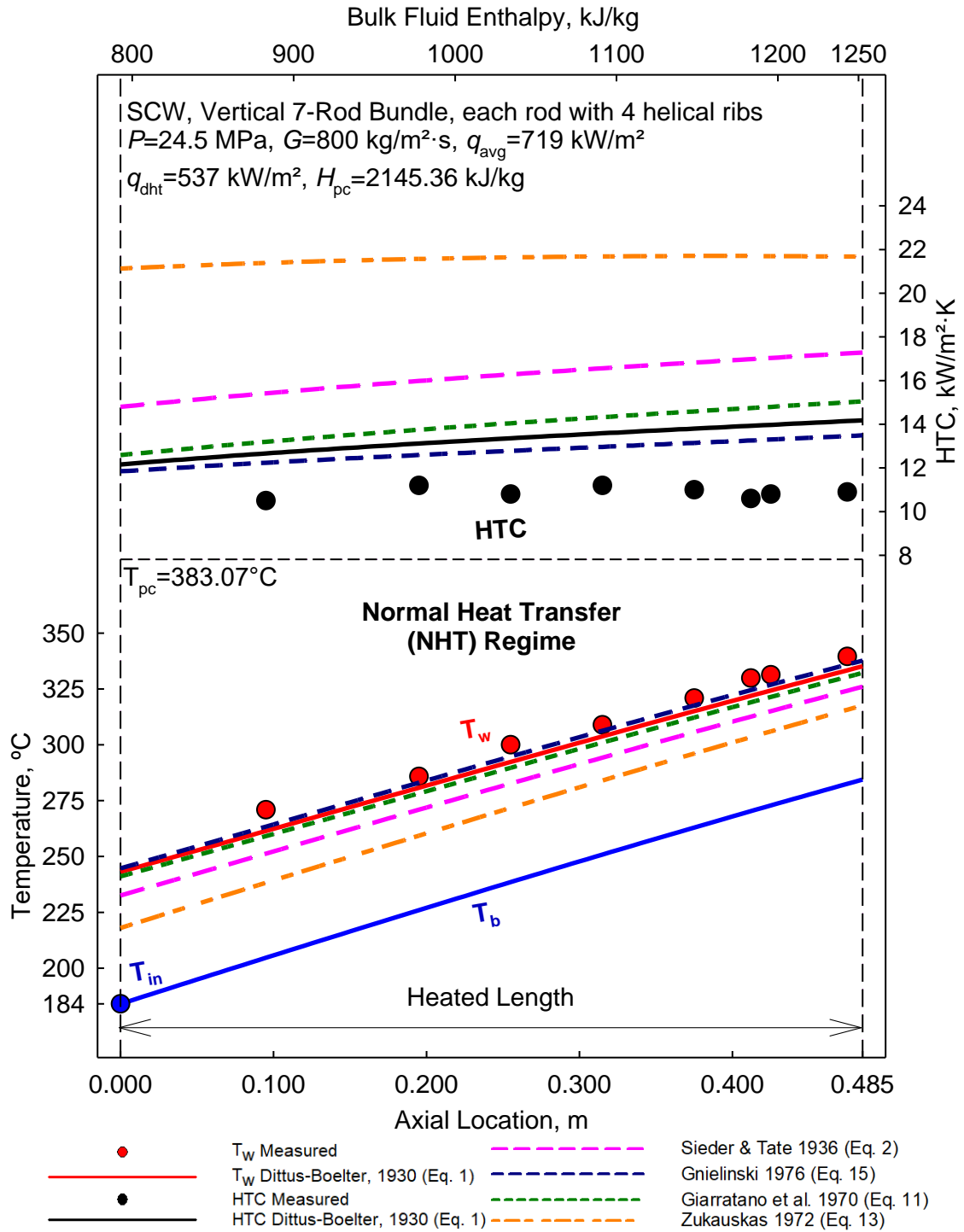


Figure 4-57: T_w and HTC Variations along 0.485m 7-rod Bundle Trial #1-2

$$q_{avg} / q_{dht} = 1.34, q_{avg} / G = 0.90, D_{hy} = 2.57 \text{ mm}$$

4.4.1.2.2 Set 2 – Trial #2

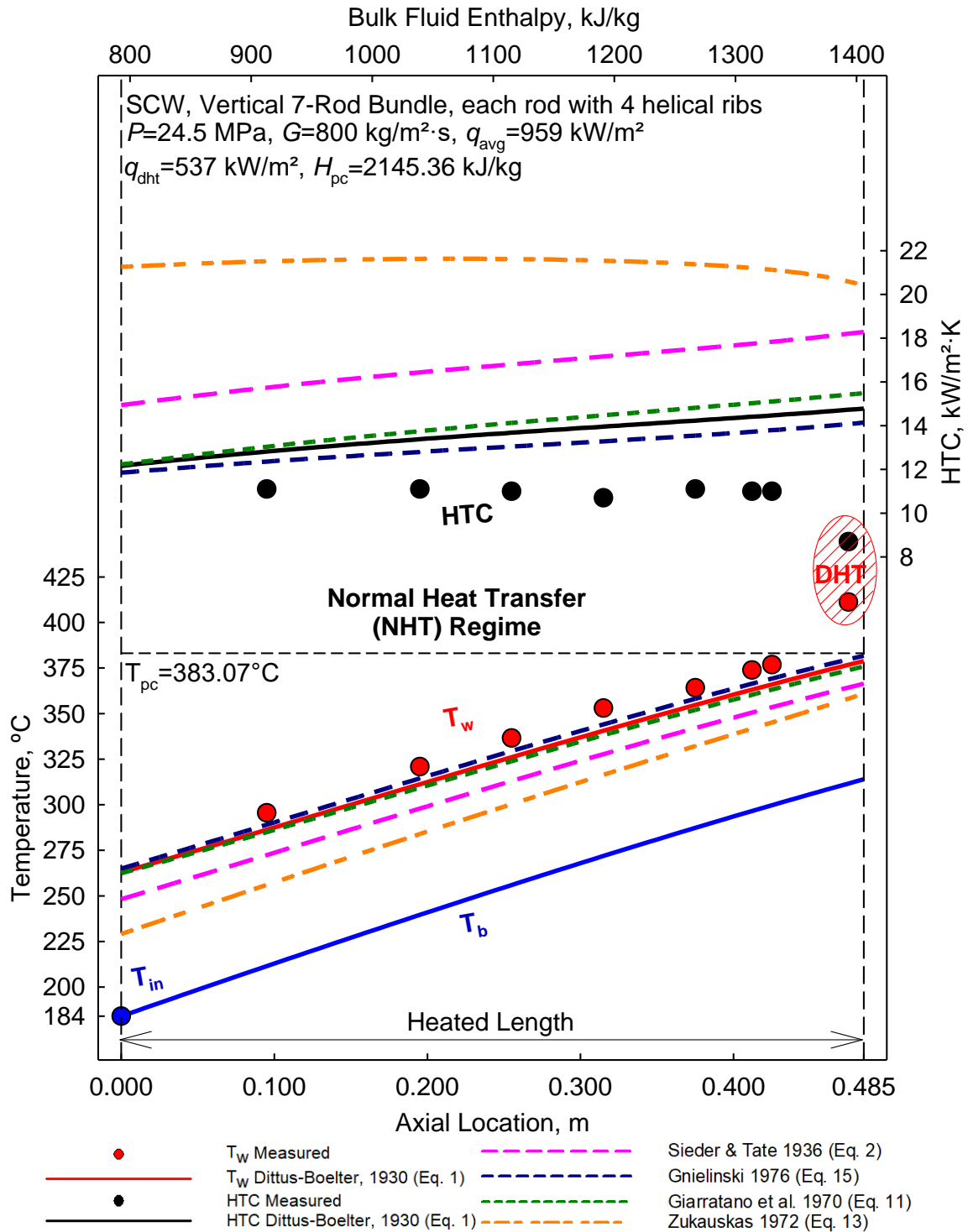


Figure 4-58: T_w and HTC Variations along 0.485m 7-rod Bundle Trial #2-2

$$q_{avg} / q_{dht} = 1.79, q_{avg} / G = 1.20, D_{hy} = 2.57 \text{ mm}$$

4.4.1.2.3 Set 2 – Trial #3

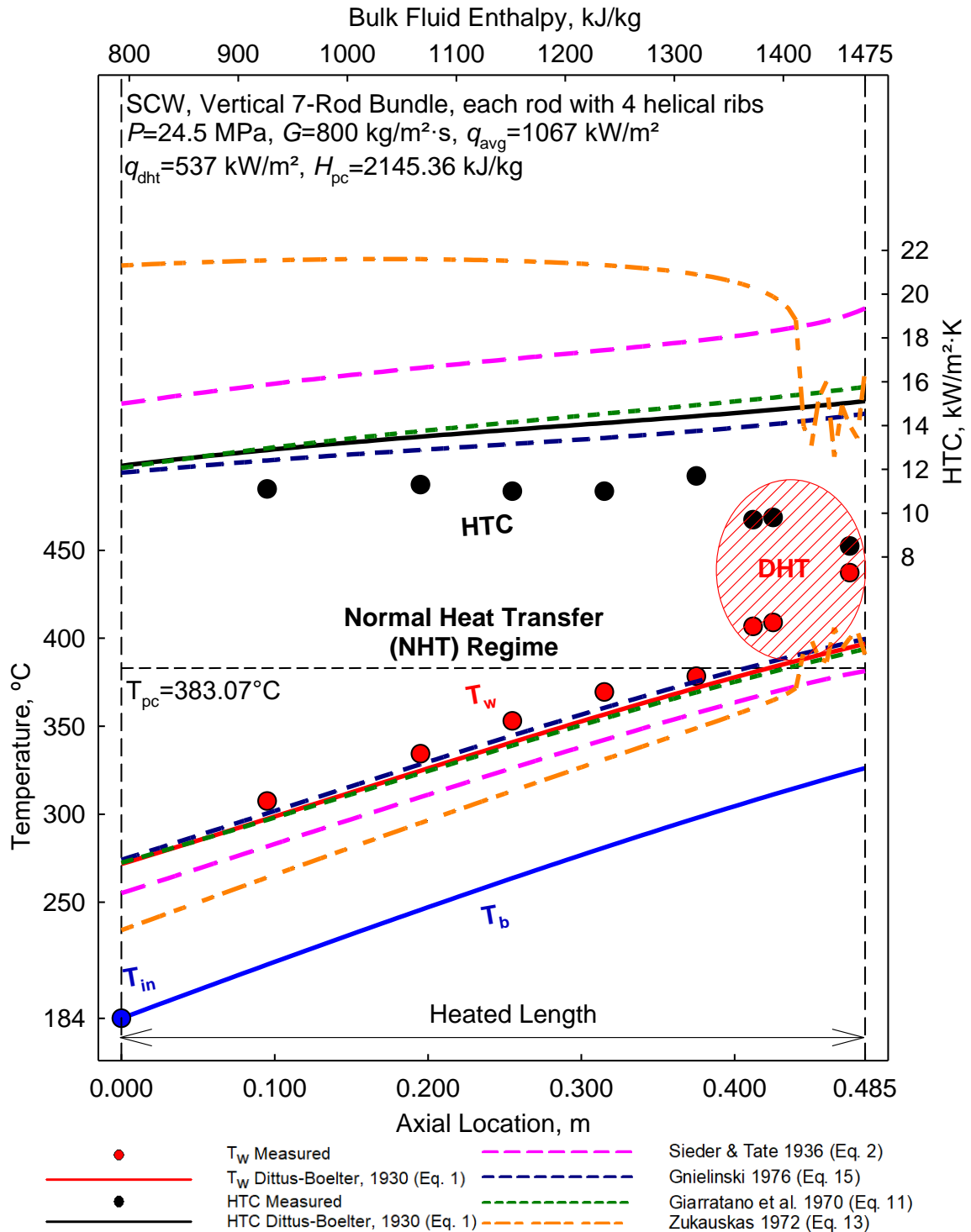


Figure 4-59: T_w and HTC Variations along 0.485m 7-rod Bundle Trial #3-2

$$q_{avg} / q_{dht} = 1.99, q_{avg} / G = 1.33, D_{hy} = 2.57 \text{ mm}$$

4.4.1.2.4 Set 2 – Trial #4

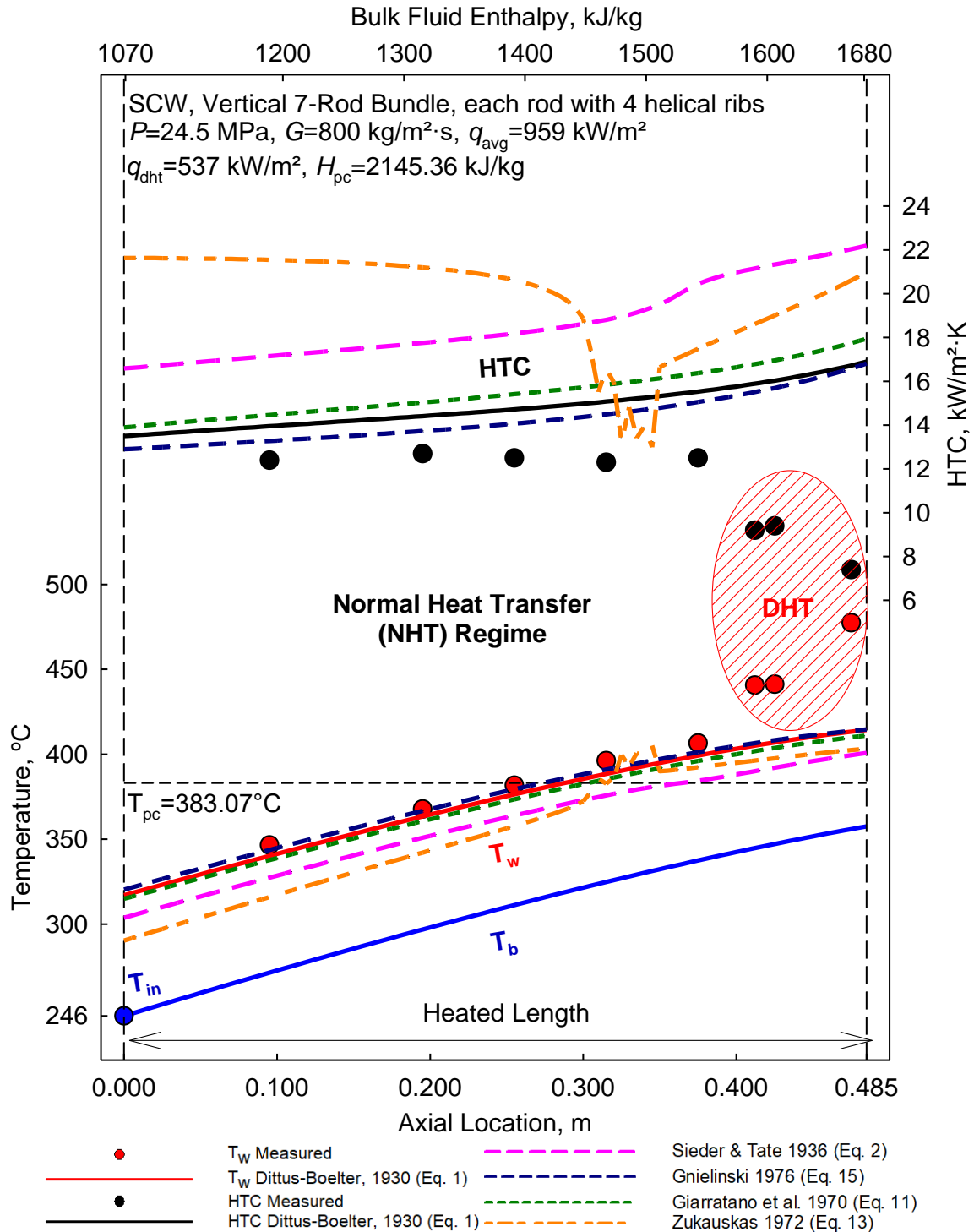


Figure 4-60: T_w and HTC Variations along 0.485m 7-rod Bundle Trial #4-2

$$q_{avg} / q_{dht} = 1.79, q_{avg} / G = 1.20, D_{hy} = 2.57 \text{ mm}$$

4.4.1.2.5 Set 2 – Trial #5/#6

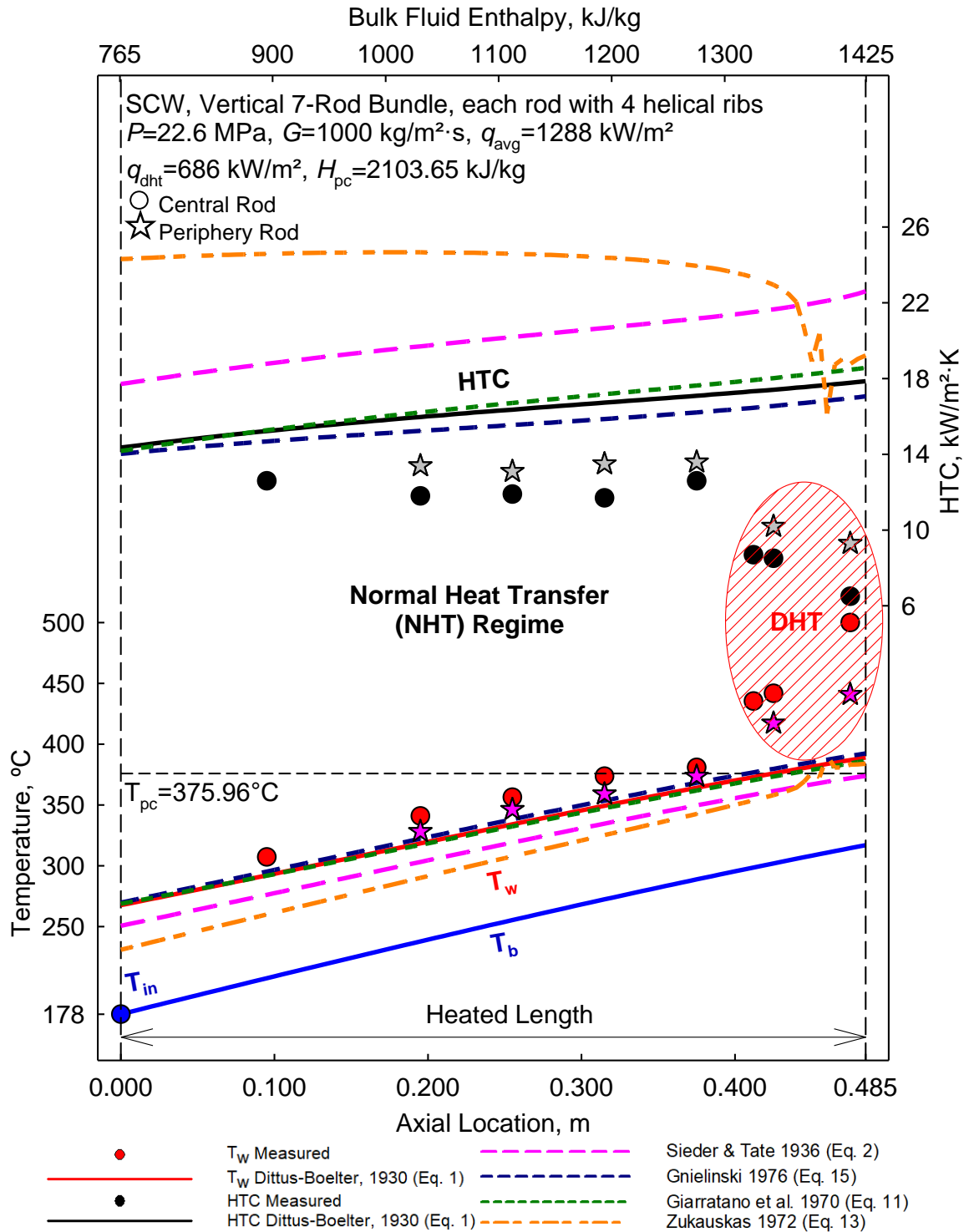


Figure 4-61: T_w and HTC Variations along 0.485m 7-rod Bundle Trial #5/#6-2

$$q_{avg} / q_{dht} = 1.88, q_{avg} / G = 1.29, D_{hy} = 2.57 \text{ mm}$$

4.4.1.2.6 Set 2 – Trial #7

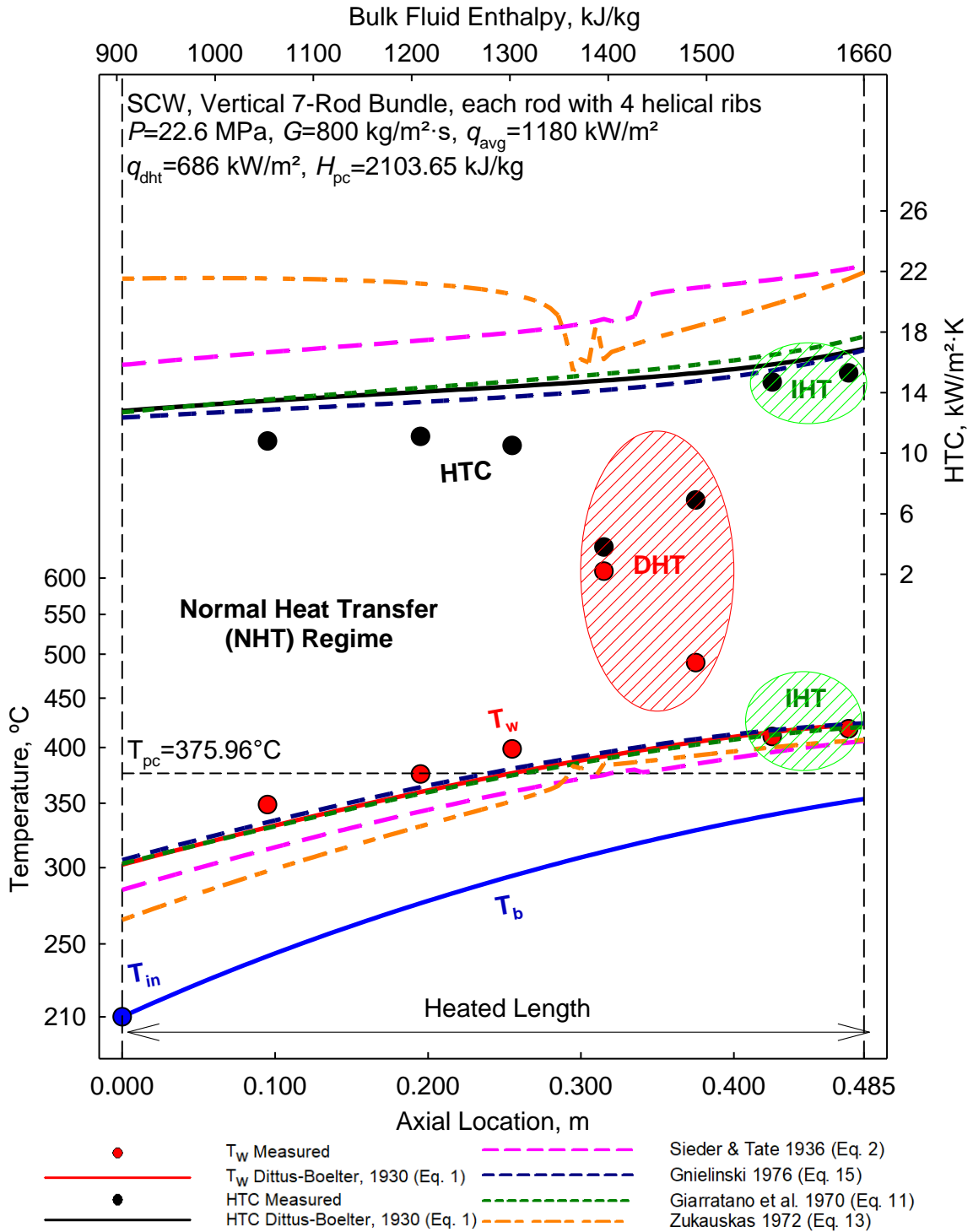


Figure 4-62: T_w and HTC Variations along 0.485m 7-rod Bundle Trial #7-2

$$q_{avg} / q_{dht} = 2.20, q_{avg} / G = 1.48, D_{hy} = 2.57 \text{ mm}$$

4.4.1.2.7 Set 2 – Trial #8

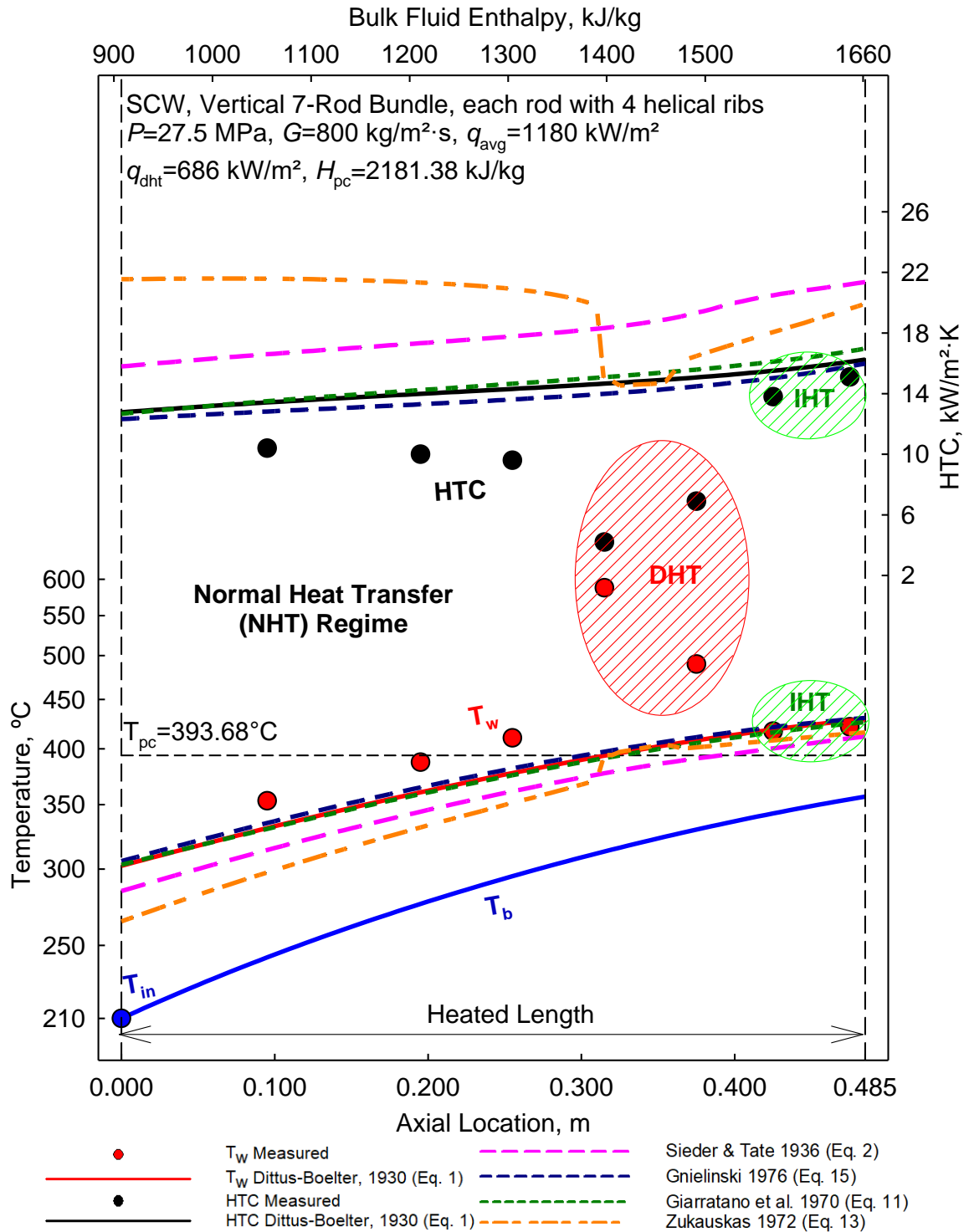


Figure 4-63: T_w and HTC Variations along 0.485m 7-rod Bundle Trial #8-2

$$q_{avg} / q_{dht} = 2.20, q_{avg} / G = 1.48, D_{hy} = 2.57 \text{ mm}$$

4.4.1.3 Set 3

Set #3 consists of the Dittus-Boelter (1930) correlation Eq. (1), the Gupta et al. (2011) correlation Eq. (29), the Gupta et al. Bulk (2013) correlation Eq. (30), Gupta et al. Wall (2013) correlation Eq. (31), and the Gupta et al. Film (2013) correlation Eq. (32).

Similar to Set 1 in section 4.4.1.1, Figure 4-64 through Figure 4-70 show the experimentally determined values for HTC and T_w for Trials #1 through #8 (symbols), the calculated values for T_b based upon the experiments, and the values predicted by the **Nu** correlations in Set 3 (solid lines).

While the T_b and the predicted T_w for all **Nu** correlations in Set 3 remained below the T_{pc} (383.07°C) throughout Trial #1, the predictions for the Gupta et al. (2011) correlation Eq. (29) and the Gupta et al. Film (2013) correlation Eq. (32) crossed the T_{pc} in Trial #2, and the predictions for T_w for all **Nu** correlations in Set 3 crossed the T_{pc} at various points throughout Trials #3 through #8.

The Gupta et al. (2011) correlation Eq. (29) under-predicts the HTC and over-predicts the T_w for Trials #1 through #8.

The Gupta et al. Bulk (2013) correlation Eq. (30) and the Gupta et al. Wall (2013) correlation Eq. (31) over-predicts the HTC and under-predicts the T_w for Trials #1 through #8 while the T_w is less than T_{pc} . After the predictions for T_w pass T_{pc} , both **Nu** correlations experience a jump, and then provide an under-prediction for the HTC and an over-prediction for the T_w , similar to the Lei et al. (2019) correlation Eq. (35) and the Mokry et al. (2009) correlation Eq. (28).

The Gupta et al. Film (2013) correlation Eq. (32) follows the HTC and T_w closely when the T_w prediction is less than the T_{pc} . Once the T_w prediction crosses the T_{pc} , this **Nu** correlation experiences one jump in prediction for Trials #2, #3, and #5/#6. However, for Trials #4, #7, and #8, this **Nu** correlation experiences two jumps, and also a band of non-convergence.

4.4.1.3.1 Set 3 – Trial #1

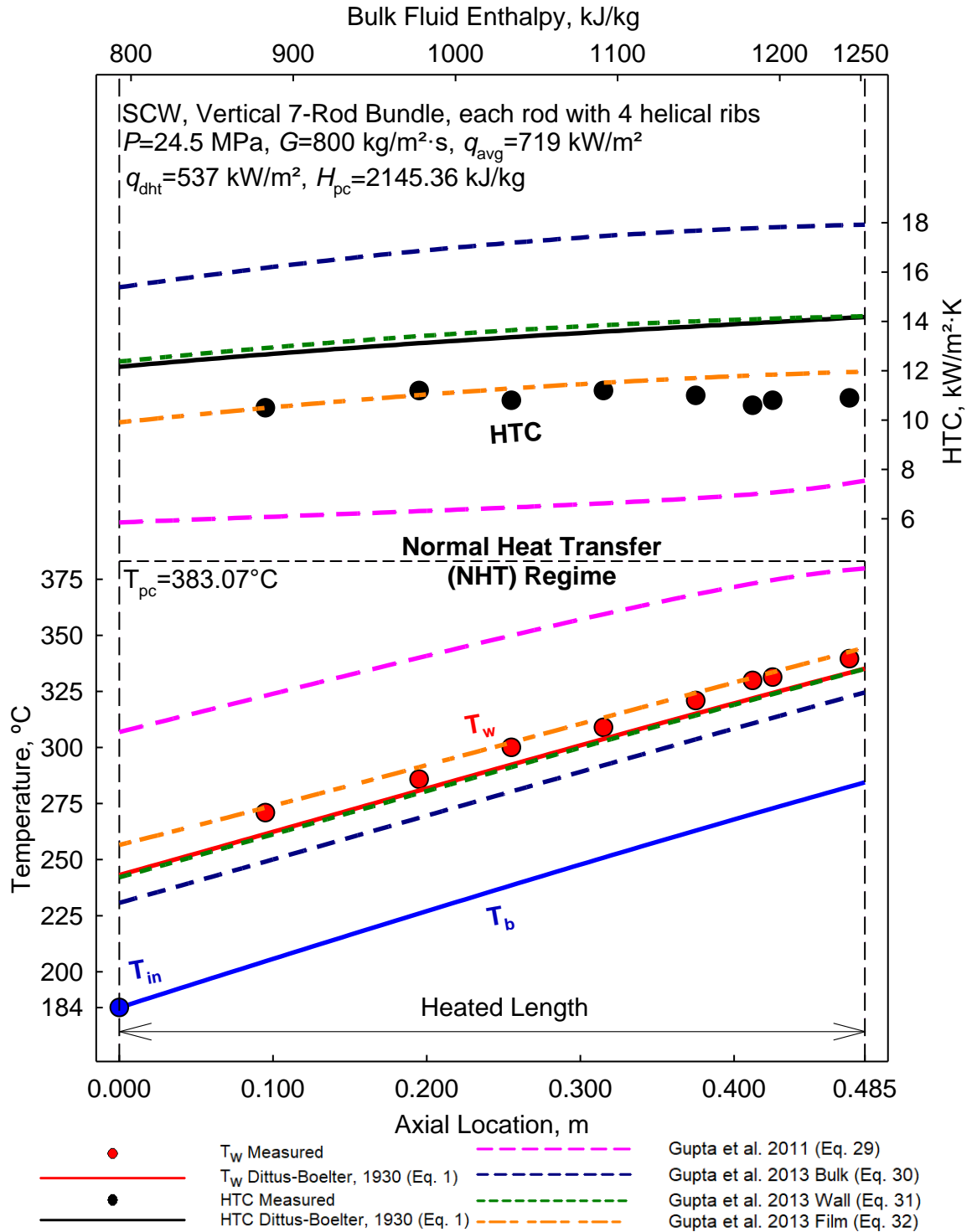


Figure 4-64: T_w and HTC Variations along 0.485m 7-rod Bundle Trial #1-3

$$q_{avg} / q_{dht} = 1.34, q_{avg} / G = 0.90, D_{hy} = 2.57 \text{ mm}$$

4.4.1.3.2 Set 3 – Trial #2

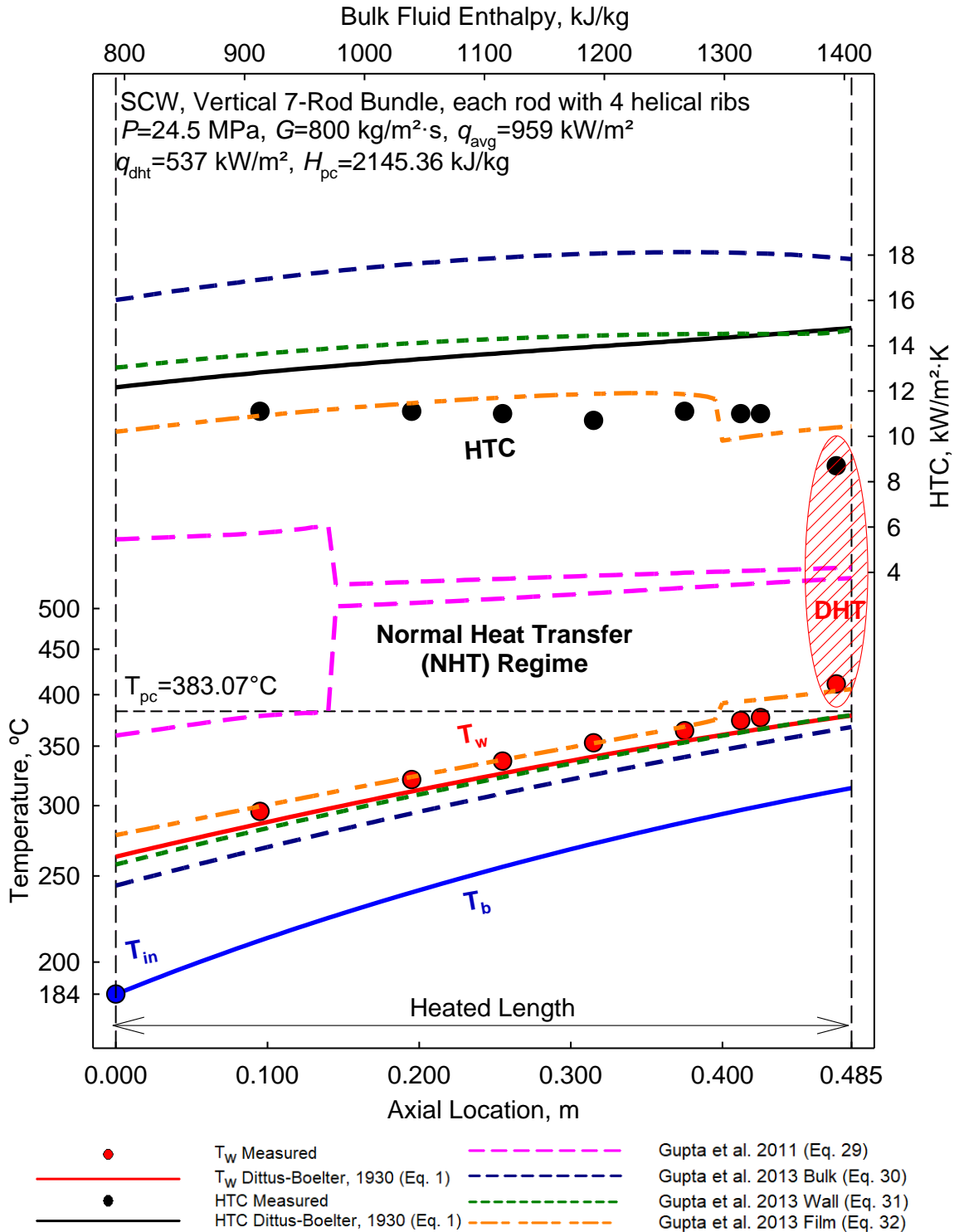


Figure 4-65: T_w and HTC Variations along 0.485m 7-rod Bundle Trial #2-3

$$q_{avg} / q_{dht} = 1.79, q_{avg} / G = 1.20, D_{hy} = 2.57 \text{ mm}$$

4.4.1.3.3 Set 3 – Trial #3

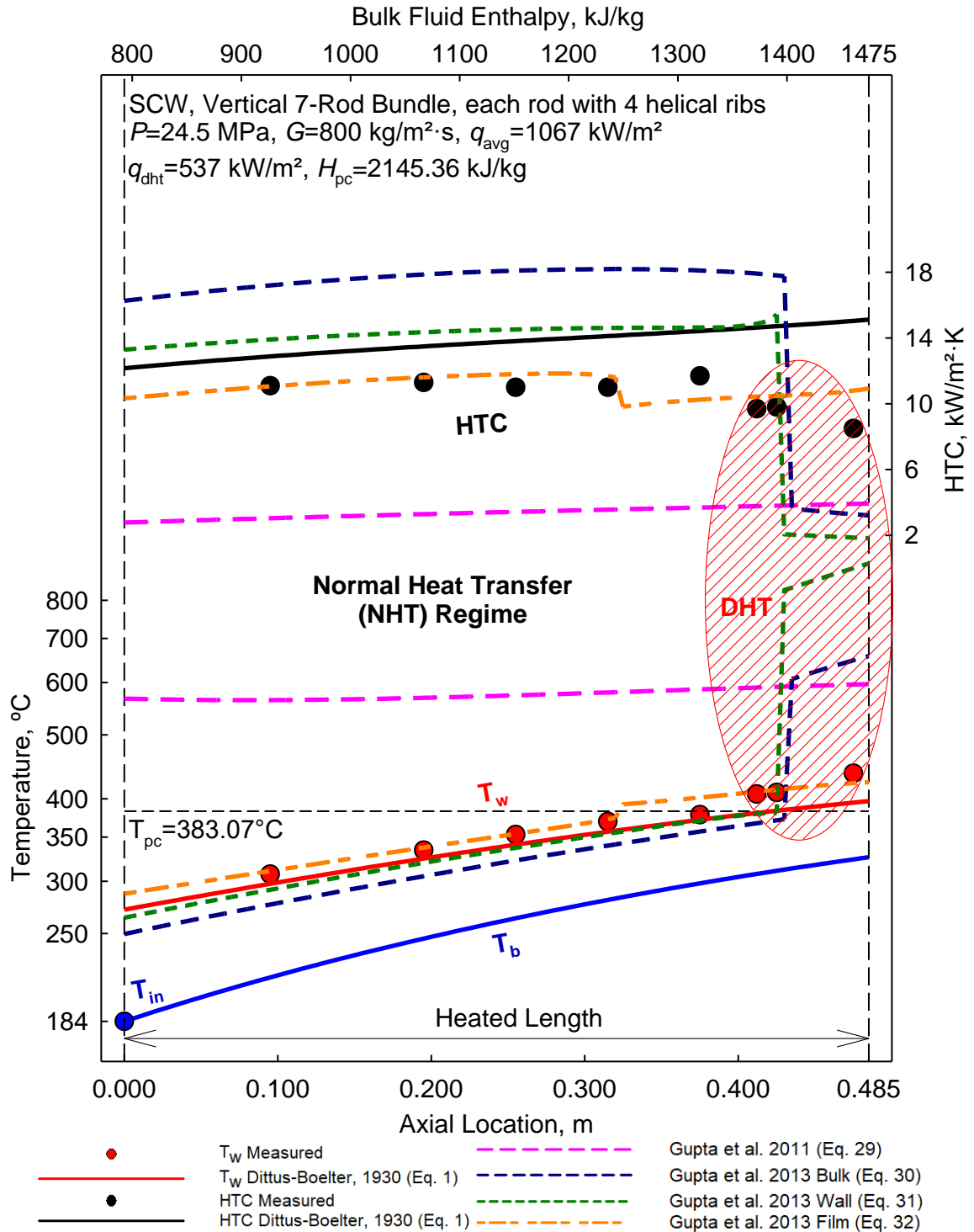


Figure 4-66: T_w and HTC Variations along 0.485m 7-rod Bundle Trial #3-3

$$q_{avg} / q_{dht} = 1.99, q_{avg} / G = 1.33, D_{hy} = 2.57 \text{ mm}$$

4.4.1.3.4 Set 3 – Trial #4

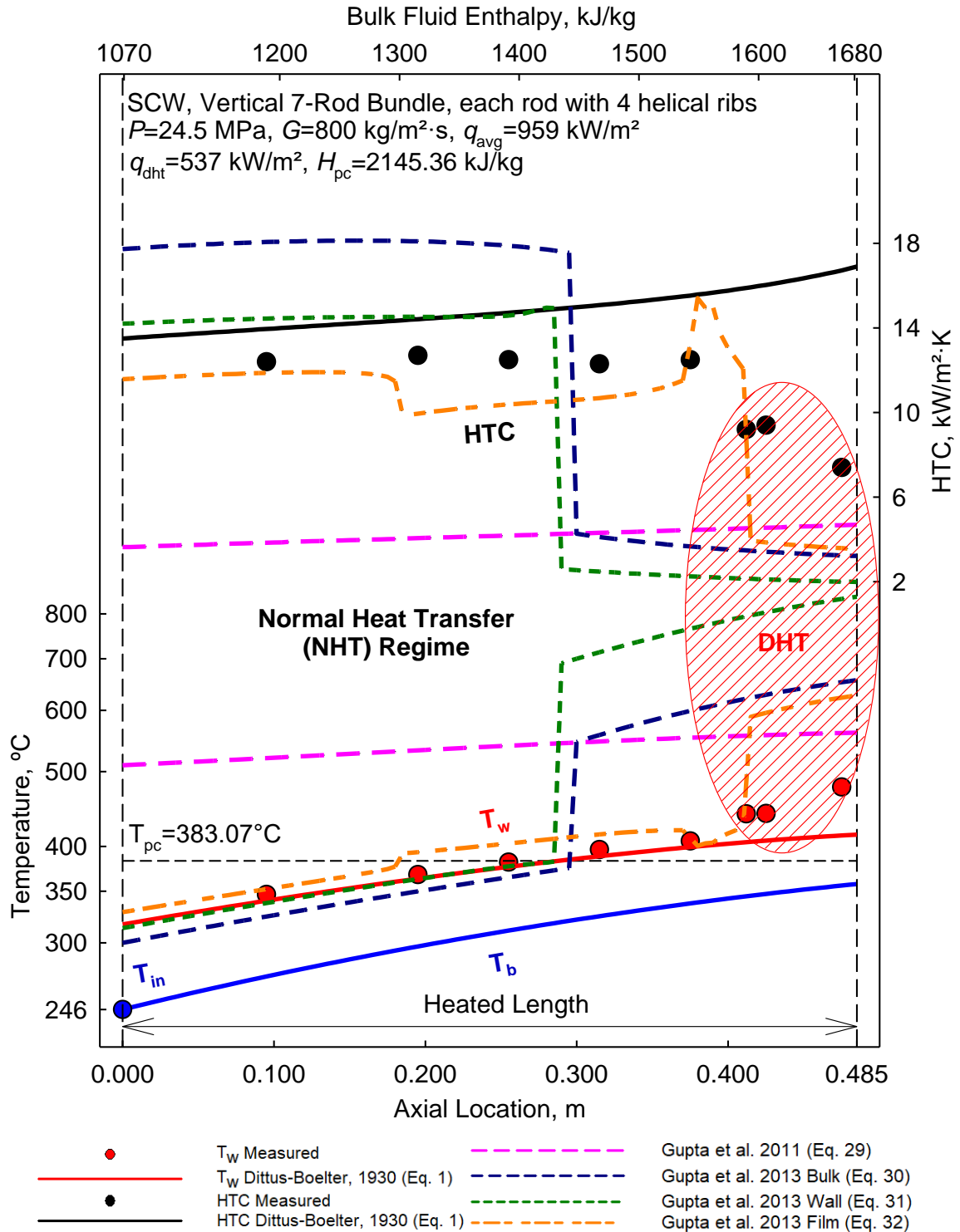


Figure 4-67: T_w and HTC Variations along 0.485m 7-rod Bundle Trial #4-3

$$q_{avg} / q_{dht} = 1.79, q_{avg} / G = 1.20, D_{hy} = 2.57 \text{ mm}$$

4.4.1.3.5 Set 3 – Trial #5/#6

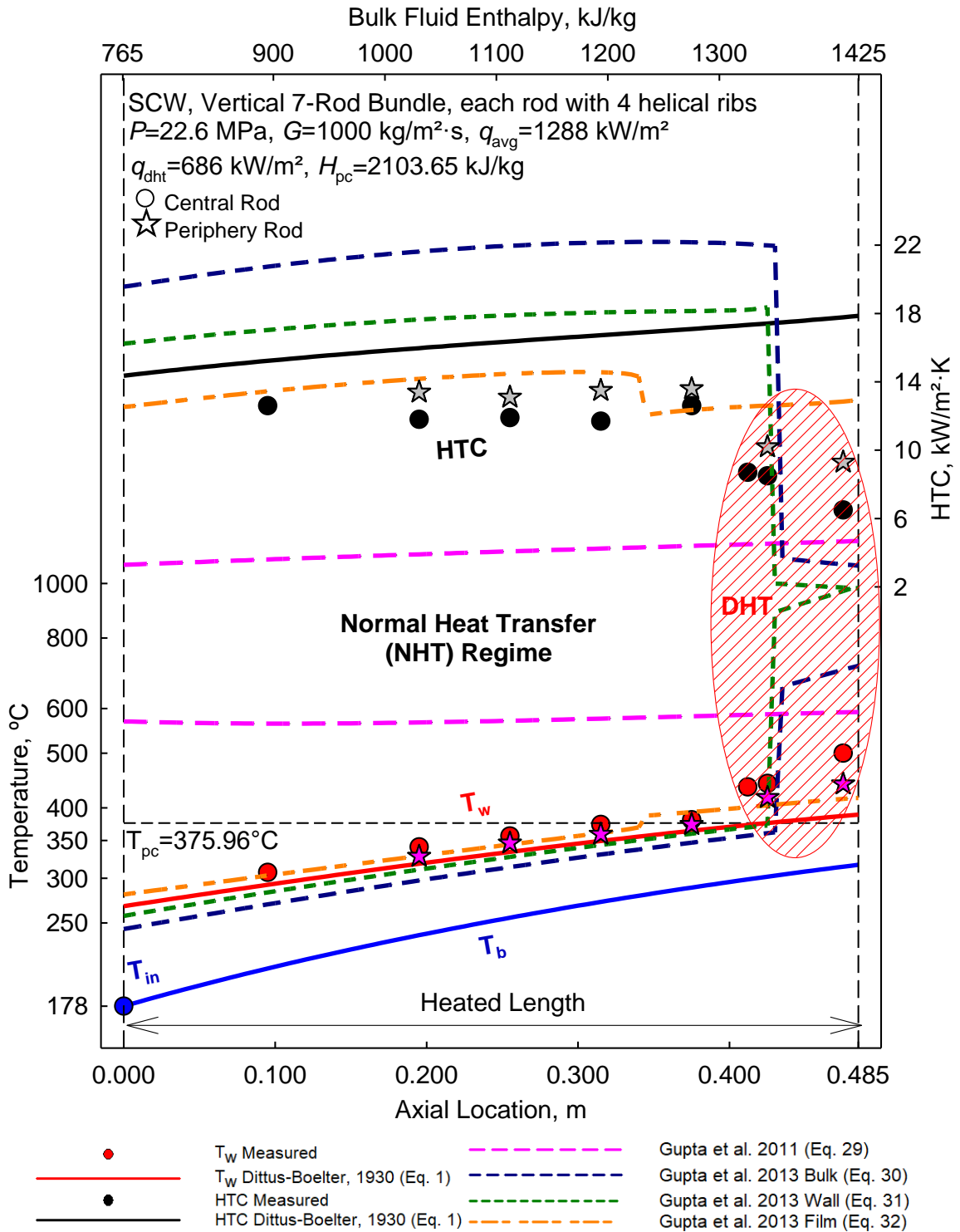


Figure 4-68: T_w and HTC Variations along 0.485m 7-rod Bundle Trial #5/#6-3

$$q_{avg} / q_{dht} = 1.88, q_{avg} / G = 1.29, D_{hy} = 2.57 \text{ mm}$$

4.4.1.3.6 Set 3 – Trial #7

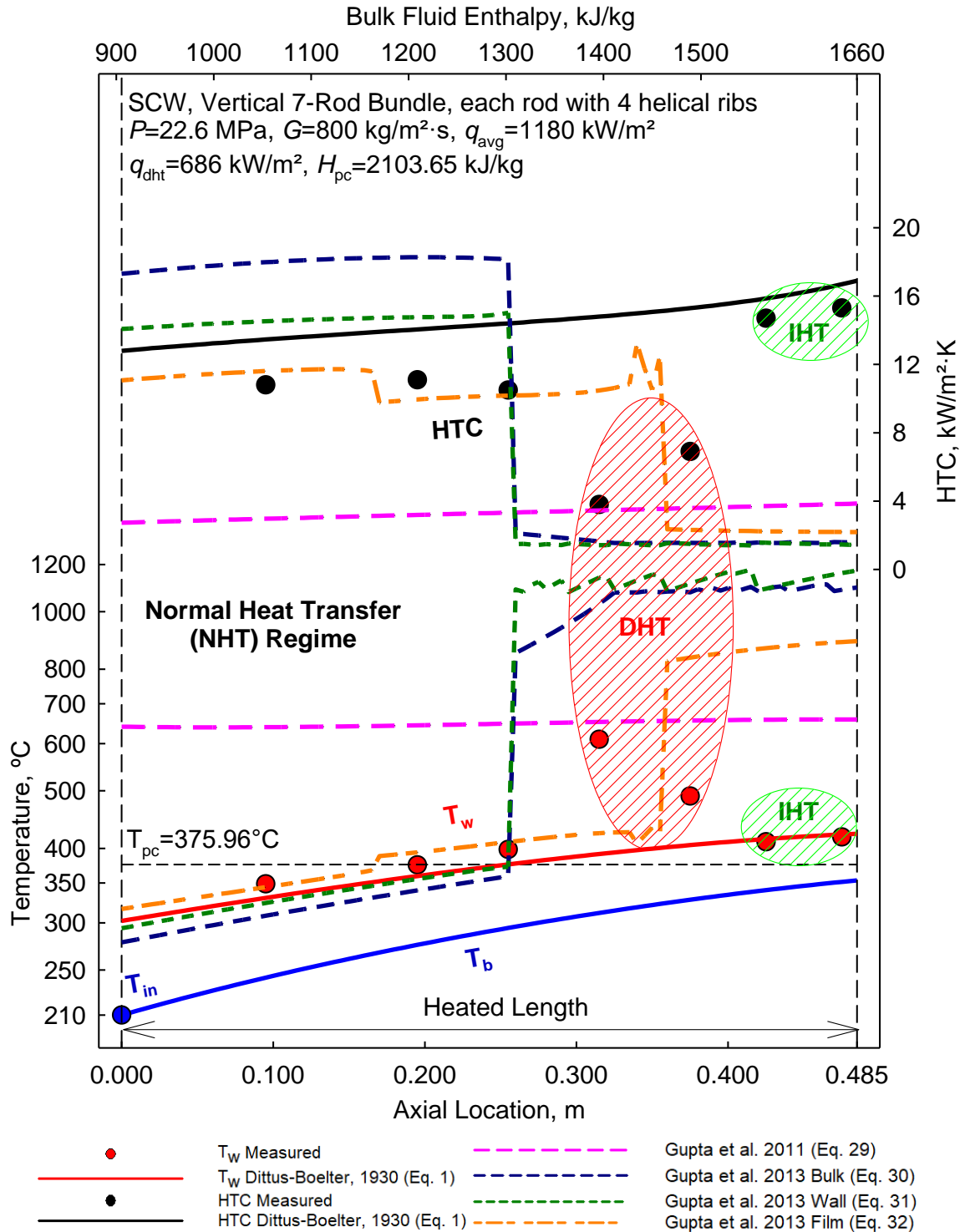


Figure 4-69: T_w and HTC Variations along 0.485m 7-rod Bundle Trial #7-3

$$q_{avg} / q_{dht} = 2.20, q_{avg} / G = 1.48, D_{hy} = 2.57 \text{ mm}$$

4.4.1.3.7 Set 3 – Trial #8

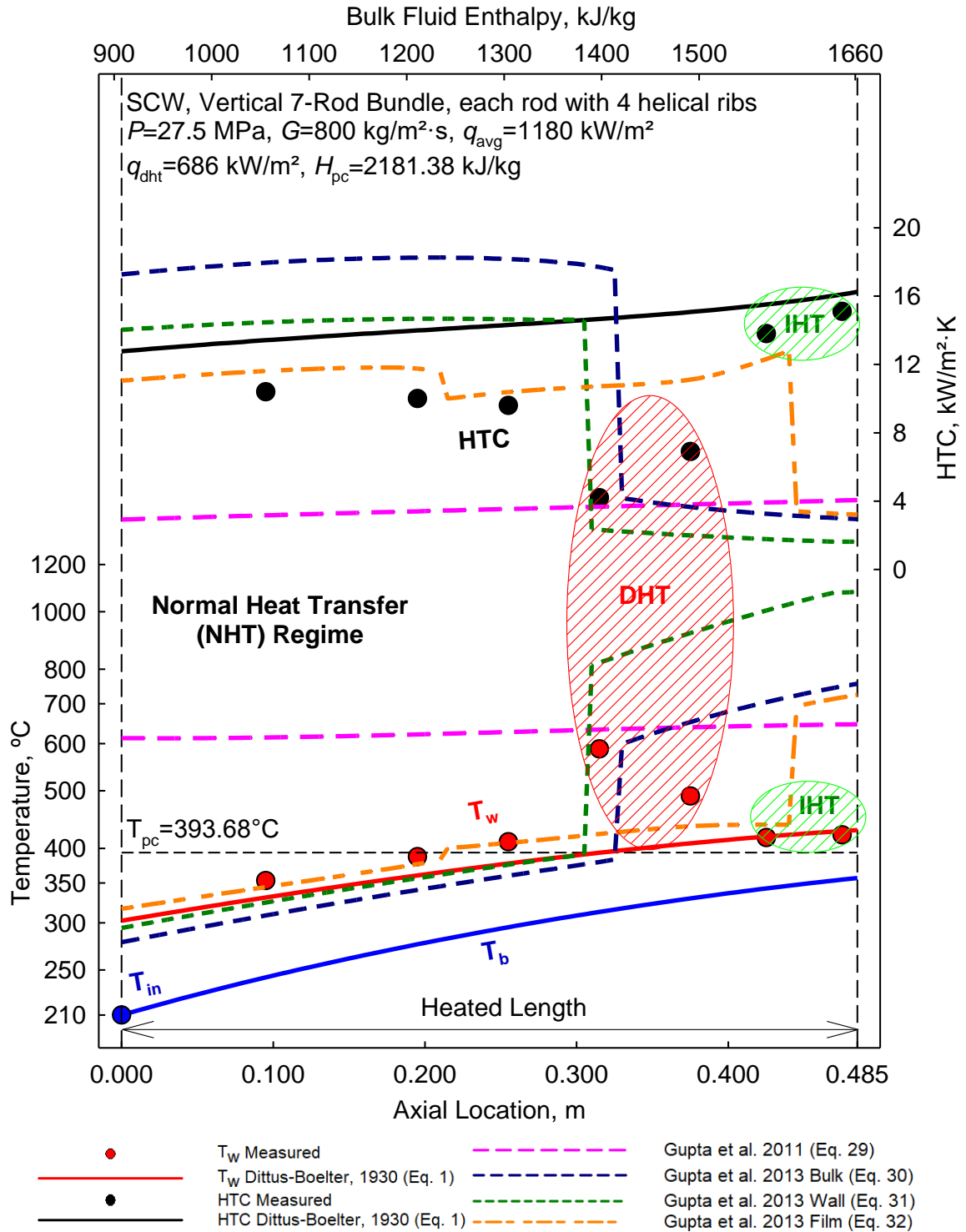


Figure 4-70: T_w and HTC Variations along 0.485m 7-rod Bundle Trial #8-3

$$q_{avg} / q_{dht} = 2.20, q_{avg} / G = 1.48, D_{hy} = 2.57 \text{ mm}$$

4.4.1.4 Set 4

Set 4 consists of the Dittus-Boelter (1930) correlation Eq. (1), Swenson et al. (1965) correlation Eq. (8), Gorban et al. (1990) correlation Eq. (18), Hu (2001) correlation Eq. (21), and the Clark et al. (2020) correlation Eq. (36).

Similar to Set 1 in section 4.4.1.1, Figure 4-71 through Figure 4-77 show the experimentally determined values for HTC and T_w for Trials #1 through #8 (symbols), the calculated values for T_b based upon the experiments, and the values predicted by the **Nu** correlations in Set 4 (solid lines).

While the T_b and the predicted T_w for all **Nu** correlations in Set 4 remained below the T_{pc} (383.07°C) throughout Trial #1, the predictions for T_w for all **Nu** correlations crossed the T_{pc} at various points throughout Trials #2 through #8.

The Gorban et al. (1990) correlation Eq. (18) follows the trends of HTC and T_w well prior to the T_w prediction crossing the T_{pc} . After crossing the T_{pc} , the **Nu** correlation experiences a large jump, resulting in large under-predictions of HTC, and large over-predictions of T_w .

The Swenson et al. (1965) correlation Eq. (8), Hu (2001) correlation Eq. (21), and the Clark et al. (2020) correlation Eq. (36) all follow the trends of HTC and T_w well prior to the T_w crossing the T_{pc} . All three **Nu** correlations experience a jump after the T_{pc} , and also experience small bands of non-convergence in Trials #2 through #7, while still providing close predictions of the HTC and T_w values. However, none of the three **Nu** correlations can predict the IHT regime, with the Clark et al. (2020) correlation Eq. (36) providing the closest predictions for all three regimes.

4.4.1.4.1 Set 4 – Trial #1

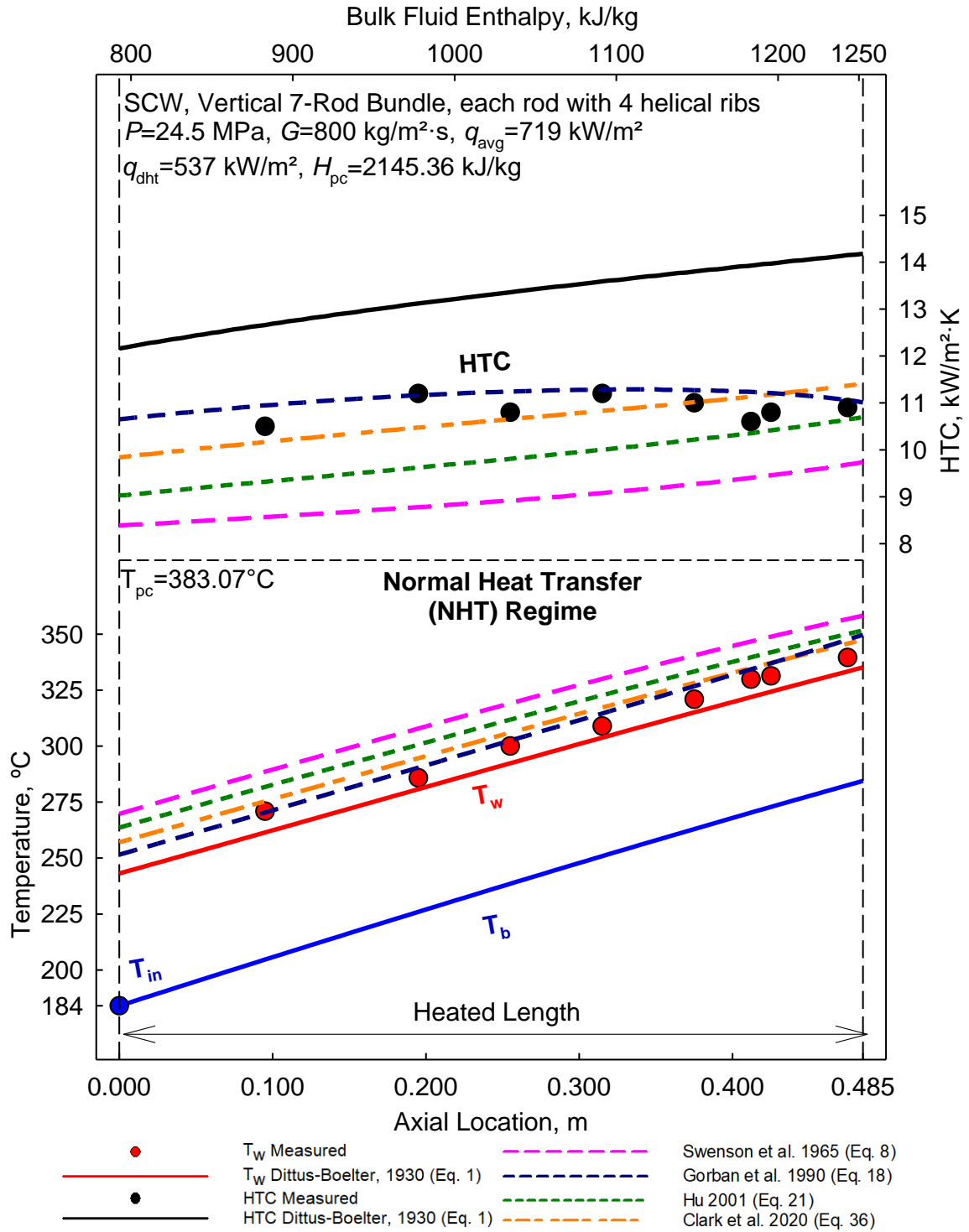


Figure 4-71: T_w and HTC Variations along 0.485m 7-rod Bundle Trial #1-4

$$q_{avg} / q_{dht} = 1.34, q_{avg} / G = 0.90, D_{hy} = 2.57 \text{ mm}$$

4.4.1.4.2 Set 4 – Trial #2

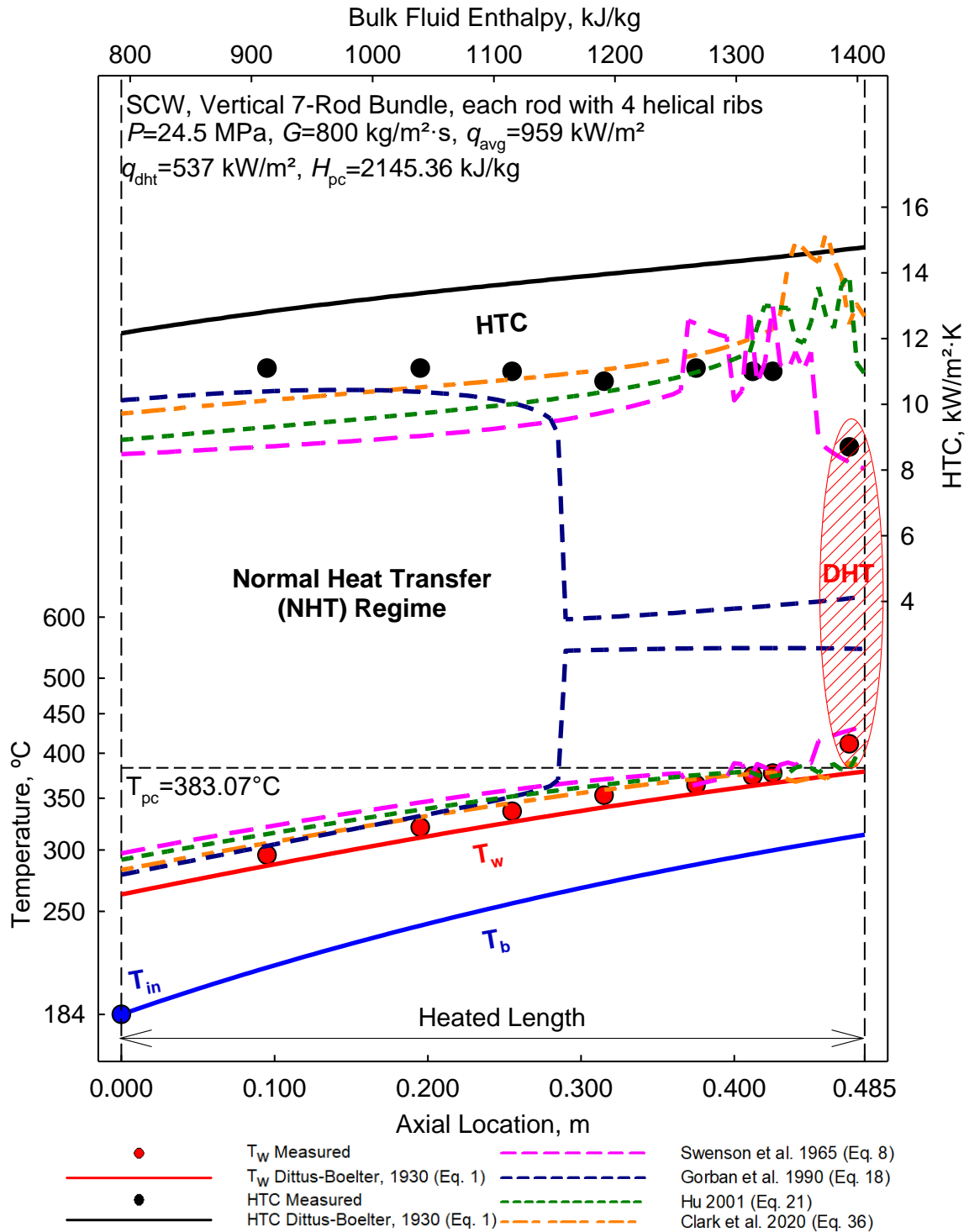


Figure 4-72: T_w and HTC Variations along 0.485m 7-rod Bundle Trial #2-4

$$q_{avg} / q_{dht} = 1.79, q_{avg} / G = 1.20, D_{hy} = 2.57 \text{ mm}$$

4.4.1.4.3 Set 4 – Trial #3

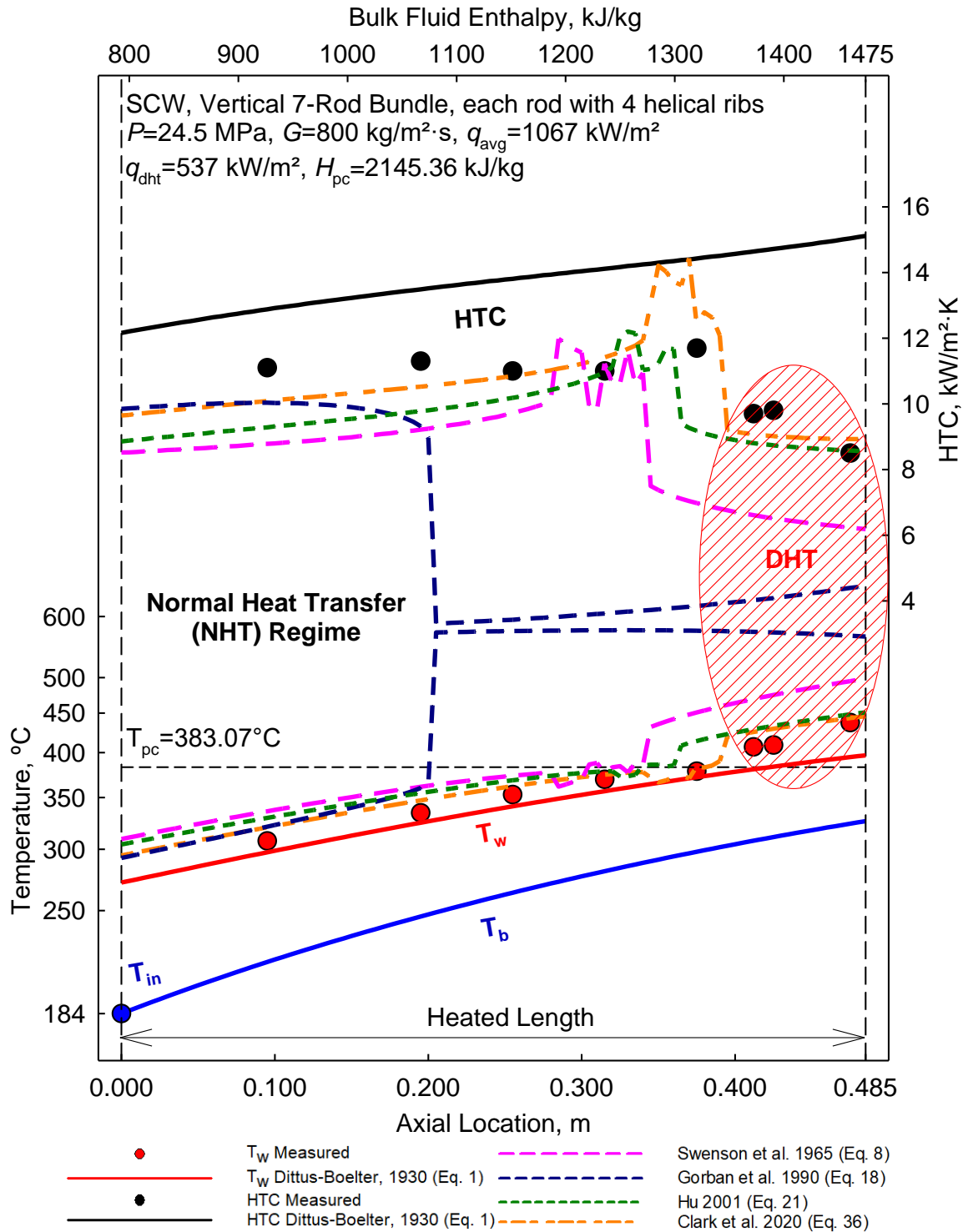


Figure 4-73: T_w and HTC Variations along 0.485m 7-rod Bundle Trial #3-4

$$q_{avg} / q_{dht} = 1.99, q_{avg} / G = 1.33, D_{hy} = 2.57 \text{ mm}$$

4.4.1.4.4 Set 4 – Trial #4

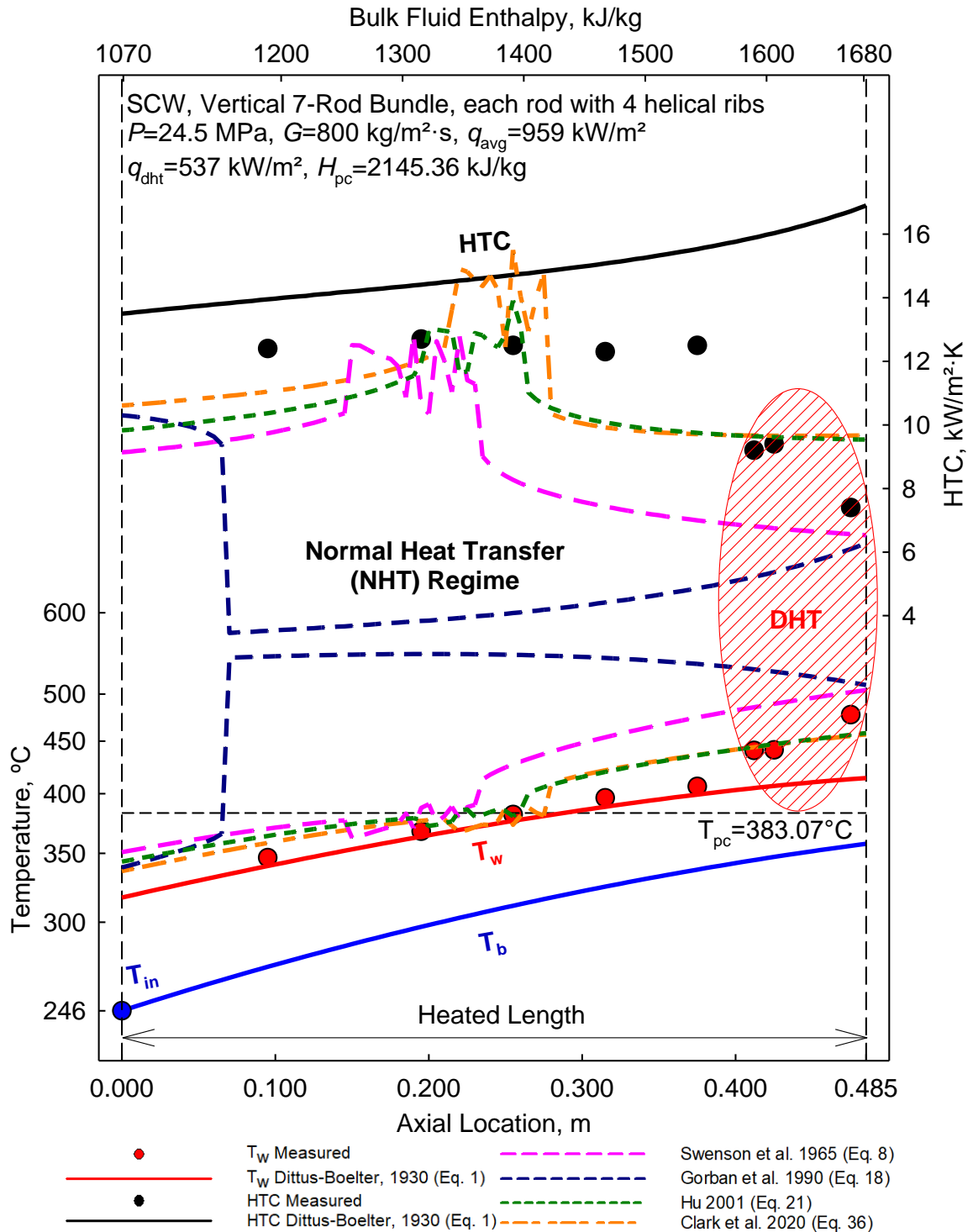


Figure 4-74: T_w and HTC Variations along 0.485m 7-rod Bundle Trial #4-4

$$q_{avg} / q_{dht} = 1.79, q_{avg} / G = 1.20, D_{hy} = 2.57 \text{ mm}$$

4.4.1.4.5 Set 4 – Trial #5/#6

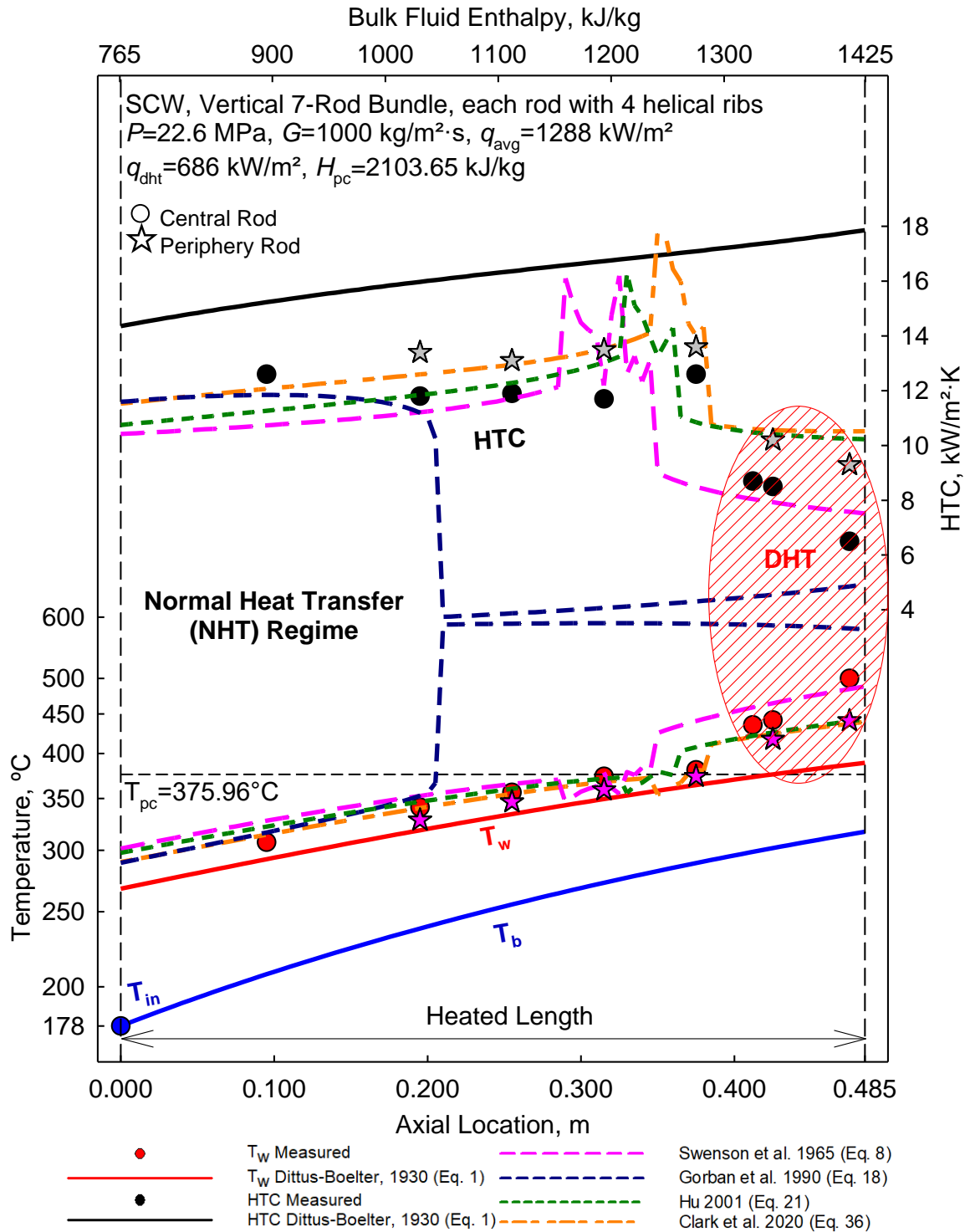


Figure 4-75: T_w and HTC Variations along 0.485m 7-rod Bundle Trial #5/#6-4

$$q_{avg} / q_{dht} = 1.88, q_{avg} / G = 1.29, D_{hy} = 2.57 \text{ mm}$$

4.4.1.4.6 Set 4 – Trial #7

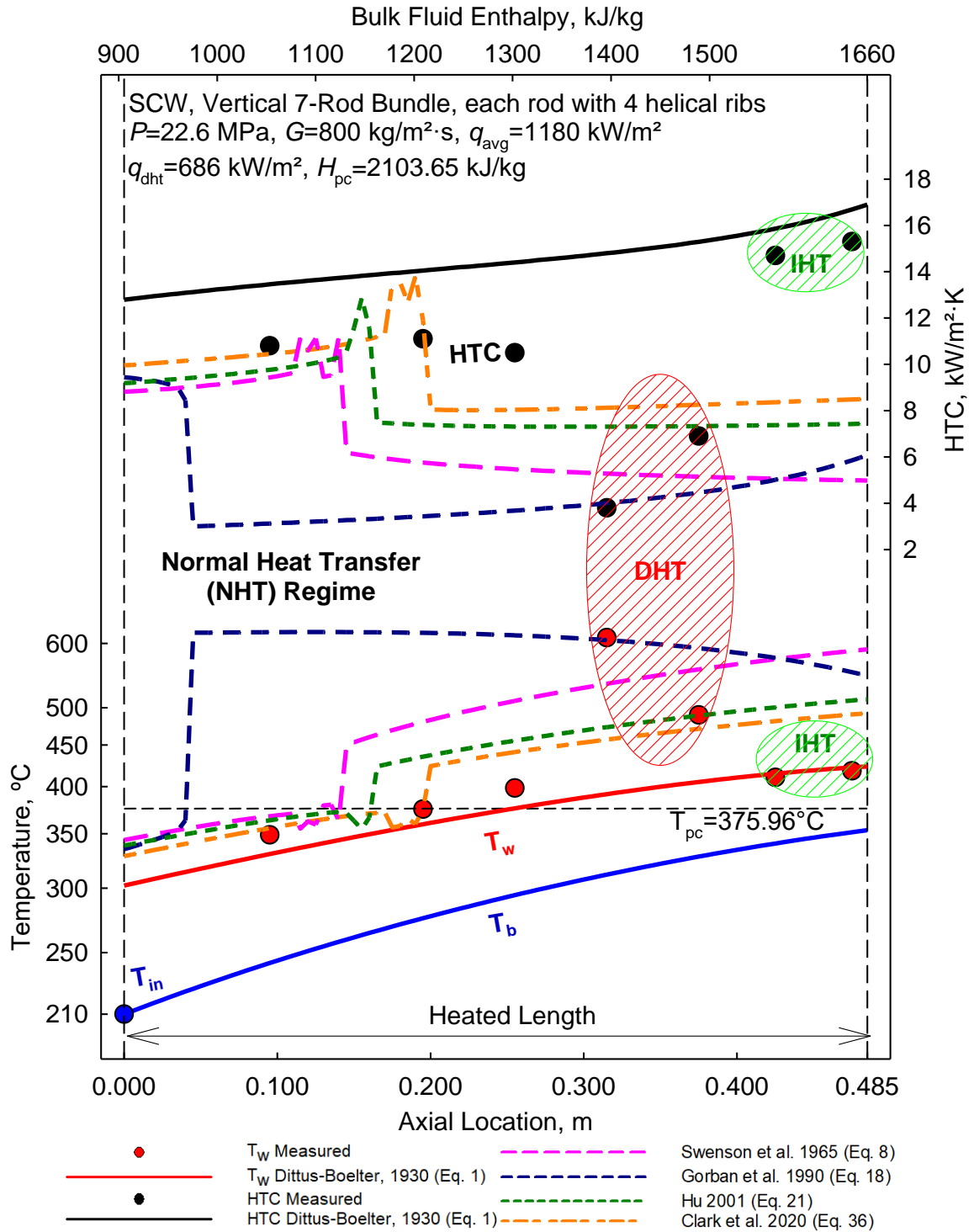


Figure 4-76: T_w and HTC Variations along 0.485m 7-rod Bundle Trial #7-4

$$q_{avg} / q_{dht} = 2.20, q_{avg} / G = 1.48, D_{hy} = 2.57 \text{ mm}$$

4.4.1.4.7 Set 4 – Trial #8

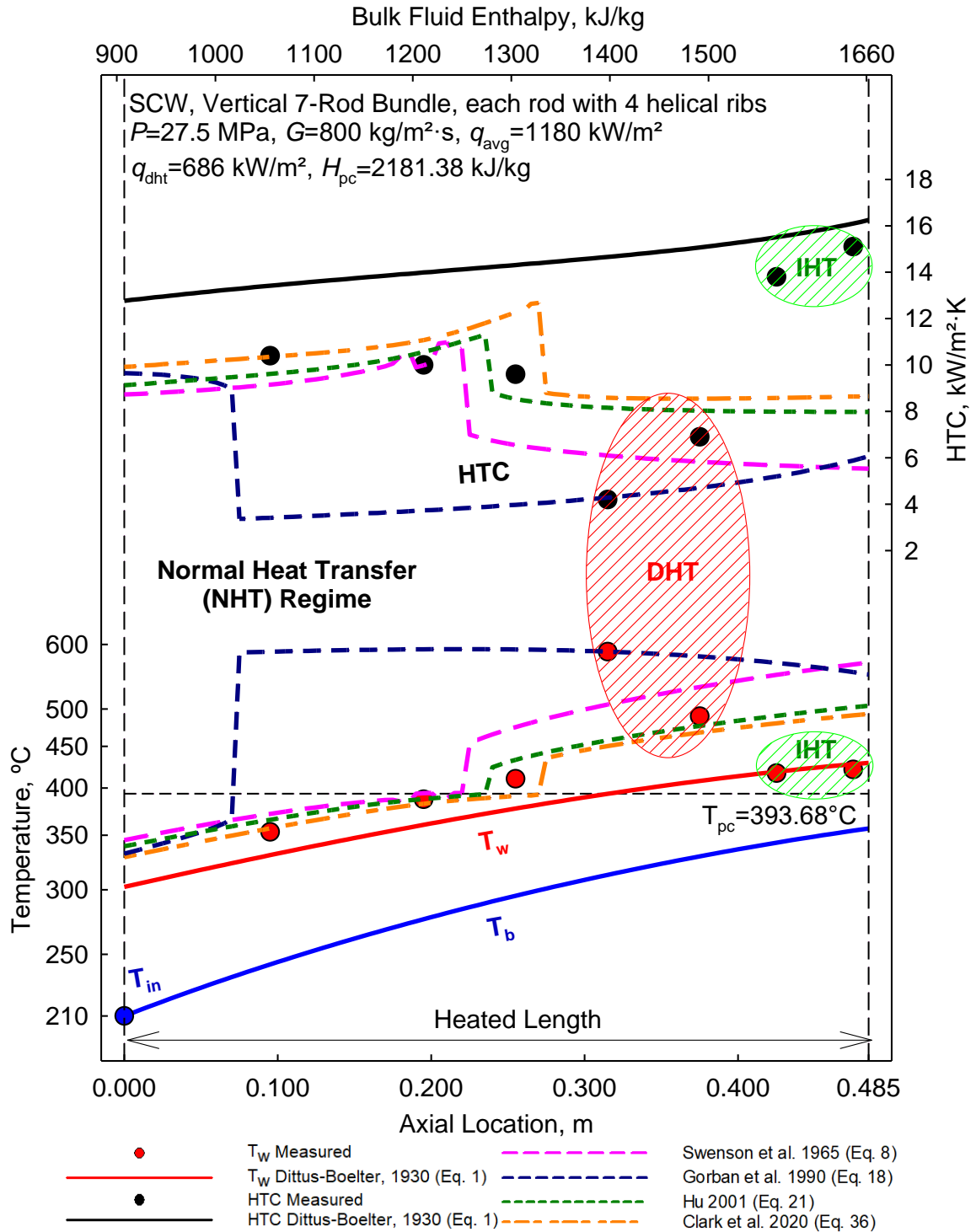


Figure 4-77: T_w and HTC Variations along 0.485m 7-rod Bundle Trial #8-4

$$q_{avg} / q_{dht} = 2.20, q_{avg} / G = 1.48, D_{hy} = 2.57 \text{ mm}$$

4.4.2 BARE TUBE DATA

Similar to Set 4, the **Nu** correlations shown in the bare tube dataset are the Dittus-Boelter (1930) correlation Eq. (1), Swenson et al. (1965) correlation Eq. (8), Gorban et al. (1990) correlation Eq. (18), Hu (2001) correlation Eq. (21), the Clark et al. (2020) correlation Eq. (36), also including the Mokry et al. (2009) correlation Eq. (28).

Figure 4-78 shows the experimentally determined values for HTC and T_w for Test 70_07 (symbols), the calculated values for T_b based upon the experiments, and the values predicted by the **Nu** correlations in Set 4 (solid lines).

The Swenson et al. (1965) correlation Eq. (8), the Hu (2001) correlation Eq. (21), and the Clark et al. (2020) correlation Eq. (36) show good agreement with the experimentally determined values and experience a small period of non-convergence as the T_w crosses the T_{pc} . The Gorban et al. (1990) correlation Eq. (18), does not follow the changing trend of HTC and T_w , resulting in a conservative prediction for the middle portion of the heated length. The Mokry et al (2009) correlation Eq. (28) over-predicts the HTC once the T_w crosses the T_{pc} , however no jump is experienced. The Dittus-Boelter (1930) correlation Eq. (1) experiences an extremely large over-prediction of the HTC as the T_b approaches the T_{pc} .

Figure 4-79 shows the data collected for Test 15_14. The Dittus-Boelter (1930) correlation Eq. (1) experiences a peak as the T_b approaches the T_{pc} , resulting in a large over-prediction of the HTC, and an under-prediction of the T_w . The remaining five **Nu** correlations follow the trends of HTC and T_w , however near the beginning of the heated length a regime of DHT occurs that no **Nu** correlation is able to predict accurately, with the Mokry et al. (2009) correlation Eq. (28) being the closest in this DHT regime.

Figure 4-80 shows the data collected for Test 49_13. The Clark et al. (2020) correlation Eq. (36), the Swenson et al. (1965) correlation Eq. (8), and the Dittus-Boelter (1930) correlation Eq. (1) provide predictive values closest to the experimental values, while the Mokry et al (2009) correlation Eq. (28), the Gorban et al. (1990) correlation Eq. (18), and the Hu (2001) correlation Eq. (21) do not appear to follow the trend of HTC or T_w , and provide variable predictions throughout the heated length.

4.4.2.1 Test 70_07

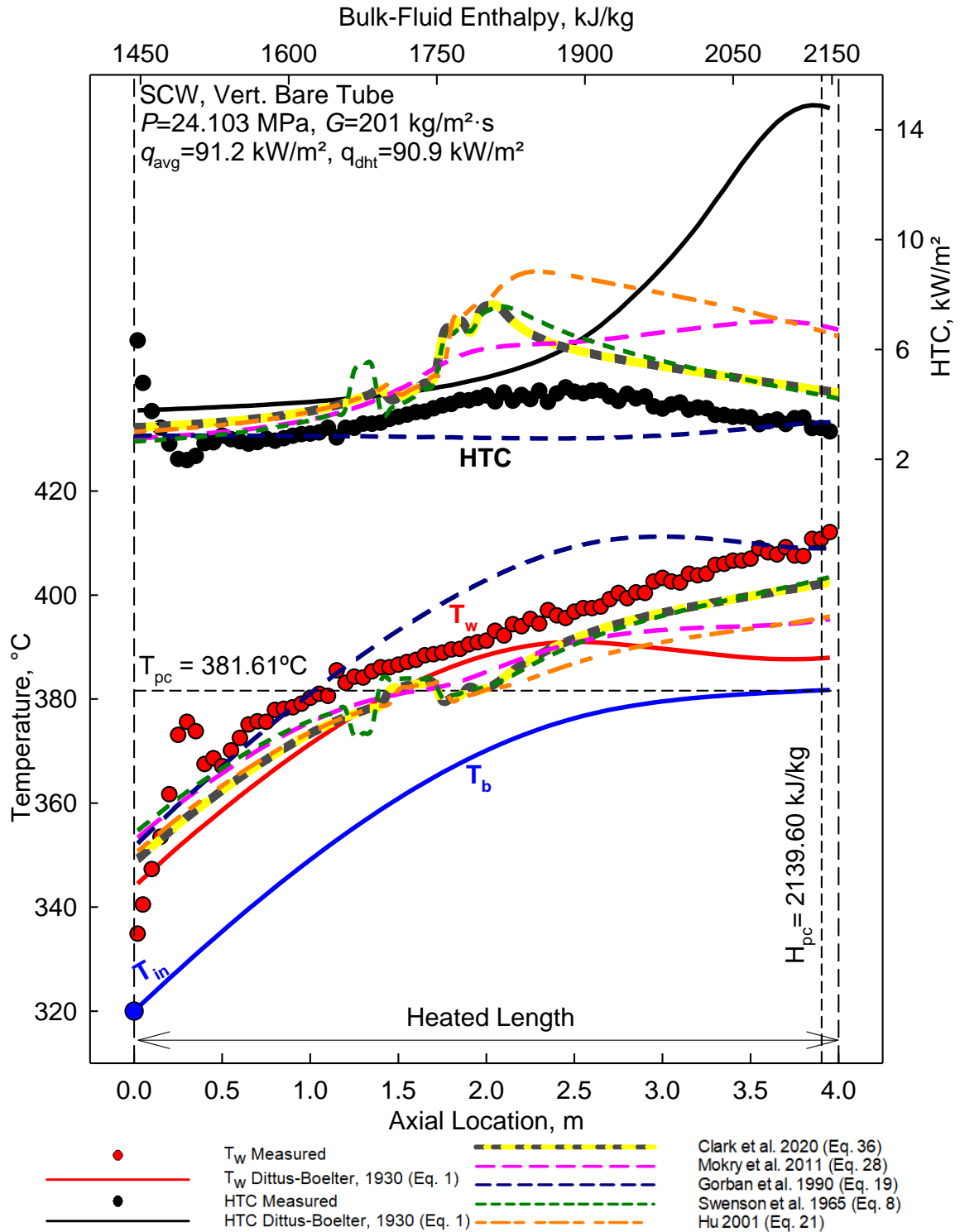


Figure 4-78: T_w and HTC Variations along 4 m bare tube Test 70_07

$$q_{avg} / q_{dht} = 1.00, q_{avg} / G = 0.45, D = 10 \text{ mm}$$

4.4.2.2 Test 15_14

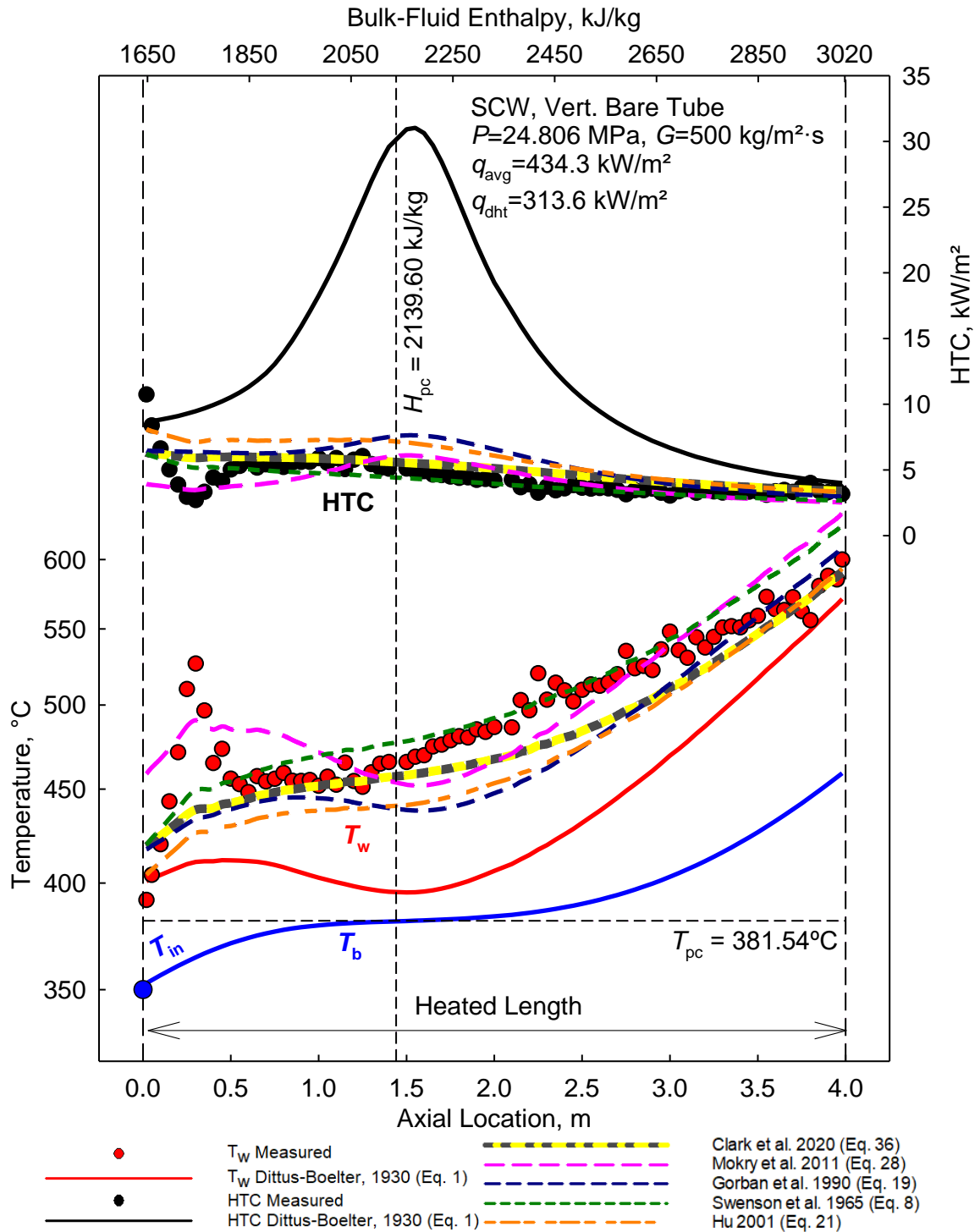


Figure 4-79: T_w and HTC Variations along 4 m bare tube Test 15_14

$$q_{avg} / q_{dht} = 1.38, q_{avg} / G = 0.87, D = 10 \text{ mm}$$

4.4.2.3 Test 49_13

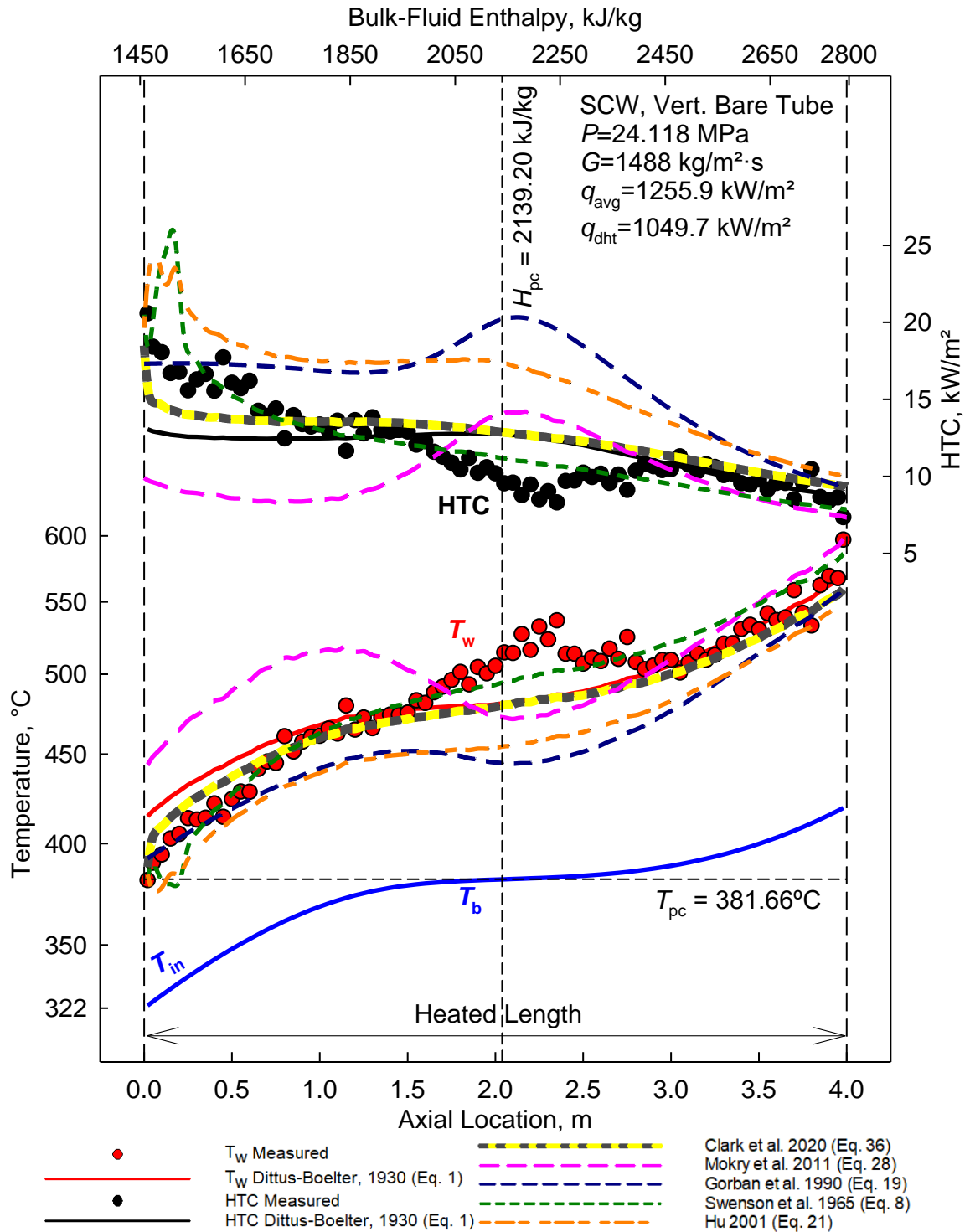


Figure 4-80: T_w and HTC Variations along 4 m bare tube Test 49_13

$$q_{avg} / q_{dht} = 1.20, q_{avg} / G = 0.84, D = 10 \text{ mm}$$

4.4.3 GRAPHICAL RESULTS SUMMARY

4.4.3.1 7-rod Bundle

4.4.3.1.1 Set #1

For the 7-rod bundle trials, the Dyadyakin and Popov (1977) correlation Eq. (16) and the Clark et al. (2020) correlation Eq. (36) predictions were very close to the measured values for the NHT regimes, and suitable for use in 7-rod bundles.

The Mokry et al. (2011) correlation Eq. (28) and the Lei et al. (2019) correlation Eq. (35) both saw a dramatic decrease in HTC predictions and increase in T_w as the T_w crossed the pc point. Due to this, they are not suitable for use in the 7-rod bundle.

4.4.3.1.2 Set #2

None of the Set #2 **Nu** correlations are suitable for use in the 7-rod bundles as they all over-predict HTC and under-predict T_w .

4.4.3.1.3 Set #3

For the 7-rod bundle trials, all **Nu** correlations experienced a dramatic decrease in HTC predictions as the T_w crossed the pc point. Due to this, none are suitable in the 7-rod bundle.

4.4.3.1.4 Set #4

For the 7-rod bundle trials, the Swenson et al. (1965) correlation Eq. (8), the Hu (2001) correlation Eq. (21), and the Clark et al. (2020) correlation Eq. (36) predict close to the measured values for the NHT regimes, and are suitable for use in 7-rod bundles. Each of these **Nu** correlations also experiences a small range of non-convergence.

Due to the jump in prediction after the T_w crosses the T_{pc} , the Gorban et al. (1990) correlation Eq. (18) is not suitable for use in the 7-rod bundle.

4.4.3.2 bare tube

For the bare tube trials, while all of the **Nu** correlations shown can predict close to the measured values at times, the Clark et al. (2020) correlation Eq. (36) and the Swenson et al. (1965) correlation Eq. (8) are the most suitable for use in bare tubes.

4.5 SIMULATED T_{SHEATH} AND $T_{\text{FUEL CL}}$

In an effort to determine the maximum fuel channel length achievable in a SCWR design, the parameters (geometric, fluid flow, and channel power) from each 7-rod bundle trial (#1-#8), and those listed for the 37-element or 64-element bundle in section 2.2, were used to perform simulations to see if the inner sheath temperature (T_{sheath}) and maximum fuel centreline temperature ($T_{\text{fuel CL}}$) would be below the industrially accepted limits of 850°C and 1850°C, respectively.

First T_b was calculated using the parameters (geometric, fluid flow, and channel power), then HTC and T_w was calculated using the Clark et al. (2020) correlation Eq. (36). Next T_{sheath} was calculated assuming A625 sheath material, and $T_{\text{fuel CL}}$ was calculated assuming that no gap between the fuel pellet and inner sheath exists, the fuel pellet is made of layers with the thermal conductivity recalculated for each layer, and that the fuel is UO_2 . Both T_{sheath} and $T_{\text{fuel CL}}$ were calculated using the methodology in section 3.3.4.

The goal for section 4.5.1 was to calculate T_{sheath} and $T_{\text{fuel CL}}$ along a heated length equivalent to 12-bundles (7-rod bundles used were the exact length as a 37-element bundle, 0.485m, current CANDU NPPs use 12 bundles per channel). This was to be performed for each of the 7-rod trials, using the parameters from each trial. However, this was not possible as the T_w predicted by Eq. (36) crossed the upper temperature limit of the NIST REFPROP 10.0 program (1350K, 1077°C) earlier than anticipated. Therefore, each trial shows only the amount of bundles required to exceed the maximum T_{sheath} . For the 7-rod trials (#1 to #8), the average heat flux and the geometry of the fuel bundle is used to determine the energy density (\dot{q} (MW/m³)), and the Channel Power.

The goal for section 4.5.2 was to calculate T_{sheath} and $T_{\text{fuel CL}}$ along a heated length equivalent to 12-bundles for the 37-element (5.82 m), and along a heated length of 5 metres for 64-element, as described in section 2.2 for the proposed SCWR designs. For the 37-element and the 64-element, the Channel Power in section 2.2.1 was used to determine the energy density. Constant power was assumed, described in section 2.2.4.

4.5.1 SIMULATED 7-ROD BUNDLES

4.5.1.1 Trial #1 Theoretical Length

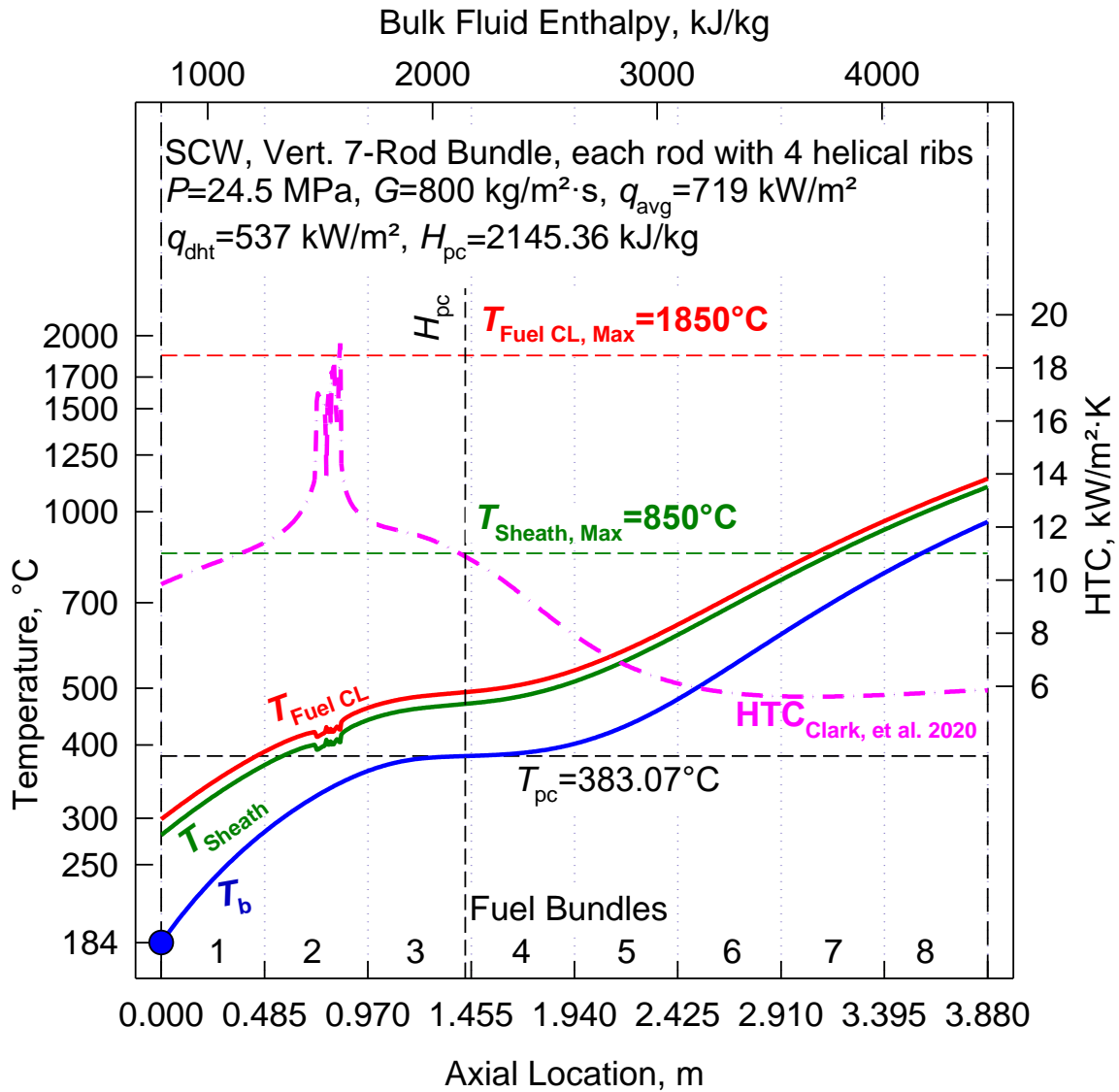


Figure 4-81: Sheath & Fuel Rod Temperature along 8 Bundles - Trial #1

Channel Power = 4.93 MW, $q_{avg}/q_{dht} = 1.34$

Figure 4-81 demonstrates that a maximum of 6 fuel bundles can be used in series with the 7-rod trial #1 conditions when only accounting for thermal aspects using the Clark, et al. (2020) correlation. The maximum Sheath temperature is surpassed in the 7th fuel bundle. The bulk-fluid temperature reaches ~960°C, well above the 625°C required from the SCWR.

4.5.1.2 Trial #2 Theoretical Length

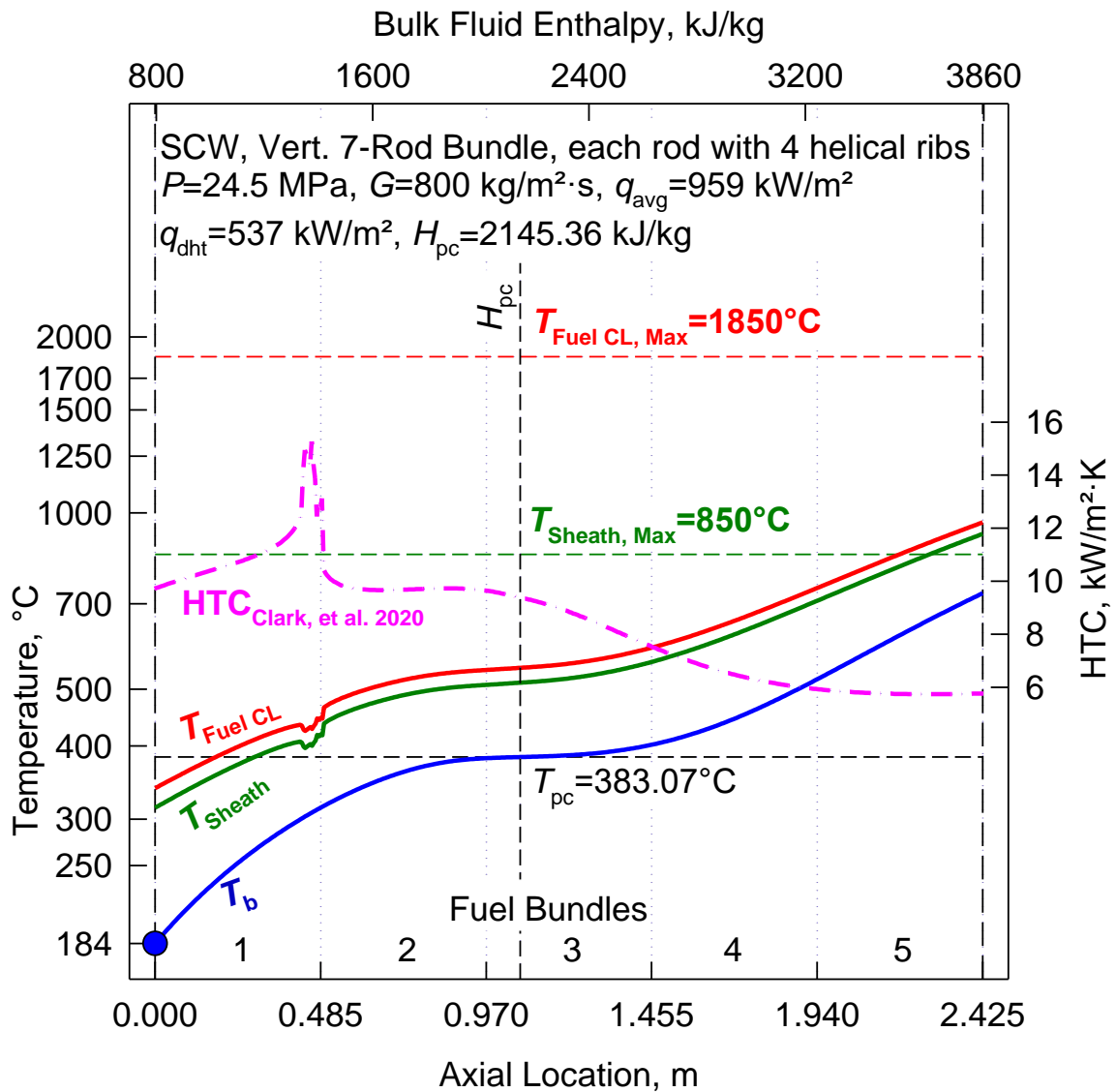


Figure 4-82: Sheath & Fuel Rod Temperature along 5 Bundles - Trial #2
Channel Power = 6.58 MW, $q_{avg}/q_{dht} = 1.79$

Figure 4-82 demonstrates that a maximum of 4 fuel bundles can be used in series with the 7-rod trial #2 conditions when only accounting for thermal aspects using the Clark, et al. (2020) correlation. The maximum Sheath temperature is surpassed in the 5th fuel bundle, and the bulk-fluid temperature reaches ~730°C.

4.5.1.3 Trial #3 Theoretical Length

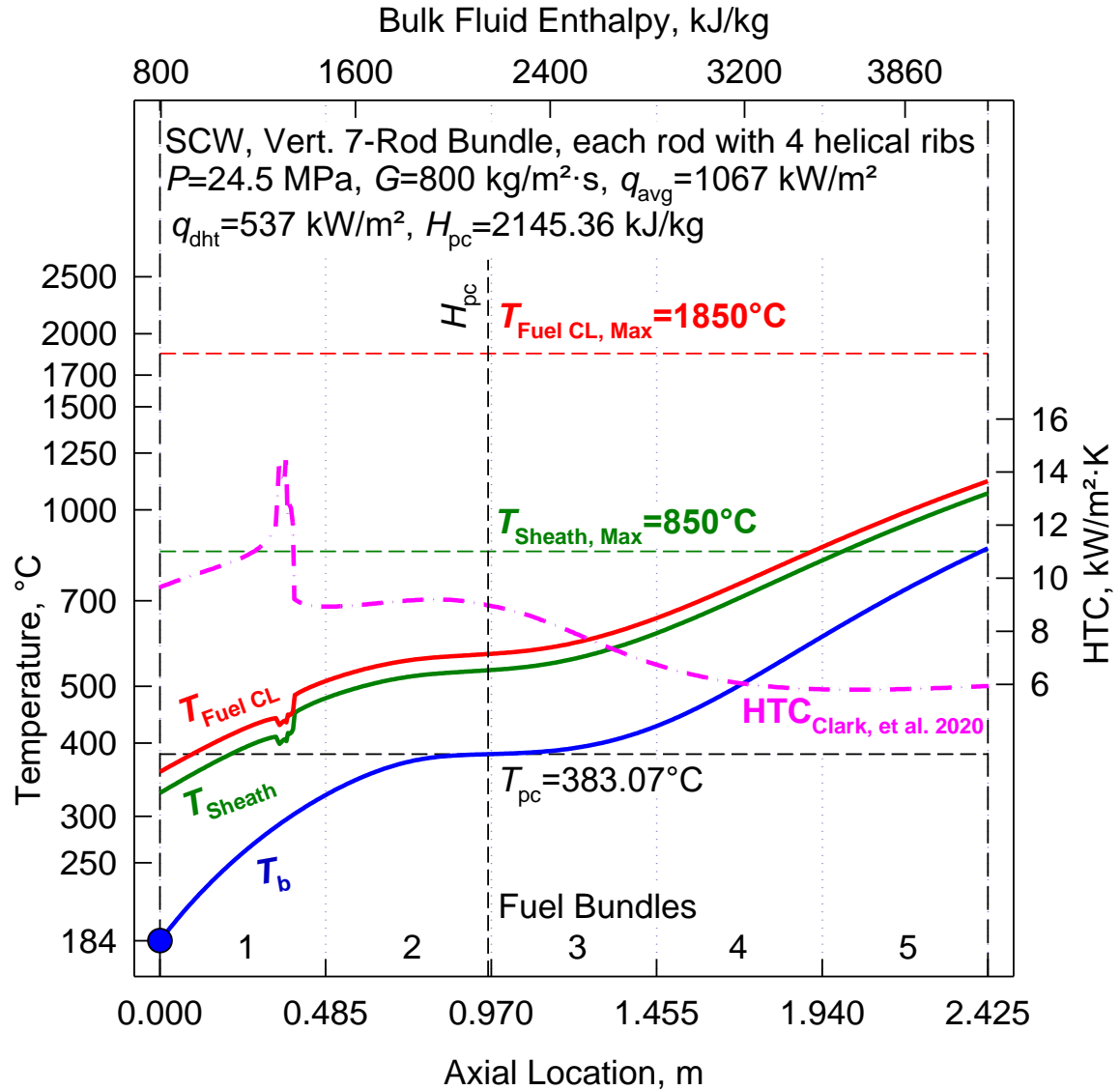


Figure 4-83: Sheath & Fuel Rod Temperature along 5 Bundles - Trial #3

Channel Power = 7.32 MW, $q_{avg}/q_{dht} = 1.99$

Figure 4-83 demonstrates that a maximum of 4 fuel bundles can be used in series with the 7-rod trial #3 conditions when only accounting for thermal aspects using the Clark, et al. (2020) correlation. The maximum Sheath temperature is surpassed in the 5th fuel bundle, and the bulk-fluid temperature reaches ~860°C.

4.5.1.4 Trial #4 Theoretical Length

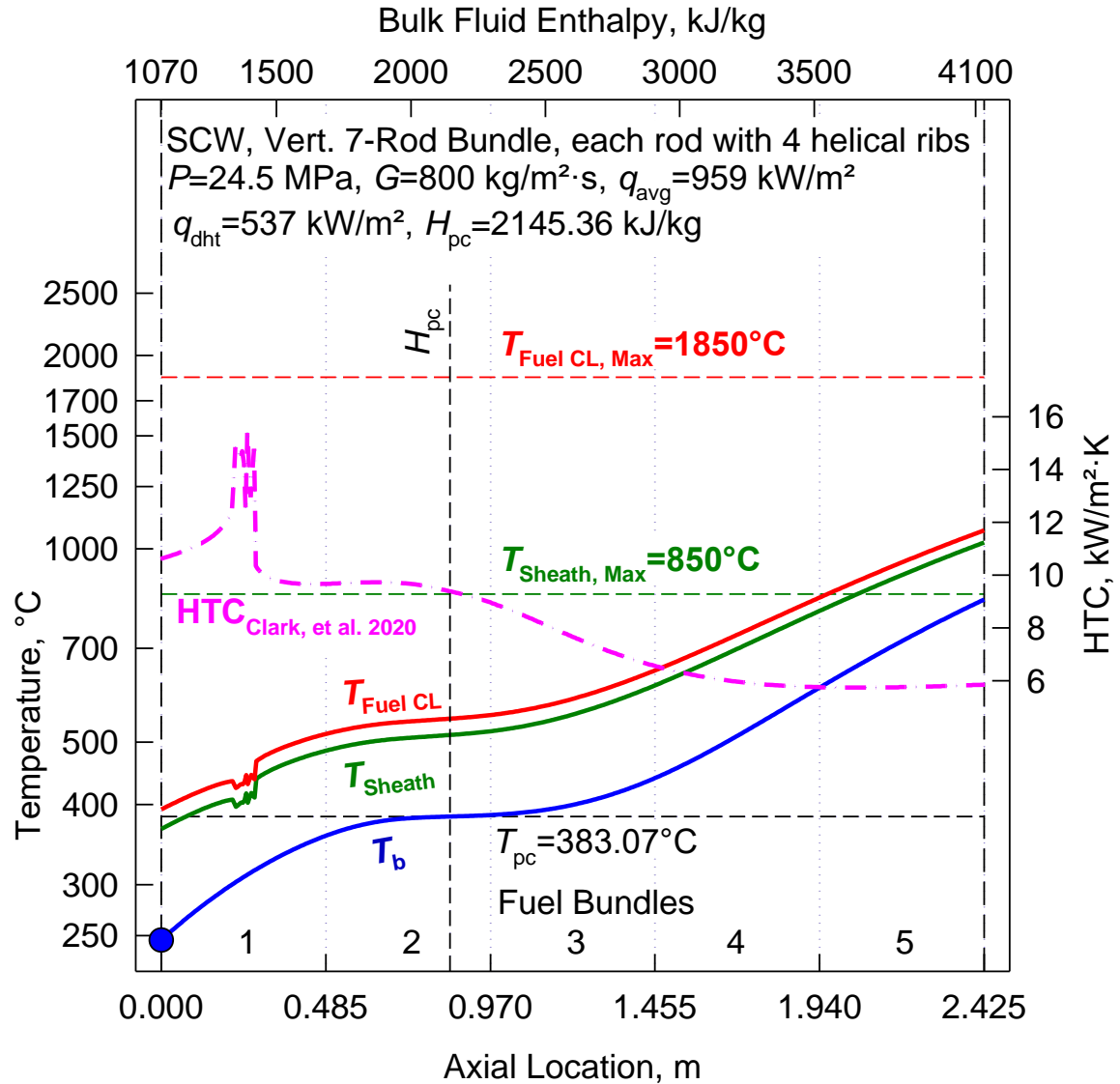


Figure 4-84: Sheath & Fuel Rod Temperature along 5 Bundles - Trial #4

Channel Power = 6.58 MW, $q_{avg}/q_{dht} = 1.79$

Figure 4-84 demonstrates that a maximum of 4 fuel bundles can be used in series with the 7-rod trial #4 conditions when only accounting for thermal aspects using the Clark, et al. (2020) correlation. The maximum Sheath temperature is surpassed in the 5th fuel bundle, and the bulk-fluid temperature reaches ~830°C.

4.5.1.5 Trial # 5 & #6 Theoretical Length

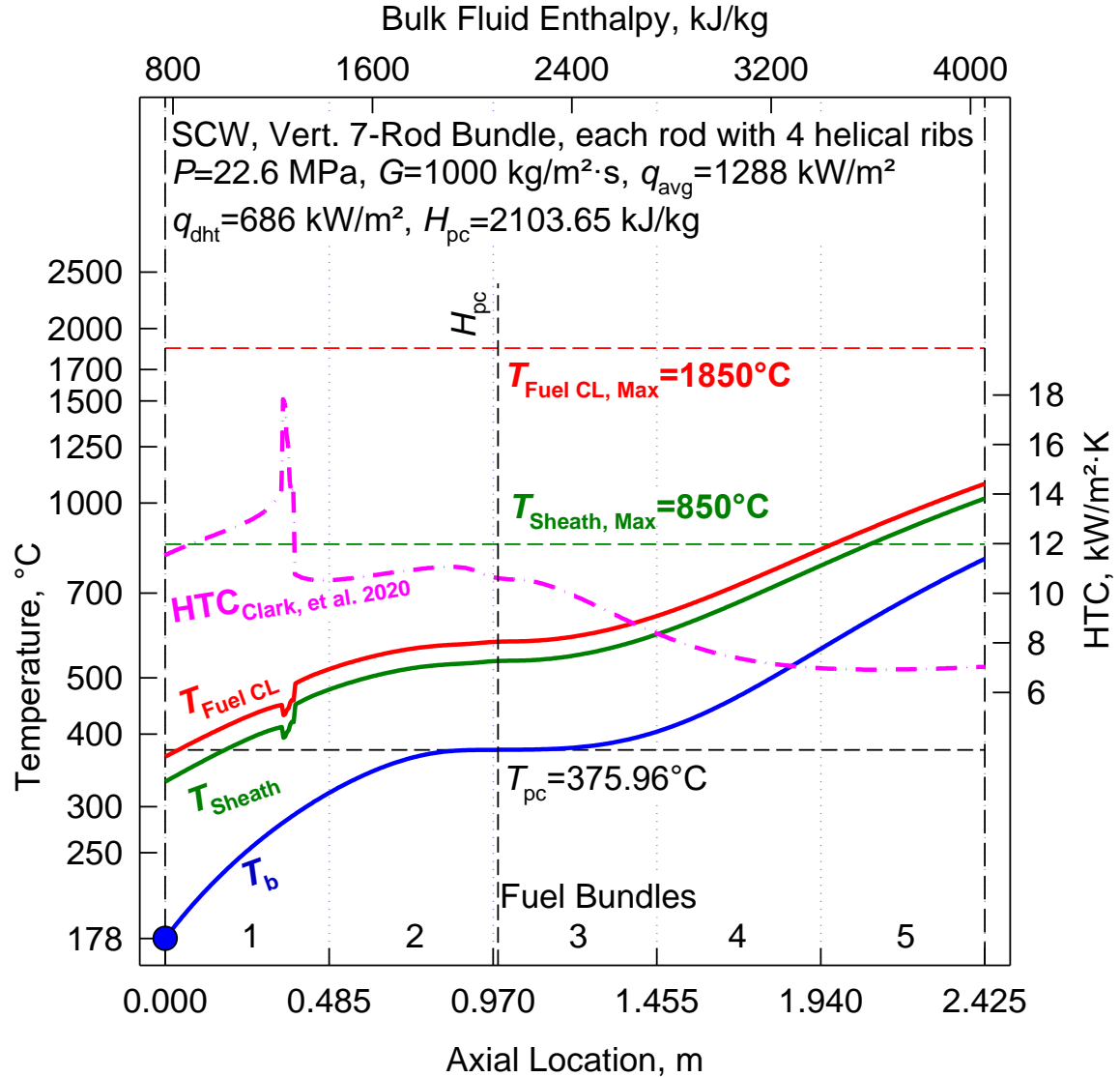


Figure 4-85: Sheath & Fuel Rod Temperature along 5 Bundles - Trial #5 & #6
Channel Power = 8.83 MW, $q_{avg}/q_{dht} = 1.88$

Figure 4-85 demonstrates that a maximum of 4 fuel bundles can be used in series with the 7-rod trial #5 & #6 conditions when only accounting for thermal aspects using the Clark, et al. (2020) correlation. The maximum Sheath temperature is surpassed in the 5th fuel bundle, and the bulk-fluid temperature reaches ~800°C.

4.5.1.6 Trial #7 Theoretical Length

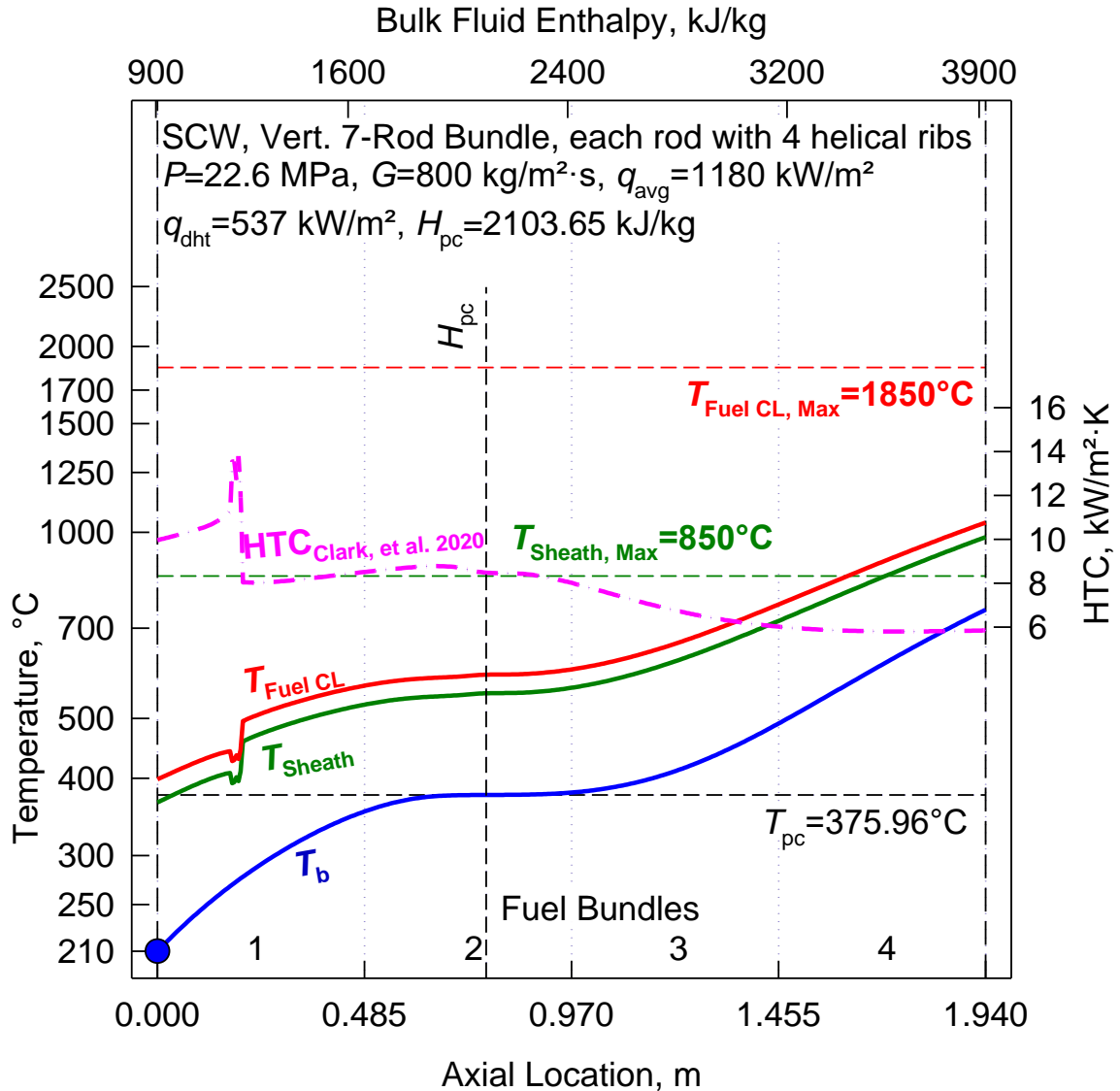


Figure 4-86: Sheath & Fuel Rod Temperature along 4 Bundles - Trial #7

Channel Power = 8.09 MW, $q_{avg}/q_{dht} = 2.20$

Figure 4-86 demonstrates that a maximum of 3 fuel bundles can be used in series with the 7-rod trial #7 conditions when only accounting for thermal aspects using the Clark, et al. (2020) correlation. The maximum Sheath temperature is surpassed in the 4th fuel bundle, and the bulk-fluid temperature reaches ~750°C.

4.5.1.7 Trial #8 Theoretical Length

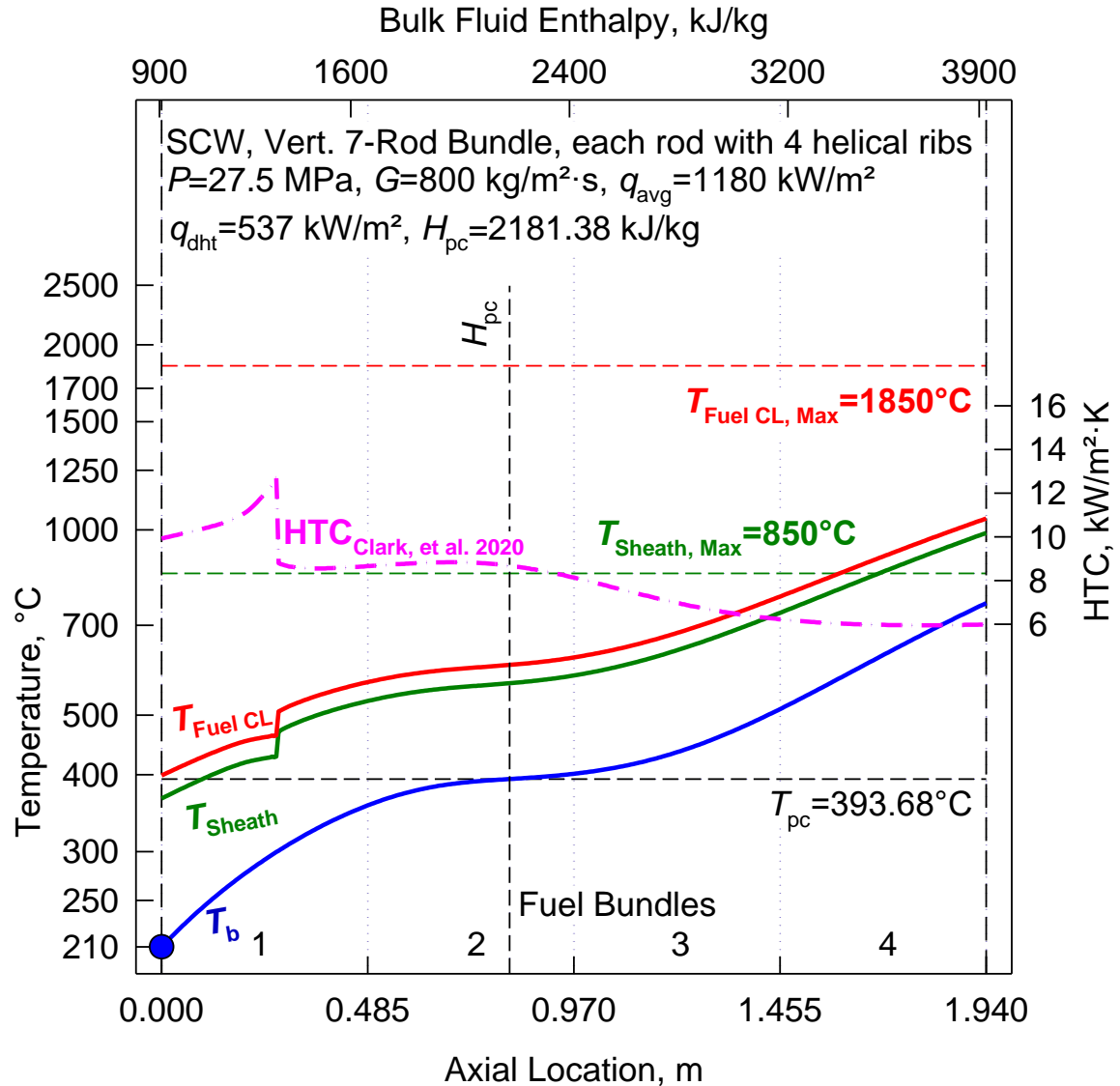


Figure 4-87: Sheath & Fuel Rod Temperature along 4 Bundles - Trial #8

Channel Power = 8.09 MW, $q_{avg}/q_{dht} = 2.20$

Figure 4-87 demonstrates that a maximum of 3 fuel bundles can be used in series with the 7-rod trial #7 conditions when only accounting for thermal aspects using the Clark, et al. (2020) correlation. The maximum Sheath temperature is surpassed in the 4th fuel bundle, and the bulk-fluid temperature reaches ~760°C.

4.5.2 SIMULATED PROPOSED SCW DESIGNS

4.5.2.1 Theoretical 37-Element Fuel Bundle SCWR

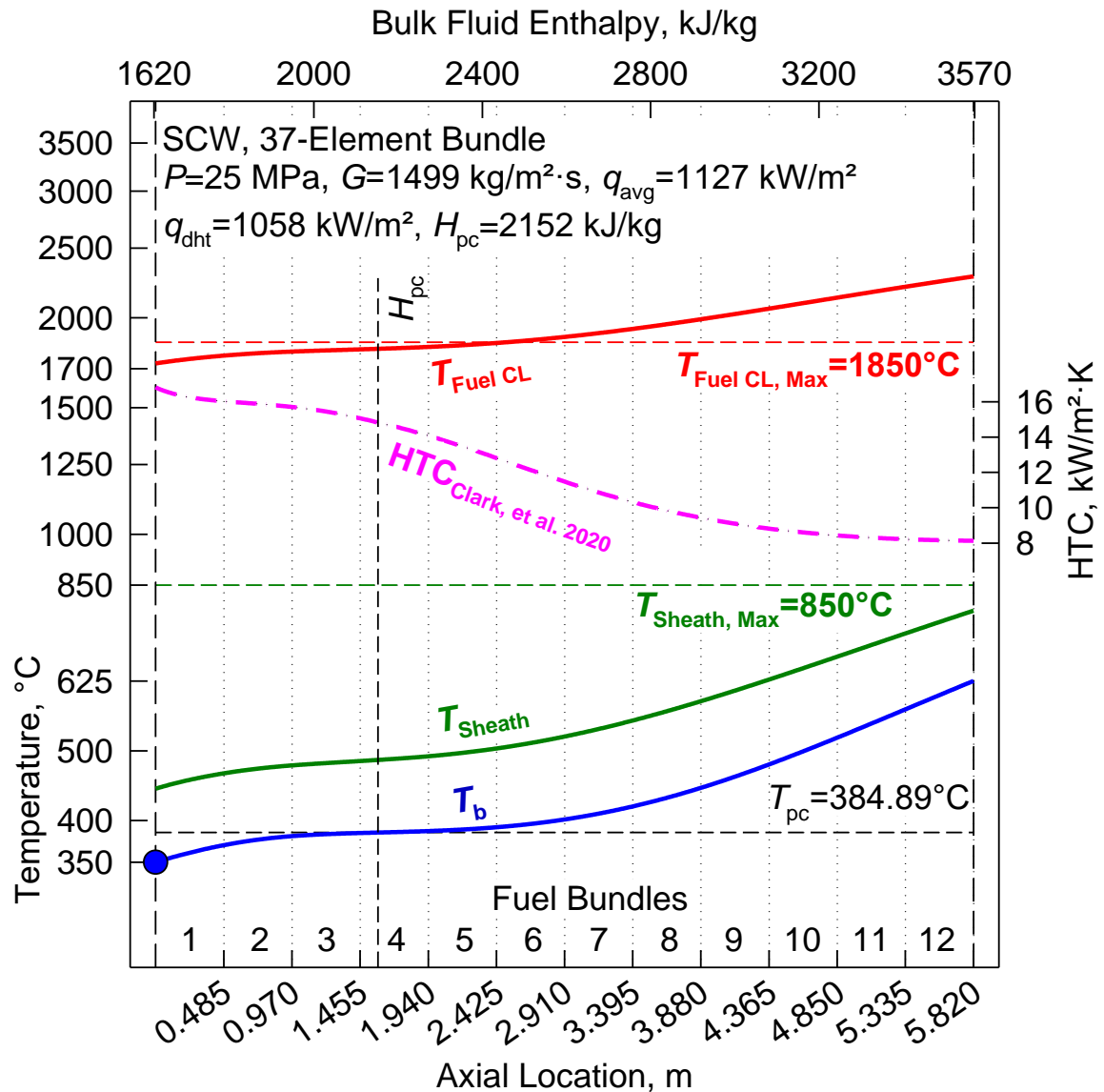


Figure 4-88: Sheath & Fuel Rod Temperature with 37-Element Bundles
Channel Power = 9.97 MW, $q_{avg}/q_{dht} = 1.07$

Figure 4-88 demonstrates that a maximum of 5 fuel bundles can be used in series with the 37-element geometry and the proposed SCWR conditions, when only accounting for thermal aspects using the Clark, et al. (2020) correlation. While the maximum Sheath temperature is not reached in the 12 bundles, the fuel centreline temperature is surpassed in the 5th fuel bundle, while the bulk-fluid temperature reaches 625°C. Thus the fuel bundles are too large in diameter for these conditions.

4.5.2.2 Theoretical 64-Element Fuel Bundle SCWR

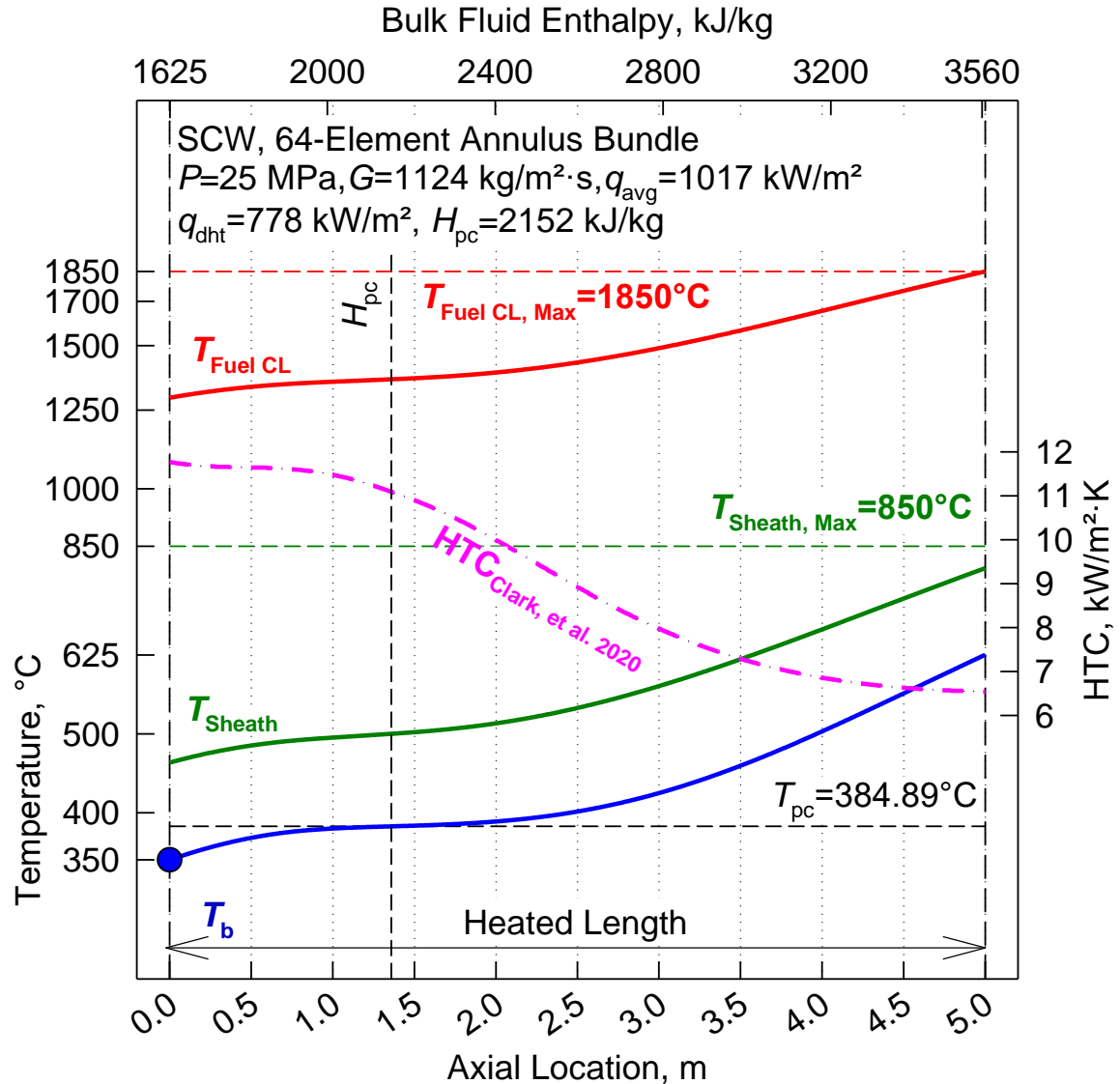


Figure 4-89: Sheath & Fuel Rod Temperature with 64-Element Bundle

Channel Power = 9.97 MW, $q_{avg}/q_{dht} = 1.07$

Figure 4-89 demonstrates that the proposed parameters for the 64-element SCWR are acceptable when only accounting for thermal aspects using the Clark, et al. (2020) correlation. The maximum Sheath temperature is not reached in the 5 m heated length section, the fuel centreline temperature reaches exactly 1850°C at the 5.0 m length, and the bulk-fluid temperature reaches 625°C.

4.5.3 SIMULATIONS SUMMARY

4.5.3.1 7-rod Bundle Simulations

In the current 37-element CANDU reactor, the fuel channel consists of 12 bundles. However, for the 7-rod bundle parameter simulations, shown in Figure 4-81 through Figure 4-87, the T_{Sheath} exceeded the industrial limit of 850°C in all simulations. At the lowest $q_{\text{avg}}/q_{\text{dht}}$ ratio of 1.34, the T_{Sheath} would exceed this limit midway through the 7th bundle (Figure 4-81), while at the highest ratio of $q_{\text{avg}}/q_{\text{dht}}$ of 2.20, the T_{Sheath} would exceed this limit midway through the 4th bundle (Figure 4-86 and Figure 4-87).

These high T_{Sheath} is due to the higher T_b experienced with these parameters. The current SCWR design calls for an inlet T_b of 350°C and an outlet temperature of 625°C. However, for the 7-rod bundle trials, the T_b was between 178°C and 246°C, while the outlets ranged from ~700-1000°C.

Therefore, the $q_{\text{avg}}/q_{\text{dht}}$ required from a SCWR design utilizing a 7-rod bundle, in a 12 bundle channel, must be less than the lowest ratio used in the 7-rod bundle trials (1.34).

4.5.3.2 Proposed SCWR Design Simulations

4.5.3.2.1 37-Element

The 37-element fuel bundle simulation shown in Figure 4-88 demonstrates that the T_b would reach the desired outlet temperature of 625°C using the proposed parameters, while the T_{Sheath} would remain below the industrial accepted limit of 850°C.

However, the $T_{\text{Fuel CL}}$ crosses industrial accepted limit of 1850°C early in the 6th bundle, or about 2.5 metres into the heated length. Considering this simulation was run with an assumed constant power, the real situation would be much worse at this midway point of the fuel channel.

In order to reduce this, the 37-element fuel diameters would need to be reduced, the channel power would have to be dropped, different fuel would have to be utilized (such as thorium fuels), and/or the SCW would have to flow at a greater rate to remove more heat. However, a greater fluid flow has practical limitations on the HTC that can be achieved, shown in Figure 4-32.

4.5.3.2.2 64-Element

The 64-element fuel bundle simulation shown in Figure 4-89 demonstrates that the proposed SCWR design parameters achieve all stated goals.

The inlet and outlet T_b are achieved, while the T_{Sheath} and $T_{\text{Fuel CL}}$ are both below the industry accepted limits, with the $T_{\text{Fuel CL}}$ reaching the limitation at the end of the fuel channel.

If the cosine shape of power were taken into consideration (described in section 2.2.4), it is anticipated that the T_{Sheath} and $T_{\text{Fuel CL}}$ would be closer to their respective industry accepted limits throughout the heated length.

As the ratio of $q_{\text{avg}}/q_{\text{dht}}$ used in this configuration is lower in comparison to the 7-rod bundle trials (1.07), and the Clark et al. (2020) correlation Eq. (36) was shown to predict quite well with a $q_{\text{avg}}/q_{\text{dht}}$ ratio < 2.0 , it is anticipated that the margin of error for the 64-element bundle T_{Sheath} and $T_{\text{Fuel CL}}$ predictions would be $\pm 7.4\%$ of the actual temperature, as described in section 4.3.3.2.

5 DISCUSSION

5.1 NPP & SCWR

In general, NPPs should be a part of the energy generating landscape for the foreseeable future due to their high energy output with large capacity factors, and low carbon emissions. However, pressure by the public out of fear of nuclear waste and nuclear proliferation, in addition to market pressure by higher efficiency fossil fuel furnaces and the rise of renewables means the long term future of nuclear energy is at present unclear.

Due to these factors, in addition to the low thermal efficiencies, the current Gen II/III/III+ NPP fleet is no longer economically competitive with SCW coal-fired power plants and combined gas cycles. Therefore, Gen IV NPPs are being considered with the following 6 concepts: 1) GFRs; 2) LFRs; 3) MSR; 4) SFRs; 5) VHTRs; 6) SCWRs.

SCWR both large and small (SMR) plants are in various stages of development, however no SCWR NPP is currently in construction anywhere in the world.

Developing SCWRs requires solid knowledge of specifics of thermophysical properties and heat transfer of SCW. While much knowledge has been gained for SC fluid behaviour in bare circular tubes, SCWRs will use bundle flow geometries (square/circular configurations, centre pins, central flow tube, etc). Therefore, experiments in various bundle flow geometries within operating conditions of SCWRs are required.

Current research is dedicated to analyzing unique datasets obtained in an electrically heated 7-rod bundle cooled with SCW with helical ribs attached to all rods. This experimental data was obtained in Kiev Polytechnic Institute (Ukraine).

5.2 LITERATURE REVIEW

Over 20 SCW Nu correlations have been developed in the past 60 years, with only 1 proposed for a bundle configuration (Dyadyakin and Popov, (1977)).

More than 10 studies on SCW Nu correlations have been performed in the past decade by various authors. Several of these studies were for various bundle configurations. No published study has been performed on a 7-rod bundle configuration, which represents the centre and inner ring of a standard 37-bundle ring configurations.

The results have generally concluded that the Mokry, et al. (2009) correlation Eq. (28) and the Swenson et al. (1965) correlation Eq. (8) were the best for bare tubes, while the Dittus-Boelter (1930) correlation Eq. (1), Jackson (2002) correlation Eq. (23), and the newly proposed Cheng (2009) correlation Eq. (27) were the best for bundle configurations. No Nu correlation exists that can predict accurately in the DHT range.

5.3 EXPERIMENTAL RESULTS

5.3.1 *DHT Regime*

Trials #1 to #3 of the 7-rod bundle in section 4.1 demonstrate that the increase in ratio of q_{avg}/q_{dht} leads to DHT occurring sooner in the bundle. Comparing Trial #3 to Trial #5/#6 illustrates that increasing the mass flux, while maintaining similar q_{avg}/q_{dht} ratios, leads to a greater DHT effect causing T_w to rise. However, this does not lead to DHT occurring earlier along the heated length. Trials #7 and #8 show that increasing the pressure produces little effect on the DHT regime or the fluid flow and thermal hydraulic characteristics.

Comparing Trial #2 and #4 in section 4.1 demonstrates that the fluid characteristics are not the only determining factor leading to DHT. Trial #2 and #4 have identical fluid parameters, with the difference being Trial #4 having a higher inlet T_b . Unexpectedly, the DHT regime in Trial #4 occurs well after T_w crosses the T_{pc} , with the T_w profile similar to that of Trial #3 and Trial #5/#6. This result is different than all other DHT regimes in the 7-rod bundle trials, suggesting the geometry of bundle configurations, entrance effects, T_w approaching T_{pc} , and other phenomena, all influence the onset of the DHT regime.

Trials #1 to #8 demonstrate that by increasing the ratio of q_{avg}/q_{dht} to 1.79 leads to an extreme DHT region that causes wall temperatures to increase significantly in 7-rod bundle geometry.

5.3.2 *IHT Regime*

Trials #7 and #8 in section 4.1 demonstrate that after the DHT regime, an IHT regime exists at high $q_{\text{avg}}/q_{\text{dht}}$ ratios (>2.0). It is unclear whether this IHT regime would exist in lower $q_{\text{avg}}/q_{\text{dht}}$ ratio trials after the emergence of the DHT regime.

5.3.3 *Central & Peripheral Rods*

Trials #5 and #6 of the 7-rod bundle in section 4.1 demonstrate that the centre fuel rod experiences a higher surface temperature than peripheral fuel rods in a 7-rod configuration.

5.4 NEW **Nu** CORRELATION

The newly proposed **Nu** correlation (Clark et al. (2020)) developed and shown in section 4.3.3.2 sufficiently predicts for 7-rod bundle data. As shown in section 4.3.3.2 (Figure 4-42 to Figure 4-45), the newly proposed **Nu** correlation predicts 80% of data within $\pm 25\%$ for HTC, and predicts 85% of data within $\pm 10\%$ for T_w .

The T_w predictions that were significantly lower than the measured T_w were primarily for $q_{\text{avg}}/q_{\text{dht}}$ ratios above 2.0. Above this ratio, under-predictions for T_w can be as high as 150°C when compared to the measured values. Therefore, designers should be cautioned against using these ratios, or against using the Clark et al. (2020) correlation Eq. (36) at $q_{\text{avg}}/q_{\text{dht}}$ ratios above 2.0 for bundle geometries. If these ratios are used with Eq. (36), differences of over 150°C just after the predicted T_w crosses the T_{pc} may be experienced.

The newly proposed **Nu** correlation also sufficiently predicts for bare tube bundle data, with 80% of data predicted within $\pm 35\%$ for HTC shown in Figure 4-44, and 98% of data predicted within $\pm 10\%$ wall temperature shown in Figure 4-45.

For $q_{\text{avg}}/q_{\text{dht}}$ ratios between 1.0 to 2.0, under-predictions for T_w can be as high as 150°C when compared to the measured values. Therefore, designers should be cautioned against using these ratios, or against using the Clark et al. (2020) correlation Eq. (36) at $q_{\text{avg}}/q_{\text{dht}}$ ratios between 1.0 - 2.0 for bare tubes. If these ratios are used with Eq. (36), differences of over 150°C may be experienced after the predicted T_w crosses the T_{pc} , or the T_b crosses the T_{pc} .

5.5 NU CORRELATION ASSESSMENTS

The initial experimental analysis error assessment outlined in section 4.2.3.2 was updated in section 4.3.4 to include the Clark et al. (2020) correlation Eq. (36). Upon examination, the Clark et al. (2020) correlation outperforms nearly all **Nu** correlations for both HTC and T_w predictions, using the RMS error and MAE metrics. The full table of data error data for the 7-rod and bare tube tests, including ME, MAE, SD, and RMS for HTC and T_w , are shown in section C.1.

For the 7-rod bundle dataset the Hu (2001) correlation Eq. (21) was the best predictor of HTC by RMS error (25.6%), while the Dyadyakin and Popov (1977) correlation Eq. (16) was the best predictor of HTC by MAE (15.6%). The Clark, et al. (2020) correlation Eq. (36) predicted HTC with an RMS error of 26.5%, and an MAE of 15.7%.

For the 7-rod dataset, the Clark, et al. (2020) correlation Eq. (36) was the best predictor of T_w by RMS error (7.4%), while the Watts and Chou (1982) correlation Eq. (17) was the best predictor of T_w by MAE (4.5%). The Clark, et al. (2020) correlation Eq. (36) predicted an MAE of 4.9%.

For the bare tube dataset, the Clark, et al. (2020) correlation Eq. (36) was the best predictor of HTC by RMS error (29.0%) and by MAE (22.2%).

For the bare tube dataset, the Clark, et al. (2020) correlation Eq. (36) was the best predictor of T_w by RMS error (3.3%), and by MAE (2.4%) (with the Wang and Li (2014) correlation Eq. (34) producing the same MAE (2.4%)).

5.6 GRAPHICAL RESULTS

After plotting the 4 sets of predictions for 7-rod data on graphs in section 4.4.1, the Clark, et al. (2020) correlation Eq. (36), the Dyadyakin and Popov (1977) correlation Eq. (16), and the Swenson, et al. (1965) correlation Eq. (8) visually appear to follow the trends of the 7-rod bundle configuration best overall.

After plotting the predictions for the bare tube data on graphs in section 4.4.2, the Mokry, et al. (2009) correlation Eq. (28), the Clark, et al. (2020) correlation Eq. (36), and the

Swenson, et al. (1965) correlation Eq. (8) visually appear to follow the trends of the bare tube best overall.

From the statistical assessments in section 4.2.3.2 and 4.3.4, and the graphical results shown in section 4.4, the Clark, et al. (2020) correlation appears to follow the trends and produce the lowest RMS error for nearly all aspects in both the 7-rod bundles and bare tubes.

5.7 SHEATH AND FUEL CENTRELINE TEMPERATURES

As shown in section 4.4.3, the theoretical maximum number of bundles that can be used is between 2 and 6 for the parameters listed in the 7-rod bundle trials, assuming UO₂ fuel with a constant heat flux and Alloy 625 sheath material. This is due to the sheath temperature crossing the industrial accepted maximum limits of 850°C for all 7-rod bundle trials. It is also noted that all T_b values are greater at the outlet than the SCWR design of 625°C. Thus the ratio of q_{avg}/q_{dht} for the 7-rod bundle trials is too high to be used in the design of an SCWR.

As a typical CANDU style reactor uses 12 fuel bundles in series, the 7-rod bundle test configuration and parameters are not suitable for use in SCWR.

The 37-Element configuration shown in section 2.2, in a 12 bundle configuration, and assuming UO₂ fuel with a constant heat flux and Alloy 625 sheath material, is not suitable for use in SCWR as the fuel centreline temperature crosses the industrial accepted limit of 1850°C in the beginning of the 6th bundle.

The 64-Element configuration shown in section 2.2 with 5-metre length, assuming UO₂ fuel with a constant heat flux and Alloy 625 sheath material, is suitable for use in SCWR as the fuel centreline temperature reaches the industrial limit of 1850°C at the 5.0 m heated length (1850.4°C), while the sheath temperature never reaches the industrially accepted limit of 850°C during the 5 m heated length. Additionally, the T_b reaches 625°C at the end of the 5 m length.

6 CONCLUSIONS

The conclusions of this thesis are as follows:

1) Specifics of HT in a 7-rod bundle Geometry

- All 3 HT regimes exist in a 7-rod bundle (NHT/IHT/DHT)
- The turbulence effect of the 7-rod bundles with the 4 helical ribs attached to each rod only slightly increases the average HTC values over that experienced by bare tubes (i.e. no significant enhancement experienced). Future SCWR does not require any helical ribs to aid in HT, as no significant improvement was observed.

2) 7-rod bundle Correlation comparisons

- Four top correlations for 7-rod bundle:
 - i. Bishop et al. (1964) correlation Eq. (7)
 - ii. Ornatsky et al. (1970) correlation Eq. (10)
 - iii. Dyadyakin & Popov (1977) correlation Eq. (16)
 - iv. Hu (2001) correlation Eq. (21)
- None of the top correlations for the 7-rod bundle can predict within an RMS error of $\pm 30\%$ for HTC and $\pm 10\%$ for T_w in bare tubes

3) New Correlation

- Clark et al. (2020) correlation Eq. (36) seems to be the best predictor of T_w for both bare tubes and 7-rod bundle configurations, based on RMS error and a visual assessment of the 36 **Nu** correlations tested.
- Clark et al. (2020) correlation Eq. (36) seems to be the best predictor of HTC for bare tubes and is second best for 7-rod bundle configurations next to the Hu (2001) correlation Eq. (21), based on RMS error and a visual assessment of the 36 **Nu** correlations tested.
- Clark et al. (2020) correlation Eq. (36) should be used in the development of future SCWR designs

4) DHT Regime Comparisons

- Onset of DHT in 7-rod bundle is greatly influenced by the turbulence effect, with a ratio of $q_{\text{avg}}/q_{\text{dht}}$ roughly 1.6 – 1.8 times higher when compared to bare tubes.
- Increasing the $q_{\text{avg}}/q_{\text{dht}}$ ratio leads to an earlier onset of DHT, with larger mass fluxes leading to a more severe DHT effect. Increasing pressure does not significantly alter the HT characteristics.
- Many **Nu** correlations developed for bare tubes cannot be used in the 7-rod bundle due to the sudden decrease of HTC prediction after the predicted T_w crosses the T_{pc} at higher ratios of $q_{\text{avg}}/q_{\text{dht}}$.

5) Typical SCWR Designs Validation

- Using the Clark et al. (2020) correlation Eq. (36) and assuming UO₂ fuel with a constant heat flux and Alloy 625 sheath material, it is predicted that the 7-rod bundle configuration with the parameters used in Trials #1 to #8 are not suitable for use in a 12 fuel bundle configuration with SCWR due to high sheath temperatures that exceed the industry accepted limit.
- Using the Clark et al. (2020) correlation Eq. (36) and assuming UO₂ fuel with a constant heat flux and Alloy 625 sheath material, it is predicted that the proposed SCWR 37-element fuel bundle configuration would not be suitable for use in the SCWR due to high fuel centreline temperatures
- Using the Clark et al. (2020 correlation Eq. (36) and assuming UO₂ fuel with a constant heat flux and Alloy 625 sheath material, it is predicted that the proposed SCWR 64-element fuel bundle configuration would be suitable for use as both sheath and fuel centreline temperatures stay below the industry accepted temperatures throughout the entire heated length.

7 FUTURE WORK

For future work three areas are identified:

1. Further investigation into the causes of DHT through additional experimentation with SCW, including geometric and/or entrance effect terms to aid in determining the onset of DHT and IHT regions during calculation (outside of predicting the onset of DHT).
2. Assessment of the newly proposed **Nu** correlation (Clark et al. (2020)) with a wider range of applicability, including both bare tubes and bundle configurations.
3. Continued investigation into sheath and fuel centreline temperatures. This assessment assumed a constant heat flux, and did not consider variable heat flux (typically a cosine function across the total heated length), which has an impact on fuel centreline temperatures.

REFERENCES

- AECL. (1984, June). *The Douglas Point Story*. Retrieved from Canadian Nuclear Society on March 21st, 2020: <https://www.cns-snc.ca/media/history/DouglasPoint/DouglasPoint.html>
- Benner, S. A., Ricardo, A. & Carrigan, M. A. (2004, December). Is there a common chemical model for life in the universe? *Current Opinion in Chemical Biology*, Vol. 8., Issue 6. Florida, USA: Elsevier. pp. 672-689.
- Berche, B., Henkel, M. & Kenna, R. (2009). Critical Phenomena: 150 years since Cagniard de la Tour. *Revista Brasileira de Ensino de Fisica*. Cornell University.
- Bergman, T., Lavine, A., Incropera, F. & Dewitt, D. (2017). Fundamentals of Heat and Mass Transfer, Ed. 8. Danvers, MA: John Wiley & Sons, Inc. p. 1045.
- Bishop, A., Sandberg, R. & Tong, L. (1964). High Temperature Supercritical Pressure Water Loop. Part IV. Forced Convection Heat Transfer to Water at Near-Critical Temperatures and Supercritical Pressures. *WCAP-2056-Part IV*. Pittsburgh, USA: Westinghouse Electric Corporation, Atomic Power Division. p. 128.
- Bringer, R. P. & Smith, J. M. (1957). Heat Transfer in the Critical Region. *AIChE Journal*. Vol. 3, No. 1, pp. 49-55.
- Brooks, G. (1993). A Short History of the CANDU Nuclear Power System. *AECL-10788*. Canada. pp. 1-39.
- Brown, A. M. (2000). A step-by-step guide to non-linear regression analysis of experimental data using a Microsoft Excel spreadsheet. *Computer Methods and Programs in Biomedicine* 65 (2001). Elsevier. pp. 191-200.
- C2ES. (2017). *Global Emissions*. Retrieved from Center for Climate and Energy Solutions on May 31st, 2020: <https://www.c2es.org/content/international-emissions/>
- Cameron, I. R. (1982). Heat Generation and Removal in Nuclear Reactors. *Nuclear Fission Reactors*. pp. 175-219.

- Cengel, Y. & Ghajar, A. (2015). Heat and Mass Transfer, a Practical Approach, 5th Ed. *McGraw-Hill*. New York, NY. p. 992.
- Chee, J. D. (2015, January). Pearson's Product-Moment Correlation: Sample Analysis. *University of Hawaii at Manoa School of Nursing*. pp. 1-15.
- Chen, W. & Fang, X. (2014). A New Heat Transfer Correlation for Supercritical Water Flowing in Vertical Tubes. *International Journal of Heat and Mass Transfer*, Vol. 78, pp. 156-160.
- Chen, W., Fang, X., Xu, Y. & Su, X. (2015). An Assessment of Correlations of Forced Convection Heat Transfer to Water at Supercritical Pressure. *Annals of Nuclear Energy*, Vol. 76. pp. 451-460.
- Cheng, X. & Schulenberg, T. (2001). Heat Transfer at Supercritical pressures - Literature Review and Application to an HPLWR. *Institut für Kern- un Energietechnik Programm Nukleare Sicherheitsforschung*. Forschungszentrum Karlsruhe GmbH, Karlsruhe. pp. 1-47.
- Cheng, X., Yang, Y. & Huang, S. (2009). A Simplified Method for Heat Transfer Prediction of Supercritical Fluids in Circular Tubes. *Annals of Nuclear Energy*, Vol. 36, Issue 8. pp. 1120-1128.
- Chow, C. K. & Khartabil, H. F. (2007). Fuel Channer Designs for CANDU-SCWR. *3rd International Symposium on SCWR - Design and Technology, Shanghai, Paper No. SCWR2007-P046, China, March 12-15*. pp. 1-11.
- Clark, S., Pioro, R., Zvorykin, A., Fialko, N. M. & Pioro, I. L. (2019, June 23-26). Comparison of Experimental and Calculated HTC Values for Short Vertical 7-Rod Bundle Cooled with SCW. *39th Annual Conference of the Canadian Nuclear Society and 43rd Annual CNS/CNA Student Conference, Paper #41*. Ottawa, ON, Canada. pp. 1-7.
- CNSC. (2020, January 13). *Pre-Licensing Vendor Design Review*. Retrieved from Government of Canada, Canadian Nuclear Safety Commission, Retrieved May 3rd,

2020: <https://nuclearsafety.gc.ca/eng/reactors/power-plants/pre-licensing-vendor-design-review/index.cfm>

- Colburn, A. (1933). A Method of Correlating Forced Convection Heat Transfer Data and a Comparison with Fluid Friction. *Trans-America Institute of Chemical Engineers (Trans-AIChE)*, Vol. 29, pp. 174-210.
- Colton, A., Bromley, B. & Dugal, C. (2017). Code-to-Code Comparisons of Lattice Physics Calculations for Thorium-Augmented and Thorium-based Fuels in Pressure Tube Heavy Water Reactors. *Annals of Nuclear Energy*, Vol. 13, pp. 194-203.
- Debrah, S., Shitsi, E., Chabi, S. & Sahebi, N. (2019). Assessment of Heat Transfer Correlations in the Sub-Channels of Proposed Rod Bundle Geometry for Supercritical Water Reactor. *Heliyon*, Vol. 5, Issue 11, pp. 1-13.
- Deissler, R. G. & Taylor, M. F. (1953). Analysis of Heat Transfer and Fluid Friction for Fully Developed Turbulent Flow of Supercritical Water with Variable Fluid Properties in a Smooth Tube. *Lewis Flight Propulsion Laboratory. NACA RM E53B17. National Advisory Committee for Aeronautics*. Cleveland, Ohio, USA. pp. 1-31.
- Dickinson, N. L. & Welch, C. P. (1958). Heat Transfer to Supercritical Water. *Transactions of the ASME*, 80, pp. 746-752.
- Dittus, F. & Boelter, L. (1930). Heat Transfer in Automobile Radiators of the Tubular Type. *University of California Publications in Engineering*, Vol. 2, No. 13, pp. 443-461.
- DOE, U. (1982, December). The First Reactor. *U.S. Department of Energy DOE/NE-0046*. Washington, D.C. pp. 1-51.
- DOE, U.S. (N.D.). The History of Nuclear Energy. *DOE/NE-0088*. Washington, D.C.: U.S. Department of Energy, Office of Nuclear Energy, Science, and Technology. pp. 1-19.

- Domin, G. (1963). Wärmeübergang in kritischen und überkritischen Bereichen von Wasser in Rohren (in German). *Brennst-Wärme-Kraft (BWK)*, Vol. 15, No. 11., pp. 527–532.
- Domínguez, A., Onder, N., Rao, Y. & Leung, L. (2016). Evolution of the Canadian SCWR Fuel-Assembly Concept and Assessment of the 64 Element Assembly for Thermalhydraulic Performance. *CNL Nuclear Review*, Vol. 5, No. 2. pp. 221-238.
- Duffey, R. & Pioro, I. L. (2019, November). Ensuring the Future of Nuclear Power. *Mechanical Engineering Magazine* Vol. 141. No. 11. pp 31 - 35. ASME.
- Duffey, R., Kirillov, P., Panchal, R. & Pioro, I. L. (2016). Chapter 1: Introduction - a survey of the status of electricity generation in the world. In I. L. Pioro, *Handbook of Generation IV Nuclear Reactors: Woodhead Publishing Series in Energy*. pp. 1-34.
- Duffey, R., Leung, L., Martin, D., Sur, B. & Yetisir, M. (2011). A Supercritical Water-Cooled Small Modular Reactor. *Proceedings of the ASME 2011 Small Modular Reactors Symposium, September 28-30, 2011, Washington, DC., USA*. pp. 1-8.
- Dyadyakin, B. V. & Popov, A. S. (1977). Heat transfer and thermal resistance of tight seven-rod bundle, cooled with water flow at supercritical pressures, (In Russian). *Transactions of VTI*, No. 11. pp. 244-253.
- Farah, A., King, K., Gupta, S., Mokry, S., Peiman, W. & Pioro, I. L. (2010). Comparison of Selected Forced-Convection Supercritical-Water Heat-Transfer Correlations for Vertical Bare Tubes. *Proceedings of the 18th International Conference on Nuclear Engineering, ICONE18, May 17-21, Xi'an, China*. pp. 1-10.
- Filonenko, G. K. (1954). Hydraulic Resistance of Pipes (in Russian). *Teploenergetika*, No. 4. pp. 40-44.
- Fink, J. (2000). Thermophysical Properties of Uranium Dioxide. *Journal of Nuclear Materials*, Vol. 279. pp. 1-18.
- Gabaraev, B. A., Ganev, I. K., Davydov, V. K., Kuznetsov, Y. N., Reshetov, V. A. & Smirnov, A. V. (2003). Vessel and Channel Fast Reactors Cooled by Boiling Water

- or Water with Supercritical Parameters. *Atomic Energy, Volume 95, Issue 4*. pp. 655-662.
- Giarratano, P. J., Arp, V. D. & Smith, R. V. (1971, October). Forced Convection Heat Transfer to Supercritical Helium. *Cryogenics Division Institute for Basic Standards, Vol. 11, Issue 5*. Boulder, Colorado, USA: Elsevier. pp. 385-393.
- GIF. (2019, August 2). *Generation IV Systems*. Retrieved from Gen IV International Forum on March 21st, 2020: https://www.gen-4.org/gif/jcms/c_40465/generation-iv-systems
- GIF. (2019, August 2). *Generation IV Systems*. Retrieved from Gen IV International Forum on March 21st, 2020: https://www.gen-4.org/gif/jcms/c_40465/generation-iv-systems
- GIF. (2019, August 2). *Origins of the GIF*. Retrieved from Gen IV International Forum on March 21st, 2020: https://www.gen-4.org/gif/jcms/c_9334/origins
- GIF. (2019, August 2). *Origins of the GIF*. Retrieved from Gen IV International Forum on March 21st, 2020: https://www.gen-4.org/gif/jcms/c_9334/origins
- GIF. (2019). *Supercritical-Water-Cooled Reactor (SCWR)*. Retrieved from GEN IV International Forum on March 21st, 2020: https://www.gen-4.org/gif/jcms/c_42151/supercritical-water-cooled-reactor-scwr
- Global Data Lab. (2020). *Subnational Human Development Index (4.0)*. Retrieved from Institute for Management Research, Radboud University, on June 5th, 2020: <https://globaldatalab.org/shdi/shdi/>
- Gnielinski, V. (1976). New Equations for heat and Mass Transfer in Turbulent Pipe and Channel Flow. *International Chemical Engineering, Vol. 16, No. 2, ISSN 0020-6318*. pp. 359-368.
- Gorban, L. M., Pomet'ko, R. S. & Khryashev, O. A. (1990). Modeling of Water Heat Transfer with Freon of Supercritical Pressure (In Russian). *Institute of Physics and Power Engineering (ФЭИ), Report No. ФЭИ-1766*. Obninsk, Russia. pp. 1-19.

- Griem, H. (1995). Investigations on Thermohydraulics with Internal Ribs Evaporator Tubes, (in German). *Dissertation. Technische Universität München.*
- Griem, H. (1996). A New Procedure for the Prediction of Forced Convection Heat Transfer at Near- and Supercritical Pressure. *Heat Mass Transfer, Vol. 31.*, pp. 301-305.
- Grosch, G. (2019). *System Arrangements and Memoranda of Understanding*. Retrieved from GEN IV International Forum on March 21st, 2020: https://www.gen-4.org/gif/jcms/c_9343/system-arrangements-mou
- Gschnaidtner, T., Schatte, G., Kohlhepp, A., Wang, Y., Wieland, C. & Spliethoff, H. (2018). A New Assessment Method for the Evaluation of Supercritical Heat Transfer Correlations, Particularly with regard to the "Multiple/No Solutions" problem. *Thermal Science and Engineering Progress, Vol. 7.* pp. 267-278.
- Gupta, S., Mokry, S. & Pioro, I. L. (2011, October 24-25). Developing A Heat-Transfer Correlation for Supercritical-Water Flow in Vertical Bare Tubes and Its Application in SCWRS. *Proceedings ICONE-19, Paper# 43503*. Osaka, Japan: p. 11.
- Gupta, S., Saltanov, E., Mokry, S., Pioro, I. L., Trevani, L. & McGillivray, D. (2013). Developing Empirical Heat-Transfer Correlations for Supercritical CO₂ Flowing in Vertical Bare Tubes. *Nuclear Engineering and Design, Vol. 261.*, pp. 116-131.
- Hall, W. & Jackson, J. (1969, August 3 - 6). Laminarisation of a turbulent pipe flow by buoyancy forces. *American Society of Mechanical Engineers Paper No. ASME 69-HT-55*. pp. 1-8.
- Herkenrath, H., Mörk-Mörkenstein, P., Jung, P. & Weckermann, F. (1967). Heat Transfer and Water at Forced Flow in Pressure Range of 140 to 250 bar, (in German). *EUR 3658d, Euratom*. pp. 1-9.
- Hilliger, B. (1916). Untersuchungen über die Wirkung von Einlagekörpern in den Rauchröhren von Lokomobilkesseln. *Zeitschr. des Vereines deutscher Ingenieure, 60.* p. 899.

- Hu, Z. H. (2001). Heat Transfer Characteristics of Vertical Up Flow and Inclined Tube in the Supercritical Pressure and Near-Critical Pressure Region. *Ph.D. Dissertation. Xi'an Jiaotong University, Xi'an, China.*
- Hussain, M., Reitsma, F., Subki, M. & Kiuchi, H. (2018). Advances in Small Modular Reactor Technology Developments: A Supplement to IAEA Advanced Reactors Information System (ARIS). *International Atomic Energy Association, SMR Book 2018. Austria.* pp. 1-258.
- IAEA. (2005). Thorium Fuel Cycle - Potential Benefits and Challenges. *International Atomic Energy Agency, IAEA-TECDOC-1450.* pp. 1-113.
- IAEA. (2014). Heat Transfer behaviour and Thermohydraulics Code Testing for Supercritical Water Cooled Reactors (SCWRs). *International Atomic Energy Agency, IAEA-TECDOC-1746.* pp. 1-510.
- IEA. (2017). *CO2 Emissions from Fuel Combustion.* Retrieved from International Energy Agency, IEA Atlas of Energy, on June 5th, 2020: <http://energyatlas.iea.org/#!/tellmap/1378539487/0>
- IEA. (2019). *Global Energy & CO2 Status Report.* All Rights Reserved.
- IEA. (2019, March 26). *Global energy demand rose by 2.3% in 2018, its fastest pace in the last decade.* Retrieved from International Energy Agency on March 21st, 2020: <https://www.iea.org/newsroom/news/2019/march/global-energy-demand-rose-by-23-in-2018-its-fastest-pace-in-the-last-decade.html>
- IEA. (2020). *Data and Statistics.* Retrieved from International Energy Agency, on June 6th, 2020: <https://www.iea.org/data-and-statistics?country=WORLD&fuel=CO2%20emissions&indicator=CO2%20emissions%20by%20energy%20source>
- IRSN. (2015). Review of Generation IV Nuclear Energy Systems. *Institut de Radioprotection et de Sûreté Nucleaire* . pp. 1-239.
- Jackson, J. D. & Fewster, J. (1975). Forced Convection Data for Supercritical Pressure Fluids. *HTFS 1975, Paper No. 21540.*

- Jackson, J. D. & Hall, W. B. (1979). Forced Convection Heat Transfer to Fluids at Supercritical Pressure. *Turbulent Forced Convection in Channels and Bundles, Vol. 2*. Hemisphere, New York, NY. pp. 563-611.
- Jackson, J. D. (2002, October 21-25). Consideration of the Heat Transfer Properties of Supercritical Pressure Water in Connection with the Cooling of Advanced Nuclear Reactors. *The 13th Pacific Basin Nuclear Conference, Vol. 34, Issue 49*, October 21-25. Shenzhen City, China, Shenzhen, China: Atomic Energy Press. p. 240.
- Jackson, J. D. (2013). Fluid Flow and Convective Heat Transfer to Fluids at Supercritical Pressure. *Nuclear Engineering Design, Vol. 264*. pp. 24-40.
- Jackson, J. D., Cotton, M. A. & Axcell, B. P. (1989). Studies of Mixed Convection in Vertical Tubes. *International Journal Heat Fluid Flow, Vol. 10, No. 1*. pp. 2-15.
- Jäger, W., Espinoza, V. & Hurtado, A. (2011). Review and Proposal for Heat Transfer Predictions at Supercritical Water Conditions using Existing Correlations and Experiments. *Nuclear Engineering and Design, Vol. 241, Issue 6*. pp. 2184-2203.
- Jo, D., Al-Yahia, O., Altamimi, R., Park, J. & Chae, H. (2014). Experimental Investigation of Convective Heat Transfer in a Narrow Rectuangular Channel for Upward and Downward Flows. *Nuclear Engineering and Technology, Vol. 46, No. 2*.
- Josse, E. (1913). Thermal Basics in the Condensation Process (in German). *Mitteilungen aus dem Maschinen-Laboratorium der Kgl. Techn. Hochschule zu Berlin, V. Heft*. p. 15.
- Kaschnitz, E., Kaschnitz, L. & Heugenhauser, S. (2019). Electrical Resistivity Measured by Millisecond Pulse Heating in Comparison with Thermal Conductivity of the Superalloy Inconel 625 at Elevated Temperature. *International Journal of Thermophysics, Vol. 40, No. 27*. pp. 1-13.
- Kim, Y., Hartanto, D. & Venneri, F. (2011). Super-Deep-Burn with the FCM (Fully Ceramic Microencapsulated) TRU Fuel in CANDU. *International Conference Future of HWRs, Ottawa, Ontario, Canada, Oct. 2-5*. pp. 1-11.

- Kirillov, P., Pomet'ko, R., Smirnov, A., Grabezhnaia, V., Pioro, I. L., Duffey, R. & Khartabil, H. (2005, Oct 9-13). Experimental Study on Heat Transfer to Supercritical Water Flowing in 1- and 4-m-Long Vertical Tubes. *Proceedings of Global 2005, Paper No. 518. ResearchGate*. Tsukuba, Japan. pp. 1-8.
- Kirillov, P., Yur'ev, Y. & Bobkov, V. (1990). Handbook of Thermal-Hydraulics Calculations (In Russian). "3.2 Flow hydraulic resistance of the working fluids with significantly changing properties". Moscow, Russia: Energoatomizdat Publishing House. pp. 66-67.
- Kitoh, K., Koshizuka, S. & Oka, Y. (2001). Refinement of Transient Criteria and Safety Analysis for a High Temperature Reactor Cooled by Supercritical Water. *Nuclear Technology Vol. 135, No. 3*, pp. 252–264.
- Knez, Ž., Markočič, E., Leitgeb, M., Primožič, M., Knez Hrnčič, M. & Škerget, M. (2014, December 1). Industrial Applications of Supercritical fluids: A Review. *Energy, Vol. 77. Elsevier*. Maribor, Slovenia. pp. 235-243.
- Kondrat'ev, N. S. (1971). About regimes of the deteriorated heat transfer at flow of supercritical pressure water in tubes, (In Russian). *Transactions of the IVth All-Union Conference on Heat Transfer and Hydraulics at Movement of Two-Phase Flow Inside Elements of Power Engineering Machines and Apparatuses*. pp. 71-74.
- Kong, X., Li, H., Zhang, Q., Guo, K., Luo, Q. & Lei, X. (2019). A New Criterion for the Onset of Heat Transfer Deterioration to Supercritical Water in Vertically-Upward Smooth Tubes. *Applied Thermal Engineering, Vol. 151*. pp. 66-76.
- Krasnoshchekov, E. A. & Protopopov, V. S. (1959). Heat Transfer at Supercritical Region in Flow of Carbon Dioxide and Water in Tubes, (in Russian). *Thermal Engineering, No. 12*. pp. 26-30.
- Krasnoshchekov, E. A. & Protopopov, V. S. (1960). About Heat Transfer in Flow of Carbon Dioxide and Water at Supercritical Region of State Parameters, (in Russian). *Thermal Engineering, No. 10*. p. 94.

- Krasnoshchekov, E. A., Protopopov, V. S., Van, F. & Kuraeva, I. V. (1967). Experimental Investigation of Heat Transfer for Carbon Dioxide in the Supercritical Region. *Proceedings of the 2nd All-Soviet Union Conference on Heat and Mass Transfer, Minsk, Belarus', May of 1964. Vol. 1*. Published as Rand Report R-451-PR, Edited by C. Gazley, Jr., J.P. Hartnett, and E.R.C. Ecker., pp. 26-35.
- Kuang, B., Zhang, Y. Q. & Cheng, X. (2008, October 5 - 9). A New, Wide-Ranged Heat Transfer Correlation of Water at Supercritical Pressures in Vertical Upward Ducts. *The 7th International Topical Meeting on Nuclear Reactor Thermal Hydraulics, Operation and Safety (NUTHOS-7), Paper No. 189*. Seoul, South Korea.
- Lei, X., Guo, Y., Zhang, W., Li, H. & Li, L. (2019). Development of Heat Transfer Correlation for Supercritical Water in Vertical Upward Tubes. *Heat Transfer Engineering, Vol. 40, No. 8.*, pp. 652-666.
- Lemmon, E. W., Bell, I. H., Huber, M. L. & McLinden, M. O. (2018). NIST Standard Reference Database 23. *Reference Fluid Thermodynamic and Transport Properties-REFPROP, Version 10.0*. Gaithersburg, Maryland, USA: National Institute of Standards and Technology, Standard Reference Data Program.
- Lesser, J. A. (2019). *Is there a Future for Nuclear Power in the United States?* Retrieved from Manhattan Institute, on June 1st, 2020: <https://www.manhattan-institute.org/nuclear-power-emissions-free-solution>
- Levelt Sengers, J. (2000). Supercritical Fluids: Their properties and applications. *Chapter 1 from: Supercritical fluids, editors: E. Kiran et al*. NATO Advanced Study Institute on Supercritical Fluids - Fundamentals and Application, NATO Science Series, Series E, Applied Sciences, Kluwer Academic Publishers, Netherlands, Vol. 366, pp. 1-29.
- Licht, J. R., Anderson, M. H., Corradini, M. L. & Bonazza, R. (2007, August). Heat Transfer Phenomena in Supercritical Water Nuclear Reactors. *University of Wisconsin - Madison Department of Engineering Physics, Final Technical Report: DE-FG07-04ID14602*. Wisconsin, USA. pp. 1-106.

- Liu, S. & Cai, J. (2014). Design & Optimization of Two Breeding Thorium-Uranium mixed SCWR fuel assemblies. *Progress in Nuclear Energy*, Vol. 70. pp. 6-19.
- McAdams, W. (1942). *Heat Transmission*, 2nd Ed. New York, NY: McGraw-Hill. pp. 167-168.
- McAdams, W. H. & Frost, T. H. (1924). Heat Transfer for Water Flowing inside Pipes. *Refridgerating Engineering*, 10. p. 23.
- Mignacca, B. & Locatelli, G. (2020). Economics and finance of Small Modular Reactors: A systematic review and research agenda. *Renewable and Sustainable Energy Reviews*, Vol. 118, Article 109519. pp. 1-15.
- Miropol'skiy, L. & Shitsman, M. E. (1957). Heat Transfer to Water and Steam at Variable Specific Heat (in Russian). *Soviet Physics, Technical Physics*, Vol. 27, pp. 2359–2372.
- Mokry, S., Gospodinov, Y., Pioro, I. L. & Kirillov, P. (2009). Supercritical Water Heat-Transfer Correlation for Vertical Bare Tubes. *Proceedings of the 17th International Conference on Nuclear Engineering (ICONE17)*, July 12-16, Brussels, Belgium, pp. 1126-1136. pp. 1-8.
- Mokry, S., Pioro, I. L., Farah, A., King, K., Gupta, S., Peiman, W. & Kirillov, P. (2011). Development of Supercritical Water Heat-Transfer Correlation for Vertical Bare Tubes. *Nuclear Engineering and Design*, Vol 241. pp. 1126-1136.
- Morris, F. H. & Whitman, W. G. (1928). Heat Transfer for Oils and Water in Pipes. *Industrial and Engineering Chemisty*, 20. p. 234.
- Munson, B. R., Okiishi, T. H., Huebsch, W. W. & Rothmayer, A. P. (2012, May 15). Fundamentals of Fluid Mechanics, 7th Ed. *John Wiley & Sons, Inc.* USA. p. 792.
- NEA. (2016). Reactivity-Initiated Accident Fuel-Code Benchmark Phase II. *Nuclear Energy Agency, Committee on the Safety of Nuclear Installations*, NEA/CSNI/R(2016)6/VOL2. pp. 1-42.

- Nusselt, W. (1909). The Heat Transfer in Pipes (in German). *Zur Habilitation an der Kgl. Sächs. Technischen Hochschule zu Dresden*.
- Oberhaus, D. (2020). *Germany Rejected Nuclear Power - and Deadly Emissions Spiked*. Retrieved from Wired, on June 6th, 2020: <https://www.wired.com/story/germany-rejected-nuclear-powerand-deadly-emissions-spiked/#:~:text=The%20German%20government%20quickly%20passed,preventing%20a%20Fukushima%2Dstyle%20disaster>.
- Office of Nuclear Energy. (2020). *Advantages and Challenges of Nuclear Energy*. Retrieved from Office of Nuclear Energy, Energy.Gov, on June 1st, 2020: <https://www.energy.gov/ne/articles/advantages-and-challenges-nuclear-energy>
- Ornatsky, A., Glushchenko, L., Siomin, E. & Kalatchev, S. I. (1970). The Research of Temperature Conditions of Small Diameter Parallel Tubes Cooled by Water Under Supercritical Pressures. *Proceedings of the 4th International Heat Transfer Conference in Paris-Versailles, France, Vol. VI, Paper No. B8.11*, Amsterdam, The Netherlands: Elsevier. pp. 1-10.
- Page, R. (1976). Canadian Power Reactor Fuel. *Atomic Energy of Canada Limited, AECL 5609*. pp. 1-63.
- Palko, D. & Anglart, H. (2008, August). Theoretical and Numerical Study of Heat Transfer Deterioration in High Performance Light Water Reactor. *Science and Technology of Nuclear Installations, Vol. 2008, Article ID 405072*. Stockholm, Sweden: Hindawi Publishing Corporation. pp. 1-5.
- Peiman, W., Pioro, I. L. & Gabriel, K. (2012, February 10). Thermal Aspects of Conventional and Alternative Fuels in SuperCritical Water-Cooled Reactor (SCWR) Applications. *Nuclear Reactors, Amir Zacarias Mesquita, IntechOpen, DOI: 10.5772/39005*. pp. 1-36.
- Pencer, J. & Hyland, B. (2011). Physics Aspects of the Pressure Tube Type SCWR Preconceptual Design. *International Conference Future of HWRs, Ottawa, Ontario, Canada, Oct. 2-5, Paper 020*. pp. 1-10.

- Petukhov, B. S. & Kirillov. (1958). About Heat Transfer at Turbulent Fluid Flow in Tubes, (in Russian). *Thermal Engineering*, (4). pp. 63-68.
- Petukhov, B. S. & Polyakov, A. F. (1974, September 3 - 7). Turbulent Flow and Heat Transfer in Horizontal Tubes with Substantial Influence of Thermal-Gravitational Forces. *International Heat Transfer Conference 5: ASME, NC4.8*. Tokyo, Japan. pp. 164-168.
- Petukhov, B. S. (1970). Heat Transfer and Friction in Turbulent Pipe Flow with Variable Physical Properties. *Advances in Heat Transfer*, Vol. 6: Elsevier. Moscow, USSR. pp. 503-564.
- Petukhov, B. S., Krasnoschekov, E. A. & Protopopov, V. S. (1961). An Investigation of Heat Transfer to Fluids Flowing in Pipes Under Supercritical Conditions, In Book: *International Developments in Heat Transfer: Papers presented at the 1961 International Heat Transfer Conference, January 8-12, Part III, Paper No. 67*. University of Colorado, Boulder, CO, USA: ASME. pp. 569-578.
- Petukhov, B. S., Kurganov, V. A. & Ankudinov, V. B. (1983). Heat Transfer and Flow Resistance in the Turbulent Pipe Flow of a Fluid with Near-Critical State Parameters, (in Russian). *High Temperature*, Vol. 21, Issue 1. pp. 92-100.
- Phillipot, S., Chernatynskiy, A., El-Azab, A. & Tulenko, J. (2011). Thermal Conductivity of UO₂ Fuel: Predicting Fuel Performance from Simulation. *Journal of the Minerals, Metals & Materials Society (JOM)*, Vol. 63, No. 8. pp. 73-79.
- Pioro, I. L. & Duffey, R. (2007). *Heat Transfer and Hydraulic Resistance at Supercritical Pressures in Power Engineering Applications*. New York, NY: ASME Press. pp. 1-361.
- Pioro, I. L. & Kirillov, P. (2013, January). Current Status of Electricity Generation at Nuclear Power Plants. *Materials and Processes for Energy: Communicating Current Research and Technological Developments* (A. Méndez-Vilas, Ed.). FORMATEX. pp. 806-817.

- Pioro, I. L. (2013, February 6). Chapter 10: Nuclear Power as a Basis for Future Electricity Production in the World: Generation III and IV Reactors. *Current Research in Nuclear Reactor Technology in Brazil and Worldwide: Amir Zacarias Mesquita, IntechOpen, DOI: 10.5772/51916*. Retrieved from IntechOpen on March 21st, 2020: <https://www.intechopen.com/books/current-research-in-nuclear-reactor-technology-in-brazil-and-worldwide/nuclear-power-as-a-basis-for-future-electricity-production-in-the-world-generation-iii-and-iv-reactors>, pp. 1-41.
- Pioro, I. L. (2016). Chapter 2: Introduction - Generation IV International Forum. In I. L. Pioro, *Handbook of Generation IV Nuclear Reactors: Woodhead Publishing Series in Energy*. pp. 37-54.
- Pioro, I. L. (2016). Handbook of Generation IV Nuclear Reactors. *Woodhead Publishing Series in Energy*, p. 942. Duxford, UK: Woodhead Publishing (WP), an imprint of Elsevier.
- Pioro, I. L. (2019). Current Status of Research on Heat Transfer in Forced Convection of Fluids at Supercritical Pressures. *Nuclear Engineering and Design*, Vol. 354, 110207. pp. 1-14.
- Pioro, I. L., Duffey, R. B., Kirillov, P. L., Pioro, R., Zvorykin, A. & Machrafi, R. (2019, April). Current Status and Future Developments in Nuclear-Power Industry of the World. *Journal of Nuclear Engineering and Radiation Science*, Vol. 5, Article 024001-1. pp. 1-27.
- Pynn, G., Brady, D., Zheng, W., Leung, L. & MacKinlay, C.-A. (2016, December). Canada's Generation IV National Program. *CNL Nuclear Review*, Vol. 5, Number 2. pp. 1-7.
- Razumovskiy, V. G., Pis'mennyi, E. N., Koloskov, A. E. & Pioro, I. L. (2008, May 11-15). Heat Transfer to Supercritical Water in Vertical 7-Rod Bundle. *Proceedings of the 16th International Conference on Nuclear Engineering, ICONE16-48954*. Orlando, Florida, USA: ASME. pp. 1-6.

- Razumovskiy, V. G., Pis'mennyi, E. N., Sidawi, K., Pioro, I. L. & Koloskov, A. E. (2015, December 9). Experimental Heat Transfer in an Annular Channel and 3-Rod Bundle Cooled with Upward Flow of Supercritical Water. *Journal of Nuclear Engineering and Radiation Science*, Vol. 2, Paper No. NERS-15-1117. ASME. pp. 1-8.
- Richards, G., Harvel, G. D., Pioro, I. L., Shelegov, A. S. & Kirillov, P. L. (2013). Heat Transfer Profiles of a Vertical, Bare, 7-element Bundle Cooled with Supercritical Freon R-12. *Nuclear Engineering and Design*, Vol. 264. pp. 246-256.
- Sabir, S. M., Chun, K., Petriw, M., Saifullah, M., Vashi, A., Zvorykin, A., . . . Pioro, I. L. (2019). Comparison of Thermophysical Properties (NIST REFPROP VER. 10) and Heat Transfer to Heavy and Light Water at Subcritical Pressures. *The 27th International Conference on Nuclear Engineering (ICONE27), The Japan Society of Mechanical Engineers, May 19-24, Article 2019.27*.
- Schulze, E. (1928). Experiments to determine the heat transfer number of air and flue gas in pipes (in German). *Mitteilung, Nr. 117 der Wärmestelle des Vereins deutscher Eisenhüttenleute*.
- Shiralkar, B. S. & Griffith, P. (1969, February 1). Deterioration in Heat Transfer to Fluids at Super-Critical Pressure and High Heat Fluxes. *Journal of Heat Transfer*, Vol. 91(1). ASME. pp. 27-36.
- Shitsman, M. (1963). Impairment of the heat transmission at supercritical pressures. *High Temperature* 1. pp. 237-244.
- Sidawi, K. (2016). Specifics of Forced-Convection Heat Transfer to Supercritical Water Flowing Upward in Annular and Bundle Flow Geometries. *Thesis Submission, The Faculty of Energy Systems and Nuclear Science, University of Ontario Institute of Technology*. pp. 1-153.
- Sieder, E. & Tate, G. (1936). Heat Transfer and Pressure Drop of Liquids in Tubes. *Industrial and Engineering Chemistry*, Vol. 28, No. 12, pp. 1429-1435.
- Special Metals. (2013). INCONEL® alloy 625. *Special Metals Corporation*. pp. 1-18.

- Styrikovich, M. A., Margulova, T. K. & Miropolskiy, Z. L. (1967). Problem in the development of designs of supercritical boilers. *Teploenergetika*, Vol. 14, No. 6. pp. 4-7.
- Swenson, H. S., Carver, J. R. & Kakarala, C. R. (1965). Heat Transfer to Supercritical Water in Smooth-Bore Tubes. *Heat Transfer*, Vol. 87, No. 4., pp. 477–484.
- Tumanovskii, A. G., Shvarts, A. L., Somova, E. V., Verbovetskii, E. K., Avrutskii, G. D., Ermakova, S. V., . . . Lazarev, M. V. (2017). Review of the Coal-Fired, Over-Supercritical and Ultra-Supercritical Steam Power Plants. *All-Russia Thermal Engineering Research Institute. Thermal Engineering*, Vol. 64, No. 2. Moscow, Russia: Pleiades Publishing. pp. 83-96.
- UNDP. (2018). *Human Development Data (1990-2018)*. Retrieved from United Nations Development Programme Human Development Reports, on June 5th, 2020: <http://hdr.undp.org/en/data>
- Waata, C. L. (2006). Coupled Neutronics/Thermal-hydraulics Analysis of a High Performance Light-Water Reactor Fuel Assembly. *Institut für Kern- und Energietechnik Programm Nukleare Sicherheitsforschung*. pp. 1-104.
- Wang, C. & Li, H. (2014). Evaluation of the Heat Transfer Correlations for Supercritical Pressure Water in Vertical Tubes. *Heat Transfer Engineering*, 35:6-8. Taylor and Francis Group, LLC. pp. 685-692.
- Wang, H., Leung, L., Wang, W. & Bi, Q. (2018). A Review on Recent Heat Transfer Studies to Supercritical Pressure Water in Channels. *Applied Thermal Engineering*, Vol. 142. pp. 573-596.
- Watts, M. & Chou, C. (1982, September 6-10). Mixed Convection Heat Transfer to Supercritical Pressure Water. *Proceedings of Seventh International Heat Transfer Conference*, pp. 495–500.
- Winterton, R. (1998). Where did Dittus and Boelter equation come from? *International Journal of Heat Mass Transfer*, Vol. 41, No. 4-5., pp. 809-810.

- WNA. (2017). *Thorium*. Retrieved from World Nuclear Association. Retrieved on May 15, 2020 from: <https://www.world-nuclear.org/information-library/current-and-future-generation/thorium.aspx>
- WNA. (2018). *Heat Values of Various Fuels*. Retrieved from World Nuclear Association, on June 1st, 2020: <https://www.world-nuclear.org/information-library/facts-and-figures/heat-values-of-various-fuels.aspx>
- WNA. (2019, January). *Nuclear Power in Canada*. Retrieved from World Nuclear Association on March 21st, 2020: <https://www.world-nuclear.org/information-library/country-profiles/countries-a-f/canada-nuclear-power.aspx>
- WNA. (2019, August). *World Nuclear Performance Report 2019*. Retrieved from World Nuclear Association: <https://www.world-nuclear.org/our-association/publications/online-reports/world-nuclear-performance-report.aspx>
- WNA. (2020). *Nuclear Power in Canada*. Retrieved from World Nuclear Association, on June 2nd, 2020: <https://www.world-nuclear.org/information-library/country-profiles/countries-a-f/canada-nuclear-power.aspx>
- WNA. (2020, March). *Small Nuclear Power Reactors*. Retrieved from World Nuclear Association on March 3rd, 2020: <https://www.world-nuclear.org/information-library/nuclear-fuel-cycle/nuclear-power-reactors/small-nuclear-power-reactors.aspx>
- WNN. (2019, April 02). *First Canadian SMR License Application Submitted*. Retrieved from World Nuclear News (WNN) on March 21st, 2020: <http://world-nuclear-news.org/Articles/First-Canadian-SMR-licence-application-submitted>
- Xu, F. & Guo, L. (2005). Mixed Convective Flow and Heat Transfer of Water in a Helicoidal Pipe Under Supercritical Pressure (original in Chinese). *Xi'an Jiaotong University, Vol. 39, No. 9.*, pp. 978-981.
- Yamagata, K., Nishikawa, K. & Hasegawa, S. (1972). Forced Convective Heat Transfer to Supercritical Water Flowing in Tubes. *International Journal of Heat and Mass Transfer, Vol. 15, No. 12.*, pp. 2575–2593.

- Yetisir, M., Diamond, W., Leung, L., Martin, D. & Duffey, R. (2011). Conceptual Mechanical Design for a Pressure-Tube Type Supercritical Water-Cooled Reactor. *The 5th International Symposium, SCWR (ISSCWR-5), Vancouver, B.C., Canada, March 13-16*. pp. 1-12.
- Yetisir, M., Gaudet, M., Pencer, J., McDonald, M., Rhodes, D., Hamilton, H. & Leung, L. (2016). Canadian Supercritical Water Cooled Reactor Core Concept and Safety Features. *Canadian Nuclear Laboratories (CNL) Nuclear Review, Vol. 5, No. 2*. pp. 189-202.
- Yetisir, M., Hamilton, H., Xu, R., Gaudet, M., Rhodes, D., King, M., . . . Benson, B. (2018). Fuel Assembly Concept of the Canadian Supercritical Water-Cooled Reactor. *Journal of Nuclear Engineering and Radiation Science, Vol. 4, 011010-1*. pp. 1-7.
- Yetisir, M., Pencer, J., McDonald, M., Gaudet, M., Licht, J. & Duffey, R. (2012, December). The Supersafe© Reactor: A Small Modular Pressure Tube SCWR. *AECL Nuclear Review, Vol 1, No. 2*. pp. 1-6.
- Yu, J., Jia, B., Wu, D. & Wang, D. (2009). Optimization of Heat Transfer Coefficient Correlation at Supercritical Pressure using Genetic Algorithms. *Heat Mass Transfer, Vol. 45, No. 6*, pp. 757-766.
- Zahlan, H., Groeneveld, D., Tavoularis, S., Mokry, S. & Piro, I. L. (2011). Assessment of Supercritical Heat Transfer Prediction Methods. *The 5th International Symposium, SCWR (ISSCWR-5), Vancouver, B.C., Canada, March 13-16*. pp. 1-20.
- Zhao, M., Gu, H. Y., Cheng, X., Li, H. B. & Yang, Q. R. (2015). Experimental and Numerical Study on Heat Transfer of Supercritical Water Flowing Upward in 2x2 Rod Bundles. *NURETH-16, Chicago, IL, Aug 30-Sep 4*. pp. 1-14.
- Zhu, Q. (2017). Innovative Power Generation Systems Using Supercritical CO₂ Cycles. *Clean Energy, Volume 1, Issue 1*. London, UK: Oxford University Press on behalf of National Institute of Clean-and-Low-Carbon Energy. pp. 68-79.

- Zhu, X. J., Bi, Q. C., Yang, D. & Chen, T. K. (2009). An Investigation on Heat Transfer Characteristics of Different Pressure Steam-Water in Vertical Upward Tube. *Nuclear Engineering and Design*, Vol. 239, No. 2. pp. 381-388.
- Žukauskas, A. (1972). Chapter 2: Heat Transfer from Tubes in Crossflow. *Advances in Heat Transfer*, Vol. 8, Edited by J.P. Hartnett and T.F. Irvine Jr. New York, USA: Academic Press. pp. 93-160.
- Zvorykin, A., Mahdi, M., Popov, R., Barati Far, K. & Pioro, I. L. (2018). Heat Transfer to Supercritical Water (Liquid-Like State) Flowing in a Short Vertical Bare Tube with Upward Flow. *Proceedings of the 2018 26th International Conference on Nuclear Engineering (ICONE26)*, July 22-26, London, England. pp. 1-12.

APPENDIX A: CODE USED

To complete the calculations listed in section 3, computer logic was developed. This logic allows a user to quickly develop new **Nu** correlations based upon a wide set of parameters, fully selectable by the user.

The computer code was developed for Microsoft Excel in VBA macro language. Excel was chosen over other software programs such as Matlab or C++ for three reasons:

- 1) The only limitation in selecting a language for development was the communication with the NIST REFPROP 10.0 software package. As REFPROP 10 is easily integrated with Excel and Matlab, these were the two languages that were considered.
- 2) The vast majority of the audience already has access to Excel on their computers and are familiar with how to operate Excel.
- 3) VBA macros are easily understood and the source code can be readily accessed if the user desires to implement changes.

The basic logic for calculating the predictions by the **Nu** correlations listed in section 3.3 is shown in Figure A-1. The code is configured to provide predictions for two types of data:

- 1) Raw inputs
 - When an experiment is performed and results such as the wall temperature, bulk temperature, heat flux, mass flux, pressure, and D_{hy} are all known
- 2) Parameter inputs
 - When only the heat flux, mass flux, pressure, inlet bulk temperature and D_{hy} , A_{fl} , p_h , and Heated Length are known, and the wall temperature is to be predicted

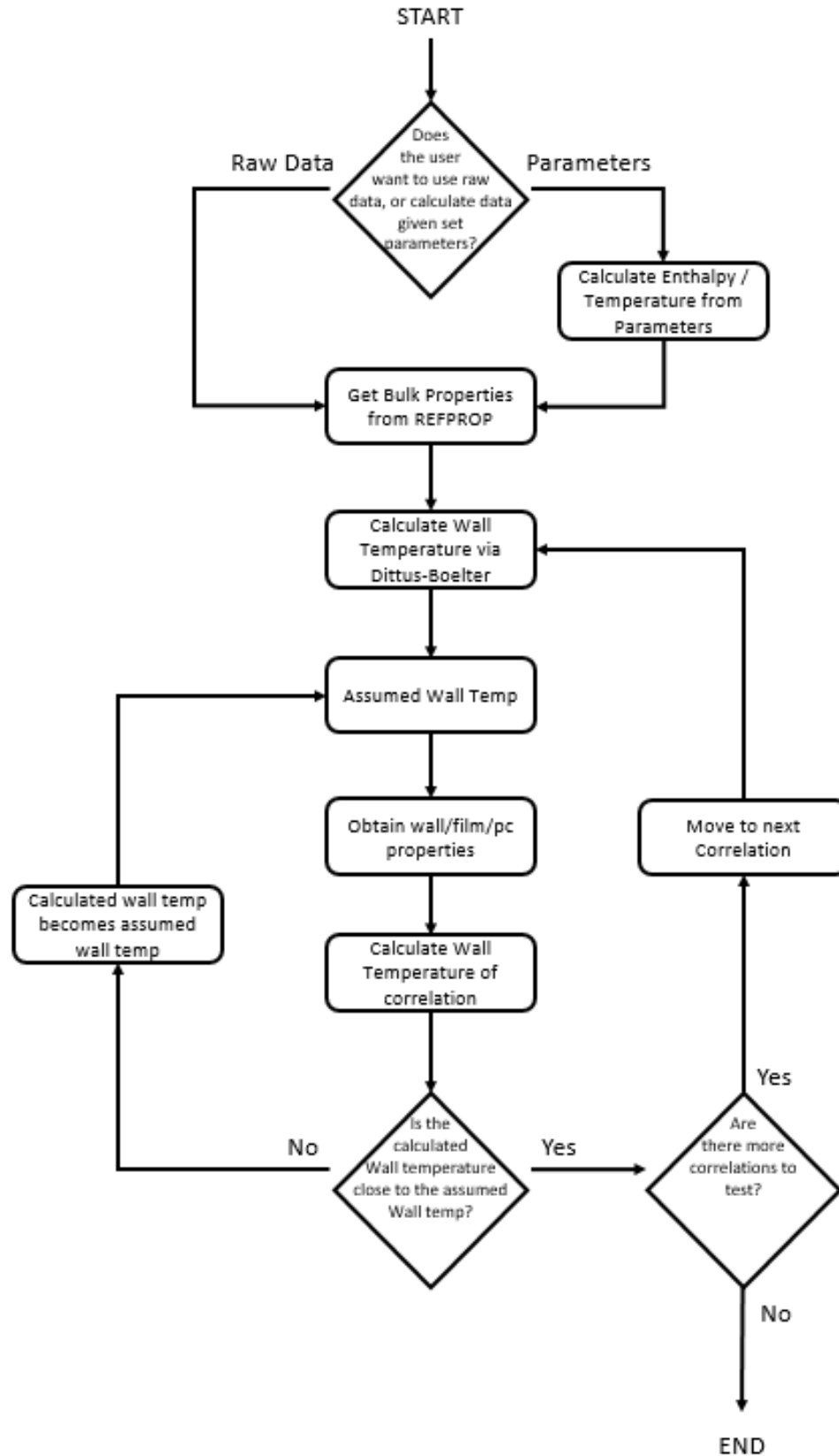


Figure A-1: Basic Algorithm for Program

A.1 CODE PARAMETERS

A.1.1 *Fluid Options*

The code was developed to allow for multi-fluid analysis and **Nu** correlation building. Therefore, there are 10 pre-set fluids built into the VBA macro:

- | | | | | |
|-------------|--------------------|---------------------|-----------|----------------------|
| 1) Air | 2) CO ₂ | 3) D ₂ O | 4) Helium | 5) Hydrogen |
| 6) Nitrogen | 7) Oxygen | 8) R-134A | 9) R-141B | 10) H ₂ O |

To change these, the ‘FluidOptions’ and ‘Fluids’ are required to be adjusted in the ‘ThesisMainCode’ module. The fluids must be compatible with the REFPROP fluids, and be the same naming convention.

A.1.2 *Additional Formulas*

If additional formulas are to be added, the ‘TotalFormulas’ parameter must be adjusted in the ‘ThesisMainCode’ module.

A.1.3 *Error Range*

When using the **Nu** correlations to calculate predictions, the loop continues until the calculated wall value is close to the assumed value. This is set to 0.01°C. To change this parameter, adjust the ‘MaxError’ parameter in the ‘ThesisMainCode’ module.

A.1.4 *Non-Convergences*

Some **Nu** correlations do not converge on one answer in a specific region (see Non-Convergent Wall Temperature).

Therefore, to avoid an endless loop, the amount of iterations has been capped at 60. To adjust the maximum iterations, the ‘MaxLoop’ parameter on the ‘ThesisMainCode’ module must be altered.

The VBA macro used is split into several modules, many submodules, and several user forms (Figure A-2). These can be accessed from the VBA menu in Excel. To see code for these modules, see section Code Body.

A.2 MODULES

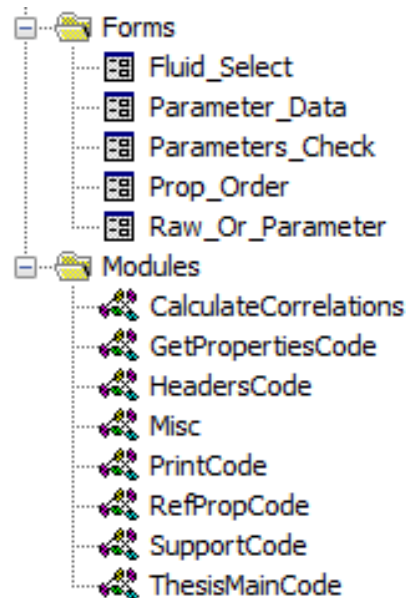


Figure A-2: VBA Macro Modules

A.3 CODE BODY

A.3.1 *ThesisMainCode Module*

```
1. 'Code written by Scott Clark, P.Eng. in aid of Masters Thesis
2. 'February 2nd, 2020
3.
4.
5. 'Setting up public variables
6. Public T() As Double, P() As Double, G() As Double, qavg() As Double, Dhy() As Double,
   xdist() As Double
7. Public Af1 As Double, ph As Double, Step As Double, Lh As Double
8. Public HTC() As Double, D() As Double, u() As Double, v() As Double, Cp() As Double,
   H() As Double, k() As Double, Pr() As Double
9. Public B() As Double, A() As Double, Re() As Double, Nu() As Double
10. Public Ta() As Double, Da() As Double, ua() As Double, va() As Double, Cpa() As Double,
   Ha() As Double, ka() As Double, Pra() As Double
11. Public Ba() As Double, Aa() As Double, Rea() As Double, Nu0() As Double, FrictF() As Double,
   Fc() As Double, FcUsed As Double
12. Public nfc() As Double, It() As Double, Errs() As Double, Din As Double, uin As Double,
   Davg() As Double, Gravg() As Double
13. Public Gamma() As Double, Grst() As Double, C1 As Integer, C2 As Integer, C3 As Integer,
   qdet() As Double, qNonD() As Double
14. Public Gr() As Double, Prw() As Double, FluidChosen As String, FormulaTitle() As String
15. Public TempChoice As String, Parameters() As Variant, RaworPar As String
16. Public HTCerrAvg() As Double, HTCerrAvgAbs() As Double, TwerrAvg() As Double, TwerrAvgAbs() As Double
17. Public ErrTotal() As Double, ErrTotalAbs() As Double, ErrSTD() As Double, PropertiesTitle() As Variant
```

```

18. Public VartoTest() As Integer, PropChosen As Integer, GlobalProperties() As Double, ExpCor() As Double, CorProperties() As Double
19. Public CorPropCorr() As Double, CorPropTitles() As String, CorCalc() As Integer
20. Public RMS() As Double, R2() As Double, Tg() As Double, Cpg() As Double
21. Public Kg() As Double, PHig() As Double, CpAVEg() As Double, Prg() As Double, Cpm
    ax1() As Double, Cpmx2() As Double, CpAVEg() As Double
22. Public Ap() As Double
23.
24.
25.
26.
27. '*****ADJUST AS NEEDED*****ADJUST AS NEEDED*****ADJUST AS NEE
    DED*****
28. 'Determines how many fluids are available to select from
29. Public Const FluidOptions As Integer = 10
30. 'Determines the fluids that are available. To input new fluids, ensure they're th
    e same type as the .FLD from refprop,
31. 'and add to Fluids string
32. Public Const Fluids As String = "Air,CO2,D2O,Helium,Hydrogen,Nitrogen,Oxygen,R134
    A,R141B,Water"
33. 'Determines how many total formulas will be tested. To add new formulas, see XXXX
    and adjust total number below
34. 'If new formulas are added, adjust here (TotalFormulas) and also on sub "Headers3
    " located in the "HeadersCode" module
35. 'If new formulas are added, add to sub "CalculateCorrelationsSub" located in the
    "CalculateCorrelations" module
36. Public Const TotalFormulas As Integer = 36
37. 'Determines the first column that will be used in the sheet
38. Public Const C0 As Integer = 1
39. 'Determines the first row that will be used in the sheet
40. Public Const R0 As Integer = 1
41. 'Determines first row that headers will be entered into for the Raw Data selectio
    n
42. Public Const R1RD As Integer = R0 + 6
43. 'Determines first row that headers will be entered into for the Parameters select
    ion
44. Public Const R1P As Integer = R0 + 17
45. 'Determines the length of the 1st header section if Raw Data is selected
46. Public Const L1RD As Integer = 11
47. 'Determines the length of the 1st header section if Parameters is selected
48. Public Const L1P As Integer = 7
49. 'Determines the length of the 2nd header section if Raw Data is selected
50. Public Const L2RD As Integer = 214
51. 'Determines the length of the 2nd header section if Parameters is selected (no se
    cond section required)
52. Public Const L2P As Integer = 16
53. 'Determines the length of the 3rd header section
54. Public Const L3 As Integer = TotalFormulas * 4
55. 'Determines amount of different styles in the headers (i.e. Header String / Lengt
    h of first part of string /
56. 'Length of second part of string/etc)
57. Public Const ms As Integer = 7
58. 'Determines the maximum amount of iterations (to avoid endless loops)
59. Public Const MaxLoop As Integer = 60
60. 'Determines the desired minimum error between predicted and calculated Tw values
    (loop continues until MaxError or MaxLoop reached)
61. Public Const MaxError As Double = 0.01
62. 'Determines the desired minimum error between values for the correlation builder
63. Public Const MaxErrorCor As Double = 0.0001
64. 'Multiple of MaxLoop for the Correlation Builder

```

```

65. Public Const MaxLoopMult As Integer = 30
66. '*****ADJUST AS NEEDED*****ADJUST AS NEEDED*****ADJUST AS NEE
    DED*****
67.
68.
69.
70.
71. Sub Heat_Transfer_Correlation_Program()
72.
73. 'Introducing the overall code timing variables
74. Dim CodeSequence As Integer, Time As Date
75.
76.
77. 'CodeSequence = 0 signifies that the code is just starting, and calls the CodeTim
    er sub
78. 'CodeSequence = 1 signifies that the code is ending
79. CodeSequence = 0
80. Call CodeTimer(Time, CodeSequence)
81.
82.
83.
84. 'Set up preliminary variables
85. Dim f As Integer, r As Integer, c As Integer, i As Integer, j As Integer, n As In
    teger, RowsR As Integer, L1 As Integer, L2 As Integer
86. Dim Selections As Integer
87. f = TotalFormulas
88.
89. ReDim FormulaTitle(1 To TotalFormulas), CorCalc(1 To TotalFormulas)
90.
91.
92. 'Row and Column that the Raw Data Headers should start on, Length of headers base
    d on parameters listed, and a
93. 'Adjust L in Headers1 sub for Nu variations as needed with change in L2 below.
94. 'Adjust f for number of formula's to test
95. Data_Template_Check
96. RaworPar = Cells(R0 + 1, C0)
97. If RaworPar = "Raw Data" Then: r = R1RD: L1 = L1RD: L2 = L2RD: ReDim PropertiesTi
    tle(1 To L2, 0 To 1) As Variant:
98. If RaworPar = "Parameters" Then: r = R1P: L1 = L1P: L2 = L2P:
99. C1 = C0 + L1: C2 = C1 + L2: C3 = C2 + L3:
100.
101.
102.
103. 'Sets the overall number of 'steps'. If the data is raw, this will count the
    rows of data pasted into the Data Template tab
104. 'and that becomes the overall number of steps (*Important not to have gaps in
    the first column!*).
105. 'If the data is parameter driven, then the Heated Length divided by the Steps
    , rounded up to the nearest '1' will become the
106. 'overall number of steps.
107. 'Number of steps also drives the size of the arrays.
108. If RaworPar = "Raw Data" Then
109.     If Cells(r + 2, C0) = "" Then: MsgBox "No data has been pasted! Paste Dat
        a!", vbOKOnly + vbExclamation, "No Data!": End:
110.     RowsR = Range(Cells(r + 2, C0), Cells(r + 2, C0).End(xlDown)).Rows.Count
111. ElseIf RaworPar = "Parameters" Then
112.     If Len(Cells(R0 + 3, C0 + 2)) > 0 And Len(Cells(R0 + 4, C0 + 2)) > 0 Then
113.         MsgBox "Must have Temperature In OR Temperature Out blank!", vbCriti
            cal, "Temperature Error"

```

```

114.         End
115.         ElseIf Len(Cells(R0 + 3, C0 + 2)) = 0 And Len(Cells(R0 + 4, C0 + 2)) = 0
116.         Then
117.             MsgBox "Parameters Missing!" & vbCrLf & "Add Temperature In OR Temperature Out!", vbCritical
118.             End
119.             ElseIf IsNumeric(Cells(R0 + 3, C0 + 2)) = False Or IsNumeric(Cells(R0 + 4, C0 + 2)) = False Then
120.             MsgBox "Temperature In OR Temperature Out must be filled out, while the other parameter remains blank." & vbCrLf & "Temperature input must be a real number.", vbCritical
121.             End
122.             ElseIf Cells(R0 + 12, C0 + 2) > Cells(R0 + 11, C0 + 2) Then
123.             MsgBox "Step cannot be larger than the Heated Length!" & vbCrLf & "Please adjust the Step/Length values.", vbOKOnly + vbCritical, "Error in Data"
124.             End If
125.         For j = 1 To 8
126.             If Len(Cells(R0 + j + 4, C0 + 2).Value) = 0 Or Cells(R0 + j + 4, C0 + 2).Value = 0 Then
127.                 MsgBox "Parameters Missing or Are ZERO!" & vbCrLf & vbCrLf & "Add or Adjust the parameter " & Cells(R0 + j + 4, C0 + 1).Value & " ", vbCritical
128.             End
129.             End If
130.         Next j
131.         Lh = Cells(R0 + 11, C0 + 2).Value
132.         Step = Cells(R0 + 12, C0 + 2).Value
133.         RowsR = Application.WorksheetFunction.RoundUp(Lh / Step, 0) + 1
134.     End If
135.     FluidChosen = ActiveSheet.Shapes("Fluid_Select").ControlFormat.List(ActiveSheet.Shapes("Fluid_Select").ControlFormat.ListIndex)
136.
137.     'Clears sheets if info already inputted
138.     If Cells(R0, C0 + L1) = C0 + L1 Then
139.         Selections = MsgBox("Do you wish to overwrite this data with a new simulation?", vbInformation + vbYesNo, "New Simulation")
140.         If Selections = 7 Then
141.             End
142.         Else
143.             'Clears all cells previously filled by code (doesn't erase user inputted data)
144.             If RaworPar = "Raw Data" Then
145.                 Cells(r + 2, C1).Select: Range(Selection, Selection.End(xlDown)).Select: Range(Selection, Selection.End(xlToRight)).Select:
146.                 Selection.Clear
147.             ElseIf RaworPar = "Parameters" Then
148.                 Rows(r + 2).Select: Range(Selection, Selection.End(xlDown)).Select: Selection.Clear
149.             End If
150.         End If
151.     End If
152.
153.     Call Headers2(r, L2, L1)
154.     Call Headers3(r, L3, L2)
155.     Call FormulaTitlesPrint(r, C2)
156.
157.     '+++++
158.     '=====

```



```

159. '+++++
+++++
160.
161. '[][][][][][][][][][][][][][][][][][][][][][][][][][]
[][][][][]
162. '[][][][][][][][][][][][][][][][][][][][][][][][][]
[][][][][]
163. 'Sets up the general variables
164. Dim CurForm As Integer, CurProp As Integer, CurPropGet As Integer
165. ReDim P(1 To RowsR) As Double, G(1 To RowsR) As Double, qavg(1 To RowsR) As Double, Dhy(1 To RowsR) As Double, HTC(1 To RowsR, 0 To f) As Double
166. ReDim xdist(1 To RowsR) As Double
167.
168.
169. 'The second variable in the properties array represents where the property is
taken from, and is as follows:
170. '1 = Bulk
171. '2 = Wall
172. '3 = Film
173. '4 = PsuedoCritical
174. '5 = Avg
175. ReDim T(1 To RowsR, 1 To 4, 0 To f) As Double, D(1 To RowsR, 1 To 4, 0 To f)
As Double, u(1 To RowsR, 1 To 4, 0 To f) As Double
176. ReDim v(1 To RowsR, 1 To 4, 0 To f) As Double, H(1 To RowsR, 1 To 4, 0 To f)
As Double, k(1 To RowsR, 1 To 4, 0 To f) As Double
177. ReDim B(1 To RowsR, 1 To 4, 0 To f) As Double, A(1 To RowsR, 1 To 4, 0 To f)
As Double, Re(1 To RowsR, 1 To 4, 0 To f) As Double
178. ReDim Nu(1 To RowsR, 1 To 4, 0 To f) As Double
179. ReDim Cp(1 To RowsR, 1 To 5, 0 To f) As Double, Pr(1 To RowsR, 1 To 5, 0 To f
) As Double
180. 'For Griem
181. ReDim Cpg(1 To RowsR, 1 To 5, 0 To f) As Double, Tg(1 To RowsR, 1 To 5, 0 To
f) As Double
182. ReDim Kg(1 To RowsR) As Double, PHIg(1 To RowsR) As Double, CpAVEg(1 To RowsR
) As Double, Prg(1 To RowsR) As Double
183. ReDim Cpmx1(1 To RowsR) As Double, Cpmx2(1 To RowsR) As Double, CpAVEgt(1 T
o RowsR) As Double
184.
185.
186. 'The second variable in the ratio of properties is the number of properties e
xamined
187. ReDim Ta(1 To RowsR, 1 To 12, 0 To f) As Double, Da(1 To RowsR, 1 To 12, 0 To
f) As Double, ua(1 To RowsR, 1 To 12, 0 To f) As Double
188. ReDim va(1 To RowsR, 1 To 12, 0 To f) As Double, Ha(1 To RowsR, 1 To 12, 0 To
f) As Double, ka(1 To RowsR, 1 To 12, 0 To f) As Double
189. ReDim Ba(1 To RowsR, 1 To 12, 0 To f) As Double, Aa(1 To RowsR, 1 To 12, 0 To
f) As Double, Rea(1 To RowsR, 1 To 12, 0 To f) As Double
190. ReDim Cpa(1 To RowsR, 1 To 20, 0 To f) As Double, Pra(1 To RowsR, 1 To 20, 0
To f) As Double, Ap(1 To RowsR, 1 To 20, 0 To f) As Double
191.
192. 'Other variables for completion of the correlation equations
193. ReDim It(1 To RowsR, 0 To f) As Double, Errs(1 To RowsR, 0 To f) As Double, N
u0(1 To RowsR, 0 To f) As Double, FrictF(1 To RowsR) As Double
194. ReDim Fc(1 To RowsR, 0 To f, 1 To 6) As Double, nfc(1 To RowsR, 1 To 2) As Do
uble, Grst(1 To RowsR) As Double
195. ReDim Davg(1 To RowsR, 0 To f) As Double, Gravg(1 To RowsR, 0 To f) As Double
, Gamma(1 To RowsR, 0 To f) As Double
196. ReDim qdet(1 To RowsR, 1 To 1) As Double, qNonD(1 To RowsR) As Double, Gr(1 T
o RowsR, 0 To f) As Double, Prw(1 To RowsR, 0 To f) As Double
197. ReDim HTCErrAvg(1 To RowsR, 1 To f) As Double, HTCErrAvgAbs(1 To RowsR, 1 To
f) As Double

```

```

198. ReDim TwErrAvg(1 To RowsR, 1 To f) As Double, TwErrAvgAbs(1 To RowsR, 1 To f)
    As Double
199. ReDim ErrTotal(1 To f, 1 To 2) As Double, ErrTotalAbs(1 To f, 1 To 2) As Double,
    ErrSTD(1 To f, 1 To 2) As Double
200. ReDim GlobalProperties(1 To RowsR, 1 To L2RD)
201.
202.
203. For i = 1 To RowsR
204.
205.     If RaworPar = "Raw Data" Then
206.         xdist(i) = Cells(r + i + 1, C0 + 2).Value 'm
207.         P(i) = Cells(r + i + 1, C0 + 3).Value 'MPa
208.         G(i) = Cells(r + i + 1, C0 + 4).Value 'kg/m2·s
209.         qavg(i) = Cells(r + i + 1, C0 + 5).Value * 1000 'W/m2
210.         Dhy(i) = Cells(r + i + 1, C0 + 6).Value / 1000 'm
211.         T(i, 1, 0) = Cells(r + i + 1, C0 + 7).Value '°C
212.         T(i, 2, 0) = Cells(r + i + 1, C0 + 8).Value '°C
213.         HTC(i, 0) = Cells(r + i + 1, C0 + 9).Value * 1000 'W/m2·K
214.         CurForm = 0: Call GetAllProperties(i, CurForm)
215.     ElseIf RaworPar = "Parameters" Then
216.         P(i) = Cells(R0 + 5, C0 + 2).Value 'MPa
217.         G(i) = Cells(R0 + 6, C0 + 2).Value 'kg/m2·s
218.         qavg(i) = Cells(R0 + 7, C0 + 2).Value * 1000 'W/m2
219.         Dhy(i) = Cells(R0 + 8, C0 + 2).Value / 1000 'm
220.         Afl = Cells(R0 + 9, C0 + 2).Value / 1000 ^ 2 'm2
221.         ph = Cells(R0 + 10, C0 + 2).Value / 1000 'm
222.         Lh = Cells(R0 + 11, C0 + 2).Value 'm
223.         Step = Cells(R0 + 12, C0 + 2).Value 'm
224.         If Cells(R0 + 3, C0 + 2) > 0 Then
225.             If i = 1 Then: T(i, 1, 0) = Cells(R0 + 3, C0 + 2): xdist(i) = 0:
                CurPropGet = 0:
226.             If i <> 1 Then: H(i, 1, 0) = H(i - 1, 1, 0) + (qavg(i) * Step * p
                h / (Afl * G(i))): xdist(i) = Round(Step + xdist(i - 1), 4): _
227.             CurPropGet = 1:
228.             ElseIf Cells(R0 + 4, C0 + 2) > 0 Then
229.                 If i = 1 Then: T(i, 1, 0) = Cells(R0 + 4, C0 + 2): xdist(i) = Lh:
                CurPropGet = 0
230.                 If i <> 1 Then: H(i, 1, 0) = H(i - 1, 1, 0) - (qavg(i) * Step * p
                h / (Afl * G(i))): xdist(i) = Round(xdist(i - 1) - Step, 4): _
231.                 CurPropGet = 1:
232.             End If
233.             CurForm = 0: CurProp = 1: Call GetProperties(i, CurForm, CurProp, Cur
                PropGet)
234.
235.         End If
236.
237.         Call CalculateCorrelationsSub(i)
238.
239.     Next i
240.
241.     Call PrintProperties(RowsR, r): Call PrintCorrelations(RowsR, r):
242.     If RaworPar = "Raw Data" Then: Call ErrorCalculations(RowsR): Call PrintError
        s(r):
243.
244.     '+++++
        +++++
245.     '=====
        =====
246.     '+++++
        +++++
247.     'This signifies that the code is ending, and calls the CodeTimer sub

```

```

248. CodeSequence = 1
249. Call CodeTimer(Time, CodeSequence)
250.
251.
252. 'Displays the Run Time
253. Cells(R0 + 1, C0 + 1) = "Run Time"
254. Cells(R0 + 1, C0 + 2) = Format(Time, "hh:mm:ss")
255. Cells(R0 + 1, C0 + 3) = "hh:mm:ss"
256. Range(Cells(R0 + 1, C0 + 1), Cells(R0 + 1, C0 + 3)).Select
257. With Selection: .HorizontalAlignment = xlCentreAcrossSelection: .VerticalAlign
    nment = xlCentre: End With
258. With Selection.Font: .FontStyle = "Bold": .Size = 9: End With
259. With Selection.Borders(xlEdgeLeft): .LineStyle = xlContinuous: .Weight = xlMe
    dium: End With
260. With Selection.Borders(xlEdgeRight): .LineStyle = xlContinuous: .Weight = xlM
    edium: End With
261. With Selection.Borders(xlEdgeTop): .LineStyle = xlContinuous: .Weight = xlMed
    ium: End With
262. With Selection.Borders(xlEdgeBottom): .LineStyle = xlContinuous: .Weight = xl
    Medium: End With
263. With Selection.Interior: .Pattern = xlSolid: .PatternColorIndex = xlAutomatic
    : .Color = 16775408: .TintAndShade = 0: .PatternTintAndShade = 0: End With
264.
265. If RaworPar = "Raw Data" Then
266.     InputFormulaTitles
267.     DisplayErrors
268.
269.     Selections = 6
270.     Do While Selections = 6
271.         Selections = MsgBox("Do you wish to test a new correlation combinatio
    n?", vbInformation + vbYesNo, "New Correlation Attempt?")
272.         If Selections = 6 Then
273.             Call ChoosePropertiesForNewCorrelation(RowsR):
274.         Else
275.             MsgBox "To test a correlation, re-
    run simulation and select Yes", vbOKOnly, "Re-Run to obtain correlation"
276.         End If
277.     Loop
278. End If
279.
280. End Sub

```

A.3.2 *SupportCode Module*

```

1. Sub CodeTimer(Time As Date, i As Integer)
2. 'This Sub is designed to calculate the total time taken to run the code. In addit
    ion, it hides screen updating to allow for faster processing
3. If i = 0 Then
4.     'Set the Time variable to the current time
5.     Time = Now()
6.     'Speed up code by hiding updates
7.     Application.Calculation = xlCalculationManual
8.     Application.ScreenUpdating = False
9.     Application.DisplayStatusBar = False
10.    Application.EnableEvents = False
11.
12. ElseIf i = 1 Then
13.     'Unhide updates

```

```

14. Application.Calculation = xlCalculationAutomatic
15. Application.ScreenUpdating = True
16. Application.DisplayStatusBar = True
17. Application.EnableEvents = True
18. Time = Now() - Time
19. End If
20.
21. End Sub
22.
23.
24. Sub TempPc(Pressure As Double, Temperature As Double)
25.
26. Dim DENS As Double, SPHT As Double, VISC As Double, THCD As Double, ENTH As Double,
    KVIS As Double, PRANDTL As Double, THXP As Double, THDF As Double
27. Dim ttemp As Double, i As Integer, Cptemp As Double, DoneFor As Integer, DoneBack
    As Integer, Inter As Double
28. 'Calculate Psuedocritical temperature for the specified pressure
29.
30. 'Gives the initial guess a closer value depending on the pressure (saves time in
    processing)
31. If Pressure >= 40 Then
32.     Temperature = 430.34
33. ElseIf Pressure >= 35 Then
34.     Temperature = 416.69
35. ElseIf Pressure >= 30 Then
36.     Temperature = 401.91
37. ElseIf Pressure >= 25 Then
38.     Temperature = 384.89
39. ElseIf Pressure >= 22.064 Then
40.     Temperature = 373.94
41. ElseIf Pressure >= 20 Then
42.     Temperature = 365.75
43. ElseIf Pressure >= 15 Then
44.     Temperature = 342.16
45. ElseIf Pressure >= 10 Then
46.     Temperature = 311
47. ElseIf Pressure >= 5 Then
48.     Temperature = 263.94
49. ElseIf Pressure >= 1 Then
50.     Temperature = 179.88
51. Else
52.     Temperature = 100
53. End If
54.
55. 'Sets up initial conditions
56. DoneFor = 0
57. DoneBack = 0
58. Inter = 50
59.
60. 'Calls the variables, specifically looking at Specific Heat. This moves forward s
    tepwise until the Cp is less than the previous one
61. Do
62.     Call REFPROPCALL(Pressure, Temperature, DENS, VISC, KVIS, SPHT, ENTH, THCD, P
        RANDTL, THXP, THDF)
63.     Cptemp = SPHT
64.     ttemp = Temperature + Inter
65.     Call REFPROPCALL(Pressure, ttemp, DENS, VISC, KVIS, SPHT, ENTH, THCD, PRANDTL
        , THXP, THDF)
66.     If Cptemp < SPHT Then
67.         Temperature = ttemp
68.     ElseIf Cptemp > SPHT And Inter = 50 Then

```

```

69.         Inter = 10
70.     ElseIf Cptemp > SPHT And Inter = 10 Then
71.         Inter = 5
72.     ElseIf Cptemp > SPHT And Inter = 5 Then
73.         Inter = 1
74.     ElseIf Cptemp > SPHT And Inter = 1 Then
75.         Inter = 0.5
76.     ElseIf Cptemp > SPHT And Inter = 0.5 Then
77.         Inter = 0.1
78.     ElseIf Cptemp > SPHT And Inter = 0.1 Then
79.         Inter = 0.01
80.     ElseIf Cptemp > SPHT And Inter = 0.01 Then
81.         DoneFor = 1
82.     End If
83. Loop While DoneFor = 0
84.
85. 'Sets the spacing at the minimum of 0.01°C apart
86. Inter = 0.01
87.
88. 'Goes backward to ensure that the forward code didn't miss the peak
89. Do
90.     Call REFPROPCALL(Pressure, Temperature, DENS, VISC, KVIS, SPHT, ENTH, THCD, P
        RANDTL, THXP, THDF)
91.     Cptemp = SPHT
92.     ttemp = Temperature - Inter
93.     Call REFPROPCALL(Pressure, ttemp, DENS, VISC, KVIS, SPHT, ENTH, THCD, PRANDTL
        , THXP, THDF)
94.     If Cptemp < SPHT Then
95.         Temperature = ttemp
96.     ElseIf Cptemp > SPHT Then
97.         DoneBack = 1
98.     End If
99. Loop While DoneBack = 0
100.
101. End Sub
102.
103.
104. Sub Data_Template_Check()
105.     'This sub is to determine if the 'Data Template' page has been created. If no
        t, it will create the
106.     'Data Template' worksheet, inform the user, and exit out of the code. If the
        'Data Template' page
107.     'has been created, this will ask the user to verify that the to allow the use
        r
108.
109.     'This section will introduce variables
110.     Dim Template As Integer, i As Integer, j As Integer, Selections As Integer, r
        As Integer, L As Integer
111.
112.     'This code starts with a looking for the 'Data Template' page for pasting all
        data into. This will search through
113.     'the workbook and determine if the 'Data Template' page has been created. If
        not, it will create the page and then
114.     'exit the code.
115.     i = Application.Sheets.Count
116.     For j = 1 To i
117.         If ActiveWorkbook.Sheets(j).Name = "Data Template" Then
118.             If ThisWorkbook.Sheets("Data Template").Cells(R0 + 1, C0) = "Raw Data
                " Then
119.                 ThisWorkbook.Sheets("Data Template").Activate

```

```

120.         Selections = MsgBox("Has the data been copied into the 'Data Temp
121. late' tab?" & vbCrLf & vbCrLf & _
122. "Data should be in ascending order according to heated length" &
123. vbCrLf & vbCrLf & "(i.e. x = 0 to x = L, not x = L to x = 0)", _
124. vbYesNo, "Data Template Check")
125.         If Selections = 7 Then
126.             End
127.         ElseIf Selections = 6 Then
128.             Exit Sub
129.         End If
130.         ElseIf ThisWorkbook.Sheets("Data Template").Cells(R0 + 1, C0) = "Para
131. meters" Then
132.             Selections = MsgBox("Are the Parameters in the Correct Units?", v
133. bYesNo, "Parameters Check")
134.             If Selections = 7 Then
135.                 MsgBox "Correct the Parameters!", vbExclamation
136.             End
137.             ElseIf Selections = 6 Then
138.                 Exit Sub
139.             End If
140.         End If
141.     Else
142.         If j = i Then
143.             Selections = MsgBox("First the 'Data Template' tab must be create
144. d, and then values must be pasted into the template." & vbCrLf & "Do you wish to
145. create the 'Data Template' tab now?", vbInformation + vbYesNo)
146.             If Selections = 6 Then
147.                 Sheets.Add.Name = "Data Template"
148.                 Raw_Or_Parameter.Show
149.                 If (RaworPar = "Raw Data") Then: r = R1RD: L = L1RD: Fluid_Se
150. lect.Show
151.                 If (RaworPar = "Parameters") Then: r = R1P: L = L1P: Paramete
152. r_Data.Show
153.                 Call ParametersPrint(r)
154.                 Cells(R0 + 1, C0) = RaworPar
155.                 Cells(R0 + 1, C0).Select
156.                 With Selection: .HorizontalAlignment = xlCentre: .VerticalAli
157. gnment = xlCentre: End With
158.                 With Selection.Font: .Name = "Calibri": .FontStyle = "Italic"
159. : .Size = 9: End With
160.                 Call Headers1(r, L)
161.                 AddButtons
162.             End
163.             ElseIf Selections = 7 Then
164.                 End
165.             End If
166.         End If
167.     End If
168. Next j
169.
170. End Sub
171.
172. Sub AddButtons()
173. 'This adds buttons for the user to run code from the Data Template screen
174. Dim btn As Button
175. ActiveSheet.Buttons.Delete
176. Dim T As Range
177. i = R0 + 1
178. 'For i = 2 To 6 Step 2
179. Set T = ActiveSheet.Range(Cells(i, C0 + 5), Cells(i + 1, C0 + 6))

```

```

171.     Set btn = ActiveSheet.Buttons.Add(T.Left, T.Top, T.Width, T.Height)
172.     With btn
173.         .OnAction = "Heat_Transfer_Correlation_Program"
174.         .Caption = "Run Code"
175.         .Name = "Run"
176.     End With
177. 'Next i
178. End Sub
179.
180. Sub showupdates()
181. Application.Calculation = xlCalculationAutomatic
182. Application.ScreenUpdating = True
183. Application.DisplayStatusBar = True
184. Application.EnableEvents = True
185. End Sub
186.
187.
188. Sub ErrorCalculations(TSteps As Integer)
189. 'Used for determining Average Error, Average Absolute Error, and Standard Error
    or for each of HTC and Tw
190.
191. Dim i As Integer, j As Integer, HTCeminE() As Double, TweminE() As Double
192. ReDim HTCeminE(1 To TSteps, 1 To TotalFormulas) As Double, TweminE(1 To TSteps
    s, 1 To TotalFormulas) As Double
193. ReDim RMS(1 To TotalFormulas, 1 To 2) As Double
194.
195. For i = 1 To TotalFormulas
196.     With Application.WorksheetFunction
197.         ErrTotal(i, 1) = .Sum(.Index(HTCErrAvg(), 0, i)) / TSteps: ErrTotalAbs
    s(i, 1) = .Sum(.Index(HTCErrAvgAbs(), 0, i)) / TSteps:
198.         ErrTotal(i, 2) = .Sum(.Index(TwErrAvg(), 0, i)) / TSteps: ErrTotalAbs
    (i, 2) = .Sum(.Index(TwErrAvgAbs(), 0, i)) / TSteps:
199.     End With
200.     For j = 1 To TSteps
201.         HTCeminE(j, i) = (HTCErrAvg(j, i) - ErrTotal(i, 1)) ^ 2
202.         TweminE(j, i) = (TwErrAvg(j, i) - ErrTotal(i, 2)) ^ 2
203.     Next j
204.     With Application.WorksheetFunction
205.         ErrSTD(i, 1) = (.Sum(.Index(HTCEminE(), 0, i)) / (TSteps - 1)) ^ 0.5:
206.         ErrSTD(i, 2) = (.Sum(.Index(TweminE(), 0, i)) / (TSteps - 1)) ^ 0.5:
207.         RMS(i, 1) = (.SumProduct(.Index(HTCErrAvg(), 0, i), .Index(HTCErrAvg(
    ), 0, i)) / TSteps) ^ 0.5
208.         RMS(i, 2) = (.SumProduct(.Index(TwErrAvg(), 0, i), .Index(TwErrAvg(),
    0, i)) / TSteps) ^ 0.5
209.     End With
210. Next i
211.
212. End Sub
213.
214. Sub ChoosePropertiesForNewCorrelation(RowsR As Integer)
215. Dim i As Integer, j As Integer
216. If RaworPar = "Raw Data" Then
217.     Parameters_Check.Show
218.     PropChosen = 0
219.     For i = 1 To L2RD - 10
220.         If PropertiesTitle(i + 10, 1) = 1 Then: PropChosen = PropChosen + 1:
221.     Next i

```

```

222.     ReDim VartoTest(1 To PropChosen + 1, 1 To 2) As Integer, ExpCor(1 To Prop
    Chosen + 1, 1 To 2) As Double
223.     ReDim CorProperties(1 To RowsR, 1 To PropChosen + 1) As Double, CorPropCo
    rr(1 To RowsR, 1 To PropChosen + 1) _
224.     As Double, CorPropTitles(1 To PropChosen)
225.     j = 1: VartoTest(j, 1) = 53: VartoTest(j, 2) = 1:
226.     For i = 1 To L2RD - 10
227.         If PropertiesTitle(i + 10, 1) = 1 Then: j = j + 1: VartoTest(j, 1) =
    i + 10: VartoTest(j, 2) = j:
228.     Next i
229.     Prop_Order.Show
230. End If
231.
232. Call CalculateExponents(RowsR)
233.
234.
235.
236. End Sub
237.
238. Sub CalculateExponents(RowsR As Integer)
239.
240. Dim i As Integer, j As Integer, Cond As Integer, ExpNum As Integer, Msgboxtes
    t As String, ExpErr() As Double
241. Dim CorDone As Integer, OK As Integer
242. ReDim ExpErr(1 To PropChosen) As Double, R2(1 To PropChosen + 1) As Double
243.
244. 'Start Conditions
245. ExpCor(1, 1) = 1: ExpCor(2, 1) = 1:
246. For i = 2 To PropChosen: ExpCor(i + 1, 1) = 0: Next i:
247. For i = 1 To RowsR
248.     For j = 1 To PropChosen + 1
249.         CorProperties(i, j) = GlobalProperties(i, VartoTest(j, 1))
250.         CorPropCorr(i, j) = CorProperties(i, j) ^ ExpCor(j, 1)
251.     Next j
252. Next i
253. For i = 1 To PropChosen: ExpErr(i) = 1: Next i:
254.
255. j = 0: OK = 1:
256. Do While OK = 1
257.     OK = 0: j = j + 1:
258.     For i = 1 To Sheets.Count
259.         If Sheets(i).Name = "Test " & j Then: OK = 1: Exit For:
260.     Next i
261. Loop
262.
263. Sheets.Add.Name = "Test " & j
264. Sheets("Test " & j).Activate
265.
266. CorDone = 0: j = 0:
267.
268. Do While CorDone = 0 And j < MaxLoop * MaxLoopMult
269.     j = j + 1
270.     For i = 1 To PropChosen:
271.         ' If ExpErr(i) <> 0 Then
272.         ExpNum = i: Call CalculateReg(RowsR, ExpNum):
273.         If j = 1 Then
274.             If ExpNum + 1 <= PropChosen Then: ExpCor(ExpNum + 2, 1) = 1:
275.
276.         End If
        ExpErr(i) = Abs(ExpCor(ExpNum + 1, 1) - ExpCor(ExpNum + 1, 2))

```



```

277.         If ExpErr(i) > MaxErrorCor Then: ExpCor(ExpNum + 1, 2) = ExpCor(E
xpNum + 1, 1):
278.         If ExpErr(i) <= MaxErrorCor Then: ExpErr(i) = 0
279.         Call RecalculateTable(RowsR)
280.     '     End If
281.     Next i
282.
283.     Call CalculateConst(RowsR)
284.
285.     For i = 1 To PropChosen + 1:
286.         If j = 1 Then
287.             If i = 1 Then
288.                 Cells(j, i) = "Trial #": Cells(j, i + 1) = "Constant": Cells(
j, i + 2 + 2 * PropChosen) = "R2 - Constant":
289.             Else
290.                 Cells(j, i + 1) = CorPropTitles(i - 1): Cells(j, i + 1 + Prop
Chosen) = "R2 - " & CorPropTitles(i - 1):
291.             End If
292.         End If
293.         Cells(j + 1, i + 1) = ExpCor(i, 1)
294.         Cells(j + 1, i + 1).NumberFormat = "0.0000"
295.         Cells(j + 1, i + 2 + PropChosen) = Format(R2(i), "0.000%")
296.         Cells(j + 1, 1) = j
297.     Next i
298.
299.     If Application.WorksheetFunction.Sum(ExpErr) = 0 Then: CorDone = 1:
300. Loop
301.
302. End Sub
303.
304. Sub RecalculateTable(RowsR As Integer)
305. Dim i As Integer, j As Integer
306. For i = 1 To RowsR
307.     For j = 2 To PropChosen + 1
308.         CorPropCorr(i, j) = CorProperties(i, j) ^ ExpCor(j, 1)
309.     Next j
310. Next i
311. End Sub
312.
313. Sub CalculateReg(RowsR As Integer, ExpNum As Integer)
314.
315. Dim i As Integer, j As Integer, Numer As Double, Denom As Double, Test() As D
ouble
316. Dim SumX As Double, SumY As Double, SumXY As Double, SumX2 As Double, xbar As
Double, ybar As Double
317. Dim xlog() As Double, ylog() As Double
318. Dim x() As Double, y() As Double, xy() As Double, x2() As Double, xsuby() As
Double, ym() As Double, xavg() As Double, yavg() As Double
319. ReDim x(1 To RowsR) As Double, y(1 To RowsR) As Double, x2(1 To RowsR) As Dou
ble, xy(1 To RowsR) As Double, xavg(1 To RowsR) As Double
320. ReDim yavg(1 To RowsR) As Double, Test(1 To 3) As Double
321. ReDim xsuby(1 To RowsR) As Double
322. ReDim xlog(1 To RowsR) As Double, ylog(1 To RowsR) As Double
323.
324.
325.
326. For i = 1 To RowsR
327.     xsuby(i) = 1
328.     For j = 1 To PropChosen
329.         If j <> ExpNum Then: xsuby(i) = xsuby(i) * CorPropCorr(i, j + 1):
330.     Next j

```

```

331.     x(i) = CorProperties(i, ExpNum + 1)
332.     y(i) = CorPropCorr(i, 1) / xsuby(i)
333.     xlog(i) = Log(x(i)) / Log(10)
334.     ylog(i) = Log(y(i)) / Log(10)
335.     xy(i) = xlog(i) * ylog(i)
336.     x2(i) = xlog(i) * xlog(i)
337. Next i
338.
339. With Application.WorksheetFunction
340.     SumX = .Sum(xlog): SumY = .Sum(ylog): SumXY = .Sum(xy): SumX2 = .Sum(x2):
341.     xbar = .Average(xlog): ybar = .Average(ylog):
342. End With
343.
344. For i = 1 To RowsR
345.     xavg(i) = xlog(i) - xbar: yavg(i) = ylog(i) - ybar:
346. Next i
347.
348. With Application.WorksheetFunction
349.     Test(1) = .SumProduct(xavg, yavg)
350.     Test(2) = .SumProduct(xavg, xavg)
351.     Test(3) = .SumProduct(yavg, yavg)
352.     R2(ExpNum) = ((Test(1) / (Test(2) * Test(3)) ^ 0.5) ^ 2)
353. End With
354.
355.
356. Numer = (RowsR * SumXY) - (SumX * SumY)
357. Denom = (RowsR * SumX2) - ((SumX) ^ 2)
358. ExpCor(ExpNum + 1, 1) = Numer / Denom:
359.
360.
361.
362.
363.
364.
365.
366. 'For i = 1 To RowsR
367. '     xsuby(i) = 1
368. '     For j = 1 To PropChosen
369. '         If j <> ExpNum Then: xsuby(i) = xsuby(i) * CorPropCorr(i, j + 1):
370. '     Next j
371. '     x(i) = CorProperties(i, ExpNum + 1)
372. '     y(i) = CorPropCorr(i, 1) / xsuby(i)
373. '     xy(i) = x(i) * y(i)
374. '     x2(i) = x(i) * x(i)
375. 'Next i
376. '
377. 'With Application.WorksheetFunction
378. '     SumX = .Sum(x): SumY = .Sum(y): SumXY = .Sum(xy): SumX2 = .Sum(x2):
379. '     xbar = .Average(x): ybar = .Average(y):
380. 'End With
381. '
382. 'For i = 1 To RowsR
383. '     xavg(i) = x(i) - xbar: yavg(i) = y(i) - ybar:
384. 'Next i
385. '
386. 'With Application.WorksheetFunction
387. '     Test(1) = .SumProduct(xavg, yavg)
388. '     Test(2) = .SumProduct(xavg, xavg)
389. '     Test(3) = .SumProduct(yavg, yavg)
390. '     R2(ExpNum) = ((Test(1) / (Test(2) * Test(3)) ^ 0.5) ^ 2)

```

```

391. 'End With
392. '
393. '
394. 'Numer = (RowsR * SumXY) - (SumX * SumY):
395. 'If (Numer < -1) Or (Numer > 0 And Numer < 1) Then: Numer = -
1 * Log(Abs(Numer)) / Log(10): Else: Numer = Log(Abs(Numer)) / Log(10)
396. '
397. 'Denom = (RowsR * SumX2) - ((SumX) ^ 2):
398. 'If (Denom < -1) Or (Denom > 0 And Denom < 1) Then: Denom = -
1 * Log(Abs(Denom)) / Log(10): Else: Denom = Log(Abs(Denom)) / Log(10)
399. '
400. 'ExpCor(ExpNum + 1, 1) = Numer / Denom
401.
402. 'If (Numer > -1 And Denom > -1) Or (Numer < -1 And Denom < -1) Then
403. '     ExpCor(ExpNum + 1, 1) = Numer / Denom:
404. 'ElseIf (Numer < -1 And Denom > -1) Or (Numer > -1 And Denom < -1) Then
405. '     ExpCor(ExpNum + 1, 1) = (Numer / Denom) * -1:
406. 'Else
407. '     ExpCor(ExpNum + 1, 1) = 0
408. 'End If
409.
410. End Sub
411.
412. Sub CalculateConst(RowsR As Integer)
413.
414. Dim i As Integer, j As Integer, Numer As Double, Denom As Double
415. Dim SumX As Double, SumY As Double, SumXY As Double, SumX2 As Double, xbar As
Double, ybar As Double
416. Dim xlog() As Double, ylog() As Double
417. Dim x() As Double, y() As Double, xy() As Double, x2() As Double, xsuby() As
Double, xavg() As Double, yavg() As Double
418. ReDim x(1 To RowsR) As Double, y(1 To RowsR) As Double, x2(1 To RowsR) As Dou
ble, xy(1 To RowsR) As Double, xavg(1 To RowsR) As Double
419. ReDim yavg(1 To RowsR) As Double, Test(1 To 3) As Double
420. ReDim xsuby(1 To RowsR) As Double
421. ReDim xlog(1 To RowsR) As Double, ylog(1 To RowsR) As Double
422.
423. For i = 1 To RowsR
424.     x(i) = 1
425.     For j = 1 To PropChosen
426.         x(i) = x(i) * CorPropCorr(i, j + 1):
427.     Next j
428.     y(i) = CorPropCorr(i, 1)
429.     xy(i) = x(i) * y(i)
430.     x2(i) = x(i) * x(i)
431. Next i
432.
433. With Application.WorksheetFunction
434.     SumX = .Sum(x): SumY = .Sum(y): SumXY = .Sum(xy): SumX2 = .Sum(x2):
435.     xbar = .Average(x): ybar = .Average(y):
436. End With
437.
438. For i = 1 To RowsR
439.     xavg(i) = x(i) - xbar: yavg(i) = y(i) - ybar:
440. Next i
441.
442. With Application.WorksheetFunction
443.     Test(1) = .SumProduct(xavg, yavg)
444.     Test(2) = .SumProduct(xavg, xavg)
445.     Test(3) = .SumProduct(yavg, yavg)
446.     R2(PropChosen + 1) = ((Test(1) / (Test(2) * Test(3)) ^ 0.5) ^ 2)

```

```

447. End With
448.
449. Numer = (RowsR * SumXY) - (SumX * SumY)
450. Denom = (RowsR * SumX2) - ((SumX) ^ 2)
451. ExpCor(1, 1) = Numer / Denom:
452.
453. End Sub

```

A.3.3 *RefPropCode Module*

```

1. 'Sub's REFPROP CALL and REFPROP developed by Eric Lemmon, Sept. 25th, 2018. Retrieved from https://github.com/usnistgov/REFPROP-wrappers/issues/64
2. DefDbl A-H, O-Z
3. DefLng I-N
4. Const ncmx = 20 'Maximum number of components in the mixture (do not change unless the Refprop Fortran code is also changed with the same number in the CONSTS.INC file)
5. Const iPropMax = 200 'Number of output properties available in ALLPROPS (also do not change).
6. 'With proper RefPROP installation, change this directory to point to the proper .DLL.
7. Private Declare PtrSafe Sub REFPROPdll Lib "C:\Program Files (x86)\Refprop\REFPRP64.DLL" (ByVal hFld As String, ByVal hIn As String, ByVal hOut As String, iUnitNum As Long, iMass As Long, iFlag As Long, A As Double, B As Double, zm As Double, Output As Double, ByVal hUnits As String, iUnits As Long, x As Double, y As Double, x3 As Double, q As Double, ierr As Long, ByVal herr As String, ln1 As Long, ln2 As Long, ln3 As Long, ln4 As Long, ln5 As Long)
8.
9.
10. Sub REFPROP CALL(Pres As Double, TEMP As Double, DENS As Double, VISC As Double, KVIS As Double, SPHT As Double, ENTH As Double, THCD As Double, PRANDTL As Double, THXP As Double, THDF As Double)
11.
12. '
13. ' Refprop uses a default set of units, these being:
14. ' K, kPa, mol/dm^3, mole fraction, J/mol, J/mol-K, m/s, uPa-s, W/m-K, and N/m
15. '
16.
17.
18. Dim hFld As String, hIn As String, hOut As String, hUnits As String, herr As String
19. Dim Output(iPropMax) As Double, z(ncmx) As Double, x(ncmx) As Double, y(ncmx) As Double, x3(ncmx) As Double
20. Dim ymass(ncmx) As Double, ymole(ncmx) As Double, KVISC As Double, Tmax As Double
21.
22. Dim f As Integer
23.
24.
25. o = 1000#
26.
27.
28.
29. '...Get the DLL number of the REFPROP DLL.
30. Call REFPROPFile(" ", " ", "DLL#", 0, 0, 0, 0, 0, z, Output, hUnits, q, ierr, herr)
31. If (ierr > 0) Then MsgBox herr

```

```

32.
33. '...Calculate the density, isobaric heat capacity, viscosity, and thermal conduct
ivity at a given
34. '...temperature and pressure with the REFPROP subroutine.
35.     Temperature = TEMP + 273.15 'K
36.     If Temperature > 1350 Then
37.         Exit Sub
38.     End If
39.     Pressure = Pres 'MPa
40.     iU = 2 'Units in mass SI (see the REFPROP.FOR file for a complete list of
the unit systems available).
41.     Call REFPROPFile(FluidChosen, "TP", "D,Cp,Vis,Tcx,H,KV,PRANDTL,BETA,TD", iU
, iMass, 0, Temperature, Pressure, z, Output, hUnits, q, ierr, herr)
42.     If (ierr > 0) Then MsgBox herr
43.     'write (*,1000) 'T,P,D,Cp,Vis,Tcx    ",ierr,iU,T,P,Output(1:4)
44.     DENS = Output(1) 'Density ----- kg/m^3
45.     Cpout = Output(2) 'Cp ----- kJ/(kg-K)
46.     VIS = Output(3) 'Viscosity ----- uPa-s
47.     tcx = Output(4) 'Thermal conductivity ----- mW/(m-K)
48.     Enthalpy = Output(5) 'Enthalpy ----- kJ/kg
49.     KVISC = Output(6) 'Kinetic Viscosity ----- cm^2/s
50.     PRANDTL = Output(7) 'Prandtl Number
51.     THXP = Output(8) 'Thermal (Volume) Expansivity - 1/K
52.     TD = Output(9) 'Thermal Diffusivity ----- cm^2/s
53.
54.     SPHT = Cpout * 1000
55.     VISC = VIS / 1000000
56.     THCD = tcx / 1000
57.     ENTH = Enthalpy * 1000
58.     KVIS = KVISC / 10000
59.     THDF = TD / (100 * 100)
60.
61. End Sub
62.
63. Sub REFPROPCALL2(Pres As Double, TEMP As Double, DENS As Double, VISC As Double,
KVISC As Double, SPHT As Double, ENTH As Double, THCD As Double, PRANDTL As Double
, THXP As Double, THDF As Double)
64.
65. '
66. '     Refprop uses a default set of units, these being:
67. '     K, kPa, mol/dm^3, mole fraction, J/mol, J/mol-K, m/s, uPa-s, W/m-
K, and N/m
68. '
69.
70.
71.     Dim hFld As String, hIn As String, hOut As String, hUnits As String, herr A
s String
72.     Dim Output(iPropMax) As Double, z(ncmax) As Double, x(ncmax) As Double, y(n
cmax) As Double, x3(ncmax) As Double
73.     Dim ymass(ncmax) As Double, ymole(ncmax) As Double, KVISC As Double, Tmax A
s Double
74.
75.     Dim f As Integer
76.
77.
78.     o = 1000#
79.
80.
81.
82. '...Get the DLL number of the REFPROP DLL.

```

```

83.     Call REFPROPFile(" ", " ", "DLL#", 0, 0, 0, 0, 0, z, Output, hUnits, q, ier
r, herr)
84.     If (ierr > 0) Then MsgBox herr
85.
86. '...Calculate the density, isobaric heat capacity, viscosity, and thermal conduct
ivity at a given
87. '...enthalpy and pressure with the REFPROP subroutine.
88.     Enthalpy = ENTH / 1000
89.     Pressure = Pres 'MPa
90.     iU = 2 'Units in mass SI (see the REFPROP.FOR file for a complete list of
the unit systems available).
91.     Call REFPROPFile(FluidChosen, "HP", "D,Cp,Vis,Tcx,T,KV,PRANDTL,BETA,TD", iU
, iMass, 0, Enthalpy, Pressure, z, Output, hUnits, q, ierr, herr)
92.     If (ierr > 0) Then MsgBox herr
93.     'write (*,1000) 'T,P,D,Cp,Vis,Tcx    ",ierr,iU,T,P,Output(1:4)
94.     DENS = Output(1)          'Density ----- kg/m^3
95.     Cpout = Output(2)         'Cp ----- kJ/(kg-K)
96.     VIS = Output(3)           'Viscosity ----- uPa-s
97.     tcx = Output(4)           'Thermal conductivity ----- mW/(m-K)
98.     Temperature = Output(5) 'Temperature ----- K
99.     KVISC = Output(6)         'Kinetic Viscosity ----- cm^2/s
100.     PRANDTL = Output(7)      'Prandtl Number
101.     THXP = Output(8)         'Thermal (Volume) Expansivity - 1/K
102.     TD = Output(9)           'Thermal Diffusivity ----- cm^2/s
103.
104.     SPHT = Cpout * 1000
105.     VISC = VIS / 1000000
106.     THCD = tcx / 1000
107.     TEMP = Temperature - 273.15
108.     KVIS = KVISC / 10000
109.     THDF = TD / (100 * 100)
110.     If (TEMP + 273.15) > 3000 Then
111.         MsgBox "Oi"
112.     End If
113.
114. End Sub
115.
116.
117.
118.
119. Sub REFPROPFile(hFld As String, hIn As String, hOut As String, iUnits As Long
, iMass As Long, iFlag As Long, A As Double, B As Double, z() As Double, Output()
As Double, hUnits As String, q As Double, ierr As Long, herr As String)
120. Dim hFld2 As String * 10000, hIn2 As String * 255, hOut2 As String * 255, hUn
its2 As String * 255, herr2 As String * 255
121. Dim iUnits2 As Long, iMass2 As Long, iFlag2 As Long, iUCode2 As Long, ierr2 A
s Long
122. Dim a2 As Double, b2 As Double, z2(ncmax) As Double, x(ncmax) As Double, y(nc
max) As Double, x3(ncmax) As Double, q2 As Double, Output2(iPropMax) As Double
123.
124. hFld2 = hFld: hIn2 = hIn: hOut2 = hOut
125. iUnits2 = iUnits: iMass2 = iMass: iFlag2 = iFlag
126. a2 = A: b2 = B
127. For i = 1 To ncmax: z2(i) = z(i): Next
128. Call REFPROPdll(hFld2, hIn2, hOut2, iUnits2, iMass2, iFlag2, a2, b2, z2(1),
Output2(1), hUnits2, iUCode2, x(1), y(1), x3(1), q2, ierr2, herr2, 10000&, 255&,
255&, 255&, 255&)
129. For i = 1 To iPropMax: Output(i) = Output2(i): Next
130. hUnits = hUnits2
131. iUCode = iUCode2
132. hUnits = hUnits2

```

```

133.     q = q2
134.     ierr = ierr2
135.     herr = herr2
136.     If Trim(hFld2) <> "" Then
137.         For i = 1 To ncmax: z(i) = z2(i): Next
138.     End If
139.
140. End Sub

```

A.3.4 *PrintCode Module*

```

1. 'This sub is meant for printing Headers
2.
3. Dim i As Integer, c As Integer, Colour(3) As Double
4.
5. Colour(1) = 10079487: Colour(2) = 5296274: Colour(3) = 16777164:
6.
7. If HeaderNum = 1 Then: c = C0
8. If HeaderNum = 2 Then: c = C1
9. If HeaderNum = 3 Then: c = C2
10.
11. For i = 1 To L
12.     Cells(r, i + c - 1) = Hd(i, 1)
13.     Cells(r, i + c - 1).Select
14.     With Selection: .HorizontalAlignment = xlCentre: .VerticalAlignment = xlCentre: End With
15.     If HeaderNum <> 3 Then
16.         With ActiveCell.Characters(Start:=1, Length:=Hd(i, 2)).Font: .Name = "Calibri": .FontStyle = "Bold": .Size = 16: End With
17.     Else
18.         With ActiveCell.Characters(Start:=1, Length:=Hd(i, 2)).Font: .Name = "Calibri": .FontStyle = "Bold Italic": .Size = 11: End With
19.     End If
20.     If Hd(i, 7) > 0 Then
21.         With ActiveCell.Characters(Start:=1 + Hd(i, 2), Length:=Hd(i, 3)).Font: .Name = "Calibri": .FontStyle = "Bold": .Size = 12: End With
22.         With ActiveCell.Characters(Start:=1 + Hd(i, 2) + Hd(i, 3), Length:=Hd(i, 4)).Font: .Name = "Calibri": .FontStyle = "Bold": .Size = 9: End With
23.         With ActiveCell.Characters(Start:=1 + Hd(i, 2) + Hd(i, 3) + Hd(i, 4), Length:=Hd(i, 5)).Font: .Name = "Calibri": .FontStyle = "Bold": .Size = 16: End With
24.         With ActiveCell.Characters(Start:=1 + Hd(i, 2) + Hd(i, 3) + Hd(i, 4) + Hd(i, 5), Length:=Hd(i, 6)).Font: .Name = "Calibri": .FontStyle = "Bold": .Size = 12: End With
25.         With ActiveCell.Characters(Start:=1 + Hd(i, 2) + Hd(i, 3) + Hd(i, 4) + Hd(i, 5) + Hd(i, 6), Length:=Hd(i, 7)).Font: .Name = "Calibri": .FontStyle = "Bold": .Size = 9: End With
26.     ElseIf Hd(i, 5) > 0 Then
27.         With ActiveCell.Characters(Start:=1 + Hd(i, 2), Length:=Hd(i, 3)).Font: .Name = "Calibri": .FontStyle = "Bold": .Size = 9: End With
28.         With ActiveCell.Characters(Start:=1 + Hd(i, 2) + Hd(i, 3), Length:=Hd(i, 4)).Font: .Name = "Calibri": .FontStyle = "Bold": .Size = 16: End With
29.         With ActiveCell.Characters(Start:=1 + Hd(i, 2) + Hd(i, 3) + Hd(i, 4), Length:=Hd(i, 5)).Font: .Name = "Calibri": .FontStyle = "Bold": .Size = 9: End With
30.     ElseIf Hd(i, 4) > 0 Then
31.         With ActiveCell.Characters(Start:=1 + Hd(i, 2), Length:=Hd(i, 3)).Font: .Name = "Calibri": .FontStyle = "Bold": .Size = 12: End With

```

```

32.         With ActiveCell.Characters(Start:=1 + Hd(i, 2) + Hd(i, 3), Length:=Hd(i,
33.         4)).Font: .Name = "Calibri": .FontStyle = "Bold": .Size = 9: End With
34.     ElseIf Hd(i, 3) > 0 Then
35.         With ActiveCell.Characters(Start:=1 + Hd(i, 2), Length:=Hd(i, 3)).Font: .
36.         Name = "Calibri": .FontStyle = "Bold": .Size = 9: End With
37.     End If
38.     Cells(r + 1, i + c - 1) = Units(i)
39.     Cells(r + 1, i + c - 1).Select
40.     With Selection: .HorizontalAlignment = xlCentre: .VerticalAlignment = xlCentr
41.     e: End With
42.     With ActiveCell.Font: .Name = "Calibri": .FontStyle = "Italic": .Size = 12: E
43.     nd With
44. Next i
45.
46. Range(Cells(r, c), Cells(r + 1, c + L - 1)).Select:
47. With Selection.Borders(xlEdgeLeft): .LineStyle = xlContinuous: .Weight = xlMedium
48. : End With
49. With Selection.Borders(xlEdgeRight): .LineStyle = xlContinuous: .Weight = xlMediu
50. m: End With
51. With Selection.Borders(xlEdgeTop): .LineStyle = xlContinuous: .Weight = xlMedium:
52. End With
53. With Selection.Borders(xlEdgeBottom): .LineStyle = xlContinuous: .Weight = xlMedi
54. um: End With
55. With Selection.Borders(xlInsideVertical): .LineStyle = xlContinuous: .Weight = xl
56. Thin: End With
57. With Selection.Borders(xlInsideHorizontal): .LineStyle = xlContinuous: .Weight =
58. xlThin: End With
59. With Selection.Interior: .Pattern = xlSolid: .PatternColorIndex = xlAutomatic: .C
60. olor = Colour(HeaderNum): .TintAndShade = 0: .PatternTintAndShade = 0: End With
61.
62. For i = c To L + c - 1
63.     Cells(R0, i) = i
64. Next i
65. Range(Cells(R0, c), Cells(R0, c + L - 1)).Select
66. With Selection: .HorizontalAlignment = xlCentre: .VerticalAlignment = xlCentre: E
67. nd With
68. With Selection.Font: .Name = "Calibri": .FontStyle = "Italic": .Size = 9: End Wit
69. h
70.
71. End Sub
72.
73. Sub ParametersPrint(r As Integer)
74. 'This code will print the parameters that were entered by the user onto the Data
75. Template tab
76. Dim i As Integer, EndNum As Integer, FluidComboBox As Object, FluidType() As Stri
77. ng, ComboRng As Range, ArrNum As Integer
78.
79. If RaworPar = "Raw Data" Then: EndNum = 1: ArrNum = 1:
80. If RaworPar = "Parameters" Then: EndNum = 11: ArrNum = 11:
81. Set ComboRng = Cells(R0 + 2 + ArrNum, C0 + 2)
82.
83. 'Gets the Parameter from the array built by the user, and then formats to the pre
84. -determined style
85. For i = 1 To EndNum
86.     Cells(R0 + 2 + i, C0 + 1) = Parameters(i, 4)
87.     Cells(R0 + 2 + i, C0 + 1).Select
88.     With ActiveCell.Characters(Start:=1, Length:=Parameters(i, 5)).Font: .Name =
89.     "Calibri": .FontStyle = "Bold": .Size = 16: End With
90.     If Parameters(i, 6) > 0 Then
91.         With ActiveCell.Characters(Start:=1 + Parameters(i, 5), Length:=Parameter
92.         s(i, 6)).Font: .Name = "Calibri": .FontStyle = "Bold": .Size = 10: End With

```



```

75.     End If
76.     If i <> EndNum Then: Cells(R0 + 2 + i, C0 + 2) = Parameters(i, 1):
77.     Cells(R0 + 2 + i, C0 + 3) = Parameters(i, 3)
78. Next i
79.
80. 'Aligns the entire table in the centre, and adds borders
81. Range(Cells(R0 + 3, C0 + 1), Cells(R0 + 3 + EndNum - 1, C0 + 3)).Select
82. With Selection: .HorizontalAlignment = xlCentre: .VerticalAlignment = xlCentre: E
    nd With
83. With Selection.Borders(xlInsideVertical): .LineStyle = xlContinuous: .Weight = xl
    Thin: End With
84. With Selection.Borders(xlInsideHorizontal): .LineStyle = xlContinuous: .Weight =
    xlThin: End With
85. With Selection.Borders(xlEdgeLeft): .LineStyle = xlContinuous: .Weight = xlMedium
    : End With
86. With Selection.Borders(xlEdgeRight): .LineStyle = xlContinuous: .Weight = xlMediu
    m: End With
87. With Selection.Borders(xlEdgeTop): .LineStyle = xlContinuous: .Weight = xlMedium:
    End With
88. With Selection.Borders(xlEdgeBottom): .LineStyle = xlContinuous: .Weight = xlMedi
    um: End With
89.
90. If RaworPar = "Parameters" Then
91.
92.     'Adds a bottom border beneath the Temperature inputs
93.     Range(Cells(R0 + 4, C0 + 1), Cells(R0 + 4, C0 + 3)).Select
94.     With Selection.Borders(xlEdgeBottom): .LineStyle = xlContinuous: .Weight = xl
        Medium: End With
95.
96.     'Adds a top border above the Step input
97.     Range(Cells(R0 + 12, C0 + 1), Cells(R0 + 12, C0 + 3)).Select
98.     With Selection.Borders(xlEdgeTop): .LineStyle = xlContinuous: .Weight = xlMed
        ium: End With
99.
100.    'Colors the inputs yellow to highlight to the user what is to be changed
        in the future
101.    Range(Cells(R0 + 3, C0 + 2), Cells(R0 + 12, C0 + 2)).Select
102.    With Selection.Interior: .Pattern = xlSolid: .PatternColorIndex = xlAutom
        atic: .Color = 65535: .TintAndShade = 0: .PatternTintAndShade = 0: End With
103.
104.    'Bolds the units column
105.    Range(Cells(R0 + 3, C0 + 3), Cells(R0 + 13, C0 + 3)).Select
106.    With Selection.Font: .FontStyle = "Bold": .Size = 12: End With
107.
108.    'Creates a side bar to inform the user of the class of parameters
109.    Cells(R0 + 5, C0) = "Operation Parameters"
110.    Range(Cells(R0 + 5, C0), Cells(R0 + 11, C0)).Select
111.    With Selection: .HorizontalAlignment = xlCentre: .VerticalAlignment = xlC
        entre: .WrapText = False: .Orientation = 90: .MergeCells = True: End With
112.    With Selection.Font: .FontStyle = "Bold Italic": .Size = 11: End With
113.    With Selection.Borders(xlEdgeLeft): .LineStyle = xlContinuous: .Weight =
        xlMedium: End With
114.    With Selection.Borders(xlEdgeRight): .LineStyle = xlContinuous: .Weight =
        xlMedium: End With
115.    With Selection.Borders(xlEdgeTop): .LineStyle = xlContinuous: .Weight = x
        lMedium: End With
116.    With Selection.Borders(xlEdgeBottom): .LineStyle = xlContinuous: .Weight
        = xlMedium: End With
117.
118.    'Creates a side bar to inform the user of the class of parameters
119.    Cells(R0 + 12, C0) = "Choices"

```

```

120.     Range(Cells(R0 + 12, C0), Cells(R0 + 13, C0)).Select
121.     With Selection: .HorizontalAlignment = xlCentre: .VerticalAlignment = xlC
entre: .WrapText = False: .Orientation = 90: .MergeCells = True: End With
122.     With Selection.Font: .FontStyle = "Bold Italic": .Size = 11: End With
123.     With Selection.Borders(xlEdgeLeft): .LineStyle = xlContinuous: .Weight =
xlMedium: End With
124.     With Selection.Borders(xlEdgeRight): .LineStyle = xlContinuous: .Weight =
xlMedium: End With
125.     With Selection.Borders(xlEdgeTop): .LineStyle = xlContinuous: .Weight = x
lMedium: End With
126.     With Selection.Borders(xlEdgeBottom): .LineStyle = xlContinuous: .Weight
= xlMedium: End With
127.
128.
129.     Else
130.         'Bolds the units column
131.         Cells(R0 + 3, C0 + 3).Select
132.         With Selection.Font: .FontStyle = "Bold": .Size = 12: End With
133.     End If
134.
135.     Columns(C0 + 2).ColumnWidth = 16:
136.
137.     FluidType = Split(Fluids, ",")
138.     'Adds a combobox for the fluid
139.     Set FluidComboBox = ActiveSheet.Shapes.AddFormControl(xlDropDown, Left:=Combo
Rng.Left, Top:=ComboRng.Top, Width:=ComboRng.Width, Height:=ComboRng.Height)
140.     With FluidComboBox
141.         .ControlFormat.DropDownLines = FluidOptions
142.         For i = 0 To FluidOptions - 1
143.             .ControlFormat.AddItem FluidType(i), i
144.             If FluidType(i) = Parameters(ArrNum, 1) Then
145.                 .ControlFormat.ListIndex = i
146.             End If
147.         Next i
148.         .Name = "Fluid_Select"
149.     End With
150.
151.
152. End Sub
153.
154. Sub PrintProperties(RowsR As Integer, r As Integer)
155.
156. Dim i As Integer, j As Integer
157.
158. For i = 1 To RowsR
159.     If RaworPar = "Parameters" Then
160.         Cells(r + i + 1, C0) = xdist(i) 'm
161.         Cells(r + i + 1, C0 + 1) = P(i) 'MPa
162.         Cells(r + i + 1, C0 + 2) = G(i) 'kg/m2·s
163.         Cells(r + i + 1, C0 + 3) = qavg(i) / 1000 'kW/m2
164.         Cells(r + i + 1, C0 + 4) = Dhy(i) * 1000 'mm
165.         Cells(r + i + 1, C0 + 5) = T(i, 1, 0) '°C
166.     End If
167.     If WallTempIn <> 6 Then: Cells(r + i + 1, C1 - 1) = "-":
168.     Cells(r + i + 1, C1) = xdist(i): GlobalProperties(i, 1) = xdist(i):
169.     Cells(r + i + 1, C1 + 1) = P(i): GlobalProperties(i, 2) = P(i):
170.     Cells(r + i + 1, C1 + 2) = G(i): GlobalProperties(i, 3) = G(i):
171.     Cells(r + i + 1, C1 + 3) = qavg(i): GlobalProperties(i, 4) = qavg(i):
172.     Cells(r + i + 1, C1 + 4) = Dhy(i): GlobalProperties(i, 5) = Dhy(i):
173.     If RaworPar = "Raw Data" Then: Cells(r + i + 1, C1 + 5) = HTC(i, 0): Glob
alProperties(i, 6) = HTC(i, 0): _

```

```

174.         Else: Cells(r + i + 1, C1 + 5) = T(i, 1, 0)
175.         If RaworPar = "Raw Data" Then
176.             For j = 1 To 4
177.                 Cells(r + i + 1, C1 + 5 + j) = T(i, j, 0): GlobalProperties(i, 6
+ j) = T(i, j, 0):
178.                 Cells(r + i + 1, C1 + 9 + j) = D(i, j, 0): GlobalProperties(i, 10
+ j) = D(i, j, 0):
179.                 Cells(r + i + 1, C1 + 13 + j) = u(i, j, 0): GlobalProperties(i, 1
4 + j) = u(i, j, 0):
180.                 Cells(r + i + 1, C1 + 17 + j) = v(i, j, 0): GlobalProperties(i, 1
8 + j) = v(i, j, 0):
181.                 Cells(r + i + 1, C1 + 21 + j) = Cp(i, j, 0): GlobalProperties(i,
22 + j) = Cp(i, j, 0):
182.                 Cells(r + i + 1, C1 + 26 + j) = H(i, j, 0): GlobalProperties(i, 2
7 + j) = H(i, j, 0):
183.                 Cells(r + i + 1, C1 + 30 + j) = k(i, j, 0): GlobalProperties(i, 3
1 + j) = k(i, j, 0):
184.                 Cells(r + i + 1, C1 + 34 + j) = Pr(i, j, 0): GlobalProperties(i,
35 + j) = Pr(i, j, 0):
185.                 Cells(r + i + 1, C1 + 39 + j) = B(i, j, 0): GlobalProperties(i, 4
0 + j) = B(i, j, 0):
186.                 Cells(r + i + 1, C1 + 43 + j) = A(i, j, 0): GlobalProperties(i, 4
4 + j) = A(i, j, 0):
187.                 Cells(r + i + 1, C1 + 47 + j) = Re(i, j, 0): GlobalProperties(i,
48 + j) = Re(i, j, 0):
188.             '         If RaworPar = "Raw Data" Then
189.                 Cells(r + i + 1, C1 + 51 + j) = Nu(i, j, 0): GlobalProperties
(i, 52 + j) = Nu(i, j, 0):
190.                 Cells(r + i + 1, C1 + 55 + j) = Ap(i, j, 0): GlobalProperties
(i, 56 + j) = Ap(i, j, 0):
191.             '         End If
192.             Next j
193.             Cells(r + i + 1, C1 + 26) = Cp(i, 5, 0): GlobalProperties(i, 27) = Cp
(i, 5, 0):
194.             Cells(r + i + 1, C1 + 39) = Pr(i, 5, 0): GlobalProperties(i, 40) = Pr
(i, 5, 0):
195.             Cells(r + i + 1, C1 + 60) = Prw(i, 0): GlobalProperties(i, 61) = Prw(
i, 0):
196.             For j = 1 To 5
197.                 Cells(r + i + 1, C1 + 60 + j) = "-
": GlobalProperties(i, 61 + j) = 0:
198.             Next j
199.             For j = 1 To 12
200.                 Cells(r + i + 1, C1 + 65 + j) = Ta(i, j, 0): GlobalProperties(i,
66 + j) = Ta(i, j, 0):
201.                 Cells(r + i + 1, C1 + 77 + j) = Da(i, j, 0): GlobalProperties(i,
78 + j) = Da(i, j, 0):
202.                 Cells(r + i + 1, C1 + 89 + j) = ua(i, j, 0): GlobalProperties(i,
90 + j) = ua(i, j, 0):
203.                 Cells(r + i + 1, C1 + 101 + j) = va(i, j, 0): GlobalProperties(i,
102 + j) = va(i, j, 0):
204.                 Cells(r + i + 1, C1 + 133 + j) = Ha(i, j, 0): GlobalProperties(i,
134 + j) = Ha(i, j, 0):
205.                 Cells(r + i + 1, C1 + 145 + j) = ka(i, j, 0): GlobalProperties(i,
146 + j) = ka(i, j, 0):
206.                 Cells(r + i + 1, C1 + 177 + j) = Ba(i, j, 0): GlobalProperties(i,
178 + j) = Ba(i, j, 0):
207.                 Cells(r + i + 1, C1 + 189 + j) = Aa(i, j, 0): GlobalProperties(i,
190 + j) = Aa(i, j, 0):
208.                 Cells(r + i + 1, C1 + 201 + j) = Rea(i, j, 0): GlobalProperties(i
, 202 + j) = Rea(i, j, 0):

```

```

209.         Next j
210.         For j = 1 To 20
211.             Cells(r + i + 1, C1 + 113 + j) = Cpa(i, j, 0): GlobalProperties(i
, 114 + j) = Cpa(i, j, 0):
212.             Cells(r + i + 1, C1 + 157 + j) = Pra(i, j, 0): GlobalProperties(i
, 158 + j) = Pra(i, j, 0):
213.         Next j
214.         ElseIf RaworPar = "Parameters" Then
215.             Cells(r + i + 1, C1 + 6) = D(i, 1, 0)
216.             Cells(r + i + 1, C1 + 7) = u(i, 1, 0)
217.             Cells(r + i + 1, C1 + 8) = v(i, 1, 0)
218.             Cells(r + i + 1, C1 + 9) = Cp(i, 1, 0)
219.             Cells(r + i + 1, C1 + 10) = H(i, 1, 0)
220.             Cells(r + i + 1, C1 + 11) = k(i, 1, 0)
221.             Cells(r + i + 1, C1 + 12) = Pr(i, 1, 0)
222.             Cells(r + i + 1, C1 + 13) = B(i, 1, 0)
223.             Cells(r + i + 1, C1 + 14) = A(i, 1, 0)
224.             Cells(r + i + 1, C1 + 15) = Re(i, 1, 0)
225.         End If
226.     Next i
227.
228. End Sub
229.
230.
231. Sub FormulaTitlesPrint(r As Integer, c As Integer)
232.
233. Dim i As Integer, Offset As Integer
234.
235. If RaworPar = "Raw Data" Then: Offset = 5:
236. If RaworPar = "Parameters" Then: Offset = 1:
237.
238. InputFormulaTitles
239.
240. If Cells(r - Offset, c) = "" Then
241.     For i = 1 To TotalFormulas
242.         Cells(r - Offset, c + 4 * (i - 1)) = FormulaTitle(i)
243.         Range(Cells(r - Offset, c + 4 * (i - 1)), Cells(r - Offset, c + 3 + 4
* (i - 1))).Select: FormatFormulaTitles
244.     Next i
245. End If
246. End Sub
247.
248. Sub FormatFormulaTitles()
249.
250. With Selection: .HorizontalAlignment = xlCentreAcrossSelection: .VerticalAlig
nment = xlCentre: End With
251. With Selection.Font: .FontStyle = "Bold Italic": .Size = 10: End With
252. With Selection.Borders(xlEdgeLeft): .LineStyle = xlContinuous: .Weight = xlMe
dium: End With
253. With Selection.Borders(xlEdgeRight): .LineStyle = xlContinuous: .Weight = xlM
edium: End With
254. With Selection.Borders(xlEdgeTop): .LineStyle = xlContinuous: .Weight = xlMed
ium: End With
255. With Selection.Borders(xlEdgeBottom): .LineStyle = xlContinuous: .Weight = xl
Medium: End With
256.
257. End Sub
258.
259. Sub PrintCorrelations(RowsR As Integer, StartRow As Integer)
260.
261. Dim i As Integer, j As Integer

```

```

262.
263.     For i = 1 To RowsR
264.         For j = 1 To TotalFormulas
265.             Cells(StartRow + i + 1, 4 * (j - 1) + C2) = HTC(i, j) / 1000
266.             Cells(StartRow + i + 1, 4 * (j - 1) + C2).NumberFormat = "0.00"
267.             ' Cells(StartRow + i + 1, 4 * (j - 1) + C2) = Format(HTC(i, j), "0.00"
                )
268.             Cells(StartRow + i + 1, 4 * (j - 1) + C2 + 1) = Format(T(i, 2, j), "0
                .00")
269.             Cells(StartRow + i + 1, 4 * (j - 1) + C2 + 2) = It(i, j)
270.             Cells(StartRow + i + 1, 4 * (j - 1) + C2 + 3) = Format(Errs(i, j), "0
                .00")
271.             If Errs(i, j) > MaxError Then
272.                 Range(Cells(StartRow + i + 1, 4 * (j - 1) + C2), Cells(StartRow +
                i + 1, 4 * (j - 1) + C2 + 3)).Select
273.                 With Selection.Interior: .Pattern = xlSolid: .PatternColorIndex =
                xlAutomatic: .Color = 16711935: .TintAndShade = 0: .PatternTintAndShade = 0: End
                With
274.                     End If
275.                 Next j
276.             Next i
277.
278.         End Sub
279.
280.     Sub PrintErrors(StRow As Integer)
281.         Dim i As Integer, ii As Integer
282.         If RaworPar = "Raw Data" Then: ii = 0: Else: ii = 1:
283.
284.         For i = 1 To TotalFormulas
285.             Cells(StRow - 4 - ii, 4 * (i - 1) + C2) = Format(ErrTotal(i, 1), "0.00%")
286.             Cells(StRow - 4 - ii, 4 * (i - 1) + C2 + 1) = Format(ErrTotal(i, 2), "0.0
                0%")
287.             Cells(StRow - 3 - ii, 4 * (i - 1) + C2) = Format(ErrTotalAbs(i, 1), "0.00
                %")
288.             Cells(StRow - 3 - ii, 4 * (i - 1) + C2 + 1) = Format(ErrTotalAbs(i, 2), "
                0.00%")
289.             Cells(StRow - 2 - ii, 4 * (i - 1) + C2) = Format(ErrSTD(i, 1), "0.00%")
290.             Cells(StRow - 2 - ii, 4 * (i - 1) + C2 + 1) = Format(ErrSTD(i, 2), "0.00%
                ")
291.             Cells(StRow - 1 - ii, 4 * (i - 1) + C2) = Format(RMS(i, 1), "0.00%")
292.             Cells(StRow - 1 - ii, 4 * (i - 1) + C2 + 1) = Format(RMS(i, 2), "0.00%")
293.
294.             Cells(StRow - 4 - ii, 4 * (i - 1) + C2 + 2) = "Average Error / Mean Error
                "
295.             Range(Cells(StRow - 4, 4 * (i - 1) + C2 + 2), Cells(StRow - 4 - ii, 4 * (
                i - 1) + C2 + 3)).Select
296.             With Selection: .HorizontalAlignment = xlCentreAcrossSelection: .Vertical
                Alignment = xlCentre: End With
297.             Cells(StRow - 3 - ii, 4 * (i - 1) + C2 + 2) = "Average Absolute Error"
298.             Range(Cells(StRow - 3, 4 * (i - 1) + C2 + 2), Cells(StRow - 3 - ii, 4 * (
                i - 1) + C2 + 3)).Select
299.             With Selection: .HorizontalAlignment = xlCentreAcrossSelection: .Vertical
                Alignment = xlCentre: End With
300.             Cells(StRow - 2 - ii, 4 * (i - 1) + C2 + 2) = "Standard Error"
301.             Range(Cells(StRow - 2, 4 * (i - 1) + C2 + 2), Cells(StRow - 2 - ii, 4 * (
                i - 1) + C2 + 3)).Select
302.             With Selection: .HorizontalAlignment = xlCentreAcrossSelection: .Vertical
                Alignment = xlCentre: End With
303.             Cells(StRow - 1 - ii, 4 * (i - 1) + C2 + 2) = "RMS"

```

```

304.     Range(Cells(StRow - 1, 4 * (i - 1) + C2 + 2), Cells(StRow - 1 - ii, 4 * (
        i - 1) + C2 + 3)).Select
305.     With Selection: .HorizontalAlignment = xlCentreAcrossSelection: .Vertical
        Alignment = xlCentre: End With
306.
307.     Range(Cells(StRow - 4 - ii, 4 * (i - 1) + C2 + 2), Cells(StRow - 1 - ii,
        4 * (i - 1) + C2 + 3)).Select
308.     With Selection.Font: .FontStyle = "Bold Italic": .Size = 9: End With
309. Next i
310.
311. End Sub
312.
313.
314. Sub DisplayErrors()
315.     Dim i As Integer, SheetCount As Integer, Selections As Integer, j As Integer,
        SheetName As String, OK As Integer
316.
317.     j = 0: OK = 1:
318.     Do While OK = 1
319.         OK = 0: j = j + 1:
320.         For i = 1 To Sheets.Count
321.             If Sheets(i).Name = "Error Output " & j Then: OK = 1: Exit For:
322.         Next i
323.     Loop
324.
325.     Sheets.Add.Name = "Error Output " & j
326.     Sheets("Error Output " & j).Activate
327.
328.     Range("A:A").ColumnWidth = 40: Range("B:I").ColumnWidth = 17.5:
329.
330.     For i = 1 To TotalFormulas
331.         Range("A" & i + 2) = FormulaTitle(i)
332.         Range("B" & i + 2) = Format(ErrTotal(i, 1), "0.00%")
333.         Range("C" & i + 2) = Format(ErrTotalAbs(i, 1), "0.00%")
334.         Range("D" & i + 2) = Format(ErrSTD(i, 1), "0.00%")
335.         Range("E" & i + 2) = Format(RMS(i, 1), "0.00%")
336.         Range("F" & i + 2) = Format(ErrTotal(i, 2), "0.00%")
337.         Range("G" & i + 2) = Format(ErrTotalAbs(i, 2), "0.00%")
338.         Range("H" & i + 2) = Format(ErrSTD(i, 2), "0.00%")
339.         Range("I" & i + 2) = Format(RMS(i, 2), "0.00%")
340.     Next i
341.
342.     Cells(2, 1) = "Correlation"
343.
344.     For i = 1 To 2
345.         Cells(2, 4 * (i - 1) + 2) = "Average Error/Mean Error"
346.         Cells(2, 4 * (i - 1) + 3) = "Average Absolute Error"
347.         Cells(2, 4 * (i - 1) + 4) = "Standard Error"
348.         Cells(2, 4 * (i - 1) + 5) = "RMS Error"
349.     Next i
350.
351.     Range(Cells(2, 1), Cells(2, 9)).Select
352.     With Selection.Font: .FontStyle = "Bold Italic": .Size = 9: End With
353.     With Selection: .HorizontalAlignment = xlCentre: .VerticalAlignment = xlCentr
        e: End With
354.
355.     Cells(1, 2) = "HTC Error"
356.     Range(Cells(1, 2), Cells(1, 5)).Select
357.     With Selection: .HorizontalAlignment = xlCentreAcrossSelection: .VerticalAlig
        nment = xlCentre: End With
358.     With Selection.Font: .FontStyle = "Bold": .Size = 16: End With

```

```

359.
360. Cells(1, 6) = "Twall Error"
361. Cells(1, 6).Select
362. With Selection.Characters(Start:=1, Length:=1).Font: .Name = "Calibri": .Font
    Style = "Bold": .Size = 16: End With
363. With Selection.Characters(Start:=2, Length:=4).Font: .Name = "Calibri": .Font
    Style = "Bold": .Size = 9: End With
364. With Selection.Characters(Start:=6, Length:=6).Font: .Name = "Calibri": .Font
    Style = "Bold": .Size = 16: End With
365. Range(Cells(1, 5), Cells(1, 9)).Select
366. With Selection: .HorizontalAlignment = xlCentreAcrossSelection: .VerticalAlign
    nment = xlCentre: End With
367.
368.
369. End Sub

```

A.3.5 *Misc*

```

1. Sub CalculateErrorsforCor()
2. '
3. Dim r As Integer, Formulas As Integer, i As Integer, j As Integer
4.
5. Dim HTC() As Double, HTCErrTotal() As Double, HTCErrTotalAbs() As Double, HTCErrTotalSq() As Double
6. Dim Tw() As Double, TwErrTotal() As Double, TwErrTotalAbs() As Double, TwErrTotalSq() As Double
7. Dim ErrAvg() As Double, ErrAvgAbs() As Double, ErrSq() As Double, RMS() As Double
8.
9. r = Range("A44", Range("A44").End(xlDown)).Rows.Count
10. Formulas = 33
11.
12. ReDim HTC(1 To r, 0 To Formulas), HTCErrTotal(1 To r, 1 To Formulas), HTCErrTotalAbs(1 To r, 1 To Formulas), HTCErrTotalSq(1 To r, 1 To Formulas)
13. ReDim Tw(1 To r, 0 To Formulas), TwErrTotal(1 To r, 1 To Formulas), TwErrTotalAbs(1 To r, 1 To Formulas), TwErrTotalSq(1 To r, 1 To Formulas)
14. ReDim ErrAvg(1 To Formulas, 1 To 2), ErrAvgAbs(1 To Formulas, 1 To 2), ErrSq(1 To Formulas, 1 To 2), RMS(1 To Formulas, 1 To 2)
15.
16. For i = 1 To r
17.     HTC(i, 0) = Cells(i + 43, 10).Value
18.     Tw(i, 0) = Cells(i + 43, 9).Value
19.
20.     For j = 1 To Formulas
21.         HTC(i, j) = Cells(i + 43, 11 + 4 * (j - 1)).Value
22.         Tw(i, j) = Cells(i + 43, 12 + 4 * (j - 1)).Value
23.         HTCErrTotal(i, j) = (HTC(i, j) - HTC(i, 0)) / HTC(i, 0)
24.         TwErrTotal(i, j) = (Tw(i, j) - Tw(i, 0)) / Tw(i, 0)
25.         HTCErrTotalAbs(i, j) = Abs(HTC(i, j) - HTC(i, 0)) / HTC(i, 0)
26.         TwErrTotalAbs(i, j) = Abs(Tw(i, j) - Tw(i, 0)) / Tw(i, 0)
27.     Next j
28. Next i
29.
30. For j = 1 To Formulas
31.     ErrAvg(j, 1) = Application.WorksheetFunction.Sum(Application.WorksheetFunction.Index(HTCErrTotal(), 0, j)) / r
32.     ErrAvg(j, 2) = Application.WorksheetFunction.Sum(Application.WorksheetFunction.Index(TwErrTotal(), 0, j)) / r

```

```

33.     ErrAvgAbs(j, 1) = Application.WorksheetFunction.Sum(Application.WorksheetFunc
tion.Index(HTCErrTotalAbs(), 0, j)) / r
34.     ErrAvgAbs(j, 2) = Application.WorksheetFunction.Sum(Application.WorksheetFunc
tion.Index(TwErrTotalAbs(), 0, j)) / r
35. Next j
36.
37. For i = 1 To r
38.     For j = 1 To Formulas
39.         HTCErrTotalSq(i, j) = (HTCErrTotal(i, j) - ErrAvg(j, 1)) ^ 2
40.         TwErrTotalSq(i, j) = (TwErrTotal(i, j) - ErrAvg(j, 2)) ^ 2
41.     Next j
42. Next i
43.
44. With Application.WorksheetFunction
45.     For j = 1 To Formulas
46.         ErrSq(j, 1) = (.Sum(.Index(HTCErrTotalSq(), 0, j)) / (r - 1)) ^ 0.5
47.         ErrSq(j, 2) = (.Sum(.Index(TwErrTotalSq(), 0, j)) / (r - 1)) ^ 0.5
48.         RMS(j, 1) = (.SumProduct(.Index(HTCErrTotal(), 0, j), .Index(HTCErrTotal(
), 0, j)) / r) ^ 0.5
49.         RMS(j, 2) = (.SumProduct(.Index(TwErrTotal(), 0, j), .Index(TwErrTotal(),
0, j)) / r) ^ 0.5
50.     Next j
51. End With
52.
53. For j = 1 To Formulas
54.     Cells(j + 2, 3) = ErrAvg(j, 1)
55.     Cells(j + 2, 4) = ErrAvgAbs(j, 1)
56.     Cells(j + 2, 5) = ErrSq(j, 1)
57.     Cells(j + 2, 6) = RMS(j, 1)
58.     Cells(j + 2, 7) = ErrAvg(j, 2)
59.     Cells(j + 2, 8) = ErrAvgAbs(j, 2)
60.     Cells(j + 2, 9) = ErrSq(j, 2)
61.     Cells(j + 2, 10) = RMS(j, 2)
62. Next j
63.
64. End Sub
65.
66.
67.
68. Sub PPc(Pressure As Double, Temperature As Double)
69.
70. Dim DENS As Double, SPHT As Double, VISC As Double, THCD As Double, ENTH As Doubl
e, KVIS As Double, PRANDTL As Double, THXP As Double, THDF As Double
71. Dim ttemp As Double, i As Integer, Cptemp As Double, DoneFor As Integer, DoneBack
As Integer, Inter As Double
72. 'Calculate Psuedocritical temperature for the specified pressure
73.
74. 'Gives the initial guess a closer value depending on the pressure (saves time in
processing)
75. If Pressure >= 40 Then
76.     Temperature = 430.34
77. ElseIf Pressure >= 35 Then
78.     Temperature = 416.69
79. ElseIf Pressure >= 30 Then
80.     Temperature = 401.91
81. ElseIf Pressure >= 25 Then
82.     Temperature = 384.89
83. ElseIf Pressure >= 22.064 Then
84.     Temperature = 373.94
85. ElseIf Pressure >= 20 Then
86.     Temperature = 365.75

```



```

87. ElseIf Pressure >= 15 Then
88.     Temperature = 342.16
89. ElseIf Pressure >= 10 Then
90.     Temperature = 311
91. ElseIf Pressure >= 5 Then
92.     Temperature = 263.94
93. ElseIf Pressure >= 1 Then
94.     Temperature = 179.88
95. Else
96.     Temperature = 100
97. End If
98.
99. 'Sets up initial conditions
100. DoneFor = 0
101. DoneBack = 0
102. Inter = 50
103.
104. 'Calls the variables, specifically looking at Specific Heat. This moves forward
    stepwise until the Cp is less than the previous one
105. Do
106.     Call REFPROPCALL(Pressure, Temperature, DENS, VISC, KVIS, SPHT, ENTH, THCD,
        PRANDTL, THXP, THDF)
107.     Cptemp = SPHT
108.     ttemp = Temperature + Inter
109.     Call REFPROPCALL(Pressure, ttemp, DENS, VISC, KVIS, SPHT, ENTH, THCD, PRA
        NDTL, THXP, THDF)
110.     If Cptemp < SPHT Then
111.         Temperature = ttemp
112.     ElseIf Cptemp > SPHT And Inter = 50 Then
113.         Inter = 10
114.     ElseIf Cptemp > SPHT And Inter = 10 Then
115.         Inter = 5
116.     ElseIf Cptemp > SPHT And Inter = 5 Then
117.         Inter = 1
118.     ElseIf Cptemp > SPHT And Inter = 1 Then
119.         Inter = 0.5
120.     ElseIf Cptemp > SPHT And Inter = 0.5 Then
121.         Inter = 0.1
122.     ElseIf Cptemp > SPHT And Inter = 0.1 Then
123.         Inter = 0.01
124.     ElseIf Cptemp > SPHT And Inter = 0.01 Then
125.         DoneFor = 1
126.     End If
127. Loop While DoneFor = 0
128.
129. 'Sets the spacing at the minimum of 0.01°C apart
130. Inter = 0.01
131.
132. 'Goes backward to ensure that the forward code didn't miss the peak
133. Do
134.     Call REFPROPCALL(Pressure, Temperature, DENS, VISC, KVIS, SPHT, ENTH, THCD,
        PRANDTL, THXP, THDF)
135.     Cptemp = SPHT
136.     ttemp = Temperature - Inter
137.     Call REFPROPCALL(Pressure, ttemp, DENS, VISC, KVIS, SPHT, ENTH, THCD, PRA
        NDTL, THXP, THDF)
138.     If Cptemp < SPHT Then
139.         Temperature = ttemp
140.     ElseIf Cptemp > SPHT Then
141.         DoneBack = 1
142.     End If

```

```

143.     Loop While DoneBack = 0
144.
145. End Sub
146.
147.
148.
149. Sub GetPpc()
150. Dim tim As Date, j As Integer
151. j = 0
152. Call CodeTimer(tim, j)
153.
154. Dim Tempforpc() As Double, Pforpc() As Double, i As Integer, StartT As Double
    , EndT As Double, Cptemp As Double, Ptemp As Double
155. Dim DENS As Double, VISC As Double, KVIS As Double, SPHT As Double, ENTH As D
    ouble, THCD As Double, PRANDTL As Double
156. Dim THXP As Double, THDF As Double
157. Dim StepRange As Double, Steps As Integer
158. StepRange = 0.05
159.
160. StartT = 373.95
161. EndT = 600
162. Steps = ((EndT - StartT) / StepRange) + 1
163.
164. ReDim Tempforpc(1 To Steps), Pforpc(1 To Steps)
165. Tempforpc(1) = 373.95
166. Pforpc(1) = 22.064
167.
168. For i = 1 To Steps
169.
170.
171.     'Sets up initial conditions
172.     DoneFor = 0
173.     DoneBack = 0
174.     Inter = 1
175.
176.     'Calls the variables, specifically looking at Specific Heat. This moves f
    orward stepwise until the Cp is less than the previous one
177.     Do
178.         Call REFPROPCALL(Pforpc(i), Tempforpc(i), DENS, VISC, KVIS, SPHT, ENT
        H, THCD, PRANDTL, THXP, THDF)
179.         Cptemp = SPHT
180.         Ptemp = Pforpc(i) + Inter
181.         Call REFPROPCALL(Ptemp, Tempforpc(i), DENS, VISC, KVIS, SPHT, ENTH, T
        HCD, PRANDTL, THXP, THDF)
182.         If Cptemp < SPHT Then
183.             Pforpc(i) = Ptemp
184.         ElseIf Cptemp > SPHT And Inter = 1 Then
185.             Inter = 0.1
186.         ElseIf Cptemp > SPHT And Inter = 0.1 Then
187.             Inter = 0.01
188.         ElseIf Cptemp > SPHT And Inter = 0.01 Then
189.             Inter = 0.001
190.         ElseIf Cptemp > SPHT And Inter = 0.001 Then
191.             DoneFor = 1
192.         End If
193.     Loop While DoneFor = 0
194.
195.     'Sets the spacing at the minimum of 0.001 MPa apart
196.     Inter = 0.001
197.
198.     'Goes backward to ensure that the forward code didn't miss the peak

```

```

199.         Do
200.             Call REFPROP_CALL(Pforpc(i), Tempforpc(i), DENS, VISC, KVIS, SPHT, ENT
H, THCD, PRANDTL, THXP, THDF)
201.             Cptemp = SPHT
202.             Ptemp = Pforpc(i) - Inter
203.             Call REFPROP_CALL(Ptemp, Tempforpc(i), DENS, VISC, KVIS, SPHT, ENTH, T
HCD, PRANDTL, THXP, THDF)
204.             If Cptemp < SPHT Then
205.                 Pforpc(i) = Ptemp
206.             ElseIf Cptemp > SPHT Then
207.                 DoneBack = 1
208.             End If
209.             Loop While DoneBack = 0
210.
211.             If i < Steps Then: Tempforpc(i + 1) = Tempforpc(i) + StepRange: Pforpc(i
+ 1) = Pforpc(i)
212.
213.         Next i
214.
215.         Sheets.Add.Name = "PC Calc"
216.         Sheets("PC Calc").Activate
217.
218.         For i = 1 To Steps + 1
219.             If i = 1 Then: Cells(i, 1) = "Temperature": Cells(i, 2) = "Pressure"
220.
221.             If i <> 1 Then: Cells(i, 1) = Format(Tempforpc(i - 1), "0.00"): Cells
(i, 2) = Format(Pforpc(i - 1), "0.000")
222.
223.             j = 1
224.             Call CodeTimer(tim, j)
225.         End Sub

```

A.3.6 *HeadersCode Module*

```

1. Sub Headers1(r As Integer, L As Integer)
2. 'This sub inputs header information and formatting
3.
4. 'Introduce general variables
5. Dim i As Integer, j As Integer
6.
7. 'Which Headers is being sent for color
8. j = 1: i = 0
9.
10. 'Introduce variant variables
11. Dim Hd() As Variant, Units() As Variant
12.
13. If RaworPar = "Raw Data" Then
14.     ReDim Hd(1 To L, 1 To ms) As Variant, Units(1 To L) As Variant
15.
16.     'Input Header string / Unit string
17.     i = i + 1: Hd(i, 1) = "#": Hd(i, 2) = 1: Units(i) = "#"
18.     i = i + 1: Hd(i, 1) = "Test": Hd(i, 2) = 4: Units(i) = "#"
19.     i = i + 1: Hd(i, 1) = "Z": Hd(i, 2) = 1: Units(i) = "m"
20.     i = i + 1: Hd(i, 1) = "P": Hd(i, 2) = 1: Units(i) = "MPa"
21.     i = i + 1: Hd(i, 1) = "G": Hd(i, 2) = 1: Units(i) = "kg/m2·s"
22.     i = i + 1: Hd(i, 1) = "q": Hd(i, 2) = 1: Units(i) = "kW/m2"
23.     i = i + 1: Hd(i, 1) = "ID": Hd(i, 2) = 2: Units(i) = "mm"

```

```

24.     i = i + 1: Hd(i, 1) = "Tb": Hd(i, 2) = 1: Hd(i, 3) = 1: Units(i) = "°C"
25.     i = i + 1: Hd(i, 1) = "Tw": Hd(i, 2) = 1: Hd(i, 3) = 1: Units(i) = "°C"
26.     i = i + 1: Hd(i, 1) = "HTC": Hd(i, 2) = 3: Units(i) = "kW/m²·K"
27.     i = i + 1: Hd(i, 1) = "Blank": Hd(i, 2) = 5: Units(i) = "Blank"
28.
29. ElseIf RaworPar = "Parameters" Then
30.     ReDim Hd(1 To L, 1 To ms) As Variant, Units(1 To L) As Variant
31.
32.     'Input Header string / Unit string
33.     i = i + 1: Hd(i, 1) = "Length": Hd(i, 2) = 6: Units(i) = "m"
34.     i = i + 1: Hd(i, 1) = "P": Hd(i, 2) = 1: Units(i) = "MPa"
35.     i = i + 1: Hd(i, 1) = "G": Hd(i, 2) = 1: Units(i) = "kg/m²·s"
36.     i = i + 1: Hd(i, 1) = "q": Hd(i, 2) = 1: Units(i) = "kW/m²"
37.     i = i + 1: Hd(i, 1) = "Dhy": Hd(i, 2) = 1: Hd(i, 3) = 2: Units(i) = "mm"
38.     i = i + 1: Hd(i, 1) = "Tbulk": Hd(i, 2) = 1: Hd(i, 3) = 4: Units(i) = "°C"
39.     If WallTempIn = 6 Then: i = i + 1: Hd(i, 1) = "Twall": Hd(i, 2) = 1: Hd(i, 3)
        = 4: Units(i) = "°C"
40.     If WallTempIn = 7 Then:: i = i + 1: Hd(i, 1) = "Blank": Hd(i, 2) = 5: Units(i
        ) = "Blank"
41. End If
42.
43.
44.
45. Call HeadersPrint(Hd(), Units(), r, L, j)
46.
47.
48. End Sub
49.
50. Sub Headers2(r As Integer, L As Integer, L1 As Integer)
51. 'This sub inputs header information and formatting
52. Dim i As Integer, j As Integer
53.
54. 'Which Headers is being sent for color
55. j = 2
56.
57. 'Introduce variant variables
58. Dim Hd() As Variant, Units() As Variant
59.
60. ReDim Hd(1 To L, 1 To ms) As Variant, Units(1 To L) As Variant
61.
62. 'Input Header string / Unit string
63. i = 1: Hd(i, 1) = "Length": Hd(i, 2) = 6: Units(i) = "m"
64. i = i + 1: Hd(i, 1) = "P": Hd(i, 2) = 1: Units(i) = "MPa"
65. i = i + 1: Hd(i, 1) = "G": Hd(i, 2) = 1: Units(i) = "kg/m²·s"
66. i = i + 1: Hd(i, 1) = "q": Hd(i, 2) = 1: Units(i) = "W/m²"
67. i = i + 1: Hd(i, 1) = "Dhy": Hd(i, 2) = 1: Hd(i, 3) = 2: Units(i) = "m"
68. If RaworPar = "Raw Data" Then: i = i + 1: Hd(i, 1) = "HTC": Hd(i, 2) = 3: Units(i
        ) = "W/m²·K":
69. 'i = 6
70. '-----
        -----
71. i = i + 1: Hd(i, 1) = "Tbulk": Hd(i, 2) = 1: Hd(i, 3) = 4: Units(i) = "°C"
72. If RaworPar = "Raw Data" Then
73.     i = i + 1: Hd(i, 1) = "Twall": Hd(i, 2) = 1: Hd(i, 3) = 4: Units(i) = "°C"
74.     i = i + 1: Hd(i, 1) = "Tfilm": Hd(i, 2) = 1: Hd(i, 3) = 4: Units(i) = "°C"
75.     i = i + 1: Hd(i, 1) = "Tpc": Hd(i, 2) = 1: Hd(i, 3) = 2: Units(i) = "°C"
76. End If
77. 'i = 10
78. '-----
        -----

```

```

79. i = i + 1: Hd(i, 1) = ChrW(961) & "bulk": Hd(i, 2) = 1: Hd(i, 3) = 4: Units(i) =
    "kg/m³"
80. If RaworPar = "Raw Data" Then
81.     i = i + 1: Hd(i, 1) = ChrW(961) & "wall": Hd(i, 2) = 1: Hd(i, 3) = 4: Units(i)
        = "kg/m³"
82.     i = i + 1: Hd(i, 1) = ChrW(961) & "film": Hd(i, 2) = 1: Hd(i, 3) = 4: Units(i)
        = "kg/m³"
83.     i = i + 1: Hd(i, 1) = ChrW(961) & "pc": Hd(i, 2) = 1: Hd(i, 3) = 2: Units(i)
        = "kg/m³"
84. End If
85. 'i = 14
86. '-----
-----
87. i = i + 1: Hd(i, 1) = "µbulk": Hd(i, 2) = 1: Hd(i, 3) = 4: Units(i) = "Pa·s"
88. If RaworPar = "Raw Data" Then
89.     i = i + 1: Hd(i, 1) = "µwall": Hd(i, 2) = 1: Hd(i, 3) = 4: Units(i) = "Pa·s"
90.     i = i + 1: Hd(i, 1) = "µfilm": Hd(i, 2) = 1: Hd(i, 3) = 4: Units(i) = "Pa·s"
91.     i = i + 1: Hd(i, 1) = "µpc": Hd(i, 2) = 1: Hd(i, 3) = 2: Units(i) = "Pa·s"
92. End If
93. 'i = 18
94. '-----
-----
95. i = i + 1: Hd(i, 1) = ChrW(957) & "bulk": Hd(i, 2) = 1: Hd(i, 3) = 4: Units(i) =
    "m²/s"
96. If RaworPar = "Raw Data" Then
97.     i = i + 1: Hd(i, 1) = ChrW(957) & "wall": Hd(i, 2) = 1: Hd(i, 3) = 4: Units(i)
        = "m²/s"
98.     i = i + 1: Hd(i, 1) = ChrW(957) & "film": Hd(i, 2) = 1: Hd(i, 3) = 4: Units(i)
        = "m²/s"
99.     i = i + 1: Hd(i, 1) = ChrW(957) & "pc": Hd(i, 2) = 1: Hd(i, 3) = 2: Units(i)
        = "m²/s"
100. End If
101. 'i = 22
102. '-----
-----
103. i = i + 1: Hd(i, 1) = "CPbulk": Hd(i, 2) = 1: Hd(i, 3) = 1: Hd(i, 4) = 4: Units(i) =
    "J/kg·K"
104. If RaworPar = "Raw Data" Then
105.     i = i + 1: Hd(i, 1) = "CPwall": Hd(i, 2) = 1: Hd(i, 3) = 1: Hd(i, 4) = 4:
        Units(i) = "J/kg·K"
106.     i = i + 1: Hd(i, 1) = "CPfilm": Hd(i, 2) = 1: Hd(i, 3) = 1: Hd(i, 4) = 4:
        Units(i) = "J/kg·K"
107.     i = i + 1: Hd(i, 1) = "CPpc": Hd(i, 2) = 1: Hd(i, 3) = 1: Hd(i, 4) = 2: U
        nits(i) = "J/kg·K"
108.     i = i + 1: Hd(i, 1) = "CPavg": Hd(i, 2) = 1: Hd(i, 3) = 1: Hd(i, 4) = 3:
        Units(i) = "J/kg·K"
109. End If
110. 'i = 27
111. '-----
-----
112. i = i + 1: Hd(i, 1) = "Hbulk": Hd(i, 2) = 1: Hd(i, 3) = 4: Units(i) = "J/kg"
113. If RaworPar = "Raw Data" Then
114.     i = i + 1: Hd(i, 1) = "Hwall": Hd(i, 2) = 1: Hd(i, 3) = 4: Units(i) = "J/
        kg"
115.     i = i + 1: Hd(i, 1) = "Hfilm": Hd(i, 2) = 1: Hd(i, 3) = 4: Units(i) = "J/
        kg"
116.     i = i + 1: Hd(i, 1) = "Hpc": Hd(i, 2) = 1: Hd(i, 3) = 2: Units(i) = "J/kg
    "

```

```

117. End If
118. 'i = 31
119. '-----
120. i = i + 1: Hd(i, 1) = "kbulk": Hd(i, 2) = 1: Hd(i, 3) = 4: Units(i) = "W/m·K"
121. If RaworPar = "Raw Data" Then
122.     i = i + 1: Hd(i, 1) = "kwall": Hd(i, 2) = 1: Hd(i, 3) = 4: Units(i) = "W/
m·K"
123.     i = i + 1: Hd(i, 1) = "kfilm": Hd(i, 2) = 1: Hd(i, 3) = 4: Units(i) = "W/
m·K"
124.     i = i + 1: Hd(i, 1) = "kpc": Hd(i, 2) = 1: Hd(i, 3) = 2: Units(i) = "W/m·
K"
125. End If
126. 'i = 35
127. '-----
128. i = i + 1: Hd(i, 1) = "Prbulk": Hd(i, 2) = 2: Hd(i, 3) = 4: Units(i) = "-"
129. If RaworPar = "Raw Data" Then
130.     i = i + 1: Hd(i, 1) = "Prwall": Hd(i, 2) = 2: Hd(i, 3) = 4: Units(i) = "-"
131.     i = i + 1: Hd(i, 1) = "Prfilm": Hd(i, 2) = 2: Hd(i, 3) = 4: Units(i) = "-"
132.     i = i + 1: Hd(i, 1) = "Prpc": Hd(i, 2) = 2: Hd(i, 3) = 2: Units(i) = "-"
133.     i = i + 1: Hd(i, 1) = "Pravg": Hd(i, 2) = 2: Hd(i, 3) = 3: Units(i) = "-"
134. End If
135. 'i = 40
136. '-----
137. i = i + 1: Hd(i, 1) = "Bbulk": Hd(i, 2) = 1: Hd(i, 3) = 4: Units(i) = "1/K"
138. If RaworPar = "Raw Data" Then
139.     i = i + 1: Hd(i, 1) = "Bwall": Hd(i, 2) = 1: Hd(i, 3) = 4: Units(i) = "1/
K"
140.     i = i + 1: Hd(i, 1) = "Bfilm": Hd(i, 2) = 1: Hd(i, 3) = 4: Units(i) = "1/
K"
141.     i = i + 1: Hd(i, 1) = "Bpc": Hd(i, 2) = 1: Hd(i, 3) = 2: Units(i) = "1/K"
142. End If
143. 'i = 44
144. '-----
145. i = i + 1: Hd(i, 1) = ChrW(945) & "bulk": Hd(i, 2) = 1: Hd(i, 3) = 4: Units(i
) = "m²/s"
146. If RaworPar = "Raw Data" Then
147.     i = i + 1: Hd(i, 1) = ChrW(945) & "wall": Hd(i, 2) = 1: Hd(i, 3) = 4: Uni
ts(i) = "m²/s"
148.     i = i + 1: Hd(i, 1) = ChrW(945) & "film": Hd(i, 2) = 1: Hd(i, 3) = 4: Uni
ts(i) = "m²/s"
149.     i = i + 1: Hd(i, 1) = ChrW(945) & "pc": Hd(i, 2) = 1: Hd(i, 3) = 2: Units
(i) = "m²/s"
150. End If
151. 'i = 48
152. '-----
153. i = i + 1: Hd(i, 1) = "Rebulk": Hd(i, 2) = 2: Hd(i, 3) = 4: Units(i) = "-"
154. If RaworPar = "Raw Data" Then
155.     i = i + 1: Hd(i, 1) = "Rewall": Hd(i, 2) = 2: Hd(i, 3) = 4: Units(i) = "-"

```

```

156.         i = i + 1: Hd(i, 1) = "Refilm": Hd(i, 2) = 2: Hd(i, 3) = 4: Units(i) = "-"
157.         i = i + 1: Hd(i, 1) = "Repc": Hd(i, 2) = 2: Hd(i, 3) = 2: Units(i) = "-"
158.     End If
159.     'i = 52
160.     '-----
161.     If RaworPar = "Raw Data" Then
162.         i = i + 1: Hd(i, 1) = "Nubulk": Hd(i, 2) = 2: Hd(i, 3) = 4: Units(i) = "-"
163.         i = i + 1: Hd(i, 1) = "Nuwall": Hd(i, 2) = 2: Hd(i, 3) = 4: Units(i) = "-"
164.         i = i + 1: Hd(i, 1) = "Nufilm": Hd(i, 2) = 2: Hd(i, 3) = 4: Units(i) = "-"
165.         i = i + 1: Hd(i, 1) = "Nupc": Hd(i, 2) = 2: Hd(i, 3) = 2: Units(i) = "-"
166.     End If
167.     'i = 56
168.     '-----
169.     If RaworPar = "Raw Data" Then
170.         i = i + 1: Hd(i, 1) = ChrW(960) & "bulk": Hd(i, 2) = 1: Hd(i, 3) = 4: Units(i) = "-"
171.         i = i + 1: Hd(i, 1) = ChrW(960) & "wall": Hd(i, 2) = 1: Hd(i, 3) = 4: Units(i) = "-"
172.         i = i + 1: Hd(i, 1) = ChrW(960) & "film": Hd(i, 2) = 1: Hd(i, 3) = 4: Units(i) = "-"
173.         i = i + 1: Hd(i, 1) = ChrW(960) & "pc": Hd(i, 2) = 1: Hd(i, 3) = 2: Units(i) = "-"
174.     End If
175.     'i = 60
176.     '-----
177.     If RaworPar = "Raw Data" Then
178.         i = i + 1: Hd(i, 1) = "Prw,avg": Hd(i, 2) = 2: Hd(i, 3) = 5: Units(i) = "-"
179.     End If
180.     'i = 61
181.     '-----
182.     If RaworPar = "Raw Data" Then
183.         i = i + 1: Hd(i, 1) = "Extra": Hd(i, 2) = 5: Units(i) = "-"
184.         i = i + 1: Hd(i, 1) = "Extra": Hd(i, 2) = 5: Units(i) = "-"
185.         i = i + 1: Hd(i, 1) = "Extra": Hd(i, 2) = 5: Units(i) = "-"
186.         i = i + 1: Hd(i, 1) = "Extra": Hd(i, 2) = 5: Units(i) = "-"
187.         i = i + 1: Hd(i, 1) = "Extra": Hd(i, 2) = 5: Units(i) = "-"
188.         'i = 66
189.         '-----
190.         i = i + 1: Hd(i, 1) = "Twall/" & vbCrLf & "Tbulk": Hd(i, 2) = 1: Hd(i, 3) = 4: Hd(i, 4) = 4: Hd(i, 5) = 4: Units(i) = "-"
191.         i = i + 1: Hd(i, 1) = "Tfilm/" & vbCrLf & "Tbulk": Hd(i, 2) = 1: Hd(i, 3) = 4: Hd(i, 4) = 4: Hd(i, 5) = 4: Units(i) = "-"
192.         i = i + 1: Hd(i, 1) = "Tpc/" & vbCrLf & "Tbulk": Hd(i, 2) = 1: Hd(i, 3) = 2: Hd(i, 4) = 4: Hd(i, 5) = 4: Units(i) = "-"
193.
194.         i = i + 1: Hd(i, 1) = "Tbulk/" & vbCrLf & "Twall": Hd(i, 2) = 1: Hd(i, 3) = 4: Hd(i, 4) = 4: Hd(i, 5) = 4: Units(i) = "-"
195.         i = i + 1: Hd(i, 1) = "Tfilm/" & vbCrLf & "Twall": Hd(i, 2) = 1: Hd(i, 3) = 4: Hd(i, 4) = 4: Hd(i, 5) = 4: Units(i) = "-"

```

```

196.      i = i + 1: Hd(i, 1) = "Tpc/" & vbCrLf & "Twall": Hd(i, 2) = 1: Hd(i, 3) =
      2: Hd(i, 4) = 4: Hd(i, 5) = 4: Units(i) = "-"
197.
198.      i = i + 1: Hd(i, 1) = "Tbulk/" & vbCrLf & "Tfilm": Hd(i, 2) = 1: Hd(i, 3)
      = 4: Hd(i, 4) = 4: Hd(i, 5) = 4: Units(i) = "-"
199.      i = i + 1: Hd(i, 1) = "Twall/" & vbCrLf & "Tfilm": Hd(i, 2) = 1: Hd(i, 3)
      = 4: Hd(i, 4) = 4: Hd(i, 5) = 4: Units(i) = "-"
200.      i = i + 1: Hd(i, 1) = "Tpc/" & vbCrLf & "Tfilm": Hd(i, 2) = 1: Hd(i, 3) =
      2: Hd(i, 4) = 4: Hd(i, 5) = 4: Units(i) = "-"
201.
202.      i = i + 1: Hd(i, 1) = "Tbulk/" & vbCrLf & "Tpc": Hd(i, 2) = 1: Hd(i, 3) =
      4: Hd(i, 4) = 4: Hd(i, 5) = 2: Units(i) = "-"
203.      i = i + 1: Hd(i, 1) = "Twall/" & vbCrLf & "Tpc": Hd(i, 2) = 1: Hd(i, 3) =
      4: Hd(i, 4) = 4: Hd(i, 5) = 2: Units(i) = "-"
204.      i = i + 1: Hd(i, 1) = "Tfilm/" & vbCrLf & "Tpc": Hd(i, 2) = 1: Hd(i, 3) =
      4: Hd(i, 4) = 4: Hd(i, 5) = 2: Units(i) = "-"
205.      'i = 78
206.      '-----
      '-----
207.      i = i + 1: Hd(i, 1) = ChrW(961) & "wall/" & vbCrLf & ChrW(961) & "bulk":
      Hd(i, 2) = 1: Hd(i, 3) = 4: Hd(i, 4) = 4: Hd(i, 5) = 4: Units(i) = "-"
208.      i = i + 1: Hd(i, 1) = ChrW(961) & "film/" & vbCrLf & ChrW(961) & "bulk":
      Hd(i, 2) = 1: Hd(i, 3) = 4: Hd(i, 4) = 4: Hd(i, 5) = 4: Units(i) = "-"
209.      i = i + 1: Hd(i, 1) = ChrW(961) & "pc/" & vbCrLf & ChrW(961) & "bulk": Hd
      (i, 2) = 1: Hd(i, 3) = 2: Hd(i, 4) = 4: Hd(i, 5) = 4: Units(i) = "-"
210.
211.      i = i + 1: Hd(i, 1) = ChrW(961) & "bulk/" & vbCrLf & ChrW(961) & "wall":
      Hd(i, 2) = 1: Hd(i, 3) = 4: Hd(i, 4) = 4: Hd(i, 5) = 4: Units(i) = "-"
212.      i = i + 1: Hd(i, 1) = ChrW(961) & "film/" & vbCrLf & ChrW(961) & "wall":
      Hd(i, 2) = 1: Hd(i, 3) = 4: Hd(i, 4) = 4: Hd(i, 5) = 4: Units(i) = "-"
213.      i = i + 1: Hd(i, 1) = ChrW(961) & "pc/" & vbCrLf & ChrW(961) & "wall": Hd
      (i, 2) = 1: Hd(i, 3) = 2: Hd(i, 4) = 4: Hd(i, 5) = 4: Units(i) = "-"
214.
215.      i = i + 1: Hd(i, 1) = ChrW(961) & "bulk/" & vbCrLf & ChrW(961) & "film":
      Hd(i, 2) = 1: Hd(i, 3) = 4: Hd(i, 4) = 4: Hd(i, 5) = 4: Units(i) = "-"
216.      i = i + 1: Hd(i, 1) = ChrW(961) & "wall/" & vbCrLf & ChrW(961) & "film":
      Hd(i, 2) = 1: Hd(i, 3) = 4: Hd(i, 4) = 4: Hd(i, 5) = 4: Units(i) = "-"
217.      i = i + 1: Hd(i, 1) = ChrW(961) & "pc/" & vbCrLf & ChrW(961) & "film": Hd
      (i, 2) = 1: Hd(i, 3) = 2: Hd(i, 4) = 4: Hd(i, 5) = 4: Units(i) = "-"
218.
219.      i = i + 1: Hd(i, 1) = ChrW(961) & "bulk/" & vbCrLf & ChrW(961) & "pc": Hd
      (i, 2) = 1: Hd(i, 3) = 4: Hd(i, 4) = 4: Hd(i, 5) = 2: Units(i) = "-"
220.      i = i + 1: Hd(i, 1) = ChrW(961) & "wall/" & vbCrLf & ChrW(961) & "pc": Hd
      (i, 2) = 1: Hd(i, 3) = 4: Hd(i, 4) = 4: Hd(i, 5) = 2: Units(i) = "-"
221.      i = i + 1: Hd(i, 1) = ChrW(961) & "film/" & vbCrLf & ChrW(961) & "pc": Hd
      (i, 2) = 1: Hd(i, 3) = 4: Hd(i, 4) = 4: Hd(i, 5) = 2: Units(i) = "-"
222.      'i = 90
223.      '-----
      '-----
224.      i = i + 1: Hd(i, 1) = "μwall/" & vbCrLf & "μbulk": Hd(i, 2) = 1: Hd(i, 3)
      = 4: Hd(i, 4) = 4: Hd(i, 5) = 4: Units(i) = "-"
225.      i = i + 1: Hd(i, 1) = "μfilm/" & vbCrLf & "μbulk": Hd(i, 2) = 1: Hd(i, 3)
      = 4: Hd(i, 4) = 4: Hd(i, 5) = 4: Units(i) = "-"
226.      i = i + 1: Hd(i, 1) = "μpc/" & vbCrLf & "μbulk": Hd(i, 2) = 1: Hd(i, 3) =
      2: Hd(i, 4) = 4: Hd(i, 5) = 4: Units(i) = "-"
227.
228.      i = i + 1: Hd(i, 1) = "μbulk/" & vbCrLf & "μwall": Hd(i, 2) = 1: Hd(i, 3)
      = 4: Hd(i, 4) = 4: Hd(i, 5) = 4: Units(i) = "-"
229.      i = i + 1: Hd(i, 1) = "μfilm/" & vbCrLf & "μwall": Hd(i, 2) = 1: Hd(i, 3)
      = 4: Hd(i, 4) = 4: Hd(i, 5) = 4: Units(i) = "-"

```



```

230.      i = i + 1: Hd(i, 1) = "μpc/" & vbCrLf & "μwall": Hd(i, 2) = 1: Hd(i, 3) =
      2: Hd(i, 4) = 4: Hd(i, 5) = 4: Units(i) = "-"
231.
232.      i = i + 1: Hd(i, 1) = "μbulk/" & vbCrLf & "μfilm": Hd(i, 2) = 1: Hd(i, 3)
      = 4: Hd(i, 4) = 4: Hd(i, 5) = 4: Units(i) = "-"
233.      i = i + 1: Hd(i, 1) = "μwall/" & vbCrLf & "μfilm": Hd(i, 2) = 1: Hd(i, 3)
      = 4: Hd(i, 4) = 4: Hd(i, 5) = 4: Units(i) = "-"
234.      i = i + 1: Hd(i, 1) = "μpc/" & vbCrLf & "μfilm": Hd(i, 2) = 1: Hd(i, 3) =
      2: Hd(i, 4) = 4: Hd(i, 5) = 4: Units(i) = "-"
235.
236.      i = i + 1: Hd(i, 1) = "μbulk/" & vbCrLf & "μpc": Hd(i, 2) = 1: Hd(i, 3) =
      4: Hd(i, 4) = 4: Hd(i, 5) = 2: Units(i) = "-"
237.      i = i + 1: Hd(i, 1) = "μwall/" & vbCrLf & "μpc": Hd(i, 2) = 1: Hd(i, 3) =
      4: Hd(i, 4) = 4: Hd(i, 5) = 2: Units(i) = "-"
238.      i = i + 1: Hd(i, 1) = "μfilm/" & vbCrLf & "μpc": Hd(i, 2) = 1: Hd(i, 3) =
      4: Hd(i, 4) = 4: Hd(i, 5) = 2: Units(i) = "-"
239.      'i = 102
240.      '-----
      '-----
241.      i = i + 1: Hd(i, 1) = ChrW(957) & "wall/" & vbCrLf & ChrW(957) & "bulk":
      Hd(i, 2) = 1: Hd(i, 3) = 4: Hd(i, 4) = 4: Hd(i, 5) = 4: Units(i) = "-"
242.      i = i + 1: Hd(i, 1) = ChrW(957) & "film/" & vbCrLf & ChrW(957) & "bulk":
      Hd(i, 2) = 1: Hd(i, 3) = 4: Hd(i, 4) = 4: Hd(i, 5) = 4: Units(i) = "-"
243.      i = i + 1: Hd(i, 1) = ChrW(957) & "pc/" & vbCrLf & ChrW(957) & "bulk": Hd
      (i, 2) = 1: Hd(i, 3) = 2: Hd(i, 4) = 4: Hd(i, 5) = 4: Units(i) = "-"
244.
245.      i = i + 1: Hd(i, 1) = ChrW(957) & "bulk/" & vbCrLf & ChrW(957) & "wall":
      Hd(i, 2) = 1: Hd(i, 3) = 4: Hd(i, 4) = 4: Hd(i, 5) = 4: Units(i) = "-"
246.      i = i + 1: Hd(i, 1) = ChrW(957) & "film/" & vbCrLf & ChrW(957) & "wall":
      Hd(i, 2) = 1: Hd(i, 3) = 4: Hd(i, 4) = 4: Hd(i, 5) = 4: Units(i) = "-"
247.      i = i + 1: Hd(i, 1) = ChrW(957) & "pc/" & vbCrLf & ChrW(957) & "wall": Hd
      (i, 2) = 1: Hd(i, 3) = 2: Hd(i, 4) = 4: Hd(i, 5) = 4: Units(i) = "-"
248.
249.      i = i + 1: Hd(i, 1) = ChrW(957) & "bulk/" & vbCrLf & ChrW(957) & "film":
      Hd(i, 2) = 1: Hd(i, 3) = 4: Hd(i, 4) = 4: Hd(i, 5) = 4: Units(i) = "-"
250.      i = i + 1: Hd(i, 1) = ChrW(957) & "wall/" & vbCrLf & ChrW(957) & "film":
      Hd(i, 2) = 1: Hd(i, 3) = 4: Hd(i, 4) = 4: Hd(i, 5) = 4: Units(i) = "-"
251.      i = i + 1: Hd(i, 1) = ChrW(957) & "pc/" & vbCrLf & ChrW(957) & "film": Hd
      (i, 2) = 1: Hd(i, 3) = 2: Hd(i, 4) = 4: Hd(i, 5) = 4: Units(i) = "-"
252.
253.      i = i + 1: Hd(i, 1) = ChrW(957) & "bulk/" & vbCrLf & ChrW(957) & "pc": Hd
      (i, 2) = 1: Hd(i, 3) = 4: Hd(i, 4) = 4: Hd(i, 5) = 2: Units(i) = "-"
254.      i = i + 1: Hd(i, 1) = ChrW(957) & "wall/" & vbCrLf & ChrW(957) & "pc": Hd
      (i, 2) = 1: Hd(i, 3) = 4: Hd(i, 4) = 4: Hd(i, 5) = 2: Units(i) = "-"
255.      i = i + 1: Hd(i, 1) = ChrW(957) & "film/" & vbCrLf & ChrW(957) & "pc": Hd
      (i, 2) = 1: Hd(i, 3) = 4: Hd(i, 4) = 4: Hd(i, 5) = 2: Units(i) = "-"
256.      'i = 112
257.      '-----
      '-----
258.      i = i + 1: Hd(i, 1) = "CPwall/" & vbCrLf & "CPbulk": Hd(i, 2) = 1: Hd(i,
      3) = 1: Hd(i, 4) = 4: Hd(i, 5) = 4: Hd(i, 6) = 1: Hd(i, 7) = 4: Units(i) = "-"
259.      i = i + 1: Hd(i, 1) = "CPfilm/" & vbCrLf & "CPbulk": Hd(i, 2) = 1: Hd(i,
      3) = 1: Hd(i, 4) = 4: Hd(i, 5) = 4: Hd(i, 6) = 1: Hd(i, 7) = 4: Units(i) = "-"
260.      i = i + 1: Hd(i, 1) = "CPpc/" & vbCrLf & "CPbulk": Hd(i, 2) = 1: Hd(i, 3)
      = 1: Hd(i, 4) = 2: Hd(i, 5) = 4: Hd(i, 6) = 1: Hd(i, 7) = 4: Units(i) = "-"
261.      i = i + 1: Hd(i, 1) = "CPavg/" & vbCrLf & "CPbulk": Hd(i, 2) = 1: Hd(i, 3
      ) = 1: Hd(i, 4) = 3: Hd(i, 5) = 4: Hd(i, 6) = 1: Hd(i, 7) = 4: Units(i) = "-"
262.
263.      i = i + 1: Hd(i, 1) = "CPbulk/" & vbCrLf & "CPwall": Hd(i, 2) = 1: Hd(i,
      3) = 1: Hd(i, 4) = 4: Hd(i, 5) = 4: Hd(i, 6) = 1: Hd(i, 7) = 4: Units(i) = "-"

```

```

264.      i = i + 1: Hd(i, 1) = "CPfilm/" & vbCrLf & "CPwall": Hd(i, 2) = 1: Hd(i,
3) = 1: Hd(i, 4) = 4: Hd(i, 5) = 4: Hd(i, 6) = 1: Hd(i, 7) = 4: Units(i) = "-"
265.      i = i + 1: Hd(i, 1) = "CPpc/" & vbCrLf & "CPwall": Hd(i, 2) = 1: Hd(i, 3)
= 1: Hd(i, 4) = 2: Hd(i, 5) = 4: Hd(i, 6) = 1: Hd(i, 7) = 4: Units(i) = "-"
266.      i = i + 1: Hd(i, 1) = "CPavg/" & vbCrLf & "CPwall": Hd(i, 2) = 1: Hd(i, 3
) = 1: Hd(i, 4) = 3: Hd(i, 5) = 4: Hd(i, 6) = 1: Hd(i, 7) = 4: Units(i) = "-"
267.
268.      i = i + 1: Hd(i, 1) = "CPbulk/" & vbCrLf & "CPfilm": Hd(i, 2) = 1: Hd(i,
3) = 1: Hd(i, 4) = 4: Hd(i, 5) = 4: Hd(i, 6) = 1: Hd(i, 7) = 4: Units(i) = "-"
269.      i = i + 1: Hd(i, 1) = "CPwall/" & vbCrLf & "CPfilm": Hd(i, 2) = 1: Hd(i,
3) = 1: Hd(i, 4) = 4: Hd(i, 5) = 4: Hd(i, 6) = 1: Hd(i, 7) = 4: Units(i) = "-"
270.      i = i + 1: Hd(i, 1) = "CPpc/" & vbCrLf & "CPfilm": Hd(i, 2) = 1: Hd(i, 3)
= 1: Hd(i, 4) = 2: Hd(i, 5) = 4: Hd(i, 6) = 1: Hd(i, 7) = 4: Units(i) = "-"
271.      i = i + 1: Hd(i, 1) = "CPavg/" & vbCrLf & "CPfilm": Hd(i, 2) = 1: Hd(i, 3
) = 1: Hd(i, 4) = 3: Hd(i, 5) = 4: Hd(i, 6) = 1: Hd(i, 7) = 4: Units(i) = "-"
272.
273.      i = i + 1: Hd(i, 1) = "CPbulk/" & vbCrLf & "CPpc": Hd(i, 2) = 1: Hd(i, 3)
= 1: Hd(i, 4) = 4: Hd(i, 5) = 4: Hd(i, 6) = 1: Hd(i, 7) = 2: Units(i) = "-"
274.      i = i + 1: Hd(i, 1) = "CPwall/" & vbCrLf & "CPpc": Hd(i, 2) = 1: Hd(i, 3)
= 1: Hd(i, 4) = 4: Hd(i, 5) = 4: Hd(i, 6) = 1: Hd(i, 7) = 2: Units(i) = "-"
275.      i = i + 1: Hd(i, 1) = "CPfilm/" & vbCrLf & "CPpc": Hd(i, 2) = 1: Hd(i, 3)
= 1: Hd(i, 4) = 4: Hd(i, 5) = 4: Hd(i, 6) = 1: Hd(i, 7) = 2: Units(i) = "-"
276.      i = i + 1: Hd(i, 1) = "CPavg/" & vbCrLf & "CPpc": Hd(i, 2) = 1: Hd(i, 3)
= 1: Hd(i, 4) = 3: Hd(i, 5) = 4: Hd(i, 6) = 1: Hd(i, 7) = 2: Units(i) = "-"
277.
278.      i = i + 1: Hd(i, 1) = "CPbulk/" & vbCrLf & "CPavg": Hd(i, 2) = 1: Hd(i, 3
) = 1: Hd(i, 4) = 4: Hd(i, 5) = 4: Hd(i, 6) = 1: Hd(i, 7) = 3: Units(i) = "-"
279.      i = i + 1: Hd(i, 1) = "CPwall/" & vbCrLf & "CPavg": Hd(i, 2) = 1: Hd(i, 3
) = 1: Hd(i, 4) = 4: Hd(i, 5) = 4: Hd(i, 6) = 1: Hd(i, 7) = 3: Units(i) = "-"
280.      i = i + 1: Hd(i, 1) = "CPfilm/" & vbCrLf & "CPavg": Hd(i, 2) = 1: Hd(i, 3
) = 1: Hd(i, 4) = 4: Hd(i, 5) = 4: Hd(i, 6) = 1: Hd(i, 7) = 3: Units(i) = "-"
281.      i = i + 1: Hd(i, 1) = "CPpc/" & vbCrLf & "CPavg": Hd(i, 2) = 1: Hd(i, 3)
= 1: Hd(i, 4) = 2: Hd(i, 5) = 4: Hd(i, 6) = 1: Hd(i, 7) = 3: Units(i) = "-"
282.      'i = 132
283.      '-----
-----
284.      i = i + 1: Hd(i, 1) = "Hwall/" & vbCrLf & "Hbulk": Hd(i, 2) = 1: Hd(i, 3)
= 4: Hd(i, 4) = 4: Hd(i, 5) = 4: Units(i) = "-"
285.      i = i + 1: Hd(i, 1) = "Hfilm/" & vbCrLf & "Hbulk": Hd(i, 2) = 1: Hd(i, 3)
= 4: Hd(i, 4) = 4: Hd(i, 5) = 4: Units(i) = "-"
286.      i = i + 1: Hd(i, 1) = "Hpc/" & vbCrLf & "Hbulk": Hd(i, 2) = 1: Hd(i, 3) =
2: Hd(i, 4) = 4: Hd(i, 5) = 4: Units(i) = "-"
287.
288.      i = i + 1: Hd(i, 1) = "Hbulk/" & vbCrLf & "Hwall": Hd(i, 2) = 1: Hd(i, 3)
= 4: Hd(i, 4) = 4: Hd(i, 5) = 4: Units(i) = "-"
289.      i = i + 1: Hd(i, 1) = "Hfilm/" & vbCrLf & "Hwall": Hd(i, 2) = 1: Hd(i, 3)
= 4: Hd(i, 4) = 4: Hd(i, 5) = 4: Units(i) = "-"
290.      i = i + 1: Hd(i, 1) = "Hpc/" & vbCrLf & "Hwall": Hd(i, 2) = 1: Hd(i, 3) =
2: Hd(i, 4) = 4: Hd(i, 5) = 4: Units(i) = "-"
291.
292.      i = i + 1: Hd(i, 1) = "Hbulk/" & vbCrLf & "Hfilm": Hd(i, 2) = 1: Hd(i, 3)
= 4: Hd(i, 4) = 4: Hd(i, 5) = 4: Units(i) = "-"
293.      i = i + 1: Hd(i, 1) = "Hwall/" & vbCrLf & "Hfilm": Hd(i, 2) = 1: Hd(i, 3)
= 4: Hd(i, 4) = 4: Hd(i, 5) = 4: Units(i) = "-"
294.      i = i + 1: Hd(i, 1) = "Hpc/" & vbCrLf & "Hfilm": Hd(i, 2) = 1: Hd(i, 3) =
2: Hd(i, 4) = 4: Hd(i, 5) = 4: Units(i) = "-"
295.
296.      i = i + 1: Hd(i, 1) = "Hbulk/" & vbCrLf & "Hpc": Hd(i, 2) = 1: Hd(i, 3) =
4: Hd(i, 4) = 4: Hd(i, 5) = 2: Units(i) = "-"
297.      i = i + 1: Hd(i, 1) = "Hwall/" & vbCrLf & "Hpc": Hd(i, 2) = 1: Hd(i, 3) =
4: Hd(i, 4) = 4: Hd(i, 5) = 2: Units(i) = "-"

```

```

298.         i = i + 1: Hd(i, 1) = "Hfilm/" & vbCrLf & "Hpc": Hd(i, 2) = 1: Hd(i, 3) =
         4: Hd(i, 4) = 4: Hd(i, 5) = 2: Units(i) = "-"
299.         'i = 144
300.         '-----
301.         i = i + 1: Hd(i, 1) = "kwall/" & vbCrLf & "kbulk": Hd(i, 2) = 1: Hd(i, 3)
         = 4: Hd(i, 4) = 4: Hd(i, 5) = 4: Units(i) = "-"
302.         i = i + 1: Hd(i, 1) = "kfilm/" & vbCrLf & "kbulk": Hd(i, 2) = 1: Hd(i, 3)
         = 4: Hd(i, 4) = 4: Hd(i, 5) = 4: Units(i) = "-"
303.         i = i + 1: Hd(i, 1) = "kpc/" & vbCrLf & "kbulk": Hd(i, 2) = 1: Hd(i, 3) =
         2: Hd(i, 4) = 4: Hd(i, 5) = 4: Units(i) = "-"
304.
305.         i = i + 1: Hd(i, 1) = "kbulk/" & vbCrLf & "kwall": Hd(i, 2) = 1: Hd(i, 3)
         = 4: Hd(i, 4) = 4: Hd(i, 5) = 4: Units(i) = "-"
306.         i = i + 1: Hd(i, 1) = "kfilm/" & vbCrLf & "kwall": Hd(i, 2) = 1: Hd(i, 3)
         = 4: Hd(i, 4) = 4: Hd(i, 5) = 4: Units(i) = "-"
307.         i = i + 1: Hd(i, 1) = "kpc/" & vbCrLf & "kwall": Hd(i, 2) = 1: Hd(i, 3) =
         2: Hd(i, 4) = 4: Hd(i, 5) = 4: Units(i) = "-"
308.
309.         i = i + 1: Hd(i, 1) = "kbulk/" & vbCrLf & "kfilm": Hd(i, 2) = 1: Hd(i, 3)
         = 4: Hd(i, 4) = 4: Hd(i, 5) = 4: Units(i) = "-"
310.         i = i + 1: Hd(i, 1) = "kwall/" & vbCrLf & "kfilm": Hd(i, 2) = 1: Hd(i, 3)
         = 4: Hd(i, 4) = 4: Hd(i, 5) = 4: Units(i) = "-"
311.         i = i + 1: Hd(i, 1) = "kpc/" & vbCrLf & "kfilm": Hd(i, 2) = 1: Hd(i, 3) =
         2: Hd(i, 4) = 4: Hd(i, 5) = 4: Units(i) = "-"
312.
313.         i = i + 1: Hd(i, 1) = "kbulk/" & vbCrLf & "kpc": Hd(i, 2) = 1: Hd(i, 3) =
         4: Hd(i, 4) = 4: Hd(i, 5) = 2: Units(i) = "-"
314.         i = i + 1: Hd(i, 1) = "kwall/" & vbCrLf & "kpc": Hd(i, 2) = 1: Hd(i, 3) =
         4: Hd(i, 4) = 4: Hd(i, 5) = 2: Units(i) = "-"
315.         i = i + 1: Hd(i, 1) = "kfilm/" & vbCrLf & "kpc": Hd(i, 2) = 1: Hd(i, 3) =
         4: Hd(i, 4) = 4: Hd(i, 5) = 2: Units(i) = "-"
316.         'i = 158
317.         '-----
318.         i = i + 1: Hd(i, 1) = "Prwall/" & vbCrLf & "Prbulk": Hd(i, 2) = 2: Hd(i,
         3) = 4: Hd(i, 4) = 5: Hd(i, 5) = 4: Units(i) = "-"
319.         i = i + 1: Hd(i, 1) = "Prfilm/" & vbCrLf & "Prbulk": Hd(i, 2) = 2: Hd(i,
         3) = 4: Hd(i, 4) = 5: Hd(i, 5) = 4: Units(i) = "-"
320.         i = i + 1: Hd(i, 1) = "Prpc/" & vbCrLf & "Prbulk": Hd(i, 2) = 2: Hd(i, 3)
         = 2: Hd(i, 4) = 5: Hd(i, 5) = 4: Units(i) = "-"
321.         i = i + 1: Hd(i, 1) = "Pravg/" & vbCrLf & "Prbulk": Hd(i, 2) = 2: Hd(i, 3
         ) = 3: Hd(i, 4) = 5: Hd(i, 5) = 4: Units(i) = "-"
322.
323.         i = i + 1: Hd(i, 1) = "Prbulk/" & vbCrLf & "Prwall": Hd(i, 2) = 2: Hd(i,
         3) = 4: Hd(i, 4) = 5: Hd(i, 5) = 4: Units(i) = "-"
324.         i = i + 1: Hd(i, 1) = "Prfilm/" & vbCrLf & "Prwall": Hd(i, 2) = 2: Hd(i,
         3) = 4: Hd(i, 4) = 5: Hd(i, 5) = 4: Units(i) = "-"
325.         i = i + 1: Hd(i, 1) = "Prpc/" & vbCrLf & "Prwall": Hd(i, 2) = 2: Hd(i, 3)
         = 2: Hd(i, 4) = 5: Hd(i, 5) = 4: Units(i) = "-"
326.         i = i + 1: Hd(i, 1) = "Pravg/" & vbCrLf & "Prwall": Hd(i, 2) = 2: Hd(i, 3
         ) = 3: Hd(i, 4) = 5: Hd(i, 5) = 4: Units(i) = "-"
327.
328.         i = i + 1: Hd(i, 1) = "Prbulk/" & vbCrLf & "Prfilm": Hd(i, 2) = 2: Hd(i,
         3) = 4: Hd(i, 4) = 5: Hd(i, 5) = 4: Units(i) = "-"
329.         i = i + 1: Hd(i, 1) = "Prwall/" & vbCrLf & "Prfilm": Hd(i, 2) = 2: Hd(i,
         3) = 4: Hd(i, 4) = 5: Hd(i, 5) = 4: Units(i) = "-"
330.         i = i + 1: Hd(i, 1) = "Prpc/" & vbCrLf & "Prfilm": Hd(i, 2) = 2: Hd(i, 3)
         = 2: Hd(i, 4) = 5: Hd(i, 5) = 4: Units(i) = "-"
331.         i = i + 1: Hd(i, 1) = "Pravg/" & vbCrLf & "Prfilm": Hd(i, 2) = 2: Hd(i, 3
         ) = 3: Hd(i, 4) = 5: Hd(i, 5) = 4: Units(i) = "-"

```

```

332.
333.     i = i + 1: Hd(i, 1) = "Prbulk/" & vbCrLf & "Prpc": Hd(i, 2) = 2: Hd(i, 3)
      = 4: Hd(i, 4) = 5: Hd(i, 5) = 2: Units(i) = "-"
334.     i = i + 1: Hd(i, 1) = "Prwall/" & vbCrLf & "Prpc": Hd(i, 2) = 2: Hd(i, 3)
      = 4: Hd(i, 4) = 5: Hd(i, 5) = 2: Units(i) = "-"
335.     i = i + 1: Hd(i, 1) = "Prfilm/" & vbCrLf & "Prpc": Hd(i, 2) = 2: Hd(i, 3)
      = 4: Hd(i, 4) = 5: Hd(i, 5) = 2: Units(i) = "-"
336.     i = i + 1: Hd(i, 1) = "Pravg/" & vbCrLf & "Prpc": Hd(i, 2) = 2: Hd(i, 3)
      = 3: Hd(i, 4) = 5: Hd(i, 5) = 2: Units(i) = "-"
337.
338.     i = i + 1: Hd(i, 1) = "Prbulk/" & vbCrLf & "Pravg": Hd(i, 2) = 2: Hd(i, 3)
      = 4: Hd(i, 4) = 5: Hd(i, 5) = 3: Units(i) = "-"
339.     i = i + 1: Hd(i, 1) = "Prwall/" & vbCrLf & "Pravg": Hd(i, 2) = 2: Hd(i, 3)
      = 4: Hd(i, 4) = 5: Hd(i, 5) = 3: Units(i) = "-"
340.     i = i + 1: Hd(i, 1) = "Prfilm/" & vbCrLf & "Pravg": Hd(i, 2) = 2: Hd(i, 3)
      = 4: Hd(i, 4) = 5: Hd(i, 5) = 3: Units(i) = "-"
341.     i = i + 1: Hd(i, 1) = "Prpc/" & vbCrLf & "Pravg": Hd(i, 2) = 2: Hd(i, 3)
      = 2: Hd(i, 4) = 5: Hd(i, 5) = 3: Units(i) = "-"
342.     'i = 178
343.     '-----
-----
344.     i = i + 1: Hd(i, 1) = "Bwall/" & vbCrLf & "Bbulk": Hd(i, 2) = 1: Hd(i, 3)
      = 4: Hd(i, 4) = 4: Hd(i, 5) = 4: Units(i) = "-"
345.     i = i + 1: Hd(i, 1) = "Bfilm/" & vbCrLf & "Bbulk": Hd(i, 2) = 1: Hd(i, 3)
      = 4: Hd(i, 4) = 4: Hd(i, 5) = 4: Units(i) = "-"
346.     i = i + 1: Hd(i, 1) = "Bpc/" & vbCrLf & "Bbulk": Hd(i, 2) = 1: Hd(i, 3) =
      2: Hd(i, 4) = 4: Hd(i, 5) = 4: Units(i) = "-"
347.
348.     i = i + 1: Hd(i, 1) = "Bbulk/" & vbCrLf & "Bwall": Hd(i, 2) = 1: Hd(i, 3)
      = 4: Hd(i, 4) = 4: Hd(i, 5) = 4: Units(i) = "-"
349.     i = i + 1: Hd(i, 1) = "Bfilm/" & vbCrLf & "Bwall": Hd(i, 2) = 1: Hd(i, 3)
      = 4: Hd(i, 4) = 4: Hd(i, 5) = 4: Units(i) = "-"
350.     i = i + 1: Hd(i, 1) = "Bpc/" & vbCrLf & "Bwall": Hd(i, 2) = 1: Hd(i, 3) =
      2: Hd(i, 4) = 4: Hd(i, 5) = 4: Units(i) = "-"
351.
352.     i = i + 1: Hd(i, 1) = "Bbulk/" & vbCrLf & "Bfilm": Hd(i, 2) = 1: Hd(i, 3)
      = 4: Hd(i, 4) = 4: Hd(i, 5) = 4: Units(i) = "-"
353.     i = i + 1: Hd(i, 1) = "Bwall/" & vbCrLf & "Bfilm": Hd(i, 2) = 1: Hd(i, 3)
      = 4: Hd(i, 4) = 4: Hd(i, 5) = 4: Units(i) = "-"
354.     i = i + 1: Hd(i, 1) = "Bpc/" & vbCrLf & "Bfilm": Hd(i, 2) = 1: Hd(i, 3) =
      2: Hd(i, 4) = 4: Hd(i, 5) = 4: Units(i) = "-"
355.
356.     i = i + 1: Hd(i, 1) = "Bbulk/" & vbCrLf & "Bpc": Hd(i, 2) = 1: Hd(i, 3) =
      4: Hd(i, 4) = 4: Hd(i, 5) = 2: Units(i) = "-"
357.     i = i + 1: Hd(i, 1) = "Bwall/" & vbCrLf & "Bpc": Hd(i, 2) = 1: Hd(i, 3) =
      4: Hd(i, 4) = 4: Hd(i, 5) = 2: Units(i) = "-"
358.     i = i + 1: Hd(i, 1) = "Bfilm/" & vbCrLf & "Bpc": Hd(i, 2) = 1: Hd(i, 3) =
      4: Hd(i, 4) = 4: Hd(i, 5) = 2: Units(i) = "-"
359.     'i = 190
360.     '-----
-----
361.     i = i + 1: Hd(i, 1) = ChrW(945) & "wall/" & vbCrLf & ChrW(945) & "bulk":
      Hd(i, 2) = 1: Hd(i, 3) = 4: Hd(i, 4) = 4: Hd(i, 5) = 4: Units(i) = "-"
362.     i = i + 1: Hd(i, 1) = ChrW(945) & "film/" & vbCrLf & ChrW(945) & "bulk":
      Hd(i, 2) = 1: Hd(i, 3) = 4: Hd(i, 4) = 4: Hd(i, 5) = 4: Units(i) = "-"
363.     i = i + 1: Hd(i, 1) = ChrW(945) & "pc/" & vbCrLf & ChrW(945) & "bulk": Hd
      (i, 2) = 1: Hd(i, 3) = 2: Hd(i, 4) = 4: Hd(i, 5) = 4: Units(i) = "-"
364.
365.     i = i + 1: Hd(i, 1) = ChrW(945) & "bulk/" & vbCrLf & ChrW(945) & "wall":
      Hd(i, 2) = 1: Hd(i, 3) = 4: Hd(i, 4) = 4: Hd(i, 5) = 4: Units(i) = "-"

```

```

366.      i = i + 1: Hd(i, 1) = ChrW(945) & "film/" & vbCrLf & ChrW(945) & "wall":
      Hd(i, 2) = 1: Hd(i, 3) = 4: Hd(i, 4) = 4: Hd(i, 5) = 4: Units(i) = "-"
367.      i = i + 1: Hd(i, 1) = ChrW(945) & "pc/" & vbCrLf & ChrW(945) & "wall": Hd
      (i, 2) = 1: Hd(i, 3) = 2: Hd(i, 4) = 4: Hd(i, 5) = 4: Units(i) = "-"
368.
369.      i = i + 1: Hd(i, 1) = ChrW(945) & "bulk/" & vbCrLf & ChrW(945) & "film":
      Hd(i, 2) = 1: Hd(i, 3) = 4: Hd(i, 4) = 4: Hd(i, 5) = 4: Units(i) = "-"
370.      i = i + 1: Hd(i, 1) = ChrW(945) & "wall/" & vbCrLf & ChrW(945) & "film":
      Hd(i, 2) = 1: Hd(i, 3) = 4: Hd(i, 4) = 4: Hd(i, 5) = 4: Units(i) = "-"
371.      i = i + 1: Hd(i, 1) = ChrW(945) & "pc/" & vbCrLf & ChrW(945) & "film": Hd
      (i, 2) = 1: Hd(i, 3) = 2: Hd(i, 4) = 4: Hd(i, 5) = 4: Units(i) = "-"
372.
373.      i = i + 1: Hd(i, 1) = ChrW(945) & "bulk/" & vbCrLf & ChrW(945) & "pc": Hd
      (i, 2) = 1: Hd(i, 3) = 4: Hd(i, 4) = 4: Hd(i, 5) = 2: Units(i) = "-"
374.      i = i + 1: Hd(i, 1) = ChrW(945) & "wall/" & vbCrLf & ChrW(945) & "pc": Hd
      (i, 2) = 1: Hd(i, 3) = 4: Hd(i, 4) = 4: Hd(i, 5) = 2: Units(i) = "-"
375.      i = i + 1: Hd(i, 1) = ChrW(945) & "film/" & vbCrLf & ChrW(945) & "pc": Hd
      (i, 2) = 1: Hd(i, 3) = 4: Hd(i, 4) = 4: Hd(i, 5) = 2: Units(i) = "-"
376.      'i = 202
377.      '-----
-----
378.      i = i + 1: Hd(i, 1) = "Rewall/" & vbCrLf & "Rebulk": Hd(i, 2) = 2: Hd(i,
      3) = 4: Hd(i, 4) = 5: Hd(i, 5) = 4: Units(i) = "-"
379.      i = i + 1: Hd(i, 1) = "Refilm/" & vbCrLf & "Rebulk": Hd(i, 2) = 2: Hd(i,
      3) = 4: Hd(i, 4) = 5: Hd(i, 5) = 4: Units(i) = "-"
380.      i = i + 1: Hd(i, 1) = "Repc/" & vbCrLf & "Rebulk": Hd(i, 2) = 2: Hd(i, 3)
      = 2: Hd(i, 4) = 5: Hd(i, 5) = 4: Units(i) = "-"
381.
382.      i = i + 1: Hd(i, 1) = "Rebulk/" & vbCrLf & "Rewall": Hd(i, 2) = 2: Hd(i,
      3) = 4: Hd(i, 4) = 5: Hd(i, 5) = 4: Units(i) = "-"
383.      i = i + 1: Hd(i, 1) = "Refilm/" & vbCrLf & "Rewall": Hd(i, 2) = 2: Hd(i,
      3) = 4: Hd(i, 4) = 5: Hd(i, 5) = 4: Units(i) = "-"
384.      i = i + 1: Hd(i, 1) = "Repc/" & vbCrLf & "Rewall": Hd(i, 2) = 2: Hd(i, 3)
      = 2: Hd(i, 4) = 5: Hd(i, 5) = 4: Units(i) = "-"
385.
386.      i = i + 1: Hd(i, 1) = "Rebulk/" & vbCrLf & "Refilm": Hd(i, 2) = 2: Hd(i,
      3) = 4: Hd(i, 4) = 5: Hd(i, 5) = 4: Units(i) = "-"
387.      i = i + 1: Hd(i, 1) = "Rewall/" & vbCrLf & "Refilm": Hd(i, 2) = 2: Hd(i,
      3) = 4: Hd(i, 4) = 5: Hd(i, 5) = 4: Units(i) = "-"
388.      i = i + 1: Hd(i, 1) = "Repc/" & vbCrLf & "Refilm": Hd(i, 2) = 2: Hd(i, 3)
      = 2: Hd(i, 4) = 5: Hd(i, 5) = 4: Units(i) = "-"
389.
390.      i = i + 1: Hd(i, 1) = "Rebulk/" & vbCrLf & "Repc": Hd(i, 2) = 2: Hd(i, 3)
      = 4: Hd(i, 4) = 5: Hd(i, 5) = 2: Units(i) = "-"
391.      i = i + 1: Hd(i, 1) = "Rewall/" & vbCrLf & "Repc": Hd(i, 2) = 2: Hd(i, 3)
      = 4: Hd(i, 4) = 5: Hd(i, 5) = 2: Units(i) = "-"
392.      i = i + 1: Hd(i, 1) = "Refilm/" & vbCrLf & "Repc": Hd(i, 2) = 2: Hd(i, 3)
      = 4: Hd(i, 4) = 5: Hd(i, 5) = 2: Units(i) = "-"
393.      'i = 214
394.      '-----
-----
395.      End If
396.      If Cells(R0, C0 + L1) <> C0 + L1 Then: Call HeadersPrint(Hd(), Units(), r, L,
      j):
397.
398.      If RaworPar = "Raw Data" Then
399.          For i = 1 To L2RD
400.              PropertiesTitle(i, 0) = Hd(i, 1)
401.              PropertiesTitle(i, 1) = 0
402.          Next i
403.      End If

```

```

404.
405.     End Sub
406.
407.
408.     Sub Headers3(r As Integer, L As Integer, L2 As Integer)
409.         Dim i As Integer, j As Integer
410.
411.         'Which Headers is being sent for color
412.         j = 3
413.
414.         'Introduce variant variables
415.         Dim Hd() As Variant, Units() As Variant
416.
417.         ReDim Hd(1 To L, 1 To ms) As Variant, Units(1 To L) As Variant
418.
419.         'Input Header string / Unit string
420.
421.         For i = 1 To TotalFormulas
422.             Hd(1 + 4 * (i - 1), 1) = "HTC" & vbCrLf & "#" & i: Hd(1 + 4 * (i - 1), 2)
               = 6 + Len(i): Units(1 + 4 * (i - 1)) = "kW/m2.K":
423.             Hd(2 + 4 * (i - 1), 1) = "Tw" & vbCrLf & "#" & i: Hd(2 + 4 * (i - 1), 2)
               = 5 + Len(i): Units(2 + 4 * (i - 1)) = "°C":
424.             Hd(3 + 4 * (i - 1), 1) = "# of Iter." & vbCrLf & "#" & i: Hd(3 + 4 * (i -
               1), 2) = 13 + Len(i): Units(3 + 4 * (i - 1)) = "#"
425.             Hd(4 + 4 * (i - 1), 1) = "Error" & vbCrLf & "#" & i: Hd(4 + 4 * (i - 1),
               2) = 8 + Len(i): Units(4 + 4 * (i - 1)) = "°C"
426.         Next i
427.
428.         If Cells(R0, C1 + L2) <> C0 + L1 Then: Call HeadersPrint(Hd(), Units(), r, L,
               j)
429.
430.     End Sub
431.
432.     Sub InputFormulaTitles()
433.         Dim i As Integer
434.         '-----
435.         '*****ADJUST AS NEEDED*****ADJUST AS NEEDED*****ADJUST AS
               NEEDED*****
436.         'Zero added in front of first 9 correlations to assist in sorting by correlat
               ion (otherwise 1 is proceeded by 10 in excel sorting)
437.         i = 1: FormulaTitle(i) = "0" & i & " - Dittus-
               Boelter, 1930" '1
438.         i = i + 1: FormulaTitle(i) = "0" & i & " - Sieder & Tate, 1936" '
               2
439.         i = i + 1: FormulaTitle(i) = "0" & i & " - Bringer & Smith, 1957" '
               3
440.         i = i + 1: FormulaTitle(i) = "0" & i & " - Miropol'skiy & Shitsman, 1957" '
               4
441.         i = i + 1: FormulaTitle(i) = "0" & i & " - Petukhov et al., 1961" '
               5
442.         i = i + 1: FormulaTitle(i) = "0" & i & " - Domin, 1963" '
               6
443.         i = i + 1: FormulaTitle(i) = "0" & i & " - Bishop et al., 1964" '
               7
444.         i = i + 1: FormulaTitle(i) = "0" & i & " - Swenson et al., 1965" '
               8
445.         i = i + 1: FormulaTitle(i) = "0" & i & " - Krasnoshchekov et al., 1967" '
               9
446.         i = i + 1: FormulaTitle(i) = i & " - Ornatsky et al., 1970" '
               10

```

```

447.   i = i + 1: FormulaTitle(i) = i & " - Giarratano et al., 1970"           '
11
448.   i = i + 1: FormulaTitle(i) = i & " - Yamagata et al., 1972"           '
12
449.   i = i + 1: FormulaTitle(i) = i & " - Zukauskas, 1972"                 '
13
450.   i = i + 1: FormulaTitle(i) = i & " - Jackson & Fewster, 1975"         '
14
451.   i = i + 1: FormulaTitle(i) = i & " - Gnielinski, 1976"               '
15
452.   i = i + 1: FormulaTitle(i) = i & " - Dyadyakin & Popov, 1977"         '
16
453.   i = i + 1: FormulaTitle(i) = i & " - Watts & Chou, 1982"             '
17
454.   i = i + 1: FormulaTitle(i) = i & " - Petukhov et al., 1983"           '
18
455.   i = i + 1: FormulaTitle(i) = i & " - Gorban et al., 1990"             '
19
456.   i = i + 1: FormulaTitle(i) = i & " - Griem, 1996"                   '
20
457.   i = i + 1: FormulaTitle(i) = i & " - Hu, 2001"                       '
21
458.   i = i + 1: FormulaTitle(i) = i & " - Kitoh et al., 2001"             '
22
459.   i = i + 1: FormulaTitle(i) = i & " - Jackson, 2002"                 '
23
460.   i = i + 1: FormulaTitle(i) = i & " - Xu & Guo, 2005"                 '
24
461.   i = i + 1: FormulaTitle(i) = i & " - Kuang et al., 2008"             '
25
462.   i = i + 1: FormulaTitle(i) = i & " - Yu et al., 2009"               '
26
463.   i = i + 1: FormulaTitle(i) = i & " - Cheng et al., 2009"            '
27
464.   i = i + 1: FormulaTitle(i) = i & " - Mokry et al., 2009"            '
28
465.   i = i + 1: FormulaTitle(i) = i & " - Gupta et al., 2011"             '
29
466.   i = i + 1: FormulaTitle(i) = i & " - Gupta et al., 2013 (Bulk)"       '
30
467.   i = i + 1: FormulaTitle(i) = i & " - Gupta et al., 2013 (Wall)"       '
31
468.   i = i + 1: FormulaTitle(i) = i & " - Gupta et al., 2013 (Film)"      '
32
469.   i = i + 1: FormulaTitle(i) = i & " - Chen & Fang, 2014"             '
33
470.   i = i + 1: FormulaTitle(i) = i & " - Wang & Li, 2014"               '
34
471.   i = i + 1: FormulaTitle(i) = i & " - Lei et al., 2019"              '
35
472.   i = i + 1: FormulaTitle(i) = i & " - Clark et al., 2020"            '
36
473.   '*****ADJUST AS NEEDED*****ADJUST AS NEEDED*****ADJUST AS
NEEDED*****
474.   '-----
-----
475.   End Sub

```

A.3.7 *GetPropertiesCode Module*

```
1. Sub GetAllProperties(i As Integer, f As Integer)
2.
3. Dim j As Integer, o As Integer, s As Integer
4.
5. T(i, 3, f) = (T(i, 1, f) + T(i, 2, f)) / 2
6. For j = 1 To 3
7.     Call REFPROPCALL(P(i), T(i, j, f), D(i, j, f), u(i, j, f), v(i, j, f), Cp(i,
8.         j, f), H(i, j, f), k(i, j, f), Pr(i, j, f), B(i, j, f) _
9.         , A(i, j, f))
10. Next j
11. If i = 1 Then
12.     Call TempPc(P(i), T(i, 4, 0))
13.     Call REFPROPCALL(P(i), T(i, 4, 0), D(i, 4, 0), u(i, 4, 0), v(i, 4, 0), Cp(i,
14.         4, 0), H(i, 4, 0), k(i, 4, 0), Pr(i, 4, 0), B(i, 4, 0) _
15.         , A(i, 4, 0))
16.     Din = D(i, 1, 0): uin = u(i, 1, 0):
17. ElseIf P(i) <> P(i - 1) Then
18.     Call TempPc(P(i), T(i, 4, 0))
19.     Call REFPROPCALL(P(i), T(i, 4, 0), D(i, 4, 0), u(i, 4, 0), v(i, 4, 0), Cp(i,
20.         4, 0), H(i, 4, 0), k(i, 4, 0), Pr(i, 4, 0), B(i, 4, 0) _
21.         , A(i, 4, 0))
22. Else
23.     T(i, 4, 0) = T(i - 1, 4, 0)
24.     D(i, 4, 0) = D(i - 1, 4, 0)
25.     u(i, 4, 0) = u(i - 1, 4, 0)
26.     v(i, 4, 0) = v(i - 1, 4, 0)
27.     Cp(i, 4, 0) = Cp(i - 1, 4, 0)
28.     H(i, 4, 0) = H(i - 1, 4, 0)
29.     k(i, 4, 0) = k(i - 1, 4, 0)
30.     Pr(i, 4, 0) = Pr(i - 1, 4, 0)
31.     B(i, 4, 0) = B(i - 1, 4, 0)
32.     A(i, 4, 0) = A(i - 1, 4, 0)
33. End If
34. Cp(i, 5, f) = (H(i, 2, f) - H(i, 1, f)) / (T(i, 2, f) - T(i, 1, f))
35. Pr(i, 5, f) = Cp(i, 5, f) * u(i, 1, f) / k(i, 1, f)
36. qNonD(i) = qavg(i) * B(i, 1, 0) / (G(i) * Cp(i, 1, 0))
37. Grst(i) = (9.81 * B(i, 1, 0) * (Dhy(i) ^ 4) * qavg(i)) / (k(i, 1, 0) * (v(i, 1, 0)
38.     ^ 2))
39. Ap(i, 1, 0) = (B(i, 1, 0) / Cp(i, 1, 0)) * (qavg(i) / G(i))
40. Ap(i, 2, 0) = (B(i, 2, 0) / Cp(i, 2, 0)) * (qavg(i) / G(i))
41. Ap(i, 3, 0) = (B(i, 3, 0) / Cp(i, 3, 0)) * (qavg(i) / G(i))
42. Ap(i, 4, 0) = (B(i, 4, 0) / Cp(i, 4, 0)) * (qavg(i) / G(i))
43. Prw(i, 0) = Cp(i, 5, 0) * u(i, 2, 0) / k(i, 2, 0)
44. For j = 1 To 4
45.     Re(i, j, f) = G(i) * Dhy(i) / u(i, j, f)
46.     If RaworPar = "Raw Data" Then
47.         Nu(i, j, 0) = HTC(i, 0) * Dhy(i) / k(i, j, 0)
48.     End If
49. Next j
50. For j = 1 To 4
51.     For o = 1 To 4
52.         If j <> o Then
53.             s = s + 1
54.             Ta(i, s, f) = T(i, o, f) / T(i, j, f)
55.             Da(i, s, f) = D(i, o, f) / D(i, j, f)
56.             ua(i, s, f) = u(i, o, f) / u(i, j, f)
57.             va(i, s, f) = v(i, o, f) / v(i, j, f)
58.             Ha(i, s, f) = H(i, o, f) / H(i, j, f)
59.             ka(i, s, f) = k(i, o, f) / k(i, j, f)
```



```

56.          Ba(i, s, f) = B(i, o, f) / B(i, j, f)
57.          Aa(i, s, f) = A(i, o, f) / A(i, j, f)
58.          Rea(i, s, f) = Re(i, o, f) / Re(i, j, f)
59.      End If
60.  Next o
61. Next j
62. s = 0
63. For j = 1 To 5
64.     For o = 1 To 5
65.         If j <> o Then
66.             s = s + 1
67.             Pra(i, s, f) = Pr(i, o, f) / Pr(i, j, f)
68.             Cpa(i, s, f) = Cp(i, o, f) / Cp(i, j, f)
69.         End If
70.     Next o
71. Next j
72.
73.
74. End Sub
75.
76. Sub GetProperties(i As Integer, f As Integer, j As Integer, e As Integer)
77. 'This code is used to get the bulk/pc properties for Parameters, and for all wall
  /film properties for correlations for
78. 'both Parameters and Raw Data
79. Dim ii As Integer
80.
81. 'If T and P are being used to call properties (e = 0)
82. If e = 0 Then
83.     Call REFPROPCALL(P(i), T(i, j, f), D(i, j, f), u(i, j, f), v(i, j, f), Cp(i,
  j, f), H(i, j, f), k(i, j, f), Pr(i, j, f), B(i, j, f) _
84.     , A(i, j, f))
85.     If i = 1 And f = 0 Then: Call TempPc(P(i), T(i, 4, 0)): Call REFPROPCALL(P(i)
  , T(i, 4, 0), D(i, 4, 0), u(i, 4, 0), v(i, 4, 0), _
86.     Cp(i, 4, 0), H(i, 4, 0), k(i, 4, 0), Pr(i, 4, 0), B(i, 4, 0), A(i, 4, 0)): Di
  n = D(i, 1, 0): uin = u(i, 1, 0):
87.     If i <> 1 Then
88.         If f = 0 And P(i) <> P(i - 1) Then: Call TempPc(P(i), T(i, 4, 0)): Call R
  EFPROPCALL(P(i), T(i, 4, 0), D(i, 4, 0), u(i, 4, 0), _
89.         v(i, 4, 0), Cp(i, 4, 0), H(i, 4, 0), k(i, 4, 0), Pr(i, 4, 0), B(i, 4, 0),
  A(i, 4, 0)):
90.         If RaworPar = "Raw Data" And xdist(i) < xdist(i - 1) Then: Din = D(i, 1,
  0): uin = u(i, 1, 0):
91.     End If
92.     Ap(i, 1, 0) = (B(i, 1, 0) / Cp(i, 1, 0)) * (qavg(i) / G(i))
93.     Ap(i, 4, 0) = (B(i, 4, 0) / Cp(i, 4, 0)) * (qavg(i) / G(i))
94. 'If H and P are being used to call properties (e = 1)
95. ElseIf e = 1 Then
96.     Call REFPROPCALL2(P(i), T(i, j, f), D(i, j, f), u(i, j, f), v(i, j, f), Cp(i,
  j, f), H(i, j, f), k(i, j, f), Pr(i, j, f), _
97.     B(i, j, f), A(i, j, f))
98.     If f = 0 And P(i) = P(i - 1) Then
99.         T(i, 4, 0) = T(i - 1, 4, 0)
100.        D(i, 4, 0) = D(i - 1, 4, 0)
101.        u(i, 4, 0) = u(i - 1, 4, 0)
102.        v(i, 4, 0) = v(i - 1, 4, 0)
103.        Cp(i, 4, 0) = Cp(i - 1, 4, 0)
104.        H(i, 4, 0) = H(i - 1, 4, 0)
105.        k(i, 4, 0) = k(i - 1, 4, 0)
106.        Pr(i, 4, 0) = Pr(i - 1, 4, 0)
107.        B(i, 4, 0) = B(i - 1, 4, 0)
108.        A(i, 4, 0) = A(i - 1, 4, 0)

```

```

109.     End If
110. End If
111.
112. 'When the bulk properties are called for (j = 1)
113. If j = 1 Then
114.     Re(i, 1, f) = G(i) * Dhy(i) / u(i, 1, f)
115.     If Re(i, 4, 0) = 0 Then
116.         Re(i, 4, 0) = G(i) * Dhy(i) / u(i, 4, 0)
117.     End If
118.     Grst(i) = (9.81 * B(i, 1, 0) * (Dhy(i) ^ 4) * qavg(i)) / (k(i, 1, 0) * (v
(i, 1, 0) ^ 2))
119.
120.
121. 'When the wall properties are called for (j = 2)
122. ElseIf j = 2 Then
123.     T(i, 3, f) = (T(i, 2, f) + T(i, 1, 0)) / 2
124.     Call REFPROPCALL(P(i), T(i, 3, f), D(i, 3, f), u(i, 3, f), v(i, 3, f), Cp
(i, 3, f), H(i, 3, f), k(i, 3, f), Pr(i, 3, f), B(i, 3, f) _
125.     , A(i, 3, f))
126.     Tg(i, 1, f) = T(i, 1, 0): Tg(i, 2, f) = (T(i, 1, 0) + T(i, 3, f)) / 2: Tg
(i, 3, f) = T(i, 3, f):
127.     Tg(i, 4, f) = (T(i, 3, f) + T(i, 2, f)) / 2: Tg(i, 5, f) = T(i, 2, f):
128.     Cp(i, 1, f) = Cp(i, 1, 0): Cp(i, 3, f) = Cp(i, 3, f): Cp(i, 5, f) = Cp
(i, 2, f):
129.     Call REFPROPCALL(P(i), Tg(i, 2, f), 0, 0, 0, Cp(i, 2, f), 0, 0, 0, 0, 0)
130.     Call REFPROPCALL(P(i), Tg(i, 4, f), 0, 0, 0, Cp(i, 4, f), 0, 0, 0, 0, 0)
131.     If i <> 1 Then
132.         If xdist(i) < xdist(i - 1) Then
133.             Din = D(i, 1, 0)
134.             uin = u(i, 1, 0)
135.         End If
136.     End If
137.     Re(i, 2, f) = G(i) * Dhy(i) / u(i, 2, f)
138.     Re(i, 3, f) = G(i) * Dhy(i) / u(i, 3, f)
139.     Cp(i, 5, f) = (H(i, 2, f) - H(i, 1, 0)) / (T(i, 2, f) - T(i, 1, 0))
140.     Pr(i, 5, f) = Cp(i, 5, f) * u(i, 1, 0) / k(i, 1, 0)
141.     nfc(i, 1) = 1.49 - 0.77 * (1 + 1 / Pr(i, 4, 0)): nfc(i, 2) = 1.44 * (1 +
1 / Pr(i, 4, 0)) - 0.53:
142.     Fc(i, f, 1) = 1: Fc(i, f, 2) = 0.67 * (Pr(i, 4, 0) ^ -
0.05) * ((Cp(i, 5, f) / Cp(i, 1, 0)) ^ nfc(i, 1)): Fc(i, f, 3) = _
143.     ((Cp(i, 5, f) / Cp(i, 1, 0)) ^ nfc(i, 2)):
144.     Davg(i, f) = (D(i, 1, 0) + D(i, 2, f)) / 2
145.     Gravg(i, f) = ((D(i, 1, 0) - Davg(i, f)) * 9.81 * (Dhy(i) ^ 3)) / (D(i, 1
, 0) * (v(i, 1, 0) ^ 2))
146.     Gamma(i, f) = Gravg(i, f) / ((Re(i, 1, 0) ^ 2.7) * (Pr(i, 5, f) ^ 0.5))
147.     qdet(i, 1) = 200 * (G(i) ^ 1.2)
148.     Fc(i, f, 4) = (2.9 * 10 ^ -8) + 0.11 / qdet(i, 1): Fc(i, f, 5) = (-
8.7 * 10 ^ -8) - 0.65 / qdet(i, 1): Fc(i, f, 6) = _
149.     (-9.7 * 10 ^ -7) + 1.3 / qdet(i, 1):
150.     Prw(i, f) = Cp(i, 5, f) * u(i, 2, f) / k(i, 2, f)
151.     Gr(i, f) = (9.81 * (Dhy(i) ^ 3) * (D(i, 1, 0) - D(i, 2, f))) / (D(i, 1, 0
) * (v(i, 1, 0) ^ 2))
152.     Cpmax1(i) = 0
153.     Cpmax2(i) = 0
154.     CpAVEgt(i) = 0
155.     For ii = 1 To 5
156.         If Cp(i, ii, f) > Cpmax1(i) Then: Cpmax2(i) = Cpmax1(i): Cpmax1(i) =
Cp(i, ii, f)
157.         CpAVEgt(i) = CpAVEgt(i) + Cp(i, ii, f)

```

```

158.     Next ii
159.     CpAVEgt(i) = (CpAVEgt(i) - Cpmx1(i) - Cpmx2(i)) / 3
160.     CpAVEg(i) = (Cpmx1(i) + Cpmx2(i) + CpAVEgt(i)) / 3
161.     Kg(i) = (k(i, 1, 0) + k(i, 2, f)) / 2
162.     Prg(i) = CpAVEg(i) * u(i, 1, 0) / Kg(i)
163.     If H(i, 1, 0) <= 1540000 Then: PHig(i) = 0.82:
164.     If H(i, 1, 0) >= 1740000 Then: PHig(i) = 1:
165.     If H(i, 1, 0) > 1540000 And H(i, 1, 0) < 1740000 Then: PHig(i) = 0.0009 *
        H(i, 1, 0) / 1000 - 0.566
166.     qNonD(i) = qavg(i) * B(i, 1, 0) / (G(i) * Cp(i, 5, f))
167.     Ap(i, 2, f) = (B(i, 2, f) / Cp(i, 2, f)) * (qavg(i) / G(i))
168.     Ap(i, 3, f) = (B(i, 3, f) / Cp(i, 3, f)) * (qavg(i) / G(i))
169. End If
170.
171. End Sub

```

A.3.8 *CalculateCorrelations Module*

```

1. Sub CalculateCorrelationsSub(i As Integer)
2. 'This sub is to calculate the Tw and HTC for each of the different correlations
3. '1 - Dittus-Boelter, 1930
4. '2 - Sieder & Tate, 1936
5. '3 - Bringer & Smith, 1957
6. '4 - Miropol'skiy & Shitsman, 1957
7. '5 - Petukhov et al., 1961
8. '6 - Domin, 1963
9. '7 - Bishop et al., 1964
10. '8 - Swenson et al., 1965
11. '9 - Krasnoshchekov et al., 1967
12. '10 - Ornatsky et al., 1970
13. '11 - Giarratano et al., 1970
14. '12 - Yamagata et al., 1972
15. '13 - Zukauskas, 1972
16. '14 - Jackson & Fewster, 1975
17. '15 - Gnielinski, 1976
18. '16 - Dyadyakin & Popov, 1977
19. '17 - Watts & Chou, 1982
20. '18 - Petukhov et al., 1983
21. '19 - Gorban et al., 1990
22. '20 - Griem, 1996
23. '21 - Hu, 2001
24. '22 - Kitoh et al., 2001
25. '23 - Jackson, 2002
26. '24 - Xu & Guo, 2005
27. '25 - Kuang et al., 2008
28. '26 - Yu et al., 2009
29. '27 - Cheng et al., 2009
30. '28 - Mokry et al., 2009
31. '29 - Gupta et al., 2011
32. '30 - Gupta et al., 2013 (Bulk)
33. '31 - Gupta et al., 2013 (Wall)
34. '32 - Gupta et al., 2013 (Film)
35. '33 - Chen & Fang, 2014
36. '34 - Wang & Li, 2014
37. '35 - Lei et al., 2019
38. '36 - Clark et al., 2020
39.

```

```

40. Dim f As Integer, exp As Double, j As Integer, TempT As Double, mm As Double, nn
    As Double, cc As Double, ffp As Double
41. Dim Eta As Double, Fmin(2) As Double, PiA(2) As Double
42.
43. For j = 1 To TotalFormulas
44.     It(i, j) = 0
45.     Errs(i, j) = MaxError + 1
46. Next j
47.
48. FrictF(i) = (1.82 * Log(Re(i, 1, 0)) / Log(10) - 1.64) ^ -2
49.
50. '-----
    -----
51. '*****ADJUST AS NEEDED*****ADJUST AS NEEDED*****ADJUST AS NEE
    DED*****
52. 'Re-arrange as needed (leave Dittus-Boelter in the first position)
53. 'Add as needed
54. '*****ADJUST AS NEEDED*****ADJUST AS NEEDED*****ADJUST AS NEE
    DED*****
55. '-----
    -----
56.
57.
58. '-----
    -----
59. '1 - Dittus-Boelter, 1930          *DO NOT REMOVE FROM FIRST POSITION!*
60. f = 1
61. If qavg(i) > 0 Then: exp = 0.4: Else: exp = 0.3:
62.
63. Nu(i, 1, f) = 0.023 * (Re(i, 1, 0) ^ 0.8) * (Pr(i, 1, 0) ^ exp)
64.
65. HTC(i, f) = Nu(i, 1, f) * k(i, 1, 0) / Dhy(i)
66.
67. T(i, 2, f) = T(i, 1, 0) + qavg(i) / HTC(i, f)
68.
69. Call GetProperties(i, f, 2, 0)
70.
71. It(i, f) = 1
72. Errs(i, f) = 0
73.
74. If RaworPar = "Raw Data" Then: HTCerrAvg(i, f) = ((HTC(i, f) / HTC(i, 0)) - 1): H
    TCErrAvgAbs(i, f) = Abs((HTC(i, f) / HTC(i, 0)) - 1):
75. If RaworPar = "Raw Data" Then: TwErrAvg(i, f) = ((T(i, 2, f) / T(i, 2, 0)) - 1):
    TwErrAvgAbs(i, f) = Abs((T(i, 2, f) / T(i, 2, 0)) - 1):
76. '-----
    -----
77. '-----
    -----
78. '2 - Sieder & Tate, 1936
79. f = f + 1
80. T(i, 2, f) = T(i, 2, 1)
81.
82. Do While Errs(i, f) > MaxError And It(i, f) < MaxLoop
83.     If T(i, 2, f) > (1300 * 1.5) - 273.15 Then: Exit Do
84.     Call GetProperties(i, f, 2, 0)
85.
86.     Nu(i, 1, f) = 0.027 * (Re(i, 1, 0) ^ 0.8) * (Pr(i, 1, 0) ^ (1 / 3)) * ((u(i,
        1, 0) / u(i, 2, f)) ^ 0.14)
87.
88.     HTC(i, f) = Nu(i, 1, f) * k(i, 1, 0) / Dhy(i)
89.     TempT = T(i, 1, 0) + qavg(i) / HTC(i, f)

```

```

90.     It(i, f) = It(i, f) + 1
91.     Errs(i, f) = Abs(T(i, 2, f) - TempT)
92.     T(i, 2, f) = TempT
93. Loop
94.
95. If RaworPar = "Raw Data" Then: HTCErrAvg(i, f) = ((HTC(i, f) / HTC(i, 0)) - 1): H
    TCErrAvgAbs(i, f) = Abs((HTC(i, f) / HTC(i, 0)) - 1):
96. If RaworPar = "Raw Data" Then: TwErrAvg(i, f) = ((T(i, 2, f) / T(i, 2, 0)) - 1):
    TwErrAvgAbs(i, f) = Abs((T(i, 2, f) / T(i, 2, 0)) - 1):
97. '-----
98. '-----
99. '3 - Bringer & Smith, 1957
100.  f = f + 1
101.  T(i, 2, f) = T(i, 2, 1)
102.
103.  Do While Errs(i, f) > MaxError And It(i, f) < MaxLoop
104.      If T(i, 2, f) > (1300 * 1.5) - 273.15 Then: Exit Do
105.      Call GetProperties(i, f, 2, 0)
106.
107.      exp = (T(i, 4, 0) - T(i, 1, 0)) / (T(i, 2, f) - T(i, 1, 0))
108.
109.      If exp < 0 Then
110.          Nu(i, 1, f) = 0.0266 * (Re(i, 1, 0) ^ 0.77) * (Pr(i, 2, f) ^ 0.55)
111.          HTC(i, f) = Nu(i, 1, f) * k(i, 1, 0) / Dhy(i)
112.      ElseIf exp >= 0 And exp <= 1 Then
113.          Nu(i, 1, f) = 0.0266 * (Re(i, 4, 0) ^ 0.77) * (Pr(i, 2, f) ^ 0.55)
114.          HTC(i, f) = Nu(i, 1, f) * k(i, 4, 0) / Dhy(i)
115.      ElseIf exp > 0 Then
116.          Nu(i, 1, f) = 0.0266 * (Re(i, 2, f) ^ 0.77) * (Pr(i, 2, f) ^ 0.55)
117.          HTC(i, f) = Nu(i, 1, f) * k(i, 2, f) / Dhy(i)
118.      End If
119.
120.      TempT = T(i, 1, 0) + qavg(i) / HTC(i, f)
121.      It(i, f) = It(i, f) + 1
122.      Errs(i, f) = Abs(T(i, 2, f) - TempT)
123.      T(i, 2, f) = TempT
124.  Loop
125.
126.  If RaworPar = "Raw Data" Then: HTCErrAvg(i, f) = ((HTC(i, f) / HTC(i, 0)) - 1
    ): HTCErrAvgAbs(i, f) = Abs((HTC(i, f) / HTC(i, 0)) - 1):
127.  If RaworPar = "Raw Data" Then: TwErrAvg(i, f) = ((T(i, 2, f) / T(i, 2, 0)) -
    1): TwErrAvgAbs(i, f) = Abs((T(i, 2, f) / T(i, 2, 0)) - 1):
128.  '-----
129.  '-----
130.  '4 - Miropol'skiy & Shitsman, 1957
131.  f = f + 1
132.  T(i, 2, f) = T(i, 2, 1)
133.
134.  Do While Errs(i, f) > MaxError And It(i, f) < MaxLoop
135.      If T(i, 2, f) > (1300 * 1.5) - 273.15 Then: Exit Do
136.      Call GetProperties(i, f, 2, 0)
137.
138.      If Pr(i, 2, f) <= Pr(i, 1, 0) Then
139.          Nu(i, 1, f) = 0.023 * (Re(i, 1, 0) ^ 0.8) * (Pr(i, 2, f) ^ (0.8))
140.      Else
141.          Nu(i, 1, f) = 0.023 * (Re(i, 1, 0) ^ 0.8) * (Pr(i, 1, 0) ^ (0.8))
142.      End If

```

```

143.
144.     HTC(i, f) = Nu(i, 1, f) * k(i, 1, 0) / Dhy(i)
145.     TempT = T(i, 1, 0) + qavg(i) / HTC(i, f)
146.     It(i, f) = It(i, f) + 1
147.     Errs(i, f) = Abs(T(i, 2, f) - TempT)
148.     T(i, 2, f) = TempT
149.     Loop
150.
151.     If RaworPar = "Raw Data" Then: HTCErrAvg(i, f) = ((HTC(i, f) / HTC(i, 0)) - 1
152.     ): HTCErrAvgAbs(i, f) = Abs((HTC(i, f) / HTC(i, 0)) - 1):
153.     If RaworPar = "Raw Data" Then: TwErrAvg(i, f) = ((T(i, 2, f) / T(i, 2, 0)) -
154.     1): TwErrAvgAbs(i, f) = Abs((T(i, 2, f) / T(i, 2, 0)) - 1):
155.     '-----
156.     '-----
157.     '5 - Petukhov et al., 1961
158.     f = f + 1
159.     T(i, 2, f) = T(i, 2, 1)
160.     Do While Errs(i, f) > MaxError And It(i, f) < MaxLoop
161.         If T(i, 2, f) > (1300 * 1.5) - 273.15 Then: Exit Do
162.         Call GetProperties(i, f, 2, 0)
163.         Nu0(i, f) = ((FrictF(i) / 8) * Re(i, 1, 0) * Pr(i, 5, f)) / (12.7 * ((Fri
164.         ctF(i) / 8) ^ 0.5) * ((Pr(i, 5, f) ^ (2 / 3)) - 1) + 1.07)
165.         Nu(i, 1, f) = Nu0(i, f) * ((u(i, 1, 0) / u(i, 2, f)) ^ 0.11) * ((k(i, 1,
166.         0) / k(i, 2, f)) ^ -0.33) * ((Cp(i, 5, f) / Cp(i, 1, 0)) ^ 0.35)
167.         HTC(i, f) = Nu(i, 1, f) * k(i, 1, 0) / Dhy(i)
168.         TempT = T(i, 1, 0) + qavg(i) / HTC(i, f)
169.         It(i, f) = It(i, f) + 1
170.         Errs(i, f) = Abs(T(i, 2, f) - TempT)
171.         T(i, 2, f) = TempT
172.     Loop
173.
174.     If RaworPar = "Raw Data" Then: HTCErrAvg(i, f) = ((HTC(i, f) / HTC(i, 0)) - 1
175.     ): HTCErrAvgAbs(i, f) = Abs((HTC(i, f) / HTC(i, 0)) - 1):
176.     If RaworPar = "Raw Data" Then: TwErrAvg(i, f) = ((T(i, 2, f) / T(i, 2, 0)) -
177.     1): TwErrAvgAbs(i, f) = Abs((T(i, 2, f) / T(i, 2, 0)) - 1):
178.     '-----
179.     '-----
180.     '6 - Domin, 1963
181.     f = f + 1
182.     T(i, 2, f) = T(i, 2, 1)
183.     Do While Errs(i, f) > MaxError And It(i, f) < MaxLoop
184.         If T(i, 2, f) > (1300 * 1.5) - 273.15 Then: Exit Do
185.         Call GetProperties(i, f, 2, 0)
186.
187.         If T(i, 2, f) >= 350 Then
188.             Nu(i, 1, f) = 0.1 * (Re(i, 1, 0) ^ 0.66) * (Pr(i, 1, 0) ^ (1.2))
189.         ElseIf T(i, 2, f) < 350 Then 'And T(i, 2, f) > 250 Then (Domin code origi
190.         nally called for the range to be between 350-250)
191.             Nu(i, 1, f) = 0.036 * (Re(i, 1, 0) ^ 0.8) * (Pr(i, 1, 0) ^ (0.4)) * (
192.             (u(i, 2, f) / u(i, 1, 0)))
193.         Else

```

```

192. ' Exit Do
193. End If
194. HTC(i, f) = Nu(i, 1, f) * k(i, 1, 0) / Dhy(i)
195. TempT = T(i, 1, 0) + qavg(i) / HTC(i, f)
196. It(i, f) = It(i, f) + 1
197. Errs(i, f) = Abs(T(i, 2, f) - TempT)
198. T(i, 2, f) = TempT
199. Loop
200.
201. If RaworPar = "Raw Data" Then: HTCErrAvg(i, f) = ((HTC(i, f) / HTC(i, 0)) - 1
): HTCErrAvgAbs(i, f) = Abs((HTC(i, f) / HTC(i, 0)) - 1):
202. If RaworPar = "Raw Data" Then: TwErrAvg(i, f) = ((T(i, 2, f) / T(i, 2, 0)) -
1): TwErrAvgAbs(i, f) = Abs((T(i, 2, f) / T(i, 2, 0)) - 1):
203. '-----
-----
204. '-----
-----
205. '7 - Bishop et al., 1964
206. f = f + 1
207. T(i, 2, f) = T(i, 2, 1)
208.
209. Do While Errs(i, f) > MaxError And It(i, f) < MaxLoop
210. If T(i, 2, f) > (1300 * 1.5) - 273.15 Then: Exit Do
211. Call GetProperties(i, f, 2, 0)
212.
213. If xdist(i) = 0 Then
214. Nu(i, 1, f) = 0.0069 * (Re(i, 1, 0) ^ 0.9) * (Pr(i, 5, f) ^ (0.66)) *
((D(i, 2, f) / D(i, 1, 0)) ^ 0.43)
215. Else
216. Nu(i, 1, f) = 0.0069 * (Re(i, 1, 0) ^ 0.9) * (Pr(i, 5, f) ^ (0.66)) *
((D(i, 2, f) / D(i, 1, 0)) ^ 0.43) * (1 + 2.4 * Dhy(i) / xdist(i))
217. End If
218.
219. HTC(i, f) = Nu(i, 1, f) * k(i, 1, 0) / Dhy(i)
220. TempT = T(i, 1, 0) + qavg(i) / HTC(i, f)
221. It(i, f) = It(i, f) + 1
222. Errs(i, f) = Abs(T(i, 2, f) - TempT)
223. T(i, 2, f) = TempT
224. Loop
225.
226. If RaworPar = "Raw Data" Then: HTCErrAvg(i, f) = ((HTC(i, f) / HTC(i, 0)) - 1
): HTCErrAvgAbs(i, f) = Abs((HTC(i, f) / HTC(i, 0)) - 1):
227. If RaworPar = "Raw Data" Then: TwErrAvg(i, f) = ((T(i, 2, f) / T(i, 2, 0)) -
1): TwErrAvgAbs(i, f) = Abs((T(i, 2, f) / T(i, 2, 0)) - 1):
228. '-----
-----
229. '-----
-----
230. '8 - Swenson et al., 1965
231. f = f + 1
232. T(i, 2, f) = T(i, 2, 1)
233.
234. Do While Errs(i, f) > MaxError And It(i, f) < MaxLoop
235. If T(i, 2, f) > (1300 * 1.5) - 273.15 Then: Exit Do
236. Call GetProperties(i, f, 2, 0)
237.
238. Nu(i, 1, f) = 0.00459 * (Re(i, 2, f) ^ 0.923) * ((Cp(i, 5, f) * u(i, 2, f)
) / k(i, 2, f)) ^ (0.613)) * ((D(i, 2, f) / D(i, 1, 0)) ^ 0.231)
239.
240. HTC(i, f) = Nu(i, 1, f) * k(i, 2, f) / Dhy(i)
241. TempT = T(i, 1, 0) + qavg(i) / HTC(i, f)

```

```

242.         It(i, f) = It(i, f) + 1
243.         Errs(i, f) = Abs(T(i, 2, f) - TempT)
244.         T(i, 2, f) = TempT
245.     Loop
246.
247.     If RaworPar = "Raw Data" Then: HTCErrAvg(i, f) = ((HTC(i, f) / HTC(i, 0)) - 1
): HTCErrAvgAbs(i, f) = Abs((HTC(i, f) / HTC(i, 0)) - 1):
248.     If RaworPar = "Raw Data" Then: TwErrAvg(i, f) = ((T(i, 2, f) / T(i, 2, 0)) -
1): TwErrAvgAbs(i, f) = Abs((T(i, 2, f) / T(i, 2, 0)) - 1):
249.     '-----
250.     '-----
251.     '9 - Krasnoshchekov et al., 1967
252.     f = f + 1
253.     T(i, 2, f) = T(i, 2, 1)
254.
255.     Do While Errs(i, f) > MaxError And It(i, f) < MaxLoop
256.         If T(i, 2, f) > (1300 * 1.5) - 273.15 Then: Exit Do
257.
258.         Call GetProperties(i, f, 2, 0)
259.         Nu0(i, f) = ((FrictF(i) / 8) * Re(i, 1, 0) * Pr(i, 5, f)) / (12.7 * ((Fri
ctF(i) / 8) ^ 0.5) * ((Pr(i, 5, f) ^ (2 / 3)) - 1) + 1.07)
260.
261.         If ((T(i, 2, f) + 273.15) / (T(i, 4, 0) + 273.15)) <= 1 Or ((T(i, 1, 0) +
273.15) / (T(i, 4, 0) + 273.15)) >= 1.2 Then
262.             exp = 0.4
263.         ElseIf ((T(i, 2, f) + 273.15) / (T(i, 4, 0) + 273.15)) >= 1 And ((T(i, 2,
f) + 273.15) / (T(i, 4, 0) + 273.15)) <= 2.5 Then
264.             exp = (0.22 + 0.18 * ((T(i, 2, f) + 273.15) / (T(i, 4, 0) + 273.15)))
265.         ElseIf ((T(i, 1, 0) + 273.15) / (T(i, 4, 0) + 273.15)) >= 1 And ((T(i, 1,
0) + 273.15) / (T(i, 4, 0) + 273.15)) <= 1.2 Then
266.             exp = (0.22 + 0.18 * ((T(i, 2, f) + 273.15) / (T(i, 4, 0) + 273.15)))
+ (5 * (0.22 + 0.18 * ((T(i, 2, f) + 273.15) / _
267.             (T(i, 4, 0) + 273.15))) - 2) * (1 - ((T(i, 1, 0) + 273.15) / (T(i, 4,
0) + 273.15)))
268.         End If
269.
270.         Nu(i, 1, f) = Nu0(i, f) * ((D(i, 2, f) / D(i, 1, 0)) ^ 0.3) * ((Cp(i, 5,
f) / Cp(i, 1, 0)) ^ exp)
271.
272.         HTC(i, f) = Nu(i, 1, f) * k(i, 1, 0) / Dhy(i)
273.         TempT = T(i, 1, 0) + qavg(i) / HTC(i, f)
274.         It(i, f) = It(i, f) + 1
275.         Errs(i, f) = Abs(T(i, 2, f) - TempT)
276.         T(i, 2, f) = TempT
277.     Loop
278.
279.     If RaworPar = "Raw Data" Then: HTCErrAvg(i, f) = ((HTC(i, f) / HTC(i, 0)) - 1
): HTCErrAvgAbs(i, f) = Abs((HTC(i, f) / HTC(i, 0)) - 1):
280.     If RaworPar = "Raw Data" Then: TwErrAvg(i, f) = ((T(i, 2, f) / T(i, 2, 0)) -
1): TwErrAvgAbs(i, f) = Abs((T(i, 2, f) / T(i, 2, 0)) - 1):
281.     '-----
282.     '-----
283.     '10 - Ornatsky et al., 1970
284.     f = f + 1
285.     T(i, 2, f) = T(i, 2, 1)
286.

```



```

287. Do While Errs(i, f) > MaxError And It(i, f) < MaxLoop
288.   If T(i, 2, f) > (1300 * 1.5) - 273.15 Then: Exit Do
289.   Call GetProperties(i, f, 2, 0)
290.
291.   If Pr(i, 2, f) <= Pr(i, 1, 0) Then
292.     Nu(i, 1, f) = 0.023 * (Re(i, 1, 0) ^ 0.8) * (Pr(i, 2, f) ^ (0.8)) * (
      (D(i, 2, f) / D(i, 1, 0)) ^ 0.3)
293.   Else
294.     Nu(i, 1, f) = 0.023 * (Re(i, 1, 0) ^ 0.8) * (Pr(i, 1, 0) ^ (0.8)) * (
      (D(i, 2, f) / D(i, 1, 0)) ^ 0.3)
295.   End If
296.
297.   HTC(i, f) = Nu(i, 1, f) * k(i, 1, 0) / Dhy(i)
298.   TempT = T(i, 1, 0) + qavg(i) / HTC(i, f)
299.   It(i, f) = It(i, f) + 1
300.   Errs(i, f) = Abs(T(i, 2, f) - TempT)
301.   T(i, 2, f) = TempT
302. Loop
303.
304. If RaworPar = "Raw Data" Then: HTCErrAvg(i, f) = ((HTC(i, f) / HTC(i, 0)) - 1
      ): HTCErrAvgAbs(i, f) = Abs((HTC(i, f) / HTC(i, 0)) - 1):
305. If RaworPar = "Raw Data" Then: TwErrAvg(i, f) = ((T(i, 2, f) / T(i, 2, 0)) -
      1): TwErrAvgAbs(i, f) = Abs((T(i, 2, f) / T(i, 2, 0)) - 1):
306. '-----
307. '-----
308. '11 - Giarratano et al., 1970
309. f = f + 1
310. T(i, 2, f) = T(i, 2, 1)
311.
312. Do While Errs(i, f) > MaxError And It(i, f) < MaxLoop
313.   If T(i, 2, f) > (1300 * 1.5) - 273.15 Then: Exit Do
314.   Call GetProperties(i, f, 2, 0)
315.
316.   Nu(i, 1, f) = 0.0259 * (Re(i, 1, 0) ^ 0.8) * (Pr(i, 1, 0) ^ (0.4)) * (((T
      (i, 2, f) + 273.15) / (T(i, 1, 0) + 273.15)) ^ -0.716)
317.
318.   HTC(i, f) = Nu(i, 1, f) * k(i, 1, 0) / Dhy(i)
319.   TempT = T(i, 1, 0) + qavg(i) / HTC(i, f)
320.   It(i, f) = It(i, f) + 1
321.   Errs(i, f) = Abs(T(i, 2, f) - TempT)
322.   T(i, 2, f) = TempT
323. Loop
324.
325. If RaworPar = "Raw Data" Then: HTCErrAvg(i, f) = ((HTC(i, f) / HTC(i, 0)) - 1
      ): HTCErrAvgAbs(i, f) = Abs((HTC(i, f) / HTC(i, 0)) - 1):
326. If RaworPar = "Raw Data" Then: TwErrAvg(i, f) = ((T(i, 2, f) / T(i, 2, 0)) -
      1): TwErrAvgAbs(i, f) = Abs((T(i, 2, f) / T(i, 2, 0)) - 1):
327. '-----
328. '-----
329. '12 - Yamagata et al., 1972
330. f = f + 1
331. T(i, 2, f) = T(i, 2, 1)
332.
333. Do While Errs(i, f) > MaxError And It(i, f) < MaxLoop
334.   If T(i, 2, f) > (1300 * 1.5) - 273.15 Then: Exit Do
335.   Call GetProperties(i, f, 2, 0)
336.

```

```

337.         exp = (T(i, 4, 0) - T(i, 1, 0)) / (T(i, 2, f) - T(i, 1, 0))
338.
339.         If exp > 1 Then: FcUsed = Fc(i, f, 1):
340.         If exp >= 0 And exp <= 1 Then: FcUsed = Fc(i, f, 2):
341.         If exp < 0 Then: FcUsed = Fc(i, f, 3):
342.
343.         Nu(i, 1, f) = 0.0135 * (Re(i, 1, 0) ^ 0.85) * (Pr(i, 1, 0) ^ (0.8)) * FcU
sed
344.
345.         HTC(i, f) = Nu(i, 1, f) * k(i, 1, 0) / Dhy(i)
346.         TempT = T(i, 1, 0) + qavg(i) / HTC(i, f)
347.         It(i, f) = It(i, f) + 1
348.         Errs(i, f) = Abs(T(i, 2, f) - TempT)
349.         T(i, 2, f) = TempT
350.     Loop
351.
352.     If RaworPar = "Raw Data" Then: HTCErrAvg(i, f) = ((HTC(i, f) / HTC(i, 0)) - 1
): HTCErrAvgAbs(i, f) = Abs((HTC(i, f) / HTC(i, 0)) - 1):
353.     If RaworPar = "Raw Data" Then: TwErrAvg(i, f) = ((T(i, 2, f) / T(i, 2, 0)) -
1): TwErrAvgAbs(i, f) = Abs((T(i, 2, f) / T(i, 2, 0)) - 1):
354.     '-----
355.     '-----
356.     '13 - Zukauskas, 1972
357.     f = f + 1
358.     T(i, 2, f) = T(i, 2, 1)
359.
360.     Do While Errs(i, f) > MaxError And It(i, f) < MaxLoop
361.         If T(i, 2, f) > (1300 * 1.5) - 273.15 Then: Exit Do
362.         Call GetProperties(i, f, 2, 0)
363.
364.         If Re(i, 1, 0) <= 40 Then: cc = 0.75: mm = 0.4:
365.         If (Re(i, 1, 0) > 40 And Re(i, 1, 0) <= 1000) Then: cc = 0.51: mm = 0.5:
366.         If (Re(i, 1, 0) > 1000 And Re(i, 1, 0) <= 2 * 10 ^ 5) Then: cc = 0.26: mm
= 0.6:
367.         If Re(i, 1, 0) > 2 * 10 ^ 5 Then: cc = 0.076: mm = 0.7: 'original correla
tion only goes up to Re = 10^6
368.         If Pr(i, 1, 0) <= 10 Then: nn = 0.37: Else: nn = 0.36:
369.
370.         Nu(i, 1, f) = cc * (Re(i, 1, 0) ^ mm) * (Pr(i, 1, 0) ^ nn) * ((Pr(i, 1, 0
) / Pr(i, 2, f)) ^ 0.25)
371.
372.         HTC(i, f) = Nu(i, 1, f) * k(i, 1, 0) / Dhy(i)
373.         TempT = T(i, 1, 0) + qavg(i) / HTC(i, f)
374.         It(i, f) = It(i, f) + 1
375.         Errs(i, f) = Abs(T(i, 2, f) - TempT)
376.         T(i, 2, f) = TempT
377.     Loop
378.
379.     If RaworPar = "Raw Data" Then: HTCErrAvg(i, f) = ((HTC(i, f) / HTC(i, 0)) - 1
): HTCErrAvgAbs(i, f) = Abs((HTC(i, f) / HTC(i, 0)) - 1):
380.     If RaworPar = "Raw Data" Then: TwErrAvg(i, f) = ((T(i, 2, f) / T(i, 2, 0)) -
1): TwErrAvgAbs(i, f) = Abs((T(i, 2, f) / T(i, 2, 0)) - 1):
381.     '-----
382.     '-----
383.     '14 - Jackson & Fewster, 1975
384.     f = f + 1

```

```

385.   T(i, 2, f) = T(i, 2, 1)
386.
387.   Do While Errs(i, f) > MaxError And It(i, f) < MaxLoop
388.       If T(i, 2, f) > (1300 * 1.5) - 273.15 Then: Exit Do
389.       Call GetProperties(i, f, 2, 0)
390.
391.       Nu(i, 1, f) = 0.0183 * (Re(i, 1, 0) ^ 0.82) * (Pr(i, 5, f) ^ 0.5) * ((D(i
, 2, f) / D(i, 1, 0)) ^ 0.3)
392.
393.       HTC(i, f) = Nu(i, 1, f) * k(i, 1, 0) / Dhy(i)
394.       TempT = T(i, 1, 0) + qavg(i) / HTC(i, f)
395.       It(i, f) = It(i, f) + 1
396.       Errs(i, f) = Abs(T(i, 2, f) - TempT)
397.       T(i, 2, f) = TempT
398.   Loop
399.
400.   If RaworPar = "Raw Data" Then: HTCErrAvg(i, f) = ((HTC(i, f) / HTC(i, 0)) - 1
): HTCErrAvgAbs(i, f) = Abs((HTC(i, f) / HTC(i, 0)) - 1):
401.   If RaworPar = "Raw Data" Then: TwErrAvg(i, f) = ((T(i, 2, f) / T(i, 2, 0)) -
1): TwErrAvgAbs(i, f) = Abs((T(i, 2, f) / T(i, 2, 0)) - 1):
402.   '-----
403.   '-----
404.   '15 - Gnielinski, 1976
405.   f = f + 1
406.   T(i, 2, f) = T(i, 2, 1)
407.
408.   Do While Errs(i, f) > MaxError And It(i, f) < MaxLoop
409.       If T(i, 2, f) > (1300 * 1.5) - 273.15 Then: Exit Do
410.       Call GetProperties(i, f, 2, 0)
411.
412.       ffp = (0.79 * Log(Re(i, 1, 0)) - 1.64) ^ -2
413.
414.       Nu(i, 1, f) = ((ffp / 8) * (Re(i, 1, 0) - 1000) * Pr(i, 1, 0)) / (1 + 12.
7 * ((ffp / 8) ^ 0.5) * ((Pr(i, 1, 0) ^ (2 / 3)) - 1))
415.
416.       HTC(i, f) = Nu(i, 1, f) * k(i, 1, 0) / Dhy(i)
417.       TempT = T(i, 1, 0) + qavg(i) / HTC(i, f)
418.       It(i, f) = It(i, f) + 1
419.       Errs(i, f) = Abs(T(i, 2, f) - TempT)
420.       T(i, 2, f) = TempT
421.   Loop
422.
423.   If RaworPar = "Raw Data" Then: HTCErrAvg(i, f) = ((HTC(i, f) / HTC(i, 0)) - 1
): HTCErrAvgAbs(i, f) = Abs((HTC(i, f) / HTC(i, 0)) - 1):
424.   If RaworPar = "Raw Data" Then: TwErrAvg(i, f) = ((T(i, 2, f) / T(i, 2, 0)) -
1): TwErrAvgAbs(i, f) = Abs((T(i, 2, f) / T(i, 2, 0)) - 1):
425.   '-----
426.   '-----
427.   '16 - Dyadyakin & Popov, 1977
428.   f = f + 1
429.   T(i, 2, f) = T(i, 2, 1)
430.
431.   Do While Errs(i, f) > MaxError And It(i, f) < MaxLoop
432.       If T(i, 2, f) > (1300 * 1.5) - 273.15 Then: Exit Do
433.       Call GetProperties(i, f, 2, 0)
434.
435.       If i = 1 Then

```

```

436.         Nu(i, 1, f) = 0.021 * (Re(i, 1, 0) ^ 0.8) * (Pr(i, 5, f) ^ 0.7) * ((D
(i, 2, f) / D(i, 1, 0)) ^ 0.45) * ((u(i, 1, 0) / uin) ^ 0.2) * _
437.         ((D(i, 1, 0) / Din) ^ 0.1)
438.     Else
439.         Nu(i, 1, f) = 0.021 * (Re(i, 1, 0) ^ 0.8) * (Pr(i, 5, f) ^ 0.7) * ((D
(i, 2, f) / D(i, 1, 0)) ^ 0.45) * ((u(i, 1, 0) / uin) ^ 0.2) * _
440.         ((D(i, 1, 0) / Din) ^ 0.1) * (1 + 2.5 * Dhy(i) / xdist(i))
441.     End If
442.
443.     HTC(i, f) = Nu(i, 1, f) * k(i, 1, 0) / Dhy(i)
444.     TempT = T(i, 1, 0) + qavg(i) / HTC(i, f)
445.     It(i, f) = It(i, f) + 1
446.     Errs(i, f) = Abs(T(i, 2, f) - TempT)
447.     T(i, 2, f) = TempT
448. Loop
449.
450. If RaworPar = "Raw Data" Then: HTCErrAvg(i, f) = ((HTC(i, f) / HTC(i, 0)) - 1
): HTCErrAvgAbs(i, f) = Abs((HTC(i, f) / HTC(i, 0)) - 1):
451. If RaworPar = "Raw Data" Then: TwErrAvg(i, f) = ((T(i, 2, f) / T(i, 2, 0)) -
1): TwErrAvgAbs(i, f) = Abs((T(i, 2, f) / T(i, 2, 0)) - 1):
452. '-----
453. '-----
454. '17 - Watts & Chou, 1982
455. f = f + 1
456. T(i, 2, f) = T(i, 2, 1)
457.
458. Do While Errs(i, f) > MaxError And It(i, f) < MaxLoop
459.     If T(i, 2, f) > (1300 * 1.5) - 273.15 Then: Exit Do
460.     Call GetProperties(i, f, 2, 0)
461.
462.     If Gamma(i, f) < 10 ^ -4 Then
463.         Nu(i, 1, f) = 0.021 * (Re(i, 1, 0) ^ 0.8) * (Pr(i, 5, f) ^ 0.55) * ((
D(i, 2, f) / D(i, 1, 0)) ^ 0.35) * ((1 - 3000 * Gamma(i, f)) ^ 0.295)
464.     Else
465.         Nu(i, 1, f) = 0.021 * (Re(i, 1, 0) ^ 0.8) * (Pr(i, 5, f) ^ 0.55) * ((
D(i, 2, f) / D(i, 1, 0)) ^ 0.35) * ((7000 * Gamma(i, f)) ^ 0.295)
466.     End If
467.
468.     HTC(i, f) = Nu(i, 1, f) * k(i, 1, 0) / Dhy(i)
469.     TempT = T(i, 1, 0) + qavg(i) / HTC(i, f)
470.     It(i, f) = It(i, f) + 1
471.     Errs(i, f) = Abs(T(i, 2, f) - TempT)
472.     T(i, 2, f) = TempT
473. Loop
474.
475. If RaworPar = "Raw Data" Then: HTCErrAvg(i, f) = ((HTC(i, f) / HTC(i, 0)) - 1
): HTCErrAvgAbs(i, f) = Abs((HTC(i, f) / HTC(i, 0)) - 1):
476. If RaworPar = "Raw Data" Then: TwErrAvg(i, f) = ((T(i, 2, f) / T(i, 2, 0)) -
1): TwErrAvgAbs(i, f) = Abs((T(i, 2, f) / T(i, 2, 0)) - 1):
477. '-----
478. '-----
479. '18 - Petukhov et al., 1990
480. f = f + 1
481. T(i, 2, f) = T(i, 2, 1)
482.
483. Do While Errs(i, f) > MaxError And It(i, f) < MaxLoop
484.     If T(i, 2, f) > (1300 * 1.5) - 273.15 Then: Exit Do

```

```

485.      Call GetProperties(i, f, 2, 0)
486.
487.      Eta = FrictF(i) * ((D(i, 2, f) / D(i, 1, 0)) ^ 0.4) * ((u(i, 2, f) / u(i,
1, 0)) ^ 0.2)
488.
489.      Nu(i, 1, f) = ((Eta / 8) / (12.7 * ((Eta / 8) ^ 0.5) * ((Pr(i, 5, f) ^ (2
/ 3)) - 1) + 1 + 900 / Re(i, 1, 0))) * _
490.      Re(i, 1, 0) * Pr(i, 1, 0)
491.
492.      HTC(i, f) = Nu(i, 1, f) * k(i, 1, 0) / Dhy(i)
493.      TempT = T(i, 1, 0) + qavg(i) / HTC(i, f)
494.      It(i, f) = It(i, f) + 1
495.      Errs(i, f) = Abs(T(i, 2, f) - TempT)
496.      T(i, 2, f) = TempT
497.      Loop
498.
499.      If RaworPar = "Raw Data" Then: HTCErrAvg(i, f) = ((HTC(i, f) / HTC(i, 0)) - 1
): HTCErrAvgAbs(i, f) = Abs((HTC(i, f) / HTC(i, 0)) - 1):
500.      If RaworPar = "Raw Data" Then: TwErrAvg(i, f) = ((T(i, 2, f) / T(i, 2, 0)) -
1): TwErrAvgAbs(i, f) = Abs((T(i, 2, f) / T(i, 2, 0)) - 1):
501.      '-----
502.      '-----
503.      '19 - Gorban et al., 1990
504.      f = f + 1
505.      T(i, 2, f) = T(i, 2, 1)
506.
507.      Do While Errs(i, f) > MaxError And It(i, f) < MaxLoop
508.          If T(i, 2, f) > (1300 * 1.5) - 273.15 Then: Exit Do
509.          Call GetProperties(i, f, 2, 0)
510.
511.          Nu(i, 1, f) = 0.0059 * (Re(i, 1, 0) ^ 0.9) * (Pr(i, 1, 0) ^ -0.12)
512.
513.          HTC(i, f) = Nu(i, 1, f) * k(i, 1, 0) / Dhy(i)
514.          TempT = T(i, 1, 0) + qavg(i) / HTC(i, f)
515.          It(i, f) = It(i, f) + 1
516.          Errs(i, f) = Abs(T(i, 2, f) - TempT)
517.          T(i, 2, f) = TempT
518.      Loop
519.
520.      If RaworPar = "Raw Data" Then: HTCErrAvg(i, f) = ((HTC(i, f) / HTC(i, 0)) - 1
): HTCErrAvgAbs(i, f) = Abs((HTC(i, f) / HTC(i, 0)) - 1):
521.      If RaworPar = "Raw Data" Then: TwErrAvg(i, f) = ((T(i, 2, f) / T(i, 2, 0)) -
1): TwErrAvgAbs(i, f) = Abs((T(i, 2, f) / T(i, 2, 0)) - 1):
522.      '-----
523.      '-----
524.      '20 - Griem, 1996
525.      f = f + 1
526.      T(i, 2, f) = T(i, 2, 1)
527.
528.      Do While Errs(i, f) > MaxError And It(i, f) < MaxLoop
529.          If T(i, 2, f) > (1300 * 1.5) - 273.15 Then: Exit Do
530.          Call GetProperties(i, f, 2, 0)
531.
532.          Nu(i, 1, f) = 0.0169 * (Re(i, 1, 0) ^ 0.8356) * (Prg(i) ^ 0.432) * PHIg(i
)
533.
534.          HTC(i, f) = Nu(i, 1, f) * Kg(i) / Dhy(i)

```

```

535.      TempT = T(i, 1, 0) + qavg(i) / HTC(i, f)
536.      It(i, f) = It(i, f) + 1
537.      Errs(i, f) = Abs(T(i, 2, f) - TempT)
538.      T(i, 2, f) = TempT
539.      Loop
540.
541.      If RaworPar = "Raw Data" Then: HTCErrAvg(i, f) = ((HTC(i, f) / HTC(i, 0)) - 1
): HTCErrAvgAbs(i, f) = Abs((HTC(i, f) / HTC(i, 0)) - 1):
542.      If RaworPar = "Raw Data" Then: TwErrAvg(i, f) = ((T(i, 2, f) / T(i, 2, 0)) -
1): TwErrAvgAbs(i, f) = Abs((T(i, 2, f) / T(i, 2, 0)) - 1):
543.      '-----
544.      '-----
545.      '21 - Hu, 2001
546.      f = f + 1
547.      T(i, 2, f) = T(i, 2, 1)
548.
549.      Do While Errs(i, f) > MaxError And It(i, f) < MaxLoop
550.          If T(i, 2, f) > (1300 * 1.5) - 273.15 Then: Exit Do
551.          Call GetProperties(i, f, 2, 0)
552.
553.          Nu(i, 1, f) = 0.0068 * (Re(i, 1, 0) ^ 0.9) * (Pr(i, 5, f) ^ 0.63) * ((D(i
, 2, f) / D(i, 1, 0)) ^ 0.17) * ((k(i, 2, f) / k(i, 1, 0)) ^ 0.29)
554.
555.          HTC(i, f) = Nu(i, 1, f) * k(i, 1, 0) / Dhy(i)
556.          TempT = T(i, 1, 0) + qavg(i) / HTC(i, f)
557.          It(i, f) = It(i, f) + 1
558.          Errs(i, f) = Abs(T(i, 2, f) - TempT)
559.          T(i, 2, f) = TempT
560.      Loop
561.
562.      If RaworPar = "Raw Data" Then: HTCErrAvg(i, f) = ((HTC(i, f) / HTC(i, 0)) - 1
): HTCErrAvgAbs(i, f) = Abs((HTC(i, f) / HTC(i, 0)) - 1):
563.      If RaworPar = "Raw Data" Then: TwErrAvg(i, f) = ((T(i, 2, f) / T(i, 2, 0)) -
1): TwErrAvgAbs(i, f) = Abs((T(i, 2, f) / T(i, 2, 0)) - 1):
564.      '-----
565.      '-----
566.      '22 - Kitoh et al., 2001
567.      f = f + 1
568.      T(i, 2, f) = T(i, 2, 1)
569.
570.      Do While Errs(i, f) > MaxError And It(i, f) < MaxLoop
571.          If T(i, 2, f) > (1300 * 1.5) - 273.15 Then: Exit Do
572.          Call GetProperties(i, f, 2, 0)
573.
574.          If H(i, 1, 0) / (1000 ^ 2) >= 0 And H(i, 1, 0) / (1000 ^ 2) < 1.5 Then: F
cUsed = Fc(i, f, 4)
575.          If H(i, 1, 0) / (1000 ^ 2) >= 1.5 And H(i, 1, 0) / (1000 ^ 2) < 3.3 Then:
FcUsed = Fc(i, f, 5)
576.          ' If H(i, 1, 0) / (1000 ^ 2) >= 3.3 And H(i, 1, 0) / (1000 ^ 2) < 4 Then:
FcUsed = Fc(i, f, 6) original correlation
577.          If H(i, 1, 0) / (1000 ^ 2) >= 3.3 Then: FcUsed = Fc(i, f, 6) 'expanded to
include all ranges for calculation
578.
579.          exp = 0.69 - (81000 / qdet(i, 1)) + FcUsed * qavg(i)
580.
581.          Nu(i, 1, f) = 0.015 * (Re(i, 1, 0) ^ 0.85) * (Pr(i, 1, 0) ^ exp)
582.

```

```

583.     HTC(i, f) = Nu(i, 1, f) * k(i, 1, 0) / Dhy(i)
584.     TempT = T(i, 1, 0) + qavg(i) / HTC(i, f)
585.     It(i, f) = It(i, f) + 1
586.     Errs(i, f) = Abs(T(i, 2, f) - TempT)
587.     T(i, 2, f) = TempT
588.     Loop
589.
590.     If RaworPar = "Raw Data" Then: HTCErrAvg(i, f) = ((HTC(i, f) / HTC(i, 0)) - 1
    ): HTCErrAvgAbs(i, f) = Abs((HTC(i, f) / HTC(i, 0)) - 1):
591.     If RaworPar = "Raw Data" Then: TwErrAvg(i, f) = ((T(i, 2, f) / T(i, 2, 0)) -
    1): TwErrAvgAbs(i, f) = Abs((T(i, 2, f) / T(i, 2, 0)) - 1):
592.     '-----
593.     '-----
594.     '23 - Jackson, 2002
595.     f = f + 1
596.     T(i, 2, f) = T(i, 2, 1)
597.
598.     Do While Errs(i, f) > MaxError And It(i, f) < MaxLoop
599.         If T(i, 2, f) > (1300 * 1.5) - 273.15 Then: Exit Do
600.         Call GetProperties(i, f, 2, 0)
601.
602.         If (T(i, 1, 0) < T(i, 2, f) And T(i, 2, f) < T(i, 4, 0)) Or (1.2 * T(i, 4
    , 0) <= T(i, 1, 0) And T(i, 1, 0) < T(i, 2, f)) Then: exp = 0.4:
603.         If (T(i, 1, 0) < T(i, 4, 0) And T(i, 4, 0) <= T(i, 2, f)) Then: exp = 0.4
    + 0.2 * (((T(i, 2, f) + 273.15) / (T(i, 4, 0) + 273.15)) - 1):
604.         If (T(i, 4, 0) < T(i, 1, 0) And T(i, 1, 0) <= 1.2 * T(i, 4, 0)) And (T(i,
    1, 0) < T(i, 2, f)) Then: exp = 0.4 + 0.2 * (((T(i, 2, f) + 273.15) -
605.         / (T(i, 4, 0) + 273.15)) - 1) * (1 - 5 * (((T(i, 2, f) + 273.15) / (T(i,
    4, 0) + 273.15)) - 1)):
606.
607.         Nu(i, 1, f) = 0.0183 * (Re(i, 1, 0) ^ 0.82) * (Pr(i, 1, 0) ^ 0.5) * ((D(i
    , 2, f) / D(i, 1, 0)) ^ 0.3) * ((Cp(i, 5, f) / Cp(i, 1, 0)) ^ exp)
608.
609.         HTC(i, f) = Nu(i, 1, f) * k(i, 1, 0) / Dhy(i)
610.         TempT = T(i, 1, 0) + qavg(i) / HTC(i, f)
611.         It(i, f) = It(i, f) + 1
612.         Errs(i, f) = Abs(T(i, 2, f) - TempT)
613.         T(i, 2, f) = TempT
614.     Loop
615.
616.     If RaworPar = "Raw Data" Then: HTCErrAvg(i, f) = ((HTC(i, f) / HTC(i, 0)) - 1
    ): HTCErrAvgAbs(i, f) = Abs((HTC(i, f) / HTC(i, 0)) - 1):
617.     If RaworPar = "Raw Data" Then: TwErrAvg(i, f) = ((T(i, 2, f) / T(i, 2, 0)) -
    1): TwErrAvgAbs(i, f) = Abs((T(i, 2, f) / T(i, 2, 0)) - 1):
618.     '-----
619.     '-----
620.     '24 - Xu & Guo, 2005
621.     f = f + 1
622.     T(i, 2, f) = T(i, 2, 1)
623.
624.     Do While Errs(i, f) > MaxError And It(i, f) < MaxLoop
625.         If T(i, 2, f) > (1300 * 1.5) - 273.15 Then: Exit Do
626.         Call GetProperties(i, f, 2, 0)
627.
628.         Nu(i, 1, f) = 0.02269 * (Re(i, 1, 0) ^ 0.8079) * (Pr(i, 5, f) ^ 0.9213) *
    ((u(i, 2, f) / u(i, 1, 0)) ^ 0.8687) * ((D(i, 2, f) / D(i, 1, 0)) -
629.         ^ 0.6638)

```

```

630.
631.     HTC(i, f) = Nu(i, 1, f) * k(i, 1, 0) / Dhy(i)
632.     TempT = T(i, 1, 0) + qavg(i) / HTC(i, f)
633.     It(i, f) = It(i, f) + 1
634.     Errs(i, f) = Abs(T(i, 2, f) - TempT)
635.     T(i, 2, f) = TempT
636. Loop
637.
638. If RaworPar = "Raw Data" Then: HTCErrAvg(i, f) = ((HTC(i, f) / HTC(i, 0)) - 1)
639. If RaworPar = "Raw Data" Then: TwErrAvg(i, f) = ((T(i, 2, f) / T(i, 2, 0)) - 1)
640. '-----
641. '-----
642. '25 - Kuang et al., 2008
643. f = f + 1
644. T(i, 2, f) = T(i, 2, 1)
645.
646. Do While Errs(i, f) > MaxError And It(i, f) < MaxLoop
647. If T(i, 2, f) > (1300 * 1.5) - 273.15 Then: Exit Do
648. Call GetProperties(i, f, 2, 0)
649.
650. Nu(i, 1, f) = 0.0239 * (Re(i, 1, 0) ^ 0.759) * (Pr(i, 5, f) ^ 0.833) * ((
651. D(i, 2, f) / D(i, 1, 0)) ^ 0.31) * ((k(i, 2, f) / k(i, 1, 0)) _
652. ^ 0.0863) * ((u(i, 2, f) / u(i, 1, 0)) ^ 0.832) * (Grst(i) ^ 0.014) * (qN
653. onD(i) ^ -0.021)
654.
655. HTC(i, f) = Nu(i, 1, f) * k(i, 1, 0) / Dhy(i)
656. TempT = T(i, 1, 0) + qavg(i) / HTC(i, f)
657. It(i, f) = It(i, f) + 1
658. Errs(i, f) = Abs(T(i, 2, f) - TempT)
659. T(i, 2, f) = TempT
660. Loop
661.
662. If RaworPar = "Raw Data" Then: HTCErrAvg(i, f) = ((HTC(i, f) / HTC(i, 0)) - 1)
663. If RaworPar = "Raw Data" Then: TwErrAvg(i, f) = ((T(i, 2, f) / T(i, 2, 0)) - 1)
664. TwErrAvgAbs(i, f) = Abs((T(i, 2, f) / T(i, 2, 0)) - 1)
665. '-----
666. '-----
667. '26 - Yu et al., 2009
668. f = f + 1
669. T(i, 2, f) = T(i, 2, 1)
670.
671. Do While Errs(i, f) > MaxError And It(i, f) < MaxLoop
672. If T(i, 2, f) > (1300 * 1.5) - 273.15 Then: Exit Do
673. Call GetProperties(i, f, 2, 0)
674.
675. Nu(i, 1, f) = 0.01378 * (Re(i, 1, 0) ^ 0.9078) * (Pr(i, 5, f) ^ 0.6171) *
676. ((D(i, 2, f) / D(i, 1, 0)) ^ 0.4356) * (Grst(i) ^ -0.012) * _
677. (qNonD(i) ^ -0.0605)
678.
679. HTC(i, f) = Nu(i, 1, f) * k(i, 1, 0) / Dhy(i)
680. TempT = T(i, 1, 0) + qavg(i) / HTC(i, f)
681. It(i, f) = It(i, f) + 1
682. Errs(i, f) = Abs(T(i, 2, f) - TempT)
683. T(i, 2, f) = TempT

```



```

680.   Loop
681.
682.   If RaworPar = "Raw Data" Then: HTCErrAvg(i, f) = ((HTC(i, f) / HTC(i, 0)) - 1
): HTCErrAvgAbs(i, f) = Abs((HTC(i, f) / HTC(i, 0)) - 1):
683.   If RaworPar = "Raw Data" Then: TwErrAvg(i, f) = ((T(i, 2, f) / T(i, 2, 0)) -
1): TwErrAvgAbs(i, f) = Abs((T(i, 2, f) / T(i, 2, 0)) - 1):
684.   '-----
685.   '-----
686.   '27 - Cheng et al., 2009
687.   f = f + 1
688.   f = 27
689.   T(i, 2, f) = T(i, 2, 1)
690.
691.   Do While Errs(i, f) > MaxError And It(i, f) < MaxLoop
692.       If T(i, 2, f) > (1300 * 1.5) - 273.15 Then: Exit Do
693.       Call GetProperties(i, f, 2, 0)
694.
695.       Fmin(1) = 0.85 + 0.776 * (Ap(i, 1, 0) * 10 ^ 3) ^ 2.4
696.       Fmin(2) = (0.48 / (Ap(i, 4, 0) * 10 ^ 3) ^ 1.55) + 1.21 * (1 - Ap(i, 1, 0
) / Ap(i, 4, 0))
697.
698.       If Fmin(1) <= Fmin(2) Then
699.           Nu(i, 1, f) = 0.023 * (Re(i, 1, 0) ^ 0.8) * (Pr(i, 5, f) ^ (1 / 3)) *
Fmin(1)
700.       Else
701.           Nu(i, 1, f) = 0.023 * (Re(i, 1, 0) ^ 0.8) * (Pr(i, 5, f) ^ (1 / 3)) *
Fmin(2)
702.       End If
703.
704.       HTC(i, f) = Nu(i, 1, f) * k(i, 1, 0) / Dhy(i)
705.       TempT = T(i, 1, 0) + qavg(i) / HTC(i, f)
706.       It(i, f) = It(i, f) + 1
707.       Errs(i, f) = Abs(T(i, 2, f) - TempT)
708.       T(i, 2, f) = TempT
709.   Loop
710.
711.   If RaworPar = "Raw Data" Then: HTCErrAvg(i, f) = ((HTC(i, f) / HTC(i, 0)) - 1
): HTCErrAvgAbs(i, f) = Abs((HTC(i, f) / HTC(i, 0)) - 1):
712.   If RaworPar = "Raw Data" Then: TwErrAvg(i, f) = ((T(i, 2, f) / T(i, 2, 0)) -
1): TwErrAvgAbs(i, f) = Abs((T(i, 2, f) / T(i, 2, 0)) - 1):
713.   '-----
714.   '-----
715.   '28 - Mokry et al., 2009
716.   f = f + 1
717.   T(i, 2, f) = T(i, 2, 1)
718.
719.   Do While Errs(i, f) > MaxError And It(i, f) < MaxLoop
720.       If T(i, 2, f) > (1300 * 1.5) - 273.15 Then: Exit Do
721.       Call GetProperties(i, f, 2, 0)
722.
723.       Nu(i, 1, f) = 0.0061 * (Re(i, 1, 0) ^ 0.904) * (Pr(i, 5, f) ^ 0.684) * ((
D(i, 2, f) / D(i, 1, 0)) ^ 0.564)
724.
725.       HTC(i, f) = Nu(i, 1, f) * k(i, 1, 0) / Dhy(i)
726.       TempT = T(i, 1, 0) + qavg(i) / HTC(i, f)
727.       It(i, f) = It(i, f) + 1
728.       Errs(i, f) = Abs(T(i, 2, f) - TempT)

```

```

729.      T(i, 2, f) = TempT
730.  Loop
731.
732.  If RaworPar = "Raw Data" Then: HTCErrAvg(i, f) = ((HTC(i, f) / HTC(i, 0)) - 1
): HTCErrAvgAbs(i, f) = Abs((HTC(i, f) / HTC(i, 0)) - 1):
733.  If RaworPar = "Raw Data" Then: TwErrAvg(i, f) = ((T(i, 2, f) / T(i, 2, 0)) -
1): TwErrAvgAbs(i, f) = Abs((T(i, 2, f) / T(i, 2, 0)) - 1):
734.  '-----
735.  '-----
736.  '29 - Gupta et al., 2011
737.  f = f + 1
738.  T(i, 2, f) = T(i, 2, 1)
739.
740.  Do While Errs(i, f) > MaxError And It(i, f) < MaxLoop
741.    If T(i, 2, f) > (1300 * 1.5) - 273.15 Then: Exit Do
742.    Call GetProperties(i, f, 2, 0)
743.
744.    Nu(i, 1, f) = 0.004 * (Re(i, 2, f) ^ 0.923) * (Prw(i, f) ^ 0.773) * ((D(i
, 2, f) / D(i, 1, 0)) ^ 0.186) *
745.    ((u(i, 2, f) / u(i, 1, 0)) ^ 0.366)
746.
747.    HTC(i, f) = Nu(i, 1, f) * k(i, 2, f) / Dhy(i)
748.    TempT = T(i, 1, 0) + qavg(i) / HTC(i, f)
749.    It(i, f) = It(i, f) + 1
750.    Errs(i, f) = Abs(T(i, 2, f) - TempT)
751.    T(i, 2, f) = TempT
752.  Loop
753.
754.  If RaworPar = "Raw Data" Then: HTCErrAvg(i, f) = ((HTC(i, f) / HTC(i, 0)) - 1
): HTCErrAvgAbs(i, f) = Abs((HTC(i, f) / HTC(i, 0)) - 1):
755.  If RaworPar = "Raw Data" Then: TwErrAvg(i, f) = ((T(i, 2, f) / T(i, 2, 0)) -
1): TwErrAvgAbs(i, f) = Abs((T(i, 2, f) / T(i, 2, 0)) - 1):
756.  '-----
757.  '-----
758.  '30 - Gupta et al., 2013 (Bulk)
759.  f = f + 1
760.  T(i, 2, f) = T(i, 2, 1)
761.
762.  Do While Errs(i, f) > MaxError And It(i, f) < MaxLoop
763.    If T(i, 2, f) > (1300 * 1.5) - 273.15 Then: Exit Do
764.    Call GetProperties(i, f, 2, 0)
765.
766.    Nu(i, 1, f) = 0.01 * (Re(i, 1, 0) ^ 0.89) * (Pr(i, 5, f) ^ -
0.14) * ((D(i, 2, f) / D(i, 1, 0)) ^ 0.93) * ((k(i, 2, f) / k(i, 1, 0)) ^ 0.22) _
767.    * ((u(i, 2, f) / u(i, 1, 0)) ^ -1.13)
768.
769.    HTC(i, f) = Nu(i, 1, f) * k(i, 1, 0) / Dhy(i)
770.    TempT = T(i, 1, 0) + qavg(i) / HTC(i, f)
771.    It(i, f) = It(i, f) + 1
772.    Errs(i, f) = Abs(T(i, 2, f) - TempT)
773.    T(i, 2, f) = TempT
774.  Loop
775.
776.  If RaworPar = "Raw Data" Then: HTCErrAvg(i, f) = ((HTC(i, f) / HTC(i, 0)) - 1
): HTCErrAvgAbs(i, f) = Abs((HTC(i, f) / HTC(i, 0)) - 1):

```

```

777.   If RaworPar = "Raw Data" Then: TwErrAvg(i, f) = ((T(i, 2, f) / T(i, 2, 0)) -
778.   1): TwErrAvgAbs(i, f) = Abs((T(i, 2, f) / T(i, 2, 0)) - 1):
779.   '-----
780.   '-----
781.   '31 - Gupta et al., 2013 (Wall)
782.   f = f + 1
783.   T(i, 2, f) = T(i, 2, 1)
784.   Do While Errs(i, f) > MaxError And It(i, f) < MaxLoop
785.       If T(i, 2, f) > (1300 * 1.5) - 273.15 Then: Exit Do
786.       Call GetProperties(i, f, 2, 0)
787.
788.       Nu(i, 1, f) = 0.0038 * (Re(i, 2, f) ^ 0.96) * (Prw(i, f) ^ -
0.14) * ((D(i, 2, f) / D(i, 1, 0)) ^ 0.84) * ((k(i, 2, f) / k(i, 1, 0)) ^ -
0.75) -
789.       * ((u(i, 2, f) / u(i, 1, 0)) ^ -0.22)
790.
791.       HTC(i, f) = Nu(i, 1, f) * k(i, 2, f) / Dhy(i)
792.       TempT = T(i, 1, 0) + qavg(i) / HTC(i, f)
793.       It(i, f) = It(i, f) + 1
794.       Errs(i, f) = Abs(T(i, 2, f) - TempT)
795.       T(i, 2, f) = TempT
796.   Loop
797.
798.   If RaworPar = "Raw Data" Then: HTCErrAvg(i, f) = ((HTC(i, f) / HTC(i, 0)) - 1
): HTCErrAvgAbs(i, f) = Abs((HTC(i, f) / HTC(i, 0)) - 1):
799.   If RaworPar = "Raw Data" Then: TwErrAvg(i, f) = ((T(i, 2, f) / T(i, 2, 0)) -
1): TwErrAvgAbs(i, f) = Abs((T(i, 2, f) / T(i, 2, 0)) - 1):
800.   '-----
801.   '-----
802.   '32 - Gupta et al., 2013 (Film)
803.   f = f + 1
804.   T(i, 2, f) = T(i, 2, 1)
805.
806.   Do While Errs(i, f) > MaxError And It(i, f) < MaxLoop
807.       If T(i, 2, f) > (1300 * 1.5) - 273.15 Then: Exit Do
808.       Call GetProperties(i, f, 2, 0)
809.
810.       Nu(i, 1, f) = 0.0043 * (Re(i, 3, f) ^ 0.94) * ((D(i, 2, f) / D(i, 1, 0))
^ 0.57) * ((k(i, 2, f) / k(i, 1, 0)) ^ -0.52)
811.
812.       HTC(i, f) = Nu(i, 1, f) * k(i, 3, f) / Dhy(i)
813.       TempT = T(i, 1, 0) + qavg(i) / HTC(i, f)
814.       It(i, f) = It(i, f) + 1
815.       Errs(i, f) = Abs(T(i, 2, f) - TempT)
816.       T(i, 2, f) = TempT
817.   Loop
818.
819.   If RaworPar = "Raw Data" Then: HTCErrAvg(i, f) = ((HTC(i, f) / HTC(i, 0)) - 1
): HTCErrAvgAbs(i, f) = Abs((HTC(i, f) / HTC(i, 0)) - 1):
820.   If RaworPar = "Raw Data" Then: TwErrAvg(i, f) = ((T(i, 2, f) / T(i, 2, 0)) -
1): TwErrAvgAbs(i, f) = Abs((T(i, 2, f) / T(i, 2, 0)) - 1):
821.   '-----
822.   '-----
823.   '33 - Chen & Fang, 2014

```

```

824.   f = f + 1
825.   T(i, 2, f) = T(i, 2, 1)
826.
827.   Do While Errs(i, f) > MaxError And It(i, f) < MaxLoop
828.       If T(i, 2, f) > (1300 * 1.5) - 273.15 Then: Exit Do
829.       Call GetProperties(i, f, 2, 0)
830.
831.       Nu(i, 1, f) = 0.46 * (Re(i, 1, 0) ^ 0.16) * ((Pr(i, 2, f) / Pr(i, 1, 0))
      ^ 0.1) * ((v(i, 2, f) / v(i, 1, 0)) ^ -0.55) *
832.       ((Cp(i, 5, f) / Cp(i, 1, 0)) ^ 0.88) * ((Grst(i) / Gr(i, f)) ^ 0.81)
833.
834.       HTC(i, f) = Nu(i, 1, f) * k(i, 1, 0) / Dhy(i)
835.       TempT = T(i, 1, 0) + qavg(i) / HTC(i, f)
836.       It(i, f) = It(i, f) + 1
837.       Errs(i, f) = Abs(T(i, 2, f) - TempT)
838.       T(i, 2, f) = TempT
839.   Loop
840.
841.   If RaworPar = "Raw Data" Then: HTCErrAvg(i, f) = ((HTC(i, f) / HTC(i, 0)) - 1
      ): HTCErrAvgAbs(i, f) = Abs((HTC(i, f) / HTC(i, 0)) - 1):
842.   If RaworPar = "Raw Data" Then: TwErrAvg(i, f) = ((T(i, 2, f) / T(i, 2, 0)) -
      1): TwErrAvgAbs(i, f) = Abs((T(i, 2, f) / T(i, 2, 0)) - 1):
843.   '-----
844.   '-----
845.   '34 - Wang and Li, 2014
846.   f = f + 1
847.   T(i, 2, f) = T(i, 2, 1)
848.
849.   Do While Errs(i, f) > MaxError And It(i, f) < MaxLoop
850.       If T(i, 2, f) > (1300 * 1.5) - 273.15 Then: Exit Do
851.       Call GetProperties(i, f, 2, 0)
852.
853.       Nu(i, 1, f) = 0.00684 * (Re(i, 1, 0) ^ 0.89765) * (Pr(i, 5, f) ^ 0.68625)
      * ((D(i, 2, f) / D(i, 1, 0)) ^ 0.31142) *
854.       ((k(i, 2, f) / k(i, 1, 0)) ^ 0.26185)
855.
856.       HTC(i, f) = Nu(i, 1, f) * k(i, 1, 0) / Dhy(i)
857.       TempT = T(i, 1, 0) + qavg(i) / HTC(i, f)
858.       It(i, f) = It(i, f) + 1
859.       Errs(i, f) = Abs(T(i, 2, f) - TempT)
860.       T(i, 2, f) = TempT
861.   Loop
862.
863.   If RaworPar = "Raw Data" Then: HTCErrAvg(i, f) = ((HTC(i, f) / HTC(i, 0)) - 1
      ): HTCErrAvgAbs(i, f) = Abs((HTC(i, f) / HTC(i, 0)) - 1):
864.   If RaworPar = "Raw Data" Then: TwErrAvg(i, f) = ((T(i, 2, f) / T(i, 2, 0)) -
      1): TwErrAvgAbs(i, f) = Abs((T(i, 2, f) / T(i, 2, 0)) - 1):
865.   '-----
866.   '-----
867.   '35 - Lei et al., 2019
868.   f = f + 1
869.   T(i, 2, f) = T(i, 2, 1)
870.
871.   Do While Errs(i, f) > MaxError And It(i, f) < MaxLoop
872.       If T(i, 2, f) > (1300 * 1.5) - 273.15 Then: Exit Do
873.       Call GetProperties(i, f, 2, 0)
874.

```

```

875.      Nu(i, 1, f) = 0.00728 * (Re(i, 1, 0) ^ 0.891) * (Pr(i, 1, 0) ^ 0.6) * ((D
      (i, 2, f) / D(i, 1, 0)) ^ 0.49)
876.
877.      HTC(i, f) = Nu(i, 1, f) * k(i, 1, 0) / Dhy(i)
878.      TempT = T(i, 1, 0) + qavg(i) / HTC(i, f)
879.      It(i, f) = It(i, f) + 1
880.      Errs(i, f) = Abs(T(i, 2, f) - TempT)
881.      T(i, 2, f) = TempT
882.      Loop
883.
884.      If RaworPar = "Raw Data" Then: HTCErrAvg(i, f) = ((HTC(i, f) / HTC(i, 0)) - 1
      ): HTCErrAvgAbs(i, f) = Abs((HTC(i, f) / HTC(i, 0)) - 1):
885.      If RaworPar = "Raw Data" Then: TwErrAvg(i, f) = ((T(i, 2, f) / T(i, 2, 0)) -
      1): TwErrAvgAbs(i, f) = Abs((T(i, 2, f) / T(i, 2, 0)) - 1):
886.      '-----
887.      '-----
888.      '36 - Clark et al., 2020"
889.      'f = f + 1
890.      f = 36
891.      T(i, 2, f) = T(i, 2, 1)
892.
893.      Do While Errs(i, f) > MaxError And It(i, f) < MaxLoop
894.          If T(i, 2, f) > (1300 * 1.5) - 273.15 Then: Exit Do
895.          Call GetProperties(i, f, 2, 0)
896.
897.          '      Nu(i, 1, f) = 0.0126 * (Re(i, 1, 0) ^ 0.8367) * (Pr(i, 5, f) ^ 0.4399) *
      ((D(i, 2, f) / D(i, 1, 0)) ^ -0.0707) *
898.          '      ((k(i, 2, f) / k(i, 1, 0)) ^ 0.4874)
899.
900.          Nu(i, 1, f) = 0.0129 * (Re(i, 1, 0) ^ 0.841) * (Pr(i, 5, f) ^ 0.5) * ((D(
      i, 2, f) / D(i, 1, 0)) ^ -0.07) *
901.          ((k(i, 2, f) / k(i, 1, 0)) ^ 0.53)
902.
903.          HTC(i, f) = Nu(i, 1, f) * k(i, 1, 0) / Dhy(i)
904.          TempT = T(i, 1, 0) + qavg(i) / HTC(i, f)
905.          It(i, f) = It(i, f) + 1
906.          Errs(i, f) = Abs(T(i, 2, f) - TempT)
907.          T(i, 2, f) = TempT
908.
909.      Loop
910.
911.      If RaworPar = "Raw Data" Then: HTCErrAvg(i, f) = ((HTC(i, f) / HTC(i, 0)) - 1
      ): HTCErrAvgAbs(i, f) = Abs((HTC(i, f) / HTC(i, 0)) - 1):
912.      If RaworPar = "Raw Data" Then: TwErrAvg(i, f) = ((T(i, 2, f) / T(i, 2, 0)) -
      1): TwErrAvgAbs(i, f) = Abs((T(i, 2, f) / T(i, 2, 0)) - 1):
913.      '-----
914.
915.      '-----
916.      '*****ADJUST AS NEEDED*****ADJUST AS NEEDED*****ADJUST AS
      NEEDED*****
917.      'Re-arrange as needed (leave Dittus-Boelter in the first position)
918.      'Add as needed
919.      '*****ADJUST AS NEEDED*****ADJUST AS NEEDED*****ADJUST AS
      NEEDED*****
920.      '-----
921.

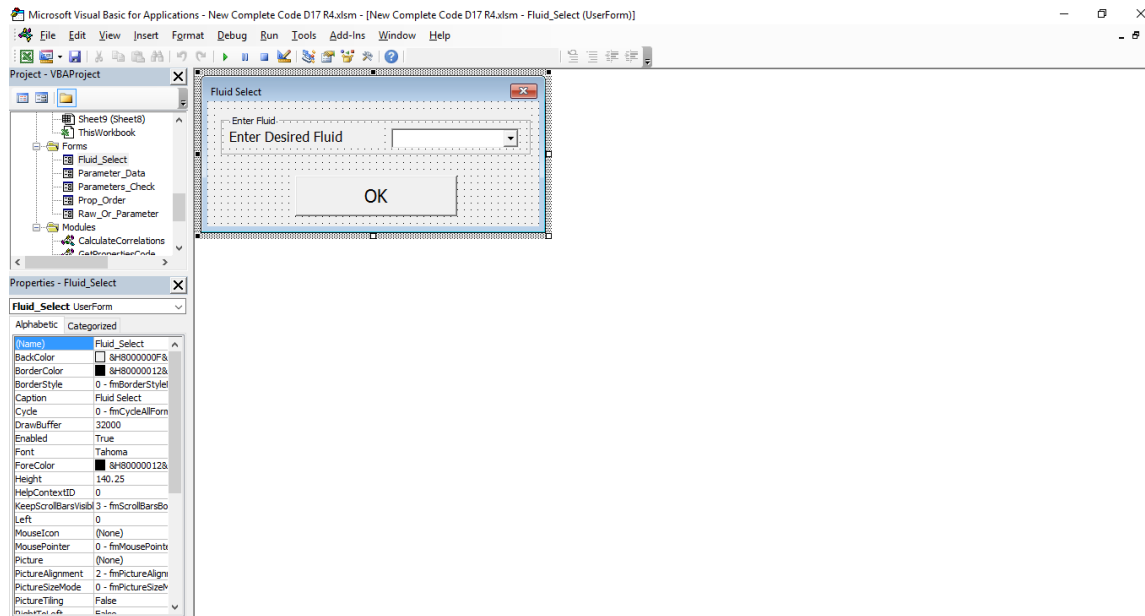
```

```

922.
923.     End Sub

```

A.3.9 *Fluid_Select Form*



```

1. Private Sub OK_CMD_Button_Click()
2. ReDim Parameters(1 To 1, 1 To 6) As Variant
3.
4. Parameters(1, 1) = Fluid_Combobox.Value: Parameters(1, 2) = "Fluid": Parameters(1
, 3) = "-": Parameters(1, 4) = "Fluid": Parameters(1, 5) = 5:
5. If Parameters(1, 1) = "" Then
6.     MsgBox "Please select Fluid!", vbCritical, "Fluid Error"
7.     Exit Sub
8. End If
9.
10. Unload Fluid_Select
11. End Sub
12.
13. Private Sub UserForm_Initialize()
14.
15.
16. Fluid_Combobox.AddItem "Air"
17. Fluid_Combobox.AddItem "CO2"
18. Fluid_Combobox.AddItem "D2O"
19. Fluid_Combobox.AddItem "Helium"
20. Fluid_Combobox.AddItem "Hydrogen"
21. Fluid_Combobox.AddItem "Nitrogen"
22. Fluid_Combobox.AddItem "Oxygen"
23. Fluid_Combobox.AddItem "R134A"
24. Fluid_Combobox.AddItem "R141B"
25. Fluid_Combobox.AddItem "Water"

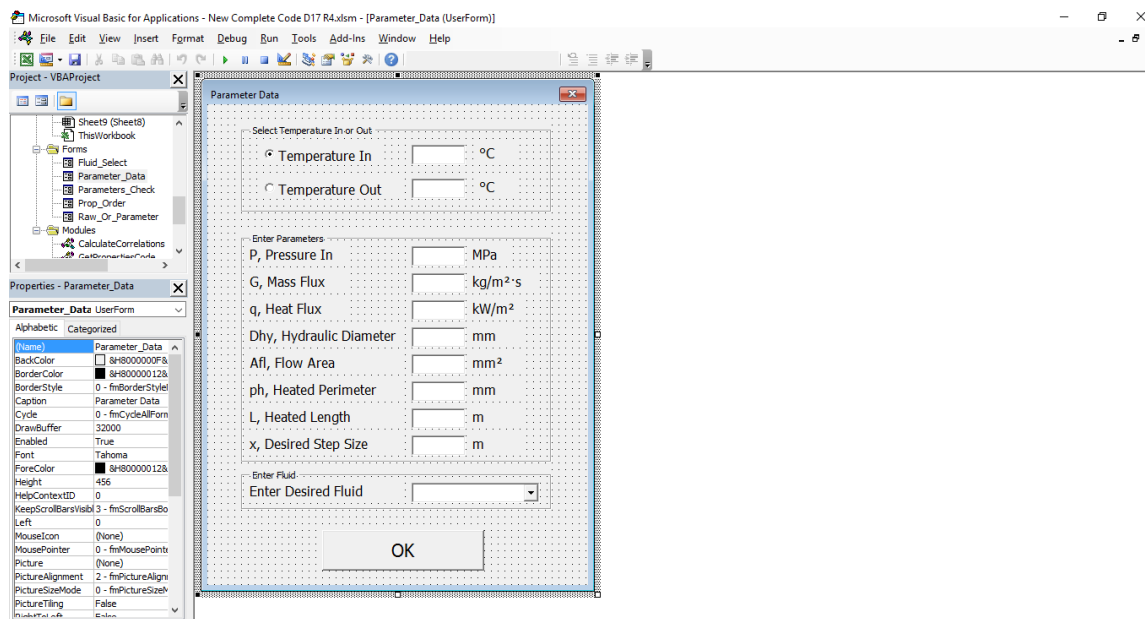
```

```

26.
27. Fluid_Combobox.ListIndex = 9
28.
29. End Sub
30.
31. Private Sub UserForm_QueryClose(Cancel As Integer, Closemode As Integer)
32.
33. If Closemode = vbFormControlMenu Then
34.     Cancel = True
35.     MsgBox "Please Select a Fluid and Click OK!"
36. End If
37.
38. End Sub

```

A.3.10 Parameter Data Form



```

1. Private Sub UserForm_Initialize()
2.
3. Fluid_Combobox.AddItem "Air"
4. Fluid_Combobox.AddItem "CO2"
5. Fluid_Combobox.AddItem "D20"
6. Fluid_Combobox.AddItem "Helium"
7. Fluid_Combobox.AddItem "Hydrogen"
8. Fluid_Combobox.AddItem "Nitrogen"
9. Fluid_Combobox.AddItem "Oxygen"
10. Fluid_Combobox.AddItem "R134A"
11. Fluid_Combobox.AddItem "R141B"
12. Fluid_Combobox.AddItem "Water"
13.
14. Fluid_Combobox.ListIndex = 9
15.
16. End Sub
17.
18. Private Sub UserForm_QueryClose(Cancel As Integer, Closemode As Integer)
19.

```

```

20. If Closemode = vbFormControlMenu Then
21.     Cancel = True
22.     MsgBox "Don't Close This Input Box!"
23. End If
24.
25. End Sub
26.
27. Private Sub OK_CMD_Button_Click()
28.
29. ReDim Parameters(1 To 11, 1 To 6) As Variant
30. Dim i As Integer
31. On Error Resume Next
32. If TempIn_Rad.Value = True Then
33.     TempChoice = "In"
34. ElseIf TempOut_Rad.Value = True Then
35.     TempChoice = "Out"
36. End If
37. Parameters(1, 1) = TempIn_Input.Value: Parameters(1, 2) = TempIn_Rad.Caption: Parameters(1, 3) = TempIn_Unit.Caption: Parameters(1, 4) = "Tin": Parameters(1, 5) = 1: Parameters(1, 6) = 2
38. Parameters(2, 1) = TempOut_Input.Value: Parameters(2, 2) = TempOut_Rad.Caption: Parameters(2, 3) = TempOut_Unit.Caption: Parameters(2, 4) = "Tout": Parameters(2, 5) = 1: Parameters(2, 6) = 3
39. Parameters(3, 1) = P_Input.Value: Parameters(3, 2) = P_Label.Caption: Parameters(3, 3) = P_Unit.Caption: Parameters(3, 4) = "Pin": Parameters(3, 5) = 1: Parameters(3, 6) = 2
40. Parameters(4, 1) = G_Input.Value: Parameters(4, 2) = G_Label.Caption: Parameters(4, 3) = G_Unit.Caption: Parameters(4, 4) = "Gin": Parameters(4, 5) = 1: Parameters(4, 6) = 2
41. Parameters(5, 1) = q_Input.Value: Parameters(5, 2) = q_Label.Caption: Parameters(5, 3) = q_Unit.Caption: Parameters(5, 4) = "q": Parameters(5, 5) = 1:
42. Parameters(6, 1) = Dhy_Input.Value: Parameters(6, 2) = Dhy_Label.Caption: Parameters(6, 3) = Dhy_Unit.Caption: Parameters(6, 4) = "Dhy": Parameters(6, 5) = 1: Parameters(6, 6) = 2
43. Parameters(7, 1) = Afl_Input.Value: Parameters(7, 2) = Afl_Label.Caption: Parameters(7, 3) = Afl_Unit.Caption: Parameters(7, 4) = "Afl": Parameters(7, 5) = 1: Parameters(7, 6) = 2
44. Parameters(8, 1) = ph_Input.Value: Parameters(8, 2) = ph_Label.Caption: Parameters(8, 3) = ph_Unit.Caption: Parameters(8, 4) = "ph": Parameters(8, 5) = 1: Parameters(8, 6) = 1
45. Parameters(9, 1) = L_Input.Value: Parameters(9, 2) = L_Label.Caption: Parameters(9, 3) = L_Unit.Caption: Parameters(9, 4) = "Lh": Parameters(9, 5) = 1: Parameters(9, 6) = 1
46. Parameters(10, 1) = x_Input.Value: Parameters(10, 2) = x_Label.Caption: Parameters(10, 3) = x_Unit.Caption: Parameters(10, 4) = "Step": Parameters(10, 5) = 4:
47. Parameters(11, 1) = Fluid_Combobox.Value: Parameters(11, 2) = "Fluid": Parameters(11, 3) = "-": Parameters(11, 4) = "Fluid": Parameters(11, 5) = 5:
48.
49. For i = 1 To 10
50.     If IsNumeric(Parameters(i, 1)) = False Or Parameters(i, 1) = 0 Then
51.         If (i = 1 And TempChoice = "In") Or (i = 2 And TempChoice = "Out") Or i > 2 Then
52.             MsgBox "All values must be non-zero, real numbers." & vbCrLf & "Please adjust " & Parameters(i, 2) & "."
53.             Exit Sub
54.         End If
55.     End If
56. Next i
57. If Parameters(11, 1) = "" Then
58.     MsgBox "Please select Fluid!", vbCritical, "Fluid Error"
59.     Exit Sub

```

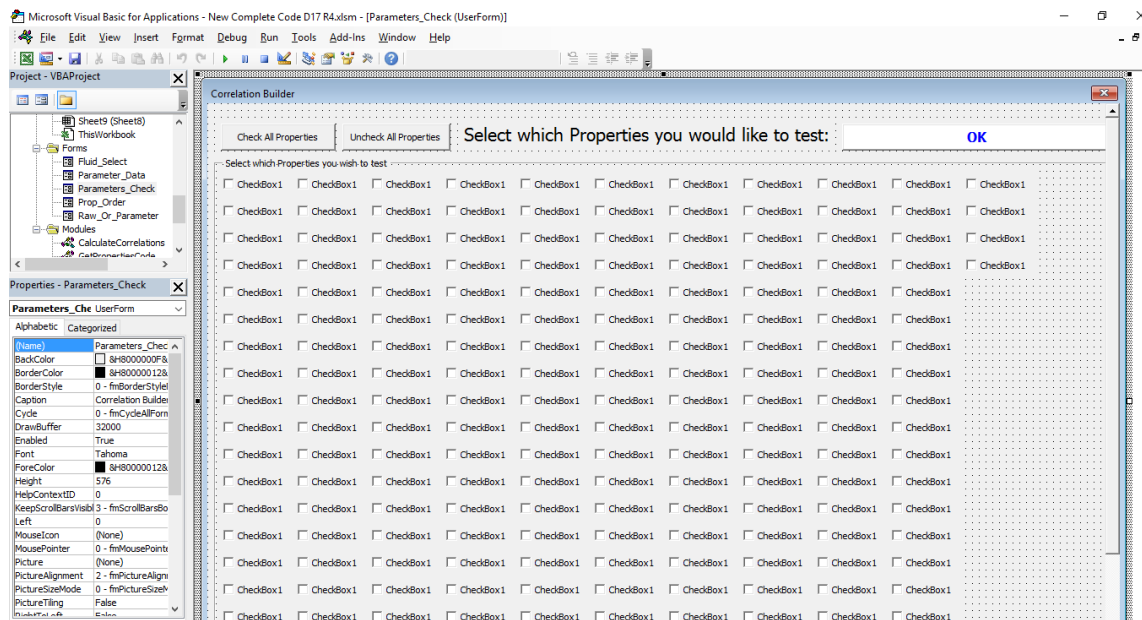


```

60. End If
61.
62. If Parameters(10, 1) > Parameters(9, 1) Then: MsgBox "Step cannot be larger than
the Heated Length!" & vbCrLf & "Please adjust the Step/Length values.", vbOKOnly
+ vbCritical, "Error in Data": Exit Sub
63.
64. Unload Parameter_Data
65. End Sub
66.
67. Private Sub TempIn_Rad_Click()
68. TempIn_Input.Locked = False
69. TempOut_Input.Locked = True
70. TempOut_Input = ""
71. TempChoice = "In"
72. End Sub
73.
74. Private Sub TempOut_Rad_Click()
75. TempIn_Input.Locked = True
76. TempOut_Input.Locked = False
77. TempIn_Input = ""
78. TempChoice = "Out"
79. End Sub

```

A.3.11 Parameters Check Form



```

1. Option Explicit
2. Public ctl As Control
3.
4.
5.
6. Private Sub Check_All_Click()
7. Dim i As Integer
8.
9. For i = 1 To L2RD - 10
10. Set ctl = Parameters_Check.Controls("CheckBox" & i)

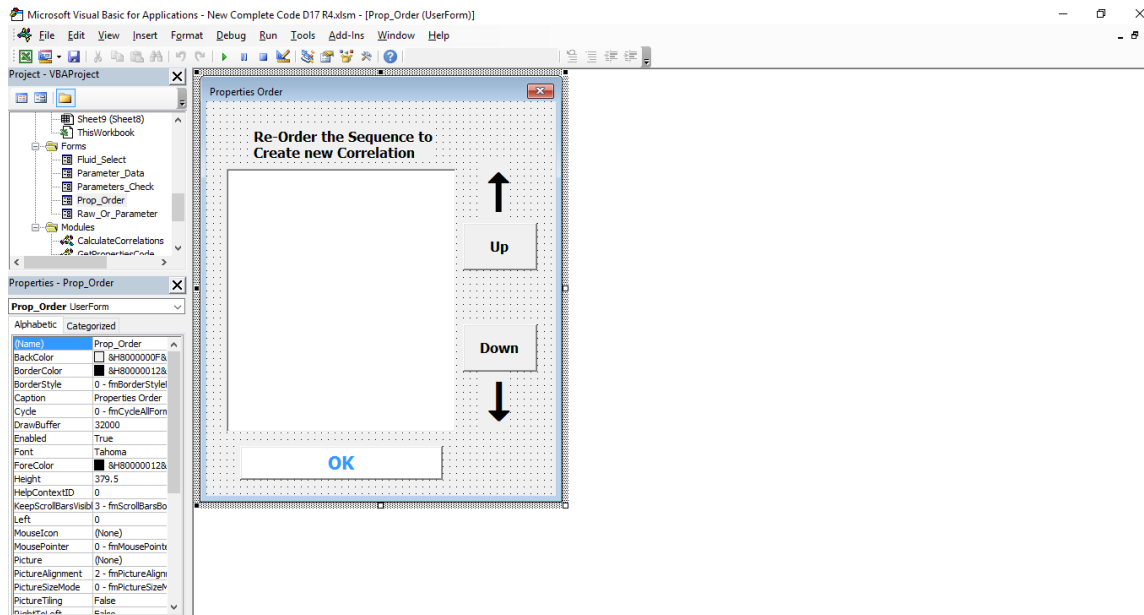
```

```

11.     If ctl.Caption <> "Extra" And InStr(ctl.Caption, "Nu") = 0 Then
12.         ctl.Value = True
13.     End If
14. Next i
15. End Sub
16.
17.
18. Private Sub OK_Btn_Click()
19. Dim i As Integer, j As Integer
20.
21. j = 0
22. For i = 1 To L2RD - 10
23.     Set ctl = Parameters_Check.Controls("CheckBox" & i)
24.     If ctl.Value = True Then: PropertiesTitle(i + 10, 1) = 1#: j = j + 1
25. Next i
26. If j = 0 Then: MsgBox "You must select at least one Property to test!", vbOKOnly,
    "Property Error": Exit Sub:
27. Unload Parameters_Check
28. End Sub
29.
30. Private Sub Uncheck_All_Click()
31. Dim i As Integer
32.
33. For i = 1 To L2RD - 10
34.     Set ctl = Parameters_Check.Controls("CheckBox" & i)
35.     ctl.Value = False
36. Next i
37. End Sub
38.
39. Private Sub UserForm_Initialize()
40.
41. Call Checkbox_Start
42.
43. End Sub
44.
45. Private Function Checkbox_Start()
46. Dim i As Integer
47.
48. For i = 1 To L2RD - 10
49.     Set ctl = Parameters_Check.Controls("CheckBox" & i)
50.     ctl.Caption = PropertiesTitle(i + 10, 0)
51.     If ctl.Caption = "Extra" Or InStr(ctl.Caption, "Nu") > 0 Then
52.         ctl.Locked = True
53.     End If
54.     'Test
55.     PropertiesTitle(i + 10, 1) = 0
56. Next i
57. End Function
58.
59. Private Sub UserForm_QueryClose(Cancel As Integer, Closemode As Integer)
60.
61. If Closemode = vbFormControlMenu Then
62.     Cancel = True
63.     MsgBox "Don't Close This Input Box!"
64. End If
65.
66. End Sub

```

A.3.12 Prop_Order Form



```

1. Private Sub Down_Btn_Click()
2. Dim ItemNum As Integer, TempItem As String, TempIndex As Integer, i As Integer
3.
4. If ListBox1.ListIndex < 0 Or ListBox1.ListIndex >= PropChosen - 1 Then: Exit Sub
5.
6. For i = 1 To PropChosen
7.     If ListBox1.Selected(i - 1) = True Then
8.
9.         TempIndex = VartoTest(i + 2, 1)
10.        VartoTest(i + 2, 1) = VartoTest(i + 1, 1)
11.        VartoTest(i + 1, 1) = TempIndex
12.
13.        ListBox1.List(i) = PropertiesTitle(VartoTest(i + 2, 1), 0)
14.        ListBox1.List(i - 1) = PropertiesTitle(VartoTest(i + 1, 1), 0)
15.        ListBox1.ListIndex = i
16.
17.        Exit Sub
18.    End If
19. Next i
20.
21. End Sub
22.
23. Private Sub OK_Btn_Prop_Order_Click()
24. Dim i As Integer
25. For i = 1 To PropChosen: CorPropTitles(i) = PropertiesTitle(VartoTest(i + 1, 1),
    0): Next i
26. Unload Prop_Order
27. End Sub
28.
29. Private Sub Up_Btn_Click()
30. Dim ItemNum As Integer, TempItem As String, TempIndex As Integer, i As Integer
31.
32. If ListBox1.ListIndex <= 0 Or ListBox1.ListIndex > PropChosen Then: Exit Sub

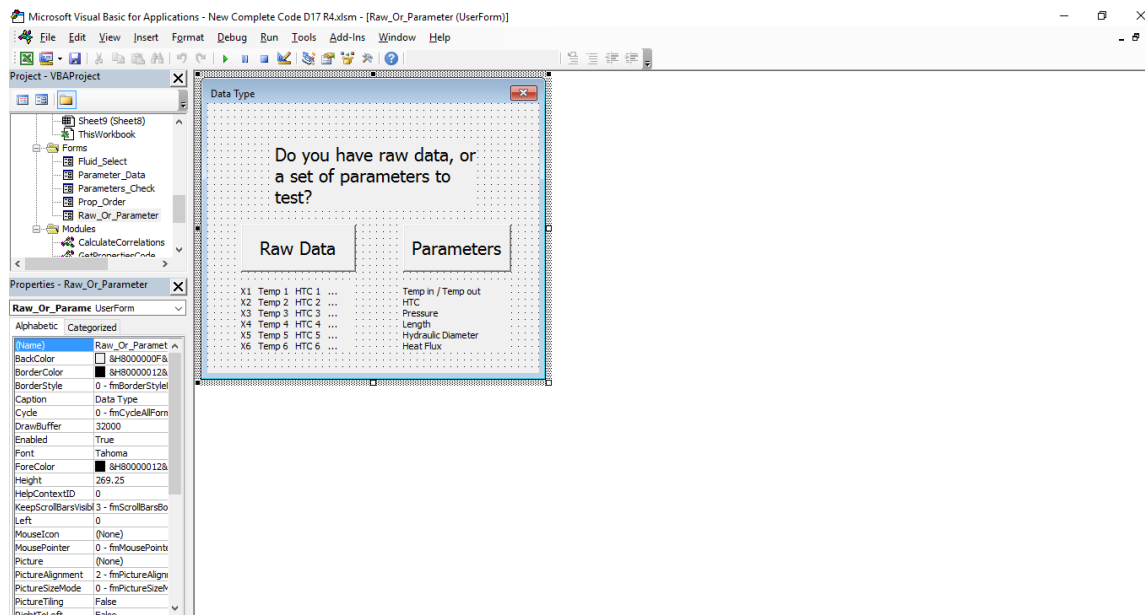
```

```

33.
34. For i = 1 To PropChosen
35.     If ListBox1.Selected(i - 1) = True Then
36.
37.         TempIndex = VartoTest(i, 1)
38.         VartoTest(i, 1) = VartoTest(i + 1, 1)
39.         VartoTest(i + 1, 1) = TempIndex
40.
41.         ListBox1.List(i - 1) = PropertiesTitle(VartoTest(i + 1, 1), 0)
42.         ListBox1.List(i - 2) = PropertiesTitle(VartoTest(i, 1), 0)
43.         ListBox1.ListIndex = i - 2
44.
45.         Exit Sub
46.     End If
47. Next i
48.
49. End Sub
50.
51. Private Sub UserForm_Initialize()
52. Dim i As Integer
53.
54. For i = 1 To PropChosen
55.     ListBox1.AddItem PropertiesTitle(VartoTest(i + 1, 1), 0)
56. Next i
57.
58. End Sub
59.
60. Private Sub UserForm_QueryClose(Cancel As Integer, Closemode As Integer)
61.
62. If Closemode = vbFormControlMenu Then
63.     Cancel = True
64.     MsgBox "Don't Close This Input Box!"
65. End If
66.
67. End Sub

```

A.3.13 Raw Or Parameter Form



```
1. Private Sub UserForm_QueryClose(Cancel As Integer, Closemode As Integer)
2.
3. If Closemode = vbFormControlMenu Then
4.     Cancel = True
5.     MsgBox "Select Either Raw Data or Parameters!"
6. End If
7.
8. End Sub
9.
10.
11. Private Sub Parameters_Button_Click()
12. RaworPar = "Parameters"
13. Unload Raw_Or_Parameter
14. End Sub
15.
16. Private Sub Raw_Data_Button_Click()
17. RaworPar = "Raw Data"
18. Unload Raw_Or_Parameter
19. End Sub
```

APPENDIX B: VERIFICATION OF CODE FUNCTION

To verify that the created code is performing calculations correctly and as intended, HTC and T_w are predicted using the Mokry et al. (2009) correlation Eq. (28), and are compared to previous Kirillov et al. (2005) datasets with Eq. (28) data already plotted. The comparisons are nearly identical, indicating the created code is functioning correctly.

B.1 TEST 27_22

Figure B-1 shows the original Mokry, et al. (2009) data (long dashed lines), and the calculated Mokry data from the computer code developed (solid green lines). As is shown, the calculations are nearly identical, with the change in properties from NIST REFPROP 10 to 9.1 accounting for the slight variation.

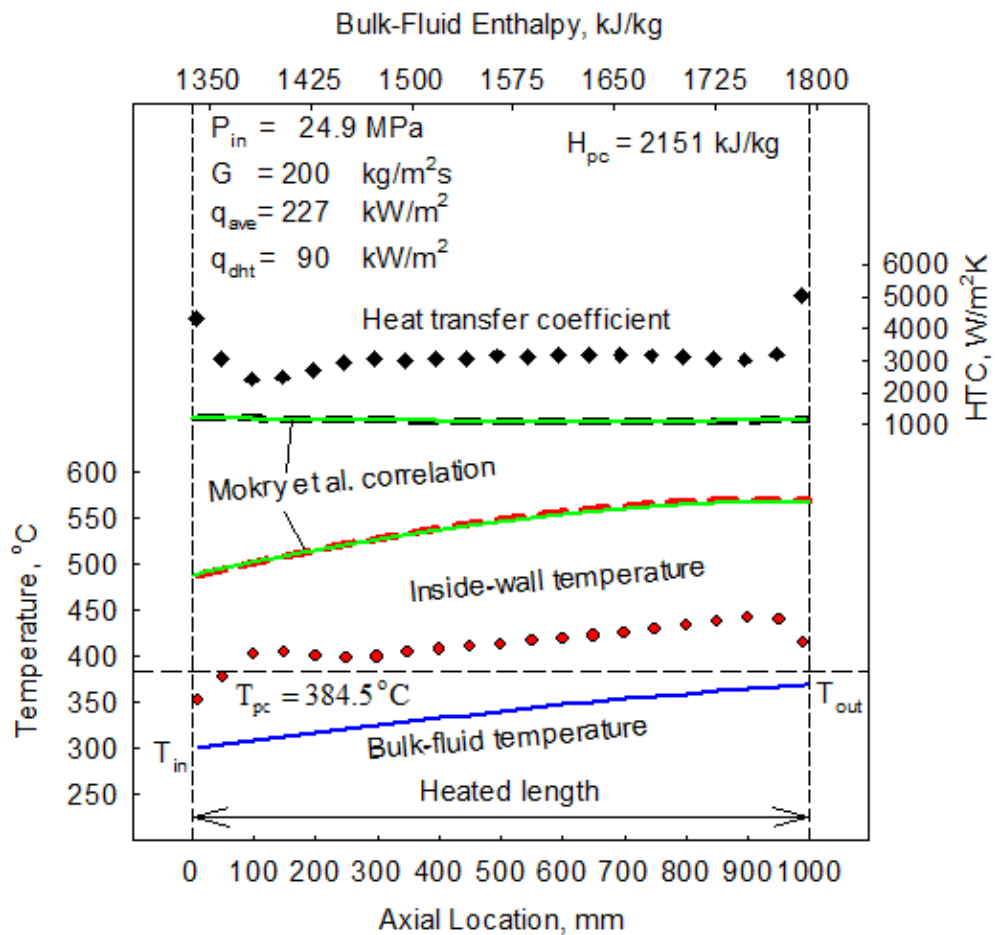


Figure B-1: T_w and HTC Variations along 1 m bare tube, Test 27_22

$P = 24.9 \text{ MPa}$, $G = 200 \text{ kg/m}^2\text{s}$, $q_{avg} = 227 \text{ kW/m}^2$, $T_{in} = 301^\circ\text{C}$, $D = 10 \text{ mm}$

B.2 TEST 27_53

Figure B-2 shows the original Mokry, et al. (2009) data (long dashed lines), and the calculated Mokry data from the computer code developed (solid green lines). As is shown, the calculations are nearly identical, with the change in properties from NIST REFPROP 10 to 9.1 accounting for the slight variation.

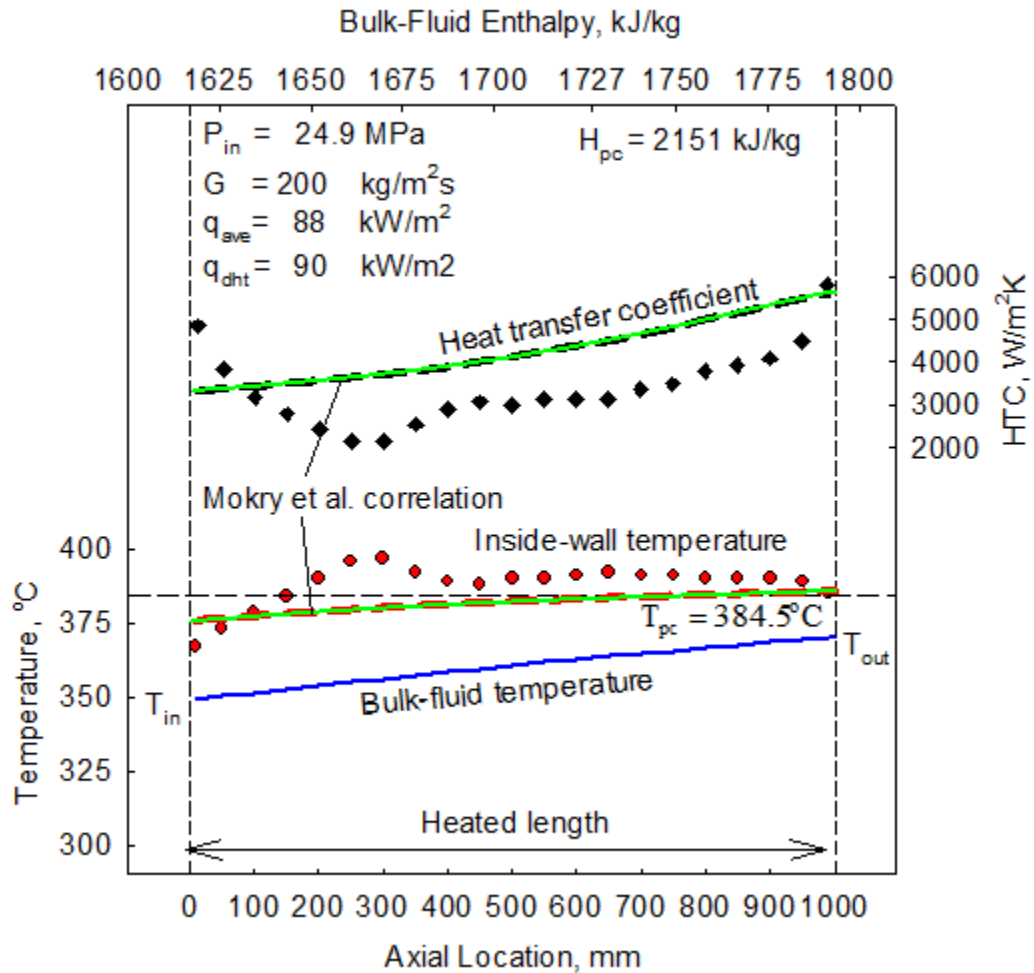


Figure B-2: T_w and HTC Variations along 1 m bare tube, Test 27_53

$P = 24.9 \text{ MPa}$, $G = 200 \text{ kg/m}^2\text{s}$, $q_{avg} = 88 \text{ kW/m}^2$, $T_{in} = 349^\circ\text{C}$, $D = 10 \text{ mm}$

B.3 TEST 27_86

Figure B-3 shows the original Mokry, et al. (2009) data (long dashed lines), and the calculated Mokry data from the computer code developed (solid green lines). As is shown, the calculations are nearly identical, with the change in properties from NIST REFPROP 10 to 9.1 accounting for the slight variation.

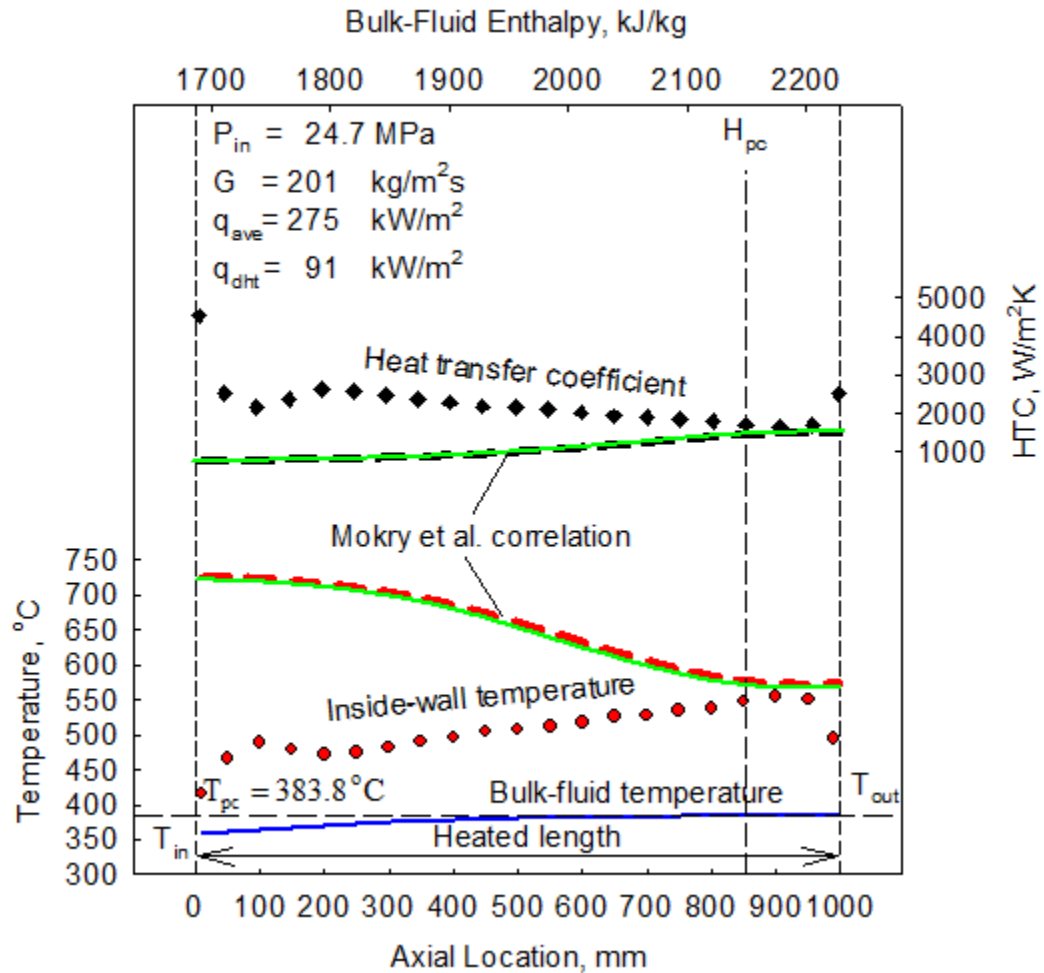


Figure B-3: T_w and HTC Variations along 1 m bare tube, Test 27_86

$P = 24.7 \text{ MPa}$, $G = 201 \text{ kg/m}^2\text{s}$, $q_{avg} = 275 \text{ kW/m}^2$, $T_{in} = 358^\circ\text{C}$, $D = 10 \text{ mm}$

B.4 TEST 27_88

Figure B-4 shows the original Mokry, et al. (2009) data (long dashed lines), and the calculated Mokry data from the computer code developed (solid green lines). As is shown, the calculations are nearly identical, with the change in properties from NIST REFPROP 10 to 9.1 accounting for the slight variation.

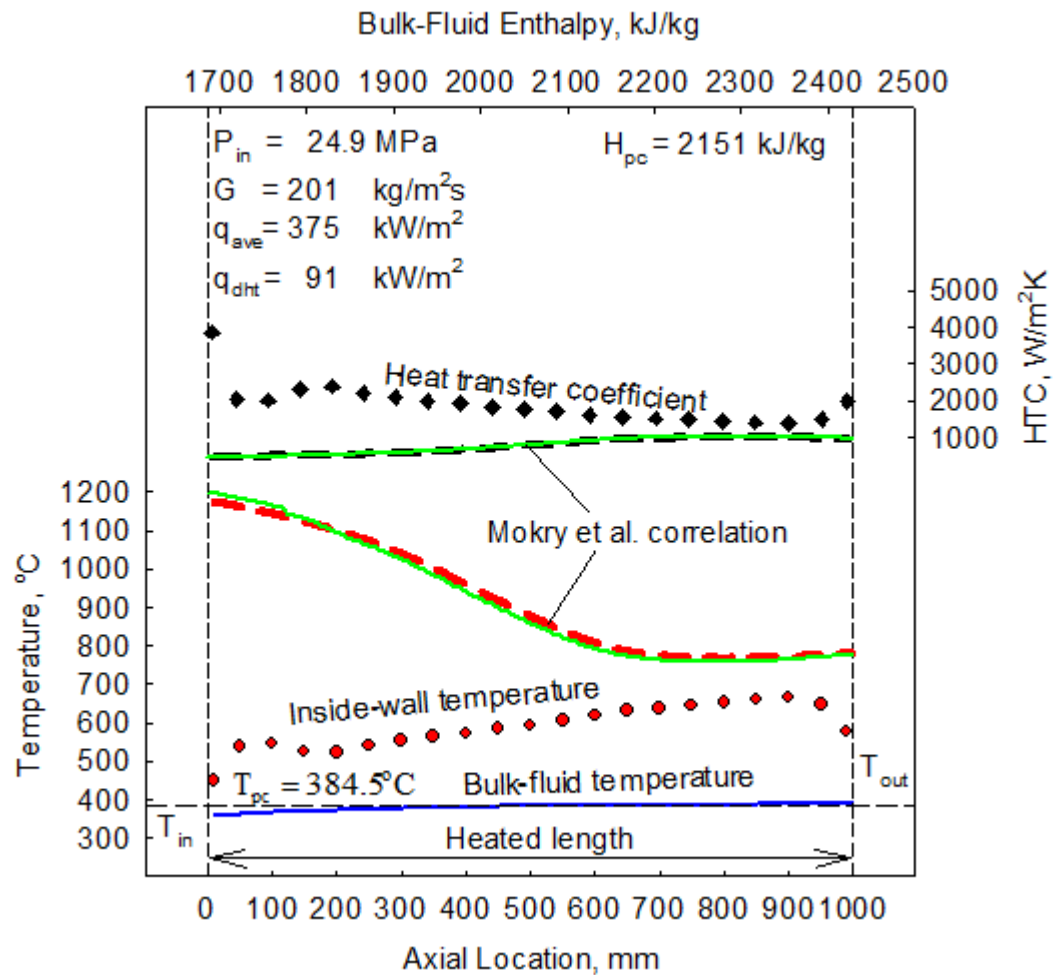


Figure B-4: T_w and HTC Variations along 1 m bare tube, Test 27_88

$P = 24.9 \text{ MPa}$, $G = 201 \text{ kg/m}^2\text{s}$, $q_{avg} = 375 \text{ kW/m}^2$, $T_{in} = 358^\circ\text{C}$, $D = 10 \text{ mm}$

B.5 TEST 49_8

Figure B-5 shows the original Mokry, et al. (2009) data (long dashed lines), and the calculated Mokry data from the computer code developed (solid green lines). As is shown, the calculations are nearly identical, with the change in properties from NIST REFPROP 10 to 9.1 accounting for the slight variation.

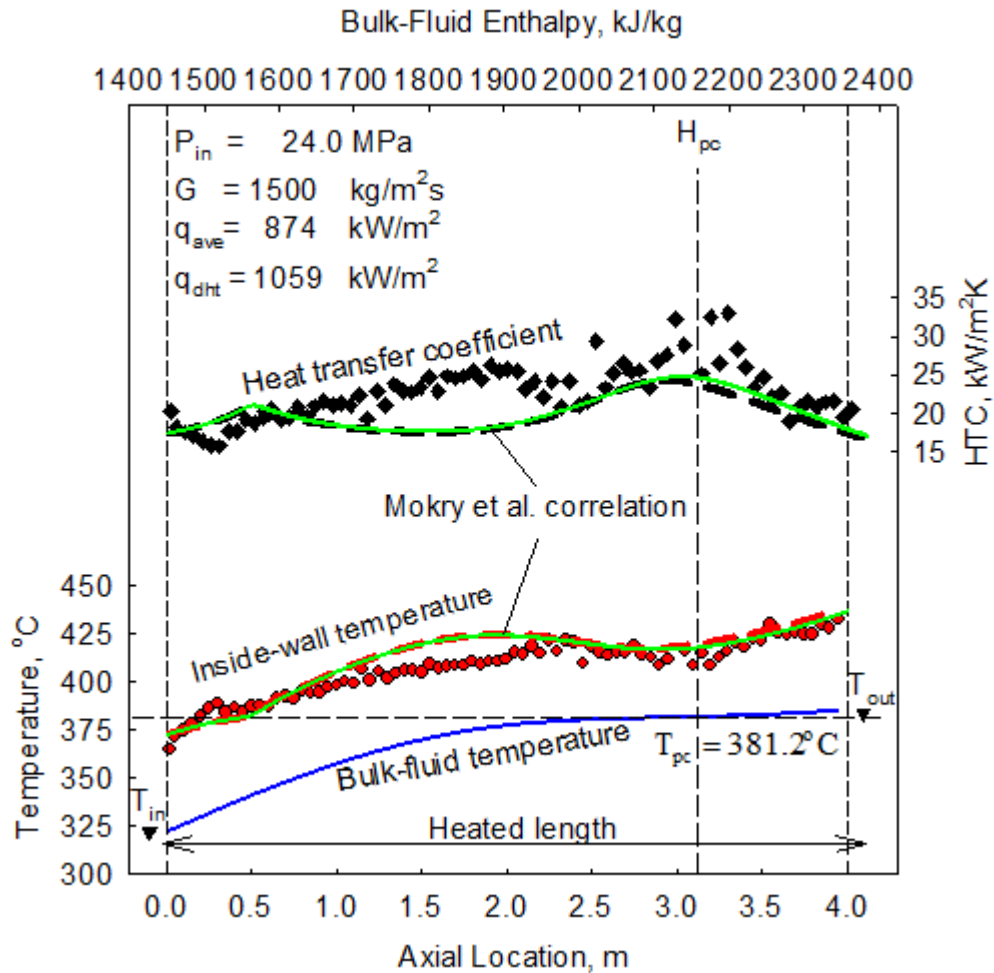


Figure B-5: T_w and HTC Variations along 1 m bare tube, Test 49_8

$P = 24 \text{ MPa}$, $G = 1500 \text{ kg/m}^2\cdot\text{s}$, $q_{avg} = 874 \text{ kW/m}^2$, $T_{in} = 322^\circ\text{C}$, $D = 10 \text{ mm}$

B.6 TEST 51_9

Figure B-6 shows the original Mokry, et al. (2009) data (long dashed lines), and the calculated Mokry data from the computer code developed (solid green lines). As is shown, the calculations are nearly identical, with the change in properties from NIST REFPROP 10 to 9.1 accounting for the slight variation.

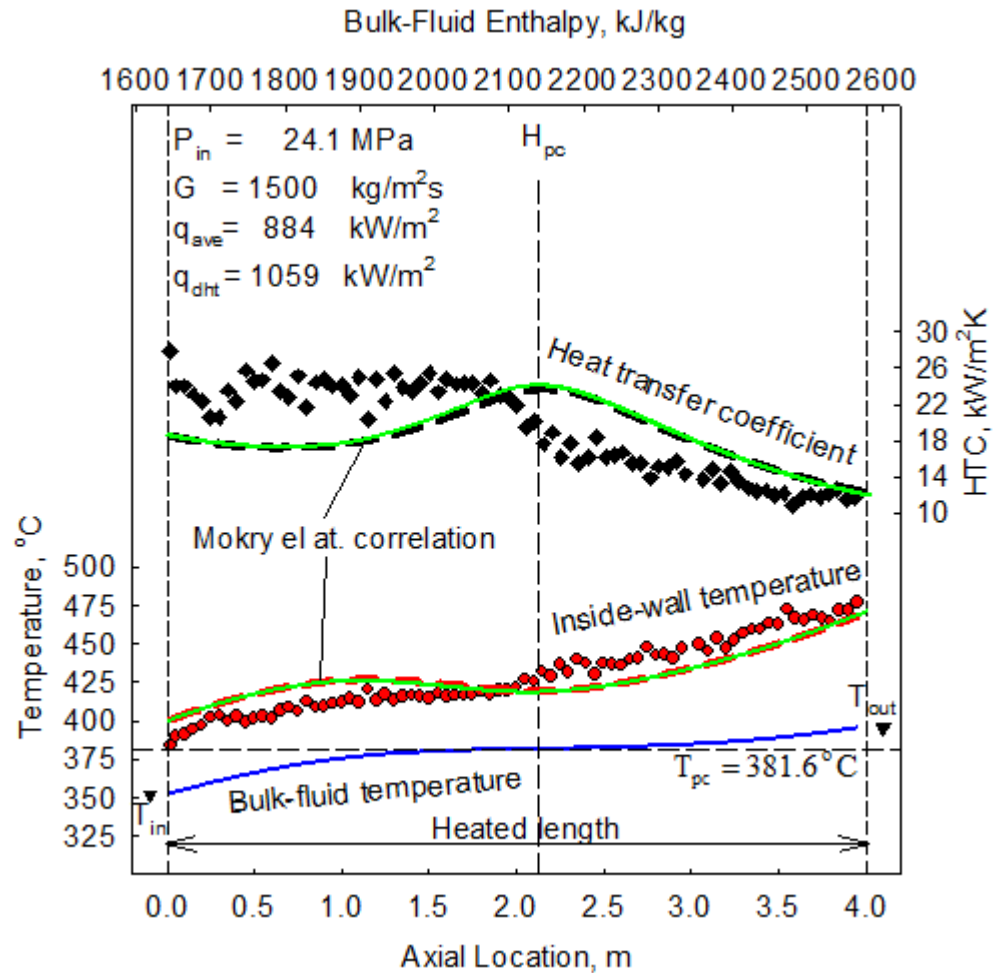


Figure B-6: T_w and HTC Variations along 1 m bare tube, Test 51_9

$P = 24.1 \text{ MPa}$, $G = 1500 \text{ kg/m}^2\text{s}$, $q_{avg} = 884 \text{ kW/m}^2$, $T_{in} = 352^\circ\text{C}$, $D = 10 \text{ mm}$

APPENDIX C: SUPPLEMENTARY DATA

C.1 T_{PC} AND C_P – PRESSURE LOOKUP TABLE

Table C-1: T_{pc} and C_p Values up to $P = 40$ MPa

P	T_{pc}	C_p	P	T_{pc}	C_p	P	T_{pc}	C_p
MPa	°C	kJ/kg·K	MPa	°C	kJ/kg·K	MPa	°C	kJ/kg·K
22.065	373.95	38,396	24.6	383.44	89.88	27.9	395.03	36.93
22.066	373.95	3,261	24.7	383.8	86.10	28	395.37	36.29
22.067	373.96	5,594	24.8	384.17	82.62	28.1	395.71	35.67
22.068	373.96	12,088	24.9	384.53	79.41	28.2	396.04	35.08
22.069	373.97	3,386	25	384.89	76.44	28.3	396.38	34.50
22.07	373.97	10,396	25.1	385.26	73.69	28.4	396.71	33.94
22.08	374.01	5,154	25.2	385.62	71.14	28.5	397.04	33.40
22.09	374.04	6,049	25.3	385.98	68.75	28.6	397.37	32.88
22.1	374.08	10,525	25.4	386.33	66.53	28.7	397.7	32.37
22.2	374.45	2,547	25.5	386.69	64.44	28.8	398.03	31.88
22.3	374.83	1,411	25.6	387.05	62.49	28.9	398.36	31.41
22.4	375.21	946.53	25.7	387.41	60.65	29	398.69	30.95
22.5	375.58	701.94	25.8	387.76	58.92	29.1	399.02	30.50
22.6	375.96	552.32	25.9	388.11	57.28	29.2	399.34	30.07
22.7	376.34	451.77	26	388.47	55.74	29.3	399.67	29.65
22.8	376.71	380.16	26.1	388.82	54.27	29.4	399.99	29.24
22.9	377.09	327.03	26.2	389.17	52.89	29.5	400.31	28.85
23	377.47	286.05	26.3	389.52	51.57	29.6	400.64	28.46
23.1	377.85	253.62	26.4	389.87	50.32	29.7	400.96	28.09
23.2	378.23	227.39	26.5	390.22	49.13	29.8	401.28	27.73
23.3	378.6	205.84	26.6	390.57	47.99	29.9	401.6	27.37
23.4	378.98	187.81	26.7	390.92	46.91	30	401.91	27.03
23.5	379.35	172.54	26.8	391.27	45.87	30.1	402.23	26.70
23.6	379.73	159.48	26.9	391.62	44.88	30.2	402.55	26.37
23.7	380.11	148.18	27	391.96	43.94	30.3	402.86	26.06
23.8	380.48	138.33	27.1	392.31	43.03	30.4	403.18	25.75
23.9	380.85	129.66	27.2	392.65	42.16	30.5	403.49	25.45
24	381.22	121.99	27.3	392.99	41.32	30.6	403.8	25.16
24.1	381.6	115.16	27.4	393.34	40.52	30.7	404.11	24.87
24.2	381.97	109.04	27.5	393.68	39.74	30.8	404.42	24.59
24.3	382.34	103.53	27.6	394.02	39.00	30.9	404.73	24.32
24.4	382.7	98.54	27.7	394.36	38.29	31	405.04	24.06
24.5	383.07	94.01	27.8	394.7	37.60	31.1	405.35	23.80

P	T _{pc}	C _p	P	T _{pc}	C _p	P	T _{pc}	C _p
MPa	°C	kJ/kg·K	MPa	°C	kJ/kg·K	MPa	°C	kJ/kg·K
31.2	405.65	23.55	34.9	416.41	17.29	38.6	426.59	14.06
31.3	405.96	23.31	35	416.69	17.18	38.7	426.86	14.00
31.4	406.26	23.07	35.1	416.97	17.06	38.8	427.13	13.93
31.5	406.57	22.83	35.2	417.25	16.95	38.9	427.4	13.87
31.6	406.87	22.61	35.3	417.53	16.85	39	427.67	13.80
31.7	407.17	22.38	35.4	417.81	16.74	39.1	427.94	13.74
31.8	407.47	22.17	35.5	418.09	16.63	39.2	428.21	13.68
31.9	407.77	21.95	35.6	418.37	16.53	39.3	428.47	13.62
32	408.07	21.75	35.7	418.64	16.43	39.4	428.74	13.56
32.1	408.37	21.54	35.8	418.92	16.33	39.5	429.01	13.50
32.2	408.66	21.35	35.9	419.2	16.23	39.6	429.27	13.44
32.3	408.96	21.15	36	419.48	16.14	39.7	429.54	13.38
32.4	409.25	20.96	36.1	419.75	16.04	39.8	429.81	13.32
32.5	409.55	20.78	36.2	420.03	15.95	39.9	430.07	13.26
32.6	409.84	20.60	36.3	420.31	15.85	40	430.34	13.21
32.7	410.13	20.42	36.4	420.58	15.76			
32.8	410.43	20.24	36.5	420.86	15.67			
32.9	410.72	20.07	36.6	421.13	15.59			
33	411.01	19.91	36.7	421.41	15.50			
33.1	411.3	19.74	36.8	421.68	15.41			
33.2	411.59	19.58	36.9	421.96	15.33			
33.3	411.87	19.43	37	422.23	15.25			
33.4	412.16	19.27	37.1	422.51	15.16			
33.5	412.45	19.12	37.2	422.78	15.08			
33.6	412.74	18.97	37.3	423.06	15.00			
33.7	413.02	18.83	37.4	423.33	14.93			
33.8	413.31	18.69	37.5	423.6	14.85			
33.9	413.59	18.55	37.6	423.88	14.77			
34	413.88	18.41	37.7	424.15	14.70			
34.1	414.16	18.28	37.8	424.42	14.62			
34.2	414.44	18.15	37.9	424.69	14.55			
34.3	414.73	18.02	38	424.97	14.48			
34.4	415.01	17.89	38.1	425.24	14.41			
34.5	415.29	17.77	38.2	425.51	14.33			
34.6	415.57	17.64	38.3	425.78	14.27			
34.7	415.85	17.52	38.4	426.05	14.20			
34.8	416.13	17.41	38.5	426.32	14.13			

C.2 ERROR TABLES FOR ALL Nu CORRELATIONS

C.2.1 7-rod Data Sorted by HTC RMS

Correlation	HTC Error				T _{wall} Error			
	Average Error/Mean Error	Average Absolute Error	Standard Error	RMS Error	Average Error/Mean Error	Average Absolute Error	Standard Error	RMS Error
21 - Hu, 2001	-3.4%	17.2%	25.6%	25.6%	3.8%	6.2%	7.8%	8.6%
36 - Clark et al., 2020	2.8%	15.7%	26.6%	26.5%	1.9%	4.9%	7.2%	7.4%
10 - Ornatsky et al., 1970	-4.4%	19.2%	26.8%	26.9%	4.3%	6.7%	8.4%	9.4%
07 - Bishop et al., 1964	2.7%	16.1%	27.9%	27.8%	2.1%	5.2%	8.0%	8.2%
08 - Swenson et al., 1965	-19.1%	23.1%	21.1%	28.3%	9.9%	10.9%	10.3%	14.3%
16 - Dyadyakin & Popov, 1977	6.5%	15.6%	28.1%	28.6%	1.3%	4.7%	9.1%	9.1%
34 - Wang & Li, 2014	-32.7%	33.4%	21.8%	39.2%	18.9%	19.1%	14.9%	23.9%
19 - Gorban et al., 1990	12.2%	22.4%	40.7%	42.2%	0.0%	5.3%	7.8%	7.8%
32 - Gupta et al., 2013 (Film)	5.4%	26.0%	43.6%	43.6%	6.9%	11.4%	25.8%	26.5%
17 - Watts & Chou, 1982	26.1%	29.8%	42.6%	49.7%	-2.8%	4.5%	7.5%	8.0%
18 - Petukhov et al., 1983	-43.8%	44.3%	27.8%	51.7%	33.4%	33.4%	24.0%	41.0%
23 - Jackson, 2002	33.7%	35.8%	44.3%	55.4%	-4.2%	5.0%	7.2%	8.3%
31 - Gupta et al., 2013 (Wall)	3.4%	50.0%	56.7%	56.3%	29.9%	37.2%	58.2%	65.0%
35 - Lei et al., 2019	-54.4%	54.4%	22.2%	58.7%	45.6%	45.6%	26.8%	52.8%
28 - Mokry et al., 2009	-53.9%	53.9%	24.7%	59.2%	51.0%	51.0%	36.4%	62.5%
29 - Gupta et al., 2011	-57.8%	57.8%	15.2%	59.7%	44.7%	44.7%	20.5%	49.1%
33 - Chen & Fang, 2014	-19.0%	48.3%	57.7%	60.3%	113.8%	117.5%	157.1%	192.9%
25 - Kuang et al., 2008	-56.6%	56.6%	25.4%	62.0%	55.0%	55.0%	35.6%	65.4%
04 - Miropol'skiy & Shitsman, 1957	37.6%	37.6%	50.6%	62.7%	-4.5%	4.7%	7.3%	8.6%
15 - Gnielinski, 1976	40.4%	40.4%	50.4%	64.3%	-5.1%	5.3%	7.2%	8.8%
14 - Jackson & Fewster, 1975	42.8%	43.9%	54.6%	69.0%	-5.2%	5.7%	7.6%	9.1%
06 - Domin, 1963	51.5%	51.5%	46.5%	69.1%	-6.6%	6.8%	6.8%	9.4%
01 - Dittus-Boelter, 1930	46.7%	46.7%	52.6%	70.0%	-5.9%	6.1%	7.1%	9.2%
12 - Yamagata et al., 1972	40.4%	40.5%	58.6%	70.8%	-4.5%	4.9%	7.9%	9.0%
22 - Kitoh et al., 2001	49.0%	49.0%	53.9%	72.5%	-6.1%	6.2%	7.2%	9.4%
11 - Giarratano et al., 1970	51.8%	51.8%	54.5%	74.8%	-6.5%	6.6%	7.1%	9.6%
03 - Bringer & Smith, 1957	48.0%	48.0%	59.0%	75.7%	-5.6%	5.7%	7.1%	8.9%
20 - Griem, 1996	44.8%	45.7%	70.3%	82.9%	-4.6%	5.5%	8.5%	9.6%
30 - Gupta et al., 2013 (Bulk)	39.8%	74.0%	73.9%	83.4%	11.0%	25.3%	42.0%	43.1%
27 - Cheng et al., 2009	57.6%	57.6%	62.3%	84.5%	-6.9%	7.0%	7.6%	10.2%
24 - Xu & Guo, 2005	-82.2%	82.2%	27.6%	86.7%	364.0%	364.0%	200.4%	414.8%
09 - Krasnoshchekov et al., 1967	62.4%	62.4%	73.4%	95.9%	-6.8%	6.8%	7.6%	10.1%
05 - Petukhov et al., 1961	66.8%	66.8%	75.0%	100.0%	-7.2%	7.2%	7.5%	10.3%
02 - Sieder & Tate, 1936	84.3%	84.3%	68.5%	108.3%	-9.7%	9.7%	7.0%	11.9%
13 - Zukauskas, 1972	97.7%	97.7%	49.3%	109.2%	-11.2%	11.3%	6.4%	12.9%
26 - Yu et al., 2009	221.2%	221.2%	116.9%	249.7%	-16.3%	16.3%	6.5%	17.5%

C.2.2 7-rod Data Sorted by T_w RMS

Correlation	HTC Error				T _{wall} Error			
	Average Error/Mean Error	Average Absolute Error	Standard Error	RMS Error	Average Error/Mean Error	Average Absolute Error	Standard Error	RMS Error
36 - Clark et al., 2020	2.8%	15.7%	26.6%	26.5%	1.9%	4.9%	7.2%	7.4%
19 - Gorban et al., 1990	12.2%	22.4%	40.7%	42.2%	0.0%	5.3%	7.8%	7.8%
17 - Watts & Chou, 1982	26.1%	29.8%	42.6%	49.7%	-2.8%	4.5%	7.5%	8.0%
07 - Bishop et al., 1964	2.7%	16.1%	27.9%	27.8%	2.1%	5.2%	8.0%	8.2%
23 - Jackson, 2002	33.7%	35.8%	44.3%	55.4%	-4.2%	5.0%	7.2%	8.3%
21 - Hu, 2001	-3.4%	17.2%	25.6%	25.6%	3.8%	6.2%	7.8%	8.6%
04 - Miropol'skiy & Shitsman, 1957	37.6%	37.6%	50.6%	62.7%	-4.5%	4.7%	7.3%	8.6%
15 - Gnielinski, 1976	40.4%	40.4%	50.4%	64.3%	-5.1%	5.3%	7.2%	8.8%
03 - Bringer & Smith, 1957	48.0%	48.0%	59.0%	75.7%	-5.6%	5.7%	7.1%	8.9%
12 - Yamagata et al., 1972	40.4%	40.5%	58.6%	70.8%	-4.5%	4.9%	7.9%	9.0%
14 - Jackson & Fewster, 1975	42.8%	43.9%	54.6%	69.0%	-5.2%	5.7%	7.6%	9.1%
16 - Dyadyakin & Popov, 1977	6.5%	15.6%	28.1%	28.6%	1.3%	4.7%	9.1%	9.1%
01 - Dittus-Boelter, 1930	46.7%	46.7%	52.6%	70.0%	-5.9%	6.1%	7.1%	9.2%
22 - Kitoh et al., 2001	49.0%	49.0%	53.9%	72.5%	-6.1%	6.2%	7.2%	9.4%
06 - Domin, 1963	51.5%	51.5%	46.5%	69.1%	-6.6%	6.8%	6.8%	9.4%
10 - Ornaty et al., 1970	-4.4%	19.2%	26.8%	26.9%	4.3%	6.7%	8.4%	9.4%
20 - Griem, 1996	44.8%	45.7%	70.3%	82.9%	-4.6%	5.5%	8.5%	9.6%
11 - Giarratano et al., 1970	51.8%	51.8%	54.5%	74.8%	-6.5%	6.6%	7.1%	9.6%
09 - Krasnoshchekov et al., 1967	62.4%	62.4%	73.4%	95.9%	-6.8%	6.8%	7.6%	10.1%
27 - Cheng et al., 2009	57.6%	57.6%	62.3%	84.5%	-6.9%	7.0%	7.6%	10.2%
05 - Petukhov et al., 1961	66.8%	66.8%	75.0%	100.0%	-7.2%	7.2%	7.5%	10.3%
02 - Sieder & Tate, 1936	84.3%	84.3%	68.5%	108.3%	-9.7%	9.7%	7.0%	11.9%
13 - Zukauskas, 1972	97.7%	97.7%	49.3%	109.2%	-11.2%	11.3%	6.4%	12.9%
08 - Swenson et al., 1965	-19.1%	23.1%	21.1%	28.3%	9.9%	10.9%	10.3%	14.3%
26 - Yu et al., 2009	221.2%	221.2%	116.9%	249.7%	-16.3%	16.3%	6.5%	17.5%
34 - Wang & Li, 2014	-32.7%	33.4%	21.8%	39.2%	18.9%	19.1%	14.9%	23.9%
32 - Gupta et al., 2013 (Film)	5.4%	26.0%	43.6%	43.6%	6.9%	11.4%	25.8%	26.5%
18 - Petukhov et al., 1983	-43.8%	44.3%	27.8%	51.7%	33.4%	33.4%	24.0%	41.0%
30 - Gupta et al., 2013 (Bulk)	39.8%	74.0%	73.9%	83.4%	11.0%	25.3%	42.0%	43.1%
29 - Gupta et al., 2011	-57.8%	57.8%	15.2%	59.7%	44.7%	44.7%	20.5%	49.1%
35 - Lei et al., 2019	-54.4%	54.4%	22.2%	58.7%	45.6%	45.6%	26.8%	52.8%
28 - Mokry et al., 2009	-53.9%	53.9%	24.7%	59.2%	51.0%	51.0%	36.4%	62.5%
31 - Gupta et al., 2013 (Wall)	3.4%	50.0%	56.7%	56.3%	29.9%	37.2%	58.2%	65.0%
25 - Kuang et al., 2008	-56.6%	56.6%	25.4%	62.0%	55.0%	55.0%	35.6%	65.4%
33 - Chen & Fang, 2014	-19.0%	48.3%	57.7%	60.3%	113.8%	117.5%	157.1%	192.9%
24 - Xu & Guo, 2005	-82.2%	82.2%	27.6%	86.7%	364.0%	364.0%	200.4%	414.8%

C.2.3 *bare tube Data Sorted by HTC RMS*

Correlation	HTC Error				T _{wall} Error			
	Average Error/Mean Error	Average Absolute Error	Standard Error	RMS Error	Average Error/Mean Error	Average Absolute Error	Standard Error	RMS Error
36 - Clark et al., 2020	4.4%	22.2%	28.7%	29.0%	-0.4%	2.4%	3.3%	3.3%
29 - Gupta et al., 2011	-8.9%	24.1%	27.9%	29.3%	2.5%	3.7%	4.5%	5.2%
08 - Swenson et al., 1965	0.3%	23.1%	29.6%	29.6%	1.0%	2.8%	3.7%	3.9%
28 - Mokry et al., 2009	5.0%	25.4%	34.2%	34.6%	0.8%	3.3%	5.0%	5.0%
34 - Wang & Li, 2014	13.1%	24.9%	33.8%	36.3%	-0.5%	2.4%	3.4%	3.5%
19 - Gorban et al., 1990	-3.2%	27.7%	36.9%	37.0%	0.0%	3.2%	4.3%	4.3%
32 - Gupta et al., 2013 (Film)	-27.4%	32.8%	25.9%	37.7%	5.3%	6.1%	5.8%	7.9%
27 - Cheng et al., 2009	3.7%	30.1%	39.7%	39.9%	1.7%	4.0%	5.5%	5.7%
30 - Gupta et al., 2013 (Bulk)	-30.7%	40.9%	34.0%	45.9%	7.3%	8.5%	8.1%	10.9%
21 - Hu, 2001	33.1%	36.2%	35.5%	48.5%	-2.7%	3.0%	3.3%	4.3%
16 - Dyadyakin & Popov, 1977	11.6%	38.2%	48.9%	50.3%	2.0%	5.1%	7.7%	8.0%
17 - Watts & Chou, 1982	30.9%	36.0%	43.2%	53.1%	-2.4%	3.1%	3.8%	4.5%
31 - Gupta et al., 2013 (Wall)	-46.7%	50.5%	27.3%	54.1%	13.5%	13.9%	10.8%	17.3%
33 - Chen & Fang, 2014	17.0%	44.1%	56.4%	58.9%	16.3%	20.6%	69.1%	71.0%
22 - Kitoh et al., 2001	23.5%	44.2%	56.9%	61.6%	-0.1%	5.6%	10.2%	10.2%
07 - Bishop et al., 1964	58.3%	59.5%	47.7%	75.3%	-4.0%	4.2%	3.8%	5.5%
14 - Jackson & Fewster, 1975	55.1%	56.6%	52.8%	76.3%	-4.1%	4.2%	4.0%	5.7%
24 - Xu & Guo, 2005	-8.3%	57.5%	82.1%	82.6%	19.1%	21.7%	36.6%	41.3%
25 - Kuang et al., 2008	36.0%	54.8%	80.2%	87.9%	-0.4%	5.0%	7.4%	7.4%
23 - Jackson, 2002	65.0%	66.6%	70.2%	95.7%	-4.4%	4.5%	4.5%	6.3%
09 - Krasnoshchekov et al., 1967	6.8%	75.5%	97.2%	97.4%	73.9%	77.5%	169.4%	184.8%
10 - Ornatsky et al., 1970	55.5%	67.1%	82.6%	99.5%	-3.2%	4.7%	5.6%	6.5%
05 - Petukhov et al., 1961	25.5%	72.6%	103.0%	106.1%	5.9%	9.8%	13.7%	14.9%
03 - Bringer & Smith, 1957	75.3%	78.3%	84.3%	113.0%	-4.4%	4.8%	4.7%	6.5%
12 - Yamagata et al., 1972	94.6%	95.4%	85.0%	127.2%	-5.3%	5.3%	4.3%	6.8%
20 - Griem, 1996	97.2%	98.0%	86.6%	130.2%	-5.6%	5.7%	4.7%	7.3%
04 - Miropol'skiy & Shitsman, 1957	116.4%	117.5%	113.4%	162.5%	-5.8%	5.9%	5.1%	7.8%
01 - Dittus-Boelter, 1930	130.6%	133.1%	156.0%	203.5%	-5.9%	6.1%	5.7%	8.2%
35 - Lei et al., 2019	101.9%	136.5%	184.9%	211.1%	-1.2%	8.4%	10.5%	10.5%
02 - Sieder & Tate, 1936	157.4%	158.0%	160.1%	224.6%	-6.9%	6.9%	5.4%	8.8%
11 - Giarratano et al., 1970	153.5%	154.7%	174.0%	232.0%	-6.4%	6.5%	5.6%	8.5%
15 - Gnielinski, 1976	169.0%	170.9%	198.3%	260.5%	-6.4%	6.6%	5.9%	8.7%
13 - Zukauskas, 1972	184.5%	189.3%	231.9%	296.3%	-6.4%	6.8%	6.1%	8.8%
18 - Petukhov et al., 1983	177.4%	214.5%	294.6%	343.9%	-1.6%	9.9%	11.9%	12.0%
26 - Yu et al., 2009	445.7%	445.7%	266.5%	519.3%	-9.8%	9.8%	5.5%	11.2%
06 - Domin, 1963	635.3%	638.2%	921.7%	1119.4%	-7.7%	8.0%	6.7%	10.2%

C.2.4 *bare tube Data Sorted by T_w RMS*

Correlation	HTC Error				T _{wall} Error			
	Average Error/Mean Error	Average Absolute Error	Standard Error	RMS Error	Average Error/Mean Error	Average Absolute Error	Standard Error	RMS Error
36 - Clark et al., 2020	4.4%	22.2%	28.7%	29.0%	-0.4%	2.4%	3.3%	3.3%
34 - Wang & Li, 2014	13.1%	24.9%	33.8%	36.3%	-0.5%	2.4%	3.4%	3.5%
08 - Swenson et al., 1965	0.3%	23.1%	29.6%	29.6%	1.0%	2.8%	3.7%	3.9%
21 - Hu, 2001	33.1%	36.2%	35.5%	48.5%	-2.7%	3.0%	3.3%	4.3%
19 - Gorbun et al., 1990	-3.2%	27.7%	36.9%	37.0%	0.0%	3.2%	4.3%	4.3%
17 - Watts & Chou, 1982	30.9%	36.0%	43.2%	53.1%	-2.4%	3.1%	3.8%	4.5%
28 - Mokry et al., 2009	5.0%	25.4%	34.2%	34.6%	0.8%	3.3%	5.0%	5.0%
29 - Gupta et al., 2011	-8.9%	24.1%	27.9%	29.3%	2.5%	3.7%	4.5%	5.2%
07 - Bishop et al., 1964	58.3%	59.5%	47.7%	75.3%	-4.0%	4.2%	3.8%	5.5%
14 - Jackson & Fewster, 1975	55.1%	56.6%	52.8%	76.3%	-4.1%	4.2%	4.0%	5.7%
27 - Cheng et al., 2009	3.7%	30.1%	39.7%	39.9%	1.7%	4.0%	5.5%	5.7%
23 - Jackson, 2002	65.0%	66.6%	70.2%	95.7%	-4.4%	4.5%	4.5%	6.3%
10 - Ornatsky et al., 1970	55.5%	67.1%	82.6%	99.5%	-3.2%	4.7%	5.6%	6.5%
03 - Bringer & Smith, 1957	75.3%	78.3%	84.3%	113.0%	-4.4%	4.8%	4.7%	6.5%
12 - Yamagata et al., 1972	94.6%	95.4%	85.0%	127.2%	-5.3%	5.3%	4.3%	6.8%
20 - Griem, 1996	97.2%	98.0%	86.6%	130.2%	-5.6%	5.7%	4.7%	7.3%
25 - Kuang et al., 2008	36.0%	54.8%	80.2%	87.9%	-0.4%	5.0%	7.4%	7.4%
04 - Miropol'skiy & Shitsman, 1957	116.4%	117.5%	113.4%	162.5%	-5.8%	5.9%	5.1%	7.8%
32 - Gupta et al., 2013 (Film)	-27.4%	32.8%	25.9%	37.7%	5.3%	6.1%	5.8%	7.9%
16 - Dyadyakin & Popov, 1977	11.6%	38.2%	48.9%	50.3%	2.0%	5.1%	7.7%	8.0%
01 - Dittus-Boelter, 1930	130.6%	133.1%	156.0%	203.5%	-5.9%	6.1%	5.7%	8.2%
11 - Giarratano et al., 1970	153.5%	154.7%	174.0%	232.0%	-6.4%	6.5%	5.6%	8.5%
15 - Gnielinski, 1976	169.0%	170.9%	198.3%	260.5%	-6.4%	6.6%	5.9%	8.7%
02 - Sieder & Tate, 1936	157.4%	158.0%	160.1%	224.6%	-6.9%	6.9%	5.4%	8.8%
13 - Zukauskas, 1972	184.5%	189.3%	231.9%	296.3%	-6.4%	6.8%	6.1%	8.8%
06 - Domin, 1963	635.3%	638.2%	921.7%	1119.4%	-7.7%	8.0%	6.7%	10.2%
22 - Kitoh et al., 2001	23.5%	44.2%	56.9%	61.6%	-0.1%	5.6%	10.2%	10.2%
35 - Lei et al., 2019	101.9%	136.5%	184.9%	211.1%	-1.2%	8.4%	10.5%	10.5%
30 - Gupta et al., 2013 (Bulk)	-30.7%	40.9%	34.0%	45.9%	7.3%	8.5%	8.1%	10.9%
26 - Yu et al., 2009	445.7%	445.7%	266.5%	519.3%	-9.8%	9.8%	5.5%	11.2%
18 - Petukhov et al., 1983	177.4%	214.5%	294.6%	343.9%	-1.6%	9.9%	11.9%	12.0%
05 - Petukhov et al., 1961	25.5%	72.6%	103.0%	106.1%	5.9%	9.8%	13.7%	14.9%
31 - Gupta et al., 2013 (Wall)	-46.7%	50.5%	27.3%	54.1%	13.5%	13.9%	10.8%	17.3%
24 - Xu & Guo, 2005	-8.3%	57.5%	82.1%	82.6%	19.1%	21.7%	36.6%	41.3%
33 - Chen & Fang, 2014	17.0%	44.1%	56.4%	58.9%	16.3%	20.6%	69.1%	71.0%
09 - Krasnoshchekov et al., 1967	6.8%	75.5%	97.2%	97.4%	73.9%	77.5%	169.4%	184.8%

C.3 CALCULATIONS

In order to analyze which **Nu** correlation provided the best predictor for HTC and T_w for the datasets, each **Nu** correlation was tested.

The **Nu** correlations in many cases require an iterative calculation process. In addition, the type of calculations performed depends on the data input type:

- 1) Raw Data
- 2) Parameter Data

For Raw data input, the outcome of experimental trials can be used to predict wall temperatures. In this data type, all inputs (T_b , T_w , HTC) and parameters are known (P , G , q_{avg} , D_{hy}) at varying locations along the heated length, depending upon where the thermocouples for each experiment are located. Each **Nu** correlation can be used to predict the T_w and the HTC, and then can be compared to the measured values.

The Parameter data input is the type that would be used by engineers when designing a system. Only the initial parameters are known (P , G , q_{avg} , D_{hy}) along with the bulk-fluid temperature at the inlet condition (T_{in} / T_b @ inlet), and all subsequent inputs (T_b , T_w , HTC) are computed along the heated length.

A sample calculation for the Parameter data input will be shown below:

*C.3.1 Sample Calculation for **Nu** Correlations*

When calculating the Parameter data, there are two stages of calculation that must be performed. The first stage calculates the T_w and HTC and can be direct or iterative depending upon the **Nu** correlation. This stage is common to both Parameter data and Raw data inputs.

The second stage calculates the T_b and is a direct calculation.

This sample calculation will use the Mokry, et al. (2009) correlation, Eq. (28).

C.3.1.1 First Stage

The first stage calculates the T_w and HTC by using the T_b , and all inlet conditions.

For this sample calculation, the input parameters are listed below in Table C-2, obtained from Razumovskiy, et al. (2008). While the D_{hy} listed in literature for the Razumovskiy 7-rod bundle is 2.76 mm, the actual value is 2.57 mm. See

Table C-2: Input Parameters for Sample Calculation
(Razumovskiy et al., 2008)

Parameter	Symbol	Value	Unit
Bulk Fluid Inlet Temperature	T_b	184	°C
Inlet Pressure	P	24.5	MPa
Mass Flux	G	800	kg/m ² ·s
Average Heat Flux	q	719	kW/m ²
Hydraulic Diameter	D_{hy}	2.5741	mm
Flow Area	A_{fl}	140.29	mm ²
Heated Perimeter	p_h	147.95	mm
Heated Length	L	0.485	m
Step Value	Δx	0.005	m
Error Value	Ev	0.01	°C

All experimental results calculated for HTC and T_w for all **Nu** correlations were obtained using properties from NIST REFPROP version 10.0.

With the bulk temperature and inlet pressure known, the bulk fluid thermophysical properties are computed using NIST REFPROP 10.0 (Lemmon et al., 2018). These properties are listed below in Table C-3.

Table C-3: Initial Bulk Fluid Thermophysical Properties

Property @ 184°C, 24.5 MPa	Symbol	Value	Unit
Density	ρ	897.8015	kg/m ³
Dynamic Viscosity	μ	0.00015264	Pa·s
Kinematic Viscosity	ν	0.000000170	m ² /s
Specific Heat Capacity	C_p	4324.1	J/kg·K
Specific Enthalpy	H	792755.1	J/kg
Thermal Conductivity	k	0.6869	W/m·K
Prandtl Number	Pr	0.96091	-
Volumetric Expansivity	β	0.001132	1/K
Thermal Diffusivity	α	0.000000177	m ² /s

With these properties known, the Reynolds number can be calculated:

$$\mathbf{Re}_b = \frac{\rho_b V_b D_{hy}}{\mu_b} = \frac{\rho_b \left(\frac{\dot{V}}{A_{fl}} \right) D_{hy}}{\mu_b} = \frac{\rho_b \left(\frac{\dot{m}/\rho_b}{A_{fl}} \right) D_{hy}}{\mu_b} = \frac{G \cdot D_{hy}}{\mu_b}$$

$$\mathbf{Re}_b = \frac{G \cdot D_{hy}}{\mu_b} = \frac{800 \text{ kg/m}^2 \cdot \text{s} \cdot 0.0025741 \text{ m}}{0.00015264 \text{ Pa} \cdot \text{s}} = 13491.09$$

For **Nu** correlations that are direct and do not require iteration, the Nusselt number would be computed here directly ending the First Stage. However, for **Nu** correlations requiring iteration, the next step is to determine an initial guess for the wall temperature. This is accomplished by using the Dittus-Boelter (1930) correlation Eq. (1).

$$\mathbf{Nu}_{DB} = 0.023 \cdot \mathbf{Re}_b^{0.8} \cdot \mathbf{Pr}_b^{0.4}$$

$$\mathbf{Nu}_{DB} = 0.023 \cdot (13491.09)^{0.8} \cdot (0.96091)^{0.4} = 45.59$$

$$h_{DB} = \frac{\mathbf{Nu}_{DB} \cdot k_b}{D_{hy}} = \frac{45.59 \cdot 0.6869 \text{ W/m} \cdot \text{K}}{0.0025741 \text{ m}} = 12164.35 \text{ W/m}^2 \cdot \text{K}$$

$$q_{AVG} = h_{DB} \cdot (T_{w,DB} - T_b) \rightarrow T_w = T_b + \frac{q_{AVG}}{h_{DB}}$$

$$T_w = 184^\circ\text{C} + \frac{719000 \text{ W/m}^2}{12164.35 \text{ W/m}^2 \cdot \text{K}} = 243.11^\circ\text{C}$$

The next step is to use this wall temperature as an initial guess to determine the fluid properties at the wall temperature:

Table C-4: 1st Iteration Properties

Property @ 243.11°C, 24.5 MPa	Symbol	Value	Unit
Density	ρ	829.63	kg/m ³
Specific Enthalpy	H	1055490.49	J/kg

Using these properties, the wall temperature can then be computed using the Mokry, et al. (2009) equation. This is an iterative process, where the average properties must first be computed:

First Iteration:

$$\overline{C_P} = \frac{H_w - H_b}{T_w - T_b} = \frac{(1055490.49 - 792755.1) \frac{J}{kg}}{(243.11 - 184)^\circ C} = 4444.86 J/kg \cdot K$$

$$\overline{Pr}_b = \frac{\overline{C_P} \cdot \mu_b}{k_b} = \frac{4444.86 \frac{J}{kg \cdot K} \cdot 0.00015264 Pa \cdot s}{0.6869 \frac{W}{m \cdot K}} = 0.98772$$

$$Nu_{MEA} = 0.0061 \cdot Re_b^{0.904} \cdot \overline{Pr}_b^{0.684} \cdot \left(\frac{\rho_w}{\rho_b} \right)^{0.564}$$

$$Nu_{MEA} = 0.0061 \cdot (13491.09)^{0.904} (0.98772)^{0.684} \cdot \left(\frac{829.63 \frac{kg}{m^3}}{897.80 \frac{kg}{m^3}} \right)^{0.564}$$

$$Nu_{MEA} = 31.32$$

$$h_{MEA} = \frac{Nu_{MEA} \cdot k_b}{D_{hy}} = \frac{31.32 \cdot 0.6869 W/m \cdot K}{0.0025741 m} = 8358.87 W/m^2 \cdot K$$

$$T_w = 184^\circ C + \frac{719000 W/m^2}{8358.87 W/m^2 \cdot K} = 270.02^\circ C$$

$$T_{w,1-2} = |270.02 - 243.11|^\circ C = 26.91^\circ C$$

The difference in temperature between the first guess (from Dittus-Boelter equation), and the Mokry prediction is 26.91°C. The next step in the procedure is to repeat this first step until the solution converges less than the specified error value (Ev). For this sample calculation, the error value specified is 0.01°C as per Table C-2.

Second Iteration:

Table C-5: 2nd Iteration properties

Property @ 270.02°C, 24.5 MPa	Symbol	Value	Unit
Density	ρ	791.86	kg/m ³
Specific Enthalpy	H	1181969.46	J/kg

$$\overline{C_P} = \frac{H_w - H_b}{T_w - T_b} = \frac{(1181969.46 - 792755.1) \frac{J}{kg}}{(270.02 - 184)^\circ C} = 4524.70 J/kg \cdot K$$

$$\overline{Pr}_b = \frac{\overline{C_P} \cdot \mu_b}{k_b} = \frac{4524.70 \frac{J}{kg \cdot K} \cdot 0.00015264 Pa \cdot s}{0.6869 \frac{W}{m \cdot K}} = 1.00546$$

$$Nu_{MEA} = 0.0061 \cdot (13491.09)^{0.904} (1.00546)^{0.684} \cdot \left(\frac{791.86 \frac{kg}{m^3}}{897.80 \frac{kg}{m^3}} \right)^{0.564} = 30.89$$

$$h_{MEA} = \frac{Nu_{MEA} \cdot k_b}{D_{hy}} = \frac{30.89 \cdot 0.6869 W/m \cdot K}{0.0025741 m} = 8241.80 W/m^2 \cdot K$$

$$T_w = 184^\circ C + \frac{719000 W/m^2}{8241.80 W/m^2 \cdot K} = 271.24^\circ C$$

$$T_{w,1-2} = |271.24 - 268.25|^\circ C = 2.99^\circ C$$

Third Iteration:

Table C-6: 3rd Iteration Properties

Property @ 271.24°C, 24.5 MPa	Symbol	Value	Unit
Density	ρ	790.02	kg/m ³
Specific Enthalpy	H	1187851.42	J/kg

$$\overline{C_P} = \frac{H_w - H_b}{T_w - T_b} = \frac{(1187851.42 - 792755.1) \frac{J}{kg}}{(271.24 - 184)^\circ C} = 4528.84 J/kg \cdot K$$

$$\overline{Pr}_b = \frac{\overline{C_P} \cdot \mu_b}{k_b} = \frac{4528.84 \frac{J}{kg \cdot K} \cdot 0.00015264 Pa \cdot s}{0.6869 \frac{W}{m \cdot K}} = 1.00638$$

$$\mathbf{Nu}_{\text{MEA}} = 0.0061 \cdot (13491.09)^{0.904} (1.00638)^{0.684} \cdot \left(\frac{790.02 \frac{\text{kg}}{\text{m}^3}}{897.80 \frac{\text{kg}}{\text{m}^3}} \right)^{0.564} = 30.86$$

$$h_{\text{MEA}} = \frac{\mathbf{Nu}_{\text{MEA}} \cdot k_b}{D_{\text{hy}}} = \frac{30.86 \cdot 0.6869 \text{ W/m} \cdot \text{K}}{0.0025741 \text{ m}} = 8236.15 \text{ W/m}^2 \cdot \text{K}$$

$$T_w = 184^\circ\text{C} + \frac{719000 \text{ W/m}^2}{8236.15 \text{ W/m}^2 \cdot \text{K}} = 271.30^\circ\text{C}$$

$$T_{w,1-2} = |271.30 - 271.24|^\circ\text{C} = 0.06^\circ\text{C}$$

Fourth Iteration:

Table C-7: 4th Iteration Properties

Property @ 271.30°C, 24.5 MPa	Symbol	Value	Unit
Density	ρ	789.92	kg/m ³
Specific Enthalpy	H	1188141.08	J/kg

$$\overline{C_P} = \frac{H_w - H_b}{T_w - T_b} = \frac{(1188141.08 - 792755.1) \frac{\text{J}}{\text{kg}}}{(271.30 - 184)^\circ\text{C}} = 4529.05 \text{ J/kg} \cdot \text{K}$$

$$\overline{\text{Pr}}_b = \frac{\overline{C_P} \cdot \mu_b}{k_b} = \frac{4529.05 \frac{\text{J}}{\text{kg} \cdot \text{K}} \cdot 0.00015264 \text{ Pa} \cdot \text{s}}{0.6869 \frac{\text{W}}{\text{m} \cdot \text{K}}} = 1.00643$$

$$\mathbf{Nu}_{\text{MEA}} = 0.0061 \cdot (13491.09)^{0.904} (1.00643)^{0.684} \cdot \left(\frac{789.92 \frac{\text{kg}}{\text{m}^3}}{897.80 \frac{\text{kg}}{\text{m}^3}} \right)^{0.564} = 30.86$$

$$h_{\text{MEA}} = \frac{\mathbf{Nu}_{\text{MEA}} \cdot k_b}{D_{\text{hy}}} = \frac{30.86 \cdot 0.6869 \text{ W/m} \cdot \text{K}}{0.0025741 \text{ m}} = 8235.82 \text{ W/m}^2 \cdot \text{K}$$

$$T_w = 184^\circ\text{C} + \frac{719000 \text{ W/m}^2}{8235.82 \text{ W/m}^2 \cdot \text{K}} = 271.30^\circ\text{C}$$

$$T_{w,1-2} = |271.30 - 271.30|^\circ\text{C} = 0.00^\circ\text{C}$$

At the end of the iteration process, the temperature converges to a singular solution.

C.3.1.2 Second Stage

The second stage is to move along the heated path length. Continuing with the example, the step size specified in Table C-2 is 0.005 m. The specific enthalpy must be calculated at this next step along the heated length (i.e. Start point + step size).

From the thermodynamic relationship:

$$\dot{Q}_{AVG} = \dot{m} \cdot (H_{i+1} - H_i)$$

where;

$$\dot{Q}_{AVG} \left(\frac{kJ}{s} \right), \quad \dot{m} \left(\frac{kg}{s} \right), \quad H_i \left(\frac{kJ}{kg} \right)$$

Transforming the thermodynamic relationship into one that uses the specified variables:

$$\begin{aligned} q_{AVG} \cdot A_h &= (G \cdot A_{fl}) \cdot (H_{i+1} - H_i) \\ q_{AVG} &= G \cdot \frac{A_{fl}}{A_h} \cdot (H_{i+1} - H_i) \rightarrow q_{AVG} = G \cdot \frac{A_{fl}}{p_h \cdot \Delta x} \cdot (H_{i+1} - H_i) \\ H_{i+1} &= H_i + \frac{q_{AVG} \cdot p_h \cdot \Delta x}{A_{fl} \cdot G} \end{aligned}$$

Using this relationship, the enthalpy values can be determined at the next step value:

$$H_{i+1} = 792755.1 \text{ J/kg} + \frac{719000 \text{ W/m}^2 \cdot 0.14795 \text{ m} \cdot 0.005 \text{ m}}{0.00014029 \text{ m}^2 \cdot 800 \text{ kg/m}^2 \cdot s} = 797494.21 \text{ J/kg}$$

Using NIST REFPROP 10.0:

Table C-8: Temperature at H_{i+1}

Property @ 797.494 kJ/kg, 24.5 MPa	Symbol	Value	Unit
Temperature	T	185.10	$^{\circ}\text{C}$

With the bulk temperature known, the First Stage can begin again to determine the wall temperature at this next distance along the heated length.

C.3.1.3 Non-Convergent Wall Temperature

An example is shown below with the Swenson, et al. (1965) correlation Eq. (8) ($P = 24.1$ MPa, $G = 1500 \text{ kg/m}^2 \cdot \text{s}$, $q = 884 \text{ kW/m}^2$, $T_b = 352.97^\circ\text{C}$, $D_{hy} = 10 \text{ mm}$, bare tube). The first two iterations are listed.

FIRST ITERATION

$$\text{Re}_b = \frac{G \cdot D_{hy}}{\mu_b} = \frac{1500 \text{ kg/m}^2 \cdot \text{s} \cdot 0.01 \text{ m}}{0.00007083 \text{ Pa} \cdot \text{s}} = 211,765.64$$

$$\text{Nu}_{DB} = 0.023 \cdot \text{Re}_b^{0.8} \cdot \text{Pr}_b^{0.4} = 0.023 \cdot (211,765.64)^{0.8} \cdot (1.09660)^{0.4} = 434.94$$

$$h_{DB} = \frac{\text{Nu}_{DB} \cdot k_b}{D_{hy}} = \frac{434.94 \cdot 0.47890 \text{ W/m} \cdot \text{K}}{0.01 \text{ m}} = 20,829.47 \text{ W/m}^2 \cdot \text{K}$$

$$T_w = T_b + \frac{q_{AVG}}{h_{DB}} = 352.97^\circ\text{C} + \frac{884000 \text{ W/m}^2}{20,829.47 \text{ W/m}^2 \cdot \text{K}} = 395.41^\circ\text{C}$$

$$\overline{C}_p = \frac{H_w - H_b}{T_w - T_b} = \frac{(2576533.38 - 1648777.01) \frac{\text{J}}{\text{kg}}}{(395.41 - 352.97)^\circ\text{C}} = 21860.49 \text{ J/kg} \cdot \text{K}$$

$$\overline{\text{Pr}}_w = \frac{\overline{C}_p \cdot \mu_w}{k_w} = \frac{21860.49 \frac{\text{J}}{\text{kg} \cdot \text{K}} \cdot 0.00002872 \text{ Pa} \cdot \text{s}}{0.16267 \frac{\text{W}}{\text{m} \cdot \text{K}}} = 3.85940$$

$$\text{Re}_w = \frac{G \cdot D_{hy}}{\mu_w} = \frac{1500 \text{ kg/m}^2 \cdot \text{s} \cdot 0.01 \text{ m}}{0.00002872 \text{ Pa} \cdot \text{s}} = 522,302.38$$

$$\text{Nu}_{w,S} = 0.00459 \cdot (522,302.38)^{0.923} \cdot (3.85940)^{0.613} \cdot \left(\frac{161.35}{611.29}\right)^{0.231} = 1463.39$$

$$h_S = \frac{\text{Nu}_{w,S} \cdot k_w}{D_{hy}} = \frac{1463.39 \cdot 0.16267 \text{ W/m} \cdot \text{K}}{0.01 \text{ m}} = 23,805.01 \text{ W/m}^2 \cdot \text{K}$$

$$T_w = T_b + \frac{q_{AVG}}{h_S} = 352.97^\circ\text{C} + \frac{884000 \text{ W/m}^2}{23,805.01 \text{ W/m}^2 \cdot \text{K}} = 390.11^\circ\text{C}$$

$$T_{w,1-2} = |390.11 - 395.41|^\circ\text{C} = 5.30^\circ\text{C}$$

SECOND ITERATION

$$\overline{C_P} = \frac{H_w - H_b}{T_w - T_b} = \frac{(2493482.36 - 1648777) \frac{J}{kg}}{(390.11 - 352.97)^\circ C} = 22746.86 J/kg \cdot K$$

$$\overline{Pr}_w = \frac{\overline{C_P} \cdot \mu_w}{k_w} = \frac{22746.86 \frac{J}{kg \cdot K} \cdot 0.00002952 Pa \cdot s}{0.19334 \frac{W}{m \cdot K}} = 3.47342$$

$$Re_w = \frac{G \cdot D_{hy}}{\mu_w} = \frac{1500 kg/m^2 \cdot s \cdot 0.01 m}{0.00002952 Pa \cdot s} = 508,082.09$$

$$Nu_{w,S} = 0.00459 \cdot (508,082.09)^{0.923} \cdot (3.47342)^{0.613} \cdot \left(\frac{180.67}{611.29}\right)^{0.231} = 1372.75$$

$$h_S = \frac{Nu_{w,S} \cdot k_w}{D_{hy}} = \frac{1372.75 \cdot 0.19334 W/m \cdot K}{0.01 m} = 26540.78 W/m^2 \cdot K$$

$$T_w = T_b + \frac{q_{AVG}}{h_S} = 352.97^\circ C + \frac{884000 W/m^2}{26540.78 W/m^2 \cdot K} = 386.28^\circ C$$

$$T_{w,1-2} = |386.28 - 389.12|^\circ C = 3.83^\circ C$$

Figure C-1 shows the results of the next 31 iterations. After the 11th iteration, the calculations enter a loop of non-convergence passing through the pc point. This non-convergence has a low range ($\sim 6^\circ C$), though this is not always the case.

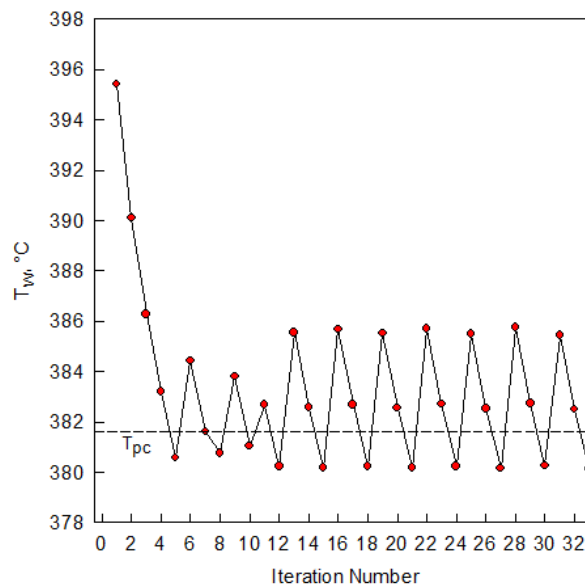


Figure C-1: Example of Non-Convergence

C.3.2 Hydraulic Diameter Calculations

C.3.2.1 7-rod Bundle

Figure 3-3 is shown below, listing the dimensions of the 7-rod bundle.

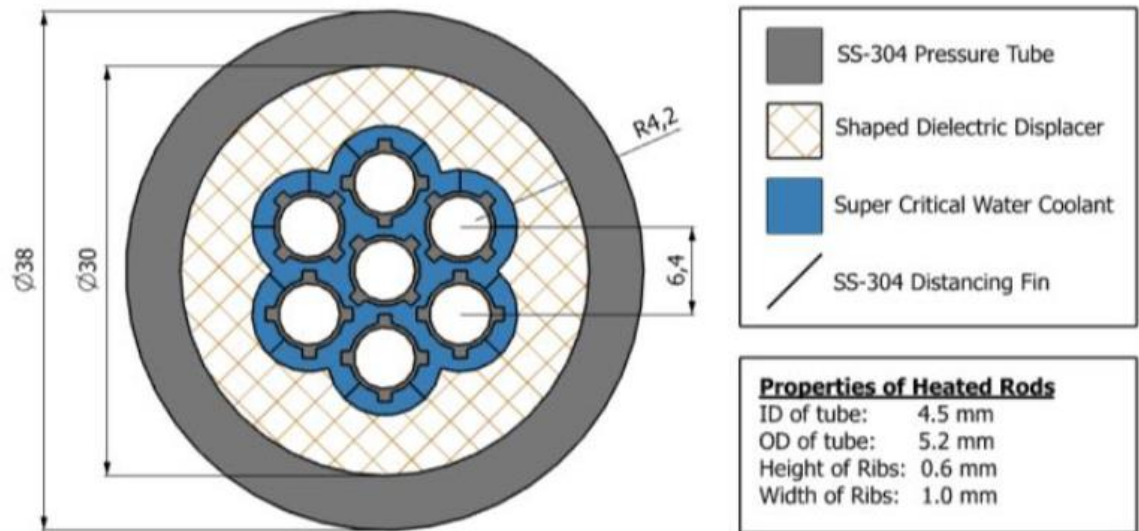


Figure 3-3: Radial Cross Section of 7-rod Bundle (repeated)

To calculate D_{hy} , the total area without fuel bundles is calculated, then the area of the fuel bundles including ribs is subtracted from the total area.

To calculate the total area without fuel bundles, the area is split into three zones shown in Figure C-2: Total Flow Area of 7-rod Fuel Bundle:

- 1) Semi Circles (in pink, bounded by red lines)
- 2) Triangles (in blue, bounded by blue lines)
- 3) Hexagon (in green)

The flow area is made up of 6 overlapping circles. Each of these 6 circles has a diameter of 8.4 mm. Therefore, the distance from the centre of these circles to the overlap point is equal to the radius of these circles (4.2 mm).

In addition, the centre of each of these circles is also the centre of the fuel bundles, having a centre-to-centre pitch of 6.4 mm.

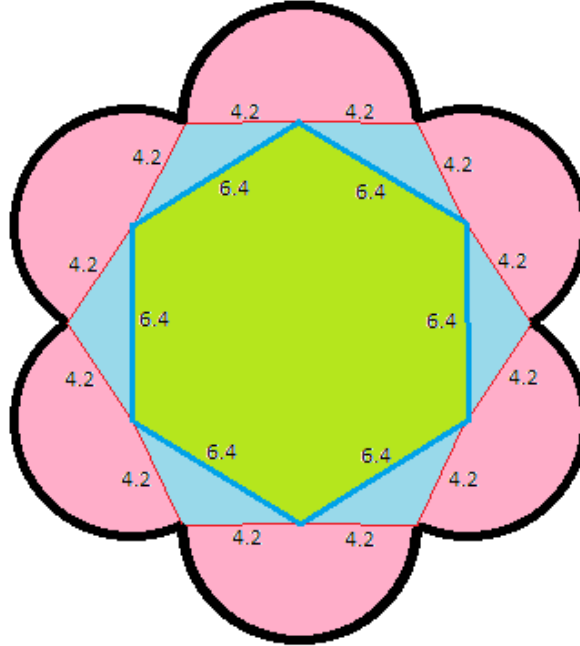


Figure C-2: Total Flow Area of 7-rod Fuel Bundle

Therefore, to calculate the total area of all 6 semi circles (in pink) the angle subtracted must be determined:

$$A_{semi-circles} = 6 * \frac{\pi}{4} \cdot D^2 \cdot \frac{Angle_{semi-circle}}{360^\circ}$$

$$Angle_{semi-circle} = 360^\circ - 2 \cdot Angle_{Triangle} - Angle_{Hexagon}$$

$$Angle_{Triangle} = \cos^{-1} \left(\frac{Pitch/2}{D/2} \right) = \cos^{-1} \left(\frac{Pitch}{D} \right)$$

$$Angle_{Triangle} = \cos^{-1} \left(\frac{6.4 \text{ mm}}{8.4 \text{ mm}} \right) = 40.37^\circ$$

$$Angle_{Hexagon} = \frac{720^\circ}{6} = 120^\circ$$

therefore;

$$Angle_{semi-circle} = 360 - 2 \cdot 40.37^\circ - 120^\circ = 159.26^\circ$$

$$A_{semi-circles} = 6 * \frac{\pi}{4} \cdot (8.4 \text{ mm})^2 \cdot \frac{159.26^\circ}{360^\circ} = 147.10 \text{ mm}^2$$

To calculate the area of the all 6 triangles (in blue), Pythagorean theorem can be used:

$$A_{Triangles} = \frac{Pitch \cdot Height_{Triangle}}{2}$$

$$A_{Triangles} = \frac{6 \cdot Pitch \cdot \sqrt{\left(\frac{D}{2}\right)^2 - \left(\frac{Pitch}{2}\right)^2}}{2} = 3 \cdot 6.4 \text{ mm} \cdot \sqrt{\left(\frac{8.4 \text{ mm}}{2}\right)^2 - \left(\frac{6.4 \text{ mm}}{2}\right)^2}$$

$$A_{Triangle} = 52.23 \text{ mm}^2$$

Finally, the area of the hexagon (in green) is calculated:

$$A_{Hexagon} = \frac{3 \cdot \sqrt{3}}{2} \cdot Pitch^2 = \frac{3 \cdot \sqrt{3}}{2} \cdot (6.4 \text{ mm})^2 = 106.42 \text{ mm}^2$$

Thus, the total area of the fuel channel, without fuel bundles is:

$$A_{fuel \text{ channel}} = A_{semi-circles} + A_{Triangles} + A_{Hexagon}$$

$$A_{fuel \text{ channel}} = 147.10 \text{ mm}^2 + 52.23 \text{ mm}^2 + 106.42 \text{ mm}^2 = 305.75 \text{ mm}^2$$

Next the total area of the fuel bundles is calculated:

$$A_{7-Rods} = 7 \cdot (A_{Rod} + 4 \cdot A_{Rib}) = 7 \cdot \left[\frac{\pi}{4} \cdot D_{Rod}^2 + 4 \cdot (Height_{Rib} \cdot Width_{Rib}) \right]$$

$$A_{7-Rods} = 7 \cdot \left[\frac{\pi}{4} \cdot (5.2 \text{ mm})^2 + 4 \cdot (0.6 \text{ mm} \cdot 1 \text{ mm}) \right] = 165.46 \text{ mm}^2$$

Therefore, the total flow area is:

$$A_{fl} = A_{fuel \text{ channel}} - A_{7-Rods} = 305.75 \text{ mm}^2 - 165.46 \text{ mm}^2 = 140.29 \text{ mm}^2$$

Next the wetted perimeter must be calculated:

$$p_{wet} = p_h + p_{unheated}$$

The heated perimeter is calculated. An assumption is made that the width of the Rib (1 mm) is the same width as the fuel rod is covers. While this is not actually the case (the projected 1 mm straight line onto the circle would be larger due to the curvature), the error associated with this assumption is small. Therefore, the Rib width considered with the Width.

$$p_h = 7 \cdot [\pi \cdot D_{Rod} + 4 \cdot (2 \cdot Width_{Rib})]$$

$$p_h = 7 \cdot [\pi \cdot 5.2 \text{ mm} + 4 \cdot (2 \cdot 0.6 \text{ mm})] = 147.95 \text{ mm}$$

The unheated perimeter is calculated next:

$$p_{\text{unheated}} = 6 \cdot \pi \cdot D \cdot \frac{\text{Angle}_{\text{semi-circle}}}{360^\circ} = 6 \cdot \pi \cdot 8.4 \text{ mm} \cdot \frac{159.26^\circ}{360^\circ} = 70.05 \text{ mm}$$

$$p_{\text{wet}} = 147.95 \text{ mm} + 70.05 \text{ mm} = 218.00 \text{ mm}$$

Therefore, the hydraulic diameter of the 7-rod fuel bundle is:

$$D_{\text{hy}} = \frac{4 \cdot A_{\text{fl}}}{p_{\text{wet}}} = \frac{4 \cdot 140.29 \text{ mm}^2}{218.00 \text{ mm}} = 2.5741 \text{ mm}$$

C.3.2.2 37-Element Bundle

To calculate flow characteristics for the 37-Element bundle, the flow area, heated perimeter, wetted perimeter, hydraulic diameter, mass flux, and heat flux must be calculated.

$$A_{\text{fl}} = \frac{\pi}{4} (D_{\text{bare tube}}^2 - 37 \cdot D_{\text{Fuel Rod}}^2) = \frac{\pi}{4} [(103.38 \text{ mm})^2 - 37 \cdot (13.08 \text{ mm})^2]$$

$$A_{\text{fl}} = 3422.16 \text{ mm}^2$$

$$p_{\text{h}} = 37 \cdot \pi \cdot D = 37 \cdot \pi \cdot 13.08 \text{ mm} = 1520.41 \text{ mm}$$

$$p_{\text{unheated}} = \pi \cdot D = \pi \cdot 103.38 \text{ mm} = 324.78 \text{ mm}$$

$$p_{\text{wet}} = p_{\text{h}} + p_{\text{unheated}} = 1520.41 \text{ mm} + 324.78 \text{ mm} = 1845.18 \text{ mm}$$

$$D_{\text{hy}} = \frac{4 \cdot A_{\text{fl}}}{p_{\text{wet}}} = \frac{4 \cdot 3422.16 \text{ mm}^2}{1845.18 \text{ mm}} = 7.42 \text{ mm}$$

To calculate the mass flux:

$$G = \frac{\dot{m}}{A_{\text{fl}}} = \frac{5.13 \text{ kg/s}}{3422.16 \text{ mm}^2 / 1000^2} = 1499.05 \frac{\text{kg}}{\text{m}^2 \cdot \text{s}}$$

Next, the heated area is determined and used with the channel power to calculate the heat flux, with a constant heat flux assumed:

$$A_{\text{h}} = 37 \cdot \pi \cdot D \cdot L = 37 \cdot \pi \cdot \frac{13.08 \text{ mm}}{1000} \cdot (0.485 \text{ m} \cdot 12) = 8.8488 \text{ m}^2$$

$$q_{\text{avg}} = \frac{\dot{Q}_{\text{nominal}}}{A_h} = \frac{9970 \text{ kW}}{8.8488 \text{ m}^2} = 1126.71 \text{ kW/m}^2$$

The length considered is 12 bundles:

$$L = 12 \cdot 0.485 \text{ m} = 5.82 \text{ m}$$

C.3.2.3 64-Element Bundle

Using the same approach as the 37-element bundle:

$$A_{\text{fl}} = A_{\text{Liner ID}} - A_{\text{Centre Flow Tube}} - A_{\text{Fuel Rods}} = \frac{\pi}{4} (D_{\text{LID}}^2 - D_{\text{CFT}}^2 - 64 \cdot D_{\text{FR}}^2)$$

$$A_{\text{fl}} = \frac{\pi}{4} [(144.0 \text{ mm})^2 - (94.0 \text{ mm})^2 - 32 \cdot (9.5 \text{ mm})^2 - 32 \cdot (10.0 \text{ mm})^2]$$

$$A_{\text{fl}} = 4564.73 \text{ mm}^2$$

$$p_h = 32\pi D_{\text{Inner Ring}} + 32\pi D_{\text{Outer Ring}} = 32\pi(9.5 + 10) \text{ mm} = 1960.35 \text{ mm}$$

$$p_{\text{unheated}} = \pi D_{\text{LID}} + \pi D_{\text{CFT}} = \pi(144 + 94) \text{ mm} = 747.70 \text{ mm}$$

$$p_{\text{wet}} = p_h + p_{\text{unheated}} = 1520.41 \text{ mm} + 324.78 \text{ mm} = 2708.05 \text{ mm}$$

$$D_{\text{hy}} = \frac{4 \cdot A_{\text{fl}}}{p_{\text{wet}}} = \frac{4 \cdot 4564.73 \text{ mm}^2}{2708.05 \text{ mm}} = 6.74 \text{ mm}$$

To calculate the mass flux:

$$G = \frac{\dot{m}}{A_{\text{fl}}} = \frac{5.13 \text{ kg/s}}{4564.73 \text{ mm}^2/1000^2} = 1123.83 \frac{\text{kg}}{\text{m}^2 \cdot \text{s}}$$

Next, the heated area is determined and used with the channel power to calculate the heat flux, with a constant heat flux assumed:

$$A_h = p_h \cdot L = \frac{1960.35 \text{ mm}}{1000} \cdot 5 \text{ m} = 9.80 \text{ m}^2$$

$$q_{\text{avg}} = \frac{\dot{Q}_{\text{nominal}}}{A_h} = \frac{9970 \text{ kW}}{9.80 \text{ m}^2} = 1017.35 \text{ kW/m}^2$$

The cladding thickness used for the calculation is 0.4 mm, as outlined by Yetisir et al. (2018). The length considered is 5 m.

C.3.3 Sheath and Fuel Centreline Temperature Calculations

C.3.3.1 Sheath Temperature

For Razumovskiy Trial #1 @ $x=0$ m, the Clark, et al. (2020) correlation predicts a T_w of 257.1°C (530.3 K) at the bulk fluid temperature of 184°C . From Figure 3-3, the OD of the sheath is 5.2 mm, while the ID is 4.5 mm.

From (2.1) the thermal conductivity for Alloy 625 at this temperature is:

$$k_{\text{A625}} \left(\frac{W}{m \cdot K} \right) = 9.7116 + 0.0176 \cdot (257.1^\circ\text{C}) = 14.24 \frac{W}{m \cdot K}$$

Therefore, the internal sheath temperature is:

$$T_{\text{int}} = 257.1^\circ\text{C} + \frac{719,000 \frac{W}{m \cdot K} \cdot \frac{5.2 \text{ mm}}{2 \cdot 1000}}{14.24 \frac{W}{m \cdot K}} \cdot \ln \left(\frac{5.2 \text{ mm} / 2}{4.5 \text{ mm} / 2} \right) = 276.0^\circ\text{C} (549.2 \text{ K})$$

C.3.3.2 Fuel Centreline Temperature, 7-rod

From the average heat flux of 719 kW/m^2 , the average energy density of each rod is:

$$\dot{q} = \frac{\dot{Q}}{V} = \frac{\frac{q}{\# \text{ Rods}} A_h}{V} = \frac{\frac{q}{\# \text{ Rods}} (\pi D L)}{\left(\frac{\pi}{4} D^2 L \right)} = \frac{4 \frac{q}{\# \text{ Rods}}}{D} = \frac{4 \frac{0.719 \frac{MW}{m^2}}{7}}{\frac{4.5 \text{ mm}}{1000}} = 91.3 \frac{MW}{m^3}$$

From section 2.2.4, the thermal conductivity of the UO_2 fuel for the first shell is calculated as:

$$k_{\text{UO}_2} = \left[\frac{100}{6.548 + 23.533 \cdot \frac{549.2 \text{ K}}{1000}} \right] + \left[\frac{6400}{\left(\frac{549.2 \text{ K}}{1000} \right)^{2.5}} \right] \cdot e^{\left(-\frac{16350}{549.2 \text{ K}} \right)} = 5.14 \frac{W}{m \cdot K}$$

The temperature inside the first shell (4 mm OD) is as below:

$$T_i = T_o + \frac{\dot{q}}{4k} (r_o^2 - r_i^2) = 276.0^\circ\text{C} + \frac{91.3 \frac{MW}{m^3}}{4 \cdot 5.14 \frac{W}{m \cdot K}} \left[\left(\frac{4.5 \text{ mm}}{2 \cdot 1000} \right)^2 - \left(\frac{4.0 \text{ mm}}{2 \cdot 1000} \right)^2 \right]$$

$$T_i = 280.8^\circ\text{C} (554.0 \text{ K})$$

The thermal conductivity of the UO₂ for the second shell:

$$k_{\text{UO}_2} = \left[\frac{100}{6.548 + 23.533 \cdot \frac{554.0 \text{ K}}{1000}} \right] + \left[\frac{6400}{\left(\frac{554.0 \text{ K}}{1000} \right)^{2.5}} \right] \cdot e^{\left(-\frac{16350}{554.0 \text{ K}} \right)} = 5.11 \frac{\text{W}}{\text{m} \cdot \text{K}}$$

The temperature inside the second shell (3.5 mm OD) is as below:

$$T_i = 280.8^\circ\text{C} + \frac{91.3 \frac{\text{MW}}{\text{m}^3}}{4 \cdot 5.11 \frac{\text{W}}{\text{m} \cdot \text{K}}} \left[\left(\frac{4.0 \text{ mm}}{2 \cdot 1000} \right)^2 - \left(\frac{3.5 \text{ mm}}{2 \cdot 1000} \right)^2 \right] = 285.0^\circ\text{C}$$

This process was repeated until a steady fuel centreline temperature was reached:

Table C-9: Fuel Centreline Layer Temperatures

Layer	Layer Size OD (mm)	Layer Size ID (mm)	Thermal Conductivity UO ₂ W/m·K	Internal Temperature (°C)
1	4.5	4.0	5.14	280.8
2	4.0	3.5	5.11	285.0
3	3.5	3.0	5.08	288.6
4	3.0	2.5	5.06	291.7
5	2.5	2.0	5.04	294.3
6	2.0	1.5	5.02	296.2
7	1.5	1.0	5.01	297.7
8	1.0	0.5	5.00	298.5
9	0.5	0.1	5.00	298.8
10	0.1	0.01	5.00	298.8

After 10 layers, down to the ID of 0.01 mm, the fuel centreline temperature was determined to be 298.8°C.

C.3.3.3 Fuel Centreline Temperature, 37-Element bundle

To calculate the fuel centreline temperature of the 37-element bundle (Sheath OD = 13.08 mm, sheath thickness = 0.38 mm, 12 bundles × 0.485 m = 5.82 m length), the energy generation density was calculated:

$$\dot{g} = \frac{\dot{Q}}{V} = \frac{\dot{Q}}{\# \text{ rods} \cdot \frac{\pi}{4} \cdot D^2 \cdot L} = \frac{9.97 \text{ MW}}{37 \cdot \frac{\pi}{4} \cdot \left(\frac{12.32 \text{ mm}}{1000} \right)^2 \cdot 5.82 \text{ m}} = 388.38 \frac{\text{MW}}{\text{m}^2}$$

Once this value is known, the process from Fuel Centreline Temperature, 7-rod can be used to determine the fuel centreline temperature.

C.3.3.4 Fuel Centreline Temperature, 64-Element bundle

To calculate the fuel centreline temperature of the 64-element bundle (Sheath #1 OD = 9.5 mm, Sheath #2 OD = 10.0 mm, sheath thickness = 0.4 mm, 5 m length), the energy generation density was calculated:

$$\dot{g} = \frac{\dot{Q}}{V} = \frac{\dot{Q}}{\# rods \cdot \frac{\pi}{4} \cdot D^2 \cdot L} = \frac{9.97 \text{ MW}}{32 \cdot \frac{\pi}{4} \cdot \left[\left(\frac{9.2 \text{ mm}}{1000} \right)^2 + \left(\frac{8.7 \text{ mm}}{1000} \right)^2 \right] \cdot 5 \text{ m}} = 494.85 \frac{\text{MW}}{\text{m}^2}$$

Once this value is known, the process from Fuel Centreline Temperature, 7-rod can be used to determine the fuel centreline temperature.

APPENDIX D: PERMISSIONS OBTAINED

D.1 WNA PERMISSION FOR USE OF CONTENT



Home / Homepage Items / Permission for Use of Content

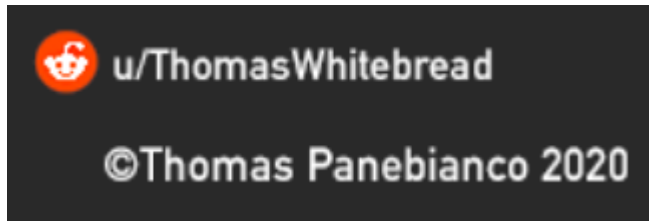
Non-exclusive permission for reuse of World Nuclear Association content

All text, photographs, graphics and other content displayed on this website are copyright the World Nuclear Association ("Our Content") or its licensors. All rights in all Our Content and other content on this website are expressly reserved.

This licence permits you to copy and distribute Our Content, provided you do so in accordance with the terms below. All use of Our Content is solely on the terms of this licence - if these terms are not acceptable to you, you are not entitled to make any use of Our Content under this licence and must seek specific permission from World Nuclear Association:

- You may reproduce sections of up to 150 words from individual pages, except where a page contains fewer than 300 words when you may only reproduce up to 50% of the words on that page. Any reproduced sections must carry attribution to the World Nuclear Association and may not materially change (or suggest a material change in) the meaning of the content. In the case of web-based reproduction the quoted content must include a link back to the original world-nuclear.org page from which it is sourced.
- You may reproduce only those charts or graphics originated by the World Nuclear Association. Such graphics are indicated by the presence of a World Nuclear Association logo on the graphic. The graphic may be resized, but should not otherwise be altered. The World Nuclear Association logo should remain clearly visible. For web-based reproduction of charts or graphics there should be a link back to the page on which they were found, or the world-nuclear.org homepage.
- You must assert World Nuclear Association's copyright in all Our Content used and must not purport to claim any copyright or other rights on behalf of your self or any third party in content sourced from the World Nuclear Association website or other World Nuclear Association publications.
- You must not attribute to the World Nuclear Association material which is not our content.
- You must not in any way do or omit to do anything which may suggest or imply: that World Nuclear Association endorses any products or services other than its own; or a misrepresentation as to the relationship between World Nuclear Association and yourself; or any false information about World Nuclear Association
- You may not make any use of World Nuclear Association's trade marks except as expressly permitted in this licence.
- You must not do or omit to do anything which may weaken, damage or be detrimental to World Nuclear Association's trade marks, goodwill or reputation.
- World Nuclear Association makes no express or implied warranty or representation as to the accuracy or adequacy of Our Content and all conditions, warranties or other terms concerning Our Content which might otherwise be implied are hereby expressly excluded.
- To the maximum extent permissible by law, World Nuclear Association shall have no liability to any party for any loss or damage arising from use made of Our Content under this licence, whether such loss or damage was foreseeable or in the contemplation of the parties and whether arising in negligence or otherwise
- This licence may be amended or terminated without notice by World Nuclear Association in its absolute discretion - you should check the currently applicable terms of this licence from time to time.
- This licence and your use of Our Content in accordance with it are subject to English law and the exclusive jurisdiction of the English courts.

D.2 THOMAS PANEBIANCO PERMISSION FOR HDI WORLDMAP



[/u/ThomasWhitebread](#)

Country Subdivisions by Human Development Index (HDI) (Original Creation):

[expand all](#) [collapse all](#)

[~] to [/u/ThomasWhitebread](#) sent an hour ago

Hi Thomas,

I really like your map on HDI worldwide, its great! I'm a Masters student at UOIT in Oshawa, Ontario, Canada, pursuing a Masters degree in Nuclear Engineering.

Part of my thesis background on heat transfer with Supercritical water is to highlight the importance of electricity, specifically the relationship between a greater electrical consumption and the resulting higher level of HDI.

I was wondering if I could get your permission to use your map in my thesis as a representation of HDI worldwide?

Thanks in advance Thomas for your consideration!

Scott Clark

[Permalink](#)

[~] from [/u/ThomasWhitebread](#) sent 59 minutes ago

Hi, Scott

I would be honored to let you use my map to help you pursue your masters! I am glad that my work can be put to such use and I wish you the best on your academic journey!

Best, Thomas

[Permalink](#) [Delete](#) [Report](#) [Block User](#) [Mark Unread](#) [Reply](#)

APPENDIX E: AUTHORS WORKS

E.1 PUBLICATIONS

Clark, S., Pioro, R., Zvorykin, A., Fialko, N. M., & Pioro, I. L. (2019, June 23-26). Comparison of Experimental and Calculated HTC Values for Short Vertical 7-Rod Bundle Cooled with SCW. 39th Annual Conference of the Canadian Nuclear Society and 43rd Annual CNS/CNA Student Conference, Paper #41. Ottawa, ON, Canada. pp. 1-7.

Sabir, S. M., Chun, K., Petriw, M., Saifullah, M., Vashi, A., Zvorykin, A., Clark, S.; Pioro, I. L. (2019). Comparison of Thermophysical Properties (NIST REFPROP VER. 10) and Heat Transfer to Heavy and Light Water at Subcritical Pressures. *The 27th International Conference on Nuclear Engineering (ICONE27), The Japan Society of Mechanical Engineers, May 19-24, Article 2019.27.*

E.2 CONFERENCES ATTENDED

39th Annual Conference of the Canadian Nuclear Society and 43rd Annual CNS/CNA Student Conference, Ottawa, Ontario, Canada, June 23-26, 2019